Characterisation of age-associated B cells in rheumatoid arthritis patients

Thesis for the degree of Doctor of Philosophy (PhD)

Gemma Vidal-Pedrola

Musculoskeletal Research Group,

Translational and Clinical Research Institute,

Faculty of Medical Sciences,

Newcastle University

Supervised by:

Dr Amy Anderson

Professor John Isaacs

Professor Dagmar Scheel-Toellner

Dr Arthur Pratt

Professor Andrew Mellor

May 2020

Newcastle University

Inflammation, Immunology & Immunotherapy

RESEARCH INTO INFLAMMATORY ARTHRITIS CENTRE VERSUS ARTHRITIS

Abstract

Rheumatoid arthritis (RA) is a chronic autoimmune disorder characterised by joint inflammation and bone destruction. The presence of autoantibodies, years before the clinical onset of disease, and the efficacy of rituximab, a B-cell depleting therapy, highlight a pathogenic role for B cells in the initiation and development of RA. Different groups have recently identified a novel subset of B cells named age-associated B cells (ABCs). Studies in murine autoimmune models and patients suffering from autoimmune diseases described these cells as CD19high CD21- CD11c+. Moreover, a subset of synovial fluid B cells with a similar phenotype, also expressing FcRL4, has been demonstrated to contribute to RA pathogenesis. I aimed to fully characterise, phenotypically, transcriptionally and functionally, peripheral blood ABCs in patients suffering from early RA.

I have shown that although my study did not show significant differences in the frequency of peripheral blood ABCs between RA patients and other disease and healthy controls, the percentage of cells with an ABC phenotype in the synovial fluid is very high in patients suffering from inflammatory arthritides. I characterised these cells phenotypically and confirmed that they have high expression of activation and co-stimulatory molecules, in addition to expressing high levels of T-bet and the members of the FcRL family (i.e. FcRL2-5). Moreover, these cells are actively proliferating and a high proportion of them have a class-switched memory B cells phenotype expressing IgG. Interestingly, the transcriptome analysis showed that the ABCs are a subset of B cells, distinct from naïve, CD5+ and memory B cell subsets, with a unique transcriptome profile. ABCs had a high expression of chemokine receptors, such as CXCR3, as well as adhesion molecules, such as integrins and CD97, supporting a role for the migration of these cells into inflammatory sites. In addition, ABCs also had high expression of apoptotic markers, such as caspases and Fas. Finally, the functional characterisation of ABCs showed that these cells are capable of secreting IgM and IgG after stimulation. However, due to low cell numbers and high cell death, very low quantities of secreted cytokines were detected; making it very difficult to determine if these cells could contribute to inflammation.

Overall, I confirmed that the ABC subset is an activated memory-like B cell subset which could potentially migrate into inflammatory sites and promote disease pathogenesis. However, exactly how these cells contribute to RA pathogenesis is still unknown and further functional work will help elucidate their role in autoimmunity.

Dedication

To my mum, Mercè, for teaching me how to fight for my dreams and for showing me that anything was achievable (“som formiguetes”). To my dad, Jesús, for always encouraging me into being curious and awakening this skill to be willing to learn a new thing every day.

To all my family, el papa, la mama, el meu germà Xavier, els padrins i padrines, els cosins i cosines, i sobretot els avis, thank you all for believing in me and for supporting me in everything I do.

To all my friends, both from home and from all over the world (I am so lucky to have had the opportunity to meet so many people during my time in the UK) for their friendship and support.

Last but definitely not least, to my grandmother Maria, who inspired me to pursue a career in science to improve people’s life and fight diseases. Gràcies iaia.

Motto

“If we knew what it was we were doing, it would not be called research, would it?"

Albert Einstein

Acknowledgements

I would like to thank my supervisors in Newcastle University, Dr Amy Anderson, Professor John Isaacs, Dr Arthur Pratt and Professor Andrew Mellor, as well as my supervisor Professor Dagmar Scheel-Toellner in University of Birmingham for their invaluable guidance and support throughout my project. I would like to thank Dr Amy Anderson, Professor John Isaacs and Professor Dagmar Scheel-Toellner for their comments on this thesis. I strongly appreciate all the support of Dr Amy Anderson for her advices and comments on the project, as well as for her scientific knowledge and support in learning new techniques.

Additionally, I would like to thank Versus Arthritis who provided the funding for this project. Thank you to the members of the Rheumatoid Arthritis Pathogenesis Centre of Excellence for proving a friendly and supportive environment in which to discuss research.

I am grateful to all individuals who disinterestedly participated giving blood for this study. I would particularly like to thank the patients attending the Newcastle Arthritis Clinics, as well as all the clinicians and nurses for helping in patient recruitment.

I would also like to thank Najib Naamane for his help with the bioinformatics analysis and Dr Dennis Lendrem for his input and advice with statistical analysis.

I am thankful to Professor Satoshi Nagata and Dr Tomoko Ise, from Osaka University, Japan, for providing the FcRL1-5 pcDNA3 plasmids used to test the flow cytometry antibodies.

I would also like to thank Dr Carmody at the University of Glasgow for providing the retroviral vectors.

I would also like to thank Dr Lilian Nwosu for her help, advice and friendship. I am also thankful to Leonie Schittenhelm (soon to be Dr Schittenhelm), Dr Inmaculada Hernandez, Dr Peter Vegh and Dr Kat Cheung for the so-needed lunch breaks and their friendship.

Finally, I would like to thank the entire Immunotherapy group, present and past members, for their help with everyday lab questions, for making the time spent here so enjoyable and for the Friday afternoons in the pub.

Table of contents

List of figures

List of tables

List of abbreviations

ABCs: Age-associated B cells

ACPA: Anti-cyclic Citrullinated Peptides Antibody

ACR: American College of Rheumatology

AF: Alexa Fluor

AID: Activation-Induced cytidine Deaminase

APCs: Antigen-Presenting Cells

APC: Allophycocyanin

ATM: Ataxia Telangiectasia-Mutated

AWERB: Animal Welfare and Ethical Review Body

BB: Brilliant Blue

BCL: B Cell Lymphoma Protein

BCR: B cell Receptor

BLAST: Basic Local Alignment Search Tool

BLIMP1: B-Lymphocyte-Induced Maturation Protein 1

BSA: Bovine Serum Albumin

BV: Brilliant Violet

BUV: Brilliant UV

CCL: C-C motif Chemokine Ligand

CCR: C-C chemokine Receptor

CD: Cluster of Differentiation

CR: Complement Receptor

CIA: Collagen-Induced Arthritis

CRP: C-Reactive Protein

csDMARDs: conventional synthetic Disease Modifying Anti-Rheumatic Drug

CTLA-4: Cytotoxic T-Lymphocyte-associated Antigen 4

CTV: CellTrace Violet

CVID: Combined Variable Immunodeficiency

CXCR: C-X-C chemokine Receptor

DAS28: Disease Activity Score-28

DC: Disease Control

DCs: Dendritic Cells

DMARDs: Disease Modifying Anti-Rheumatic Drug

DMEM: Dulbecco's Modified Eagle Medium

DMSO: Dimethyl Sulfoxide

DNA: Deoxyribonucleic Acid

EBNA: Epstein-Barr Nuclear Antigen

EBV: Epstein - Barr Virus

EDTA: Ethylenediaminetetraacetic Acid

eIA: early Inflammatory Arthritis

ELISA: Enzyme-Linked ImmunoSorbent Assay

eQTL: expression Quantitative Trait Locus

eRA: early Rheumatoid Arthritis

ERK: Extracellular signal-Regulated Kinases

ERV: Endogenous Retrovirus

ESR: Erythrocyte Sedimentation Rate

EstIA: Established Inflammatory Arthritis

EstRA: Established Rheumatoid Arthritis

EULAR: European League Against Rheumatism

FACS: Fluorescence-Activated Cell Sorting

FCGR: Fc Gamma Receptor

FcRL: Fc Receptor Like

FCS: Foetal Calf Serum

FDCs: Follicular Dendritic Cells

FITC: Fluorescein isothiocyanate

FLS: Fibroblast-Like Synoviocytes

FMO: Fluorescence Minus One

FO: Follicular

FSC: Forward-Scattered light

GFP: Green Fluorescent Protein

GLM: Generalized Linear Model

GM-CSF: Granulocyte-Macrophage Colony-Stimulating Factor

GWAS: Genome Wide Association Studies

GZM: Granzyme

HC: Healthy Control

HCQ: Hydroxychloroquine

HEK: Human embryonic kidney

HERV: Human Endogenous Retrovirus

HIV: Human Immunodeficiency Virus

HLA: Human Leukocyte Antigen

ICAM: Intercellular Adhesion Molecule

Ig: Immunoglobulin

IFN: Interferon

IFNAR: Interferon Alpha and Beta Receptor

IL: Interleukin

ILCs: Innate Lymphoid Cells

IRES: Internal Ribosome Entry Site

IRF: Interferon Regulatory Factor

ITAM: Immunoreceptor Tyrosine-based Activation Motif

ITIM: Immunoreceptor Tyrosine- based Inhibitory Motif

ITSM: Immunoreceptor Tyrosine- based Switch Motif

JIA: Juvenile Idiopathic Arthritis

KIR: Killer cell Immunoglobulin-like Receptor

KLR: Killer cell Lectin like Receptors

LAIR: Leukocyte Associated Immunoglobulin like Receptor

LB: Luria Broth

LEAF: Low Endotoxin Azide-Free

LILR: Leukocyte Immunoglobulin Like Receptor

LINE-1: Long interspersed nuclear element 1

LTR: Long Terminal Repeat

MACS: Magnetic Cell Sorting

MALT: Mucosa-Associated Lymphoid Tissues

MAPK: Mitogen-Activated Protein Kinase

MFI: Median Fluorescence Intensity

MHC: Major Histocompatibility Complex

mQTL: methylation Quantitative Trait Locus

mRNA: messenger RNA

MS: Multiple Sclerosis

MSD: Meso Scale Discovery

MTX: Methotrexate

MZ: Marginal Zone

NEAC: Newcastle Early Arthritis Clinic

NFATC: Nuclear Factor of Activated T Cells

NF-κB: Nuclear Factor Kappa-light-chain-enhancer of activated B cells

NFKBI: NFKB Inhibitor

NIHR: National Institute for Health Research

NK: Natural Killer

NZB: New Zealand Black

OIA: Other Inflammatory Arthritis

PAMPs: Pathogen-Associated Molecular Patterns

PB: Peripheral Blood

PBMCs: Peripheral Blood Mononuclear Cells

PBS: Phosphate Buffered Saline

PC: Plasma cells

PCA: Principal Component Analysis

PCR: Polymerase Chain Reaction

PE: Phycoerythrin

pIG: Puromycin IRES GFP

PRF: Perforin

PRRs: Pattern Recognition Receptors

PsA: Psoriatic Arthritis

PTPN22: Protein Tyrosine Phosphatase Non-receptor type 22

PWM: Poke Weed Mitogen

RA: Rheumatoid Arthritis

RACE: Rheumatoid Arthritis pathogenesis Centre of Excellence

RANKL: Receptor Activator of Nuclear factor Kappa-B Ligand

RARRES3: Retinoic Acid Receptor Responder 1

RBC: Red Blood Cells

RF: Rheumatoid Factor

RPMI: Roswell Park Memorial Institute

qPCR: quantitative Polymerase Chain Reaction

RT: Room Temperature

SEM: Standard Error of the Mean

SF: Synovial Fluid

SFMCs: Synovial Fluid Mononuclear Cells

SHM: Somatic Hypermutation

SINE: Short interspersed nuclear element

SLE: Systemic Lupus Erythematosus

SLEDAI: Systemic Lupus Erythematosus Disease Activity Index

SNP: Single Nucleotide Polymorphisms

SOC: Super Optimal Broth or SOB

SOCS: Suppressor Of Cytokine Signalling

SSC: Side-Scattered light

SSc: Systemic sclerosis

SSZ: Sulfasalazine

STAT: Signal Transducer and Activator of Transcription

TAE: Tris base, Acetic acid and EDTA.

TBX21: T-Box Transcription Factor 21

TCR: T cell Receptor

TD: T-Dependent

Tfh: T follicular helper

Th: T helper

TI: T-Independent

TLR: Toll Like Receptor

TNF: Tumor Necrosis Factor

TNFRSF: TNF Receptor Superfamily Member

Tregs: T regulatory cells

UIA: Undifferentiated Inflammatory Arthritis

VAS: Visual Analogue Scale

VSVG: Vesicular Stomatitis Virus G glycoprotein

WT: Wild Type

XBP1: X-box Binding Protein 1

ZUV: Zombie UV

Chapter 1. Introduction

1.1 Rheumatoid Arthritis

1.1.1 Rheumatoid Arthritis Pathogenesis

Rheumatoid arthritis (RA) is a chronic autoimmune disorder characterised by joint inflammation and bone destruction. RA was regarded as an autoimmune disease resulting from immune dysregulation after the discovery of a genetic association with the Human Leukocyte Antigen (HLA) class II molecules and other innate and adaptive immune system molecules, presence of autoantibodies, and the development of a murine model for RA using immunisation with type II collagen, a candidate autoantigen in RA (McInnes and Schett, 2011). RA has a prevalence of around 1% in the UK population, affecting adults of working age (Humphreys *et al.*, 2013). Moreover, RA is associated with high morbidity and mortality, which shortens the patient's lifespan and increases the risk of work-related disability and impaired quality of life (Innala *et al.*, 2016). Interestingly, RA has a higher prevalence in females compared to males, with a ratio of 3 females per 1 male being affected (Kvien *et al.*, 2006). The risk factors for the development of RA include both genetic and environmental, with the strongest associations being seen with female sex, a family history of RA, the presence of certain HLA class II alleles and exposure to tobacco smoke (Deane *et al.*, 2017). Evidence suggest that the risk factors have an effect before the clinical onset of the disease presents, due to the presence of autoantibodies and other biomarkers many years before symptoms appear (Deane and El-Gabalawy, 2014).

RA is a heterogeneous disease both in terms of clinical presentation and pathogenesis. RA patients can be divided into two major subgroups based on the presence or absence of autoantibodies against citrullinated proteins, called anti-citrullinated protein antibodies (ACPAs), and autoantibodies specific for the Fc part of immunoglobulin G, known as rheumatoid factor (RF). The presence of ACPA and/or RF defines the form of RA known as seropositive RA that constitutes approximately two-thirds of all the disease cases (Malmstrom *et al.*, 2017). Interestingly, ACPA is specific for RA, but RF is not and can be found in other arthritides. The seropositive form of RA causes typically more bone and joint destruction and the patients respond better to B cell depletion therapy using the anti-CD20 antibody, Rituximab (Chatzidionysiou *et al.*, 2011).

At diagnosis patients present classically with a symmetrical polyarthritis of the small joints of the hands and feet. The inflammation of the joints, or synovitis, occurs when a wide range of immune cells, such as T cells, B cells, macrophages and neutrophils, infiltrate the

synovial compartment (McInnes and Schett, 2011). All these cells contribute to RA pathogenesis by producing proinflammatory mediators, such as TNF-α, IFN-γ and IL-6. These pro-inflammatory mediators in turn create a positive feedback loop and further activate adaptive and innate immune pathways. These mediators also activate other resident cells, such as synovial fibroblasts, chondrocytes and osteoclasts, which promote tissue damage and remodelling, culminating in cartilage and bone destruction. All in all, this persistent inflammation drives the chronic phase in the pathogenesis of RA (Figure 1.1).

The current approach used to treat RA firstly involves global immune suppression using conventional synthetic disease-modifying anti-rheumatic drugs (csDMARDs), such as methotrexate. If the patient does not respond to this treatment the next phase is the introduction of a newer therapy called biologics that cause more specific immunomodulation. The first biologic developed was Infliximab, a monoclonal antibody directed against TNF (Elliott *et al.*, 1994). The following years saw an explosion of other biologic therapies, of interest in this thesis is Rituximab, an anti-CD20 antibody, which can be used to deplete B cells. Biologic therapies are generally more effective than DMARDs and have significantly improved the outcome of patients suffering from RA (Cheung and McInnes, 2017). Unfortunately, these treatments do not work on all patients, as only two thirds of patients respond to therapy. Consequently, there is an unmet need for new therapies in RA and therefore, exploring novel targets of pathogenic cellular subsets will bring insights into other ways of treating RA (Strand et al., 2007).

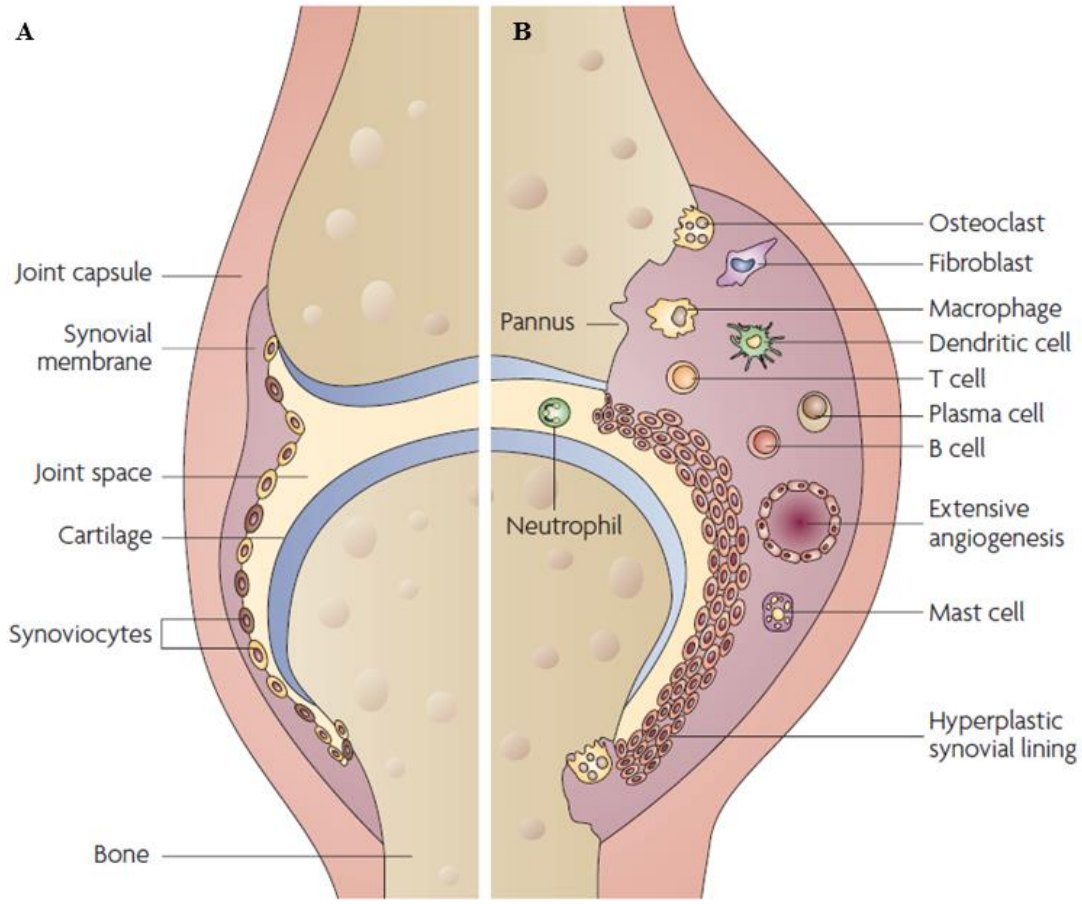

Figure 1. 1. Representative diagram of a healthy joint and a rheumatoid arthritis joint. A. Schematic of a healthy joint with the thin synovial membrane which produces lubricating synovial fluid. **B.** Schematic of a rheumatoid arthritis joint. In RA, the synovial membrane is invaded by inflammatory cells as T and B cells. Moreover, the synoviocytes proliferate and the membrane becomes hyperplastic destroying the cartilage and the bone. Image obtained from Strand *et al*., 2007.

1.1.2 Early Rheumatoid Arthritis

Understanding the triggering event of RA continues to be challenging and identifying the possible triggers has proved remarkably difficult. A model for the longitudinal disease course of RA proposed by Malmström *et al.* and review by Smolen *et al.* divides the disease development in four phases (Malmstrom *et al.*, 2017; Smolen *et al.*, 2018). Phase 1 represents triggering of the disease by an environmental stimulus plus the genetic risk at mucosal surfaces. Phase 2, maturation, occurs when the autoimmune response gradually matures, epitopes start spreading and autoantibody titres (ACPAs and RF) increase. This phase happens in regional lymph nodes and other secondary lymphoid organs. In Phase 3, the targeting, leukocytes are recruited into the joints and there is production of pro-inflammatory mediators, which further activate cells and cause joint swelling. Moreover, ACPAs and RF autoantibodies also contribute to this inflammation. In phase 4, a second hit in the joints produced by a microtrauma or an infection could lead to synovial vascular activation, leading to additional recruitment of more pro-inflammatory cells into the joints. This leads to cartilage destruction, bone loss and joint damage. This phase 4 corresponds with the development of the classical symptomatology of RA caused by chronic inflammation of the joint (Figure 1.2).

Different studies have demonstrated that treating patients at an early stage (phase 3), in the so-called window of opportunity, has better long-term outcomes in terms of patient morbidity and disease control (Smolen *et al.*, 2016; Stoffer *et al.*, 2016). This is translated in the clinic by the rapid initiation and escalation of DMARDs in the early stages after diagnosis. The aim of this approach is to achieve rapid and sustained low disease activity as soon as a patient has been diagnosed (Lard *et al.*, 2001).

In the clinic, the 2010 ACR/European League Against Rheumatism (EULAR) classification criteria was designed in part to make earlier diagnosis of RA feasible (Aletaha *et al.*, 2010). However, from a research context, identifying the pathological processes that occur in early disease would provide new therapeutic targets and strategies with long term benefits. Moreover, studying the immune dysregulation in RA patients treated with DMARDs and glucocorticoids can limit our understanding of the disease process as these treatments can mask the immunological processes that are taking place.

There is a great deal of interest in, and an advantage to studying the early onset of RA. It is thought that in RA a break of tolerance to self-antigens leads to the development of

autoimmunity. However, the point when this breach happens is still unknown and may vary between individuals (Deane and Holers, 2019). In recent years studies have shown that autoantibodies can be detected in the blood of individuals at risk years before the onset of the disease (Deane and El-Gabalawy, 2014). Moreover, there is emerging evidence that initiation and propagation of RA autoimmunity could occur at mucosal sites (Catrina *et al.*, 2014).

In summary, studying early diagnosed patients before the start of therapy (i.e. drug naïve) will bring insights into the early pathogenesis of RA, which will help identify RA suffers and enable early, tailored treatment initiation, which will in turn improve their response to treatment and life quality.

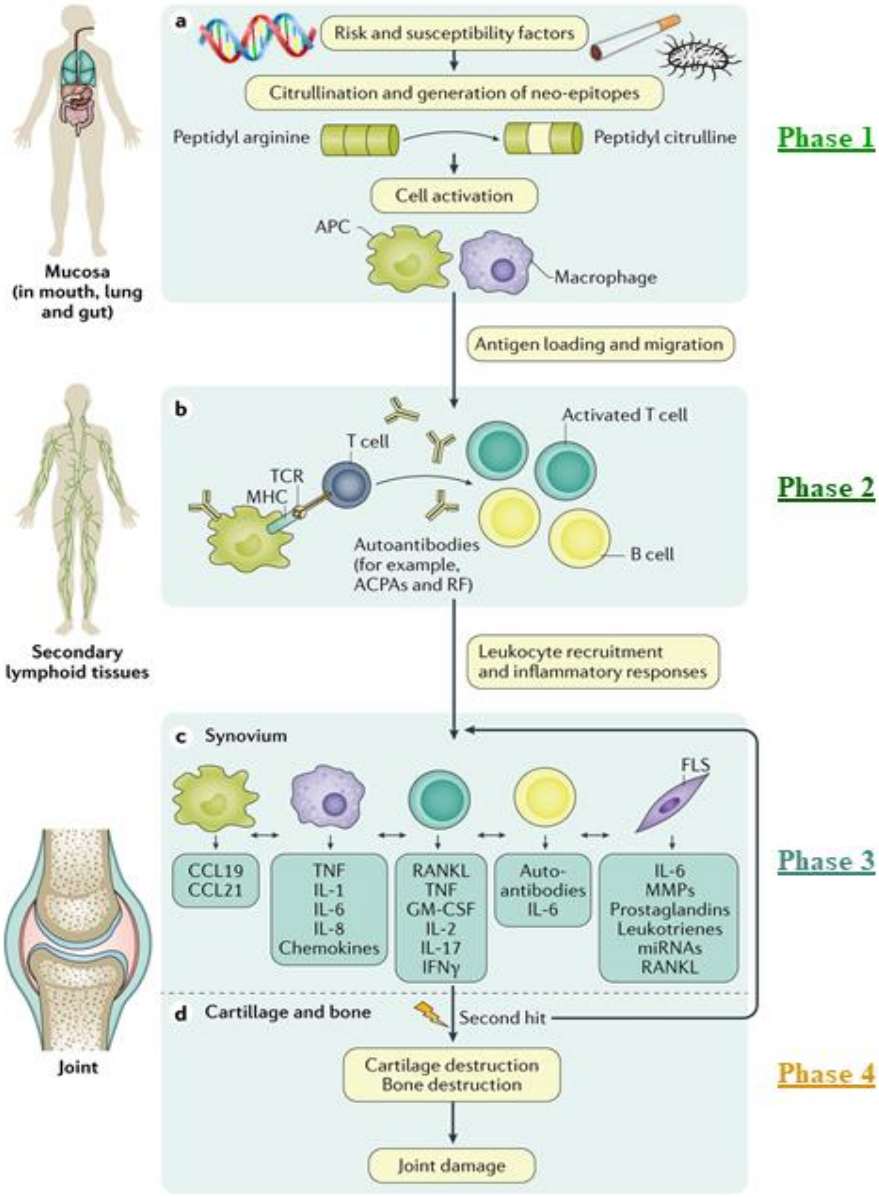

Figure 1. 2. Mechanisms involved in initiation and progression of rheumatoid arthritis. A. Phase 1 represents triggering of the disease -by an environmental stimuli plus the genetic risk at mucosal surfaces such as the lungs, the gum or the gut. **B. Phase 2**, maturation, occurs when the autoimmune response gradually matures, epitopes start spreading and autoantibody titres (ACPAs and RF) increase. This phase is thought to happen in regional lymph nodes and other secondary lymphoid organs. **C.** In **Phase 3**, the targeting, the recruitment of leukocyte into the joints together with ACPAs and RF autoantibodies cause joint swelling. A wide range of recruited cells, as well as resident cells produce pro-inflammatory mediators which further promote inflammation. **D.** A second hit in the joints produced by a microtrauma or an infection could lead to synovial vascular activation, leading to additional recruitment of more pro-inflammatory cells into the joints. This leads to cartilage destruction, bone loss and joint damage. This phase 4 would correspond with the development of the classical symptomatology of RA caused by chronic inflammation of the joint. Adapted from Smolen *et al.,* 2018.

1.2 Immune system overview

The function of the immune system is to protect us from organisms that can cause disease. We are constantly in contact with organisms via inhalation, skin contact or ingestion and whether these organisms cause disease or not depends on their pathogenicity and also on the integrity of our immune system (Parkin and Cohen, 2001). The immune system is composed of lymphoid organs, cells and cytokines, which together protects the body from pathogens. The immune response is divided into two arms: an innate response, characterised by a rapid reaction, which provides immediate host defence, and an adaptive response, which takes more time to develop but it is characterised by an antigen specific response (Figure 1.3). A key function of the immune system is the recognition of self and non-self. This feature is essential to prevent damage to the body and when it fails an autoimmune, self-reactive response can develop resulting in destruction of organs (Kumar *et al.*, 2017).

1.2.1 Innate immunity

Innate immunity is the first line of host defence against pathogens. Its importance in survival is demonstrated by the highly conserved innate response mechanisms across species (Yatim and Lakkis, 2015). The innate immune system is composed of physical barriers, such as mucosal surfaces, the complement system and innate immune cells. This group of cells consists of neutrophils, eosinophils, basophils, dendritic cells (DCs), monocytes/macrophages, innate lymphoid cells (ILCs), mast cells and natural killer cells (Janeway and Medzhitov, 2008).

Although pathogens are very diverse, they all express conserved molecular structures not present in the eukaryotic organisms. Because related species of microbes have similar structures, this allows for the recognition of infectious non-self organisms by the immune system. These structures include components of microbial membranes, cell walls, proteins and DNA, and are called pathogen-associated molecular patterns (PAMPs) (Dempsey *et al.*, 2003). These common structures are recognised by highly conserved receptors named pattern recognition receptors (PRRs). The best known of these PRRs are Toll-like receptors (TLRs), which detect the presence of pathogens and induce activation of inflammatory innate immune responses (Medzhitov, 2001).

The innate immune system is the first line of defence, it is a rapid response, but its lack of specificity can lead to tissue damage. Therefore, a more specific response, the adaptive immune response, is also needed.

1.2.2 Adaptive immunity

Adaptive immunity provides a more specific response to pathogens. This response involves antigen-presenting cells (APCs) directing T and indirectly, B lymphocytes (cells) to facilitate pathogen-specific effector pathways and generate immunologic memory. Lymphocytes are derived from progenitor cells in the bone marrow. T cells then develop and mature in the thymus and B cells do the same in the bone marrow. As part of this development/maturation process gene rearrangement of the antigen-recognition receptors, the T cell receptor (TCR) in T cells and the B cell receptor (BCR) in B cells, leads to the generation of unique antigen-specific receptors for T cells and B cells, with each individual T cell and B cell expressing receptors for a single specificity that recognises a single cognate antigen (Bonilla and Oettgen, 2010). Once a developed T cell or B cell enters the periphery, as a naïve cell, they can be activated in lymphoid organs, resulting in initiation of an adaptive immune response. In addition, some of these activated antigen-specific cells will became long-lived memory cells, which upon a second encounter with the same pathogen, will activate and produce a more rapid and robust protective response.

The cells of the innate and adaptive immune system interact and work together to fight pathogens. Briefly, DCs, as professional antigen-presenting cells, present antigens in the form of peptides (processed forms of protein) to both to CD8+ and CD4+ cells via major histocompatibility complex (MHC) class I and class II molecules, respectively. The T cell recognises the presented antigen via their TCR, but only if the TCR is specific for that particular peptide. This interaction of MHC molecule-peptide complexes with the TCR is the first step in T cell activation and is known as signal 1(Williams and Bevan, 2007). But signal 1, antigen presentation, is not the only signal required for full T cell activation. DCs also provide co-stimulatory signals and cytokines (den Haan *et al.*, 2014). The second signal (signal 2) is provided through co-stimulatory molecules, for example CD80 and CD86, expressed by DCs, which bind to CD28 on the T cell. Finally, a third signal (signal 3) is transmitted through the release of cytokines. The cytokines milieu where the T cell activation happens will drive T helper (Th) cells towards one of several different differentiation pathways and will therefore result in different effector functions (Bonilla

and Oettgen, 2010). These three signals are required for the T cell to reach its expansion potential and fully activate (Curtsinger and Mescher, 2010).

B cells are activated in a different manner to T cells. In brief, mature, naïve B cells can recognise antigens through their BCR, which, at this stage, includes both IgM and IgD isotypes (den Haan *et al.*, 2014). B cells can be activated in two ways, depending on the type of antigen: T-dependent (TD) antigens, requiring T cell help, and T-independent (TI) antigens, which do not require T cell help. For TD antigens in order for B cells to fully activate, in addition to antigen recognition via their BCR, B cells also need help from T cells, particularly T follicular helper (Tfh) cells found in germinal centres. Recognition of antigen via the BCR, together with co-stimulatory signals and cytokines produced by T cells, leads to B cell activation, resulting in B cell proliferation, antibody affinity maturation and immunoglobulin (Ig) class switch recombination (MacLennan, 1994). For TI antigens, B cells respond to the antigen independently of T cell help through BCR and other PRR receptor signalling or throughout chronic BCR stimulation by a specific antigen (Weller *et al.*, 2001). Activation of B cells via the TD route leads to the generation of antigen-specific memory B cells, which results in a recall response that occurs more rapidly and consists of high affinity antibodies of the IgG, IgA or IgE isotypes (Ahmed and Gray, 1996). However, activation of B cells via the TI route induces very poor and short-lived memory responses, mainly producing antibodies of the IgM isotype.

B cell maturation and differentiation as well as their role in the pathogenesis of RA are discussed in more detail below, in section 1.3.

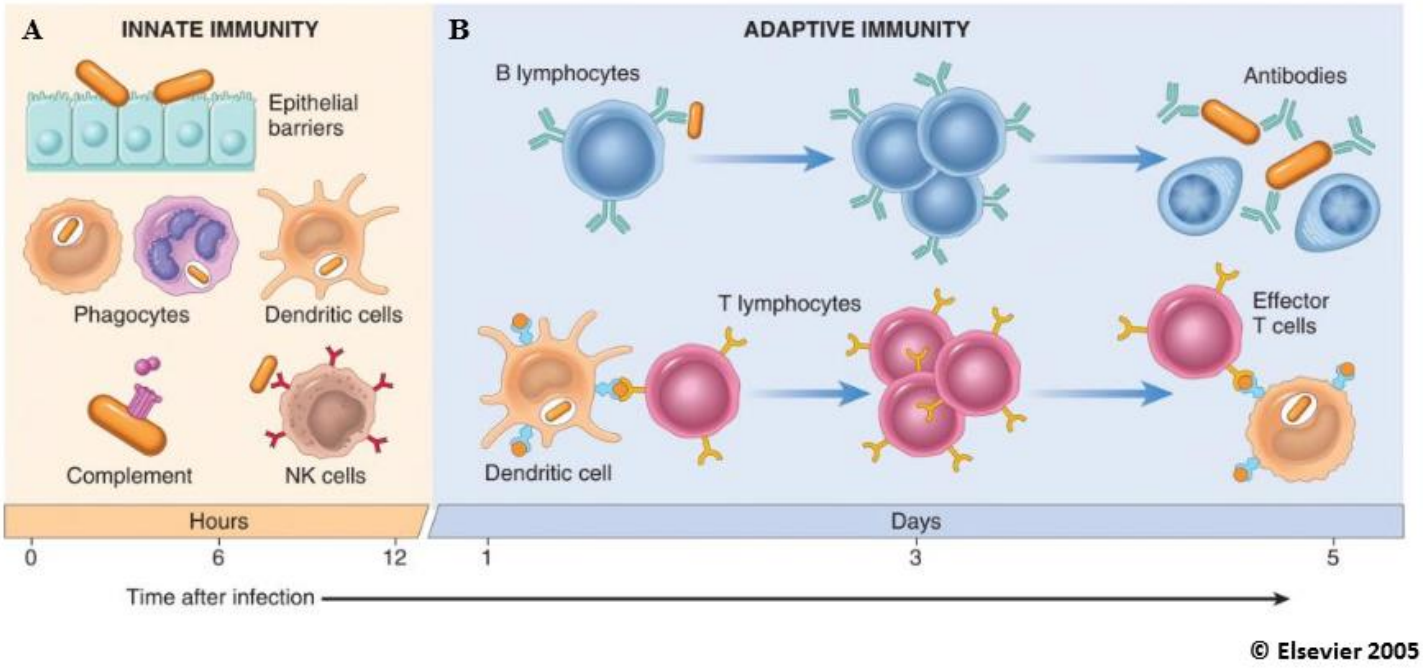

Figure 1. 3. The immune response consists of two arms: an innate response and an adaptive response. A. The innate response is the first line of host defence against pathogens. It is composed of epithelial barriers, the complement system and a group of innate cell populations. Their function is to detect the presence of pathogens and induce activation of inflammatory immune responses. **B.** The adaptive response provides a more specific response to antigens. This response involves B cells recognising a specific antigen and with T cell help differentiating into antibody secreting cells. Moreover, dendritic cells present antigens to T cells, which will expand and become effector T cells. This response facilitates pathogen-specific effector pathways and generates immunologic memory. Image obtained from Kumar *et al.*, 2017.

1.2.3 Immune system dysfunction in RA

As explained before, RA has been regarded as an autoimmune disease resulting from immune dysregulation since the discovery of a genetic association between allelic HLA class II variants and the presence of autoantibodies. However, our understanding of how the immune response contributes to RA disease pathogenesis is constantly evolving as more research is conducted in the area. The immune dysregulation present in RA affects both types of immune response, innate and adaptive, as well as stromal cells, such as fibroblast and osteoclasts (Firestein and McInnes, 2017). In terms of the dysregulation of the innate response, macrophages present in the inflamed joints have been shown to secrete pro-inflammatory cytokines, such as IL-1 and TNF-α and enzymes, such as metalloproteinases, which contribute to joint damage (Kinne *et al.*, 2000). In addition, macrophages have high expression of HLA molecules which allows them to act as antigen presenting cells and therefore perpetuate the dysregulated adaptive response via the activation of T cells and B cells.

Regarding the adaptive response, over recent years T cells have been acknowledged as one of the main pathological cell subsets in RA (Cope, 2008). The most convincing evidence that T cells play a role in RA pathogenesis is their high levels of infiltration in synovial biopsies (Duke *et al.*, 1982). Moreover, genome wide association studies (GWAS) confirmed the association of HLA-DRB1 and other non-HLA regions such as protein tyrosine phosphatase-22 (PTPN22) and cytotoxic T-lymphocyte-associated antigen 4 (CTLA-4) to the genetic risk of RA (Plenge *et al.*, 2005). Additionally, inhibition of T cell co-stimulation by abatacept, a soluble antibody fusion protein of the CTLA-4 extracellular domain, which binds the co-stimulatory molecules CD80 and CD86 with higher affinity than CD28, improved the symptoms of RA (Kremer *et al.*, 2003). However, describing a specific pathogenic T cell subset has been proven very difficult. RA was historically considered a Th1 disease due to IFN-γ expression in murine RA models (McInnes and Schett, 2007). Nevertheless, more recent studies using murine models suggested a Th17 population may be a potent effector T cell subset in RA and other autoimmune diseases. IL-17 is present in the synovial fluid and the cytokine environment of the synovial fluid could potentially support Th17 differentiation. Th2 cytokines have also been suggested to play a role in early RA pathogenesis (Raza *et al.*, 2005). Moreover, dysregulation of regulatory T cells (Tregs), a subset of T cells that dampens immune response, has also been

hypothesised to have reduced functional abilities in RA patients, which would make them less efficient at supressing inflammatory responses (Cooles *et al.*, 2013).

The presence of autoantibodies in RA patients, years before the onset of the disease confirms a role for B cells in RA disease initiation and progression (Conigliaro *et al.*, 2016). The presence of ACPA autoantibodies has been associated with a progressive and destructive disease outcome, showing erosion lesions earlier and at a greater frequency in ACPA+ patients (Burska *et al.*, 2014). Moreover, RF autoantibodies recognise IgG Fc fragments, crosslinking them and creating immune complexes. This immune complexes can then trigger complement activation, which initiates innate immune responses and inflammation (Brown *et al.*, 1982). B cells can further contribute to disease pathogenesis through their production of cytokines, and via their ability to present antigens and activate T cells. Moreover, B cells have also been shown to be increased in the inflamed synovial compartment in RA (Page and Miossec, 2004). The contribution of B cells to RA pathogenesis is further discussed in section 1.3.3.

As mentioned previously, there is growing evidence that autoimmunity may initiate at mucosal surfaces, such the lungs, the oral mucosa and the gastrointestinal tract. The exact mechanisms for this initiation are not fully understood. However, it is thought that local tissue stress leads to the post-translational modification of peptides, such as citrullination, which in turn drives subsequent antibody formation (Yap *et al.*, 2018). Nevertheless, how the disease emerges in the joints is still unknown. Some groups hypothesise that a second "hit" in the joints produced by a microtrauma or an infection could lead to synovial vascular activation. Innate cells in the synovia, like mast cells, may then release vasoactive mediators and increase antibody access to the joint. Autoantibodies in the joint may therefore activate the complement cascade and release chemoattractants. This would lead to the activation of other resident cells, the recruitment of new innate and adaptive immune cells, and the promotion of stromal cell activation (Tan and Smolen, 2016). The recruitment of immune cells could in turn drive the production of more pro-inflammatory cytokines and chemokines self-perpetuating a positive feedback loop and eventually producing chronic inflammation (Firestein and McInnes, 2017).

In summary, for years, CD4+ T cells have been thought to orchestrate the immune cascade in RA, as evidenced by the efficacy of blocking T cell co-stimulation for reducing RA activity (Kremer *et al.*, 2003). Activated CD4+ T cells, as well as producing pro-

inflammatory mediators, provide help for autoreactive B cells to differentiate into autoantibody-producing plasma cells. These factors, together with cytokines secreted by macrophages and fibroblast stimulated by activated CD4+ T cells, are crucial to perpetuate and maintain the chronic inflammation in the joints.

1.3 B cells

The first discovery of a subset of cells, now known as B cells, came in 1890 with the discovery of circulating antitoxins in immunity to diphtheria and tetanus by Emil von Behring and Shibasaburo Kitasato. Later, Paul Ehrlich proposed that an immune cell carrying many different antibody receptors would bind an antigen and release receptors which would specifically bind that antigen (Cooper, 2015). The elucidation and purification of the antibodies led to rapid discoveries and to the recognition of B cells as a separate lymphocyte lineage.

1.3.1 Naïve and memory B cells

B cells develop from stem cells in the bone marrow and go through several maturation and activation stages in peripheral lymph nodes and spleen, until, as plasma cells, they can return to the bone marrow (Hardy and Hayakawa, 2001). B cells can be divided into two main subtypes: naïve and memory B cells.

Immature B cells in the bone marrow undergo recombination of the V, D and J segments to produce an IgD or IgM BCR expressed on the cell surface. If this immature B cell succeeds in producing a functional BCR, it differentiates into a mature, naïve B cell. Mature naïve B cells are found in peripheral blood and lymphoid organs (Figure 1.4). They are characterised by the expression of IgD and IgM but lack switched-class IgG and the activation marker CD27 (LeBien and Tedder, 2008). Each mature naïve B cell expresses a unique BCR, which leads to a wide repertoire of naïve B cells capable of recognising a huge range of antigens. Many naïve B cells that leave the bone marrow contain autoreactive BCRs (Grimaldi *et al.*, 2005).

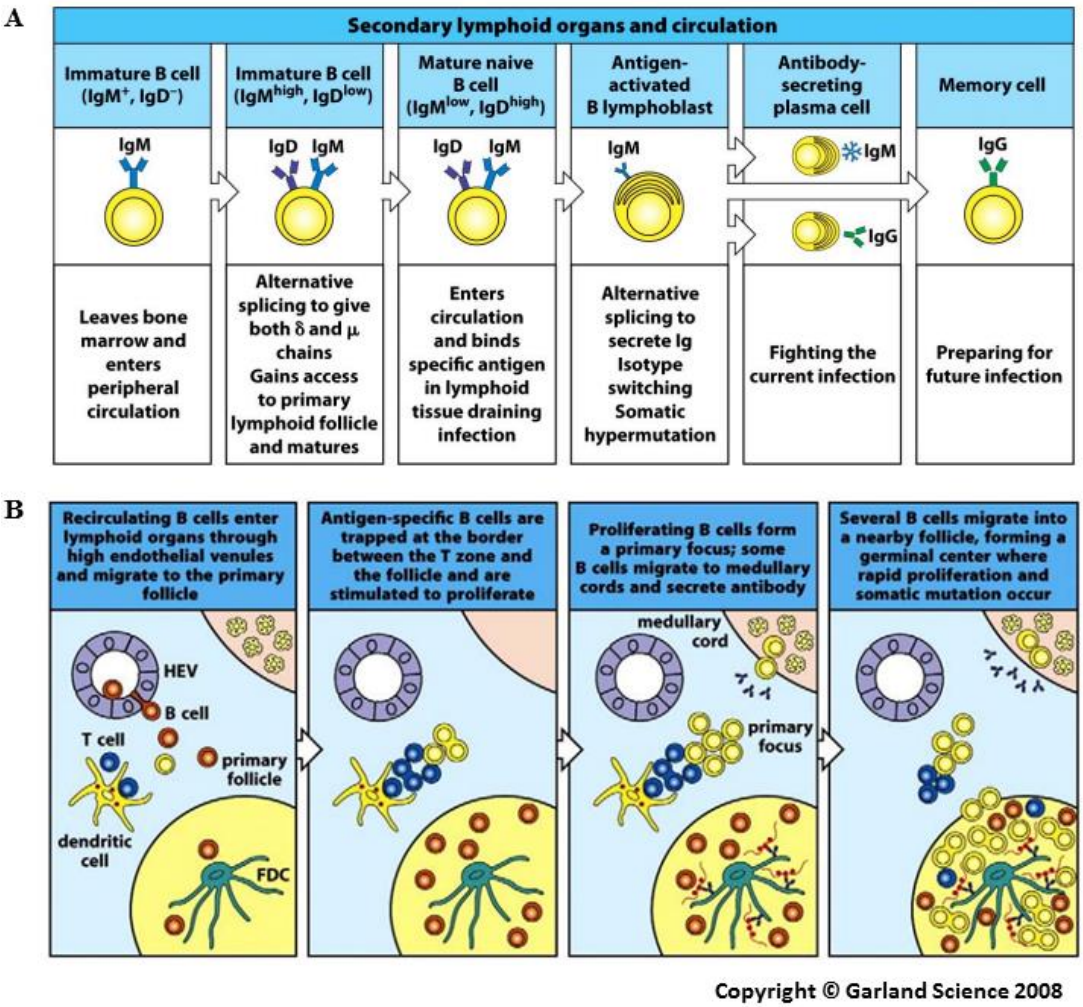

Figure 1. 4. B cell maturation and differentiation in secondary lymphoid organs. A. Summary of the development of human B cells. Immature B cells leave the bone marrow and enter a lymphoid follicle where they mature and express IgM and IgD. Mature naïve B cells expressing mainly IgD enter circulation looking for an antigen to bind. Antigen-activated B cells will proliferate and differentiate with some of these going on to secrete IgM, whereas others undergo somatic hypermutation to improve antigen affinity. If affinity binding is improved the cell will undergo class switching and some will become IgG-secreting plasma cells, whereas others will become circulating memory B cells preparing for future infections. **B.** B cells enter the lymphoid organ and migrate to the primary follicle. Stimulated antigen-specific B cells will interact with antigen-specific T helper cells at the interface between T and B zone. There B cells are stimulated and proliferate forming a primary focus. Some B cells will migrate to medullary cords and secrete antibody whereas other will migrate to the follicle and form a germinal centre where rapid proliferation, somatic mutation, selection and isotype switching will occur. Images obtained from Janeway *et al.*, 2008.

Mature B cells can be activated through the BCR following crosslinking with soluble or particulate antigens. The antigens recognise by the BCR are usually soluble antigens, however, B cells can also acquire and present antigens which are part of the surface of follicular dendritic cells (FDCs) and resident macrophages in the lymph node (Suzuki *et al.*, 2009), as well as from apoptotic immune cells (Ciechomska *et al.*, 2011). Importantly, they can internalise and process these antigens to present them to T cells in the context of MHCII. Following this interaction, B cells will receive stimulatory signals from the T cells such as CD40L/CD40 crosslinking and cytokines and a TD immune response is initiated. Mature naïve B cells are activated by the antigen through the BCR and at the border of the T cell and the B cell zone encounter antigen-specific T cells (Jacob and Kelsoe, 1992) (Figure 1.4). This interaction leads to further activation and proliferation of the B cells; some of the cells will become IgM short-lived plasma cells, whereas other will migrate into the B cell zone. Here, a germinal centre will develop: the B cells undergo proliferation and somatic hypermutation (SHM), which introduces mutations in the BCR variable region genes leading to generation of a diverse range of clones. Many of the mutations will produce a BCR with lower affinity and the B cells will be deleted via apoptosis (Rajewsky, 1996). However, if the new BCR has improved affinity for its cognate antigen, the B cell will be positively selected. They will be selected for specificity and affinity through competition for native antigen captured on the surface of FDCs. The B cells with high affinity BCR will internalise and process the captured antigen and present it to antigen-specific Tfh cells, allowing them to receive a second survival signal. The selected B cells can return to the dark zone of the germinal centre for further cycles of hypermutation and selection to optimise affinity. Furthermore, the B cells with high affinity BCR will undergo class-switch recombination in order to allow for the production of other immunoglobulin isotypes with the capacity of being secreted and distinct effector functions. This cell will undergo proliferation and depending on the transcription factor profile, some cells will differentiate into long-lived plasma cells with high antibody production, which will migrate to the bone marrow (Shapiro-Shelef and Calame, 2005). Other cells will differentiate into memory B cells, which will circulate as resting cells until they are reactivated by recognition of their cognate antigen. Although plasma cell differentiation transcription factors are well known the program that drives memory B cell differentiation is poorly understood (Seifert and Kuppers, 2016).

The circulating memory B cell pool, upon reactivation by their cognate antigen, can differentiate into plasma cells and help increase antibody titres during reinfection. In addition, memory B cells can re-enter germinal centres and undergo further affinity maturation rounds to readapt to the pathogen (Yoshida *et al.*, 2010).

The functions of antibodies are well known; antibodies can bind pathogens to target them for killing. Antibodies can also activate the complement system through the classical pathway and or can target pathogens to be phagocytosed by macrophages (Forthal, 2014). However, memory B cells can perform other functions apart from antibody production, for example they are capable of presenting antigens to T cells, as well as having multiple effects via the secretion of cytokines (LeBien and Tedder, 2008). A part from presenting antigens to T cells, B cells can influence T cell differentiation via expression of co-stimulatory molecules as well as via the production of cytokines which will regulate T cell fate (Gray *et al.*, 2007a). B cell activation can develop without T cell help, leading to a TI immune response. The resulting plasma cells will produce antibodies, commonly of an IgM isotype, of low affinity and usually they do not give rise to long-lived memory B cells (Defrance *et al.*, 2011). These TI responses generally depend on further B cell activation through TLRs or enhanced crosslinking through repetitive epitopes for example on carbohydrate antigens.

1.3.2 CD5+ B cells

CD5 expression on B cells was first described in mice (Berland and Wortis, 2002). In mice, three populations of B cells have been characterised, B1 B cells, B2 B cells and marginal zone (MZ) B cells. B1 B cells play an important role in innate immunity in opposition to B2 B cells which are involved in adaptive responses (Duan and Morel, 2006). MZ B cells are found in the spleen and have characteristics of both B1 and B2 B cells (Martin *et al.*, 2001). B1 B cells in mice have expression of CD5 and spontaneously produce low affinity IgM antibodies, reactive to self-antigens (Hayakawa *et al.*, 1984). However, only a subset of B1 B cells expresses CD5, called B1a. The rest of B1 cells are negative for CD5 and are called B1b B cells. In humans, CD5 expression has also been observed in a B cell population. CD5 expression in humans marks a naïve B cell population and nearly all the B cells in neonates have expression of CD5. However, this expression decreases in peripheral blood with age, resulting in around 10-20% of B cells in blood in healthy adult individuals which are positive for CD5 (Carsetti *et al.*, 2004). Like in mice, human CD5+

B cells secrete polyreactive natural antibodies recognising self-antigens (Prieto and Felippe, 2017).

Due to their ability to spontaneously produce autoantibodies, CD5+ B cells have been suggested to be implicated in autoimmune diseases. Some studies have found the CD5+ B cell subset is expanded in autoimmune diseases, such as RA or primary Sjogren's syndrome (Berland and Wortis, 2002). However, their role in autoimmune diseases remains disputed. Some studies suggest CD5+ B cells protect against autoimmunity by producing the regulatory cytokine IL-10 (Dalloul, 2009). Other studies suggest CD5+ B cells contribute to autoimmune pathogenesis by producing polyreactive IgM antibodies that have low affinity and broad specificities (Duan and Morel, 2006). Treatment of RA patients with alemtuzumab, an anti-CD52 antibody that causes lymphocyte depletion, induced DMARD-free clinical remission on 6 of 25 patients (Lorenzi *et al.*, 2008). Our group followed a cohort of alemtuzumab treated patients 12 and 20 years after treatment and showed that alemtuzumab causes long-term alterations in lymphocyte subsets, with a reduction of CD4+ and CD8+ memory T cells and a decline in total CD19+ B cells as well as the CD5+ B cell subset and transitional regulatory B cells (CD9+ CD24high CD38high) (Anderson *et al.*, 2012; Cooles *et al.*, 2016). From the B cell data, the CD5+ B cells results were interesting and were therefore chosen as a B cell subset to further characterise.

1.3.3 B cells in RA

As mentioned before, autoantibodies are a hallmark of RA. This suggests an important role for B cells in the initiation and the progression of RA. The most frequent autoantibodies are RF and ACPAs, but the specific autoantigen for these antibodies has not been well defined (Conigliaro *et al.*, 2016). Moreover, these antibodies are present in individuals at risk, years before the onset of the disease. Recently, other autoantibodies have been associated with RA, such as anti-carbamylated protein antibodies (anti-CarP) (Brink *et al.*, 2015).

Many naïve B cells containing autoreactive BCRs arise regularly (Grimaldi *et al.*, 2005). In healthy individuals, most of the autoreactive B cells are removed through central or peripheral tolerance checkpoints. These checkpoints prevent B cells recognising self-antigens or not functioning correctly to proliferate and differentiate. However, in RA, both mechanisms are defective, a defective central tolerance checkpoint in the bone marrow leads to an increase percentage of polyreactive early B cell precursors (Wardemann *et al.*,

2003). The later peripheral tolerance checkpoint in RA has also been shown to be defective, which results in the accumulation of large numbers of self-reactive B cells in the mature naïve B cell compartment. This failure in removing autoreactive B cells may favour the development of autoimmunity (Bugatti *et al.*, 2014). Therefore, a defect in B cell development might explain the presence of autoantibodies years before the disease onset (Yurasov and Nussenzweig, 2007).

The interaction between B cells and T cells is the basis for the theory that in some autoimmune diseases, an amplification cycle, triggered by a certain factor, allows persistent inflammation and immunopathology. In RA, RF producing B cells provide one example of how autoreactive B cells might become self-perpetuating in this disease. RF is a soluble antibody specific for the Fc region of IgG, which can polymerise with the complement protein C3d. This complex can then bind to the complement receptor CR2, also known as CD21, on B cells, which can then provide a positive-feedback signal to the cell. Moreover, the BCR specific for RF can endocytose foreign antigens and consequently stimulate T cells that will then help activate the B cell by cytokines release (Leadbetter *et al.*, 2002; Edwards and Cambridge, 2006). In the case of the ACPA antibodies, it is clear that T cells may be needed for B cell stimulation and production of autoantibodies as they are mainly, but not exclusively, IgG, so they require T cell-dependent class switching (Alivernini *et al.*, 2019). This is not as clear in the case of RF, since these autoantibodies are often IgM, but can also be IgG and IgA.

Furthermore, a pathogenic role for B cells is confirmed by the efficacy of rituximab, an anti-CD20 antibody depleting therapy, in RA. Plasma cells are not targeted by anti-CD20 antibodies, as they do not express CD20, and autoantibody levels are altered to varying degrees after treatment. These data suggest that the role of B cells in the pathogenesis of RA is not just linked to autoantibody production (McInnes and Schett, 2011). B cells can further contribute to disease pathogenesis due to their antigen presentation ability, leading to T cell activation, as well as production of cytokines (Figure 1.5). B cells can effectively present antigens to stimulate T cells and support optimal development of memory CD4+ T cells. RF+ B cells can uptake antigen immune complexes through their RF-specific receptor and process and present the peptides from the antigen, inducing T cell activation (Leadbetter *et al.*, 2002).

In addition to antigen presentation, B cells can stimulate pathogenic immune responses through cytokine secretion (Figure 1.5). These cytokines, such as IL-6, IL-17 and TGF-β, can target T cells, and are known to have an effect on Th cell differentiation (Wong *et al.*, 2006). Furthermore, there is growing evidence that B cells in RA can contribute to the local synthesis of cytokines acting on other pathogenic cell types, including immune and non-immune. There have been reports showing that synovial B cells have high expression of RANKL and TNF-α, which can act on osteoclasts promoting osteoclastogenesis (Yeo *et al.*, 2015). Moreover, lymphocyte aggregates have been detected in the synovium of patients with early arthritis (van de Sande *et al.*, 2011).

In addition, regulatory B cells (Bregs) have been proven important in autoimmunity. Bregs, which have suppressive abilities that dampen an immune response, have been reported to be decreased in the blood of RA patients compared to healthy controls (Ma *et al.*, 2014) (Figure 1.5). Moreover, injection of apoptotic cells into a collagen-induced arthritis (CIA) model prevented the development of CIA. Elucidation of the cellular mechanisms revealed that apoptotic cells have a direct effect on B cells, inducing production of IL-10, which in turn leads to the differentiation of an IL-10 producing regulatory T cell subset (Gray *et al.*, 2007b).

Interestingly, growing evidence show that B cells activated via T-independent responses could play an important role in autoimmunity. Collaboration between T and B cells creates a positive loop that amplifies and perpetuates the activation of autoreactive responses (Shlomchik *et al.*, 2001). Nevertheless, it has been published that activation of autoreactive B cells which produced autoantibodies did not require T cell help (Herlands *et al.*, 2008), indicating that B cell activation is an initial step in systemic autoimmunity, which would be followed by consecutive activation of autoreactive T cells by these B cells. Moreover, TLR7 and TLR9 activation of the autoreactive B cells is a critical requirement for the activation of these cells with or without T cell help. Additionally, because somatic hypermutation can lead to the formation of autoreactive B cells, mechanisms of control are important in GC (Shokat and Goodnow, 1995). However, in the presence of chronic antigen stimulation and innate pathways activation, B cells can escape these mechanisms to control autoreactive B cells activating in the GC and the cells can undergo class switch outside GCs (William *et al.*, 2002). This leading role of autoreactive B cells initiating autoimmune responses would explain the efficacy of B cell depletion therapies in autoimmune diseases and the lack of success of CD4-depleting treatment in RA (Mason *et al.*, 2002).

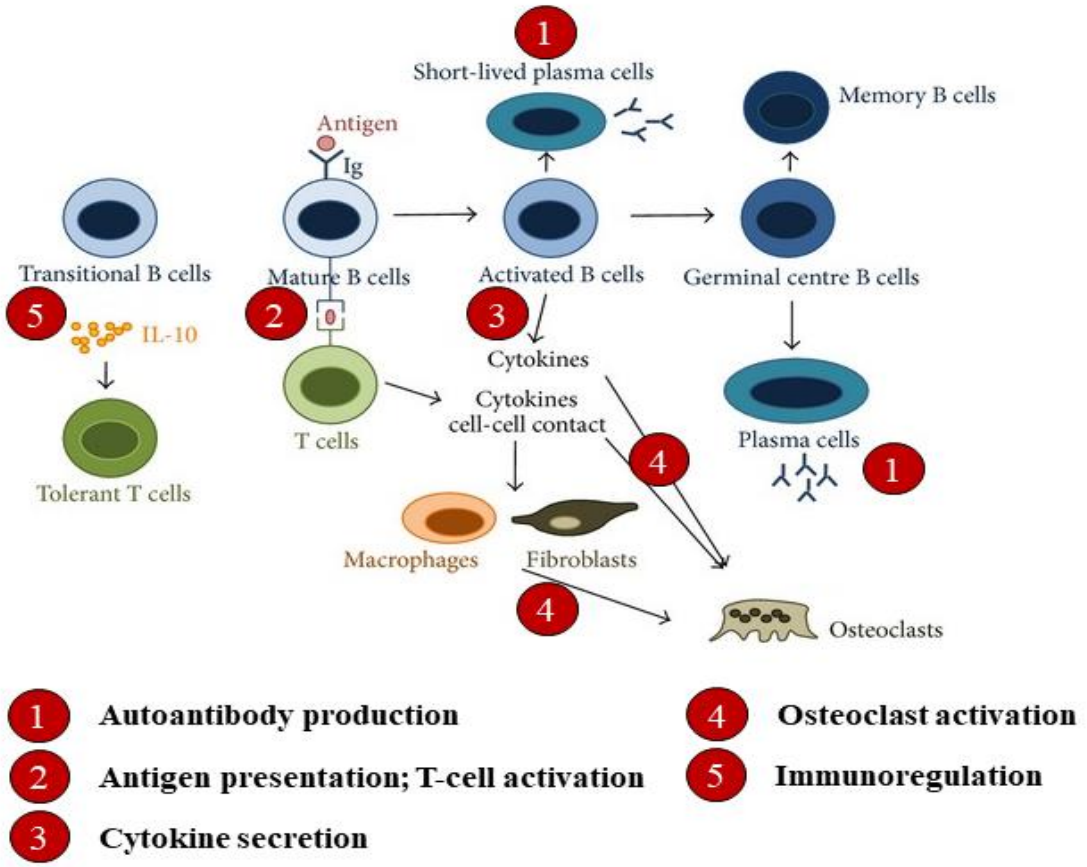

Figure 1. 5. Potential B cell functional roles which may contribute to rheumatoid arthritis pathogenesis. 1. Antigen specific B and T cell interactions leads to the activation and differentiation of plasma cells, which are responsible for the production of autoantibodies. **2.** Additionally, activated B cells provide help to T cells and induce differentiation of effector T cells which produce pro-inflammatory cytokines. **3.** B cells can secrete pro-inflammatory cytokines, such as interleukin IL-1, IL-6, TNF-α and IL-17A. **4.** Pro-inflammatory cytokines and RANKL produced by activated B cells, as well as T cells, macrophages, and synovial fibroblasts, promote the differentiation and activation of osteoclasts, leading to bone destruction. **5.** However, B cells can also be immunoregulatory through the production of IL-10. Adapted from Bugatti *et al.*, 2014.

1.4 ABC-like cells

Several groups have recently identified a novel subset of B cells named age-associated B cells (ABCs). These cells could potentially be involved in RA pathogenesis due to their potential ability to produce autoantibodies, cytokines and present antigens. Studies to characterise this subset have been performed in murine models, as well as a handful of human studies using healthy individuals and patients with autoimmune diseases. Table 1.1 and 1.2, at the end of this section, summarise the different studies and shows the different characteristics of the ABC-like cells described by the different groups.

1.4.1 Murine ABCs

Rubtsov *et al.*, described a population of murine B cells that express the integrins, CD11b and CD11c, but lack the complement receptor type 2, CD21(Rubtsov *et al.*, 2011). It was found that these cells are increased in the spleen of aged female mice compared to young females or males of any age. Because this subpopulation appears in high frequency in aged mice, they were named ABCs. Characterisation of these cells revealed that they are slightly larger in size than follicular B cells (FO B cells). Moreover, these cells were positive for CD5 and expressed high levels of the co-stimulatory molecules, CD80 and CD86, as well as MHC-class II, suggesting they have an activated phenotype. This subset was increased in mice prone to autoimmune disease (NZB/WF1 and Mer-/- mice, which develop a lupus-like disease) when compared to age-matched healthy mice (C57BL/6 mice). Hao *et al.*, also described a similar B cell subset that lacked expression of CD21 in healthy old female mice (Hao *et al.*, 2011). However, this subset lacked expression of CD5 and did not have an activated phenotype, as levels of MHC class II and CD86 were comparable with FO B cells. They described the subset as an exhausted B cell population but called them ABCs as they emerge with age.

Murine ABCs, when stimulated by a TLR7 agonist, produce IgM similar to other B cell subsets, but also produce higher amounts of IgG (Rubtsov *et al.*, 2013; Rubtsova *et al.*, 2017). These IgG antibodies recognise chromatin, demonstrating that ABCs may be a source of autoantibodies, and the higher frequency of ABCs in autoimmune-susceptible mice may directly affect the onset of autoimmunity. Interestingly, simultaneous stimulation with TLR and BCR ligation produce a strong response, resulting in extensive division and high numbers of responding cells (Hao *et al.*, 2011). Moreover, chronic stimulation of B cells via TLR7 was sufficient to induce accumulation of ABCs, resulting in autoantibody

production (Rubtsov *et al.*, 2011). Other studies using mice showed that accumulation of CD11c+T-bet+ ABCs induced dysregulation in T follicular helper differentiation through their potent antigen-presenting function which lead to a compromised formation of antigen-specific GC B cell responses and antibody maturation (Zhang *et al.*, 2019b). These findings provide a link between ABCs and autoantibody production.

Gene expression analysis and flow cytometry showed overexpression of CD11c, in addition to transcripts of Ig heavy chain and CD138 (Syndecan-1), supporting their role as a unique antibody-secreting population that may be a plasma cell precursor (Rubtsov *et al.*, 2011). Curiously, ABCs expressed genes are also found in helper and cytotoxic T cells such as T-bet, perforin and granzyme A. Therefore, T-bet was described as a specific transcription factor for ABCs and other papers that characterised this subset used T-bet as an indicator of a B cell subset with an ABC-like phenotype. Rubstova *et al.*, went on to demonstrate that T-bet expression in B cells is critical for the development of pathology and the rapid mortality in systemic lupus erythematosus (SLE) mice (Rubtsova *et al.*, 2017). Moreover, they found that in the absence of T-bet expression, ABCs frequencies and numbers were reduced and that there was a significant reduction of anti-chromatin IgG2a levels.

Despite the growing appreciation for the importance of T-bet in B cells, the signals that result in B cell expression of T-bet are not well understood. Studies using knockout mice show that IL-21 and IFN-γ together with TLR engagement promotes T-bet expression in B cells (Naradikian *et al.*, 2016b). Moreover, IL-21 alone also induced CD11c expression. Conversely, IL-4 antagonised the induction of T-bet. Other studies in knockout mice demonstrated a role of interferon-regulatory factors (IRFs), IRF5 in the absence of SWEF proteins in the generation of ABC-like cells. SWAP-70 and DEF6 are the only two members of a Rho-family GTPase proteins, which regulate interferon-regulatory factors (IRFs). In the absence of SWEF proteins, there was a dysregulated activity of IRF5 in response to stimulation with IL-21 and this led to an enhanced generation of ABC-like cells in these mice (Manni *et al.*, 2018).

Other studies in T-bet+ B cells showed that T-bet expression was required for the formation of long-lived antibody-secreting cells (Stone *et al.*, 2019). This study showed that T-bet facilitates differentiation of IFN-γ activated inflammatory effector B cells into antibody secreting cells in IFN-γ induced inflammatory responses.

1.4.2 Human ABCs

In autoimmune patients suffering from SLE and autoimmune cytopenia, a population of B cells, which are CD19high CD21- and that share features with murine ABCs, has been identified (Warnatz *et al.*, 2002; Wehr *et al.*, 2004). One of the main differences between murine ABCs and this human CD21low B cell subset is that only a proportion of autoimmune patients have high frequencies of this CD21low B cell subset in their peripheral blood. Rubtsov *et al.*, investigated human ABCs, defined as CD19high CD21-CD11c+ B cells, in the peripheral blood of RA, Systemic sclerosis (SSc) and SLE patients, and found high frequencies of this subset in a proportion of patients with RA and SSc (Rubtsov *et al.*, 2011). The expanded ABC population was observed at a higher frequency in women over 60 years old suffering from RA compared to younger women and men of any age. Another study, which compared healthy controls and patients with RA and defined ABC-like cells as CD21lowCD86+, found that the RA patients had higher frequencies than the healthy controls (Shimabukuro-Vornhagen *et al.*, 2017).

CD21low B cells have been described in different diseases ranging from infections to autoimmunity (Isaak *et al.*, 2006; Charles *et al.*, 2011; Ma *et al.*, 2019). The common feature in all these diseases is chronic immune stimulation. CD21, also known as complement receptor type 2, binds to complement fragments bound to antigens. On B cells, CD21 forms a complex with CD19 and CD81 and functions as a co-receptor for the BCR (Cherukuri *et al.*, 2001). Therefore, through its complement binding ability, CD21 can enhance B cell responses to an antigen, and via the CD21/CD19/CD81 complex can modulate the strength of the BCR signal. Activation of B cells can lead to a reduction in expression of CD21 (Masilamani *et al.*, 2003), suggesting that the CD21low B cell subset may be maintained in situations in which low-level chronic antigen stimulation is present, such as in chronic inflammatory conditions (Winslow *et al.*, 2017).

With regard to the phenotype of these CD21low B cells there are some discrepancies in the reported expression of several surface molecules, such as CD27. This discrepancy could be due to the presence of more than one subset within the CD21low population. Focusing on RA, two CD21low B cell subsets have been found to be expanded in peripheral blood: one expresses CD27, while the other lacks expression of this receptor (Thorarinsdottir *et al.*, 2015). Rubtsov *et al.*, found that the CD27+ subset also express CD11c and CD5, in addition to activation markers, such as CD80 and CD86, and were considered to be memory

B cells as they were class-switched (Rubtsov *et al.*, 2011). The CD27- cells, characterised by Isnardi *et al.*, also express CD11c but displayed unmutated IgM (Isnardi *et al.*, 2010). Moreover, this particular CD27-CD21low B cell subset responded poorly to BCR stimulation and displayed autoreactive traits and were therefore, described as anergic naïve B cells.

The CD21low B cell subset described by the three different groups had high expression of the co-stimulatory molecules CD80 and CD86, as well as the MHC class II molecule, HLA-DR (Isnardi *et al.*, 2010; Rubtsov *et al.*, 2011; Shimabukuro-Vornhagen *et al.*, 2017). These CD21-CD11c+ B cells were also positive for T-bet. Rubtsova *et al*., demonstrated that T-bet expression in B cells is critical for B cell activation and generation of germinal centre B cells (Rubtsova *et al.*, 2017). In addition, B cell expression of T-bet was also required for effective T cell activation, possibly due to T-bet expressing ABCs being potent antigen presenting cells. This highlights two possible roles of ABCs in autoimmune pathogenesis, autoantibody production and antigen-presentation to T cells. Figure 1.6 shows a model for the generation and possible function of T-bet+ ABC-like cells (Knox *et al.*, 2019).

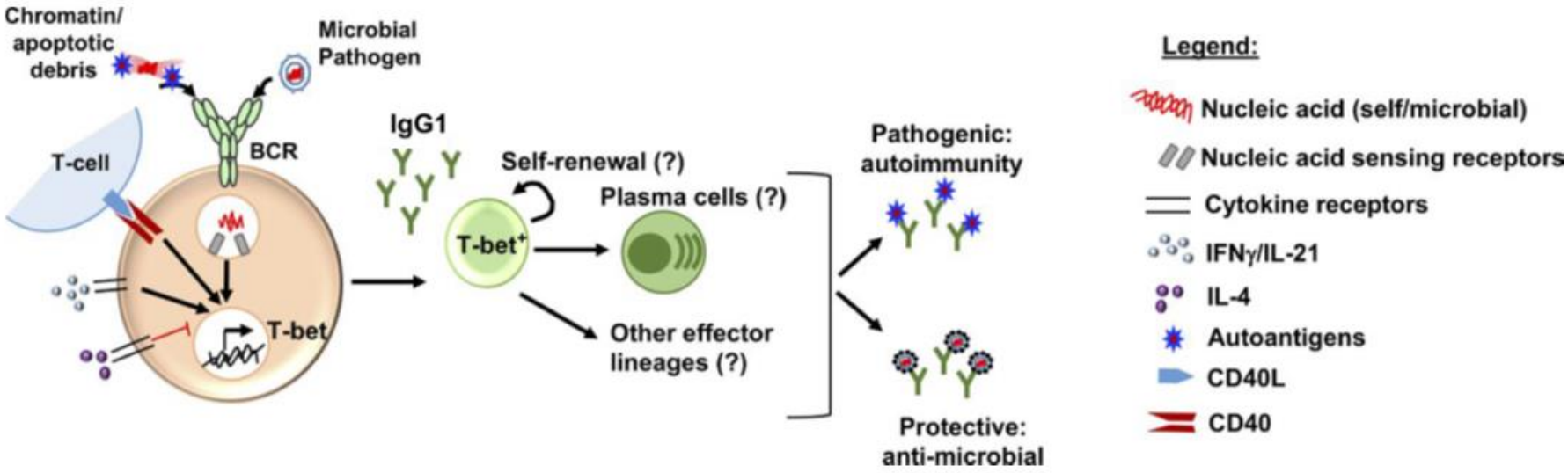

Figure 1. 6. Origin, fate and function of T-bet+ B cells. Microbial pathogens and apoptotic debris can trigger signalling of innate receptors recognising nucleic acids. These signals in conjunction with a Th1 cytokine milieu composed of IL-21 and IFN-γ (and absence of IL-4, which is inhibitory) can induce expression of T-bet in B cells. There is evidence suggesting that there is a requirement for cognate help and germinal centre-dependent formation of T-bet+ B cells. However, these cells can also develop extrafollicularly under certain circumstances. T-bet expression drives class switching to IgG1 isotype antibodies. T-bet+ memory B cells are persistent, most likely due to self-renewal, and can be progenitors of plasma cells or differentiate into other effector cell lineages upon re-challenge. Because of their persistence and roles in antibody secretion and other B cell functions, T-bet+ B cells are key players in protective humoral immunity, as well as in pathogenic processes. Adapted from Knox et al., 2019.

Recent studies have investigated the origin of these cells. Similar to murine studies, in patients with SLE, IL-21 was able to induce CD11c+T-bet+ B cells and promote the differentiation of these cells into autoreactive antibody-secreting plasma cells (Wang *et al.*, 2018). This study highlights a role for IL-21 in the generation of cells with an ABCs-like phenotype. This is further supported by studies in mice which show that IL-21 and IFN-γ together with TLR engagement promotes T-bet expression in B cells (Naradikian *et al.*, 2016b).

Other studies have also investigated expression of antibodies by ABCs to determine if these cells have undergone class switching, in addition to determining their replicative ability. The subset described by Shimabukuro-Vornhagen *et al.,* as CD21lowCD86+ B cells contained a large proportion of proliferating cells, assessed by the expression of Ki67, and a high degree of class-switched cells which were IgM and IgD negative (Shimabukuro-Vornhagen *et al.,* 2017). In line with these results, Rubtsov *et al.,* found that ABCs were negative for IgD and IgM, but positive for IgG (Rubtsov *et al.*, 2011). However, Isnardi *et al.,* found that CD21low B cells from RA patients preferentially expressed IgM and/or IgD, whereas CD21low B cells from healthy donors were class-switched B cells (Isnardi *et al.*, 2010). This further supports the idea that the CD21low B cell subset described by some groups is a heterogeneous, mixed B cell population.

Transcriptome analysis was also performed to assess gene expression in ABCs and CD21low B cells. Shimabukuro-Vornhagen *et al.,* reported that CD21lowCD86+ B cells had high gene expression of chemokine receptors and adhesion molecules involved in extravasation and recruitment to sites of inflammation, such as *CD11a*, *CCR3*, *CCR5*, *CCR10* and *CXCR2* (Shimabukuro-Vornhagen *et al.*, 2017). In addition, their gene expression for lymph node homing receptors was low. On the contrary, transcriptome analysis by Isnardi *et al.,* found that CD21low B cells downregulate genes encoding survival and activation proteins, as well as cytokine and chemokine receptors that stimulate B cell proliferation. In contrast, this subset up-regulated inhibitory receptors to supress B cell activation and proliferation (Isnardi *et al.,* 2010).

Isnardi *et al.,* characterised CD21low B cells as lacking the ability to become activated, proliferate or secrete antibodies upon BCR triggering (Isnardi *et al.,* 2010). This subset was referred to as anergic and their irresponsive state was suggested to result from chronic BCR exposure to self-antigens. This result is consistent with Shimabukuro-Vornhagen *et al.*,

who found that CD21lowCD86+ B cells have impaired BCR-induced signalling (Shimabukuro-Vornhagen *et al.*, 2017). The results from Shimabukuro-Vornhagen *et al.*, agree with the suggestion that, if this B cell subset is already in an activated state, they will be less responsive to BCR stimulation. Although Isnardi *et al.*, found that the CD21low B cells are prone to die by apoptosis, and stimulation by their BCR, or via CD40 or TLR9 ligation, does not rescue them from cell death (Isnardi *et al.*, 2010), other groups have shown that murine ABC-like cells do respond to TLR engagement; TLR7 and TLR9 stimulation was sufficient to induce proliferation and antibody production (Hao *et al.*, 2011; Rubtsov *et al.*, 2011). These reported differences with regard to response to stimuli could be explained by the fact that the CD21low B cell subset investigated by Isnardi *et al.*, is a different subset to other ABC-like B cells or ABCs, as their CD21low B cells are described as being anergic, and only one marker, CD21, in addition to CD19, is used to identify the population. Additionally, these differences could be due to species variation as the Hao *et al.*, and Rubtsov *et al.*, studies were done using mouse cells.

There is some debate on whether these ABCs and CD21low B cells are naïve B cells, memory B cells or plasma cells. As explained before, there could be two subsets of CD21low CD11c+ B cells. The CD21low B cell subset described by Isnardi *et al.*, are naïve B cells because they are not class-switched B cells (Isnardi *et al.*, 2010). Nevertheless, the CD21lowCD86+ B cell subset characterised by Shimaburuko-Vornhagen *et al.*, could be in a translational state between germinal centre B cells and early plasmablasts based on their phenotypic and functional characterisation (Shimabukuro-Vornhagen *et al.*, 2017).

As ABCs and CD21low B cells are increased in inflammatory diseases, such as RA, they could be involved in the pathophysiology of this disease and would therefore, be a promising target for the development of new therapies for the treatment of autoimmune diseases. As explained before, Rituximab is effective in some patients with RA (Tavakolpour *et al.*, 2019), but development of more specific therapies could be more efficient and be effective in a larger number of patients. Nevertheless, new markers for these newly discovered ABCs and CD21low B cell subsets are still needed in order to develop therapies against novel targets.

Sadly, our knowledge of these cells is obscured by the fact that the cells are defined in different ways by different investigators, in addition to the fact that the ABC population is heterogeneous in surface marker expression, and presumably, function (Phalke and

Marrack, 2018). For this reason, more studies on the phenotype, gene expression and function of these subsets of B cells will help characterise these cells and elucidate their role in health and disease.

1.4.3 FcRL4+ B cells

An interesting new subset of the synovial fluid B cells has recently investigated by my co-supervisor, Professor Dagmar Scheel-Toellner. This subset express FcRL4 and produce the cytokines Receptor Activator of Nuclear factor Kappa-B Ligand (RANKL) and TNF-α, which stimulates the differentiation and activation of osteoclasts (Yeo *et al.*, 2011). This FcRL4+ B cell subset shows some similarities with the ABCs described in peripheral blood. These cells express low levels of CD21 and were positive for CD11c. Moreover, other studies in mice have shown that CD21low B cells display altered ataxia telangiectasia-mutated (ATM) function, leading to increased RANKL production and bone erosion, as well as a rise in circulating CD21low B cells (Mensah *et al.*, 2019). The FcLR4+ synovial B cells are considered class-switched memory B cells because they express CD27, IgG and IgA but do not express IgD and CD38. Moreover, this FcRL4+ subset shows elevated expression of adhesion molecules and the chemokines receptors CCR1 and CCR5, in addition to high expression of co-stimulatory molecules, CD80 and CD86. Interestingly, FcRL4 has been shown to attenuate BCR signalling but augment B cell activation through TLR9 signalling (Sohn *et al.*, 2011). Ligands for TLR9, like bacterial DNA containing CpG motifs, have been found in the synovial fluid of patients with RA (Zhao *et al.*, 2018). It is feasible that FcRL4 expression on the B cells in RA patients, may enhance immune activation through TLR9, or via other receptors known to be potently activated by disease-relevant ligands, such as immune complexes containing citrullinated proteins. FcRL4+ B cells express more IgA, a mucosal immunity-associated Ig, than FcRL4- B cells, which is interesting as currently there is growing evidence supporting the hypothesis that RA pathogenesis could start with mucosal inflammation in the gum, the gut and the lungs (Catrina *et al.*, 2014). Additional studies are needed to determine if these FcRL4+IgA+ B cells are generated due to an IgA immune response in the mucosa and later they migrate to the joints. Moreover, since the ABCs and CD21low B cell subsets described in this review share several surface markers with the FcRL4+ B cells in synovia, it may be possible that the ABCs are the blood precursors of these FcRL4+ B cells found in RA joints (Amara *et al.*, 2017). Further work is needed to investigate the relationship of ABCs and ABC-like cells with the novel joint FcRL4+ B cell population.

		Main markers	Other markers	Stimulated by	Immunoglobulin expression
Mouse	Rubtsov *et al.*, 2011 Rubtsova *et al.*, 2017	CD19 high CD11c+ CD21-	High: CD5, CD80, CD86 and HLA-DR Positive: CD27, CD11b, CD138, T-bet	Accumulate after TLR7	IgM anti-chromatin IgG
	Hao *et al.*, 2011	CD19+ CD21-	Normal CD86 and HLA-DR Negative: CD5	TLR9 and TLRs + BCR	IgM and low IgD
Human	Rubtsov *et al.*, 2011	CD19 high CD11c+ CD21-	High: CD5, CD80, CD86, CD20 and CD27 Negative: CD23- and CD38low	-	IgG
	Wang *et al.*, 2018	CD19 high CD11c high T-bet+	High: CD32, CD95, CD20 and FcRL5 Negative: CD5, CD21, CD23 and CD138 Low: CD27, CD38 and CD40	Respond to coculture with anti-CD3-activated T cells	IgG Autoantibody production
	Shimabukuro-Vornhagen *et al.*, 2017	CD19+ CD21low CD86+	High: CD80, HLA-DR and HLA-ABC Positive: CD27 and Ki67 Low: CD40	Chronic CD40L No response to BCR	IgG
	Isnardi *et al.*, 2010	CD19+ CD21-	High: CD5, CD80, MHC class II and CD20 Positive: T-Bet Negative: CD27, CD10 and CD40low	No proliferation by BCR-CD40 A bit by TLR9	IgM and/or IgD
RA synovia	Yeo *et al.*, 2015 Amara *et al.*, 2017	CD19high FcRL4+	High: CD80, CD86 and CD11c Positive: CD27+ and FcRL5+ Negative: CD21- and CD38-	TLR9	IgG IgA

Table 1. 1. ABC-like cell characteristics described by different groups. ABC-like cells have been characterised in mice, human and RA synovia. Summary of the markers used to describe ABC-like cells by each group, as well as information on their response to stimulation and their immunoglobulin expression profile is shown.

		Main markers	Activation status	B cell type	Increased in	Function
Mouse	Rubtsov *et al.*, 2011 Rubtsova *et al.*, 2017	CD19 high CD11c+ CD21-	Activated B cells	Plasmablast (precursors of plasma cells)	Elderly female WT mice Autoimmune-prone mice	Possibly antigen presenting cells Autoantibody secretion
	Hao *et al.*, 2011	CD19+ CD21-	Exhausted B cells	Expanded mature B cells	Elderly female WT mice	Present antigens Th17 polarisation
Human	Rubtsov *et al.*, 2011	CD19 high CD11c+ CD21-	Activated B cells	-	RA and SSc	Possibly antigen presenting cells Autoantibody secretion
	Wang *et al.*, 2018	CD19 high CD11c high T-bet+	Activated B cells	Memory B cells, rapidly differentiate into plasma cells	SLE	Autoantibody secretion
	Shimabukuro-Vornhagen *et al.*, 2017	CD19+ CD21low CD86+	Activated B cells	Translation state: between germinal centre and early plasmablasts	RA blood and synovial fluid	Potent antigen presenting cells
	Isnardi *et al.*, 2010	CD19+ CD21-	Anergic B cells	Naïve B cells	RA and CVID	-
RA synovia	Yeo *et al.*, 2015 Amara *et al.*, 2017	CD19high FcRL4+	Activated B cells	Switched memory B cells	Synovial fluid in RA	Possibly potent antigen presenting cells

Table 1. 2. ABC-like cell characteristics described by different groups. ABC-like cells have been characterised in mice, human and RA synovia. Summary of the activation status, as well as the classification of the ABC-like cells by each group. Information on the disease in which these cells were described as well as they postulated function is shown.

1.5 Fc Receptor Like (FcRLs) family

Fc receptor-like (FcRL) molecules were identified around 15 years ago. In 2006, a uniform nomenclature was established to designate the FcRL family, as prior to this the members of this family were given different names when they were first discovered by several groups (Maltais *et al.*, 2006; Li *et al.*, 2014a). A summary of the information for each FcRL family member can be found in Table 1.3, at the end of this section.

FcRL1 to FcRL5 are located in what is called the human *FcRL1-5* gene cluster. It spans approximate a 300 kb region of the chromosome 1q21-22 and it encodes type I transmembrane glycoproteins with 3-9 extracellular Ig-like domains and cytoplasmic tails with immunoreceptor tyrosine-based-activating (ITAM), -switch (ITSM) and/or -inhibitory (ITIM) motifs (Figure 1.7) (Mechetina *et al.*, 2002). *FcRL6* codes for a transmembrane receptor with similar features, but it is located at a separate locus. Finally, two additional relatives were discovered; FcRLA and FcRLB, which lack transmembrane segments and are intracellular proteins. All the FcRLs members, except for FcRL6, are preferentially expressed by B cells (Ehrhardt *et al.*, 2007).

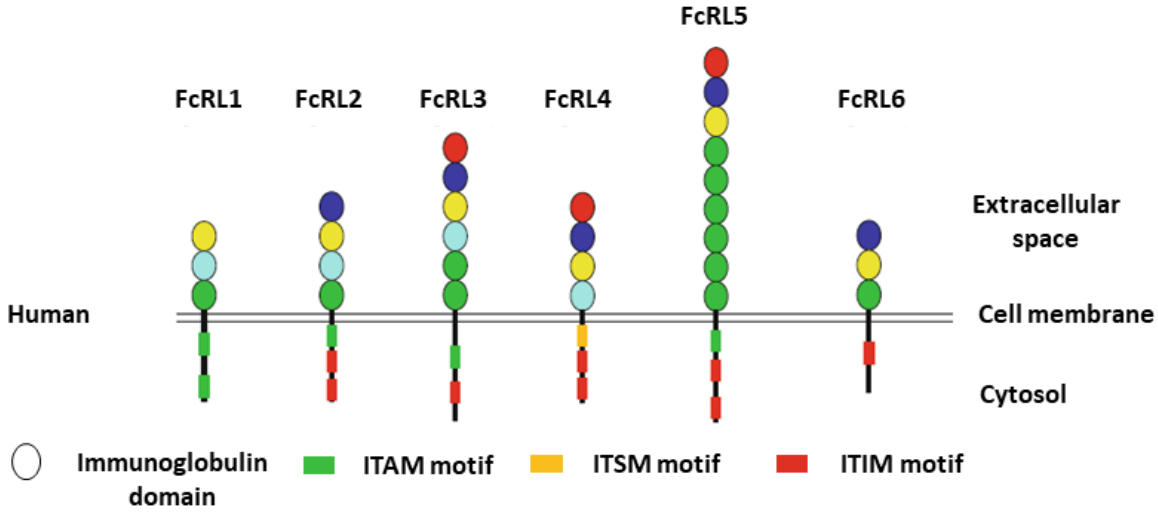

Figure 1. 7. Protein structure of the human FcRL family molecules. In the extracellular space, immunoglobulin domains are shown as circles. These are colour-coded to indicate their phylogenetic relationships. FcRL cytoplasmic tails possess consensus sequences for immunoreceptor tyrosine-based activating motifs (ITAM) in red, immunoreceptor tyrosine-based inhibitory motifs (ITIM) in green and immunoreceptor tyrosine-based switch motifs (ITSM) in orange. Adapted from Li *et al.*, 2014.

The cellular distribution of FcRL1-5 varies between each member of the family. However, in general, their expression increases with B cell differentiation and peaks in circulating cells and those localised to secondary lymphoid tissues (Davis *et al.*, 2001). FcRL1 emerges at the pre-B cell stage and increases with B cell maturation, with higher expression in naïve and memory subpopulations. FcRL2 and FcRL3 both peak on memory B cells in the periphery and mark a circulation innate-like MZ B cell equivalent (Polson *et al.*, 2006). However, FcRL3 is also expressed outside the B cell lineage by subpopulations of cytotoxic NK cells and CD8+ T cells, as well as a dysfunctional population of CD4+ regulatory T cells (Swainson *et al.*, 2010). FcRL4 is expressed in a subpopulation of tissue-based memory B cells located in mucosa-associated lymphoid tissues (MALT) and its expression in circulating B cells is scarce (Falini *et al.*, 2003). Additionally, FcRL4 is expressed by a B cell subset found in the synovial fluid of patients suffering from RA (Yeo *et al.*, 2015). Lastly, FcRL5 has a broader distribution that reaches the highest surface density on terminally differentiated plasma cells derived from the bone marrow (Polson *et al.*, 2006).

Unfortunately, the ligands for most of the FcRLs family members are still unknown. Only the ligands for FcRL4 and FcRL5, and recently for FcRL3, have been described. Previous reports suggested that FcRLs might be Fc receptors as for their high homology to FcγRI (Hatzivassiliou *et al.*, 2001). Wilson *et al*. showed that FcRL4 and FcRL5, but not the other FcRLs, can bind heat-aggregated IgA and IgG, respectively (Wilson *et al.*, 2012). Transfected cells with the different FcRL family members where incubated with heat-aggregated IgA, IgG and IgM and binding of the immunoglobulins to FcRLs expressing cells was assessed by flow cytometry. No binding of human IgM to any of the FcRL family members was observed, however FcRL4 showed binding to IgA and FcRL5 to IgG. The FcRL5 findings were confirmed by Franco *et al.* demonstrating that FcRL5 binds IgG not through the Fc receptor fragment but via other mechanisms (Franco *et al.*, 2013). Additionally, the FcRL4 findings were confirm by my co-supervisor in Birmingham, Professor Dagmar Scheel-Toellner (unpublished). Recently, the ligand for FcRL3 has been postulated to be secreted IgA (Agarwal *et al.*, 2020). Nevertheless, the IgA found to bind FcRL3 was not heat-aggregated but was secretory IgA from human colostrum. Secretory IgA binding to FcRL3 was assessed by surface plasmon resonance and further confirmed by flow cytometry on transfected cell lines and primary B cells and Treg cells.

The role of these receptors in both innate and adaptive immunity is still under investigation. The cytoplasmic properties of FcRLs are complex. Most FcRLs cytoplasmic tail possess

both ITAM-like and ITIM elements. The possession of these intracellular sequences indicates that most of these molecules may be capable of exerting a dual-modulation, i.e. they may activate or inhibit responses (Ehrhardt *et al.*, 2007). FcRL1 is the only FcRL family member with two ITAM-like sequences and appears to act as a co-activation receptor. Its ligation by receptor-specific monoclonal antibodies and crosslinking with the BCR enhances calcium flux augmenting B cell activation and proliferation (Leu *et al.*, 2005).

Regarding the other FcRLs, several groups have carried out work exploring the contributions of the FcRL2-5 cytoplasmic tyrosine-based motifs on BCR-mediated activation (Haga *et al.*, 2007; Kochi *et al.*, 2009; Jackson *et al.*, 2010). Their engagement alone does not appear to impact basal B cell function. Nevertheless, crosslinking the FcRL and the BCR induces phosphorylation of intracellular tyrosine residues of the BCR and promotes docking of the SHP-1 and/or SHP-2 SH-2 domain-containing phosphatases at consensus ITIMs (Figure 1.8). The outcome of these repressive signals is, therefore, an attenuation of antigen receptor-mediated calcium mobilisation and MAPK activation that results in apoptosis.

Nonetheless, recent work has begun to explore the effects of human FcRLs on innate-driven responses. Different studies on FcRL3 and FcRL4 provided evidence that these proteins promote TLR-mediated signalling. Exposure of FcRL4 expressing B cells to the TLR9 agonist CpG prompted co-localisation of these receptors in endosomes and the upregulation of CD23, an indicator of TLR activation (Sohn *et al.*, 2011). FcRL3 studies show that engagement of FcRL3 with specific monoclonal antibodies enhanced TLR9 triggered blood B cell proliferation, survival, and induction of CD25, CD86 and HLA-DR activation markers (Li *et al.*, 2013). FcRL3 had inverse effects on antibody production and blocked the differentiation of antibody-secreting cells. Flow cytometry analysis revealed that FcRL3 enhances CpG-mediated NF-kB p65 and MAPK pERK and p38 activation (Figure 1.8).

In T cells, Agarwal *et al.*, showed that stimulation of Tregs with FcRL3 ligand, secreted IgA, impaired Treg-mediated inhibition of responder cell proliferation, concluding that secreted IgA through its binding to FcRL3, inhibits Treg cell suppressive function (Agarwal *et al.*, 2020). Moreover, FcRL3 stimulation promoted the transition of Treg cells towards a

Th17-like phenotype, which in inflammatory environments with secretion of IgA, might contribute to pathogen and tumour clearance.

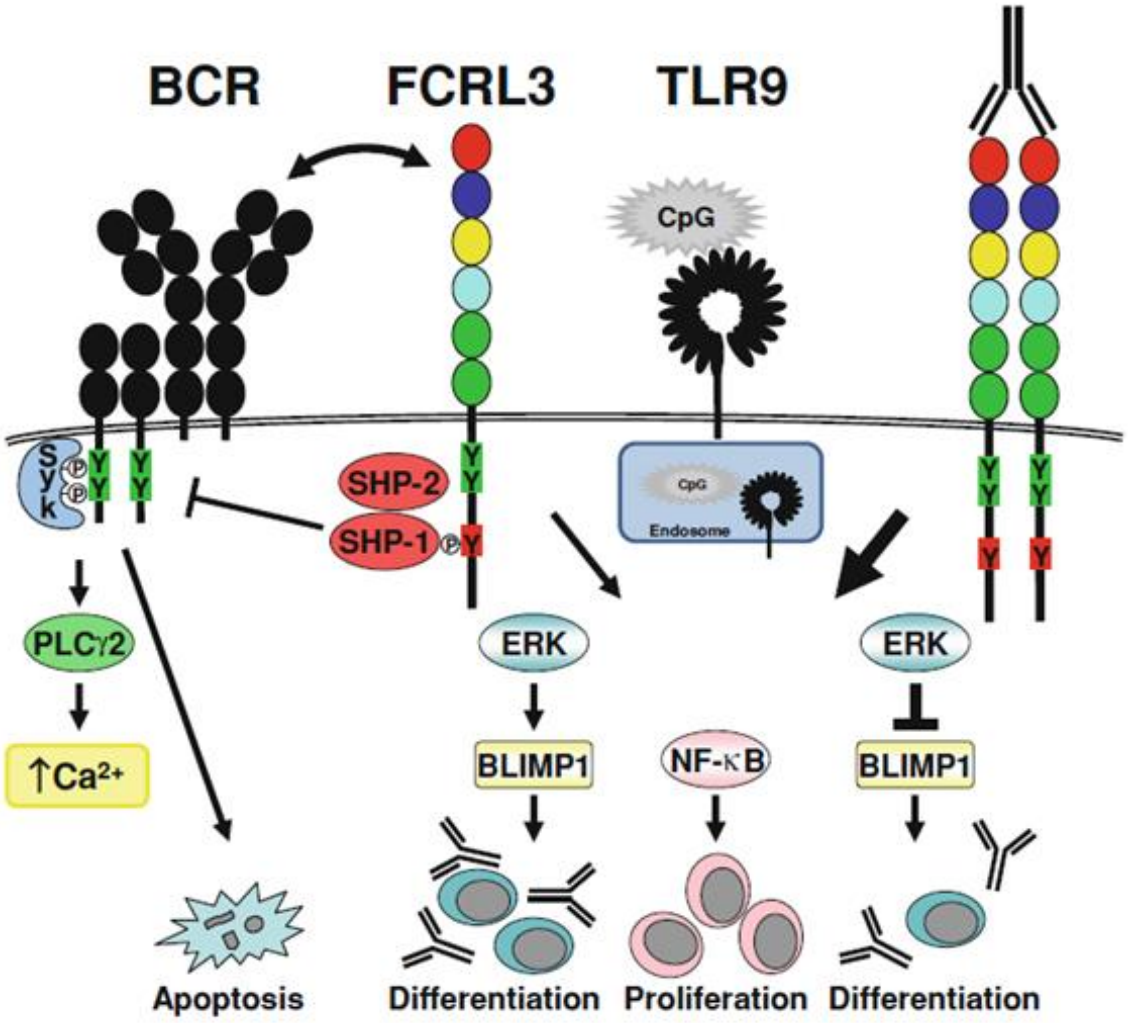

Figure 1. 8. FcRL3 regulation of adaptive and innate signalling pathways. Co-ligation of FcRL3 with the BCR facilitates the recruitment of SHP-1 and SHP-2 that inhibit Syk and PLCγ2 phosphorylation on the BCR and suppresses downstream calcium signalling and induces apoptosis. Nevertheless, after exposure to CpG, a TLR9 agonist, FcRL3 expressing B cells activate the NF-κB and MAPK/pERK pathways that drive proliferation. Phosphorylated ERK additionally induces expression of the BLIMP1 plasma cell commitment factor which stimulates B cell differentiation and antibody production. In addition, simultaneous crosslinking of FcRL3 in TLR9-activated B cells significantly elevates NF-κB and pERK to promote proliferation and survival. However, this augmented pERK activation in TLR9 and FcRL3 co-stimulated B cells represses BLIMP1 induction and therefore abolishes plasma cell differentiation and antibody production. Image obtained from Li *et al.*, 2014.

In addition, expression of FcRLs and their involvement with immune-mediated disorders has also been investigated. Multiple groups have detected expression and dysregulation of FcRLs in various lymphoproliferative disorders. FcRL2 was upregulated in the mutated-indolent subtype of leukaemia and emerged as an aggression biomarker (Li *et al.*, 2008). Several FcRLs have also drawn interest because of their upregulation in lymphocyte populations in individuals with infectious diseases. For example, in patients afflicted with chronic viral diseases, such as HIV and hepatitis C, there is appearance of an FcRL4+ population of B cells (Moir *et al.*, 2008).

Regarding tolerance and autoimmunity, disease risk associations for single nucleotide polymorphisms (SNP) located in regions of the FcRL genes have arisen in a variety of disorders. The principal variant (rs7528684) was located in a potential NF-κB consensus binding motif within the FcRL3 promoter region (Kochi *et al.*, 2005). The C susceptibility allele of this SNP (169T → C) generated a more orthodox NF-κB binding sequence, with higher promoter activity via p50, p65 and c-Rel binding and exerted a dose-dependent regulatory effect on FcRL3 transcript and protein expression. These results suggesting that the FcRL3 polymorphism may be a risk factor for RA were confirmed by our group (Clark *et al.*, 2020). Clark *et al.* identified both a methylation and an expression quantitative trait locus (mQTL and eQTL, respectively) in the FcRL3 region on B cells and T cells from patients with RA. However, there have been conflicting results as many studies found no link for FcRL3 with autoimmune disease susceptibility (Eyre *et al.*, 2006). These discrepancies may reflect differences in racial and ethnic backgrounds.

In summary, expression of FcRLs and their link to both innate and adaptive immune responses, for example the preferential expression of FcRL2 and FcRL3 by innate-like MZ B cells and their capacity to promote T-cell independent responses, is an interesting new avenue to explore with regard to autoimmune diseases. As several FcRLs appear to serve as facilitators of innate stimulation, and as TLR stimulation of ABCs, or ABC-like B cells, seems to be important for not only generation of these cells, but also plays a role in their function, determining the role of FcRLs on cell function is another interesting area for investigation. Finally, the significance of FcRLs as pathologic, diagnostic, prognostic and therapeutic agents is showing great promise in a large number of lymphoid malignancies and immune-mediated disorders, so FcRLs may be useful biomarkers or therapeutic targets for RA.

	FcRL1	FcRL2	FcRL3	FcRL4	FcRL5	FcRL6	FcRLA	FcRLB
Cytoplasmic tail	2 ITAMs	1 ITAM and 2 ITIMs	1 ITAM and 1 ITIM	2 ITIMs and 1 ITSM	1 ITAM and 2 ITIMs	1 ITIM	Mucin-like regions	Mucin-like regions
Cellular location	Cell surface	Cell surface	Cell surface	Cell surface	Cell surface	Cell surface	Intracellular protein	Intracellular protein
Distribution	Pan B cell	Memory B cells (circulating MZ)	B cells, T cells and NK cells	Memory B cells (tissue MZ)	Pan B cell and Plasma cells	Cytotoxic T cells and NK cells	Germinal centre B cells	Germinal centre B cells
Ligand	Unknown	Unknown	Secreted IgA	IgA immune complexes	Heat-aggregated or intact IgG	MHC class II / HLA-DR	Intracellular IgM, IgG, and IgA	Unknown

Table 1. 3. Summary table of the FcRL family members' characteristics. Each FcRL family member is shown in a different colour. Information about their cytoplasmic tail motifs, the cellular location, the distribution and their ligands is shown in each row.

1.6 Hypothesis, aims and objectives

I hypothesised that ABCs represent a differentiated, activated and pathogenic B cell population in RA. These cells are capable of migrating to sites of inflammation and perpetuate inflammation and disease pathogenesis via the secretion of autoantibodies and pro-inflammatory mediators.

The aims of my study were to:

1. Determine the frequency of ABCs in peripheral blood and synovial fluid in early and established RA patients compared to disease controls and age-matched healthy controls.
2. Phenotypically characterise peripheral blood ABCs.
3. Determine the transcriptomic profile of ABCs from early RA patients compared to disease controls and age-matched healthy controls.
4. Investigate the function of ABCs.
5. Conduct a preliminary study to elucidate the role of FcRL3 expression on B cell function.

The specific objectives were to:

1. Compare ABCs frequency in peripheral blood in different inflammatory arthritides as well as healthy controls using flow cytometry.
2. Compare expression of different markers (co-stimulatory, activation, transcription factors, immunoglobulin, etc.) between ABCs and other B cell subsets using flow cytometry.
3. Determine the transcriptomic profile of ABCs and other B cell subsets from early RA patients compared to disease controls and healthy controls using NanoString Technology.
4. Investigate the function of ABCs by assessing their secretion of immunoglobulins and their cytokine production profile after culture and stimulation.
5. Explore the potential role for FcRL3 on B cell function using a stably transduced B cell line overexpressing FcRL3.

Chapter 2. Materials and methods

2.1 Patient recruitment

2.1.1 Ethics

Ethical approval for the recruitment of patients was provided by North East – Newcastle & North Tyneside 2 Research Ethics Committee, for the project entitled *Prognostic and therapeutic biomarkers in an observational inception cohort: the Northeast Early Arthritis Cohort*: REC reference 12/NE/0251. In addition, ethics for healthy volunteers were provided by two ethically approved projects: 1. For the project entitled *The role of inflammation in human immunity*, ethical approval was provided by the County of Durham and Tees Valley Research Ethics Committee, REC reference 12/NE/0121; and 2. For the project titled *Understanding Mechanisms of Immune Mediated Disease*, ethical approval was obtained from The Animal Welfare and Ethical Review Body (AWERB), Newcastle University, project ID Number: ID 633.

2.1.2 Early Arthritis Clinic

Patients were recruited from the Newcastle Early Arthritis Clinic (NEAC), in the Musculoskeletal Unit at the Freeman Hospital, Newcastle-upon-Tyne. Patients referred to the NEAC from their primary healthcare provider have suspected inflammatory arthritis and are seen within 14 weeks of symptoms onset. At visit 1 (week 1) patients are reviewed by the nurse specialist, their disease activity is assessed, an ultrasound examination is performed and routine blood test is collected for clinical tests to assess inflammation and rheumatology markers. Disease activity is measured by the DAS28, DAS stands for "Disease Activity Score" and 28 refers to the 28 joints examined in this assessment. This score is calculated by the number of tender joints, the number of swollen joints, the patient's assessment on their global health using the visual analogue scale and with the inflammatory markers CRP or ESR. At visit 2, a week later, a consultant rheumatologist examines the patient and considering the patient's clinical history, the examination and the above investigations, a diagnosis is made.

Patients diagnosed with RA following the 2010 ACR/EULAR classification criteria were, where possible, recruited. Other disease controls were also recruited, which included patients diagnosed with psoriatic arthritis, ACPA+ arthralgia, undifferentiated, crystal and reactive arthritis. All these patients were naïve to disease modifying anti-rheumatic drugs (DMARDs) and biological therapies.

For all these patients, where possible, RF and CCP antibody titres, ESR and CRP values, DAS28 score (only for RA patients), smoking status, age and sex were recorded.

2.1.3 Established RA patients

Patients with a diagnosis of RA and a disease duration of more than 12 months were also recruited. These patients were recruited from the rheumatology clinics/day unit services at the Musculoskeletal Unit at the Freeman Hospital, Newcastle-upon-Tyne. All the patients recruited were treated only with DMARDs, methotrexate (MTX), hydroxychloroquine (HCQ) and sulfasalazine (SSZ), but not with biological therapies. Any patient that had received any oral, intramuscular or intra-articular glucocorticoid steroids in the last 3 months were excluded. For all the patients an attempt was made to record the anti-rheumatic treatments, the RF and CCP antibody titres, ESR and CRP values, DAS28 score, smoking status, age and sex.

2.1.4 Healthy controls

An effort was made to recruit healthy volunteers that would match in age and sex the patients. Volunteers over 50 years old were recruited mainly from staff at Newcastle University. In addition, through Voice Global, a group led by Newcastle University whose members support a range of research activity, age-matched healthy volunteers were also recruited. All the volunteers had no personal history of autoimmunity or other musculoskeletal conditions.

2.2 Primary cellular techniques

2.2.1 Cell isolation

Peripheral blood mononuclear cells (PBMCs) isolation

Blood was collected into BD EDTA Vacutainer® tubes (BD Biosciences, CA, USA) and diluted 1:1 with room temperature (RT) Hanks Balanced Salt Solution (HBSS, Lonza, Switzerland) containing 2mM EDTA (Fisher Scientific, NH, USA). 20ml of the diluted blood was layered slowly onto 15ml of Lymphoprep (Axis-Shield Diagnostics Ltd, UK) and was then centrifuged at 895g for 30 minutes at RT. PBMCs were recovered from the surface of the density centrifugation medium (Figure 2.1). PBMCs from up 2 tubes were pooled together and topped up to 50ml with cold HBSS containing 1% Foetal Calf Serum (FCS, Labtech, UK). The resultant cell suspension was centrifuged at 600g for 8 minutes at 4°C. The supernatant was aspirated and the cells were topped up to 50ml with cold HBSS

containing 1% FCS and centrifuged again at 250g for 8 minutes at 4°C to remove platelets. Cells from the different tubes were pooled together and strained through a 70µm nylon filter to remove any debris/clumps. Cells were then counted using a Burker counting chamber with Trypan Blue (Sigma-Aldrich, MO, USA) exclusion and were used for subsequent downstream assays.

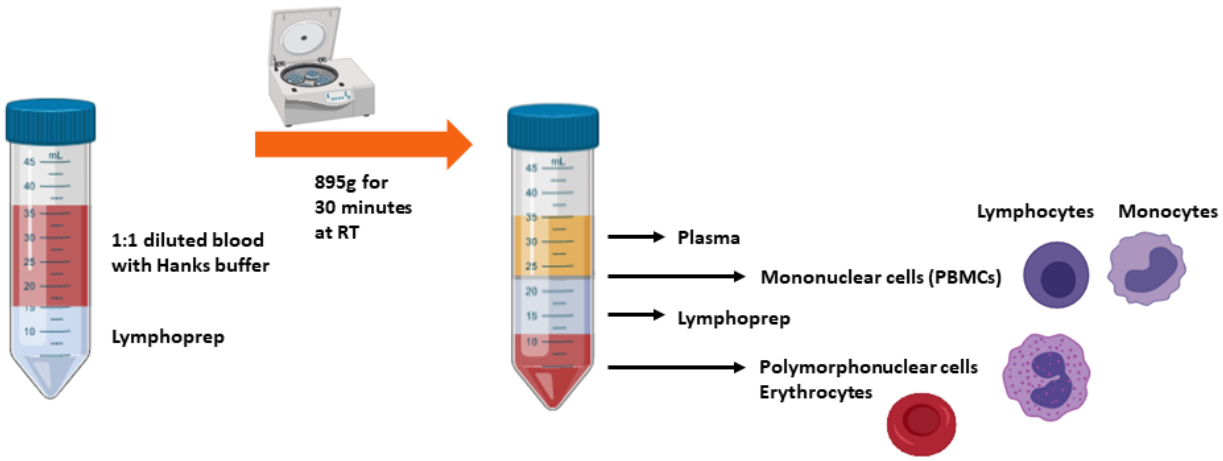

Figure 2. 1. Scheme of separation of PBMCs using the density centrifugation medium Lymphoprep. 20ml of blood were diluted 1:1 with HBSS and slowly layered onto 15ml of Lymphoprep. The tubes were centrifuged at 895g for 30 minutes at room temperature. PBMCs were recovered from the surface of the density centrifugation medium and washed for downstream applications. Created with Biorender.com.

CD3+ T cell depletion of PBMCs

For the functional work, CD3+ T cells were depleted from the PBMCs in order to reduce the flow cytometry sorting time needed for the isolation of the different B cell subsets. CD3+ T cells were depleted by positive selection using a CD3 MicroBead Kit (Miltenyi Biotech, Germany). Depletion was performed as per manufacturer's instructions. For the magnetic separation LS columns from Miltenyi Biotech were used. Because depletion was performed to exclude the T cells, the flow through was used for flow cytometry sorting, and therefore, purity of the CD3+ T cell population was not assessed.

Synovial fluid mononuclear cells (SFMCs) isolation

Synovial fluid (SF) was collected into a universal tube and diluted 1:1 with RT HBSS containing 2mM EDTA. Hyaluronidase (Sigma-Aldrich, MO, USA) was added to the SF at a concentration of 10 U/ml and heparin (Wockhardt, UK) at 1 IU/ml. The SF was then incubated in a water bath at 37°C for 40 minutes. 20ml of the treated SF was layered slowly

onto 15ml of Lymphoprep and this was then centrifuged at 895g for 30 minutes at RT. Cells in the interface were harvested and topped up to 50ml with cold HBSS containing 1% FCS. The cell suspension was centrifuged at 600g for 8 minutes at 4°C. The supernatant was aspirated and the cells were topped up to 50ml with cold HBSS containing 1% FCS and centrifuged again at 250g for 8 minutes at 4°C. Cells were then counted using a Burker counting chamber with Trypan Blue exclusion and were used for subsequent downstream assays.

2.2.2 Cell culture

Sorted B cell activation

Sorted B cells were cultured in RPMI 1640 medium (Sigma-Aldrich, MO, USA) containing 10% (v/v) FCS and supplemented with 2 mM L-glutamine, 100 U/ml penicillin and 100 µg/ml streptomycin (all Sigma-Aldrich, MO, USA). B cells were cultured at a density of 20,000 cells per well in 96-well round-bottom plates in a final volume of 200µl of culture medium. At initiation of culture, B cells were stimulated with a combination of the TLR7 ligand, Imiquimod (1µg/ml, InvivoGen, CA, USA), TLR9 agonists, ODN 2216 – CpG A and ODN 2006 – CpG B (both 1µg/ml, InvivoGen, CA, USA), Poke Weed Mitogen (PWM, 5µg/ml, Sigma-Aldrich, MO, USA), anti-CD40 antibody (10µg/ml, clone HB14, mouse IgG1, Biolegend, CA, USA), human IL-21 (0.05µg/ml, Miltenyi Biotech, Germany), human IL-4 (0.05µg/ml, Immunotools, Germany) and IFN-gamma (0.02µg/ml, Peprotech, UK). B cells were cultured for 5 days at 37°C with 5% CO_2 prior to analysis by flow cytometry. Supernatants were frozen at -80°C prior to further analysis by MSD or ELISA.

Whole blood activation

Blood was collected into BD Heparin Vacutainer® tubes. Heparinised blood was required rather than EDTA-treated blood because EDTA chelates Ca^{2+} which is necessary for the activation of the cells. Heparin does not chelate Ca^{2+} and is therefore the preferred anti-coagulant for whole blood functional assays. In a 24-well plate, 500µl of blood were diluted 1:1 with RT RPMI 1640 medium. Two different stimulation cocktails were added to the corresponding wells: 1. PWM (5µg/ml), the TLR7 ligand, Imiquimod (1µg/ml) and TLR9 agonists ODN 2216 – CpG A and ODN 2006 – CpG B (both 1µg/ml); 2. TLR7 and TLR9 ligands as described above, but PWM was substituted by anti-IgM/IgG antibody (10µg/ml, polyclonal, goat IgG, eBioscience, CA, USA). Blood was stimulated for 24 and 48 hours at 37°C with 5% CO_2. After the incubation time, cells were analysed by flow cytometry for

the expression of activation markers (see Table 2.1) following the whole blood staining protocol (see section 2.5.1) adjusting the volumes of antibodies used to higher amounts of blood used.

2.2.3 Cell freezing and thawing

Cell freezing

Cells were pelleted at 400g for 8 minutes at 4°C and resuspended in FCS with a maximum concentration of 20 x 10^6 cells in 500µl. FCS containing 20% dimethyl sulfoxide (DMSO; Sigma-Aldrich, MO, USA) was added drop wise in equal volume, resulting in a final concentration of 10% DMSO. This suspension was added to cryovials (1ml per vial) and the cryovials were placed in a CoolCell® (BioCision, CA, USA), which was then stored at -80°C overnight to facilitate controlled freezing at a rate of -1°C/minute. The frozen cryovials of cells were then moved to liquid nitrogen for long term storage.

Cell thawing

Frozen cryovials were warmed to 37°C for 5 minutes in a standard water bath submerging the lower half of the vial only. Cells were mixed and transferred drop wise to a universal container containing warmed (37°C) thawing medium (HBSS supplemented with 10% FCS) to a final volume of 25 ml. Suspensions were centrifuged at 400g for 8 minutes at RT and the pellet was resuspended in warm thawing medium and centrifuged as stated above. Cells were then counted with a Burker counting chamber using Trypan Blue exclusion and were then used for subsequent downstream assays.

2.2.4 Cytospins

Sorted cells were pelleted and resuspended in 50µl of FCS. Slides were placed in the cytospin cartridges along with a carbon filter facing the centre of the cytospin. Cells were transferred to each cytospin well and centrifuged at 350 rpm for 8 minutes (Shandon Cytospin 4, ThermoFisher Scientific, MA, USA). The slides were left to dry overnight. The next day, they were placed in a jar containing cold methanol for 30 seconds to fix the slide. Giemsa staining was performed using the Hematek 3000 machine (Siemens Healthineers, Germany) and the Wright-Giemsa Stain Pack (Siemens Healthineers, Germany). Slides were left for at least one hour to dry before being imaged.

2.3 Cytokine and antibody measurement

2.3.1 Enzyme-linked immunosorbent assays (ELISAs)

Enzyme-linked immunosorbent assays, ELISAs, was used to quantify secreted IgG from the supernatants of the stimulated B cell subsets. IgG was detected using the Human IgG total ELISA Ready-SET-Go!™ Kit (eBioscience, CA, USA). IgG quantification was done as per manufacturer's instructions following the kit's two day protocol: The plate was coated overnight and the blocking and incubation with the sample and the secondary antibody were all done on the second day.

Because the B cells used in the cell culture activation assays were from seropositive patients (RF and CCP antibody positives), and as RF is a heterophilic antibody, i.e. binds immunoglobulins, there was a potential interference of RF with the accuracy of the ELISA results. Supernatants from stimulated memory B cells and ABCs were sent to the Newcastle laboratories (Newcastle Hospitals NHS Trust) for the detection of RF. The lower end of detection was 10 IU/ml for the RF antibody. CCP antibodies were also measured out of interest, with its lower end of detection being 0.5 U/ml. However, no autoantibodies either for RF and CCP were detected, for that reason, the ELISAs were run as per manufacturer's protocol and no further action regarding heterophilic antibodies was taken.

2.3.2 MSD plates

Meso Scale Discovery (MSD, Meso Scale Discovery, Maryland, USA) biomarker assays provide a rapid and convenient method for measuring the levels of targets within a single, small-volume sample. MSD multiplex plate allows for the detection of up to 10 targets in a single volume. This is achieved as the well surface is composed of a carbon electrode onto which each different capture antibody is coated in one of the ten spots (Figure 2.2). Like in a sandwich immunoassay, the sample to be analysed is loaded and the analyte binds to the capture antibody. Then a detection antibody, labelled with SULFO-TAG™, an electrochemiluminescent compound, binds the analyte and emits light when a voltage is applied to the electrodes on the plate surface. The light intensity is measured by the analyser and allows quantification of each analyte.

Using the MSD multiplexing technology, 9 cytokines were measured from culture supernatants of the sorted B cell subsets, as well as from the FcRL3 transfected Ramos B cells and controls after stimulation. The chosen assay was a U-PLEX Custom Biomarker

(human) plate with the following cytokines: GM-CSF, IL-2, IL-6, IL-10, IL-12p70, IL-23 and TNF-alpha.

The Isotyping Panel 1 (Human/NHP) Kit also from MSD was used to measure immunoglobulin isotype in the supernatants of sorted B cell subsets and transfected Ramos B cells as per manufacturer's instructions.

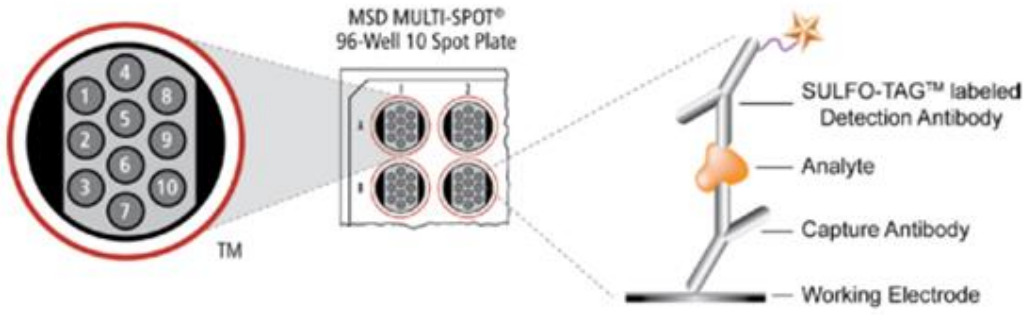

Figure 2. 2. MSD multiplex assay. MSD multiplex plate surface is composed of a carbon electrode onto which each capture antibody is coated in one of the ten spots. Like in a sandwich immunoassay, the analyte binds to the capture antibody. Then a detection antibody, labelled with SULFO-TAGTM, an electrochemiluminescent compound, bind the analyte and emits light when a voltage is applied to the electrodes on the plate surface. The light intensity is measured by the analyser and allows quantification of each analyte. Image taken from the MSD Multispot manual (https://www.mesoscale.com/~/media/files/product%20inserts/human%20proinflam%209-plex%20us.pdf).

2.4 Flow Cytometry

2.4.1 Cell surface protein expression in whole blood

Blood was collected into BD EDTA Vacutainer® tubes. Reverse pipetting was used to transfer 200µl of blood into a 2ml microcentrifuge tube. Each antibody (see Tables 2.1 – 2.4 for fluorophore labelled antibody panels used) at a pre-titrated dilution was added to the blood and the tubes were then incubated in a water bath at 37°C for 30 minutes. After this time, red blood cells (RBC) were immediately lysed by adding 10 volumes of pre-warmed 1x BD FACS Lysing solution (BD Biosciences, CA, USA) and the tubes were incubated at 37°C for 12 minutes. Tubes were then centrifuged at 600g for 8 minutes at RT and the supernatant was decanted. The cell pellet was washed with FACS buffer

(Dulbecco's Phosphate Buffered Saline (D-PBS) containing 0.5% BSA, 1mM EDTA and 0.01% Sodium azide) and centrifuged at 600g for 8 minutes at RT. The supernatant was decanted and the cell pellet was resuspended in 300µl of FACS buffer and transferred to a FACS tube (BD Biosciences, CA, USA) to be acquired on a BD LSR Fortessa X20™ (Becton Dickinson, NJ, USA).

For the intracellular staining panel (Table 2.2) cells were first surface stained as outlined above and then processed accordingly to the intracellular protein expression protocol (see section 2.5.2).

Surface marker	Fluorophore	Clone	Dilution factor	Company
CD3	PE-CF594	UCHT1	1:200	BD Biosciences, CA, USA
CD33	PE-CF594	WM53	1:33	BD Biosciences, CA, USA
CD19	BUV395	SJ25C1	1:100	BD Biosciences, CA, USA
CD20	BV510	2H7	1:200	Biolegend, CA, USA
CD11c	APC	S-HCL-3	1:200	BD Biosciences, CA, USA
CD21	PE	BU32	1:200	Biolegend, CA, USA
CD5	PE-Cy7	UCHT2	1:100	eBioscience, CA, USA
CD27	BV650	O323	1:200	Biolegend, CA, USA
IgD	AF700	IA6-2	1:100	Biolegend, CA, USA
CD80	BB515	L307.4	1:100	BD Biosciences, CA, USA
CD86	BV711	IT2.2	1:200	Biolegend, CA, USA
CD69	APC-Vio770	FN-50	1:50	Miltenyi Biotech, Germany
HLA-DR	PerCP	L203	1:50	RnD Systems, MN, USA
CD40	BV421	5C3	1:50	Biolegend, CA, USA

Table 2. 1. Fluorophore labelled antibodies used for the activation panel.

Surface marker	Fluorophore	Clone	Dilution factor	Company
CD3	PE-CF594	UCHT1	1:200	BD Biosciences, CA, USA
CD33	PE-CF594	WM53	1:33	BD Biosciences, CA, USA
CD19	BUV395	SJ25C1	1:100	BD Biosciences, CA, USA
CD20	BV510	2H7	1:200	Biolegend, CA, USA
CD11c	APC	S-HCL-3	1:200	BD Biosciences, CA, USA
CD21	PE	BU32	1:200	Biolegend, CA, USA
CD5	PE-Cy7	UCHT2	1:100	eBioscience, CA, USA
CD27	FITC	M-T271	1:100	BD Biosciences, CA, USA
IgD	AF700	IA6-2	1:100	Biolegend, CA, USA
T-bet	BV421	O4-46	1:10	BD Biosciences, CA, USA
Ki67	BV711	Ki-67	1:10	Biolegend, CA, USA

Table 2. 2. Fluorophore labelled antibodies used for the intracellular panel.

Surface marker	Fluorophore	Clone	Dilution factor	Company
CD3	PE-CF594	UCHT1	1:200	BD Biosciences, CA, USA
CD33	PE-CF594	WM53	1:33	BD Biosciences, CA, USA
CD19	BUV395	SJ25C1	1:100	BD Biosciences, CA, USA
CD20	BV510	2H7	1:200	Biolegend, CA, USA
CD11c	BV421	B-LY6	1:50	BD Biosciences, CA, USA
CD21	PE-Cy7	BU32	1:100	Biolegend, CA, USA
CD5	APC-Cy7	L17F12	1:200	Biolegend, CA, USA
CD27	BV650	O323	1:200	Biolegend, CA, USA
IgD	AF700	IA6-2	1:100	Biolegend, CA, USA
FcRL3	BB515	H5	1:200	BD Biosciences, CA, USA
FcRL4	PE	413D12	1:100	Biolegend, CA, USA
FcRL5	APC	509f6	1:50	Biolegend, CA, USA

Table 2. 3. Fluorophore labelled antibodies used for the FcRL3-5 panel.

Surface marker	Fluorophore	Clone	Dilution factor	Company
CD3	PE-CF594	UCHT1	1:200	BD Biosciences, CA, USA
CD33	PE-CF594	WM53	1:33	BD Biosciences, CA, USA
CD19	BUV395	SJ25C1	1:100	BD Biosciences, CA, USA
CD20	BV510	2H7	1:200	Biolegend, CA, USA
CD11c	BV421	B-LY6	1:50	BD Biosciences, CA, USA
CD21	PE-Cy7	BU32	1:100	Biolegend, CA, USA
CD5	APC-Cy7	L17F12	1:200	Biolegend, CA, USA
CD27	BV650	O323	1:200	Biolegend, CA, USA
IgD	AF700	IA6-2	1:100	Biolegend, CA, USA
FcRL2	PE	REA474	1:20	Miltenyi Biotech, Germany
FcRL1	APC	REA440	1:100	Miltenyi Biotech, Germany
FcRL2	PE	B24	1:100	Gift from Prof Nagata, Japan

Table 2. 4. Fluorophore labelled antibodies used for the FcRL1-2 panel.

Surface marker	Fluorophore	Clone	Dilution factor	Company
CXCR3	AF488	1C6	1:50	BD Biosciences, CA, USA
CXCR4	APC	REA649	1:100	Miltenyi Biotech, Germany
CXCR5	BV510	J252D4	1:100	Biolegend, CA, USA
CD95/FAS	PE	REA738	1:100	Miltenyi Biotech, Germany
CD97	FITC	VIM3b	1:100	Biolegend, CA, USA
Granzyme B	PE-CF594	GB11	1:10	BD Biosciences, CA, USA
Perforin	PE-Cy7	B-D48	1:10	Biolegend, CA, USA

Table 2. 5. Fluorophore labelled antibodies used for the validation of the NanoString markers.

2.4.2 Intracellular protein expression

To assess intracellular expression of Ki67 and T-bet, whole blood was first stained for surface antibodies (as described in 2.5.1 above). The surface stained cells were resuspended in 200µl FACS buffer and transferred to a 96-well v-bottom plate (CoStar, DC, USA). Cells were then permeabilised in 300µl of 1x Perm buffer (eBioscience, CA USA) for 30 minutes at 4°C in the dark. To reduce background staining, the cells were blocked with 2% mouse serum (Sigma-Aldrich, MO, USA) in 50µl volume for 15 minutes at 4°C in the dark before

adding Ki67 and T-bet antibodies at the pre-titrated dilution (Table 2.2). Cells were incubated for 30 minutes at 4°C in the dark. After this time, the cells were washed, resuspended in 300µl of FACS buffer and transferred to a FACS tube (BD Biosciences, CA, USA) to be acquired on a BD LSR Fortessa X20™.

2.4.3 Cell surface protein expression in PBMCs

1 x 10^6 cells were transferred to a 96-well v-bottom plate and centrifuged at 400g for 3 minutes. To reduce background staining, cells were resuspended in 50µl of FACS buffer containing 2% mouse serum and incubated for 15 minutes at 4°C in the dark. Wells were then topped up with FACS buffer and centrifuged at 400g for 3 minutes. Cells were resuspended in 50µl of FACS buffer mastermix containing each antibody (see Table 2.6 for the fluorophore labelled antibodies used). The cells were incubated at 4°C for 30 minutes in the dark. After this time, the plate was centrifuged at 400g for 3 minutes, blotted and resuspended in 100µl of PBS (Sigma-Aldrich, MO, USA) containing 1µl of Zombie Aqua (Biolegend, CA, USA) to stain dead cells. Cells were incubated at 4°C for 15 minutes in the dark, then washed twice with FACS buffer, resuspended in a final volume of 300µl of FACS buffer and fixed in 1% formaldehyde (TAAB laboratories, UK) before acquisition on a BD LSR Fortessa X20™.

Surface marker	Fluorophore	Clone	Dilution factor	Company
CD3	PE-CF594	UCHT1	1:50	BD Biosciences, CA, USA
CD33	PE-CF594	WM53	1:50	BD Biosciences, CA, USA
CD19	BUV395	SJ25C1	1:100	BD Biosciences, CA, USA
CD11c	BV421	B-LY6	1:20	BD Biosciences, CA, USA
CD21	PE-Cy7	BU32	1:50	Biolegend, CA, USA
CD5	APC-Cy7	L17F12	1:100	Biolegend, CA, USA
CD27	BV650	O323	1:10	Biolegend, CA, USA
IgD	AF700	IA6-2	1:50	Biolegend, CA, USA
IgM	BB515	G20-127	1:20	BD Biosciences, CA, USA
IgG	BV786	G18-145	1:50	BD Biosciences, CA, USA
IgA	PE	IS11-8E10	1:50	Miltenyi Biotech, Germany

Table 2. 6. Fluorophore labelled antibodies used for the immunoglobulin panel.

2.4.4 Flow cytometry analysis

All the flow cytometry data was analysed using the software FlowJo Version 10 (Treestar Inc, OR, USA). For the phenotypic characterisation and the determination of the frequency of ABCs, the gating strategy shown in Figure 3.1 in Chapter 3 was used to create the gates for each of the four populations of B cells of interest. First, doublets and autofluorescent cells were excluded. Lymphocytes were gated using SSC-A vs FSC-A, and from the lymphocyte gate, the B cells were gated. A dump channel was used to exclude other cell types, CD3 for T cells, CD16 and CD14 for all monocytes, CD56 for NK cells and most importantly CD33 for dendritic cells. Exclusion of dendritic cells is very important as these cells are positive for CD11c and may contaminate the ABC population, therefore I used an antibody to exclude CD33+ cells. From the B cell gate, ABCs were gated as CD11c+ CD21-, from the remaining CD19+ cells, CD5+ cells were gated as CD5+ CD19+. From the CD5- fraction, naïve B cells (IgD+ CD27-) and memory B cells (IgD- CD27+) were gated.

Expression of each of the phenotypic markers in each of the subsets was determined by creating a quadrant gate in the lymphocytes gate of the marker against CD19 and copying that gate into the subsets to assess the number of positive cells for that marker in each subset (Figure 4.1 in Chapter 4).

In some cases, the expression of a particular antigen was clear bimodal, resulting in clear positives and negatives meaning gates could be easily determined. However, for most phenotypic markers, gates were set on fluorescence minus one (FMO) controls, and in a few cases the gates were set based in an unstained population of cells. The use of unstained cells informs us about the background fluorescence and the autofluorescence properties of the sample and gates can be set to delineate the negative population. An FMO control includes all of the antibody conjugates present in the test sample except one. The use of an FMO control helps to identify the positive population when the expression of that marker is low. This method allows the assessment of the spread of fluorescence as another fluorophore from another channel may leak into the channel of interest causing a false positive staining.

2.4.5 Flow cytometry cell sorting

Previously isolated PBMCs or the CD3-depleted PBMC fraction were resuspended in cold FACS buffer to a final concentration of 20 x 10^6 cells/ml and 1ml of this cell suspension

was added to a microcentrifuge tube. The cells were centrifuged at 400g for 8 minutes at 4°C. The cell pellet was resuspended in the fluorophore labelled antibody mix (see Table 2.7) which also contained 4µg/ml of human IgG (Gift from Professor Sophie Hambleton, Newcastle University, UK) in a total volume of 50µl FACS buffer. The cells were incubated for 30 minutes at 4°C in the dark. After this incubation time, cells were washed with PBS and centrifuged at 400g for 8 minutes at 4°C. Cell pellets were resuspended in 100µl of PBS containing 2µl of Zombie UV (Biolegend, CA, USA) to stain for dead cells. Cells were incubated at 4°C for 15 minutes in the dark and then washed twice with FACS buffer. Cells from each microcentrifuge tube were transferred to a FACS tube and the volume was made up to 2ml with FACS buffer, resulting in a cell density of 10 x 10^6 cells/ml.

Right before sorting, the cells were transferred into a new FACS tube and strained through a 30µm cell strained (CellTrics - Sysmex, IL, USA). This was performed immediately prior to sorting to avoid small cell clumps blocking the sorter's nozzle. The BD FACSARIA II (Becton Dickinson, NJ, USA) with a 70µm nozzle was used to sort the four immune cell subsets. The gating strategy is shown in Figure 5.1 in Chapter 5 and the fluorophore labelled antibodies used are shown in Table 2.7.

Surface marker	Fluorophore	Clone	Dilution factor	Company
CD3	PE-CF594	UCHT1	1:12.5	BD Biosciences, CA, USA
CD33	PE-CF594	WM53	1:12.5	BD Biosciences, CA, USA
CD19	BUV395	SJ25C1	1:10	BD Biosciences, CA, USA
CD20	BV510	2H7	1:12.5	Biolegend, CA, USA
CD11c	APC	S-HCL-3	1:10	BD Biosciences, CA, USA
CD21	PE	BU32	1:16.5	Biolegend, CA, USA
CD5	PE-Cy7	UCHT2	1:12.5	eBioscience, CA, USA
CD27	FITC	M-T271	1:12.5	BD Biosciences, CA, USA
IgD	AF700	IA6-2	1:16.5	Biolegend, CA, USA

Table 2. 7 Fluorophore labelled antibodies used for the sorting panel.

2.5 NanoString Technologies

The NanoString Technologies uses the nCounter® gene expression platform to capture and count individual mRNA transcripts (Geiss *et al.*, 2008). Briefly, the assay consists of a multiplexed probe library with two sequence-specific probes for each gene of interest, which has been previously tested and optimised by NanoString. The first probe is a capture probe of around 50 nucleotides plus a short common sequence coupled to an affinity tag such as biotin (Figure 2.3.A). The second probe, the reporter probe also consists of 50 nucleotides and is coupled to a specific colour barcode per each target gene, providing the detection signal. Both probes hybridise with the target of interest in a solution phase (Figure 2.3.B). Excess probes are removed by affinity purification and the remaining target- probe complexes are bound the nCounter cartridge surface, aligned and immobilised using electrophoresis (Figure 2.3.C). Finally, the cartridge is placed in a digital analyser for image acquisition and data processing (Figure 2.3.D). The level of expression is measured by counting the number of codes for each mRNA.

The main advantages of the nCounter® system are the ability of measuring total mRNA transcripts without requiring amplification, meaning no gene-specific biases are introduced. Moreover, unlike in microarrays, hybridisation of the probe and the target happens in solution, allowing for a higher sensitivity, especially of lower expressed genes.

Additionally, nCounter® technology is ideal for small samples with limited amounts of RNA, such as tissue biopsies or cells sorted by flow cytometry.

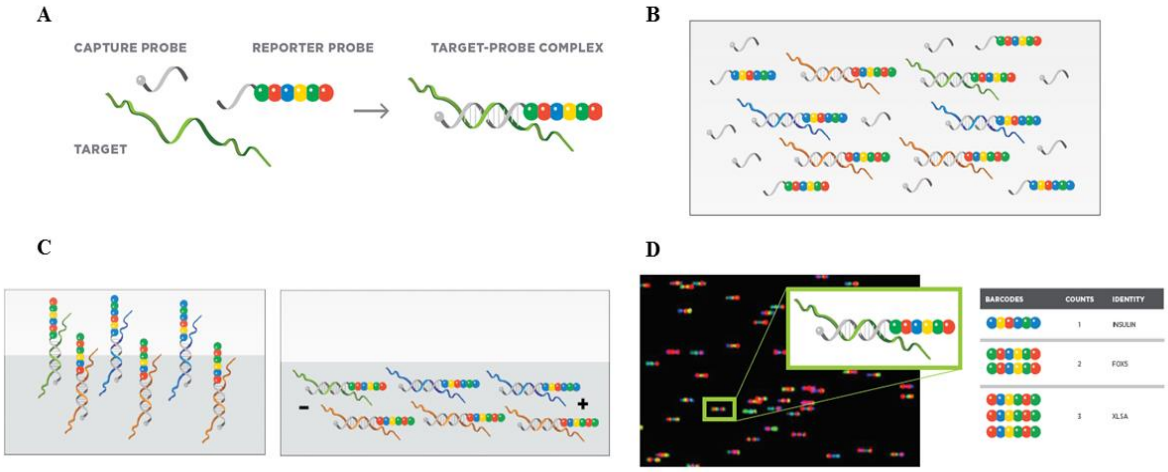

Figure 2. 3. NanoString nCounter technology. A. NanoString probes. Each gene of interest (target) is detected using a capture probe and a target probe, which will bind the mRNA of the gene and make the target-probe complex. **B. Probe and target gene hybridisation.** Probes hybridise with the target in a solution phase. **C. Target-probe complex is immobilised in the cartridge.** Target-probe complex binds the cartridge via the capture probe and is then immobilised by electrophoresis in the cartridge. **D. Barcode count.** The cartridge is then placed in a digital analyser which counts each reporter barcode and gives, therefore gene counts.

Adapted from https://www.nanostring.com/scientific-content/technology-overview/ncounter-technology on 27/05/2019.

2.5.1 Methodology and genes analysed

The transcriptome of the flow cytometry sorted B cell subsets were analysed using the NanoString nCounter Human immunology V2 Panel (NanoString Technologies Inc, WA, USA). For the full list of genes assessed see Appendix A.1. An additional 20 custom genes were added to the plate, in order to expand B cell relevant markers, identify DNA/RNA intracellular sensing pathways and identify retrotransposon activity (Table 2. 8, sequences included in Appendix A.2).

Standard probes	Customised probes
CD38	AluYa5
CXCR5	AluYb9
DDX58 (RIG-1)	L1_5prime
FcRL4	L1_ORF2
IDO2	LTR_3prime
IRF9	LTR_5prime
KMO	
MAVS	
cGAS	
SAMHD1	
CD138	
TDO2	
TPH1	
TREX1	

Table 2. 8 Additional genes (probes) included in the NanoString nCounter Human immunology V2 Panel.

Due to the small numbers of ABCs I was able to sort from samples, when RNA was directly extracted from these cells it resulted in very small amounts of RNA purified. The amount of RNA was lower than the recommended amount, 100ng, to use in the NanoString assay. Using low amounts of RNA would lead to a loss of detection of low expressed genes, which could be very important for the characterisation of ABCs. I therefore, used whole cell lysates to load on the chip as the starting material. For each subset, 15,000 cells were sorted into a 1.5ml microcentrifuge tubes containing 280µl of RF10 (RPMI +10% FCS). After sorting, the cells were transferred into a 96-well plate and spun at 400g for 4 minutes. Cells were then resuspended in 1.6µl of RLT buffer (Qiagen, Germany), transferred, together with the residual RF10 volume, to a 0.2ml microcentrifuge tube and stored in the -80 freezer until all the samples were collected from recruited donors. Once the recruitment was finished and the NanoString plates were ready to run, a total volume of 5µl of lysate for each of the cell subsets was loaded into the chip and the protocol was followed according to standard nCounter instructions.

Each nCounter CodeSet includes 15 housekeeping genes used as an internal control due to their low variability across sample types and high counts to correct for differences in sample quality and amount of RNA.

2.5.2 NanoString nCounter data analysis

The analysis of the data generated with NanoString was performed by Najib Naamane, a bioinformatician in our group. R software version 3.5.3 was used in association with the Bioconductor repository (Huber *et al.*, 2015) for this analysis.

Data pre-processing and quality assessment

A quality control step was conducted using the arrayQualityMetrics (Kauffmann *et al.*, 2009) Bioconductor package to detect and remove any outlier samples. This was done after normalisation to the NanoString housekeeping genes. For each sample, arrayQualityMetrics computes three different metrics: 1. The sum of the distances to all other samples, 2. The Kolmogorov-Smirnov statistic between the sample's distribution and the pooled distribution from all samples, and 3. The Hoeffding's statistic on the joint distribution of M (log-ratio) and A (mean of logarithms) values, corresponding to the gene counts of the studied sample and a "pseudo"-sample (i.e. the median across samples). A threshold is then determined for each metric based on the distribution of its values across all samples (i.e. the third quartile plus 1.5 times the interquartile range). Samples with at least two metrics exceeding the threshold were considered as outliers. Four samples were flagged as outliers and were thus excluded from further analysis.

Lowly expressed genes were filtered out to improve the mean-variance relationship estimation and reduce the number of tests to be performed during downstream differential expression analysis, hence increasing the statistical power. A gene was considered to be expressed in a given sample if its counts were greater than the corresponding background estimate (i.e. the mean of the negative controls in that sample added by two standard deviations). Only genes that were expressed in all the samples of at least one condition (i.e. a cell subset of a disease group) were retained.

Differential gene expression analysis

The DESeq2 R package (Love *et al.*, 2014) was used to compare the gene expression profiles between different B cell subsets and disease groups. DESeq2 tests for differential expression by fitting negative binomial generalized linear models (GLMs) to the data (Love

et al., 2014). The analysis was performed in three steps. First, sample-specific size factors were estimated using the median ratio method (Anders and Huber, 2010) implemented by the estimateSizeFactors function. Then, the gene-specific dispersions estimates were obtained using the estimateDispersions function. Finally, the nbinomWaldTest function was used to fit a GLM that uses the previously calculated size factors and dispersion estimates to normalize the raw count data for library size and compute the Wald statistics for the following comparisons:

- ABCs against each cell type in early RA - each B cell subset was compared with the ABCs in patients with early RA.
- Cell types in early RA against DC - each B cell subset was compared between early RA and disease controls.
- Cell types in eRA against HC - each B cell subset was compared between early RA and age-matched healthy controls.

Genes with a Benjamini-Hochberg adjusted p-value < 0.05 and a fold change > 1.5 were considered to be differentially expressed when comparing B cell subtypes within the same disease group while a less stringent cut-off (unadjusted p-value < 0.05 and a fold change > 1.5) was required for disease group comparisons within the same cell subpopulation.

2.6 Cell lines

2.6.1 HEK293T cells

The cell line HEK293T (Human Embryonic Kidney 293T, ATCC® CRL-3216™) was used. The HEK293T cell line, originally referred to as 293tsA1609neo, is a highly transfectable cell line which contains the SV40 T-antigen. It is a semi adherent cell line. Due to its high transfectable capacity and its ability to produce recombinant retroviruses, they were used to both check FcRLs antibody specificity and for FcRL3 retroviral particle assembly.

HEK293T cells were cultured in Dulbecco's Modified Eagle Medium with high glucose and L-Glutamine (all Gibco - Thermo Fisher Scientific, MA, USA), supplemented with 100 U/ml penicillin, 100µl/ml streptomycin and 8% FCS.

Upon thawing a cryovial of frozen HEK293T cells, cells were mixed and transferred drop wise to a universal container containing warmed (37 °C) culture medium DMEM with 8% FCS to a final volume of 25ml. These were then centrifuged at 400g for 8 minutes. The cell

pellet was resuspended in 20ml of warmed culture medium and centrifuged again at 400g for 8 minutes. Cells were resuspended in 12ml of warmed medium and transferred to a T75 culture flask (Greiner Bio-one, Austria). The flask was incubated at 37 °C with 5% CO_2 until the cells were 80-90% confluent. When the cells were confluent, the media was removed, the cells were detached by flushing PBS and centrifuged at 400g for 8 minutes. The cell pellet was resuspended in 12ml of pre-warmed culture medium, and the cells were then split (1:10 or 1:20) and incubated at 37 °C with 5% CO_2 until confluent or counted using a Burker counting chamber with Trypan Blue exclusion and used for their desired application.

2.6.2 Ramos and Raji cells

For the functional work with FcRL3, Ramos (RA 1, ATCC® CRL-1596™) and Raji (ATCC® CCL-86™) B cell lines were used. The Ramos B cell line was established from a Burkitt's lymphoma of a 3-year-old Caucasian male and the Raji B cell line was established from a Burkitt's lymphoma of the left maxilla of an 11-year-old black male. Both cell lines grow in suspension and have a lymphoblast morphology. However, Raji B cells are positive for the presence of Epstein Barr virus (EBV) viral DNA sequences and EBNA protein whereas Ramos B cells are negative for EBV.

Ramos and Raji cells were cultured in RPMI 1640 medium containing 2 mM L-glutamine, 100 U/ml penicillin and 100 µg/ml streptomycin and supplemented with 10% FCS.

Upon thawing a cryovial of frozen Ramos or Raji cells, cells were mixed and transferred drop wise to a universal container containing warmed (37 °C) culture medium RPMI 1640 with 10% FCS to a final volume of 25ml. These were then centrifuged at 400g for 8 minutes. The cell pellet was resuspended in 20ml of warmed culture medium and centrifuged again at 400g for 8 minutes. Cells were resuspended in 12ml of warmed medium and transferred to a T75 culture flask. The flask was incubated at 37 °C with 5% CO_2 until the cell density was 80-90%. When the cell density was high, they were split 1:10 or 1:20 by transferring the cells to a new T75 flask with warmed culture medium and incubated at 37 °C with 5% CO_2. If the cells were needed for another application, these were counted using a Burker counting chamber with Trypan Blue exclusion after splitting them and used for downstream experiments.

2.7 FcRL family transfection of HEK293T cells

The cell line HEK293T was used to check FcRLs antibody specificity. The plasmids containing transcripts for the FcRL family were kindly provided by Professor Nagata, Osaka University, Japan. Briefly, in order to have enough plasmid to test the antibody specificity, *Escherichia coli* (*E. coli*) bacteria were transformed and the plasmids were extracted. Then HEK293T cells were transfected with the plasmids using a lipid-based approach and stained for all the antibodies against the FcRL family members.

2.7.1 Agar plates preparation and bacterial LB broth preparation

Agar plates were used to grow transformed *E. coli* bacteria. To make 10 plates, 7.63g of Luria Broth (LB) containing 15g/L of agar (Sigma-Aldrich, MO, USA) was added to 250ml of distilled water in a 500ml glass bottle. The solution was mixed and autoclaved to sterilise. After autoclaving, the bottle was placed into a 55°C water bath and left for at least 15 minutes to decrease the temperature. Then, under a Bunsen burner flame, to maintain sterility, ampicillin was added at a final concentration of 100µg/ml. Close to the open flame, 25ml of sterile LB broth with agar and ampicillin was pipetted into previously labelled Petri dishes. The Petri dishes were left to set and were parafilmed and store at 4°C (in the cold room) upside down for future use.

2.7.2 Bacteria transformation

Plasmid concentration and quality were determined using a NanoDrop ND-1000 spectrophotometer (NanoDrop Technologies, DE, USA). *E. coli* competent cells, LS2001 (Promega, WI, USA), were used for all the bacterial transformations. Close to an open Bunsen burner flame, 100µl of competent cells were transferred to a chilled sterile tube. Plasmid DNA was then added to the *E. coli*. For the positive control, 0.1ng of control DNA was used, and for the plasmids of interest 50ng was used. The competent cells with the DNA were placed on ice and incubated for 10 minutes. After this time, the bacteria were heat-shocked by placing the tubes in a water bath at exactly 42°C for 50 seconds. After the 50 seconds, bacteria were placed immediately back on ice and incubated for 2 minutes before the addition of 900µl of cold SOC medium (Sigma-Aldrich, MO, USA). The competent cells were then incubated for 1 hour at 37°C with shaking at 300rpm. After this incubation period, each transformation reaction was diluted with warm SOC medium before plating. For the positive control, bacteria were diluted 1:10, and for the plasmid of interest transformations bacteria were diluted 1:10 and 1:100. Finally, 100µl of the diluted

transformed bacteria was pipetted into an agar plate with ampicillin and the bacteria was spread using a glass spreader previously sterilised in 90% ethanol. Plates were incubated upside down in a bacterial incubator at 37°C for 12-14 hours. The next morning, plates were checked, parafilmed and stored at 4°C (cold room) upside down until future use.

2.7.3 Plasmid extraction

For the FcRLs antibody specificity checking (Chapter 4.4.5), the plasmids were extracted using the PureLink™ HiPure Plasmid DNA Purification Kit – MidiPrep (Invitrogen - Thermo Fisher Scientific, MA, USA) according to manufacturer's protocol. Briefly, transformed cells were grown overnight. Cells were pelleted, lysed and loaded into the kit's column. The column was washed and the plasmid was eluted. Then the eluate was precipitated with isopropanol and washed with ethanol. Finally, the pellet was air-dried and resuspended in RNase/DNase-free water (Sigma-Aldrich, MO, USA). The extracted plasmids were stored in the -20 °C freezer.

2.7.4 Concentration of plasmids

For downstream applications, such as transfecting cells, the generated plasmids were needed at a high concentration. Upon thawing of the plasmids, the microcentrifuge tube caps were cut and the tube was covered with parafilm (Bemis, WI, USA). Using a 25G BD Micolance™ needle (Becton Dickinson, NJ, USA), holes were placed in the parafilm to allow controlled evaporation. The microcentrifuge tube was centrifuged using the DNA 120 SpeedVac system (Thermo Fisher Scientific, MA, USA) until about 10-15µl volume remained. The plasmid concentration was then quantified using a NanoDrop ND-1000 spectrophotometer (NanoDrop Technologies, DE, USA) and was re-frozen at -20 °C until further use.

2.7.5 Restriction enzyme digestion

For the antibody specificity checking, the plasmids were digested to check that the insert length was the expected one. All the restriction enzymes used were purchased from Thermo Fisher Scientific, MA, USA. As described in Table 2.9, plasmids encoding for FcRL4 and FcRL3 were digested using the restriction enzymes EcoRV and NotI, plasmids encoding FcRL5 and FcRL2 were digested using BamHI and NotI, and the plasmid encoding FcRL1 was digested using EcoRI and NotI. Figure 2.4 shows a scheme of the restriction enzyme digestion protocol. Each plasmid was digested with both enzymes to check that the insert length was the expected one. However, a single digestion with only one of the enzymes

was also performed to linearize the plasmid and check for the total plasmid length. Plasmid concentration was determined using a NanoDrop ND-1000 spectrophotometer. In a microcentrifuge tube, for each digestion, 1µg of each plasmid was added, together with 1x O buffer and 20 units of enzyme (see Table 2.9 for enzyme compatibility with buffer). Because the plasmids concentration was low, and in order to not have to dilute the enzymatic reaction by adding big volumes of plasmids, all the volumes were scaled up to 80µl final volume. The tubes were topped up to 80µl final volume with RNase/DNase free water. The reactions were mixed gently and incubated at 37°C overnight. The next morning, the restriction enzymes were heat-inactivated at 65°C for 20 minutes. Finally, 5µl of the restriction enzyme digestion and 2µl of undigested plasmid were run in a 1% agarose gel with a DNA ladder, to check that the gene and the plasmid sizes were the correct ones (see section 2.8.2 for detailed protocol).

	FcLR1	FcLR2	FcLR3	FcLR4	FcLR5
5' enzyme	EcoRI	BamHI	EcoRV	EcoRV	BamHI
3' enzyme	NotI	NotI	NotI	NotI	NotI
Buffer used	O buffer	O buffer	O buffer	O buffer	O buffer
RE fold excess	Same amount of both	4-fold excess of BamHI	2-fold excess of EcoRV	2-fold excess of EcoRV	4-fold excess of BamHI
Whole plasmid size	6,790 bp	7,027 bp	7,525 bp	7,048 bp	8,434 bp
FcRL transcript size	1,290 bp	1,527 bp	2,205 bp	1,548 bp	2,934 bp

Table 2. 9. Restriction enzymes and buffers used to digest each of the FcRLs plasmids, and the expected size for each plasmid.

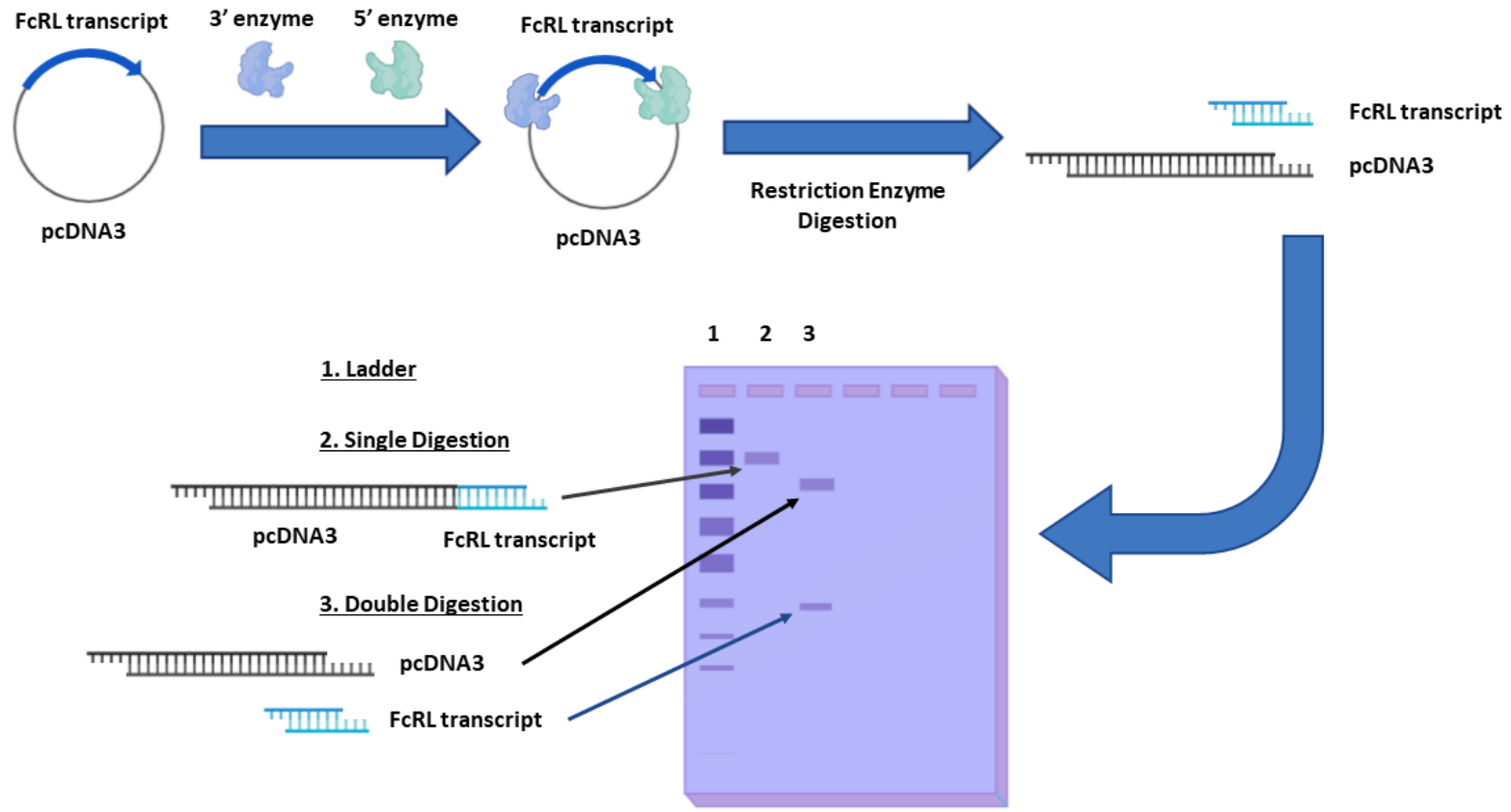

Figure 2. 4. Scheme of restriction enzyme digestion of the plasmids coding the FcRL family members. Each plasmid coding one FcRL family member was digested using the correspondent restriction enzymes for a 3' and a 5' digestion. After the incubation time, each restriction enzyme digestion was run in a 1% agarose gel with a DNA ladder (lane 1). For each plasmid, a single digestion, shown in lane 2, was performed to linearize the plasmid and check for the total plasmid length. Additionally, as shown in lane 3, a double digestion was performed, resulting in two bands in the gel: one corresponding to the plasmid backbone (pcDNA3) and the other corresponding to the size of the FcRL family member transcript examined. Created with Biorender.com.

2.7.6 HEK293T cells transfection

To check specificity of each FcRL antibody, HEK293T cells were transfected using a lipid-based approach. Lipofectamine ®LTX and Plus™ Reagent (Thermo Fisher Scientific, MA, USA) were used to transfect the cells with each FcRL family member plasmid.

Between 2-0.5 x 10^5 HEK293T cells were cultured into a 24-well plate (CoStar, DC, USA) in a final volume of 500µl of DMEM with 8% FCS. The cells were incubated at 37°C with 5% CO_2 overnight, so the next day they were 70-90% confluent. As for the manufacturer's protocol, when cells were confluent, 50µl of serum free medium and 4µl of lipofectamine were added to a microcentrifuge tube. In another tube, 250µl of a serum free medium was mixed with 5µl of plus reagent and 5µg of the plasmid. For the final mix, in a new microcentrifuge tube, 50µl of the mix containing lipofectamine was combined with 50µl of the mix containing the plasmid and the plus reagent. This mix was then incubated for 5 minutes at RT and a final volume of 50µl was added dropwise to the cells in the plate. Cells were incubated for one day at 37°C with 5% CO_2. The next day, cells were harvested by pipetting up and down to detach them, transferred into a universal flask and spun at 400g for 8 minutes. Cell were then resuspended in FACS buffer and transferred to a 96-well plate for antibody staining. To reduce background staining, the cells were blocked with 2% mouse serum for 15 minutes at 4°C. Cells were then washed and resuspended in the FcRL1 to FcRL5 antibody mixes (Tables 2.10 and 2.11) at the pre-titrated dilution in FACS buffer. Cells were incubated for 30 minutes at 4°C in the dark. After this time, cells were washed and resuspended in 100µl of PBS containing 1µl of Zombie UV to stain dead cells. Cells were incubated at 4°C for 15 minutes in the dark, then washed twice with FACS buffer, resuspended in a final volume of 300µl of FACS buffer and fixed in 1% formaldehyde before acquisition on a BD LSR Fortessa X20.

Surface marker	Fluorophore	Clone	Dilution factor	Company
FcRL3	BB515	H5	1:200	BD Biosciences, CA, USA
FcRL4	PE	413D12	1:100	Biolegend, CA, USA
FcRL5	APC	509f6	1:50	Biolegend, CA, USA

Table 2. 10 Fluorophore labelled antibodies used for the specificity check (FcRL3-5).

Surface marker	Fluorophore	Clone	Dilution factor	Company
FcRL2	PE	REA474	1:20	Miltenyi Biotech, Germany
FcRL1	APC	REA440	1:100	Miltenyi Biotech, Germany
FcRL2	PE	B24	1:100	Gift from Prof Nagata, Japan

Table 2. 11 Fluorophore labelled antibodies used for the specificity check (FcRL1-2).

2.8 FcRL3 cloning

The FcRL3 transcript from the pcDNA3 plasmid was cloned into the pIG plasmid in order to create retroviral particles and transduce the Ramos and Raji cell lines. See Figure 2.5 for an overview of the cloning steps.

2.8.1 Polymerase chain reaction (PCR)

Standard PCR was used to amplify the FcRL3 transcript in order to clone it into the retroviral pMSCV PIG plasmid (referred to as pIG). Primers were designed to amplify a product containing the start and stop codons of the FcRL3 transcript with the introduction of restriction enzyme digestion sites for two different restriction enzymes at the 5' and the 3' end of the product (Table 2.12). The restriction enzyme sites were identical to two sites within the pIG plasmid. From the pcDNA3 plasmid, 2ng were mixed with 2.5µl of 10µM of forward and reverse primers (Sigma-Aldrich, MO, USA), 1µl of 10mM of dNTPs and 10µl of 5x Phusion HF buffer (both from Invitrogen - Thermo Fisher Scientific, MA, USA). The volume of the reaction was then topped up with RNase/DNase free water to a final volume of 50µl. Finally, 0.5µl of 2 U/µl of Phusion Hot Start II DNA Polymerase (Invitrogen - Thermo Fisher Scientific, MA, USA) was added. The mixture was covered with a StarSeal adhesive lid (StarLab, Germany) and pulse spun to >800g before being placed in a PCRmax alpha thermal cycler (PCRmax, UK). The following cycle was performed after preheating the lid to 98 °C: an initial denaturation at 98 °C for 30 seconds and then 25 cycles of denaturation at 98 °C for 10 seconds and annealing and extension at 72 °C for 45 seconds, finally a final extension at 72 °C for 5 minutes. All the PCR product was loaded onto an agarose gel to check for the correct size and extract the amplified sequence (see section 2.8.2).

FcRL3 gene	
Forward	CTAGCTCGAGATGCTTCTGTGGCTG
Reverse	GATCGTTAACCTAGTGGTCTGAGGCCAGTA

Table 2. 12 FcRL3 forward and reverse primer sequences used to clone the FcRL3 transcript. The XhoI restriction enzyme site is highlighted in yellow in the forward primer. The HpaI restriction enzyme site is highlighted in green in the reverse primer Start codon is underlined in the forward primer and the stop codon is underlined in the reverse primer.

2.8.2 Gel electrophoresis and fragment purification

The PCR amplification product was run in an agarose gel in order to check the size of the amplicon and purify the fragment. A 1% weight/volume agarose gel was made by mixing 1g of agarose (Sigma-Aldrich, MO, USA) with 100ml of 1x TAE (made of 2M Tris base (Sigma-Aldrich, MO, USA), 0.5M EDTA (Thermo Fisher Scientific, MA, USA), 1M acetic acid (Fisher Scientific, NH, USA) and up to 1L with distilled water). The agarose mix was heated in the microwave until melted, when cool to touch 5µl of 10mg/ml ethidium bromide (Sigma-Aldrich, MO, USA) were added and the mix was poured in the gel tank and left until solid. For fragment purification steps downstream, all the PCR product, 50µl, was loaded onto the gel mixed with 8µl of 6x loading dye (Thermo Fisher Scientific, MA, USA). A 1Kb DNA ladder (Thermo Fisher Scientific, MA, USA) was used to assess the band sizes. The gel was run at 100 V for 1 hour and 30 minutes and visualised under the UV light using an Odyssey Fc Imaging System (Licor Biosciences, NE, USA).

Fragment purification was performed using the Wizard® SV Gel and PCR Clean-Up System (Promega, WI, USA) as per manufacturer's instructions. The DNA fragment of interest was cut from the gel, dissolved in a ratio of 10µl of Membrane Binding Solution from the kit per 10mg of agarose gel slice, and incubated at 60°C until the gel slice was completely dissolved. The solution was loaded on the SV Minicolumn provided in the kit and spun at 16,000g. Then the column was washed twice with Membrane Wash Solution previously diluted with 95% ethanol (Thermo Fisher Scientific, MA, USA). Finally, DNA was eluted in 50µl of RNase and DNase free water and quantified using a NanoDrop ND-1000 spectrophotometer.

2.8.3 Restriction enzyme digestion

For the cloning of the FcRL3 transcript into the pIG plasmid, both the FcRL3 transcript and the pIG plasmid were restriction enzyme digested in order to be able to ligate the FcRL3 transcript into the pIG plasmid. The two restriction enzymes used, XhoI and HpaI, were purchased from New England Biolabs, MA, USA. As for the other plasmids, a single digestion, to check the size of the whole plasmid (size of 9,874 bp) and a double digestion, to check the insert length was performed (plasmid backbone size was 7,649 bp and FcRL3 transcript size was 2,225 bp). For this restriction enzyme digestion, 500ng of plasmid was used, together with 10 units of each enzymes and 1x CutSmart buffer (New England Biolabs, MA, USA). The tubes were topped up to a final volume of 50µl with RNase/DNase free water. The reactions were mixed gently and incubated at 37°C for 1 hour. After this time, the restriction enzymes were heat-inactivated at 65°C for 20 minutes. The digestion products were all loaded onto a 1% agarose gel and purified as described in section 2.8.2.

2.8.4 DNA ligation

The products of the restriction enzyme digestion were ligated in order to introduce the FcRL3 transcript sequence into the pIG plasmid. The concentration of both digestion products was determined using a NanoDrop ND-1000 spectrophotometer. The New England Biolabs Ligation Calculator (NEBs, MA, USA) was used to calculate the mass of insert required to ligate 50ng of vector DNA. Two ratios of insert: vector were used, 2:1 and 5:1. A higher ratio of FcRL3 gene to plasmid increases the chances of FcRL3 being inserted in the plasmid.

In a microcentrifuge tube on ice, the calculated amount of plasmid and FcRL3 for the two ratios reaction was added, together with 1x T4 DNA ligase buffer (10x stock) and 400 Units of T4 DNA ligase (stock at 400,000 U/ml; both from New England Biolabs, MA, USA). The reaction was topped up to a final volume of 20µl with RNase/DNase free water. The contents were mixed by pipetting up and down and the tubes were incubated at RT for 2 hours. After this time, the T4 DNA ligase was heat-inactivated at 65°C for 10 minutes. The tubes were then chilled on ice, then frozen at -20°C and stored. The reaction product was thawed on ice and 2µl were used for bacterial transformation (see section 2.7.2).

2.8.5 Plasmid extraction

To check if the plasmid incorporated into the bacteria in the colonies that grew on the agar plate had the correct inserted FcRL3 transcript, a QIAprep® Spin Miniprep Kit (Qiagen, Germany) was used following manufacturer's instructions for the high-yield protocol. After checking all the colonies using restriction enzyme digestion analysis (see section 2.8.3), one colony was picked and a Maxiprep, using the PureYield^{TM} Plasmid Maxiprep System (Promega, WI, USA) following the manufacturer's protocol, was performed to obtain high amounts of the plasmid.

2.8.6 Plasmid sequencing

The two FcRL3 plasmids, FcRL3-pcDNA3 and the FcRL3-pIG, were sent for sequencing, to make sure that the FcRL3 transcript was the correct one and the sequence did not contain any mutations. Two labelled 1.5ml microcentrifuge tubes with plasmids were prepared: One for the forward sequencing, and the other for the reverse sequencing. 100 ng of plasmid in a final volume of 20µl of RNase/DNase free water were sent to GATC Services (Eurofins Scientific, Luxembourg) for sequencing in both directions. The primers were designed using Primer3Plus (Free Software Foundation, MA, USA) and their synthesis was ordered from GATC Services (Eurofins Scientific, Luxembourg). For primers details see Tables 2.13 and 2.14.

FcRL3-pcDNA3 plasmid		
FcRL3 Forward primers	1	CMV promoter primer
	2	TCTGAGATGTCAGGGGAAAGA
	3	CAGAGAGTCCCTGTGTCTAATGTG
	4	CCAGCACAGTCATGGAGTGA
	5	GTGAGTGTCAGGAGCCTTCC
FcRL3 Reverse primers	6	AATATGTGTCTCCCTGGGCTA
	7	AGCTGGACATCTGGCCTCT
	8	GGAATTCTCACGGTGACTCG
	9	TGAGTGTCACCACTTTACTGTGC
	10	GGCCAGTAATACACGTGGTACA

Table 2. 13. Forwards and reverse primer sequences used to sequence the FcRL3-pcDNA plasmid.

FcRL3-pIG plasmid		
FcRL3 - pIG Forward primers	pBABE 5’	CTTTATCCAGCCCTCAC
	2	TCTGAGATGTCAGGGGAAAGA
	3	CAGAGAGTCCCTGTGTCTAATGTG
	4	CCAGCACAGTCATGGAGTGA
	5	GTGAGTGTCAGGAGCCTTCC
FcRL3 - pIG Reverse primers	6	AATATGTGTCTCCCTGGGCTA
	7	AGCTGGACATCTGGCCTCT
	8	GGAATTCTCACGGTGACTCG
	9	TGAGTGTCACCACTTTACTGTGC
	MSCV rev	CAGCGGGGCTGCTAAAGCGCATGC

Table 2. 14 Forwards and reverse primer sequences used to sequence the FcRL3-pIG plasmid.

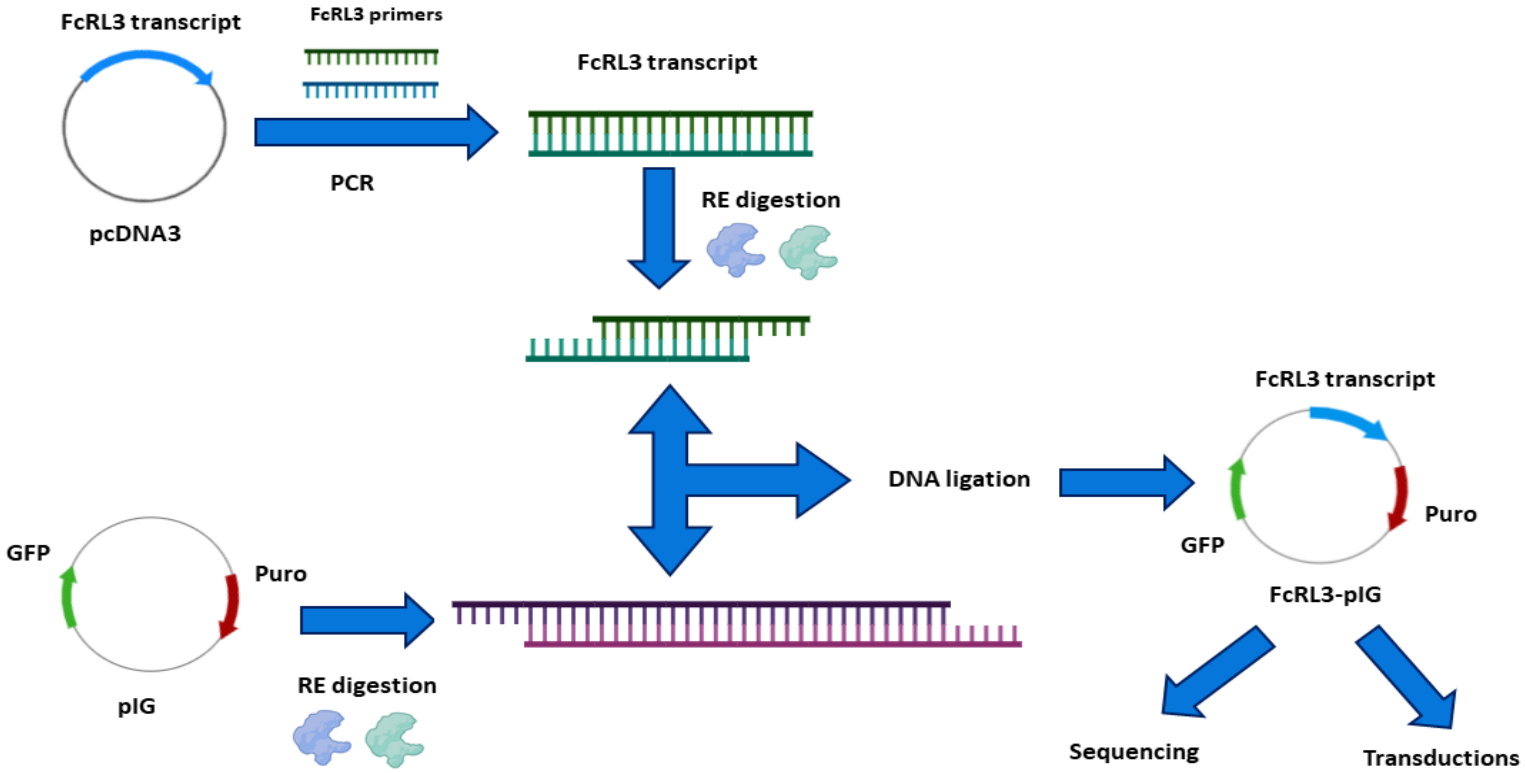

Figure 2. 5. Overview of protocol used to clone the FcRL3 transcript into the pIg plasmid. The FcRL3 transcript was amplified from the pcDNA3 plasmid by PCR. The primers contained the start and the stop codons, as well as two different restriction enzyme sites. These restriction enzymes were identical to two sites within the pIG plasmid. Both the PCR product containing FcRL3 transcripts and the pIG plasmid were restriction enzyme digested to create sticky ends. Finally, the two digestion products were ligated using a T4 DNA ligase, resulting in the FcRL3 transcript being incorporated in the pIG plasmid. The ligation product was checked by transforming bacteria and digesting the plasmid grown by selected colonies. A colony showing the right restriction enzyme digestion was picked and the plasmid was sent for sequencing to check that the transcript sequence was the same as the reference one. After validation of the sequence, the FcRL3-pIG plasmid was used to transduce a Ramos B cell line. Created with Biorender.com.

2.9 FcRL3 transfection/transduction of Ramos B cells

2.9.1 Ramos and Raji cells Neon® Kit Transfection

The Neon® Transfection System (Invitrogen - Thermo Fisher Scientific, MA, USA) was used for the transfection of Ramos and Raji B cells with the FcRL3-pcDNA3 plasmid using electroporation. Cells from each cell line were harvested and washed in PBS. Then, the cells were resuspended in Resuspension Buffer R to a final density of 2×10^7 cells/ml. Cells were resuspended up and down gently to ensure a single cell suspension and 9µl were transferred to a tube with 3µg of FcRL3-pcDNA3 plasmid, making up a final volume of 10µl. Then, using the Neon® Pipette with a 10µl Neon® Tip the cell-DNA suspension was slowly aspirated, carefully avoiding air bubbles. The Neon® Tip was then vertically inserted into the Neon® Tube which was previously filled with 3ml of Electrolytic Buffer (Buffer E). Next, the desired pulse conditions were set; the pulse conditions used were tested and optimised for Ramos and Raji cells by Invitrogen and were as following: a pulse voltage of 1,350V, a pulse width of 30ms and a pulse number of 1. After the electroporation, the Neon® Tip was slowly removed from the Neon® Pipette Station and cells were immediately transferred to a previously prepared 24-well plate containing 0.5ml of pre-warmed RF10 (RPMI +10% FCS). Cells were incubated for three days at 37°C with 5% CO_2 in RF10 without any antibiotics. After the three days, the selection antibiotic G418 (Geneticin, Thermo Fisher Scientific, MA, USA) was added at a final concentration of 600µg/ml. The cells which were successfully transfected would be resistant to G418 as the FcRL3-pcDNA3 plasmid contained a neomycin resistance gene. Transfection efficiency was assessed by expression of FcRL3 using flow cytometry.

2.9.2 HEK293T cells retroviral transfection

Lipofectamine ®LTX and Plus™ Reagent was also tested for its ability to transfect HEK293T cells with the plasmids to assemble the FcRL3 retroviral particles needed to transduce the B cell lines. See Figure 2.6 for an overview of the protocol.

To create the retroviral particles, three plasmids were used. Two of the plasmids, VSVG and pCGP create the viral particles: VSVG codes for the vesicular stomatitis virus G-protein making the envelope, and the pCGP plasmid codes for the Gag protein, a major component of the virus capsid and the Pol protein, responsible for synthesis of viral DNA and integration into the host genome. The third plasmid used is the pIG transfer plasmid (Puromycin IRES GFP plasmid), this plasmid is packed into the retroviral particles and

once in the transduced cells the puromycin resistance gene confers puromycin resistance and the IRES (Internal Ribosome Entry Site) induces GFP production and in the case of the FcRL3-pIG plasmid of GFP and FcRL3, as two separate protein products.

2.5 x 10^6 HEK293T cells were cultured in a 6-well plate (CoStar, DC, USA) in a final volume of 10ml of DMEM with 8% FCS. The cells were incubated at 37°C with 5% CO_2 overnight, so the next day they were 70-90% confluent. As for the manufacturer's protocol, when cells were confluent, 150µl of the mix containing serum free medium and 15µl of lipofectamine was combined with 150µl of a mix containing serum free medium, 14µl of plus reagent and 14µg of the FcRL3-pIG transfer plasmid, the pCGP packaging plasmid and the VSVG envelope plasmid. As a control, the empty pIG transfer plasmid was added together with the packaging and the envelope plasmids to generate control viral particles that will do not contain the FcRL3 transcript and will only express GFP. The final mixes were incubated for 5 minutes at RT and a final volume of 250µl was added dropwise to the cells in the plate. Cells were incubated for two days at 37°C with 5% CO_2. After two days, cells were harvested by pipetting up and down to detach them, transferred into a universal tube and spun at 400g for 10 minutes. Supernatants were collected and used on the same day to transfect the Ramos and Raji cell lines.

2.9.3 Ramos and Raji cells retroviral transduction

Cells from each cell line were harvested and count Burker counting chamber with Trypan Blue. 0.5 x 10^6 cells from each cell line, were cultured in a 12-well plate (CoStar, DC, USA) in a final volume of 1ml of RPMI 1640 with 10% FCS. Mastermixes containing 8µg/ml of polybrene and various volumes (250µl, 500µl, 750µl and 1000µl) of either only RF10, or 48-hour HEK293T cell culture supernatants from cells transfected either with the control retroviral particles or the FcRL3 retroviral particles, were added to the cell lines. Cells were then centrifuged at 600g for 2 hours at RT in order to force the retroviral particles towards the cells at the bottom of the plate. Cells were then incubated for 72 hours at 37°C with 5% CO_2. After 3 days, cells were harvested and centrifuged at 400g for 8 minutes. Cells transduced with either the control retroviral particles or the FcRL3 retroviral particles, were resuspended in pre-warmed RPMI 1640 containing 10% FCS and supplemented with 1µg/ml puromycin. Cells were split and plated at a cell density of 0.5 x 10^6 cells/well of a 12-well plate. A control well with wild-type cells from each cell line was cultured in RPMI 1640 containing 10% FCS without puromycin. The cells which were

successfully transduced would be resistant to puromycin as the pIG plasmid contained a puromycin resistance gene. Cells were incubated for an additional 72 hours. After these three days, cells were harvested, layered under 10ml of Lymphoprep and centrifuged at 700g for 10 minutes at RT (acceleration 9, deceleration 0). Live cells deposited at the interface were harvested and the cells were washed twice in RPMI 1640 with 10% FCS to remove any contaminating Lymphoprep. The first wash centrifugation spin was at 600g for 8 minutes and the second at 400g for 8 minutes. Cells were then resuspended in 5ml of RPMI 1640 with 10% FCS and 1μg/ml of puromycin and transferred to a T25 culture flask (Greiner Bio-one, Austria). Once confluent, cells were transferred to a T75 culture flask and were kept in culture in the presence of puromycin to select the transduced cells. Transduction efficiency was assessed by expression of FcRL3 and GFP using flow cytometry.

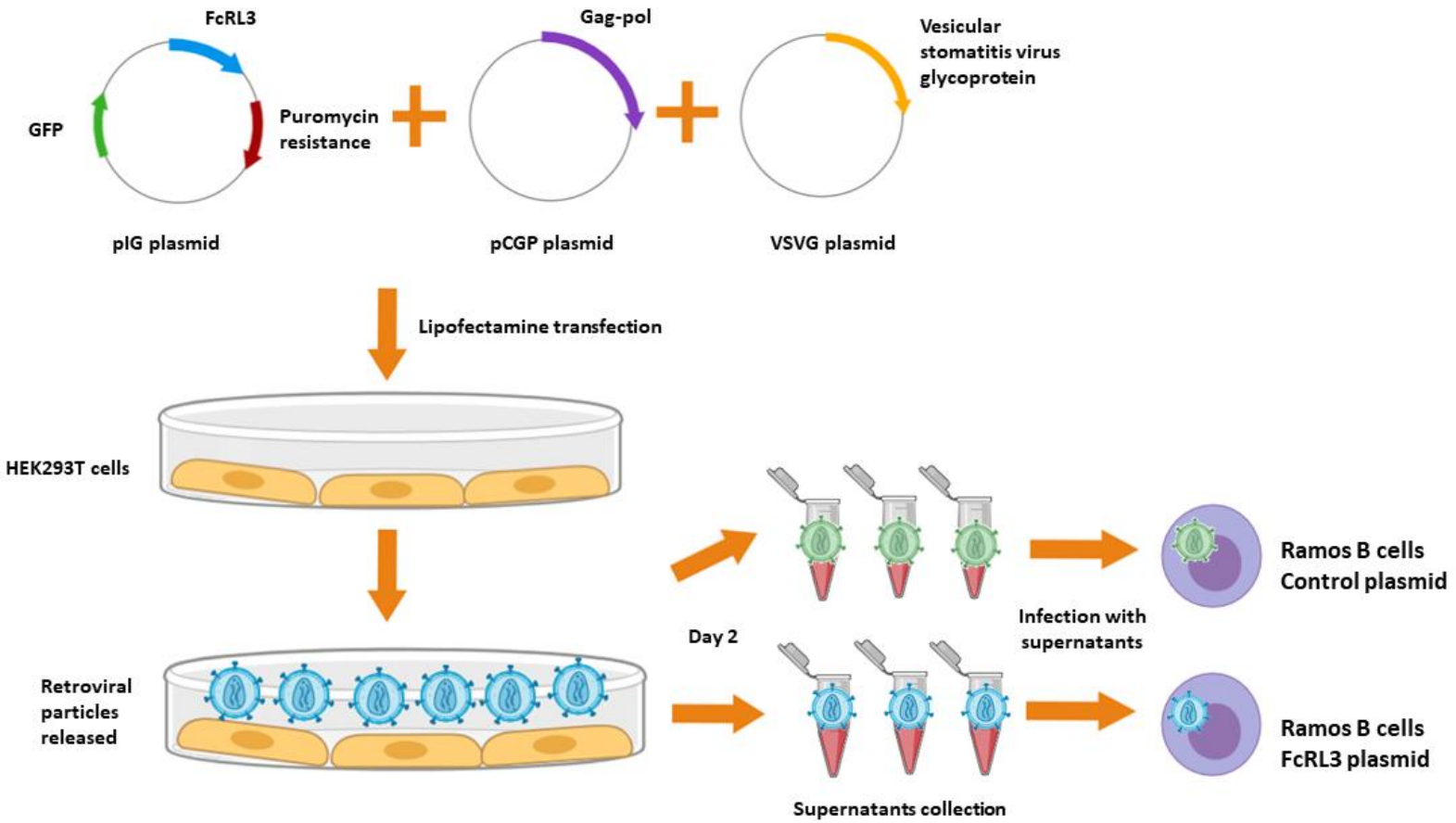

Figure 2. 6. Overview of protocol used to transduce Ramos cells using a retroviral approach. HEK293T cell were transfected using lipofectamine with the three plasmids needed to create the retroviral particles. After two days, supernatants containing the virus particles were collected. Ramos cell lines were then incubated with the HEK293T supernatants containing the viruses. Selection of the infected cells was achieved by the addition of puromycin three days post-transfection. Created with Biorender.com.

Due to the presence of a heterogeneous mixed population in the FcRL3 Ramos transduced cells, expressing either GFP alone or both GFP and FcRL3, flow cytometry cell sorting was used to purify the double positive population (GFP+FcRL3+). 30 x 10^6 cells were stained for FcRL3-PE (Biolegend, CA, USA) and the lineage marker CD19-BV421 (Biolegend, CA, USA). Cells were stained with 2µl of Zombie UV in 100µl of PBS for exclusion of dead cells. Cells were transferred to a FACS tube and the volume was made up to 2ml with FACS buffer, resulting in a cell density of 10 x 10^6 cells/ml.

Immediately before sorting, the cells were transferred into a new FACS tube and strained through a 50µm cell strained (CellTrics - Sysmex, IL, USA). The BD FACSARIA II with a 100µm nozzle was used to sort three cell subsets: GFP bright cells (GFP high FcRL3-), GFP intermediate cells (GFP+ FcRL3-) and double positive cells (GFP+ FcRL3+). Around 0.8 x 10^6 cells per subset were sorted into 350µl of RLT Plus Lysis Buffer from Qiagen RNeasy Plus Micro Kit, to which β-mercaptoethanol had been added at ratio 1:100. Cells were sorted into RLT as FcRL3 expression was also checked at the mRNA level (see sections 2.9.4-6). The lysate was then added to a QIAshredder column (Qiagen, Germany) and spun at full speed (1,700g) for 2 minutes. The eluate was then frozen at -80 °C prior to RNA extraction. The rest of the cells, about 1 x 10^6 cells, were sorted into RF20 (RPMI 1640 medium containing 20% (v/v) Foetal Calf Serum and supplemented with 2 mM L-glutamine, 100 U/ml penicillin and 100 µg/ml streptomycin) for cell culture. The sorting gating strategy is shown in Chapter 7, Figure 7.5. After sorting, cells were spun at 400g for 8 minutes at RT and resuspended in 5ml of RPMI 1640 with 10% FCS and 1µg/ml of puromycin and transferred to a T25 culture flask.

Transduction efficiency was assessed throughout the process of expanding the transduced population, by GFP fluorescence using a fluorescent microscope (Invitrogen™ EVOS™ FL Digital Inverted Fluorescence Microscope - Life Technologies - Thermo Fisher Scientific, MA, USA), as well as by flow cytometry, acquiring the cells on a BD LSR Fortessa X20™. In addition to GFP detection, transduction was assessed by flow cytometry staining transduced cells with the FcRL3 antibody (FcRL3 – PE clone H5/FcRL3, from Biolegend CA, USA).

2.9.4 RNA extraction

Transduced Ramos cells were flow cytometry sorted straight into 350µl of RLT Plus Lysis Buffer containing β-mercaptoethanol at ratio 1:100. Sorting straight into RLT buffer

increases RNA recovery and integrity. The lysate was then added to a QIAshredder column and spun at full speed (1,700g) for 2 minutes. The eluate was then frozen at -80 °C prior to RNA extraction.

The Qiagen RNeasy Mini Kit (Qiagen, Germany) was used to extract the RNA following manufacturer's instructions apart from one modification. To ensure that any DNA contamination was removed, the optional DNase digestion steps were performed as described in the appendix D protocol in the Qiagen RNeasy Mini Kit Handbook. Extracted RNA was eluted in 30µl of RNase-free water (provided in the kit). The concentration of RNA in this final eluate was determined using the NanoDrop ND-1000 spectrophotometer and the RNA was frozen at -80 °C if not used immediately for downstream applications.

2.9.5 Reverse Transcription

Reverse transcription (cDNA synthesis) was performed in a 0.2ml PCR strip. Due to different amounts of extracted RNA, the same total amount of RNA, 160 ng, was reverse transcribed for each sample used in a volume of 10µl. Two negative controls were included, a water control where RNA was replaced with RNase/DNase-free water and a reverse transcriptase (RT) control where RT enzyme (SuperScript II, Thermo Fisher Scientific, MA, USA) was replaced with RNase/DNase-free water. To all wells 1µl of random hexamers (1 µg/µl, Integrated DNA Technologies, Inc, IA, USA) was added and the mixture was covered with a StarSeal adhesive lid (StarLab, Germany) and pulse spun to >800g. In a PCRmax alpha thermal cycler (PCRmax, UK) the strip was heated to 70 °C for 10 minutes and then chilled at 4 °C for an extra 10 minutes. A mastermix containing 0.01M DTT, 0.25mM dNTP, 1 unit SuperScript II and 2.2X First Strand Buffer (all Invitrogen - Thermo Fisher Scientific, MA, USA) was generated and 9µl of the mastermix were added in each well except the RT negative control, giving a final volume of 20 µl. For the RT negative controls, an additional mastermix was made up where the SuperScript II was replaced by RNase/DNase-free water. The strip was then heated for 1 hour at 42 °C in the PCRmax thermal cycler. The synthesised cDNA was diluted down to 1:2.5 and 1:100 with RNase/DNase-free water and stored at -20 °C until used for downstream applications.

2.9.6 Quantitative Polymerase chain reaction (q-PCR)

qPCR was used to check FcRL3 expression on the transfected cell lines. A mastermix containing 0.2µl of 10µM Universal ProbeLibrary probe (Roche, Switzerland), 0.4µl of 10mM forward and reverse primers (Sigma-Aldrich, MO, USA), 4µl RNase/DNase Free

water and 10µl 2X TaqMan® Gene Expression Mastermix (Life Technologies - Thermo Fisher Scientific, MA, USA) was prepared and 15µl were mixed with 5µl of 1:2.5 diluted cDNA in a MicroAmp Fast Optical PCR plate (Applied Biosystems - Thermo Fisher Scientific, MA, USA). Probe and primer sequences for FcRL3 are shown in Table 2.15. The expression of the housekeeper gene, 18S, was used to normalise the results. For the 18S expression, 5µl of a separate mastermix containing 0.1µl of 10µM 18S Probe (Sigma-Aldrich, MO, USA), 0.1µl of 10mM forward and reverse primers (Sigma-Aldrich, MO, USA), and 4.7µl of 2X TaqMan® Gene Expression Mastermix were added to 5µl of 1:100 diluted cDNA. Probe and primer sequences for the 18S gene are shown in Table 2.15.

mRNA expression was quantified using a TaqMan 7900HT fast-real time PCR system (Life Technologies - Thermo Fisher Scientific, MA, USA) with the thermal cycler set to 50 °C for 2 minutes, 95 °C for 10 minutes and then 95 °C for 15 seconds and 60 °C for 1 minute repeated for 40 cycles.

FcRL3 gene	
Forward	CAGTCATGGAGTGAGTCTCAGG
Reverse	CTCACAGTGAAGCTCCAGCA
Roche Universal Probe Library	Number 64
18S housekeeping gene	
Forward	CGAATGGCTCATTAAATCAGTTATGG
Reverse	TATTAGCTCTAGAATTACCACAGTTATCC
Probe	FAM-TCCTTTGGTCGCTCGCTCCTCTCCC-TAMRA

Table 2. 15 FcRL3 and housekeeper 18S primer and probe information.

2.10 FcRL3 functional work

2.10.1 Apoptosis assay

Untransduced (wild type) and transduced Ramos cells (Ramos GFP control cells and Ramos FcRL3+ cells) were plated at a cell density of 1 x 10^6 cells per well in 24-well plate in a final volume of 1ml of RF10 with or without 1µg/ml of puromycin. A separate plate was used for each of the three time points: Day 1, Day 2 and Day 3. The LEAF™ Purified anti-human CD95 (Fas) antibody (clone EOS9.1; Biolegend, CA, USA) was used to induce apoptosis. Three different final concentrations of the antibody were used: 10ng/ml,

100ng/ml and 200ng/ml. Cells were cultured for different days at 37°C with 5% CO_2 prior to assessment by flow cytometry. After the different time points, cells were harvested from the culture plate and transferred to a previously labelled 1.5ml microcentrifuge tube. The tubes were then spun at 400g for 8 minutes at RT, supernatants were discarded and cells were resuspended and transferred to a 96-well v-bottom plate (CoStar, DC, USA) for flow cytometry staining. The plate was centrifuged at 400g for 3 minutes, blotted and resuspended in 100µl of PBS containing 1µl of Zombie UV to stain dead cells. Cells were incubated at 4°C for 15 minutes in the dark, then washed once with FACS buffer. Cells were then resuspended in 100µl of 1x Binding Buffer (10x stock containing 0.1 M HEPES (at pH 7.4), 1.4 M NaCl, 25 mM $CaCl_2$) containing 5µl of Annexin V – APC (Biolegend, CA, USA). Cells were incubated at room temperature for 15 minutes in the dark. After the incubation time, cells were washed with 100µl of 1x Binding Buffer and resuspended in a 150µl of 1x Binding Buffer and fixed in 1% formaldehyde through the addition of 50µl of 4% formaldehyde.

2.10.2 Cell Trace Violet staining

2 x 10^6 untransduced and (wild type) and transduced Ramos cells (Ramos GFP control cells and Ramos FcRL3+ cells) were resuspended in a final volume of 1ml of warmed PBS and stained with CellTrace™ Violet (CTV; ThermoFisher Scientific, MA, USA). CellTrace dyes are used for *in vivo* labelling of cells to trace multiple generations using dye dilution by flow cytometry. CellTrace dyes easily cross the plasma membrane and covalently bind to all free amines on the surface and inside cells. Due to their high stability and well-retained fluorescence, these dyes provide a consistent signal, even after several days in a cell culture environment. When a cell divides, the amount of dye in their membrane is divided by half, allowing for proliferation measurement by successive halving of the fluorescent dye intensity. As per manufacturer's instructions, a vial of CTV was reconstituted by adding 20µl of DMSO (included in the CTV Kit) to a final concentration of 5 mM, immediately prior to use. The recommended final concentration of CellTrace™ dye per 1 x 10^6 cells is of 5µM, therefore a 2x stock of 10µM in warm PBS was prepared by mixing 2µl of CTV and 1ml of warm PBS. Finally, the 2x stock solution was mixed with an equal volume of the cells giving a final concentration of 5µM CTV per 1 x 10^6 cells/ml. The mixture was gently mixed and incubated at 37°C for 30 minutes (in an incubator), protected from light. After the incubation time, at least 5x the staining volume of complete culture medium, RF10, was added and incubated at 37°C for 5 minutes to

quench any remaining dye. After 5 minutes, cells were spun at 400g for 8 minutes at RT. Supernatants were discarded, and cells were resuspended in 12ml of RPMI 1640 with 10% FCS with or without 1µg/ml of puromycin and transferred to a T75 culture flask. At the different time points, a 500µl aliquot of cells were transferred to a FACS tube topped to 2ml with FACS buffer and spun at 400g for 8 minutes. The supernatant was blotted and the cells were resuspended in a final volume of 200µl of FACS buffer and fixed in 1% formaldehyde before acquisition on a BD LSR Fortessa X20™.

2.10.3 Cell Stimulation

Untransduced (wild type) and transduced Ramos cells (Ramos GFP control cells and Ramos FcRL3+ cells) were plated at a cell density of 250,000 cells per well in 24-well plate in a final volume of 1ml of RF10 with or without 1µg/ml of puromycin, respectively. Cells were stimulated with two different cocktails: Stimulus 1 was a combination of the TLR7 ligand, Imiquimod (1µg/ml), TLR9 agonists ODN 2216 – CpG A and ODN 2006 – CpG B (both 1µg/ml), PWM (5µg/ml), anti-CD40 antibody (10µg/ml, clone HB14), human IL-21 (0.05µg/ml), human IL-4 (0.05µg/ml) and IFN-gamma (0.02µg/ml). Stimulus 2 was the same stimulation reagents as stimulus 1 but no IL-4 was added to the mastermix. Cells were cultured for 3 days at 37°C with 5% CO_2 prior to assessment by flow cytometry. For the staining protocols see section 2.4.3 for surface staining and 2.4.2 for intracellular staining. For information on the antibodies used see Tables 2.16-2.18. Supernatants were frozen at -80°C prior to further analysis by MSD assay.

Surface marker	Fluorophore	Clone	Dilution factor	Company
FcRL3	PE	H5/FcRL3	1:25	Biolegend CA, USA
CD19	BUV395	SJ25C1	1:100	BD Biosciences, CA, USA
HLA-DR	PerCP	L203	1:20	RnD Systems, MN, USA
FcRL4	APC	413D12	1:10	Biolegend CA, USA
CD69	APC-Vio770	FN-50	1:20	Miltenyi Biotech, Germany
CD40	BV421	5C3	1:20	Biolegend CA, USA
CD86	BV711	IT2.2	1:50	Biolegend CA, USA

Table 2. 16 Fluorophore labelled antibodies used for the activation panel.

Surface marker	Fluorophore	Clone	Dilution factor	Company
FcRL3	PE	H5/FcRL3	1:25	Biolegend CA, USA
CD19	BUV395	SJ25C1	1:100	BD Biosciences, CA, USA
IgM	PerCP-Cy5.5	MHM-88	1:20	Biolegend CA, USA
FcRL5	APC	509f6	1:50	Biolegend CA, USA
IgD	AF700	IA6-2	1:50	Biolegend CA, USA
CD11c	BV421	B-LY6	1:20	BD Biosciences, CA, USA
IgG	BV786	G18-145	1:50	BD Biosciences, CA, USA

Table 2. 17 Fluorophore labelled antibodies used for the immunoglobulin panel.

Surface marker	Fluorophore	Clone	Dilution factor	Company
FcRL3	PE	H5/FcRL3	1:25	Biolegend CA, USA
CD19	BUV395	SJ25C1	1:100	BD Biosciences, CA, USA
CD55	APC	JS11	1:25	Biolegend CA, USA
CD5	PE-Cy7	UCHT2	1:50	eBioscience, CA, USA
T-bet	BV421	O4-46	1:10	BD Biosciences, CA, USA
CD27	BV650	O323	1:10	Biolegend CA, USA
Ki67	BV711	Ki-67	1:10	Biolegend CA, USA
CD97	BV786	VIM3b	1:25	BD Biosciences, CA, USA

Table 2. 18. Fluorophore labelled antibodies used for the intracellular panel.

2.11 Statistical analysis

For the flow cytometric analyses percentage positive cells and MFI values were visualised as graphs using GraphPad Prism (version 8, GraphPad Software, CA, USA). Various statistical analyses were carried out on the data of three replicates or more. For statistical tests where a non-parametrical analysis was performed due to the non-normal distribution of the data, two tests were used: a Mann-Whitney U test to compare 2 groups and a Kruskal-Wallis test for 3 or more groups. For the Kruskal-Wallis test a subsequent Dunn's test was used to perform multiple comparisons and assess which comparisons are significantly different. For frequency data, like the percentage of females in each cohort, a non-

parametric test like the Fisher exact probability test was used to compare 2 groups and a Chi-squared test to compare more than 2 groups. To study linear correlations, like the correlation of ABC frequency with inflammation markers, a Pearson Correlation coefficient was calculated to assess if there is a correlation and if this correlation is positive or negative. These tests were performed using GraphPad Prism and significance was defined when $p<0.05$.

As mentioned above, for the NanoString transcriptomic analysis, R core (The R Foundation) was used together with the Bioconductor repository both to analyse and plot the data.

Some tests were performed using JMP Statistical Visualization Software (version 13, SAS Inc, NC). Functional work readouts from RA patients and healthy control B cell subsets were analysed using the JMP Software. Data was transformed to ranks permitting parametric tests, such as a Two-way ANOVA, comparing established RA patients and healthy controls, to be performed. Also using JMP Software, a regression analysis was performed to evaluate the influence of key patient variables on ABC frequency. These data was logit transformed to take into account that the lower bound is zero, as for some patients the frequency of ABCs is in the range of 0 (from 0.5 to 1) the logit transformation was used to change these values so a fitted Full Model assessing the contribution of each variable to variation in ABC frequency could be performed.

Chapter 3. Peripheral blood detection of ABCs in RA patients

3.1 Introduction

Different groups have recently identified a novel subset of B cells named age-associated B cells (ABCs), which are linked to aging and autoimmunity (Hao *et al.*, 2011; Rubtsov *et al.*, 2011). Studies to characterise this subset have been done in mice models, as well as in healthy individuals and autoimmune patients. Because of their increased frequencies in autoimmune patients, these cells have been hypothesised to potentially be involved in autoimmune pathogenesis due to their ability to produce antibodies, cytokines and present antigens.

In mice, Rubtsov *et al*., described these cells as CD11c and CD11b positive but CD21 negative and found them in increased frequencies in mice prone to autoimmune diseases like lupus-like disease and systemic autoimmunity (NZB/WF1 and Mer-/- mice) when compared to age-matched healthy mice (C57BL/6 mice) (Rubtsov *et al.*, 2011).

In autoimmune patients suffering from SLE and autoimmune cytopenia, a similar population of B cells has been identified as CD21-CD19high B cells (Warnatz *et al.*, 2002; Wehr *et al.*, 2004). However, unlike in mice, only a proportion of autoimmune patients displayed high frequencies of CD21low B cells in peripheral blood. Rubtsov *et al.*, also investigated human ABCs, defined as CD21-CD11c+CD19high B cells, in the peripheral blood of RA, SSc and SLE patients and found high frequencies of this subset in a proportion of patients with RA and SSc (Rubtsov *et al.*, 2011). The expanded ABC population was observed at a higher frequency in women suffering from RA compared to younger women and men of any age. Other studies also compared healthy, age- and sex- matched controls with patients with RA and found that the patients had higher frequencies than the controls (Shimabukuro-Vornhagen *et al.*, 2017). The CD21low population has also been studied in synovial fluid of patients with active RA, where it has been demonstrated that the CD21low B cell subset is a major B cell subset (Illges *et al.*, 2000; Thorarinsdottir *et al.*, 2019).

CD21low B cells have been described in different diseases ranging from infections to autoimmunity (Charles *et al.*, 2011; Thorarinsdottir *et al.*, 2015). The common feature in all of these diseases is chronic immune stimulation. However, none of the published papers have correlated ABCs frequency with clinical parameters as markers of inflammation and disease activity scores.

Therefore, I assessed the frequency of ABCs in peripheral blood and synovial fluid in early and established RA patient cohorts compared to other disease controls as well as age-matched healthy controls.

3.2 Chapter hypothesis and aims

In this chapter, I hypothesised that ABCs are found in increased frequencies in patients with RA and they correlate with inflammation markers and disease activity.

Therefore, the aims of this chapter were to:

1. Assess the frequency of ABCs in peripheral blood and synovial fluid in early and established RA patient cohorts compared to other disease controls and age-matched healthy controls.
2. Correlate the frequency of these cells with the patients' clinical parameters.

The specific objectives were:

1. Determine the best staining protocol to assess ABC frequency by flow cytometry.
2. Compare ABC frequency in peripheral blood in different inflammatory arthritides as well as healthy controls.
3. Correlate the frequency of these cells with different clinical parameters such as disease activity and inflammation markers.
4. Assess the frequency of ABCs in synovial fluid of patients with inflammatory arthritides.

3.3 Methods

3.3.1 Flow cytometry gating strategy used to determine the frequency of ABCs

ABC frequency in blood of patients and healthy controls was determined by flow cytometry. See methods chapter 2 for staining protocols from whole blood and from previously isolated PBMCs (sections 2.5.1 and 2.5.3 respectively). The flow cytometry data were analysed using the software FlowJo Version 10 (Treestar Inc, OR, USA).

Figure 3.1 shows an example of the gating strategy used to determine the percentage of ABCs from the total B cell population from an RA patient. First, doublets and autofluorescent cells were excluded. Lymphocytes were gated using SSC-A vs FSC-A, and from the lymphocyte gate, the B cells were gated. A dump channel was used to exclude other cell types, CD3 for T cells, CD16 and CD14 for all monocytes, CD56 for NK cells and most importantly CD33 for dendritic cells. Exclusion of dendritic cells is very important as these cells are positive for CD11c and could contaminate our ABC population. From the B cell gate, ABCs were identified as CD11c+CD21- and, from the non-ABC B cells, CD5+ cells were gated as CD5+CD19+. From the CD5- fraction, naïve B cells (IgD+CD27-) and memory B cells (IgD-CD27+) were identified.

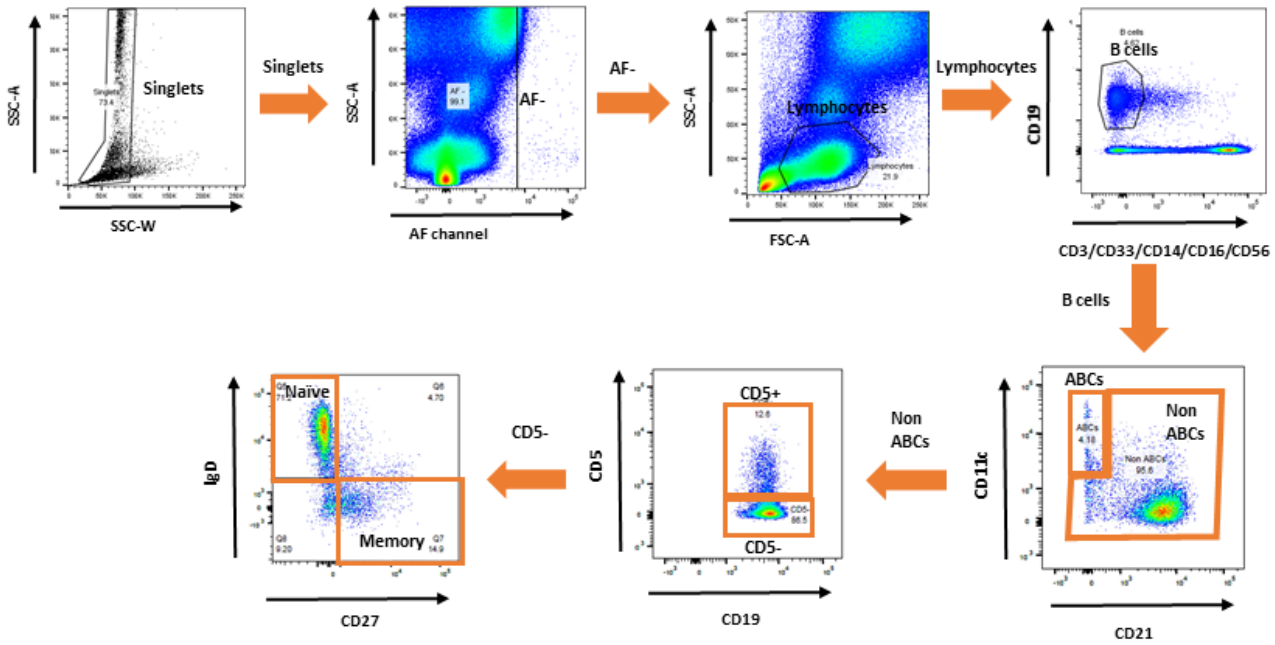

Figure 3. 1. Gating strategy for each B cell subset. Example of the gating strategy used to create each of the B cell subsets of interest from whole blood from an RA patient. Singlet cells are gated first using SSC-A against SSC-W, then autofluorescent cells are excluded. From the AF- gate, the lymphocyte gate is created on a SSC-A against FSC-A. Then B cells are gated excluding NK cells, T cell, monocytes and most importantly dendritic cells with a dump channel. From the B cell gate, ABCs were identified as CD11c+CD21- and from the non-ABCs, CD5+ B cells were identified as CD5+CD19+. From the CD5- populations, naïve cells are identified as IgD+CD27- and memory B cells as IgD-CD27+.

3.4 Results

3.4.1 Detection of ABCs using different staining techniques and centrifugation medium

Using flow cytometry, ABCs were identified as CD19+CD11c+CD21- in the peripheral blood of patients and healthy controls (Figure 3.1), as previously described by other groups (Rubtsov *et al.*, 2011).

I have demonstrated that ABCs are detectable in peripheral blood using flow cytometry. However, as I planned to isolate ABCs for downstream analysis, I needed to determine whether ABCs were detectable after PBMCs isolation using a density centrifugation medium. ABCs have previously been described as slightly larger than other B cell subsets (Rubtsov *et al.*, 2011). Due to their larger size, it is possible that I might lose some ABCs when isolating PBMCs with a density centrifugation medium, such as Lymphoprep. This technique uses the cell density to isolate mononuclear cells from red blood cells and granulocytes, which are denser and pass through the Lymphoprep solution and sediment during centrifugation. If ABCs are bigger and denser than other B cells it would be possible that they also sediment and therefore are lost from the isolated PBMC fraction.

To test this, an ABCs detection panel was used to stain cells isolated using different density centrifugation medium. From the same sample, an aliquot of whole blood was stained with an antibody panel to detect ABCs, and the remaining blood was used to isolate mononuclear cells with different density centrifugation medium and stained with the same panel of antibodies. ABCs frequency, as a percentage of total CD19+ B cells was used to determine if there was any cell loss during cell isolation.

There were no significant differences between the frequency of ABCs detected from stained whole blood and different centrifugation media (Figure 3.2.A). When comparing whole blood and Lymphoprep in matched donors, no differences were seen in the percentage of ABCs detected (Figure 3.2.B). I therefore used whole blood flow cytometry to detect and phenotype the different B cell populations as this involves minimal manipulation of the cells. When isolating cells for downstream work, the centrifugation media chosen was Lymphoprep.

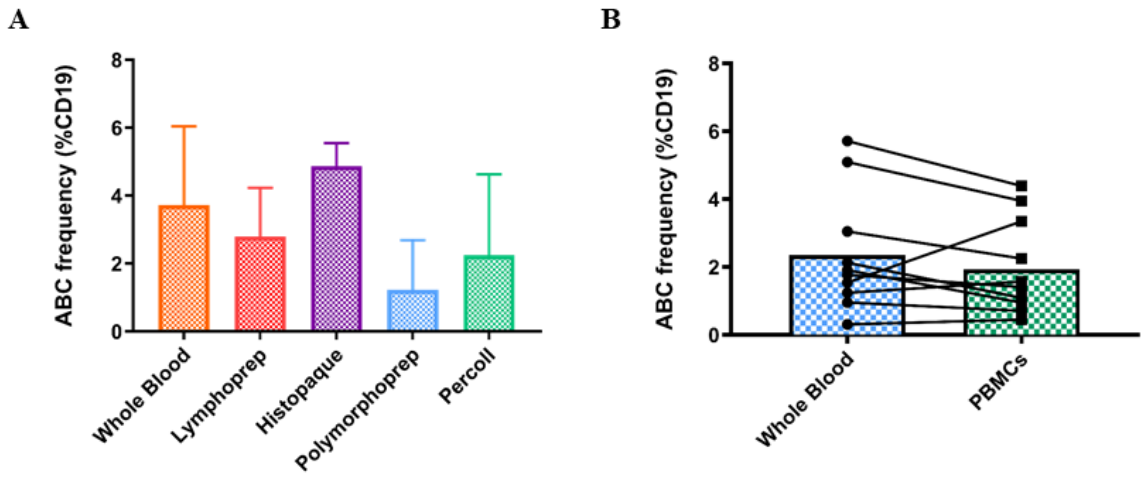

Figure 3. 2. Determination of ABCs frequency using different staining protocols. A. ABCs were detected by flow cytometry from whole blood staining and from different centrifugation media protocols used to isolate PBMCs. The frequency of ABCs is shown as a percentage of total CD19+ B cells. N numbers vary between each method: whole blood n = 4, Lymphoprep n = 3, Histopaque n = 2, Polymorphoprep n = 2 and Percoll n = 2. **B.** ABCs were detected in the same donor by flow cytometry from whole blood staining (n = 11) and from Lymphoprep isolated peripheral blood mononuclear cells (n = 11). The frequency of ABCs is shown as a percentage of total CD19+ B cells. Samples are from HCs (n = 3) and RA patients (n = 8).

3.4.2 ABCs frequency and cohorts' demographical data

Using the ABCs gating strategy described in Figure 3.1, percentages of ABCs in peripheral blood were determined. The percentage of ABCs found in blood was measured in four different cohorts: early drug naïve RA (eRA), established RA (estRA), early drug naïve other inflammatory arthitides (disease controls, DC) and age-matched healthy controls (HC).

There were 50 patients in the early RA cohort. The demographical and clinical data are shown in Table 3.1. All patients met the 2010 ACR/EULAR RA classification criteria. For the early disease control cohort with the other inflammatory arthritides, 39 patients were recruited. The comparison between the different disease groups is shown in Table 3.2. There were statistically significant differences between the groups in terms of sex. Analysis of the participants' age in each group revealed significant differences between the cohorts. There were differences in disease activity between the early and the established RA cohorts. Regarding seropositive status the differences between the groups were also significant.

The percentage of ABCs present in peripheral blood in the different cohorts was assessed by flow cytometry. There were no significant differences between early RA patients when compared to other cohorts (Figure 3.3). However, established RA patients had significantly higher percentages of ABCs in peripheral blood than ACPA+ patients and the Undifferentiated Inflammatory Arthritis (UIA) patients.

Early RA patients	Number = 50
Age (years; median and range)	68 (21 - 89)
Number of females (percentage)	34 (68%)
DAS28 (median and range)	4.47 (1.33 – 8.53)
CRP (mg/ml; median and range)	9 (4 - 127)
ESR (mm/hr; median and range)	28 (2 - 116)
Tender joint count (median and range)	3 (0 - 25)
Swollen joint count (median and range)	4 (0 – 21)
Patient VAS (median and range)	50 (2 – 100)
Anti-CCP positive (n and percentage)	30 (60%)
Rheumatoid factor positive (n and percentage)	31 (62%)
Seropositive – anti-CCP+ or RF+ (n and percentage)	34 (68%)
Smoker (n and percentage)	29 (58%)

Table 3. 1. Demographic characteristics of the early RA cohort. Demographical data for the drug naïve RA patients' cohort used to determine the frequency of ABCs in peripheral blood. All patients were diagnosed with rheumatoid arthritis following the 2010 ACR/EULAR classification criteria. All these patients were naïve to disease modifying anti-rheumatic drugs (DMARDs) at the time that blood was taken. CRP = C - reactive protein, ESR = erythrocyte sedimentation rate, anti- CCP = anti-cyclic citrullinated peptide antibody, RF = rheumatoid factor.

	Early RA patients	Established RA patients	PsA patients	ACPA+ arthralgia patients	Undifferentiated Arthritis patients	Healthy controls	Difference between groups
Number	50	12	17	3	7	13	-
Age (years; median and range)	68 (21 - 89)	62.5 (31 - 84)	47.8 (22-79)	60.5 (52-75)	53.8 (37-76)	61 (50 - 73)	0.0198[#]
Number of females (percentage)	34 (68%)	9 (75%)	8 (47%)	1 (33%)	3 (43%)	8 (61.5%)	0.04[+]
DAS28 (median and range)	4.47 (1.33 – 8.53)	1.38 (0.68 – 3.74)	-	-	-	-	0.0001[ǂ]
Seropositive – anti-CCP+ or RF+ (n and percentage)	34 (68%)	11 (92%)	3 (18%)	3 (100%)	2 (29%)	-	<0.0001[+]

Table 3. 2. Demographic characteristics for all the cohorts. Demographical data for the disease cohorts: early RA patients, n=50; established RA patients, n=12; Psoriatic Arthritis patients, n=17; ACPA+ arthralgia patients, n=3; Undifferentiated Arthritis patients, n=7 and the healthy control cohort (n=13) used to determine the frequency of ABCs in blood. # Kruskal-Wallis test with Dunn's multiple comparisons. + Chi-square test. ǂ Mann-Whitney test.

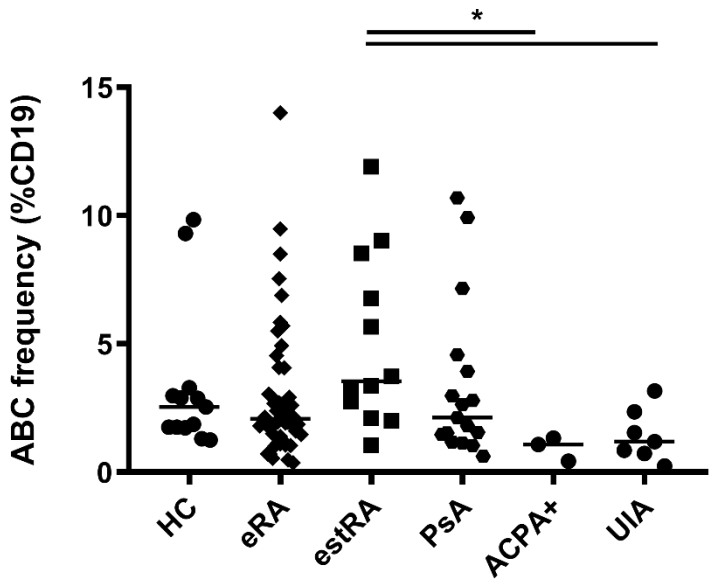

Figure 3. 3. Detection of ABCs in different disease groups and age-matched healthy controls. ABCs frequency in healthy controls older than 50 years old (HC, n=13), early RA patients (eRA, n=50), established RA patients (estRA, n=12), Psoriatic Arthritis patients (PsA, n=17), ACPA+ patients (ACPA+, n=3) and Undifferentiated Inflammatory Arthritis patients (UIA, n=7). ABCs were detected by flow cytometry using whole blood. The frequency of ABC is shown as a percentage of total CD19+ B cells. The median value is represented by the horizontal line for each group. Statistical significance was assessed using a Kruskal-Wallis test with Dunn's multiple comparisons of each group against the others. * $p < 0.05$. Kruskal-Wallis test $p = 0.0092$.

3.4.3 ABCs frequency and patients' serostatus in RA patients

Due to the implication of B cells in autoantibody production in autoimmune diseases, all early RA patients (n=50) and established RA patients (n=12) were then separated by serostatus as defined by their RF and anti-CCP titres, which were positive or negative as determined by the clinical labs' standards. Patients were further split into double negative (anti-CCP-, RF-), and positive, including both single positive for either autoantiboy (anti-CCP+, RF- and anti-CCP-, RF+) as well as double positive (anti-CCP+, RF+). There were no significant differences in the frequency of ABCs found in blood and the serostatus of the patients (Figure 3.4).

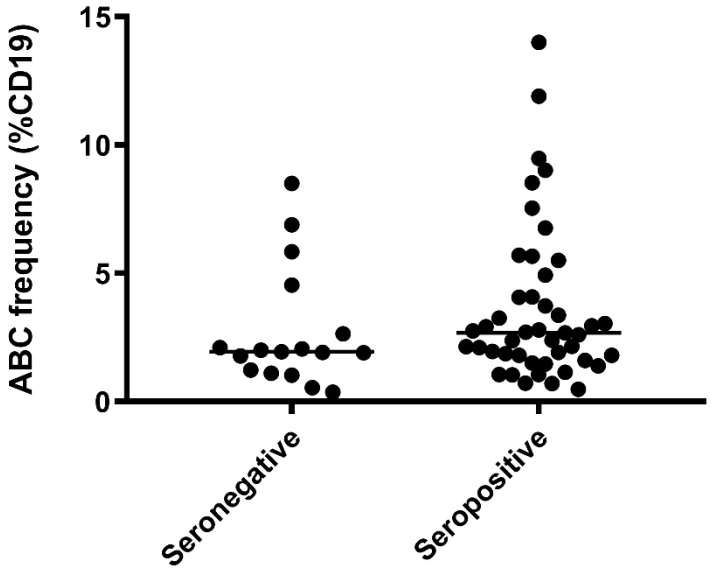

Figure 3. 4. ABCs frequency in early RA patients separated by their serostatus. Early RA patients were divided in seronegative (double negative, anti-CCP-, RF-) where n=16 or in seropositive, including single positive (anti-CCP+, RF- and anti-CCP-, RF+) as well as double positive (anti-CCP+, RF+), where n=34. The median is represented by the horizontal line. Statistical significance was assessed using a Mann- Whitney U test.

3.4.4 ABCs frequency and correlation with age and sex in the RA cohort

Due to significant differences in age and sex between the cohorts, RA patients were separated by sex and age into four groups, females younger than 54 years, females older than 55 years, males younger than 54 years and males older than 55 years. An age range of over or below 55 was chosen based on other published work reporting higher frequencies in young females compared to young males (Shimabukuro-Vornhagen *et al.*, 2017), and because it was a cut-off that give enough number of patients in each group to compare. There were no significant differences in the percentage of ABCs found in peripheral blood in each of the groups (Figure 3.5).

Nevertheless, when RA patients were separated by sex, higher frequencies of ABCs were seen in females compared to male patients (Figure 3.6).

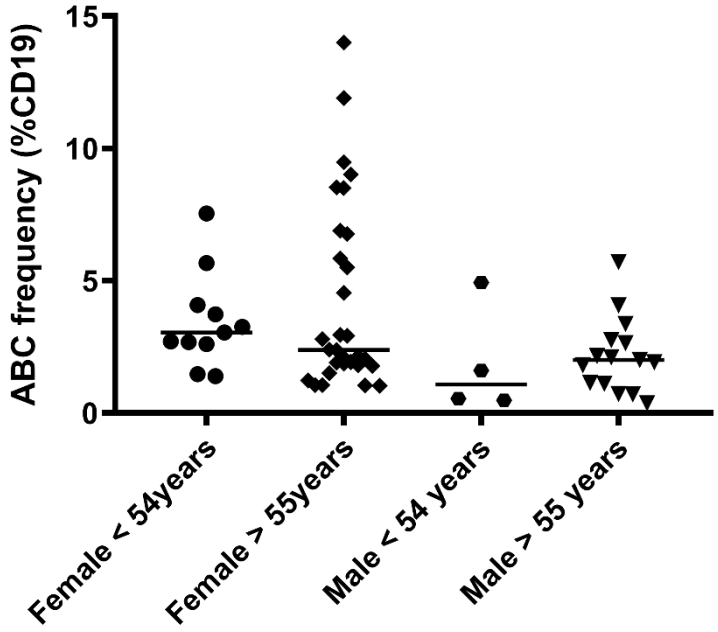

Figure 3. 5. ABCs frequency in RA patients separated by age and sex. Both early and established RA patients were separated according to their age and sex: females younger than 54 years old (n=11); females older than 55 years old (n=32); males younger than 54 years old (n=4); and males older than 55 years old (n=15). The median value is represented by the horizontal line for each group. Statistical significance was assessed using a Kruskal-Wallis test with Dunn's multiple comparisons. Kruskal-Wallis test p = 0.0860.

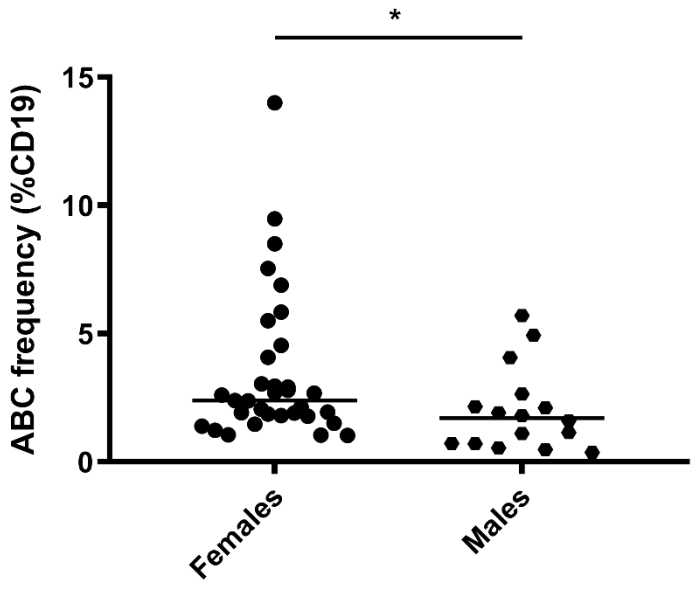

Figure 3. 6. ABCs frequency in RA patients separated by sex. Both early and established RA patients were separated according to their sex. Females (n=34) and males (n=16). The median value is represented by the horizontal line for each group. Statistical significance was assessed using a Mann- Whitney U test; * $p < 0.05$.

3.4.5 ABCs frequency and correlation with inflammatory markers in eRA patients

The correlation of inflammatory markers, erythrocyte sedimentation rate (ESR) and C - reactive protein (CRP), in early RA patients with ABCs frequencies was also assessed. ESR and CRP values were determined by the clinical labs according to their standards. Unfortunately, no significant correlation with ESR or CRP was seen (Figure 3.7-8).

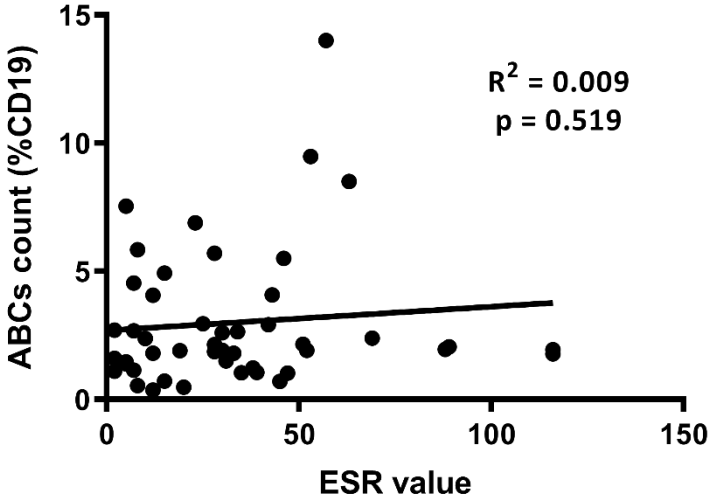

Figure 3. 7. Correlation of the frequency of ABCs with the ESR value. ABCs frequency in early RA patients were correlated with the patients' ESR value as determined by the clinical labs; n=47. Pearson R test was used.

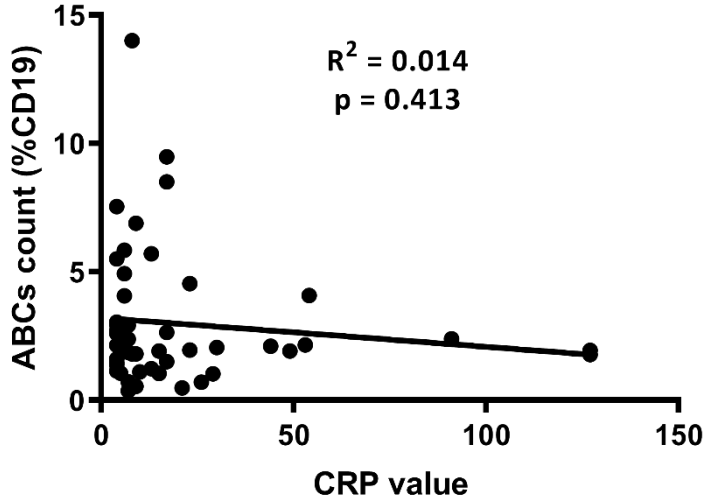

Figure 3. 8. Correlation of the frequency of ABCs with the CRP value. ABCs frequency in early RA patients were correlated with the patients' CRP value as determined by the clinical labs; n=49. Pearson R test was used.

3.4.6 ABCs frequency and correlation with disease activity in eRA patients

Early RA patients (n= 50) were then separated by disease activity at the time of the visit in three groups, patients with a low disease activity (DAS28 < 3.2), patients with moderate disease activity (DAS28 ≥ 3.2 but < 5.1) and patients with high disease activity (DAS28 ≥ 5.1). There were no significant differences between the ABCs frequencies in each of the disease activity groups (Figure 3.9). There were also no significant differences when patients' DAS28 score was correlated with the frequency of ABCs (Figure 3.10).

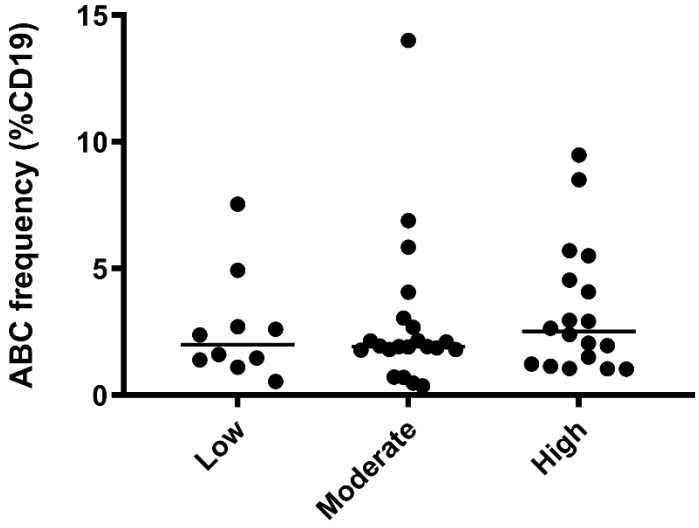

Figure 3. 9. ABCs frequency in early RA patients separated by the disease activity at the time of the visit. Early RA patients were separated by their disease activity depending on their DAS28 score in patients with a low disease activity (DAS28 < 3.2; n=10), and patients with moderate disease activity (DAS28 ≥ 3.2 but < 5.1; n=22) and patients with high disease activity (DAS28 ≥ 5.1; n=18). The horizontal lines represent the median value. Statistical significance was assessed using a Kruskal-Wallis test with Dunn's multiple comparisons. Kruskal-Wallis test p = 0.6211.

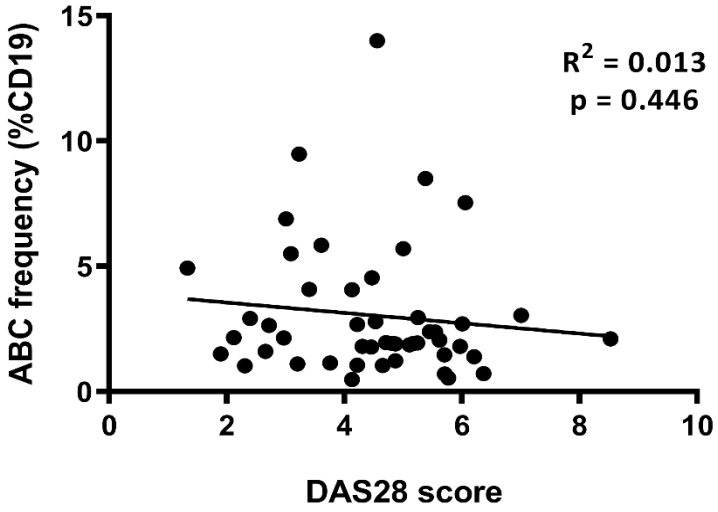

Figure 3. 10. Correlation of the number of ABCs with the disease activity score, DAS28. ABCs frequency in early RA patients were correlated with the patients' DAS28 score; n=47 using a Pearson R test.

3.4.7 Regression analysis

In order to integrate all the patient variables and assess which effect they have on the ABC frequency, a single regression analysis was performed using JMP Software. The variables analysed were age, sex, RF positivity, CCP positivity, CRP value, ESR value, DAS28 score, disease activity and smoking status. The data was logit transformed in order to take into account that the lower bound is zero. A fitted Full Model was run assessing the effect of each variable. As seen in Figure 3.11, the only significant effect was found on sex, which confirms the results found when the variables were analysed separately.

Effect Summary

Source	LogWorth	PValue
Sex	1.449	0.03558
DAS28	0.393	0.40486
Smoker	0.387	0.41053
RF status	0.253	0.55865
ESR	0.213	0.61272
Age	0.204	0.62483
CCP status	0.202	0.62740
Disease activity	0.150	0.70825
CRP	0.052	0.88630

Figure 3. 11. Summary of the effect of each variable in ABC frequency using a single regression analysis. The contribution of each variable in the frequency of ABCs was assessed using a fitted full model in JMP. The blue line is set at a p value of 0.01. After adjustment for differences in age, smoking status and other covariates, there is a significant difference in sex: ABCs were more prevalent in females ($p<0.05$).

3.4.8 ABCs frequency in synovial fluid from patients with inflammatory arthritides

Other groups (Amara *et al.*, 2017; Thorarinsdottir *et al.*, 2019) reported that ABC frequencies were much higher in synovial fluid than in peripheral blood. I, therefore, wanted to replicate this in my own inflammatory arthritis cohort. Synovial fluid mononuclear cells from inflammatory arthritis patients collected throughout three years were thawed and stained for the detection of ABCs. Patients were separated by disease diagnosis into early RA patients (n=3), established RA patients (n=6), Psoriatic Arthritis patients (n=3), Other Inflammatory Arthritis patients (n=5), Juvenile Idiopathic Arthritis patients (n=2), ACPA+ patients (n=1) and Reactive Arthritis patients (n=1). There were no significant differences in patients' demographics between all the disease groups regarding sex (Table 3.3). However, differences were seen in terms of age between the cohorts. Unfortunately, serostatus was not available for these patient samples. No differences were seen in age and sex when the patients were separated in early inflammatory arthritis and established inflammatory arthritis (Table 3.4).

The flow cytometry gating strategy used was the same as for the blood samples (Figure 3.1). There were no significant differences between the different inflammatory arthritides groups (Figure 3.12). However, when all the patients were separated into early drug naïve and established patients, there were higher frequencies of ABCs in the synovium of patients with established disease (Figure 3.13).

	Early RA patients	Established RA patients	Psoriatic Arthritis patients	Other Inflammatory Arthritis patients	Juvenile Idiopathic Arthritis patients	ACPA + Arthralgia patients	Reactive Arthritis patients	Difference between groups
Number	2	6	3	5	2	1	1	-
Age (years; median and range)	76 (72-81)	71.5 (58 - 86)	37 (24-53)	36.8 (20-54)	42.5 (34-51)	55	64	0.0171[#]
Percentage of females (n and percentage)	1 (50%)	3 (50%)	1 (33.3)	3 (60%)	2 (100%)	1 (100%)	1 (100%)	0.69[+]

Table 3. 3. Demographic characteristics for all the cohorts. Demographical data for the disease cohorts: early RA patients (n=3), established RA patients (n=6), Psoriatic Arthritis patients (n=3), Other Inflammatory Arthritis patients (n=5), Juvenile Idiopathic Arthritis patients (n=2), ACPA+ patients (n=1) and Reactive Arthritis patients (n=1) used to determine the frequency of ABCs in synovial fluid. # Kruskal-Wallis test with Dunn's multiple comparisons. + Chi-square test.

	Early Inflammatory Arthritis patients	Established Inflammatory Arthritis patients	Difference between groups
Number	6	10	-
Age (years; median and range)	46.2 (22-84)	60.6 (20-86)	0.3535#
Percentage of females (n and percentage)	2 (33.3%)	6 (60%)	0.6084+

Table 3. 4. Demographic characteristics for all the cohorts. Demographical data for the disease cohorts separated into early Inflammatory Arthritis patients (n=6), established Inflammatory Arthritis patients (n=10). # Mann-Whitney test. + Fisher's exact test.

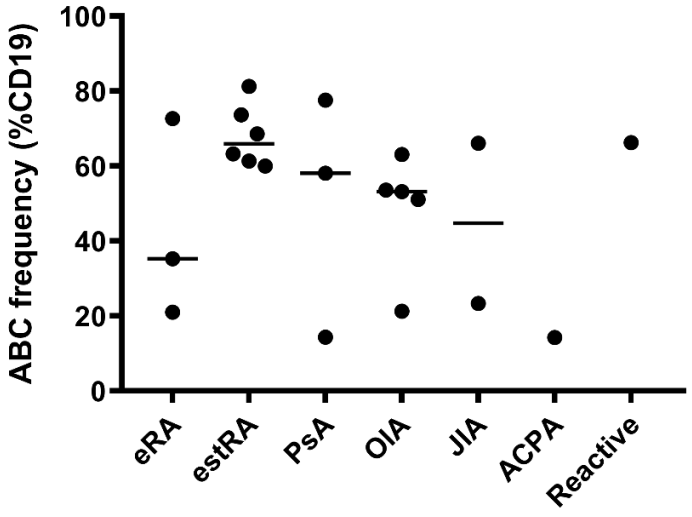

Figure 3. 12. ABCs detection in synovial fluid in different disease groups. ABCs frequency in early RA patients (eRA, n=3), established RA patients (estRA, n=6), Psoriatic Arthritis patients (PsA, n=3), Other Inflammatory Arthritis patients (OIA, n=5), Juvenile Idiopathic Arthritis patients (JIA, n=2), ACPA+ patients (ACPA+, n=1) and Reactive Arthritis patients (Reactive, n=1). ABCs were detected by flow cytometry from isolated synovial fluid mononuclear cells. The frequency of ABC is shown as a percentage of total CD19+ B cells. The median value is shown as a horizontal line for each group. Statistical significance was assessed using a Kruskal-Wallis test with Dunn's multiple comparisons of each group against the others. Kruskal-Wallis test p = 0.2358.

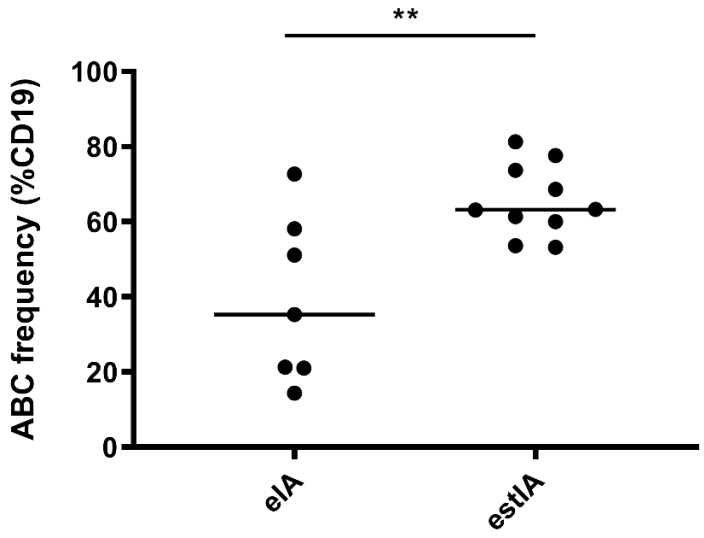

Figure 3. 13. ABCs detection in synovial fluid in patients with inflammatory arthritis separated into early and established disease. ABCs frequency in early Inflammatory Arthritis patients (n=7) and in established Inflammatory Arthritis patients (n=10). The median value is shown as a horizontal line for each group. Statistical significance was assessed using a Mann- Whitney U test; ** $p < 0.01$.

3.5 Discussion

In this chapter, I explored the frequency of ABCs in the peripheral blood of RA patients, disease controls and healthy controls. I found that the percentage of ABCs in early and established RA patients is not significantly higher than in age-matched healthy controls. However, I did see an increase in the percentage of ABCs in females with RA compared to males. The frequency of ABCs did not correlate with disease activity or with blood inflammatory markers. Importantly, high percentages of ABCs were found in the synovial fluid of patients with inflammatory arthritides, especially in those with established disease.

Previous studies found that these cells were slightly larger than follicular B cells. They were also reported to have high expression of granzymes and could have a granular appearance (Rubtsov *et al.*, 2011; Shimabukuro-Vornhagen *et al.*, 2017). For that reason, I first investigated if due to their bigger size and granularity these cells would pass through the density centrifugation medium, as happens with granulocytes, and therefore we would lose them from the PBMC preparation. Consequently, I determined the frequency of these cells comparing whole blood and PBMCs isolated with Lymphoprep and found no significant differences between the two isolation methods (Figure 3.2). I subsequently used whole blood for the phenotyping of these cells. This only requires a small amount of blood, which is advantageous as samples are shared between different researchers; reassuringly, however, my data suggested that I could use Lymphoprep isolated PBMCs to sort ABCs for transcriptome analysis and functional assays, which would reduce flow sorting time and costs. For PBMC isolation I also compared different density centrifugation media and found a similar frequency of ABCs between them, I decided to use Lymphoprep for downstream work as this is the standard density centrifugation medium used in the lab.

Multiple studies have shown increased frequencies of ABCs in patients with RA compared to healthy donors (Isnardi *et al.*, 2010; Shimabukuro-Vornhagen *et al.*, 2017; Wang *et al.*, 2018). However, I could not replicate these results (Figure 3.3). This could be due a few differences in the studies. None of the other groups used age-matched healthy controls, therefore if their healthy controls were younger, they could have lower percentages of ABCs in blood purely reflecting their age, and explaining the difference from RA patients. Finding healthy controls to match the patients was difficult as I had to match patients who were over the age of 75. This age group are hard to find and most volunteers of this age have comorbidities which could influence the data. Recently NIHR Newcastle Biomedical

Research Centre has established a "healthy ageing" bioresource, which provides a recallable population of elderly patients willing to provide blood samples for studies such as mine.

Furthermore, there is no consensus on how to gate ABCs in humans. Each group uses different markers; some groups describe them as CD21-/low B cells (Shimabukuro-Vornhagen *et al.*, 2017), others use CD19+ and CD11c+ B cells but do not look at CD21 expression (Wang *et al.*, 2018) and others use CD11c+ CD21- B cells (Rubtsov *et al.*, 2011). In this project, I defined the ABCs as CD11c+ and CD21- CD19+ B cells as described initially by Rubtsov *et al.*, in mice spleen (Rubtsov *et al.*, 2011) (Figure 3.1). Nonetheless, I could not replicate the results shown by Rubtsov *et al.*, with RA patients having significantly higher percentages of ABCs in the blood compared to healthy controls. Other studies found that CD11c+ double negative B cells (CD27- IgD-), which have a similar phenotype to ABCs, were increased in a cohort of patients with a predominance of African-American ethnicity (Jenks *et al.*, 2018). Although Rubtsov *et al.*, did not described the ethnicity of the population used in their study, differences in ethnicity could be the reason I was unable to replicate their data. Therefore, there could be differences in the accumulation of these cells in different ethnic groups.

A common feature seen in all studies is the variability in ABCs frequency. As shown in Figure 3.3, the percentage of ABCs is variable between individuals. Most of the patients have similar percentages of ABCs in blood, ranging from 0.5 to 3% but a small number of patients have higher than 5%, especially in early RA, established RA and PsA patients. Similar results can also be seen in the RA cohorts used by different groups (Isnardi *et al.*, 2010; Rubtsov *et al.*, 2011; Shimabukuro-Vornhagen *et al.*, 2017). In order to reduce "noise" due to inherent variability seen in human studies, more patients and healthy controls could be recruited. However, due to time limitations and the finite timing of the PhD that was not possible.

In terms of the association of ABC frequency with sex and age, these cells have been reported to be increased in the spleen of elderly female mice (Hao *et al.*, 2011; Rubtsov *et al.*, 2011). Rubtsov *et al.*, checked ABC frequencies in RA patients and found that these cells were increased in females and, furthermore, in females their frequency correlated with age. However, I could only detect an increase in the frequency of ABCs in females compared to males but no differences in age was found (Figure 3.5-6). Other groups also

reported sex and age differences in healthy controls; however, Shimabukuro-Vornhagen et al observed an increase frequency of CD21low CD86+ cells in young female (Shimabukuro-Vornhagen *et al.*, 2017). All these differences could be explained by the use of different markers in each study used to define ABCs or, as explained before, due to discrepancies in ethnicity.

Since ABCs are known to play an important role in clearing viral infections (Charles *et al.*, 2011) and are reported to be increased in autoimmune diseases (Thorarinsdottir *et al.*, 2019), I hypothesised that these cells could be associated with inflammatory state and I further investigated if their frequency correlated with disease activity or with blood inflammatory markers. It has been reported before that the frequency of ABCs in SLE patients correlates with the disease activity score SLEDAI (Wang *et al.*, 2018). Nevertheless, I was unable to reproduce this correlation in patients with RA, finding no correlation between the frequency of ABCs and the DAS28 score or inflammatory markers (Figure 3.7-10).

Because many variables could potentially affect the frequency of ABCs, a single regression analysis was used to assess the effect of each variable in the frequency of ABCs (Figure 3.11). Unfortunately, the only variable showing a significant effect was sex, as shown in the separated analysis.

The lack of differences between the frequency of ABCs in HCs and RA patients, it could be the case that peripheral blood is not the most appropriate organ to study these cells. Murine studies have looked at the spleen instead of the blood (Hao *et al.*, 2011; Rubtsov *et al.*, 2011; Rubtsov *et al.*, 2013), however, in patients the most accessible tissue is blood. A possibility to keep in mind would be the hypothesis that these cells are harboured in the spleen and when they reach a certain threshold they appear in the blood. This would explain why ABCs are only detected in the peripheral blood of elderly women, as it could be that they are present in the spleen in younger women but are not detected until they egress into peripheral blood during aging. However, in inflammatory conditions, ABCs could be migrating from the spleen to inflammatory sites as reported previously in RA synovial fluid (Illges *et al.*, 2000; Yeo *et al.*, 2015) and in multiple sclerosis central nervous system (van Langelaar *et al.*, 2019).

The frequencies of ABCs in synovial fluid of patients with inflammatory arthritides was much higher than the frequencies found in blood, reaching almost 90% of the total B cell

population (Figure 3.12). These results are in line with other previously published studies (Illges *et al.*, 2000; Yeo *et al.*, 2015; Amara *et al.*, 2017). A better option would have been obtaining matched PBMCs and SFMCs in order to correlate the frequencies seen in blood and synovial fluid, however, this has proven difficult and only one patient had matched samples. Interestingly, this patient showed a small frequency of ABCs in peripheral blood, of around 1% but very high percentages in synovial fluid, reaching up to 72%.

The reason for this increase in ABCs in the synovial fluid is unknown. The high vascularisation and release of proinflammatory mediators in the joints increases mononuclear cells recruitment in the synovial tissue (Ziff, 1989). The migration of cells into the synovial fluid could be due to the presence of chemokines, ligands and antigens facilitating cell activation and inflammation.

Even though ABCs are found in much higher frequencies in synovial fluid than in blood, further research is needed to understand their origin. It is still unknown if ABCs migrate from the blood into the tissue or if B cells from the blood infiltrate the inflammatory tissue and once there, they are skewed towards an ABC phenotype.

3.6 Conclusions

I assessed the frequency of ABCs in different arthritic diseases. I hypothesised that ABCs are present in peripheral blood of patients and controls and that they can be found in increased frequencies in patients suffering from RA. The frequency of these cells, due to their contribution to inflammation, might correlate with disease activity and inflammation. I also hypothesised that the frequency of these cells in the synovial fluid is increased compared to peripheral blood.

I showed that ABCs are detectable in blood from patients and controls by flow cytometry. I described ABCs as CD11c+ CD21- CD19+ B cells. Contrary to my hypothesis, assessment of the frequency of B cells with this phenotype showed no significant differences in patients with RA compared to other arthritic diseases and age-matched healthy controls. Moreover, no correlation was found with inflammation and disease activity. In addition, the previously described correlation between the age and sex of RA patients and the frequency of these cells could not be reproduced. However, I did see a much higher frequency of these cells in synovial fluid of patients with arthritides, composing almost all the B cell population found in the joint of some patients.

In summary, I could not demonstrate a higher frequency of ABCs in RA patients. However, these cells constitute a unique subset of B cells which are of interest in inflammatory conditions and therefore more research on their phenotype and their function is needed to elucidate their contribution in health and inflammatory diseases.

Chapter 4. Phenotypic characterisation of ABCs

4.1 Introduction

In addition to determining the frequency of ABCs in blood and synovial fluid of patients with RA, I also aimed to characterise this subset of B cells in terms of surface and intracellular expression of relevant markers.

Studies in mice mainly described ABCs as expressing CD11b and CD11c but lacking CD21 (Rubtsov *et al.*, 2011). Characterisation of these cells revealed that they were positive for CD5 and expressed high levels of CD80, CD86 and MHC class II. When stimulated by TLR7 agonist, these cells produced high amounts of anti-chromatin IgG autoantibodies compared to other B cell subsets, demonstrating that ABCs may be a source of autoantibodies (Rubtsov *et al.*, 2013).

In humans, ABCs have been described by different groups generally as CD21low B cells. However, some studies reported these cells as being functionally exhausted and anergic, whereas others have described them as activated B cells. The discrepancies in expression of several surface molecules could be justified by the presence of more than one subset within the CD21low population. Focusing on RA, two CD21low B cell subsets have been found to be expanded in peripheral blood: one expresses CD27 while the other lacks expression of this receptor (Thorarinsdottir *et al.*, 2015). Rubtsov *et al.*, found that the CD27+ subset also expresses CD11c and CD5 in addition to activation markers such as CD80 and CD86, and were considered to be memory cells as they were class-switched (Rubtsov *et al.*, 2011). The CD27- cells, characterised by Isnardi *et al.*, also expressed CD11c but displayed unmutated IgM (Isnardi *et al.*, 2010). Besides some differences, the CD21low B cell subset described by all the different groups had high expression of CD86, CD80 and HLA-DR (Isnardi *et al.*, 2010; Rubtsov *et al.*, 2011; Shimabukuro-Vornhagen *et al.*, 2017).

These CD21-CD11c+ B cells also expressed the transcription factor T-bet (Rubtsova *et al.*, 2017). T-bet expression in B cells has been proven to play a critical role during anti-viral immune responses (Rubtsova *et al.*, 2013), however, their role in human autoimmunity is still understudied (Rubtsov *et al.*, 2017).

Studies have also investigated expression of Ig by ABCs to determine if these cells have undergone class switching, in addition to determining their replicative ability. The subset described by Shimabukuro-Vornhagen *et al.*, had a large fraction of proliferating cells, assessed by the expression of Ki67, and a high degree of class-switching cells (IgM- and

IgD-negative) (Shimabukuro-Vornhagen *et al.*, 2017). In line with these results, Rubtsov *et al.*, found that ABCs were negative for IgD and IgM but positive for IgG (Rubtsov *et al.*, 2011). However, Isnardi *et al.*, found that CD21low B cells from RA patients preferentially expressed IgM and/or IgD, whereas CD21low B cells from healthy donors were switched-class B cells (Isnardi *et al.*, 2010).

Moreover, a subset of synovial fluid B cells described as FcRL4+ B cells showed a similar phenotype to the ABCs as they had low expression of CD21 and high expression of CD11c. These cells also showed expression of the co-stimulatory molecules CD80 and CD86 in addition to expression of CD27, IgG and IgA (Yeo *et al.*, 2015; Amara *et al.*, 2017).

Therefore, I assessed expression of different activation markers as well as intracellular molecules by flow cytometry on the ABC population (CD19+CD11c+CD21-) compared to the other three B cell subsets, CD5+ B cells (CD19+CD5+), naïve B cells (CD19+IgD+CD27-) and memory B cells (CD19+IgD-CD27+).

4.2 Chapter hypothesis and aims

The underlying hypothesis for the work detailed in this chapter is: the involvement of ABCs in RA pathogenesis can be confirmed if they have an activated phenotype and are class-switched, actively proliferating B cells.

Therefore, the aims of this chapter were to:

1. Characterise the phenotype of ABCs compared to other B cell subsets.
2. Determine if the phenotype of ABCs is different between different diseases, as well as healthy controls.

The specific objectives were:

1. Measure expression of different markers (co-stimulatory, activation, transcription factors, immunoglobulin, etc.) using flow cytometry.
2. Compare expression of those markers between ABCs and other B cell subsets.
3. Compare expression of the markers in ABCs from different disease groups as well as healthy controls.

4.3 Methods

4.3.1 Flow cytometry gating strategy for the determination of expression of phenotypic markers in the different B cell subsets

I designed 5 different antibody panels to investigate the expression of a range of phenotypic markers. Each of the panels included the markers used to identify B cells and exclude other cell types, as well as the markers to create the four B cell subsets: ABCs (CD19+CD11c+CD21-), CD5+ B cells (CD19+CD5+), naïve B cells (CD19+IgD+CD27-) and memory B cells (CD19+IgD-CD27+). In addition, the different phenotypic markers were included in the various panels to be able to determine the percentage of positive cells in each subset for each marker. See section 2.5.1 in the methods chapter for whole blood staining protocol and tables 2.1 to 2.5 for the antibodies used. The gating strategy used is shown in Figure 4.1, showing an RA patient as an example. First, following the gating strategy explain in Chapter 3 Figure 3.1, the different B cell subsets were created. Then, expression of each of the phenotypic markers in each of the subsets was determined by creating a quadrant gate in the lymphocytes population of the marker against CD19 and copying that gate into the subsets to assess the number of positive cells for that marker in each subset. Most of the phenotypic marker's gate were set using an FMO. However, for some markers, only expressed by B cells, the gates were set from the non-expressing CD19- population.

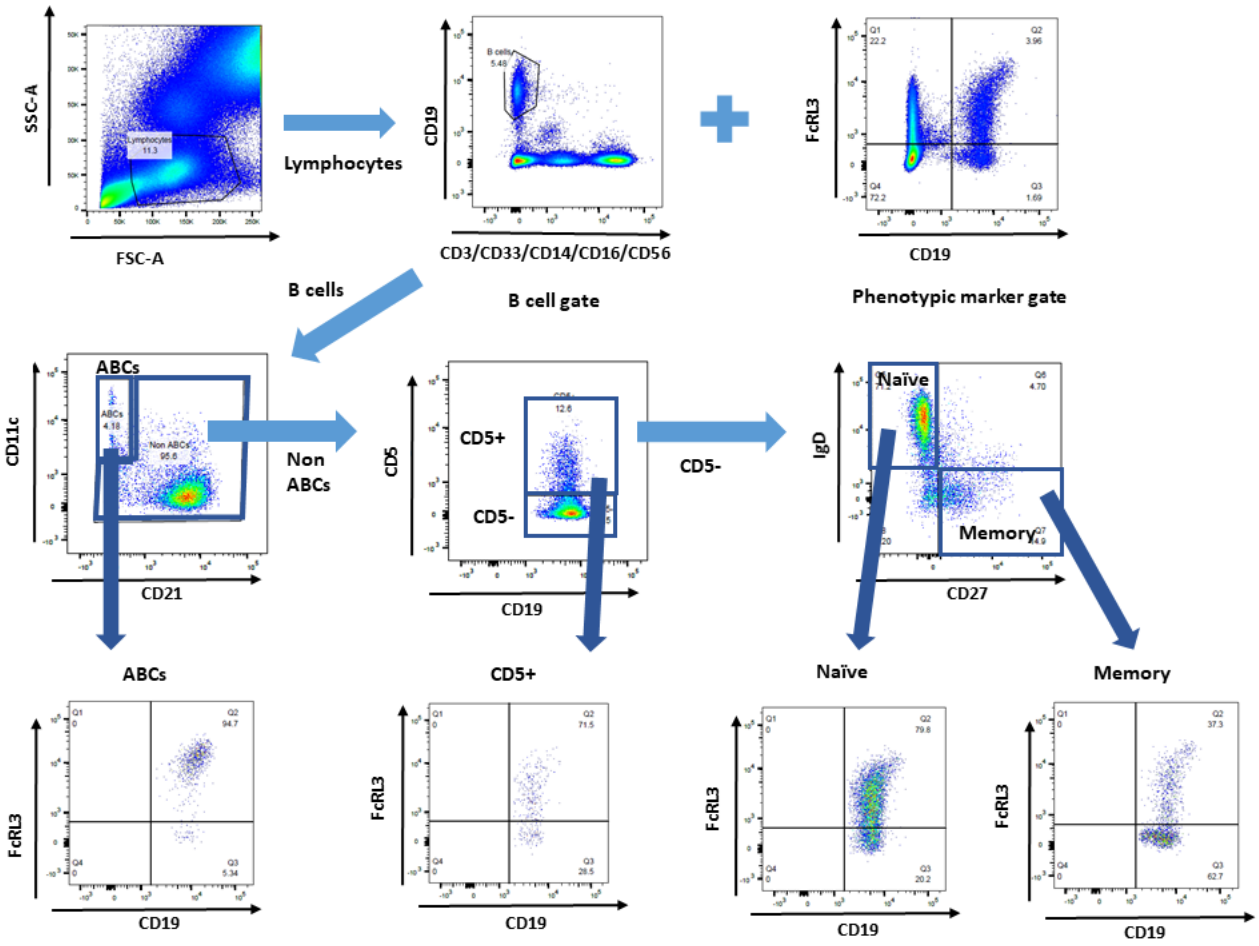

Figure 4. 1. Gating strategy for all the phenotypic markers. The gating strategy for determination of FcRL3 expression in B cell subsets from an RA patient is shown as an example. A similar strategy was used for all the other phenotype markers. Dead cells and doublets were excluded. Lymphocytes were selected based on their forward and sideward scatter signal, B cells were identified as CD19+ and negative for CD3, CD33, CD14, CD16 and CD56. Among the selected B cells the four B cell subsets were defined. From the lymphocyte gate, the phenotypic marker against CD19 expression is gated and the phenotypic marker gate is copied in each B cell subset, allowing determination of expression of a set of markers in each subset. The phenotypic marker's gate is set on the expression of that marker in the CD19- fraction of cells. If the CD19- population also expresses the phenotypic marker, for example with FcRL3, the FMO strategy was used to set the gate.

4.4 Results

4.4.1 ABCs have high expression of HLA-DR but low expression of the co-stimulatory molecule CD40

As expected, all B cell subsets have high expression of the antigen presentation MHC class II molecule, HLA-DR (Figure 4.2.A-C). However, MFI values showed that ABCs have significantly higher expression of HLA-DR compared to the memory B cells (Figure 4.2.D).

In terms of CD40 expression, all B cells are positive for this co-stimulatory molecule (Figure 4.3). Nevertheless, significantly lower percentages of positive cells are found in the ABC population compared to the naïve B cells and the CD5+ subsets (Figure 4.3.C). However, no significant differences were seen in terms of MFI values (Figure 4.3.D).

4.4.2 In the ABC population there are higher percentages of cells positive for activation markers

Expression of B cell activation markers was assessed. CD80, a co-stimulatory molecule that is upregulated on activated B cells was highly expressed in the memory and ABC population (Figure 4.4). There were significantly higher percentages of positive cells in the ABCs compared to naïve and CD5+ cells (Figure 4.4.C). Moreover, CD80 expression, measured as a MFI value, was also higher in ABCs compared to naïve and CD5+ cells (Figure 4.4.D).

Another co-stimulatory molecule, which is also upregulated on B cells after stimulation, is CD86. A higher percentage of CD86 positive B cells was found on the ABCs population (Figure 4.5. A-C), these differences were significant in ABCs compared to naïve and CD5+ B cells. CD86 expression was also higher in ABCs compared to naïve and CD5+ cells (Figure 4.5.D).

Finally, CD69 expression was also assessed (Figure 4.6). CD69 is an early indicator of leukocyte activation and although being more variable between patients, there are significantly higher percentages of positive cells in the ABC population compared to the memory B cell subset (Figure 4.6.C). CD69 expression is also higher in ABCs than in memory B cells (Figure 4.6.D).

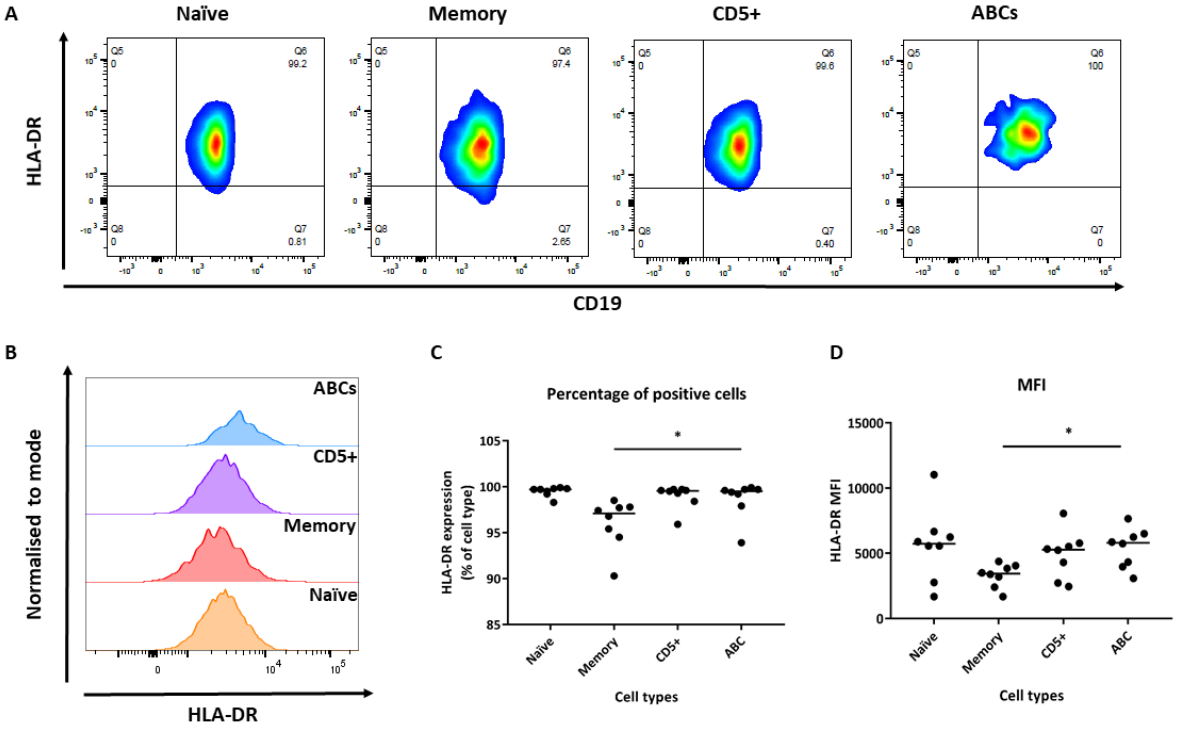

Figure 4. 2. Expression of the antigen-presentation molecule HLA-DR in each B cell subset in early RA patients. A. Flow cytometry plots for each B cell subset. HLA-DR expression against CD19, gate set from the lymphocyte population. **B.** HLA-DR expression overlay for each of the subsets. Naïve B cells are shown in orange; memory B cells in red, CD5+ B cells in purple and ABCs are shown in blue. The peaks are normalised to the same height to normalise different numbers of cells in each population. **C.** Percentage of HLA-DR positive cells in the B cell subsets (n=8). The bar represents the median. **D.** HLA-DR median fluorescence intensity (MFI) in the different B cell subsets (n=8). The bar represents the median. Statistical significance was assessed using a Kruskal-Wallis test with Dunn's multiple comparisons of the ABCs against the other subsets; * $p < 0.05$. Kruskal-Wallis test $p = 0.0029$ for percentages; $p = 0.048$ for MFI values.

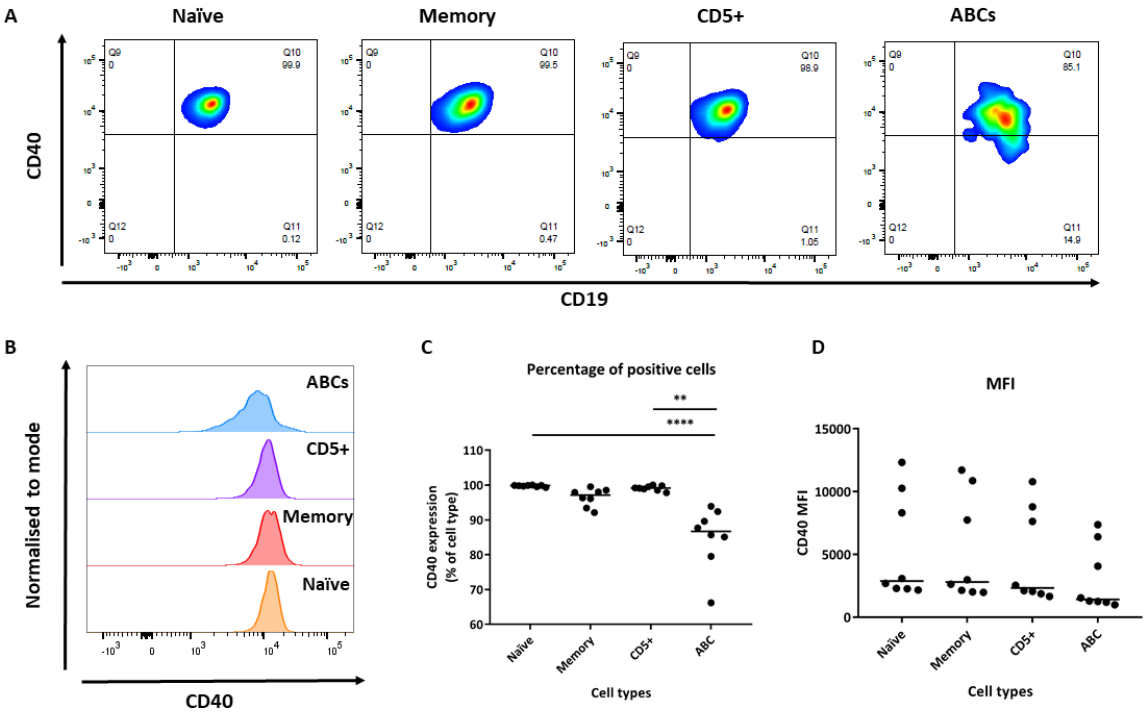

Figure 4. 3. Expression of the co-stimulatory molecule CD40 in each B cell subset in early RA patients. A. Flow cytometry plots for each B cell subset. CD40 expression against CD19, gate set from the lymphocyte population. **B.** CD40 expression overlay for each of the subsets. Naïve B cells are shown in orange; memory B cells in red, CD5+ B cells in purple and ABCs are shown in blue. The peaks are normalised to the same height to normalise different numbers of cells in each population. **C.** Percentage of CD40 positive cells in the B cell subsets (n=8). The bar represents the median. **D.** CD40 median fluorescence intensity (MFI) in the different B cell subsets (n=8). The bar represents the median. Statistical significance was assessed using a Kruskal-Wallis test with Dunn's multiple comparisons of the ABCs against the other subsets; **$p < 0.01$, **** $p < 0.0001$. Kruskal-Wallis test $p < 0.0001$ for percentages; $p = 0.1189$ for MFI values.

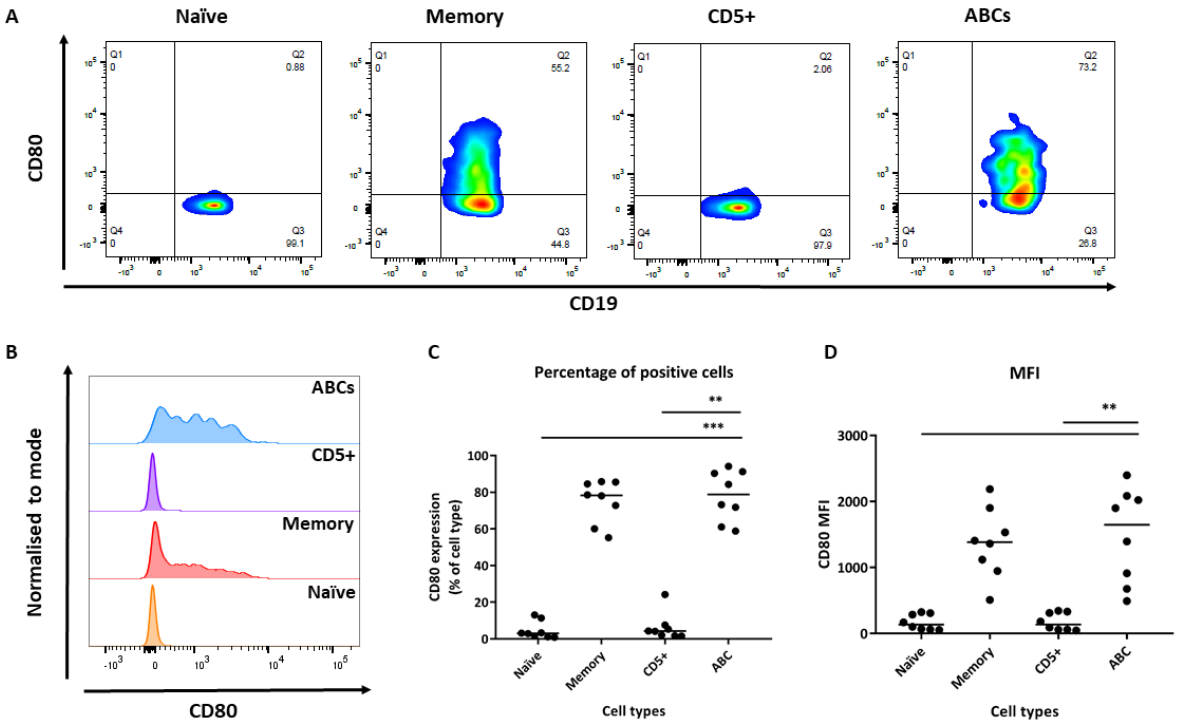

Figure 4. 4. Expression of the co-stimulatory molecule CD80 in each B cell subset in early RA patients. A. Flow cytometry plots for each B cell subset. CD80 expression against CD19, gate set from the lymphocyte population. **B.** CD80 expression overlay for each of the subsets. Naïve B cells are shown in orange; memory B cells in red, CD5+ B cells in purple and ABCs are shown in blue. The peaks are normalised to the same height to normalise different numbers of cells in each population. **C.** Percentage of CD80 positive cells in the B cell subsets (n=8). The bar represents the median. **D.** CD80 median fluorescence intensity (MFI) in the different B cell subsets (n=8). The bar represents the median. Statistical significance was assessed using a Kruskal-Wallis test with Dunn's multiple comparisons of the ABCs against the other subsets; **p < 0.01, *** p < 0.001. Kruskal-Wallis test p < 0.0001 for percentages; p < 0.0001 for MFI values.

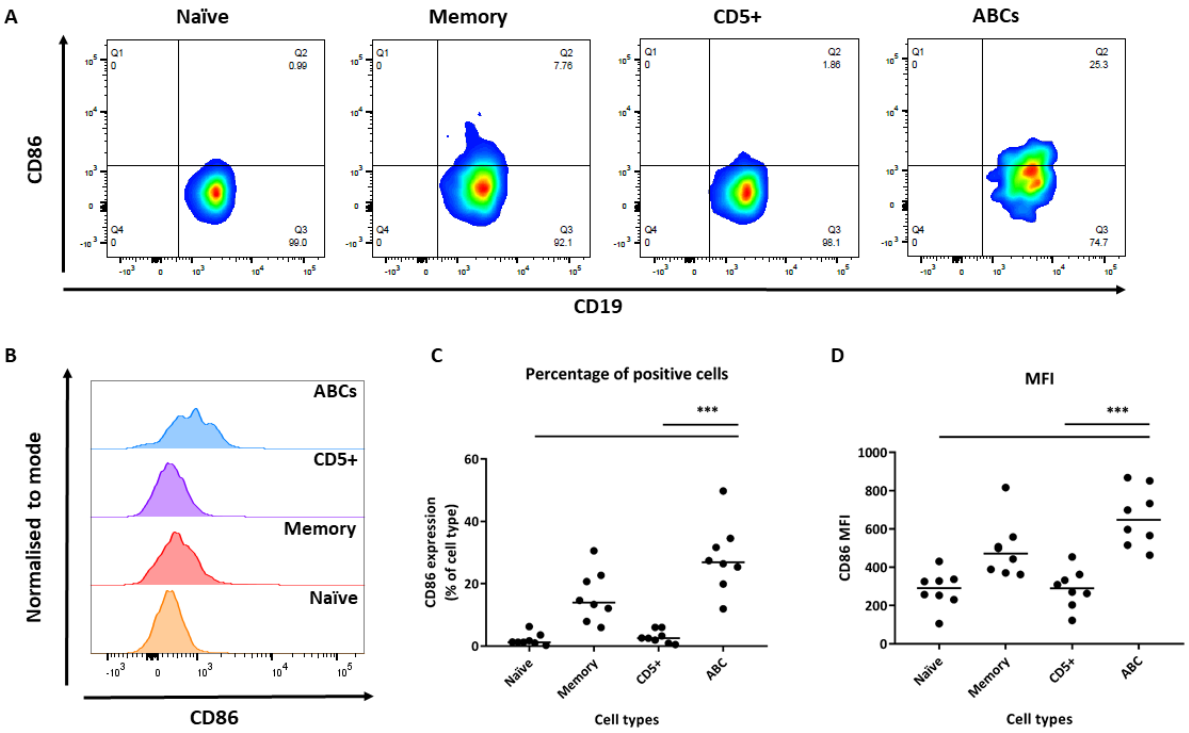

Figure 4. 5. Expression of the co-stimulatory molecule CD86 in each B cell subset in early RA patients. A. Flow cytometry plots for each B cell subset. CD86 expression against CD19, gate set from the lymphocyte population. **B.** CD86 expression overlay for each of the subsets. Naïve B cells are shown in orange; memory B cells in red, CD5+ B cells in purple and ABCs are shown in blue. The peaks are normalised to the same height to normalise different numbers of cells in each population. **C.** Percentage of CD86 positive cells in the B cell subsets (n=8). The bar represents the median. **D.** CD86 median fluorescence intensity (MFI) in the different B cell subsets (n=8). The bar represents the median. Statistical significance was assessed using a Kruskal-Wallis test with Dunn's multiple comparisons of the ABCs against the other subsets; *** $p < 0.001$. Kruskal-Wallis test $p < 0.0001$ for percentages; $p < 0.0001$ for MFI values.

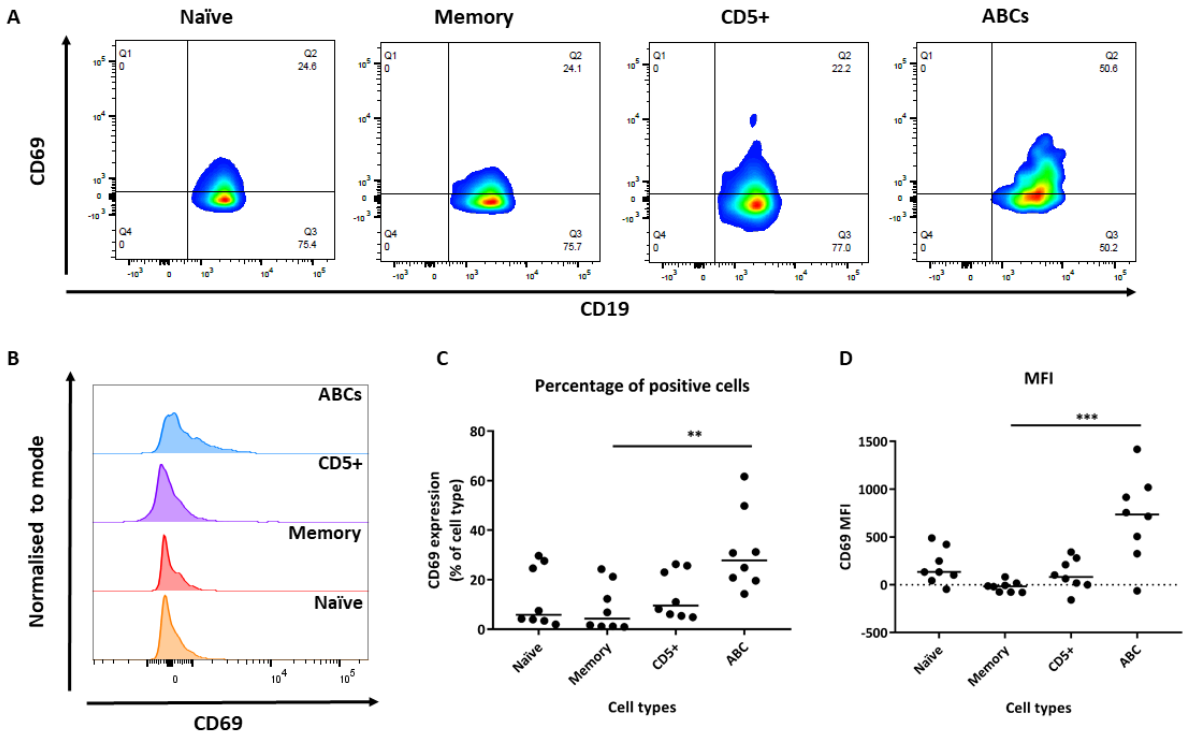

Figure 4. 6. Expression of the activation molecule CD69 in each B cell subset in early RA patients. A. Flow cytometry plots for each B cell subset. CD69 expression against CD19, gate set from the lymphocyte population. **B.** CD69 expression overlay for each of the subsets. Naïve B cells are shown in orange; memory B cells in red, CD5+ B cells in purple and ABCs are shown in blue. The peaks are normalised to the same height to normalise different numbers of cells in each population. **C.** Percentage of CD69 positive cells in the B cell subsets (n=8). The bar represents the median. **D.** CD69 median fluorescence intensity (MFI) in the different B cell subsets (n=8). The bar represents the median. Statistical significance was assessed using a Kruskal-Wallis test with Dunn's multiple comparisons of the ABCs against the other subsets; **$p < 0.01$, *** $p < 0.001$. Kruskal-Wallis test $p = 0.0133$ for percentages; $p = 0.0014$ for MFI values.

4.4.3 A high percentage of the ABC population is actively proliferating

In order to assess cell proliferation, an intracellular staining was performed. Ki67 was used as a cell proliferation marker as it is expressed during all the phases of the cell cycle but not in resting cells (Schwarting *et al.*, 1986). As expected, in the memory B cell population there was a small proportion of cells positive for Ki67, and in the ABC population there was a similar percentage of positive cells (Figure 4.7). This high percentage of positive cells in the ABC subset was significant when compared to the naïve and the CD5+ cells (Figure 4.7.C). However, no significant differences were seen in terms of MFI values between the populations (Figure 4.7.D).

4.4.4 A high percentage of the ABC population expresses the transcription factor T-bet

The T cell-associated transcription factor T-bet has been described as a specific transcription factor for the ABC-like subset (Rubtsov *et al.*, 2011; Rubtsova *et al.*, 2015; Karnell *et al.*, 2017), therefore I explored this in RA patients. T-bet expression was determined by flow cytometry using the intracellular staining protocol (Figure 4.8). The percentage of T-bet positive B cells was very low in the naïve and CD5+ B cell populations, but in the ABC subset there was a significantly higher number of B cells expressing this transcription factor (Figure 4.8.C). MFI values also showed that T-bet expression was higher in ABCs compared to the naïve and the CD5+ populations (Figure 4.8.D).

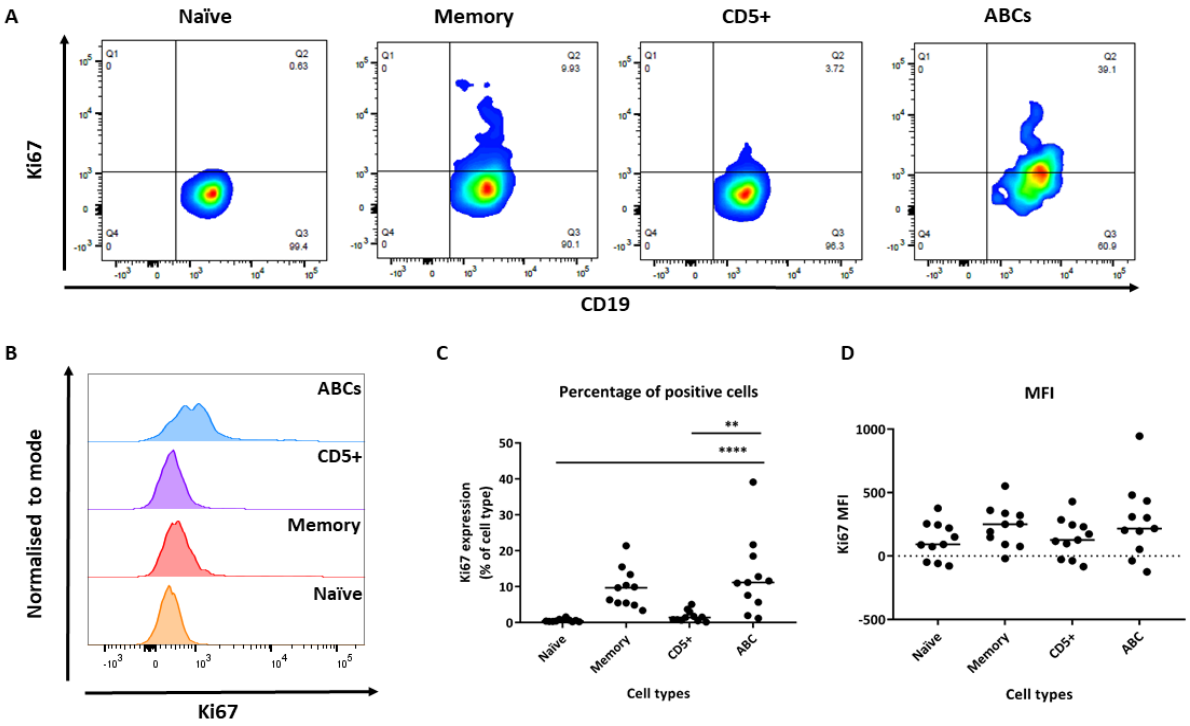

Figure 4. 7. Expression of the proliferation marker Ki67 in each B cell subset in early RA patients. A. Flow cytometry plots for each B cell subset after intracellular staining. Ki67 expression against CD19, gate set from the lymphocyte population. **B.** Ki67 expression overlay for each of the subsets. Naïve B cells are shown in orange; memory B cells in red, CD5+ B cells in purple and ABCs are shown in blue. The peaks are normalised to the same height to normalise different numbers of cells in each population. **C.** Percentage of Ki67 positive cells in the B cell subsets (n=11). The bar represents the median. **D.** Ki67 median fluorescence intensity (MFI) in the different B cell subsets (n=11). The bar represents the median. Statistical significance was assessed using a Kruskal-Wallis test with Dunn's multiple comparisons of the ABCs against the other subsets; **p < 0.01, **** p < 0.0001. Kruskal-Wallis test p < 0.0001 for percentages; p = 0.2723 for MFI values.

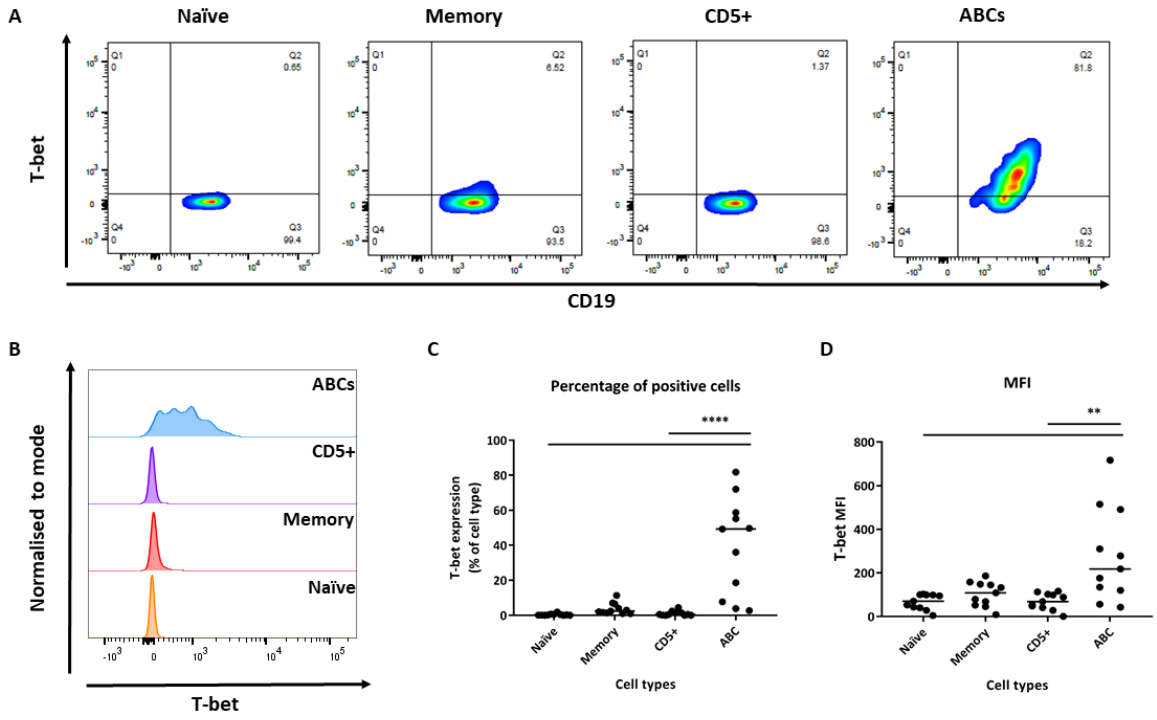

Figure 4. 8. Expression of the transcription factor T-bet in each B cell subset in early RA patients. A. Flow cytometry plots for each B cell subset after intracellular staining. T-bet expression against CD19, gate set from the lymphocyte population. **B.** T-bet expression overlay for each of the subsets. Naïve B cells are shown in orange; memory B cells in red, CD5+ B cells in purple and ABCs are shown in blue. The peaks are normalised to the same height to normalise different numbers of cells in each population. **C.** Percentage of T-bet positive cells in the B cell subsets (n=11). The bar represents the median. **D.** T-bet median fluorescence intensity (MFI) in the different B cell subsets (n=11). The bar represents the median. Statistical significance was assessed using a Kruskal-Wallis test with Dunn's multiple comparisons of the ABCs against the other subsets; **p < 0.01, **** p < 0.0001. Kruskal-Wallis test p < 0.0001 for percentages; p = 0.0025 for MFI values.

4.4.5 ABCs resemble a memory B cell population regarding class switch immunoglobulin expression

In order to assess the immunoglobulin expression on each of the B cell subsets, PBMCs were isolated from EDTA blood and stained with the immunoglobulin panel for flow cytometry analysis. Isolated PBMCs were used instead of whole blood due to circulating IgG and IgM present in plasma that would bind the flow cytometry antibodies and therefore reduce staining of the cells.

As expected, most of the cells in the naïve and the CD5+ population are positive for IgM (Figure 4.9). However, in the ABC population there was significantly lower percentages of cells expressing IgM compared to the CD5+ subset but higher percentages of positive cells than in the memory population (Figure 4.9.C). In terms of MFI, ABCs have significant lower expression of IgM compared to the naïve and CD5+ B cells (Figure 4.9.D).

Expression of IgD was also assessed. IgD is expressed in mature B cells until somatic hypermutation and class switching occurs (Treanor, 2012). Accordingly, the percentage of positive cells for IgD was significantly higher in naïve (expected as this subset is gated on IgD expression) and CD5+ B cells (Figure 4.10). In the ABC population there was a significantly lower percentage of cells expressing IgD compared to the naïve subset but higher percentages of positive cells than in the memory population (Figure 4.10.C). MFI values show that ABCs have significantly lower expression of IgD than naïve and CD5+ B cells but higher than memory B cells (Figure 4.10.D).

I also evaluated expression of the class switched immunoglobulins, IgG and IgA. Both IgG and IgA are immunoglobulins expressed after B cells are antigen-activated and undergo somatic hypermutation and class switching (Treanor, 2012). Regarding IgG expression, in the naïve and the CD5+ B cells there very few cells positive for IgG (Figure 4.11). As expected, in the memory B cells we found around half of the cells positive for IgG. However, in the ABC population there are also significantly higher percentages of positive cells for this class switched immunoglobulin compared to the naïve and the CD5+ subsets (Figure 4.11.C). In addition, ABCs have significantly higher expression of IgG than naïve B cells (Figure 4.11.D).

Expression of another class switched immunoglobulin, IgA, showed that higher percentages of positive cells were found in the memory subset (Figure 4.12). Nevertheless,

the ABC population has significantly higher percentages and higher expression of IgA compared to the naïve and the CD5+ subsets (Figure 4.12.C-D).

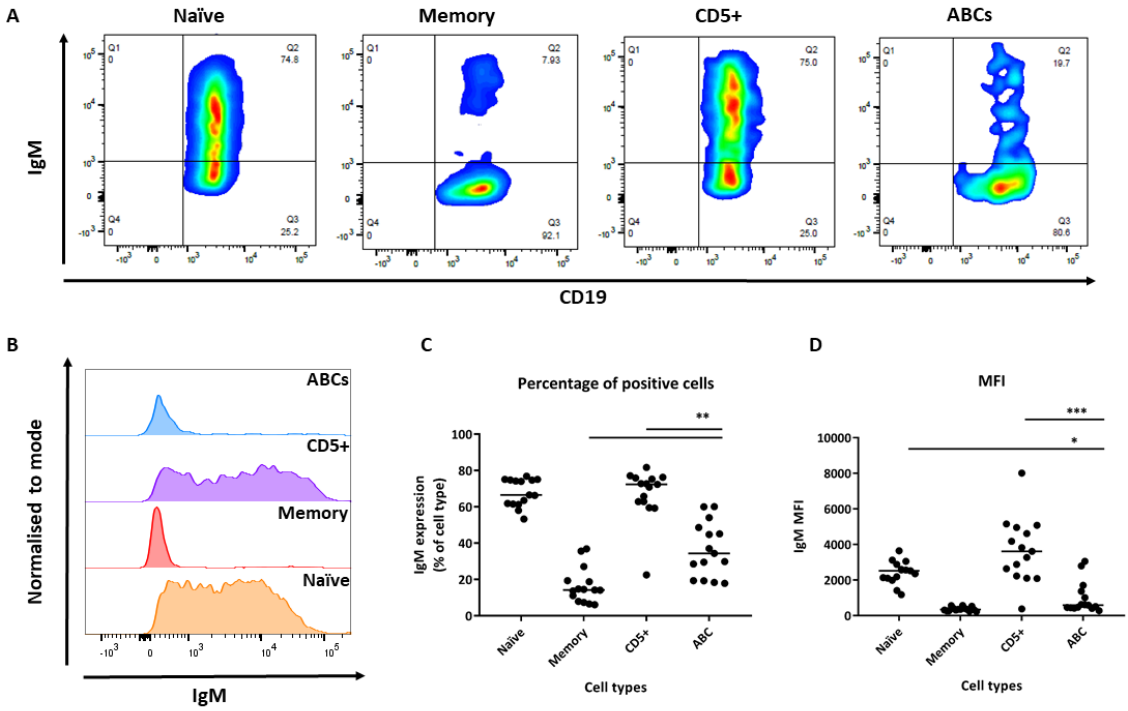

Figure 4. 9. IgM expression in each B cell subset in early RA patients. A. Flow cytometry plots for each B cell subset after PBMCs isolation and staining. IgM expression against CD19, gate set from the lymphocyte population. **B.** IgM expression overlay for each of the subsets. Naïve B cells are shown in orange; memory B cells in red, CD5+ B cells in purple and ABCs are shown in blue. The peaks are normalised to the same height to normalise different numbers of cells in each population. **C.** Percentage of IgM positive cells in the B cell subsets (n=15). The bar represents the median. **D.** IgM median fluorescence intensity (MFI) in the different B cell subsets (n=15). The bar represents the median. Statistical significance was assessed using a Kruskal-Wallis test with Dunn's multiple comparisons of the ABCs against the other subsets; * $p < 0.05$, **$p < 0.01$, *** $p < 0.001$. Kruskal-Wallis test $p < 0.0001$ for percentages; $p < 0.0001$ for MFI values.

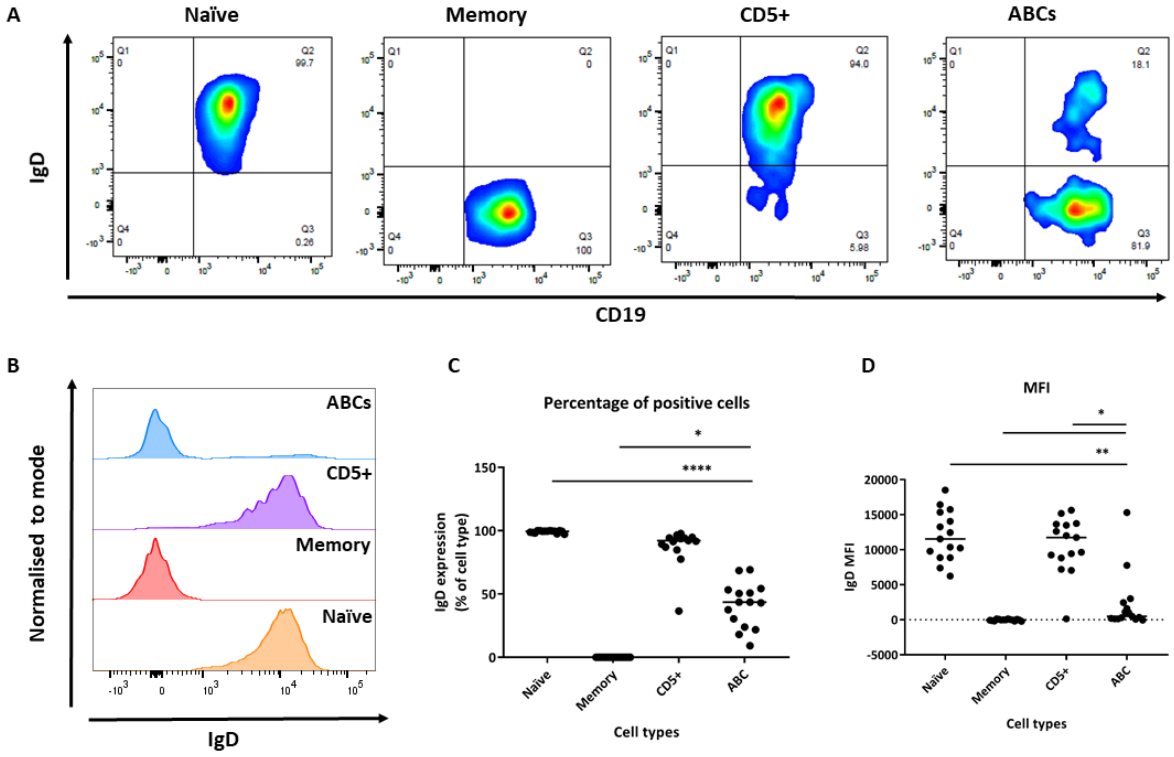

Figure 4. 10. IgD expression in each B cell subset in early RA patients. A. Flow cytometry plots for each B cell subset after PBMCs isolation and staining. IgD expression against CD19, gate set from the lymphocyte population. **B.** IgD expression overlay for each of the subsets. Naïve B cells are shown in orange; memory B cells in red, CD5+ B cells in purple and ABCs are shown in blue. The peaks are normalised to the same height to normalise different numbers of cells in each population. **C.** Percentage of IgD positive cells in the B cell subsets (n=15). The bar represents the median. **D.** IgD median fluorescence intensity (MFI) in the different B cell subsets (n=15). The bar represents the median. Statistical significance was assessed using a Kruskal-Wallis test with Dunn's multiple comparisons of the ABCs against the other subsets; * $p < 0.05$, **$p < 0.01$, **** $p < 0.0001$. Kruskal-Wallis test $p < 0.0001$ for percentages; $p < 0.0001$ for MFI values.

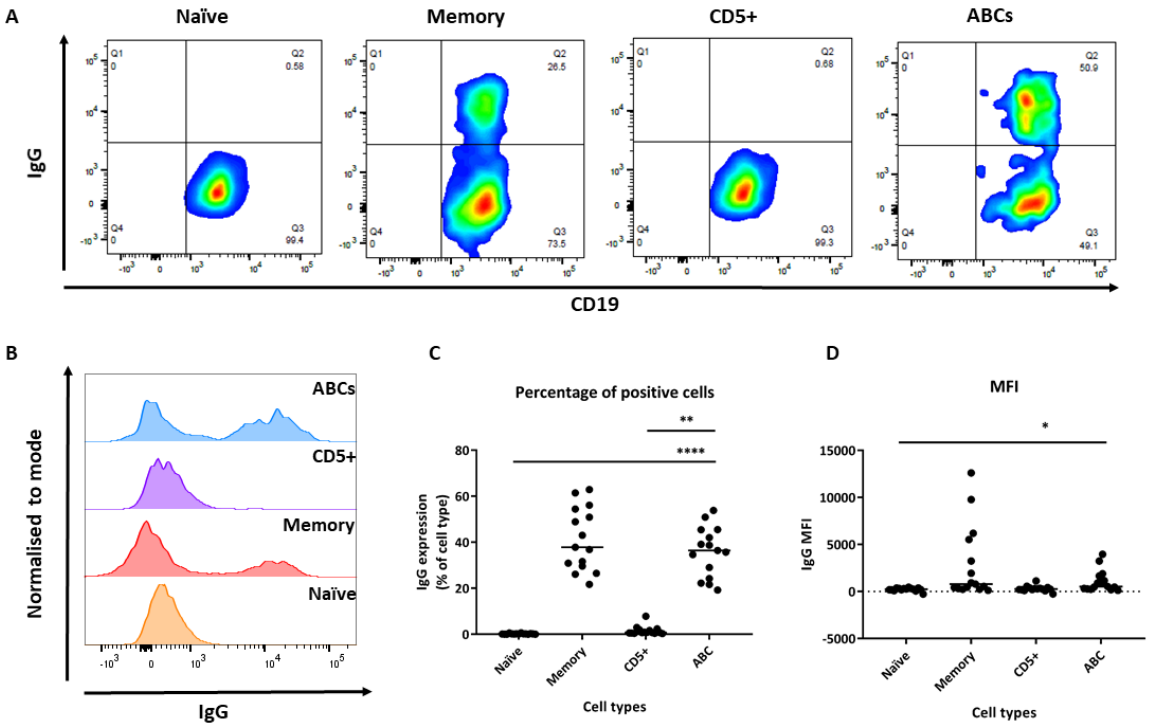

Figure 4. 11. Expression of class switch IgG in each B cell subset in early RA patients. **A.** Flow cytometry plots for each B cell subset after PBMCs isolation and staining. IgG expression against CD19, gate set from the lymphocyte population. **B.** IgG expression overlay for each of the subsets. Naïve B cells are shown in orange; memory B cells in red, CD5+ B cells in purple and ABCs are shown in blue. The peaks are normalised to the same height to normalise different numbers of cells in each population. **C.** Percentage of IgG positive cells in the B cell subsets (n=15). The bar represents the median. **D.** IgG median fluorescence intensity (MFI) in the different B cell subsets (n=15). The bar represents the median. Statistical significance was assessed using a Kruskal-Wallis test with Dunn's multiple comparisons of the ABCs against the other subsets; * $p < 0.05$, **$p < 0.01$, **** $p < 0.0001$. Kruskal-Wallis test $p < 0.0001$ for percentages; $p = 0.0005$ for MFI values.

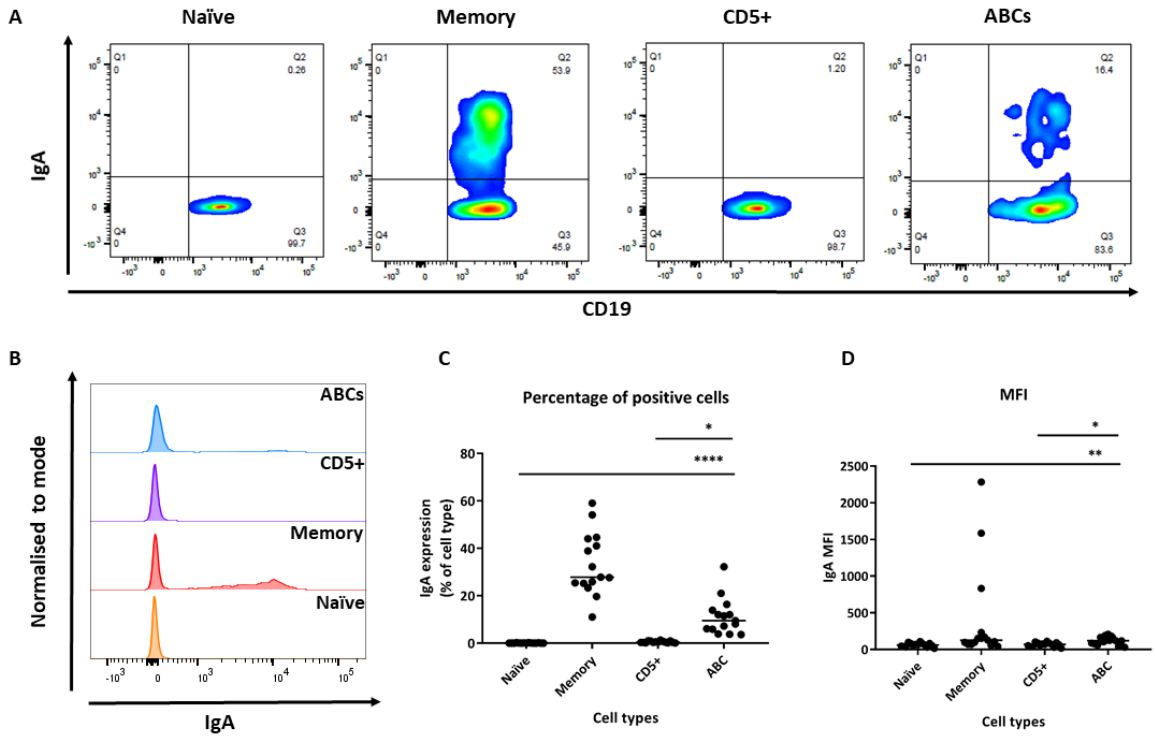

Figure 4. 12. Expression of class switch IgA in each B cell subset in early RA patients. **A.** Flow cytometry plots for each B cell subset after PBMCs isolation and staining. IgA expression against CD19, gate set from the lymphocyte population. **B.** IgA expression overlay for each of the subsets. Naïve B cells are shown in orange; memory B cells in red, CD5+ B cells in purple and ABCs are shown in blue. The peaks are normalised to the same height to normalise different numbers of cells in each population. **C.** Percentage of IgA positive cells in the B cell subsets (n=15). The bar represents the median. **D.** IgA median fluorescence intensity (MFI) in the different B cell subsets (n=15). The bar represents the median. Statistical significance was assessed using a Kruskal-Wallis test with Dunn's multiple comparisons of the ABCs against the other subsets; * $p < 0.05$, **$p < 0.01$, **** $p < 0.0001$. Kruskal-Wallis test $p < 0.0001$ for percentages; $p = 0.0003$ for MFI values.

4.4.6 Expression of members of the FcRL family is enriched in the ABC population

In view of my supervisor's work in Birmingham on FcRL4+ cells in the synovial fluid of RA patients and their similar phenotype to peripheral blood ABCs (Yeo *et al.*, 2015), I designed a panel to assess FcRL4 expression in blood. Moreover, due to FcRL3 implication in RA (Lin *et al.*, 2016) and FcRL5 in IgG binding (Franco *et al.*, 2013), these two other FcRLs were included in the panel.

Considering the high homology present between each of the members of the FcRLs family (Li *et al.*, 2014b), I first needed to validate that the antibodies used to determine expression of these markers were specific for each of the FcRLs and were not cross-reacting and binding another FcRL family members. In order to check the antibodies' specificity, I transfected HEK293T cells with individual plasmids coding each of the FcRLs (kind gift from Professor Nagata, Osaka University) and stained transfected cells with each of the antibodies.

In Figure 4.13, the rows show each of the transfected cell lines and the columns the FcRLs antibody clones used to stain the transfected cells. The antibodies raised against each FcRLs are only recognised by their cognate FcRL. However, the FcRL2 antibody, in addition to recognising FcRL2 transfected cells, it also binds cells transfected with the FcRL3 and FcRL5 plasmid; meaning that FcRL2 antibody clone REA474 apart from partially binding FcRL2 also binds FcRL3 and FcRL5 (Figure 4.13).

In the view of these results, a previously verified FcRL2 antibody by the Nagata's group was tested and FcRL2 expression was assessed using the transfected HEK293T cells. FcRL2 antibody clone B24 was a kind gift from Professor Nagata (Osaka University). As shown in Figure 4.14, the new FcRL2 clone was specific and there was no binding of the antibody to other FcRLs.

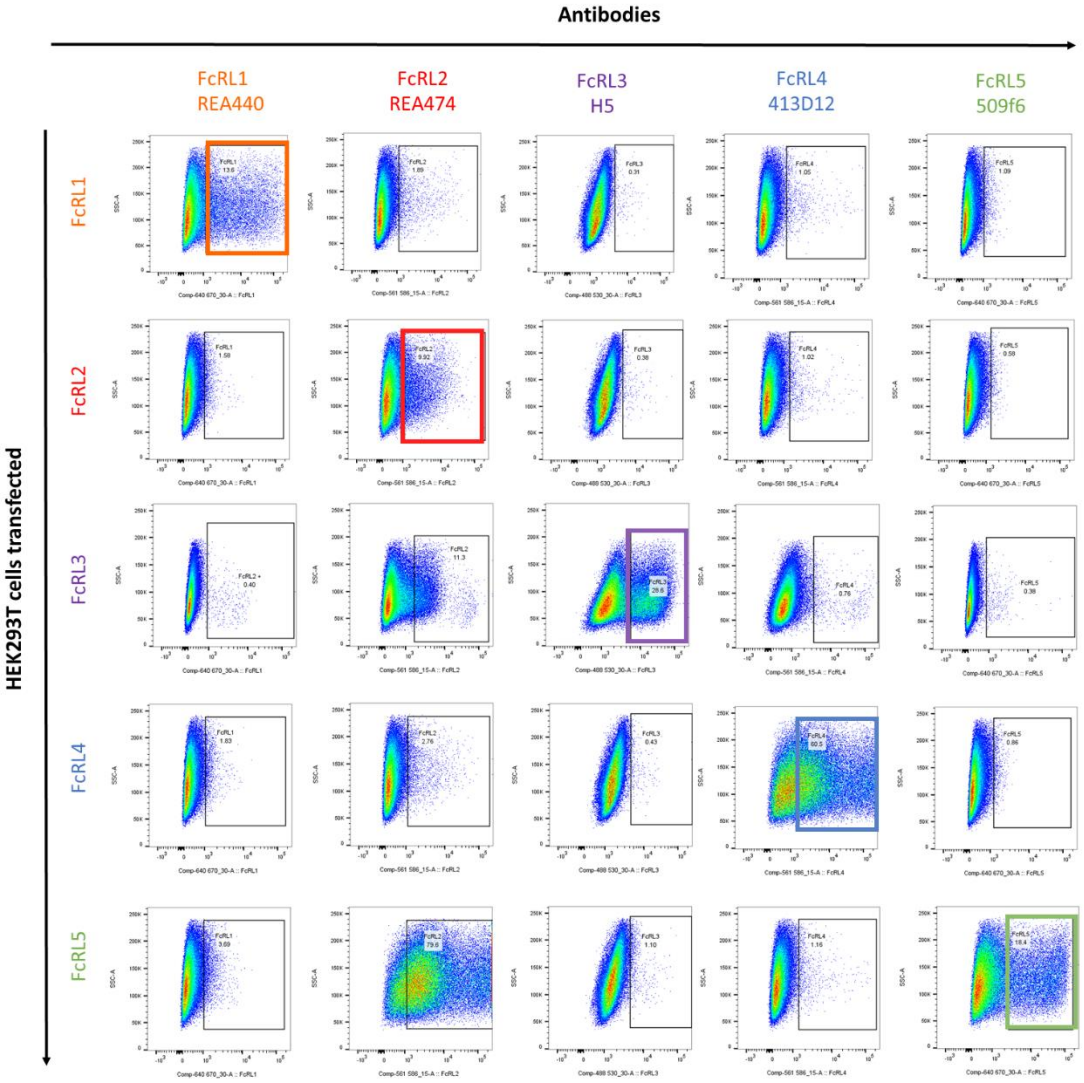

Figure 4. 13. FcRLs antibodies check using transfected HEK293T cells expressing a single FcRL. Rows show each of the HEK293T cells transfected with a single FcRLs. Columns show staining of the cells with each of FcRLs antibody clones. The diagonal marks each of the antibodies recognising the correspondent FcRL. Gates were set based on isotype controls.

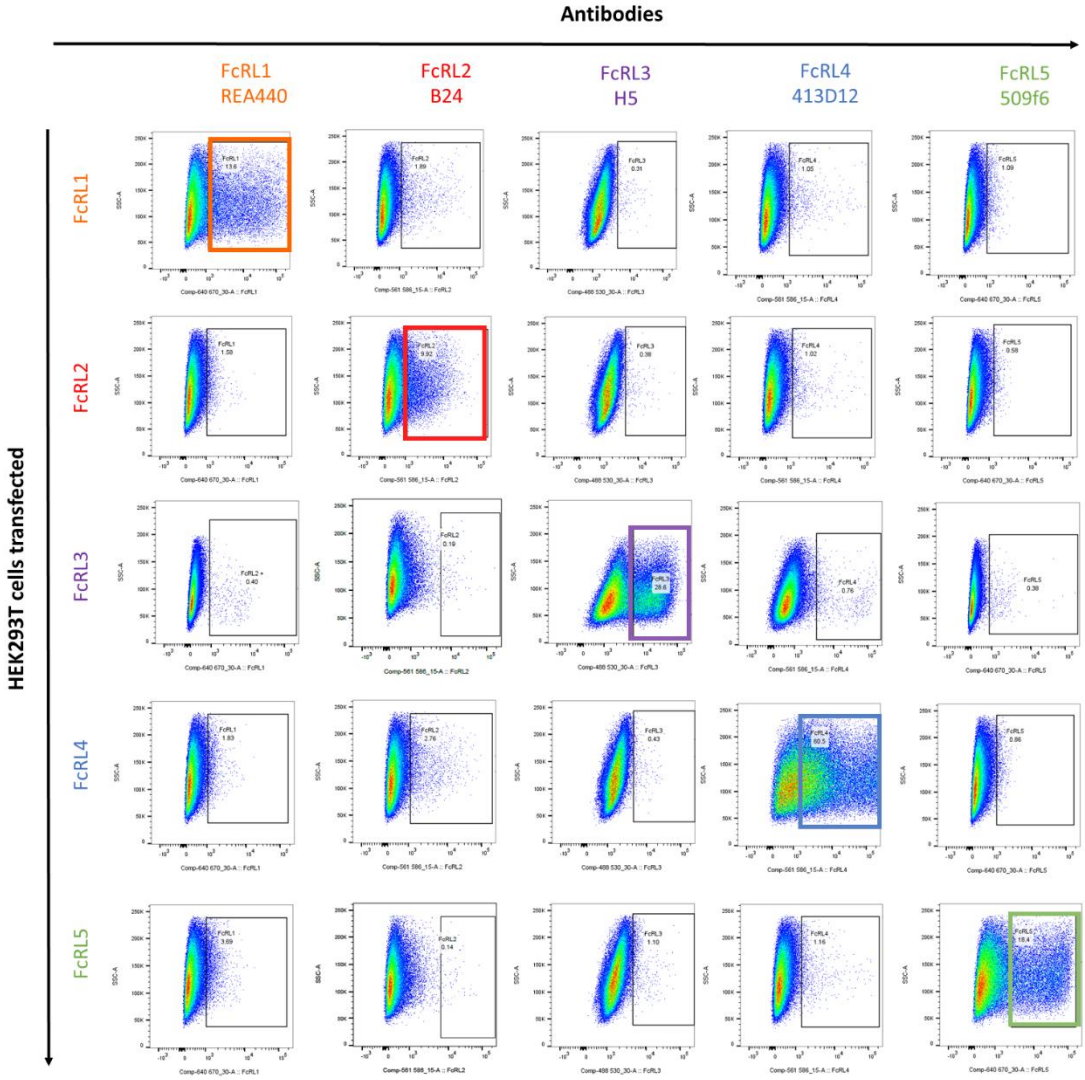

Figure 4. 14. New FcRL2 clone B24 antibody check using transfected HEK293T cells expressing a single FcRL. Rows show each of the HEK293T cells transfected with a single FcRLs. Columns show staining of the cells with each of FcRLs antibody clones. The diagonal marks each of the antibodies recognising the correspondent FcRL. Gates were set based on isotype controls.

Once the antibodies were validated, early RA patients were recruited and expression of the FcRL family members in each of the B cell subsets of interest was determined.

FcRL4 expression is scarce on circulating B cell subsets (Figure 4.15) but there were significantly higher percentages of positive cells in the ABC population compared to naïve and CD5+ subsets (Figure 4.15.C). However, no significant differences were seen in terms of MFI values between the populations (Figure 4.15.D).

In terms of FcRL5 expression, there were significantly higher percentages of FcRL5 and higher expression in the ABC population compared to the naïve and the memory B cell subsets (Figure 4.16).

Regarding FcRL3 expression, this marker is more widely expressed by peripheral B cells than FcRL4 and FcRL5, as around 60% of the cells in each subset expressed FcRL3. However, in the ABC population, all the cells are positive for FcRL3 (Figure 4.17). There are significantly higher percentages of FcRL3 positive cells in the ABCs population compared to all the other subsets (Figure 4.17.C). The MFI shows that FcRL3 is significantly expressed in ABCs compared to all the other B cell subsets (Figure 4.17.D).

FcRL1 and FcRL2 are also expressed in B cells (Miller *et al.*, 2002), therefore expression of these other two FcRLs was also assessed. FcRL1 is highly expressed on all the B cells, although memory B cells and ABCs have lower expression (Figure 4.18). The percentage of ABCs positive for FcRL1 is significantly lower compared to naïve and the CD5+ B cells (Figure 4.18.C). However, no significant differences were seen in terms of MFI values between the populations (Figure 4.18.D).

FcRL2 was expressed at a low level in peripheral B cells but in the ABCs population a significantly higher percentage of FcRL2 positive cells compared to all the other B subsets was found (Figure 4.19.C). Moreover, MFI values revealed significantly higher expression of FcRL2 in ABCs compared to all the subsets (Figure 4.19.D).

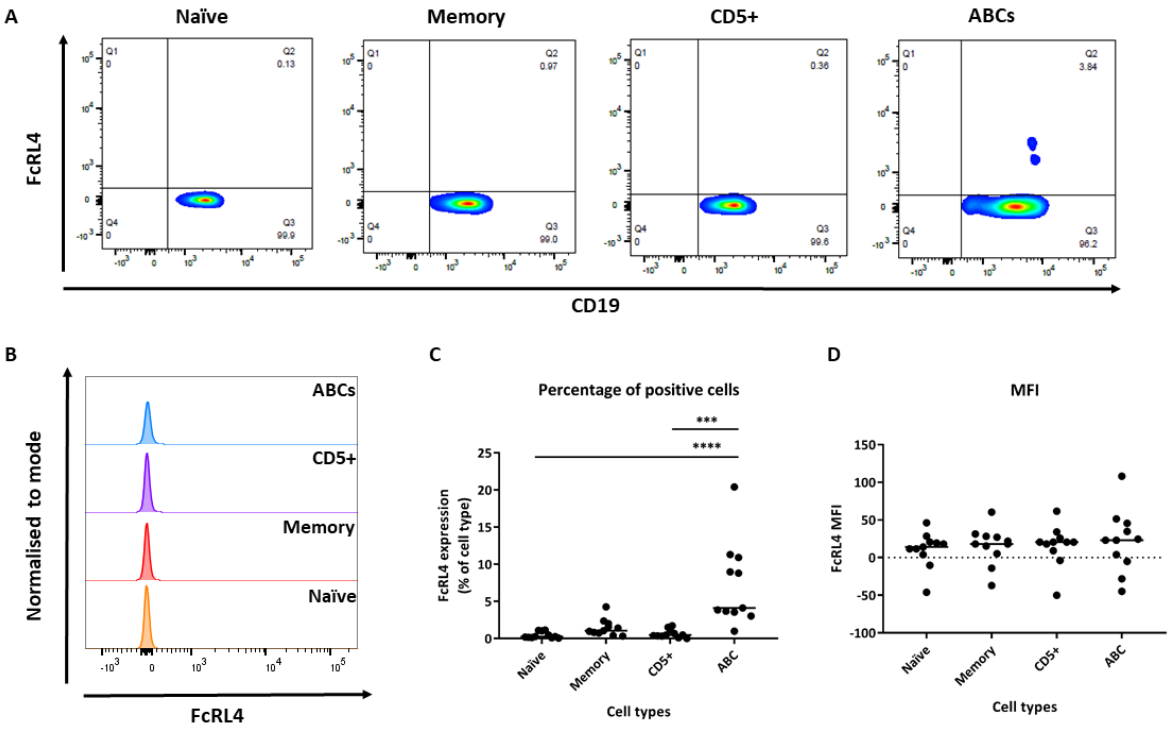

Figure 4. 15. Expression of FcRL4 in each B cell subset in early RA patients. A. Flow cytometry plots for each B cell subset after whole blood staining. FcRL4 expression against CD19, gate set from the lymphocyte population. **B.** FcRL4 expression overlay for each of the subsets. Naïve B cells are shown in orange; memory B cells in red, CD5+ B cells in purple and ABCs are shown in blue. The peaks are normalised to the same height to normalise different numbers of cells in each population. **C.** Percentage of FcRL4 positive cells in the B cell subsets (n=11). The bar represents the median. **D.** FcRL4 median fluorescence intensity (MFI) in the different B cell subsets (n=11). The bar represents the median. Statistical significance was assessed using a Kruskal-Wallis test with Dunn's multiple comparisons of the ABCs against the other subsets; * $p < 0.05$, ** $p < 0.01$, *** $p < 0.001$, **** $p < 0.0001$. Kruskal-Wallis test $p < 0.0001$ for percentages; $p = 0.6787$ for MFI values.

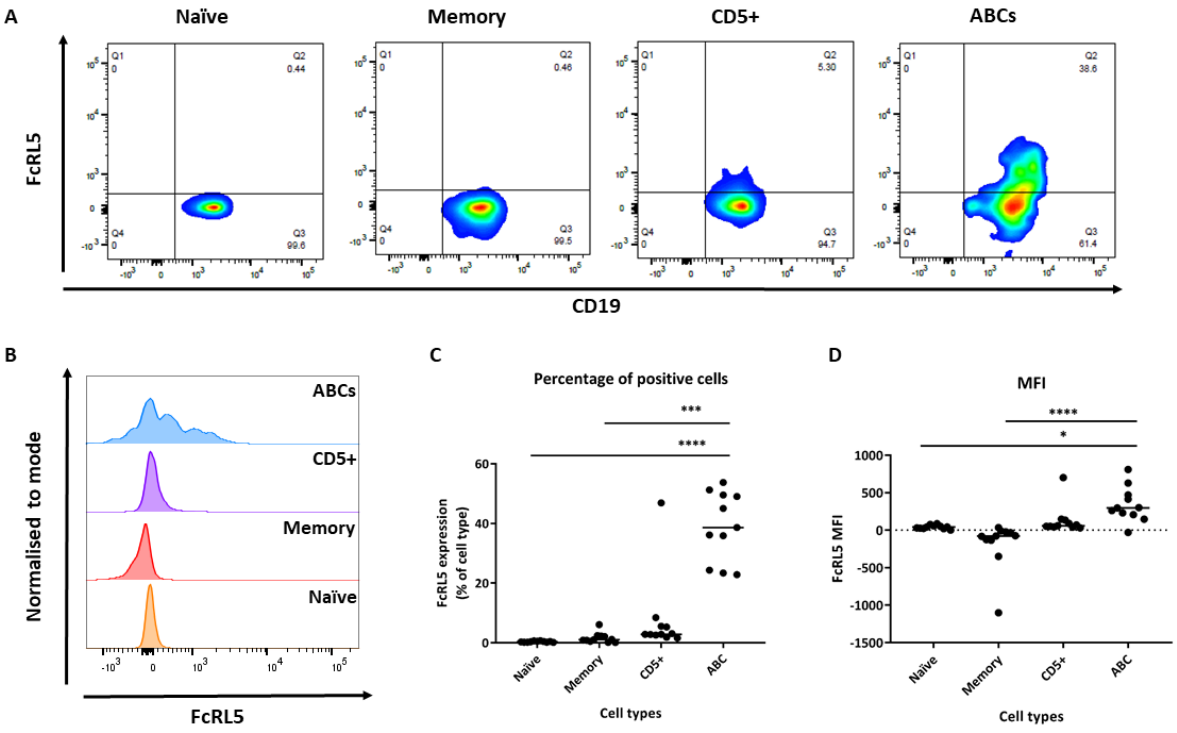

Figure 4. 16. Expression of FcRL5 in each B cell subset in early RA patients. A. Flow cytometry plots for each B cell subset after whole blood staining. FcRL5 expression against CD19, gate set from the lymphocyte population. **B.** FcRL5 expression overlay for each of the subsets. Naïve B cells are shown in orange; memory B cells in red, CD5+ B cells in purple and ABCs are shown in blue. The peaks are normalised to the same height to normalise different numbers of cells in each population. **C.** Percentage of FcRL5 positive cells in the B cell subsets (n=11). The bar represents the median. **D.** FcRL5 median fluorescence intensity (MFI) in the different B cell subsets (n=11). The bar represents the median. Statistical significance was assessed using a Kruskal-Wallis test with Dunn's multiple comparisons of the ABCs against the other subsets; * $p < 0.05$, ** $p < 0.01$, *** $p < 0.001$, **** $p < 0.0001$. Kruskal-Wallis test $p < 0.0001$ for percentages; $p < 0.0001$ for MFI values.

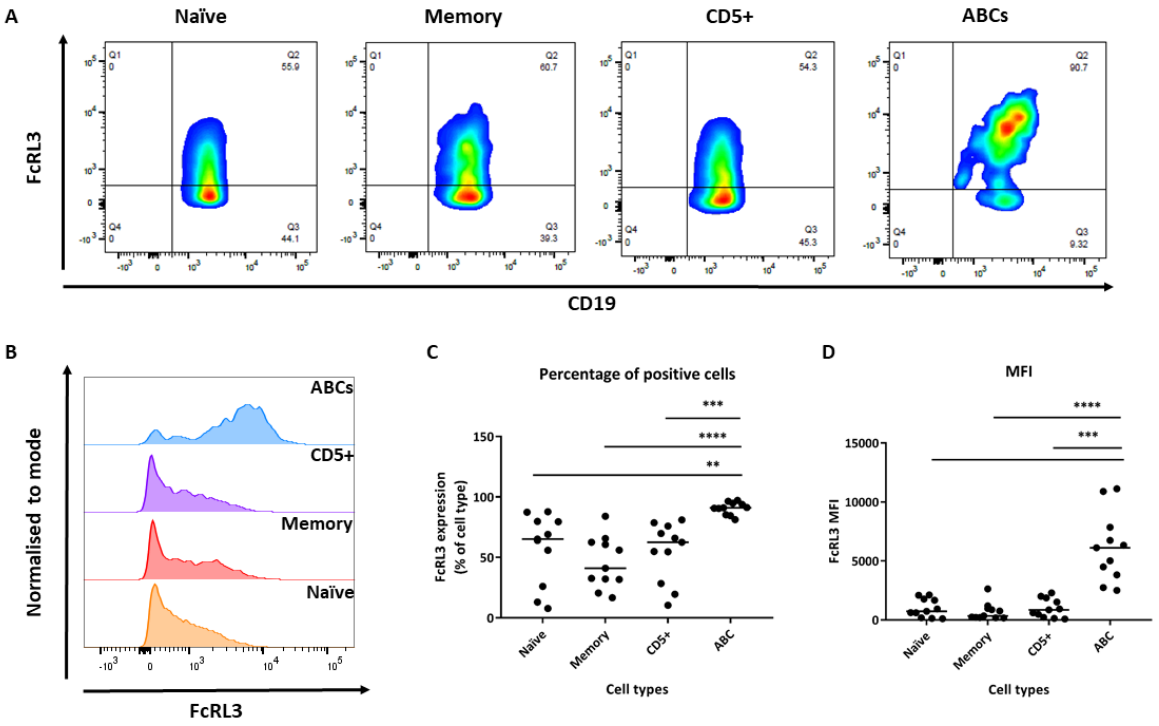

Figure 4. 17. Expression of FcRL3 in each B cell subset in early RA patients. A. Flow cytometry plots for each B cell subset after whole blood staining. FcRL3 expression against CD19, gate set from the lymphocyte population. **B.** FcRL3 expression overlay for each of the subsets. Naïve B cells are shown in orange; memory B cells in red, CD5+ B cells in purple and ABCs are shown in blue. The peaks are normalised to the same height to normalise different numbers of cells in each population. **C.** Percentage of FcRL3 positive cells in the B cell subsets (n=11). The bar represents the median. **D.** FcRL3 median fluorescence intensity (MFI) in the different B cell subsets (n=11). The bar represents the median. Statistical significance was assessed using a Kruskal-Wallis test with Dunn's multiple comparisons of the ABCs against the other subsets; * $p < 0.05$, **$p < 0.01$, *** $p < 0.001$, **** $p < 0.0001$. Kruskal-Wallis test $p < 0.0001$ for percentages; $p < 0.0001$ for MFI values.

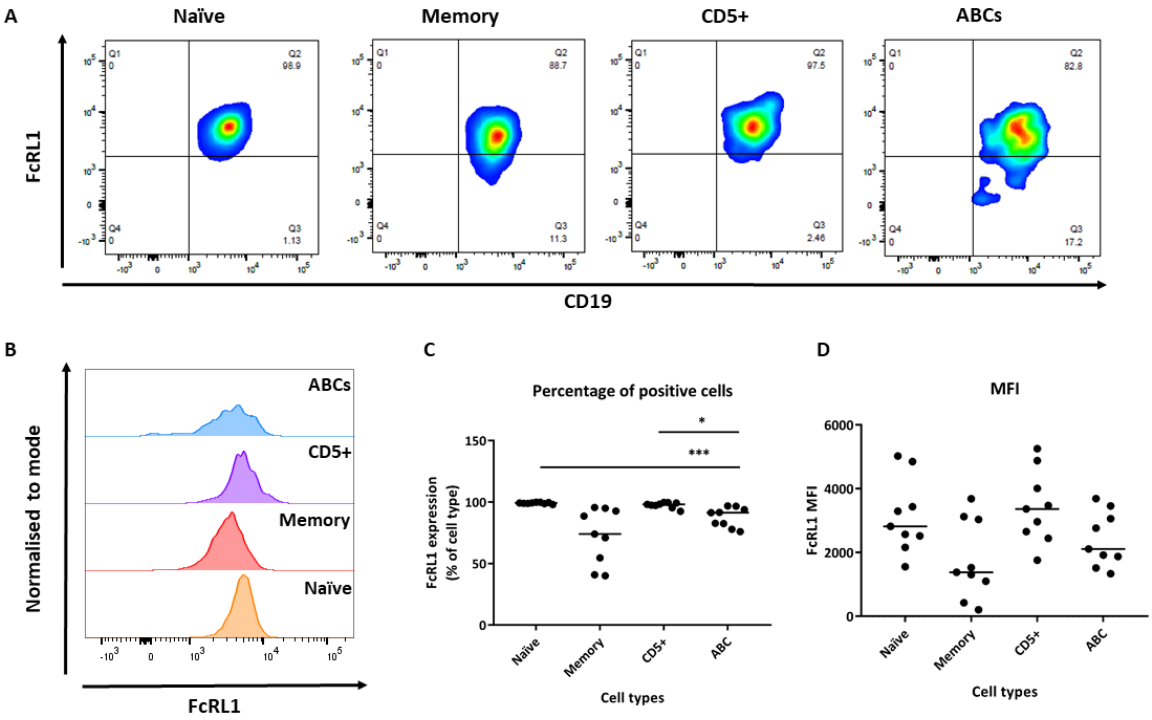

Figure 4. 18. Expression of FcRL1 in each B cell subset in early RA patients. A. Flow cytometry plots for each B cell subset after whole blood staining. FcRL1 expression against CD19, gate set from the lymphocyte population. **B.** FcRL1 expression overlay for each of the subsets. Naïve B cells are shown in orange; memory B cells in red, CD5+ B cells in purple and ABCs are shown in blue. The peaks are normalised to the same height to normalise different numbers of cells in each population. **C.** Percentage of FcRL1 positive cells in the B cell subsets (n=9). The bar represents the median. **D.** FcRL1 median fluorescence intensity (MFI) in the different B cell subsets (n=9). The bar represents the median. Statistical significance was assessed using a Kruskal-Wallis test with Dunn's multiple comparisons of the ABCs against the other subsets; * $p < 0.05$, **$p < 0.01$, *** $p < 0.001$, **** $p < 0.0001$. Kruskal-Wallis test $p < 0.0001$ for percentages; $p = 0.0355$ for MFI values.

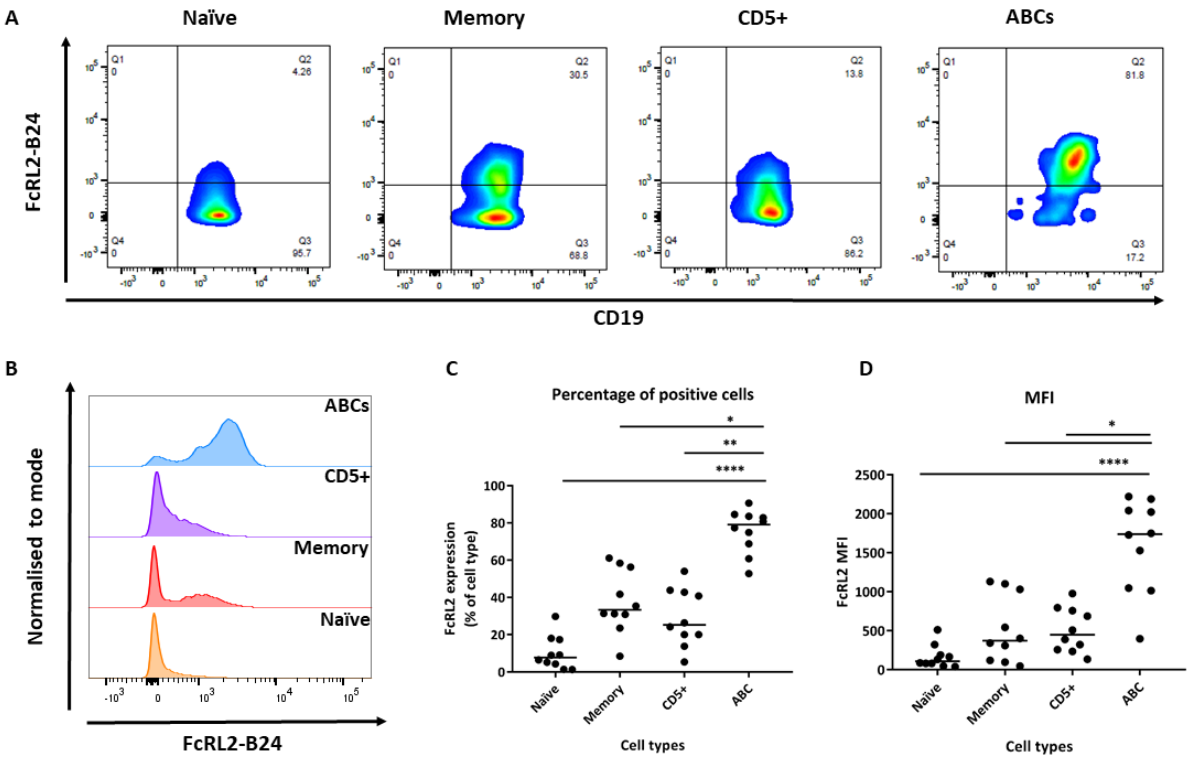

Figure 4. 19. Expression of FcRL2 in each B cell subset in early RA patients, tested using the specific FcRL2 antibody. A. Flow cytometry plots for each B cell subset after whole blood staining. FcRL2 expression against CD19, gate set from the lymphocyte population. **B.** FcRL2 expression overlay for each of the subsets. Naïve B cells are shown in orange; memory B cells in red, CD5+ B cells in purple and ABCs are shown in blue. The peaks are normalised to the same height to normalise different numbers of cells in each population. **C.** Percentage of FcRL2 positive cells in the B cell subsets (n=11). The bar represents the median. **D.** FcRL2 median fluorescence intensity (MFI) in the different B cell subsets (n=11). The bar represents the median. Statistical significance was assessed using a Kruskal-Wallis test with Dunn's multiple comparisons of the ABCs against the other subsets; * $p < 0.05$, **$p < 0.01$, *** $p < 0.001$, **** $p < 0.0001$. Kruskal-Wallis test $p < 0.0001$ for percentages; $p < 0.0001$ for MFI values.

4.4.7 Phenotypically, ABCs from eRA patients are similar to ABCs from other disease controls and healthy controls

To determine whether ABCs from early RA patients were phenotypically different from ABCs from RA patients with established disease, as well as ABCs from disease controls and healthy controls, I recruited donors for each group and assessed ABCs phenotype using flow cytometry. See Appendix A.3 and A.4 for the tables showing demographic differences between each group in each of the panels used. Due to the donors in each cohort being recruited longitudinally over two years, MFI values variate substantially and therefore only percentage of positive cells are used to assess phenotypical differences in ABCs from different disease controls and healthy controls.

Regarding percentage of positive cells for the MHC class II molecule, HLA-DR, there were no significant differences between the different groups (Figure 4.20.A). Comparing the percentage of positive cells for the co-stimulatory molecule CD40 revealed no differences between the different groups (Figure 4.20.B).

Expression of molecules upregulated after activation such as CD80 and CD86, also demonstrated no significant difference between the groups (Figure 4.21. A-B). Expression of the activation marker CD69 showed a trend for increased expression in RA patients compared to healthy controls, however, these differences did not reach significance (Figure 4.21.C).

With regard to expression of intracellular markers as Ki67 in ABCs, there were no significant differences between the groups (Figure 4.22.A). In terms of T-bet expression, the ABC-associated transcription factor, ABCs from established patients had significantly fewer positive cells than the age-matched healthy controls (Figure 4.22.B).

Immunoglobulin expression on these cells in the different groups was also assessed. IgM expression was not significantly different among the groups although established RA patients showed a trend for decreased IgM positive cells in the ABC population that did not reach significance (Figure 4.23.A). However, more established patients are needed to confirm this trend as n = 4. IgD expression was very similar between the groups (Figure 4.23.B). The percentage of IgG positive cells was slightly increased in established RA patients compared to the other group, but these differences were not significant (Figure 4.23.C). There was no difference in cells positive for IgA between groups (Figure 4.23.D).

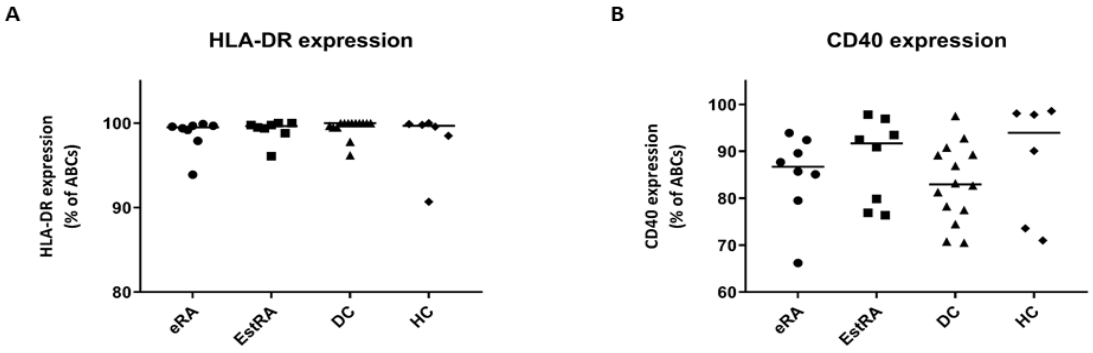

Figure 4. 20. HLA-DR and CD40 expression in ABCs from different diseases and healthy control groups. Disease controls and healthy controls donors were recruited and whole blood was stained for different flow cytometry panels. Percentage of HLA-DR positive cells (**A**) and CD40 positive cells (**B**) in the ABC subset in early RA patients (n=8), established RA patients (n=8), disease controls (n=14) and age-matched healthy controls (n=6). The bar represents the median. Statistical significance was determined using a Kruskal-Wallis test with Dunn's multiple comparisons of each groups against the others.

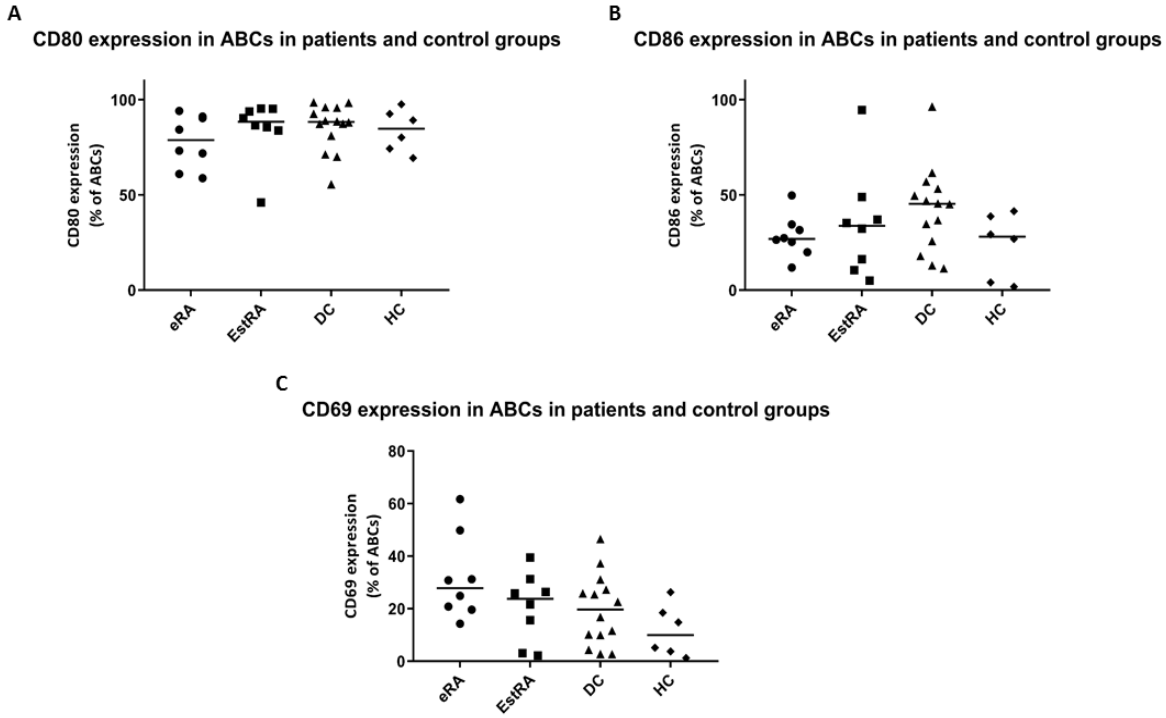

Figure 4. 21. Expression of the co-stimulatory molecules, CD80 and CD86 and the activation marker CD69 in ABCs from different diseases and healthy control groups. Disease controls and healthy controls donors were recruited and whole blood was stained for different flow cytometry panels. Percentage of CD80 positives (**A**), of CD86 positives (**B**) and of CD69 positives (**C**) in the ABC population in early RA patients (n=8), established RA patients (n=8), disease controls (n=14) and age-matched healthy controls (n=6). The bar represents the median. Statistical significance was assessed using a Kruskal-Wallis test with Dunn's multiple comparisons of each groups against the others.

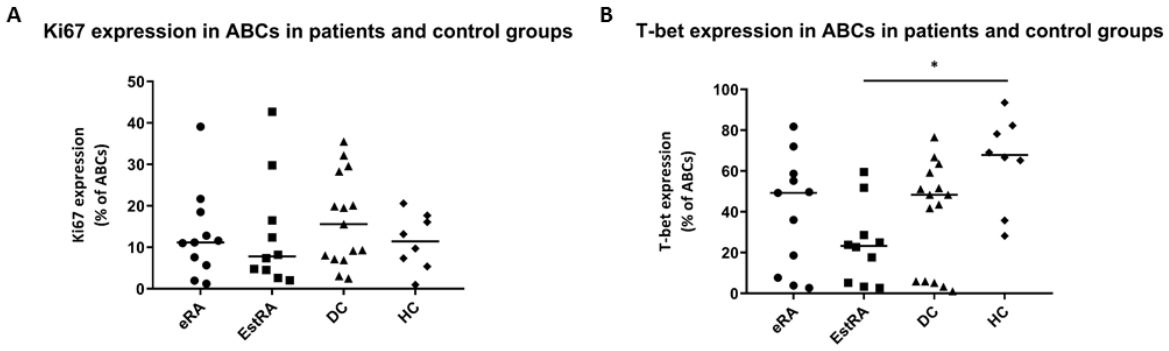

Figure 4. 22. Expression of the proliferation marker Ki67 and the transcription factor T-bet in ABCs from different diseases and healthy control groups. Disease controls and healthy controls donors were recruited and whole blood was stained for different flow cytometry panels. Percentage of Ki67 positive cells (**A**) and percentage of T-bet positive cells (**B**) in the ABC population in early RA patients (n=11), established RA patients (n=10), disease controls (n=15) and age-matched healthy controls (n=8). The bar represents the median. Statistical significance was determined using a Kruskal-Wallis test with Dunn's multiple comparisons of each groups against the others. * $p < 0.05$.

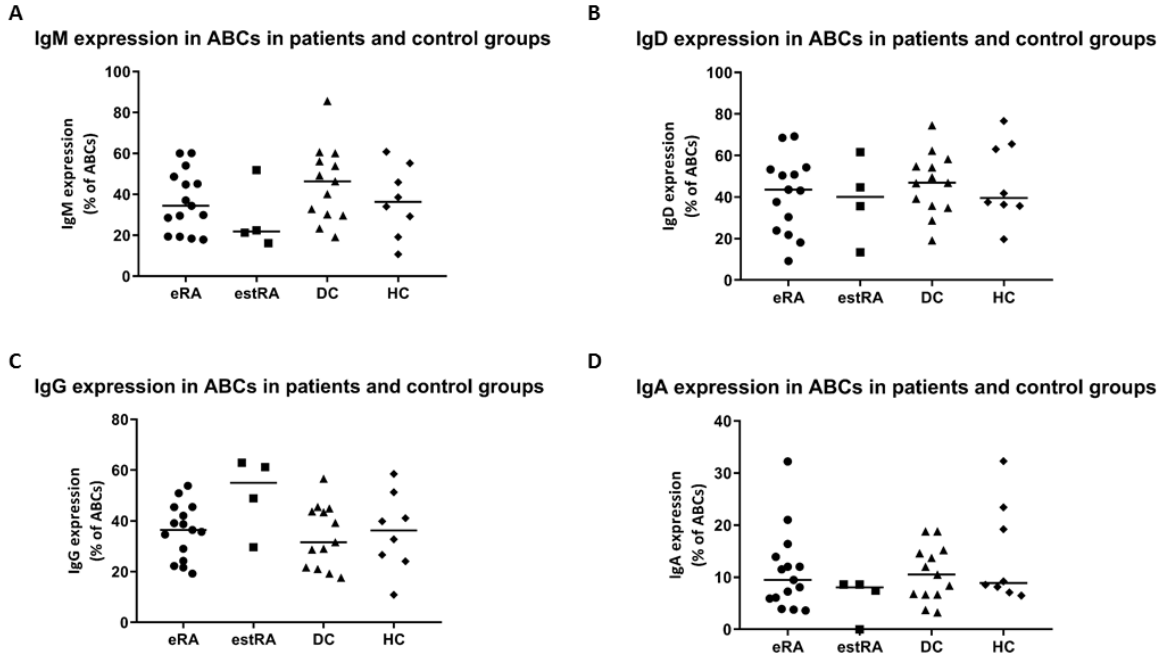

Figure 4. 23. Expression of the immunoglobulin markers in ABCs from different diseases and healthy control groups. Disease controls and healthy controls donors were recruited and whole blood was stained for different flow cytometry panels. Percentage of IgM positive cells (**A**), percentage of IgD positive cells (**B**), percentage of IgG positive cells (**C**) and percentage of IgA positive cells (**D**) in the ABC subset in early RA patients (n=15), established RA patients (n=4), disease controls (n=13) and age-matched healthy controls (n=8). The bar represents the median. Statistical significance was determined using a Kruskal-Wallis test with Dunn's multiple comparisons of each groups against the others.

Regarding FcRLs expression in the different groups, there were no significant differences in FcRL3, FcRL4 and FcRL5 expression in ABCs among the groups (Figure 4.24).

In addition, expression of FcRL1 and FcRL2 in the ABC population from the different groups was very similar and there were no differences (Figure 4.25).

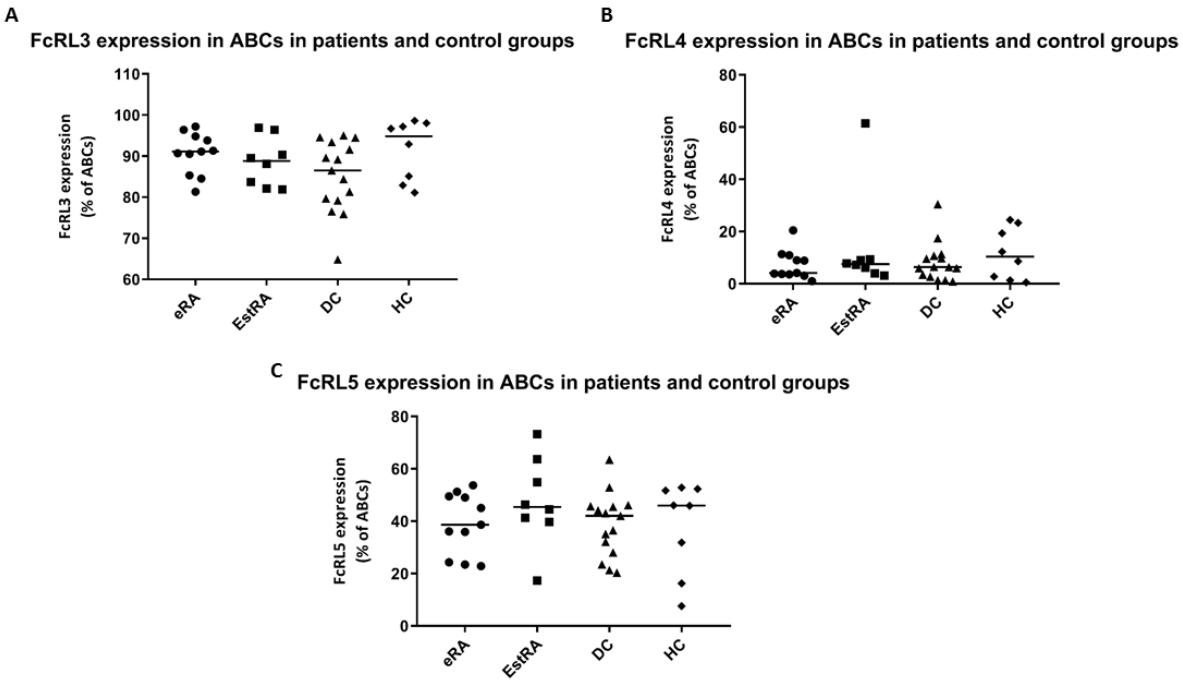

Figure 4. 24. Expression of the FcRL3 to FcRL5 in ABCs from different diseases and healthy control groups. Disease controls and healthy controls donors were recruited and whole blood was stained for different flow cytometry panels. Percentage of FcRL3 positive cells (**A**), percentage of FcRL4 positive cells (**B**) and percentage of FcRL5 positive cells (**C**) in the ABC subset in early RA patients (n=11), established RA patients (n=8), disease controls (n=15) and age-matched healthy controls (n=8). The bar represents the median. Statistical significance was determined using a Kruskal-Wallis test with Dunn's multiple comparisons of each groups against the others.

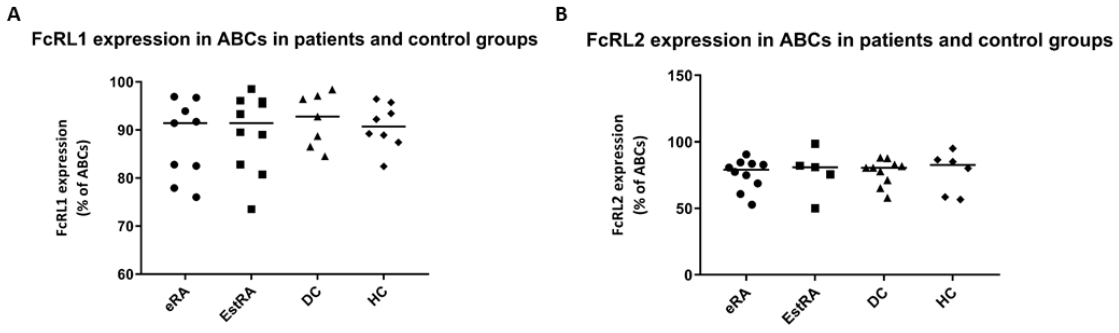

Figure 4. 25. Expression of the FcRL1 and FcRL2 in ABCs from different diseases and healthy control groups. A. Disease controls and healthy controls donors were recruited and whole blood was stained for different flow cytometry panels. Percentage of FcRL1 positive cells in the ABC subset in early RA patients (n=9), established RA patients (n=10), disease controls (n=7) and age-matched healthy controls (n=8). **B.** Percentage of FcRL2 positive cells in the ABC subset in early RA patients (n=10), established RA patients (n=5), disease controls (n=10) and age-matched healthy controls (n=6). The bar represents the median. Statistical significance was assessed using a Kruskal-Wallis test with Dunn's multiple comparisons of each groups against the others.

4.5 Discussion

In this chapter, I characterised the ABC subset from RA patients phenotypically in depth, using several flow cytometry panels. Their high expression of activation markers like CD80 and CD69 suggests that they are an activated cell population. Moreover, expression of the cell cycle marker, Ki67, indicated that some cells in the ABC subset are actively replicating and that, as reported before. B cells with this phenotype express the T-bet transcription factor. Immunoglobulin expression analysis showed that most of these cells are class-switched B cells expressing IgG. Interestingly, expression of FcRL molecules is elevated in ABCs compared to the other B cell subsets. Despite the differences between cell types, no major differences were seen between ABCs in different arthritic diseases and the healthy controls.

In the initiation of an adaptive immune response, the first signal for the engagement of an antigen-presenting cell and a T cell is interaction of MHC class II molecules bound with peptide to the T cell receptor (Katikaneni and Jin, 2019). HLA-DR is an MHC class II molecule found on the surface of antigen-presenting cells such as dendritic cells and B cells. In the view of this, HLA-DR is considered a marker of antigen-presenting cells, and the fact that it is highly expressed in ABCs (Figure 4.2) confirms the hypothesis that one of the functions of these cells might be to present antigens to T cells, thus initiating and directing immune responses, although specific functional work is needed to confirm this hypothesis. This result fits with published literature as other studies, in mice and in autoimmune patients, also reported ABCs to have higher expression of the MHC class II molecule HLA-DR (Isnardi *et al.*, 2010; Rubtsov *et al.*, 2011).

Subsequent signals to initiate the immune response include co-stimulatory receptors binding their ligands. One of these co-stimulatory molecules is CD40, which is expressed by antigen-presenting cells and it binds its ligand CD40L on activated T cells (Elgueta *et al.*, 2009). These two signals together with other complementary cytokine signals lead to an activation of the antigen-presenting cells, such as B cells. I investigated CD40 expression on ABCs compared to other B cells subsets and interestingly in the ABC population I found fewer cells positive for this marker (Figure 4.3). Contrary to the HLA-DR, expression of CD40 suggest that ABCs may not be capable of productive interactions with T cells expressing CD40L. Low CD40 expression was also reported before on B cells from SLE patients with a similar ABC phenotype described as CD11c+ B cells (Wang *et*

al., 2018). These cells in the Wang *et al.*, study quickly differentiated into plasma cells that produced IgG when co-cultured with T cells, suggesting that ABCs may already be activated B cells in a translation state between germinal centre B cells and early plasmablasts. Other studies suggested that ABCs arise from conventional B cells after a sustained CD40 stimulation (Shimabukuro-Vornhagen *et al.*, 2017). This chronic CD40 stimulation could therefore result in the CD40 downregulation seen on ABCs.

Two other co-stimulatory receptors found on B cells are CD80 and CD86. These co-stimulatory molecules are upregulated upon B cell activation and are therefore used as markers of activation (Shimabukuro-Vornhagen *et al.*, 2017). My results show higher expression of these molecules in ABCs compared to naïve B cells in addition to a high expression by memory B cells (Figure 4.4-5). These results are in line with other published phenotyping studies (Isnardi *et al.*, 2010; Rubtsov *et al.*, 2011; Shimabukuro-Vornhagen *et al.*, 2017). These results together with the HLA-DR expression results, strengthen the hypothesis that these cells are potentially potent antigen-presenting cells.

CD69 has also been described as an activation marker. Kinetic studies show this marker to increase early after infection in mice (Purtha *et al.*, 2008) and decrease during the course of infection in B cells. My results show that higher percentages of CD69+ B cells can be found in the ABC population (Figure 4.6). The only other group to assess CD69 expression on ABC-like cells was Isnardi *et al.*, which found that CD21low B cells failed to induce CD69 after BCR and CD40 triggering (Isnardi *et al.*, 2010). A possible explanation for the contradictory results is that my results are on resting ABCs, whereas Isnardi *et al.*, stimulated the cells. In addition, Isnardi *et al.*, described these cells only using CD21 and therefore, it is not possible to confirm that their CD21low B cell is the same as my ABC subset. The CD69 results reinforces the hypothesis that these cells are activated cells which may function as antigen-presenting cells.

I next assessed if there were actively proliferating cells in the ABC population (Figure 4.7). My results do show a fairly high percentage of cells in the ABC subset are positive for the proliferation marker Ki67, the percentages are similar to memory B cells which are known to proliferate. Ki67 expression is strictly associated with cell proliferation. This protein is expressed during all phases of the cell cycle except in resting cells (Scholzen and Gerdes, 2000). Only one other group has investigated Ki67 expression in ABC-like cells

(Shimabukuro-Vornhagen *et al.*, 2017); the results were in accordance with mine, with very similar percentages of positive cells in their ABC-like cells.

T-bet was originally described as a transcription factor skewing T cells towards a Th1 linage (Szabo *et al.*, 2000). However, in the last years expression of T-bet has been reported in other cell types such as dendritic cells, NK cells and B cells (Rubtsov *et al.*, 2017). Most of the published work on ABC-like cells, found that these cells express the transcription factor T-bet (Isnardi *et al.*, 2010; Rubtsov *et al.*, 2011). Because most of the T-bet+ B cells also express CD11c and these cells have similar expression of other activation markers as well as a similar chemokine receptor profile, T-bet+ B cells have also been called ABCs (Karnell *et al.*, 2017). For this reason, I assessed expression of T-bet in my ABC population. My results showed that T-bet is lowly expressed by B cells but high percentages of positive cells are found in the ABC-like population (Figure 4.8). On B cells, groups have focused on the requirement of T-bet for class-switching to IgG2a on mice (Gerth *et al.*, 2003), as well as elucidating which receptors are needed for its expression (Liu *et al.*, 2003). Nonetheless, the role of T-bet expression on B cells is still under investigation. It has been demonstrated to play an important function on viral clearance (Rubtsova *et al.*, 2013) as well as in controlling chronic viral infections (Barnett *et al.*, 2016). Additionally, T-bet expression has also been reported to play an important role in autoimmunity. ABCs expressing T-bet+ were increased in autoimmune-prone mice (Rubtsov *et al.*, 2011) and these cells were able to produced autoantibodies (Rubtsov *et al.*, 2013). In humans, some studies showed increase frequencies of these cells in patients with scleroderma, RA and SLE (Rubtsova *et al.*, 2017; Shimabukuro-Vornhagen *et al.*, 2017; Wang *et al.*, 2018). The main question still to be answered is why these cells are involved both in protective humoral responses and autoimmune diseases. Although most of the times these cells are described as CD11c+ or T-bet+ B cells, not all the CD11c+ B cells are T-bet+ and not all the T-bet+ cells are CD11c+. Therefore, there is some heterogeneity within this subset regarding origin and function of these cells that could explain these contrasting roles (Myles *et al.*, 2019).

I also explored the immunoglobulin expression profile of ABCs. Studies in mice demonstrated that after TLR7 agonist stimulation, ABCs produced some IgM and high amounts of IgG (Rubtsov *et al.*, 2011). Moreover, this IgG could recognise chromatin, proving that ABCs could be a source of autoantibodies. As described before, T-bet+ ABCs also produced IgG2a in response to viral infections (Rubtsova *et al.*, 2013). However, in humans, some discrepancies have been reported. Both subsets reported by Shimabukuro-

Vornhagen *et al.*, and Rubtsov *et al.*, described these cells as IgD-IgM- but IgG+, being therefore, class-switched B cells (Rubtsov *et al.*, 2011; Shimabukuro-Vornhagen *et al.*, 2017). On the contrary, Isnardi *et al.*, found that CD21low B cells from RA patients preferentially expressed IgM and/or IgD, whereas CD21low B cells from healthy donors were switched-class B cells enriched for polyreactive and autoreactive clones (Isnardi *et al.*, 2010). My results show that around half the population of ABCs are IgG+ (Figure 4.11). However, in this population there are still some cells positive for IgM and IgD (Figure 4.9-10). I think that these results show that the ABC population found in the blood could be heterogeneous. This is confirmed by the discrepancies in expression of other markers such as CD27 or T-bet in my ABC subset compared to other ABC subsets (Thorarinsdottir *et al.*, 2015). As explained before about T-bet expression, these studies defined ABCs as CD21low B cells, so no expression of CD11c was assessed. Not all the CD21low B cells are positive for CD11c, therefore the CD21 low population is a different population with a different phenotype to my ABCs. However, taking all the studies into account, ABCs as described in this thesis are more similar to the studies describing them as class-switched, as half of the cells are IgG+, rather than Isnardi's cells which look more like exhausted B cells which are not class-switched.

Focusing on the FcRLs, I successfully tested all the antibody clones and made sure that these are specific for each FcRL (Figure 4.14). This is very important as due to the high homology between the FcRLs, antibodies could be cross-reacting and giving false positive results (Sullivan *et al.*, 2015).

FcRL4 expression on blood cells is very scarce, which is in accordance to other published studies (Ehrhardt and Cooper, 2011). FcRL4 expression is limited to a subset of memory B cells found in mucosal-associated lymphoid tissues (Falini *et al.*, 2003). Transcriptome analysis of this subset of FcRL4+ B cells revealed expression of similar genes to ABCs, as they had low expression of CD21 and had high expression of CD80 and CD11c (Ehrhardt *et al.*, 2005). Additionally, a subset of B cells characterised by the expression of FcRL4 was described by my supervisor in Birmingham, Professor Dagmar Scheel-Toellner (Yeo *et al.*, 2015). These cells had a phenotype similar to blood ABCs, with low expression of CD21 and high expression of CD11c. The common expression of FcRL4 by mucosal B cells and synovial fluid B cells and the enrichment of IgA expressing cells reinforces the hypothesis that RA pathogenesis could start within mucosal inflammation in the gum, the gut and the lungs (Catrina *et al.*, 2014). However, additional studies are needed to

determine if these FcRL4+ B cells are generated in the mucosa and later migrate to the synovia to contribute to RA pathogenesis. Another interesting role for FcRL4, shared by ABCs, is its ability to attenuate BCR signalling but augment B cell activation through TLR9 signalling (Sohn *et al.*, 2011). The ligand for FcRL4 has been postulated to be heat-aggregated IgA (Wilson *et al.*, 2012) and the ligand for TLR9 is DNA fragments containing CpG motifs. Interestingly, both these ligands are found in the synovial fluid of patients with RA (Hajizadeh *et al.*, 2003; Aleyd *et al.*, 2016), so it is feasible that FcRL4 in RA, may enhance immune activation through TLR9 signalling.

FcRL5 has been reported to be expressed by naïve and memory B cells from the blood, with high expression levels found on plasma cells from the spleen, the bone marrow and the tonsils (Polson *et al.*, 2006). There are some discrepancies between FcRL5 expression in blood in the literature; Polson et al detected expression in blood B cells, however, other studies showed no expression on primary B cells (Ise *et al.*, 2005). These differences could be due to different antibody clones used in each study, as both groups generated their antibodies. My results showed low expression of FcRL5 on most of the B cell subsets except for the ABCs, with about half the cells positive for this receptor (Figure 4.16). FcRL5 expression on ABCs have been previously described by other groups at the mRNA levels and the protein levels (Isnardi *et al.*, 2010; Lau *et al.*, 2017; Wang *et al.*, 2018). FcRL5 function is still under investigation and there is some disagreement on whether this receptor inhibits B cell activation (Haga *et al.*, 2007) or if it is able to enhance B cell proliferation and drive the development of IgG+ and IgA+ B cells (Dement-Brown *et al.*, 2012). These differences could be due to the use of different cells, as one study used cell lines and the other used primary B cells from blood.

My results for FcRL3 expression by ABCs are especially interesting. Some studies reported very low expression of FcRL3 on peripheral blood B cell (Polson *et al.*, 2006), however, other studies show some expression of FcRL3 by circulating B cells with an increase in expression by memory B cells (Li *et al.*, 2013). However, my results, while confirming some expression on memory, as well as naïve and CD5+ B cells, show that FcRL3 expression on ABCs is extremely high and that all the ABCs have expression of this receptor (Figure 4.17). Studies that have investigated FcRL3 expression on B cells reported a potential role for FCRL3 in memory B cells with innate-like characteristics (Li *et al.*, 2013). The influence of FcRL3 on innate-like responses has shown that FcRL3 engagement increased TLR9 triggered peripheral blood B cell activation, survival and activation

markers expression. On the contrary, this signal inhibited antibody production and plasma cell differentiation (Li *et al.*, 2013). These findings together with the fact that ABCs are not fully differentiated into plasma cells and have high expression of HLA-DR and co-stimulatory molecules, reinforces the hypothesis that ABCs are potential antigen-presenting cells which respond to innate-like stimuli via TLRs. Another fascinating aspect of FcRL3 is its implication in autoimmune diseases. For a variety of disorders, disease risk associations for single nucleotide polymorphisms (SNP) located in regions of FcRL genes have been reported (Kochi *et al.*, 2005). A SNP on the FcRL3 promoter region generated a more orthodox NF-κB binding sequence that exerted a regulatory effect on FcRL3 transcript and protein expression as well as on auto-antibody production (Gibson *et al.*, 2009). Moreover, our group has reported that site-specific DNA methylation upstream of the FcRL3 gene mediates expression of this gene (Clark *et al.*, 2020). Due to its very high expression on ABCs and its potential role as an innate mediator, together with its association in autoimmune disease, I decided to further investigate the role of FcRL3 in B cell function (see Chapter 7).

FcRL1 expression is present on all B cells and for this reason, it can be considered a pan B cell marker. It appears at the pre-B cell stage and it increases with maturation, peaking on naïve and memory B cells (Polson *et al.*, 2006). My results show that FcRL1 is expressed by all the B cell subsets (Figure 4.18); however, we see lower numbers of FcRL1+ cells in the memory and the ABC population. FcRL1 is the only FcRLs family member with two ITAM-like sequences and appears to act as a co-activation receptor. Its ligation by receptor-specific monoclonal antibodies results in its tyrosine phosphorylation (pTyr) and stimulates human B cell proliferation (Leu *et al.*, 2005). Moreover, crosslinking FcRL1 with the BCR enhances calcium flux augmenting B cell activation and proliferation. Accordingly, the lower expression of FcRL1 seen in ABCs is in line with other studies showing that ABCs do not respond to BCR stimulation, but they do respond to TLRs (Rubtsov *et al.*, 2011). FcRL1 acts as a co-activator in adaptive signals, however, other FcRLs such as FcRL3, which are increased in ABCs, tend to respond together with colligation of TLRs and would be better at amplifying innate immune responses (Ehrhardt and Cooper, 2011). These findings support a role for ABCs as innate immune cells (Rubtsov *et al.*, 2017).

Lastly, FcRL2 expression in peripheral blood has been described in circulating CD20+ B cells (Polson *et al.*, 2006). My results show that most of these B cells are found on the memory B cell subset and in the ABCs (Figure 4.19). This is the first time FcRL2 protein

expression is reported on ABCs, as all the previous studies have only checked expression of FcRL3-5 (Isnardi *et al.*, 2010; Lau *et al.*, 2017; Wang *et al.*, 2018). FcRL2 function is still unknown. There are some studies investigating FcRL2 function together with FcRL3 and FcRL5 and mutated receptors which indicate that FcRL2 co-engagement with the BCR leads to an inhibition of BCR signalling (Jackson *et al.*, 2010). More studies investigating the role of FcRL2 in B cell function, are needed. This is especially important because FcRL2 is highly expressed on malignant B cell leukaemia and it could, therefore, be a potential therapeutic target (Ise *et al.*, 2005).

In terms of phenotypic expression in the different disease groups, there are no differences in expression of the different phenotypic markers I assessed (Figure 4.20-25). As explained in Chapter 3, one of the reasons for this finding could be that the blood is not the most informative tissue to investigate. In patients with RA, it has been demonstrated that most of the B cells that infiltrate the synovia have a similar phenotype as ABCs, with high expression of CD11c and low expression of CD21 (Amara *et al.*, 2017). Therefore, I hypothesised that circulating ABCs found in peripheral blood are similar phenotypically between HCs and inflammatory arthritis patients, but in inflammatory arthritis, ABCs also migrate to sites of inflammation where they become activated and contribute to pathology and joint damage.

The only difference between ABCs from HCs and RA patients was in T-bet expression (Figure 4.22). Even though expression seems to be quite variable between individuals in all the disease groups, there is significantly higher expression in healthy controls compared to established RA patients. In addition, RA and disease controls with early disease also have higher expression of T-bet than established patients, although these differences are not significant. This could be due to the treatment the patients with established disease receive. It is difficult to record the treatment established patients are receiving, due to the structure of the established clinics. These patients with chronic disease are treated with immune system suppressant drugs and these could influence ABCs function and alter their transcriptional profile, as it has been reported before on T cells (Ponchel *et al.*, 2005). Interestingly, three patients with low percentages of T-bet positive cells had been treated with steroids, being therefore a possible explanation for their low expression of the transcription factor. T-bet has been shown to induce CXCR3 expression in T cells (Koch *et al.*, 2009), and CXCR3 promotes cell migration into sites of inflammation (Groom and Luster, 2011b). Another explanation for the decreased T-bet expression in established

patients would be that cells with higher expression of T-bet, would have higher expression of CXCR3 and therefore migrate into the inflamed joints. These results are in line with my results from Chapter 3, which show that established patients have higher percentages of ABCs in the synovial fluid than early RA patients.

4.6 Conclusions

In this chapter, I performed an extensive phenotypic characterisation of the ABCs subset using flow cytometry. Based on previously published literature, I hypothesised that ABCs are activated B cells with a potential capacity for antigen presentation.

I confirmed this hypothesis and showed that ABCs have high expression of co-stimulatory and activation molecules, like CD80, CD86 and CD69. Moreover, a high proportion of B cells in the ABC subset are actively proliferating and express the transcription factor T-bet. Immunoglobulins expression analysis revealed that the ABCs population is heterogeneous. A high percentage of ABCs, similar to memory B cells, are class-switched IgG-expressing B cells. However, some ABCs also express IgD and IgM. This reinforces the hypothesis that, although being a heterogeneous population, some of these cells are antigen-experienced B cells and could be producing antibodies. Additionally, to my knowledge, this is the first time that a deep phenotyping looking at all five FcRL receptors has been performed on ABCs at a protein level. My results showed a very high expression of FcRL2-5 and a lower expression of FcRL1 on ABCs compared to the other B cell subsets. As discussed before, the effect of FcRL2-5 signalling in conjunction to BCR and TLRs is still under investigation. Nevertheless, FcRL2-5 engagement seems to enhance TLRs signalling and therefore potentially marks an innate-like B cell subset which is in concordance to ABCs responding to TLR7 and TLR9. Differences in the ABC phenotype in different diseases and healthy controls was not found; ABCs from different disease groups have a similar protein expression profile.

In summary, I confirmed the hypothesis that ABCs are an active, proliferating and class-switched B cell subset with a potential role in antigen presentation. Despite the surface expression results, functional work is needed in order to confirm the role of these cells.

Chapter 5. Transcriptional characterisation of ABCs

5.1 Introduction

Alongside characterisation of ABC surface marker expression in early RA patients and controls, I also aimed to assess the transcriptome profile of these cells and compare gene expression between the different B cell subsets, as well as between RA patients and controls.

Murine studies showed that ABCs express transcripts of Ig heavy chain, transcription factors involved in plasma cell differentiation and the marker *CD138*, supporting their role as a unique precursor of antibody-secreting plasma cells (Rubtsov *et al.*, 2011). Curiously, ABCs also expressed genes found in helper and cytotoxic T cells such as *T-bet*, *perforin* and *granzyme A* as well as high expression of adhesion molecules such as integrins.

Human studies in ABCs/CD21low B cells from healthy donors showed that these cells had high expression of chemokine receptors and adhesion molecules involved in extravasation and recruitment to sites of inflammation, such as *CD11a*, *CCR3*, *CCR5*, *CCR10* and *CXCR2* (Shimabukuro-Vornhagen *et al.*, 2017). In addition, their expression of lymph node homing receptors was low. Transcriptome analysis of ABCs from patients with SLE confirmed that these cells have highly upregulated plasma cell transcripts such as *BLIMP1*, *AID* and *XBP1*. Nevertheless, their low expression of CD38 and CD138 suggests that these cells may be precursors of plasmablasts (Wang *et al.*, 2018). In addition, these cells had upregulation of inflammation homing chemokine receptors such as *CXCR3* and downregulation of lymph node homing receptors such as *CXCR4* and *CXCR5*, confirming the conclusions of other groups.

Alternatively, some studies described CD21low B cells as anergic and found that this subset downregulated genes encoding survival and activation proteins, as well as cytokine and chemokine receptors (Isnardi *et al.*, 2010). In contrast, this subset up-regulated inhibitory receptors known to suppress B cell activation and proliferation. Other studies also showed that CD11c+T-bet+ B cells had high expression of inhibitory receptors such as *FcRLs*, *CD72* and *CD32B*, in contrast to low expression of markers associated with B cell activation such as *CD40* and *NFKBIA* (Karnell *et al.*, 2017). This would support the idea that ABCs poorly respond to BCR stimulation. In addition, these cells had upregulation of apoptosis-related transcripts such as caspases, suggesting they are prone to cell death. This together with their downregulation of survival genes such as cyclins, supports the suggestion that these cells might have reduced survival and proliferation (Isnardi *et al.*,

2010; Saadoun *et al.*, 2013). Additionally, some studies showed that ABCs had high expression of *TNF* and *IFN* receptors, reinforcing the hypothesis that these cells play an important role in autoimmune diseases (Isnardi *et al.*, 2010; Saadoun *et al.*, 2013).

Transcriptional analysis of the FcRL4+ B cell subset with a similar phenotype as the ABCs showed high expression of the cytokines *RANKL* and *TNF-α* (Yeo *et al.*, 2015). Moreover, these cells had high expression of the chemokine receptors *CCR1* and *CCR3* which would explain their homing and retention to the inflamed synovium. In support of this finding, RNA sequencing confirmed that FcRL4 expressing B cells had high expression of *RANKL* and *CD11c* as well as inflammatory recruitment chemokine receptors such as *CCR1* (Amara *et al.*, 2017). Nonetheless, these cells showed low expression of *BLIMP1* and *XBP1* suggesting that these cells are not differentiating into antibody-secreting plasma cells.

All in all, although the discrepancies in whether these cells are an anergic or an activated subset, gene expression analysis revealed high expression of adhesion molecules and inflammatory chemokine receptors suggesting that ABCs are able to migrate into inflamed tissue. Moreover, all the studies conclude that these cells are not plasma cells but probably a precursor of them. The origin of ABCs remains unknown, studies in the generation of T-bet+ B cells show that they would be generated via BCR stimulation together with triggering of endosomal TLRs in a Th1 cytokine milieu composed of IL-21 and IFN-γ and absence of IL-4 (Knox *et al.*, 2019).

Additionally, previous work done in our group compared expression of six retrotransposons in different white blood cells from early RA patients (Cooles *et al.*, unpublished results). Higher expression of these retrotransposons was found in the B cell and the CD4+ T cell populations compared to CD14+ monocytes, plasmacytoid DCs and myeloid DCs (Figure 5.1 and 5.2). In the case of the endogenous retrovirus sequence LTR5 5' expression on B cells was significanlty higher compared to all the other cell subsets (Figure 5.1.A). Interestingly, retroelements have been shown to be transcribed to RNA and bind and signal through TLRs (Mu *et al.*, 2016). These results together with the evidence showing that ABCs are generated through TLR7 signalling (Rubtsov *et al.*, 2011; Rubtsov *et al.*, 2013) lead to the hypothesis that the high expression of retrotransposons could activate TLR7 in the B cells and drive ABC skewing. Accordingly, expression of these retroelements would be higher in ABCs compared to other B cells. Moreover, previous work done on RA and retrotransposons showed high expression of the LINE-1 retroelement in RA synovial tissue

compared to reactive arthritis' synovium (Neidhart *et al.*, 2000; Ali *et al.*, 2003). Therefore, expression of retroelements in the different subset of B cells as well as in the different cohorts was evaluated.

Due to the lack of studies of ABCs from RA patients, I used NanoString Technologies to analyse the gene expression profile of the ABC subset from RA patients and compare this to other B cell subsets from RA patients. I also compared the ABC transcriptome from RA patients to the ABC transcriptome from psoriatic arthritis (PsA) patients and age-matched healthy controls, to identify RA-specific gene expression in this novel B cell subset.

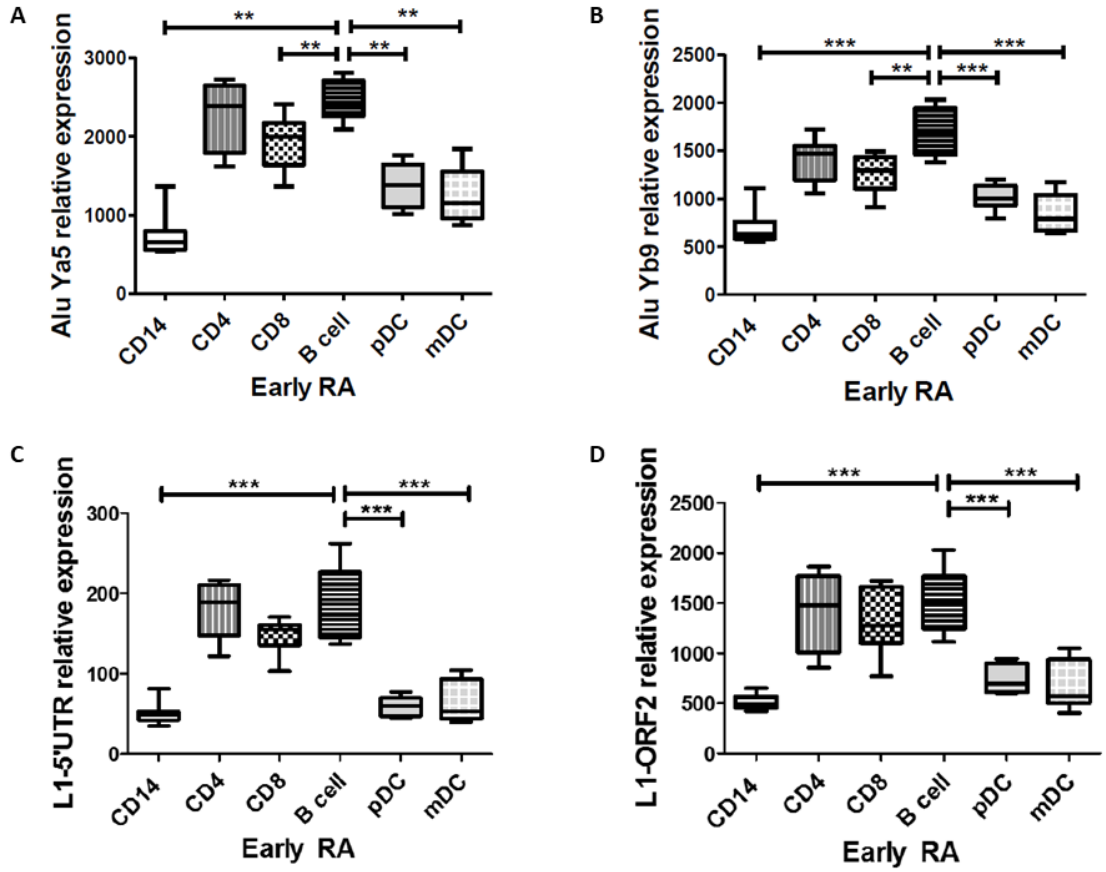

Figure 5. 1. Expression of non-long terminal repeat retroelements in different immune cell subsets in early RA. Peripheral blood immune cells (plasmacytoid dendritic cells, pDCs; myeloid dendritic cells, mDCs; B cells, CD4+ T cells, CD4; CD8+ T cells, CD8; CD14+ monocytes, CD14) from early RA patients (n=8) were flow cytometry cell sorted and cellular RNA was analysed using NanoString nCounter technology for non-long terminal repeat retroelements. **A.** AluYa5 activity. **B.** AluYb9 activity. **C.** L1-5'UTR activity. **D.** L1-ORF2 activity. Data are presented as box and whisker plots, in which the horizontal line represents the median value, the box represents upper and lower quartiles and the error bars represent range. Kruskal-Wallis test. ** $p<0.01$, ***$p<0.001$. Taken from (Cooles *et al.*, unpublished results).

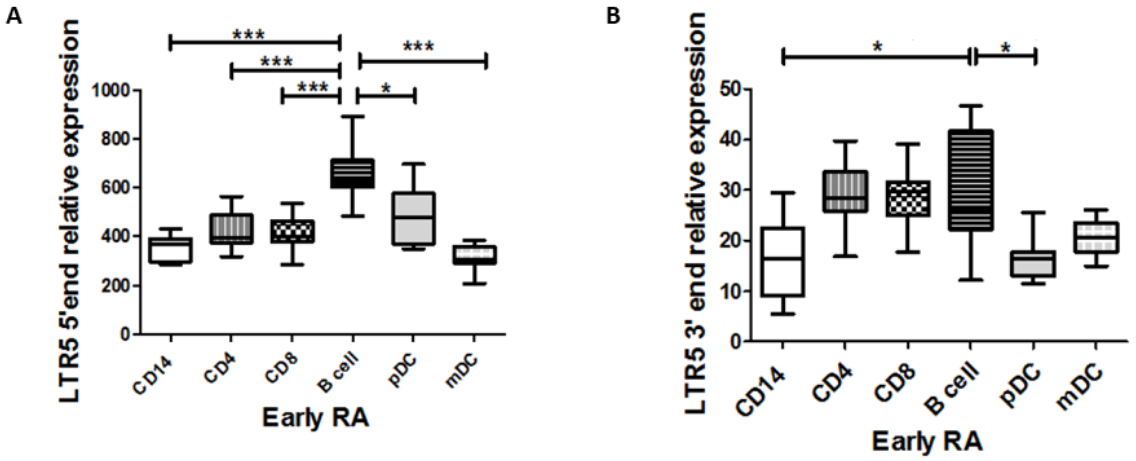

Figure 5. 2. Expression of long terminal repeat retroelements in different immune cell subsets in early RA. Peripheral blood immune cells (plasmacytoid dendritic cells, pDCs; myeloid dendritic cells, mDCs; B cells, CD4+ T cells, CD4; CD8+ T cells, CD8; CD14+ monocytes, CD14) from early RA patients (n=8) were flow cytometry cell sorted and cellular RNA was analysed using NanoString nCounter technology for non-long terminal repeat retroelements. **A.** LTR5 5' activity. **B.** LTR5 3' activity. Data are presented as box and whisker plots, in which the horizontal line represents the median value, the box represents upper and lower quartiles and the error bars represent range. Kruskal-Wallis test. *p<0.05, ** p<0.01, ***p<0.001. Taken from (Cooles *et al*., unpublished results).

5.2 Chapter hypothesis and aims

The work described in this chapter addresses the hypothesis that ABCs have a unique transcriptome compared to other B cell subsets and that ABCs from RA patients show a different gene expression profile to ABCs from PsA disease controls and healthy controls.

Therefore, the aims of this chapter were to:

1. Characterise the gene expression profile of ABCs compared to other B cell subsets.
2. Determine if the ABC transcriptome from RA patients is different to that from PsA patients and age-matched healthy controls.
3. Determine if ABCs show higher expression of retroelements compared to other B cell subsets.
4. Determine if eRA B cells have higher expression of retroelements compared to B cells from PsA and healthy controls.

The specific objectives were:

1. Optimise the sorting of pure B cell populations.
2. Compare gene expression between ABCs and other B cell subsets in RA patients.
3. Compare gene expression between ABCs from RA patients and ABCs from PsA patients and healthy controls.
4. Compare gene expression of the retroelements between ABCs and other B cell subsets in RA patients.
5. Compare gene expression of the retroelements between B cells from RA patients and B cells from PsA patients and healthy controls.

5.3 Methods

5.3.1 Flow cytometry cell sorting of B cell subsets for NanoString analysis

Briefly, isolated PBMCs were resuspended in cold FACS buffer to a final concentration of 20 x 10^6 cells/ml. To each tube, 1ml of this cell suspension was added and centrifuged at 400g for 8 minutes at 4°C. The cell pellet was resuspended in the fluorophore labelled antibody mix (see table 2.6 in Chapter 2 for the list of antibodies used). After the staining time, cells were stained for Zombie UV (Biolegend, CA, USA) in PBS to identify dead cells. Cells were incubated at 4°C for 15 minutes in the dark and then washed twice with FACS buffer. Cells from each tube were transferred to a FACS tube and the volume was made up to 2ml with FACS buffer, resulting in a cell density of 10 x 10^6 cells/ml.

Right before sorting, the cells were strained through a 30µm cell strainer (CellTrics - Sysmex, IL, USA). This was performed immediately prior to sorting to avoid small cell clumps blocking the sorter's nozzle. The BD FACSARIA II (Becton Dickinson, NJ, USA) with a 70µm nozzle was used to sort the four immune cell subsets.

The gating strategy used to sort the four subsets is shown in Figure 5.3. After excluding dead cells and doublets using two doublet gates, lymphocytes were gated using SSC-A vs FSC-A. From the lymphocyte gate, B cells were gated using CD19 vs CD3/CD33, therefore excluding T cells and dendritic cells. From the B cell gate, the ABCs were gated using CD11c vs CD21. From the rest of the cells, CD5+ cells were gated using CD5 and CD19. Finally, from the CD5- fraction, naïve (IgD+CD27-) and memory (IgD-CD27+) B cells were gated.

5.3.2 Post-sorting sample preparation for NanoString analysis

For each subset, 15,000 cells were sorted into 1.5ml microcentrifuge tubes containing 280µl of RF10 (RPMI +10% FCS) at 4°C. After sorting, the cells were transferred into a 96-well plate and spun at 400g for 4 minutes. The supernatant was removed by flicking and blotting the plate. Cells were then resuspended in 1.6µl of RLT buffer, transferred, together with the residual RF10 volume (resulting in 5µl total volume), to a 0.2ml PCR tube and stored in the -80 freezer until all the patients were recruited. Once the recruitment was completed and the NanoString chips were ready to run, a total volume of 5µl of lysate for each of the cell subsets was loaded onto the NanoString chip and the protocol was followed according to standard nCounter instructions.

See Chapter 2 section 2.5 on NanoString Technologies for the methodology, the genes analysed and the computational analysis performed in collaboration with our group's bioinformatician, Najib Naamane.

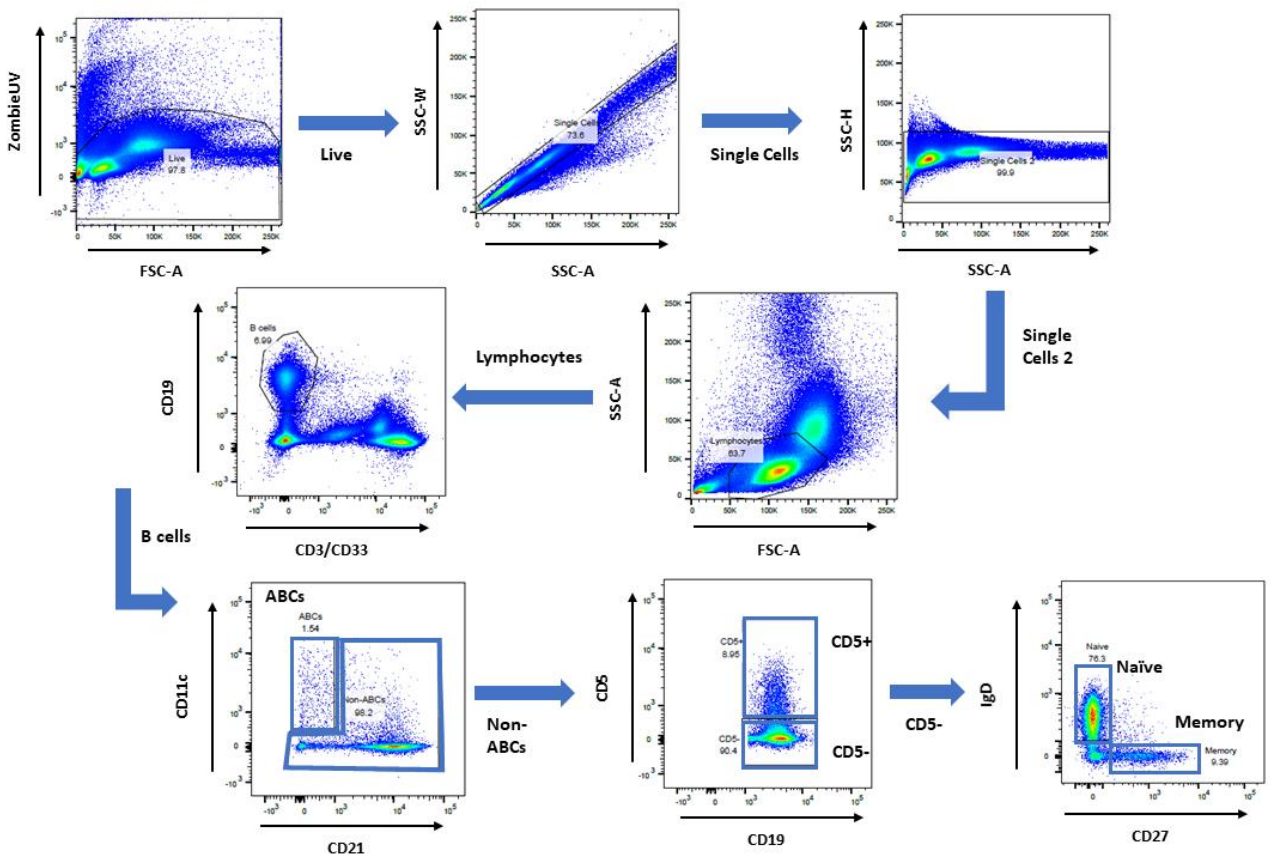

Figure 5. 3. Gating strategy used for the sorting of each B cell subset for gene expression analysis. Example of the gating strategy used to sort the four B cell populations for the gene expression analysis. After excluding dead cells and doublets twice, lymphocytes were gated using SSC-A vs FSC-A. From the lymphocyte gate, B cells were gated using CD19 vs CD3/CD33. From the B cell gate, the ABCs were gated using CD11c vs CD21. From the rest of the cells, CD5+ cells were gated using CD5 and CD19. Finally, from the CD5- fraction, naïve (IgD+CD27-) and memory (IgD-CD27+) B cells were gated. Gates were set based on an initial FMO and every time that a donor was recruited the gates were checked to ensure that the populations were inside the gate.

5.4 Results

5.4.1 Sorted B cell populations show a purity greater than 85%

For the gene expression analysis, the four B cell subsets had to be isolated from the rest of the PBMC fraction. For this reason, I flow cytometry cell sorted the four B cell subsets; naïve, memory, CD5+ B cells and ABCs. However, due to the importance for high purity sorting, the gating strategy was optimised to make sure highly pure populations were isolated. In order to check whether the sorted cells were pure, some of the sorted cells were reacquired on the FACSAria II sorter to check their purity (Figure 5.4). Figure 5.4.A shows the gates for each subset before sorting, from the mixed population. Figure 5.4.B shows each of the purified B cell subsets after reacquisition. The purity of ABCs was greater than 85%, the purity of CD5+ B cells was 91.3%, the naïve B cell purity was 98.6% and the memory B cells 93.2%. These purities may be underestimated due to slight changes in morphology and fluorescence of sorted cells causing spreading of the population.

In addition to purity checks, the cells were cytospun and stained with a Wright-Giemsa staining in order to assess cell morphology and appearance (Figure 5.5). The Wright-Giemsa staining colours the cytoplasm light pink and the nuclei dark purple. Examples of naïve B cells are shown in Figure 5.5.A. Memory B cells are shown in Figure 5.5.B; these cells are slightly bigger than naïve B cells. Similar to naïve B cells, CD5+ B cells (Figure 5.5.C) are round and smaller than memory B cells. ABCs are shown in Figure 5.5.D; ABCs are very much like memory B cells in terms of size. Moreover, memory and ABCs show a less round shape with some small dendrites and a bigger and more granular cytoplasm.

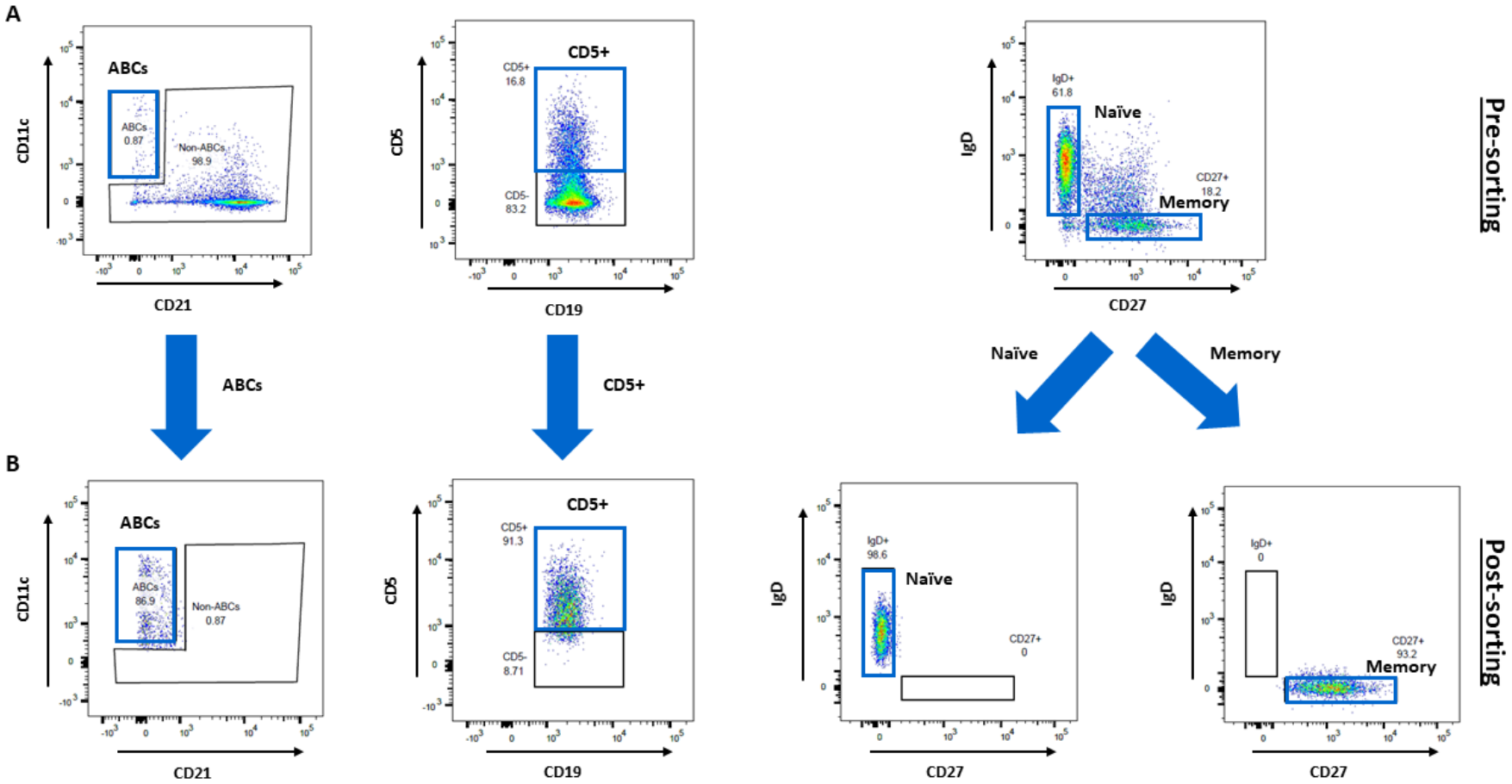

Figure 5. 4. Purity check of the sorted B cell subsets. A. Flow cytometry plots of the gates used to sort each of the B cell subsets from the pre-sorted mixed population of B cells. Subsets of interest are squared in blue. **B.** After sorting, some cells from each of the subsets were rerun in the FACSAria II sorter to check if the sorted populations were pure. Each sorted population is found in the correct gate. Gates for the pre-sorting were set based on an initial FMO as explained before. To check for purity, gates for the post-sorting were the same as for the pre-sorting sample.

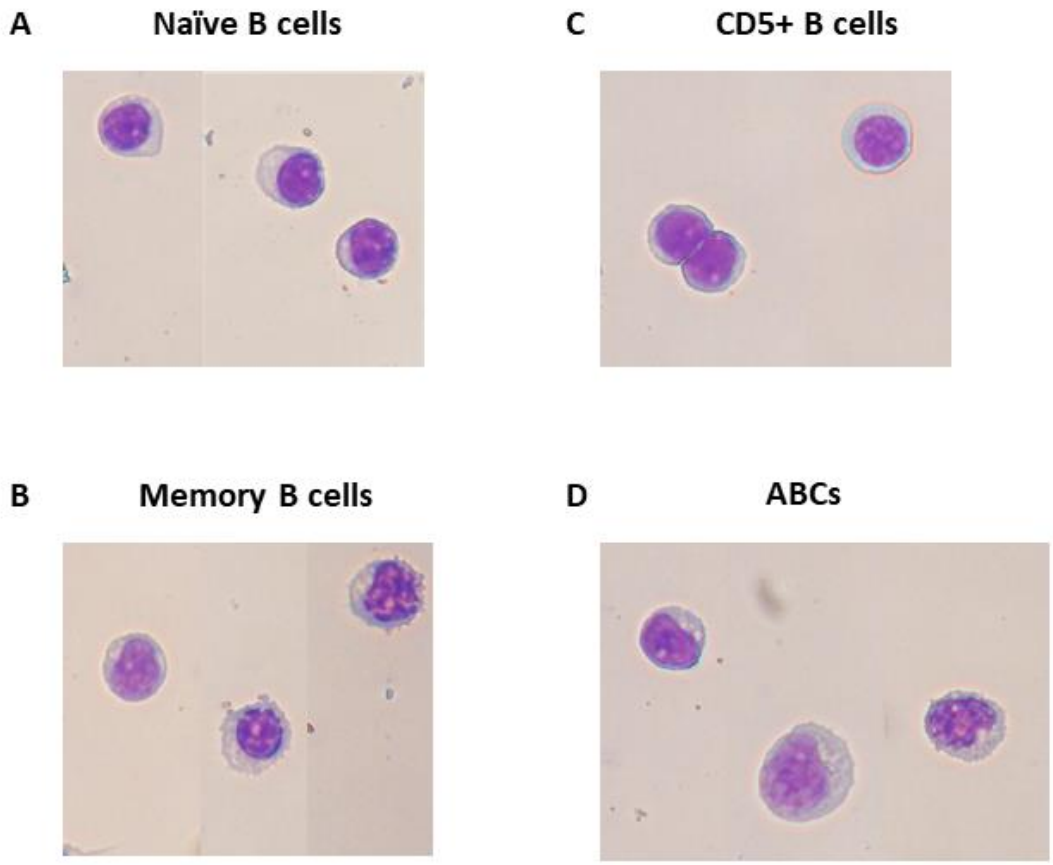

Figure 5. 5. Cytospin images of the sorted B cell subsets. Cytospin pictures to assess morphology and appearance were performed on the four sorted B cell subsets. Cytospins were stained with Wright-Giemsa stain, which stains the cytoplasm light pink and the nucleus dark purple. **A.** Naïve B cells, **B.** Memory B cells, **C.** CD5+ B cells and **D.** Age-associated B cells.

5.4.2 Cohorts demographics

Once I had confirmed that the sorted populations were pure, I recruited early RA and PsA patients, as well as age-matched healthy controls for B cell subset sorting. Early RA patients were recruited from the Newcastle Early Arthritis Clinic (NEAC) and were therefore naïve to any DMARDs or other drug treatment. These patients were double positive for RF and anti-CCP antibodies. As a disease control, patients diagnosed with psoriatic arthritis were used; these patients were also early-untreated patients. Early PsA patients were double negative for RF and anti-CCP antibodies. Healthy controls were volunteers who had no personal history of rheumatological or autoimmune disease. Demographic data are shown in Table 5.1. There were no significant differences between the age and the sex of the groups. There was a significant difference, as expected, in the autoantibody seropositivity between the two disease groups. The differences between groups for the age and the sex were calculated comparing all three groups, however, for the serostatus only RA and PsA were compared.

	Early RA patients	**Early PsA patients**	**Healthy controls**	**Difference between groups**
Number	4	4	4	-
Age (years; median and range)	70 (60 - 80)	70 (63 - 79)	63 (61 - 73)	>0.9[#]
Percentage of females (n and percentage)	2 (50%)	2 (50%)	2 (50%)	>0.9[+]
DAS28 (median and range)	5.74 (4.65 - 6.37)	-	-	-
Seropositive – anti-CCP+ and RhF+ (n and percentage)	4 (100%)	0 (0%)	-	0.03[*]

Table 5. 1. Demographic characteristics for all the cohorts used for NanoString gene expression analysis. Flow cytometry cell sorting was performed on the disease cohorts (early RA patients, n = 4 and early PsA patients, n = 4) and the healthy control cohort (n = 4) to assess gene expression using NanoString Technologies. # Kruskal-Wallis test with Dunn's multiple comparisons. + Chi-square test. * Fisher's exact test.

5.4.3 Data pre-processing and quality assessment

Before performing differential gene analysis, data quality was assessed using the arrayQualityMetrics (Kauffmann *et al.*, 2009) Bioconductor package to detect and remove any outlier samples. An overview of the bioinformatics performed can be found in Chapter 2 section 2.5. NanoString, like other methods to assess gene expression, uses gene counts to quantify gene expression, meaning it counts the number of times a gene is detected. First, the gene counts for each sample are normalised to the housekeeping genes to correct for differences in amounts of mRNA. Then, for each normalised sample, arrayQualityMetrics computes three different metrics corresponding to the gene counts. Samples with at least two metrics exceeding the threshold were considered as outliers. After running the arrayQualityMetrics and excluding the outliers, the normalisation was run again and further outliers were also removed. On the third cycle of arrayQualityMetrics, no outliers exceeded the threshold, in total four samples were flagged as outliers (2 ABCs samples from disease controls, 1 ABC sample from a healthy control and 1 memory B cell sample from a disease control) and were excluded from further analysis. Because the gene counts dataset is a multivariate data set with a lot of variables, a PCA plot helps extracting the important information and plotting it in new variables called principal components. These new variables correspond to a combination of the original variables, therefore, PCA reduces the dimensionality of a multivariate data to two principal components that can be visualised in a graph. The PCA plot shown in Figure 5.6 represent one of the metrics used to assess data quality. These plots show variance in the data set, allowing for the detection of outlier samples. Figure 5.6.A shows the results of the first cycle of arrayQualityMetrics. In this cycle, three ABCs samples, two from PsA patients and one from a HC were flagged (circled). Figure 5.6.B shows the results of the second cycle. One more sample was flagged and excluded, it corresponded to memory B cells from a PsA patient. Figure 5.6.C shows the last cycle of quality control, no outliners were detected in more than two methods therefore no more samples were excluded.

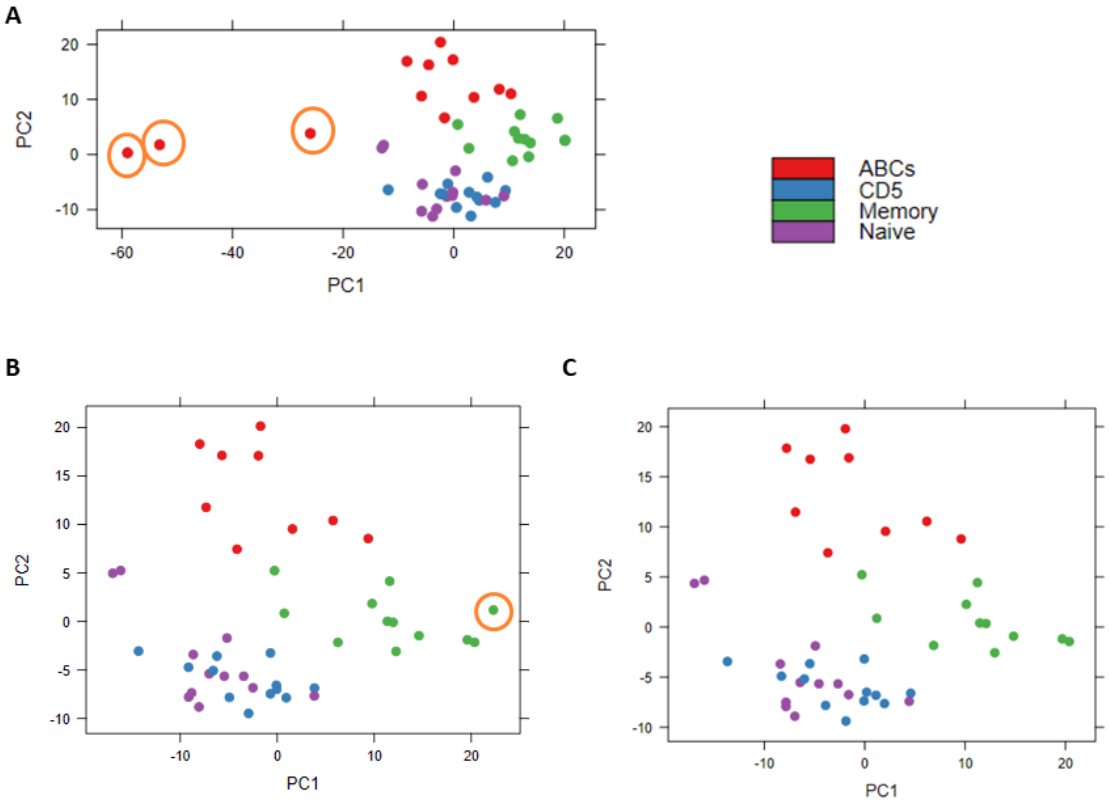

Figure 5. 6. Principal component analysis of the normalised samples. Principal component analysis was run on the normalised data from the NanoString chip using the arrayQualityMetrics Bioconductor package in R software. Each dot represents a donor and the cell types can be distinguished by the colour code. **A.** PCA plot generated after the first round of quality control. Circled samples show high and significant variance in the data set as assessed by this metric. These samples were, therefore, excluded. **B.** PCA plot generated after the second round of quality control. Another outlier was detected and excluded from further analysis. **C.** PCA plot generated after the third round of quality control. No outliers were flagged and therefore all the remaining samples were used for further analysis.

5.4.4 Differential gene expression in the distinct B cell subsets from early RA patients

After assessing data quality and excluding outliers, ABCs gene expression was compared with this of the other B cell subsets in early RA. An overview of the bioinformatics analysis can be found in Chapter 2 section 2.6. Briefly, the DESeq2 R package (Love *et al.*, 2014) was used to compare the gene expression profiles between different B cell subsets and disease groups. DESeq2 package was chosen as it is a standard method for the analysis of count data. This package estimates the dispersion and the fold change of the counts to enable for a more quantitative analysis focused on the strength of the differential expression rather than the simple presence of differential expression. Differences were regarded significant when the Benjamini-Hochberg adjusted p value was <0.05 and the fold change was >1.5.

Heatmaps were used to visualize clustering differences between cell types (Figure 5.7). Figure 5.7.A shows that ABCs and naïve B cells are two distinct subsets with different gene expression profiles. The same is shown for the comparison of ABCs to CD5+ B cells (Figure 5.7.B) and memory B cells (Figure 5.7.C). The ABCs display different gene expression profiles to the rest of the B cell subsets.

Differentially expressed genes between the ABCs and the naïve B cells were assessed (Figure 5.8). The differentially expressed genes identified are shown in the volcano plot (Figure 5.8.A). This analysis revealed a wide range of downregulated genes such as *CR2* and *CR1*, which encode CD21 and CD35 respectively, and chemokine receptors which mediate recruitment to lymphoid organs such as *CCR7, CXCR4* and *CXCR5* (Figure 5.8.B). Moreover, the upregulated genes were mainly enriched for previously described ABC markers such as integrins (*ITGAX, ITGB2*), adhesion molecules (*CD97*) and *TBX21*, which encodes T-bet (Figure 5.8.C).

ABCs' gene expression was compared to the CD5+ B cells' gene profile (Figure 5.9). Differentially expressed gene analysis between the two subsets is shown in the volcano plot (Figure 5.9.A). Gene expression analysis revealed a similar profile of downregulated genes as compared to naïve B cells, with downregulation of chemokine receptors mediating recruitment to lymphoid organs and *CD21* (Figure 5.9.B). Additionally, upregulated genes comprised T-bet, integrins and adhesion molecules as with the naïve B cells (Figure 5.9.C).

Finally, ABCs' gene expression was also compared to the memory B cells' gene profile (Figure 5.10). The volcano plot shows the differentially expressed genes between the two

subsets (Figure 5.10.B). Downregulated genes include complement receptors and regulators such as *CR1*, *CR2*, and *CD59*, in addition to the plasma cell marker *CD138* and *CD38* (Figure 5.10.C). Upregulated genes comprised integrin genes, *CD19* and the coding T-bet gene. Moreover, there was upregulation of inhibitory receptors such as *LAIR1* and the transcription factors *NFATC2* and *NFATC3*, involved in B cell activation and differentiation (Figure 5.10.D).

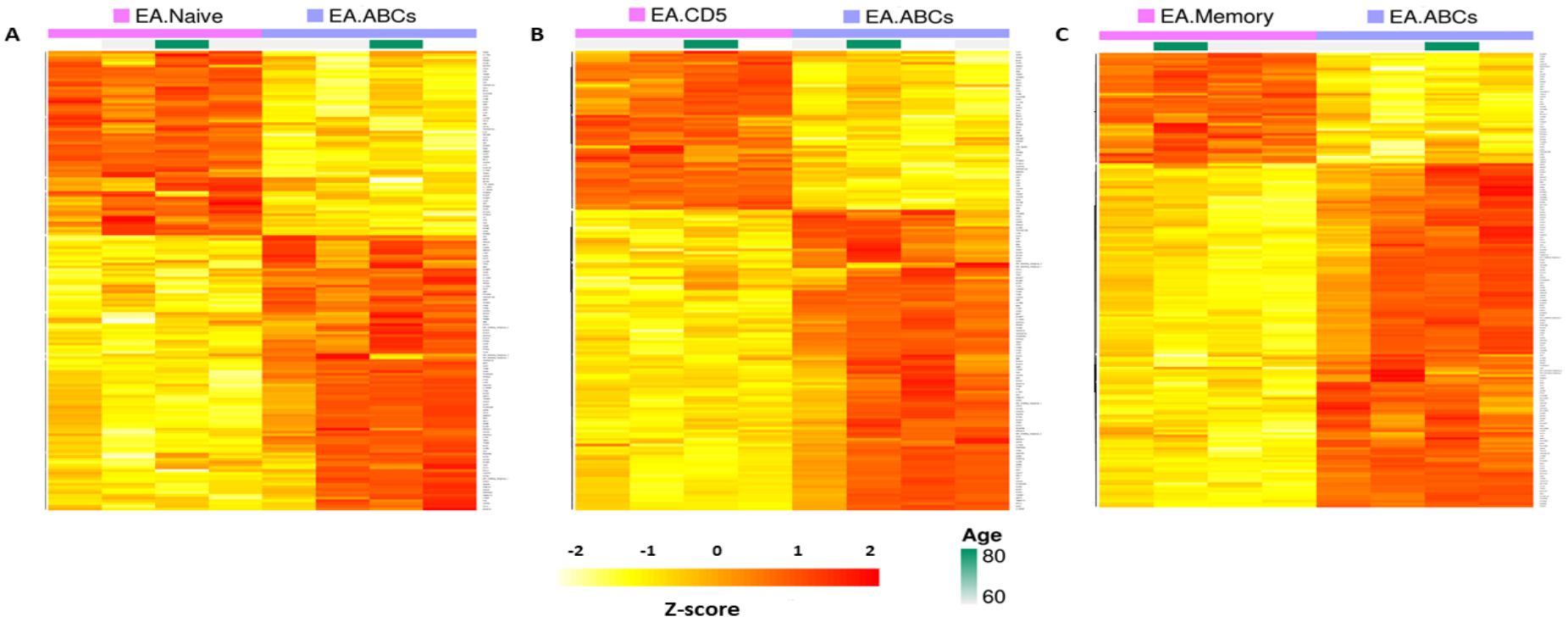

Figure 5. 7. Heatmap of the differentially expressed genes between ABCs and the other subsets of B cells. B cell subsets from early RA patients were sorted by flow cytometry. Cells were lysed and the cell lysates were loaded to the NanoString nCounter Technologies chip to assess gene expression. Raw counts were normalised to the housekeeping genes. Sample quality was then assessed using the arrayQualityMetrics package and 4 outliers were excluded. Gene expression profiles between different B cell subsets was assessed using the DESeq2 R package. Gene expression intensities were log10 transformed and are displayed as colours ranging from yellow to red as shown in the key. **A.** Heatmap of the differentially expressed genes between naïve B cells and ABCs. ABCs are shown in purple and naïve B cells in pink. **B.** Heatmap of the differentially expressed genes between CD5+ B cells and ABCs. ABCs are shown in purple and CD5+ B cells in pink. **C.** Heatmap of the differentially expressed genes between memory B cells and ABCs. ABCs are shown in purple and memory B cells in pink. Each column represents a different early RA patient.

A

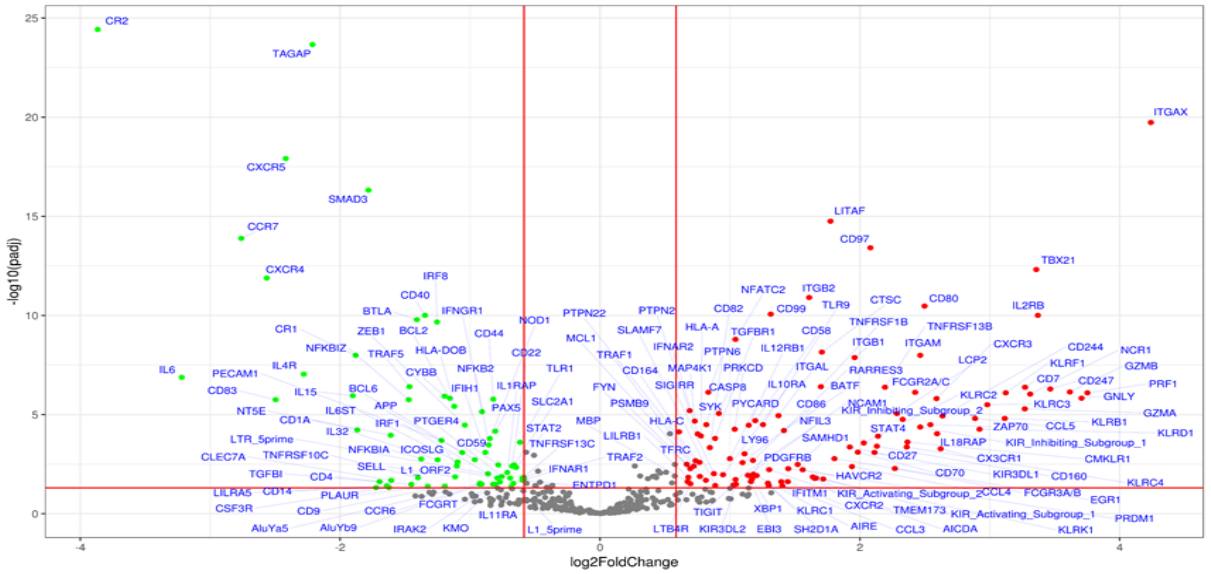

B

Gene	Log2 Fold Change	Adjusted p value
CR2	-3.86576	3.81E-25
TAGAP	-2.21268	2.19E-24
CXCR5	-2.41883	1.23E-18
SMAD3	-1.78242	4.84E-17
CCR7	-2.76143	1.31E-14
CXCR4	-2.56433	1.31E-12
CD40	-1.34696	9.96E-11
BTLA	-1.40893	1.64E-10
IRF8	-1.25436	2.16E-10
CR1	-1.88115	1.03E-8

C

Gene	Log2 Fold Change	Adjusted p value
ITGAX	4.23960	1.86E-20
LITAF	1.77373	1.78E-15
CD97	2.08084	3.89E-14
TBX21	3.35745	4.87E-13
ITGB2	1.60949	1.25E-11
CD80	2.49788	3.38E-11
CD99	1.31361	8.66E-11
IL2RB	3.36979	9.95E-11
NFATC2	1.04227	1.62E-9
CTSC	1.70717	7.06E-9

Figure 5. 8. Gene expression analysis of sorted ABCs compared to naïve B cells from early RA patients. Cell lysates from sorted ABCs and naïve B cells from early RA patients were loaded to the NanoString nCounter Technologies chip to assess gene expression. Raw counts were normalised to the housekeeping genes. Sample quality was then assessed using the arrayQualityMetrics package and 4 outliers were excluded. Gene expression profiles between different B cell subsets was assessed using the DESeq2 R package. Genes achieved statistical significance when the adjusted p value was <0.05 (FDR corrected) and the fold change was >1.5. **A.** Volcano plot showing the Log2Fold change against the –log10 Adjusted p value where genes plotted in red are upregulated and genes in green are downregulated in ABCs compared to naïve. **B.** Table showing the 10 most significant downregulated genes, with their fold change and adjusted p value. **C.** Table showing the 10 most significant upregulated genes, with their fold change and adjusted p value.

A

B

Gene	Fold Change	Adjusted p value
TAGAP	-2.19189	8.42E-24
CR2	-3.63759	5.26E-23
SMAD3	-1.82123	1.99E-18
CXCR5	-2.24942	2.01E-16
CXCR4	-2.48264	6.04E-12
IRF8	-1.23567	3.09E-10
CCR7	-2.25823	3.88E-10
CD40	-1.27774	5.24E-10
CR1	-1.97748	8.52E-10
CD1A	-2.59428	1.74E-09

C

Gene	Fold Change	Adjusted p value
CD97	2.60563	3.5E-22
ITGAX	4.11506	1.92E-20
LITAF	1.76934	2.01E-16
TBX21	3.60869	6.32E-16
CD80	2.47105	1.83E-13
IL2RB	3.71392	3.33E-13
CD99	1.43532	3.77E-13
TNFRSF1B	2.29763	8.32E-13
ITGB2	1.55655	2.81E-11
ITGB1	2.21949	4.42E-11

Figure 5. 9. Gene expression analysis of sorted ABCs compared to CD5+ B cells from early RA patients. Cell lysates from sorted ABCs and CD5+ B cells from early RA patients were loaded to the NanoString nCounter Technologies chip to assess gene expression. Raw counts were normalised to the housekeeping genes. Sample quality was then assessed using the arrayQualityMetrics package and 4 outliers were excluded. Gene expression profiles between different B cell subsets was assessed using the DESeq2 R package. Genes achieved statistical significance when the adjusted p value was <0.05 (FDR corrected) and the fold change was >1.5. **A.** Volcano plot showing the Log2Fold change against the –log10 Adjusted p value where genes plotted in red are upregulated and genes in green are downregulated in ABCs compared to CD5+ B cells. **B.** Table showing the 10 most significant downregulated genes, with their fold change and adjusted p value. **C.** Table showing the 10 most significant upregulated genes, with their fold change and adjusted p value.

A

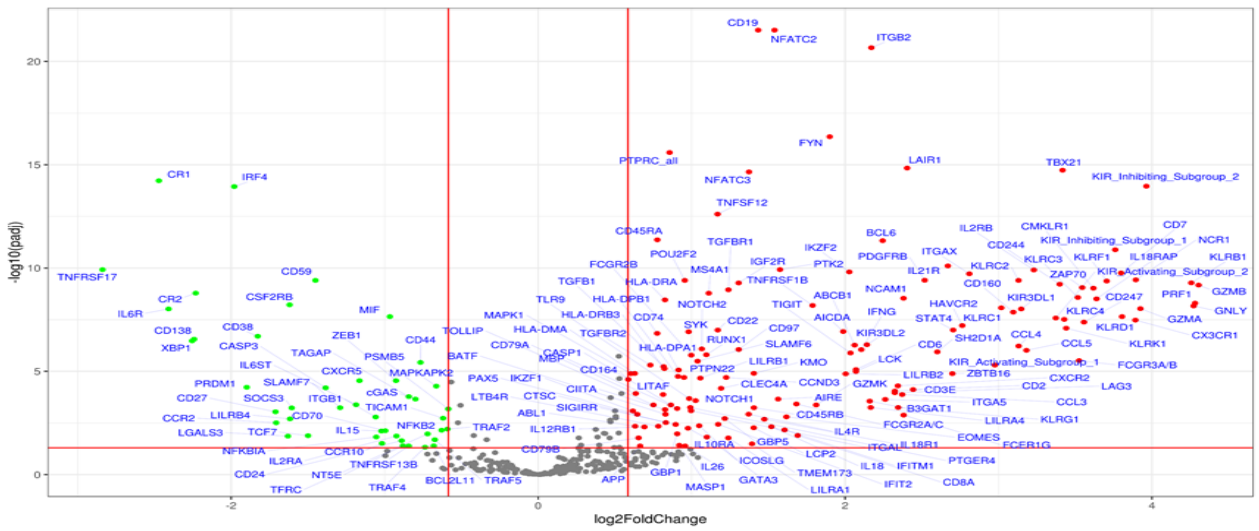

B

Gene	Log2 Fold Change	Adjusted p value
CR1	-2.47143	5.93E-15
IRF4	-1.98025	1.14E-14
TNFRSF17	-2.83845	1.2E-10
CD59	-1.45094	3.97E-10
CR2	-2.23117	1.64E-09
CSF2RB	-1.61953	6.01E-09
IL6R	-2.40806	9.56E-09
MIF	-0.96626	2.25E-08
CD38	-1.82704	2.00E-07
CD138	-2.24169	2.78E-07

D

Gene	Log2 Fold Change	Adjusted p value
CD19	1.43382	3.04E-22
NFATC2	1.54024	3.04E-22
ITGB2	2.17134	2.15E-21
FYN	1.89988	4.39E-17
PTPRC_all	0.85661	2.56E-16
LAIR1	2.40449	1.45E-15
TBX21	3.41734	1.83E-15
NFATC3	1.37402	2.22E-15
KIR_Inhibiting_Subgroup_2	3.96343	1.09E-14
TNFSF12	1.16911	2.44E-13

Figure 5. 10 Gene expression analysis of sorted ABCs compared to memory B cells from early RA patients. Cell lysates from sorted ABCs and memory B cells from early RA patients were loaded to the NanoString nCounter Technologies chip to assess gene expression. Raw counts were normalised to the housekeeping genes. Sample quality was then assessed using the arrayQualityMetrics package and 4 outliers were excluded. Gene expression profiles between different B cell subsets was assessed using the DESeq2 R package. Genes achieved statistical significance when the adjusted p value was <0.05 (FDR corrected) and the fold change was >1.5. **A.** Volcano plot showing the Log2Fold change against the –log10 Adjusted p value where genes plotted in red are upregulated and genes in green are downregulated in ABCs compared to memory B cells. **B.** Table showing the 10 most significant downregulated genes, with their fold change and adjusted p value. **C.** Table showing the 10 most significant upregulated genes, with their fold change and adjusted p value.

5.4.5 Expression of selected genes of interest in B cell subsets

Considering the previous results showing different gene expression between ABCs and the other B cell subsets, I decided to further investigate some of the enriched and previously reported pathways.

Further inspection of the genes which were differentially expressed by ABCs compared to the other B cell subsets revealed that the high expression of some of the previously assessed protein phenotypic markers were confirmed at the mRNA level. The markers comprising the ABC phenotype were *CD19*, *ITGAX* (*CD11c*), *TBX21* (*T-bet*), *CR2* (*CD21*), *MS4A1* (CD20) and *CD27* (Figure 5.11.A).

Gene expression analysis of genes related to B cell differentiation and activation markers showed higher expression of genes involved in plasma cell differentiation (*AICDA*, *PRDM1* (*BLIMP1*) and *XBP1*) compared to naïve B cells, although lower expression compared to memory B cells (Figure 5.11.B), supporting the idea that ABCs might be precursors of plasma cells. However, low expression by ABCs of molecules associated to B cell activation, for example *NFKBIA* and *NFKBIZ* support the notion that ABCs might be unresponsive to BCR stimulation (Figure 5.11.B).

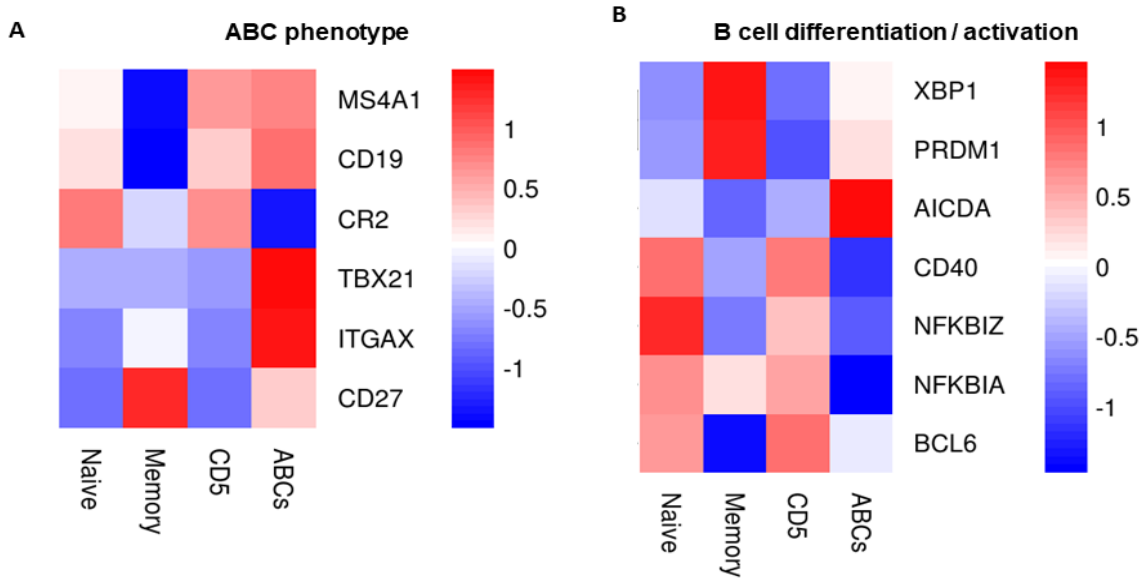

Figure 5. 11. Expression of selected genes of interest in the different B cell subsets from RA patients. Heat map showing expression pattern of representative genes with relevant functions. **A.** Group of genes encoding the ABCs phenotype. **B.** Genes encoding B cell differentiation and activation factors. For plotting, median log2 expression for each cell population was used. Red indicates higher expression, and blue indicates lower expression. Colour bar indicates Z score or adjusted p value.

Furthermore, analysis of migration and adhesion molecules showed high expression of alpha and beta integrins (like *ITGAL* and *ITGB1*) as well as *NCAM1*, but not *PECAM* (Figure 5.12.A).

Moreover, the gene expression results confirm a unique ABC-expression profile of cytokine receptors. These cytokines include the gamma-c family receptor *IL2RB*, members of the TNF receptor super family (*TNFRSF1B* and *TNFRSF13B*) and the interferon alpha receptor 2, *IFNAR2* (Figure 5.12.B). The unique chemokine receptor profile includes high expression of chemokine receptors which mediate recruitment to inflammatory sites and low expression of chemokine receptors which mediates migration of leukocytes into lymphoid organs (Figure 5.12.B).

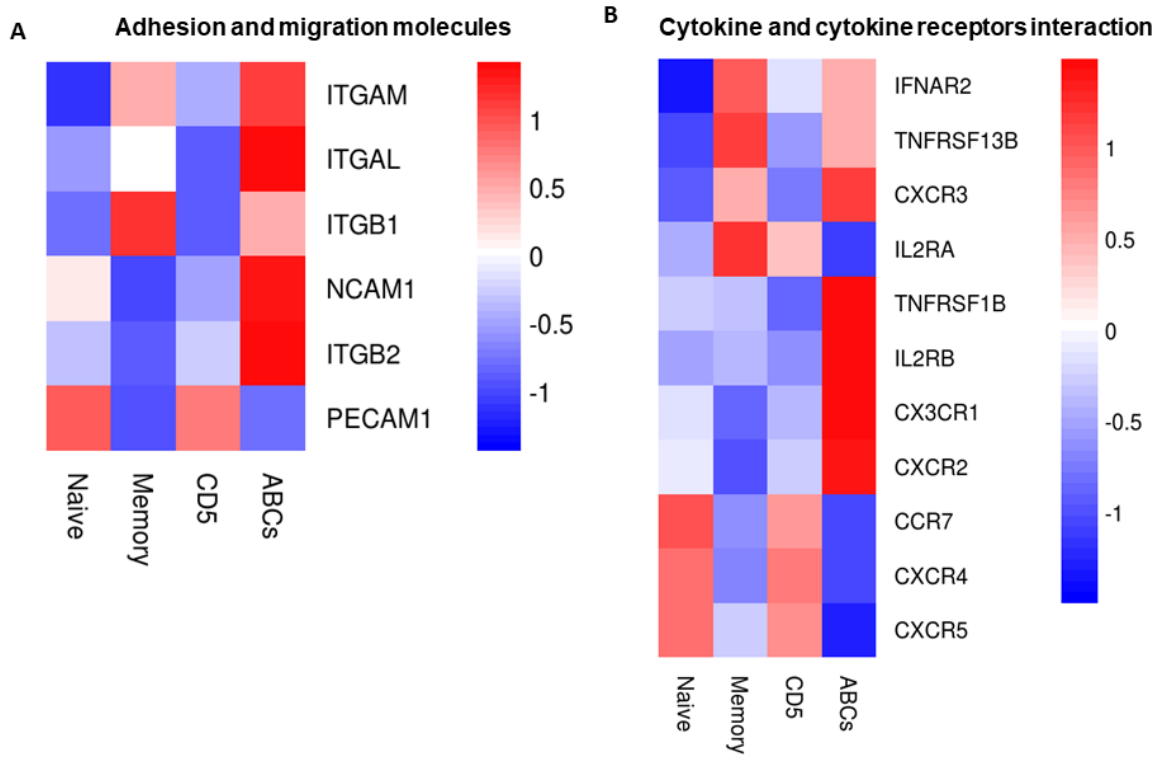

Figure 5. 12. Expression of selected genes of interest in the different B cell subsets from RA patients. Heat map showing expression pattern of representative genes with relevant functions. **A.** Group of genes encoding adhesion molecules. **B.** Genes encoding cytokines and chemokines receptors. For plotting, median log2 expression for each cell population was used. Red indicates higher expression, and blue indicates lower expression. Colour bar indicates Z score or adjusted p value.

Moreover, ABCs also show high expression of apoptosis-related genes as expression of caspases (*CASP8* and *CASP1*), the apoptotic antigen *FAS*, and the apoptosis regulator *MCL1*, primarily compared to naïve B cells (Figure 5.13.A).

Interestingly, gene expression results demonstrated very high expression of genes associated with NK cell cytotoxicity. ABCs upregulate genes encoding granzymes (*GZMA*, *GZMB* and *GNLY*) and perforin (*PRF1*) as well as Killer cell Lectin like Receptors (*KLRC3*, *KLRF1* and *KLRD1*) and Killer cell Immunoglobulin-like Receptor (*KIR3DL1*) (Figure 5.13.B).

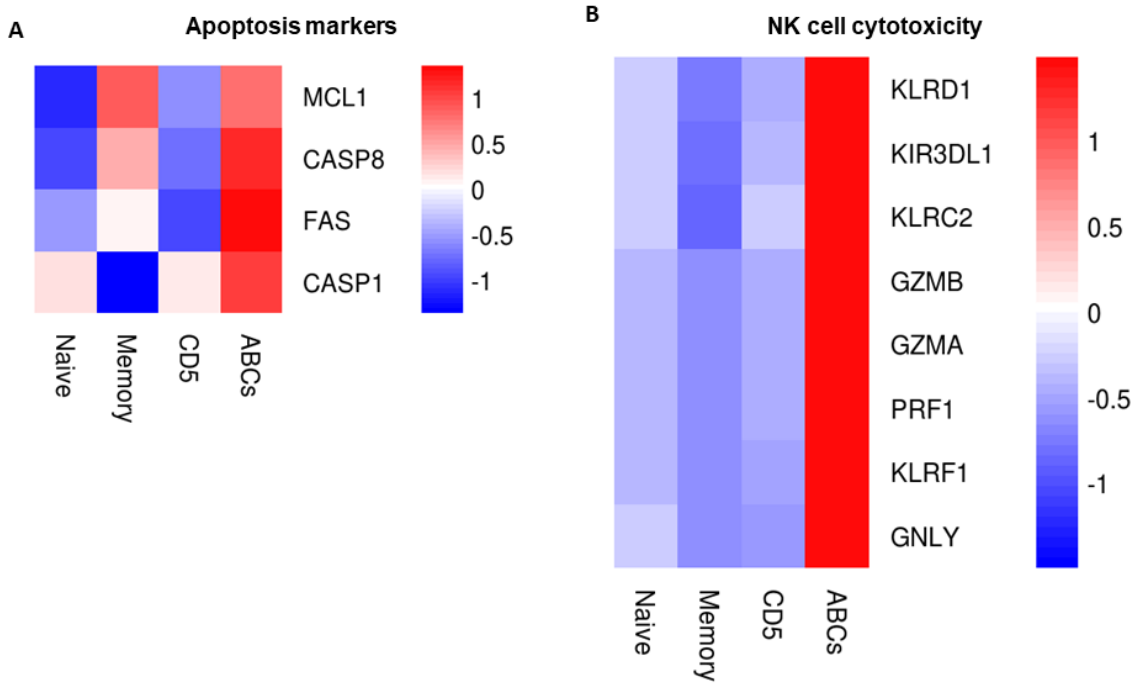

Figure 5. 13. Expression of selected genes of interest in the different B cell subsets from RA patients. Heat map showing expression pattern of representative genes with relevant functions. **A.** Group of genes related to apoptosis. **B.** Genes involved in NK cell cytotoxicity. For plotting, median log2 expression for each cell population was used. Red indicates higher expression, and blue indicates lower expression. Colour bar indicates Z score or adjusted p value.

Additionally, ABCs show high expression of inhibitory receptors such as *FCGR*, and *LILRB*, as well as immunomodulatory molecules including *TLR9*, *CD80* and *CD86* (Figure 5.14).

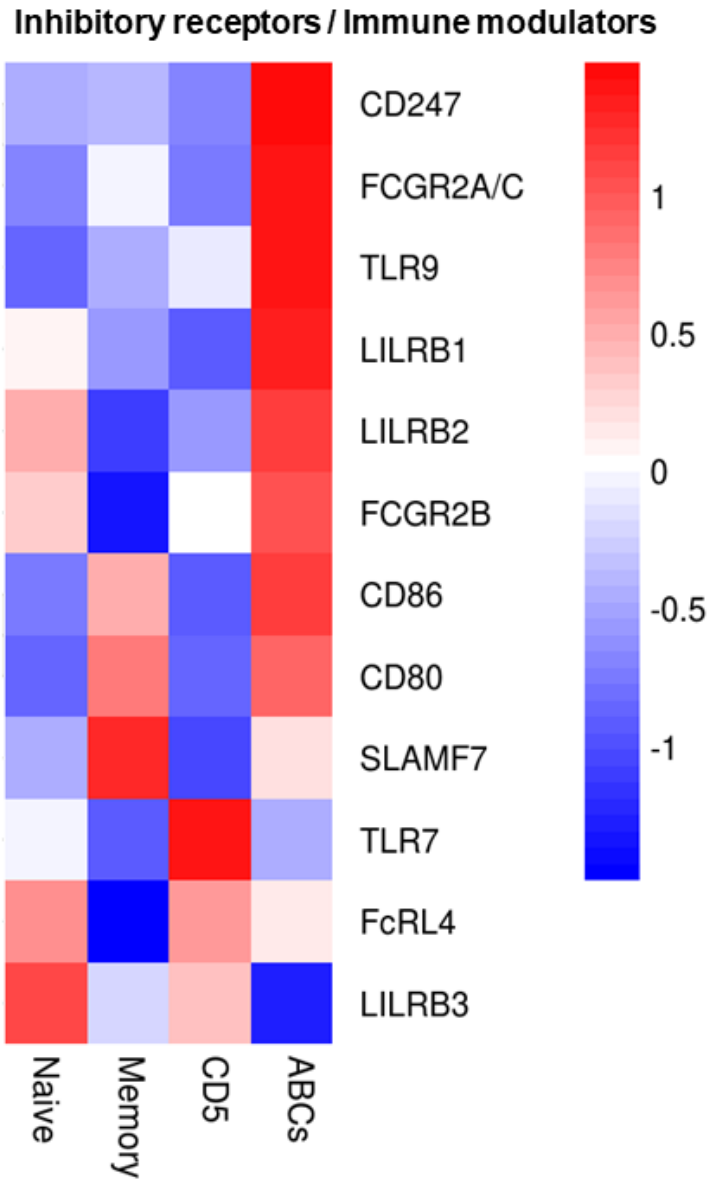

Figure 5. 14. Expression of selected genes of interest in the different B cell subsets from RA patients. Heat map showing expression pattern of representative genes with relevant functions. **A.** Group of genes encoding inhibitory receptors and immune modulators. For plotting, median log2 expression for each cell population was used. Red indicates higher expression, and blue indicates lower expression. Colour bar indicates Z score or adjusted p value.

As a different way to compare key pathways between the B cell subsets, gene expression after normalisation to housekeeping genes was compared using dot plots. Figure 5.15 highlights genes involved in cellular migration.

Analysis of chemokine receptor gene expression showed high expression of the chemokine receptors which mediate migration into inflammatory sites (Figure 5.15.A-B). High expression on ABCs was significant when compared to naïve B cells for *CXCR3* and memory B cells for *CX3CR1*. On the contrary, expression of chemokine receptors known to mediate recruitment to lymphoid organs such as *CXCR4* and *CXCR5*, was significantly downregulated in ABCs compared to naïve B cells (Figure 5.15.C-D).

Additionally, expression of *ITGB2*, an integrin also known as CD18 and involved, together with CD11c, in B cell attachment to fibrinogen (Postigo *et al.*, 1991), was plotted as a representative of the different integrins and adhesion molecules upregulated in ABCs compared to other subsets. *ITGB2* expression was significantly higher in ABCs compared to memory B cells (Figure 5.16.A). Expression of the adhesion and activation marker *CD97* was also assessed (Figure 5.16.B). *CD97* expression was higher in ABCs than the other subsets but the differences were significant only in ABCs compared to CD5+ B cells.

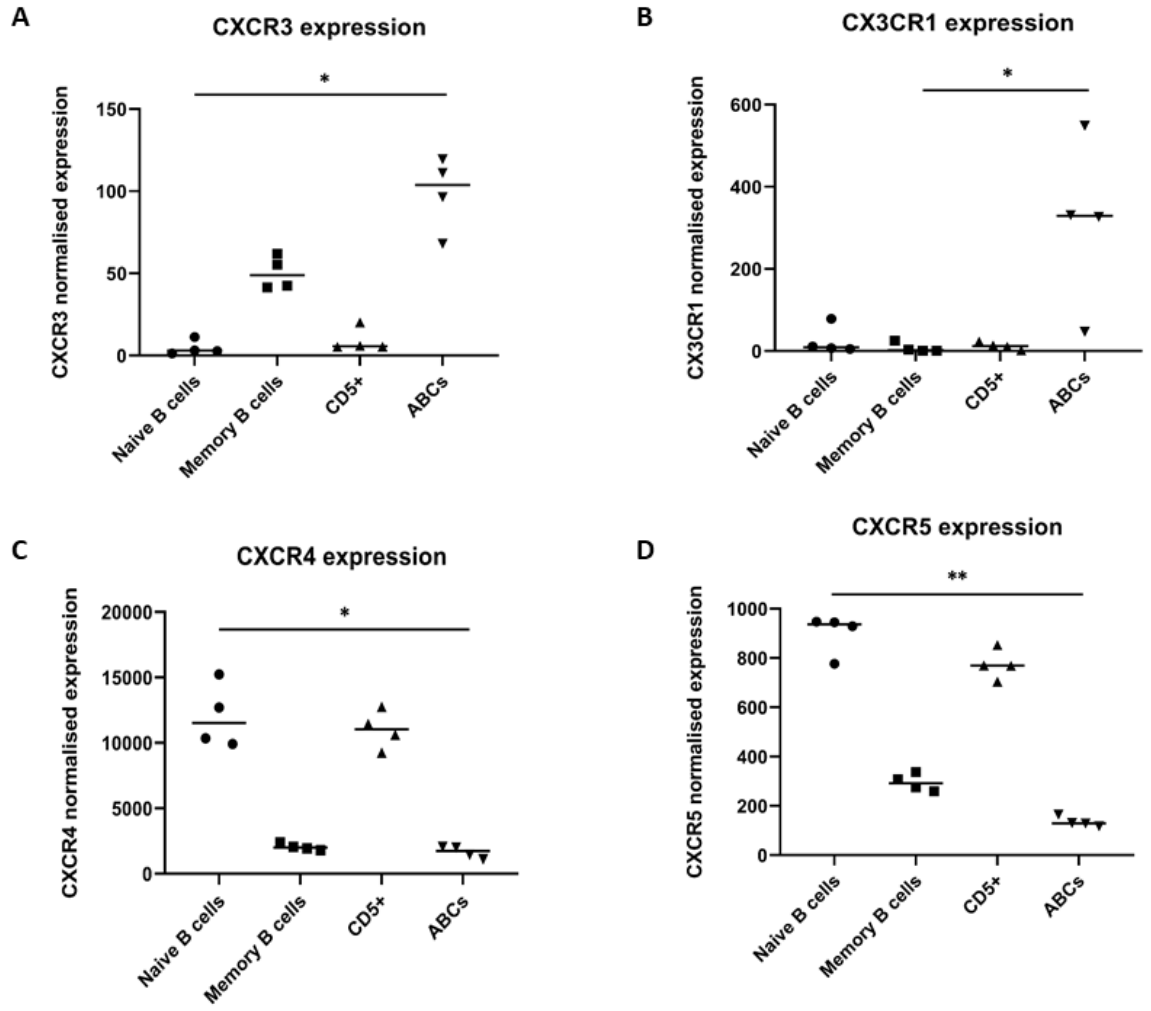

Figure 5. 15. Normalised gene expression of chemokine receptors in the different B cell subsets in early RA patients. A-B. Normalised gene expression of chemokine receptors which mediate recruitment of cells to inflammatory sites (n=4). **C-D.** Normalised gene expression of chemokine receptors which mediate recruitment of cells to lymphoid organs (n=4). The bar represents the median. Statistical significance was assessed using a Friedman test with Dunn's multiple comparisons of the ABCs against the other subsets; * $p < 0.05$, ** $p < 0.01$. Friedman test $p = 0.0009$ for A, $p = 0.0190$ for B, $p = 0.0027$ for C and $p < 0.0001$ for D.

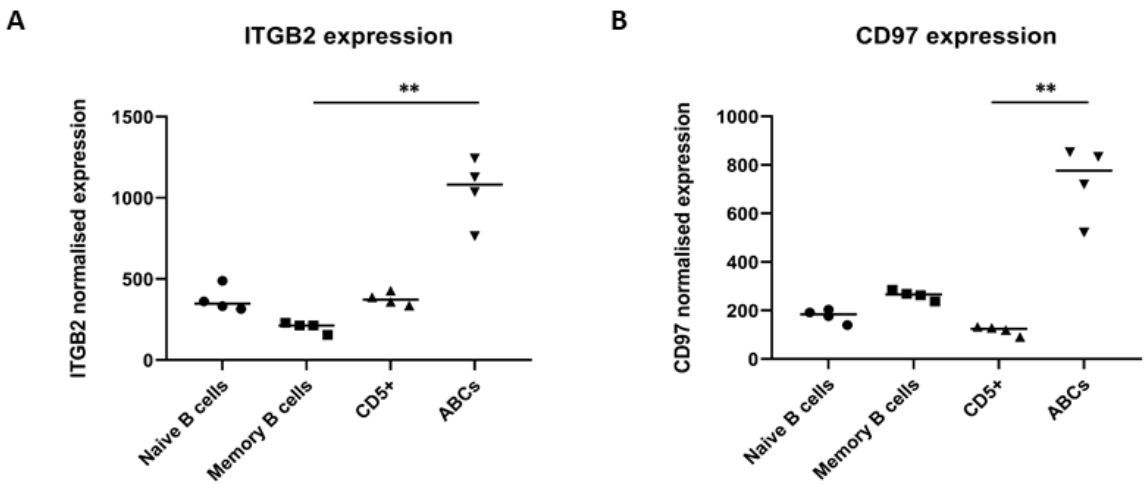

Figure 5. 16. Normalised gene expression of adhesion molecules in the different B cell subsets in early RA patients. A. Normalised gene expression of the adhesion receptor integrin subunit β2 in the different B cell subsets (n=4). **B.** Normalised gene expression of the adhesion molecule CD97 in each of the B cell subsets (n=4). Statistical significance was assessed using a Friedman test with Dunn's multiple comparisons of the ABCs against the other subsets; * $p < 0.05$, **$p < 0.01$, **** $p < 0.0001$. Friedman test $p = 0.0016$ for A and $p < 0.0001$ for B.

5.4.6 Validation of transcriptomic data at the protein level

Considering the previous results showing different gene expression between ABCs and other B cell subsets, I validated the expression of selected genes at the protein level, using flow cytometry.

CXCR3 expression, known to recruit cells into sites of inflammation, showed higher percentages of CXCR3 positive cells in the ABC population (Figure 5.17.A-C), confirming the gene expression analysis. These differences were significant in ABCs compared to naïve and CD5+ B cells (Figure 5.17.C). CXCR3 expression, as measured by MFI, was also higher in ABCs compared to naïve and CD5+ B cells (Figure 5.17.D).

CXCR4 expression, a chemokine receptor that recruits cells into lymph nodes, was downregulated in the ABC population (Figure 5.18.A-B). There were significantly lower percentages of positive cells in the ABCs compared to naïve and CD5+ B cells (Figure 5.18.C). Moreover, CXCR4 expression, as measured by MFI, was also lower in ABCs compared to naïve and CD5+ B cells (Figure 5.18.D).

Another chemokine receptor which recruits lymphocytes into lymphoid organs is CXCR5. A lower percentage of CXCR5 positive B cells was found on the ABCs population (Figure 5.19.A-C), these differences were significant in ABCs compared to naïve and CD5+ B cells. CXCR5 expression was also higher in ABCs compared to the rest of the B cell subsets (Figure 5.19.D).

Expression of the death receptor CD95 (Fas) was also validated. CD95 expression was highly expressed in the memory and ABC population (Figure 5.20.A-C). There were significantly higher percentages of positive cells in the ABCs compared to naïve and CD5+ cells (Figure 5.20.C). Moreover, CD95 expression, as measured by MFI, was also higher in ABCs compared to naïve and CD5+ cells (Figure 5.20.D).

Expression of the adhesion and activation marker CD97 was additionally validated. Higher percentages of CD97 positive cells can be found in the ABC population compared to naïve and CD5+ B cells (Figure 5.21. A-C). MFI values confirmed the higher expression of CD97 in ABCs compared to naïve and CD5+ B cells (Figure 5.21. D).

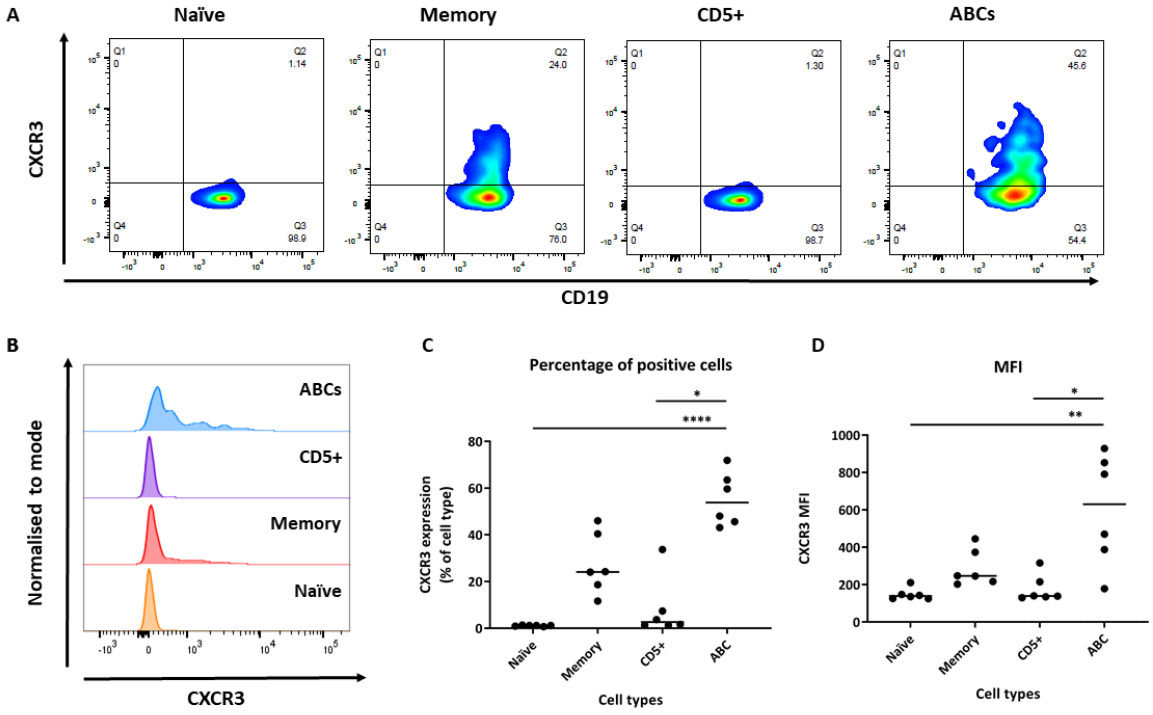

Figure 5. 17. Expression of CXCR3 in each B cell subset in early RA patients. A. Flow cytometry plots for each B cell subset after whole blood staining. CXCR3 expression against CD19, gate set from the lymphocyte population. **B.** CXCR3 expression overlay for each of the subsets. Naïve B cells are shown in orange; memory B cells in red, CD5+ B cells in purple and ABCs are shown in blue. The peaks are normalised to the same height to normalise different numbers of cells in each population. **C.** Percentage of CXCR3 positive cells in the B cell subsets (n=6). The bar represents the median. **D.** CXCR3 median fluorescence intensity (MFI) in the different B cell subsets (n=6). The bar represents the median. Statistical significance was assessed using a Kruskal-Wallis test with Dunn's multiple comparisons of the ABCs against the other subsets; * $p < 0.05$, **$p < 0.01$, **** $p < 0.0001$. Kruskal-Wallis test $p = 0.0002$ for percentages; $p = 0.0022$ for MFI values.

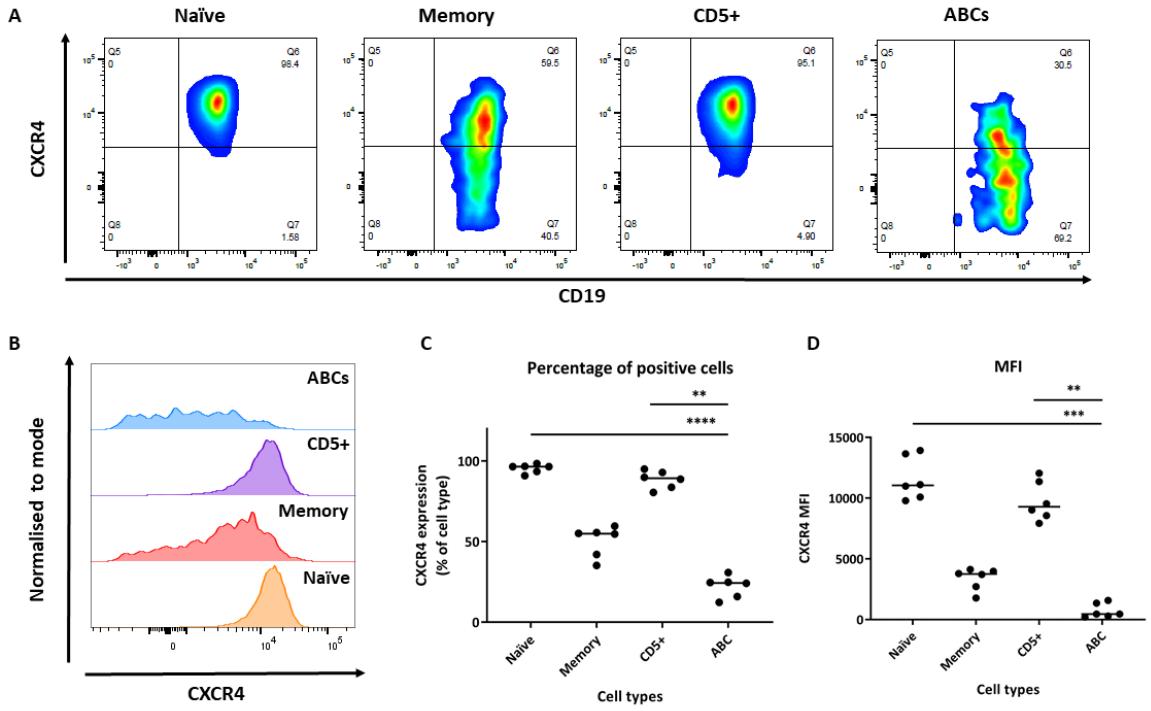

Figure 5. 18. Expression of CXCR4 in each B cell subset in early RA patients. A. Flow cytometry plots for each B cell subset after whole blood staining. CXCR4 expression against CD19, gate set from the lymphocyte population. **B.** CXCR4 expression overlay for each of the subsets. Naïve B cells are shown in orange; memory B cells in red, CD5+ B cells in purple and ABCs are shown in blue. The peaks are normalised to the same height to normalise different numbers of cells in each population. **C.** Percentage of CXCR4 positive cells in the B cell subsets (n=6). The bar represents the median. **D.** CXCR4 median fluorescence intensity (MFI) in the different B cell subsets (n=6). The bar represents the median. Statistical significance was assessed using a Kruskal-Wallis test with Dunn's multiple comparisons of the ABCs against the other subsets; **p < 0.01, *** p < 0.001, **** p < 0.0001. Kruskal-Wallis test p = 0.0001 for percentages; p = 0.0002 for MFI values.

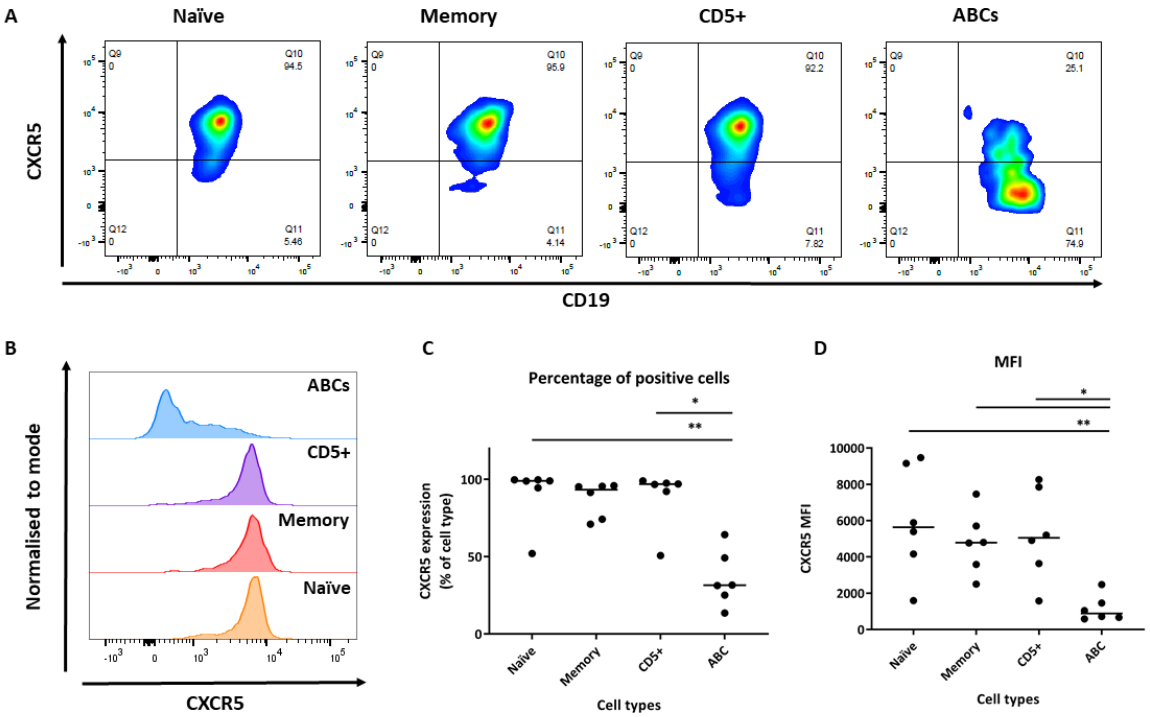

Figure 5. 19. Expression of CXCR5 in each B cell subset in early RA patients. A. Flow cytometry plots for each B cell subset after whole blood staining. CXCR5 expression against CD19, gate set from the lymphocyte population. **B.** CXCR5 expression overlay for each of the subsets. Naïve B cells are shown in orange; memory B cells in red, CD5+ B cells in purple and ABCs are shown in blue. The peaks are normalised to the same height to normalise different numbers of cells in each population. **C.** Percentage of CXCR5 positive cells in the B cell subsets (n=6). The bar represents the median. **D.** CXCR5 median fluorescence intensity (MFI) in the different B cell subsets (n=6). The bar represents the median. Statistical significance was assessed using a Kruskal-Wallis test with Dunn's multiple comparisons of the ABCs against the other subsets; * $p < 0.05$, **$p < 0.01$. Kruskal-Wallis test $p = 0.0030$ for percentages; $p = 0.0057$ for MFI values.

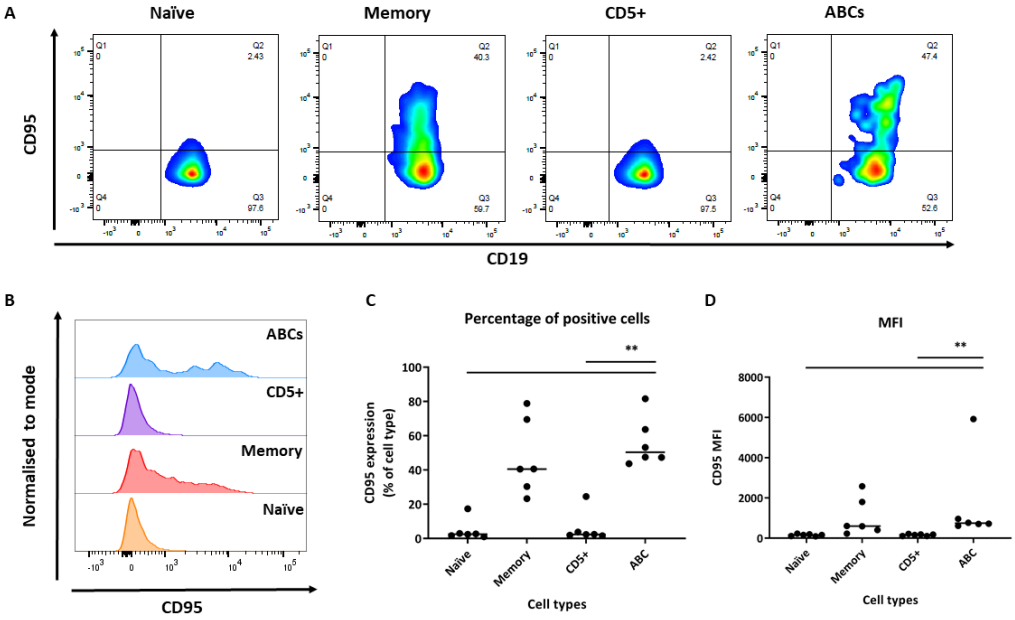

Figure 5. 20. Expression of CD95 in each B cell subset in early RA patients. A. Flow cytometry plots for each B cell subset after whole blood staining. CD95 expression against CD19, gate set from the lymphocyte population. **B.** CD95 expression overlay for each of the subsets. Naïve B cells are shown in orange; memory B cells in red, CD5+ B cells in purple and ABCs are shown in blue. The peaks are normalised to the same height to normalise different numbers of cells in each population. **C.** Percentage of CD95 positive cells in the B cell subsets (n=6). The bar represents the median. **D.** CD95 median fluorescence intensity (MFI) in the different B cell subsets (n=6). The bar represents the median. Statistical significance was assessed using a Kruskal-Wallis test with Dunn's multiple comparisons of the ABCs against the other subsets; **p < 0.01. Kruskal-Wallis test p = 0.0006 for percentages; p = 0.0005 for MFI values.

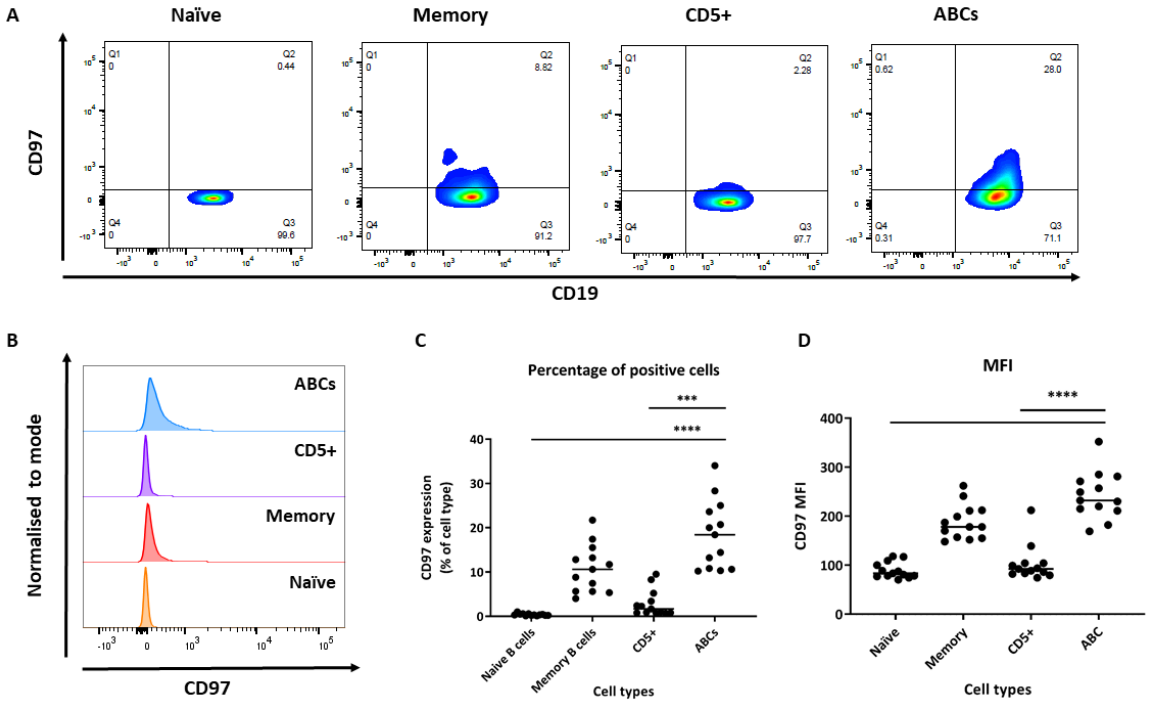

Figure 5. 21. Expression of CD97 in each B cell subset in early RA patients. A. Flow cytometry plots for each B cell subset after whole blood staining. CD97 expression against CD19, gate set from the lymphocyte population. **B.** CD97 expression overlay for each of the subsets. Naïve B cells are shown in orange; memory B cells in red, CD5+ B cells in purple and ABCs are shown in blue. The peaks are normalised to the same height to normalise different numbers of cells in each population. **C.** Percentage of CD97 positive cells in the B cell subsets (n=13). The bar represents the median. **D.** CD97 median fluorescence intensity (MFI) in the different B cell subsets (n=13). The bar represents the median. Statistical significance was assessed using a Kruskal-Wallis test with Dunn's multiple comparisons of the ABCs against the other subsets; *** $p < 0.001$, **** $p < 0.0001$. Kruskal-Wallis test $p < 0.0001$ for percentages; $p < 0.0001$ for MFI values.

Two NK cell related genes were also validated at the protein level using intracellular flow cytometry staining.

Granzyme B, a serine protease that induces apoptosis in target cells, was expressed by all NK cells (Figure 5.22.A). NK cells were gated by the exclusion of the CD19 and the CD3 and CD33 cells to assess staining. The higher mRNA expression of this protease in ABCs could not be confirmed at the protein level (Figure 5.22.B). Granzyme B expression in the NK cell population was very high, however, no differences in the MFI values were seen between B cell subsets (Figure 5.22.C).

The higher mRNA expression of perforin, another cytotoxic protein which mediates pore formation in target cells, by ABCs could also not be validated by flow cytometry (Figure 5.23). Perforin expression in NK cells confirmed that the staining worked as most of the cells were positive for perforin (Figure 5.23.A). Unfortunately, there were no perforin positive cells in any of the B cell subsets (Figure 5.23.B). Moreover, no differences in the MFI values were seen between B cell subsets (Figure 5.23.C).

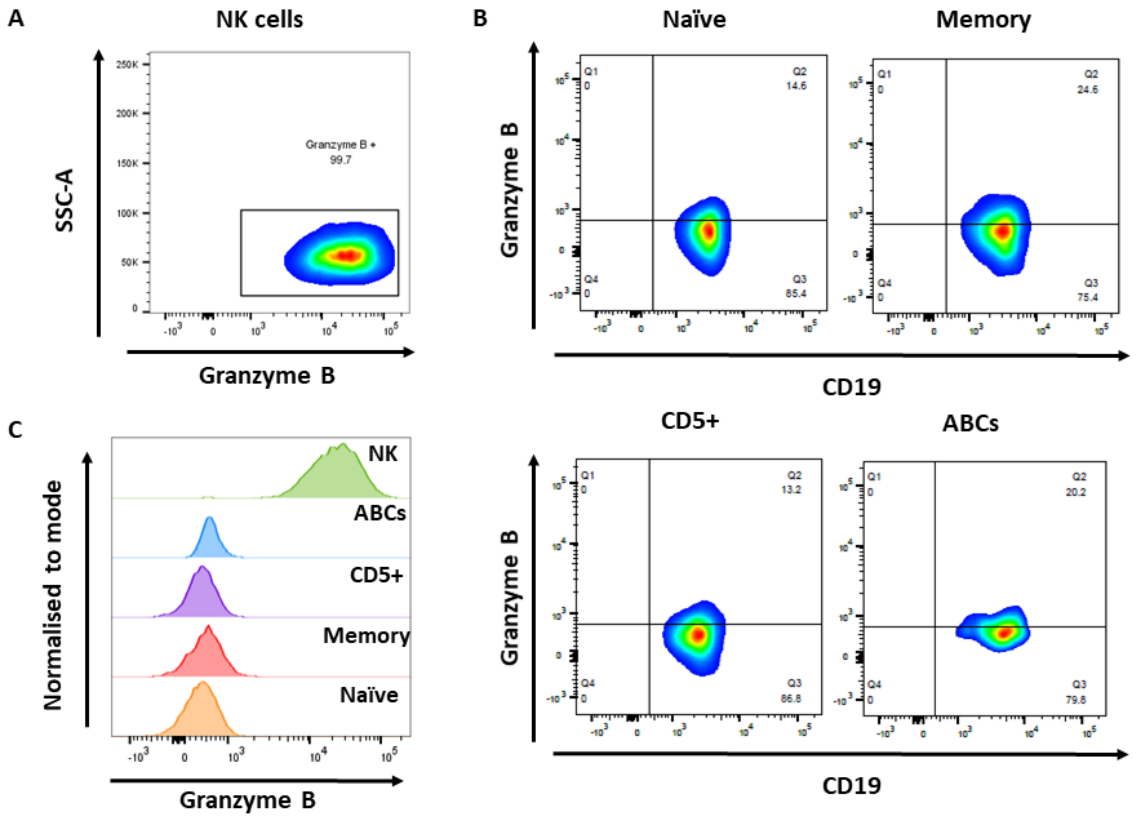

Figure 5. 22. Expression of Granzyme B in each B cell subset in early RA patients. A. Flow cytometry plot showing expression of granzyme B against SSC-A in the NK cell population after intracellular staining. Gate set using an FMO. **B.** Flow cytometry plots for each B cell subset after intracellular staining. Granzyme B expression against CD19, gate set using an FMO **C.** Granzyme B expression overlay for each of the subsets. Naïve B cells are shown in orange; memory B cells in red, CD5+ B cells in purple, ABCs in blue and NK cells in green. The peaks are normalised to the same height to normalise different numbers of cells in each population.

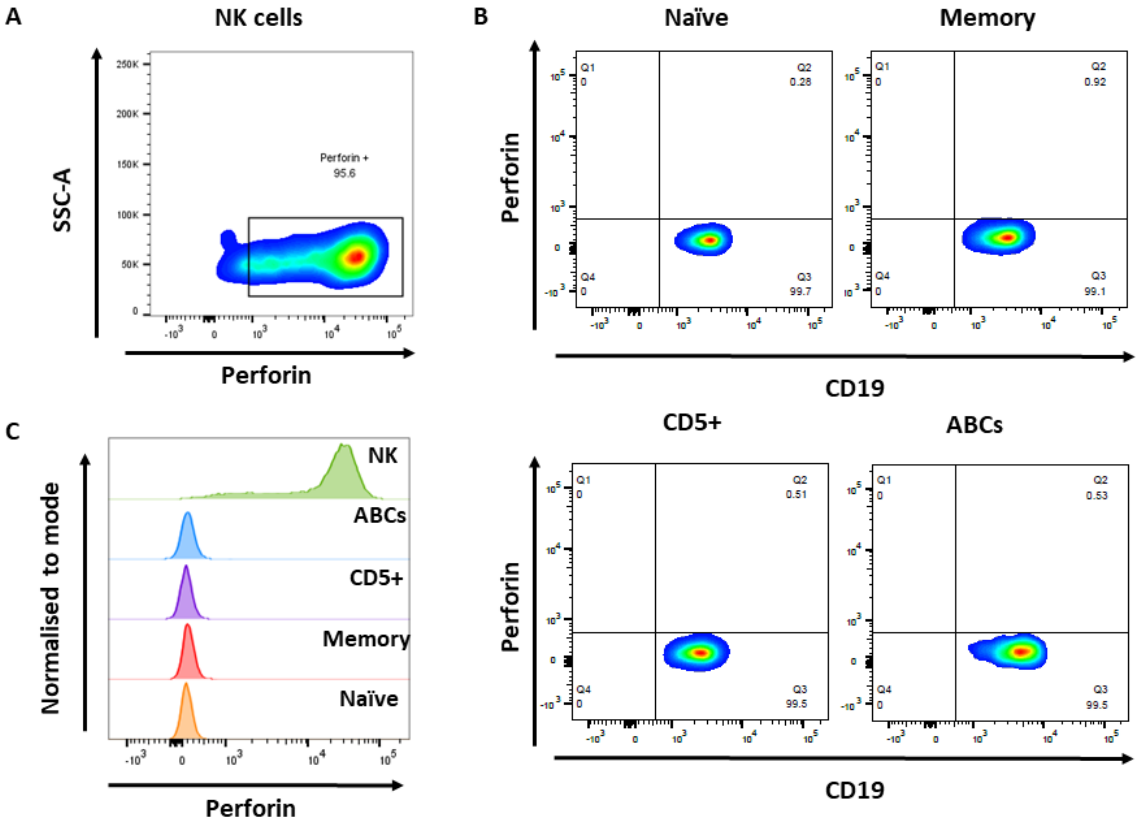

Figure 5. 23. Expression of perforin in each B cell subset in early RA patients. A. Flow cytometry plot showing expression of perforin against SSC-A in the NK cell population after intracellular staining. Gate set using an FMO. **B.** Flow cytometry plots for each B cell subset after intracellular staining. Perforin expression against CD19, gate set using an FMO **C.** Perforin expression overlay for each of the subsets. Naïve B cells are shown in orange; memory B cells in red, CD5+ B cells in purple, ABCs in blue and NK cells in green. The peaks are normalised to the same height to normalise different numbers of cells in each population.

5.4.7 Differential gene expression in ABCs from early RA patients compared to early PsA patients and healthy controls

A comparison of ABCs' gene expression between the different groups, eRA, ePsA and healthy controls was also performed. The DESeq2 R package (Love *et al.*, 2014) was used to compare the gene expression profiles between different B cell subsets and disease groups. For this analysis a less stringent cut-off was used. Differences were regarded significant when the unadjusted p value was < 0.05 and the fold change was > 1.5. Unadjusted p values were used as applying adjusted p values did not result in any differentially expressed genes between the RA patients and the two control groups. This is probably due to the small number of samples per group, as only four donors were recruited in each group, and not all samples passed quality controls. Further validation in a bigger cohort is needed to confirm these exploratory results.

Heatmaps were used to visualize clustering differences between the RA patients and the disease controls and the healthy controls (Figure 5.24). Figure 5.24.A shows that ABCs from eRA patients and ePsA patients cluster separately, with the exception of one eRA patient. As explained before, two ABC samples from ePsA patients did not pass quality control and were therefore excluded, leaving only two ePsA ABC samples. For the comparison of ABCs from eRA patients and healthy controls, cells from each group cluster separately (Figure 5.24.B). An ABC sample from a healthy control was also excluded as it did not pass quality control.

Differentially expressed genes between eRA and ePsA ABCs were assessed (Figure 5.25). The differentially expressed genes identified are shown in the volcano plot (Figure 5.25.A). This analysis revealed a few downregulated genes in eRA, such as the transcription factors *BCL6* and *SOCS3*, as well as extracellular receptors such as *IFNAR2, FCGRT* and *LILRB4* (Figure 5.25.B). Moreover, the genes upregulated in eRA were coding for subunits of interleukin receptors such as *IL2RG* and *IL13RA1*, as well as the killer cell receptor *KIR3DL1* (Figure 5.25.C). Interestingly, two of the upregulated genes were related to the chemerin pathway, with upregulation of retinoid acid receptor (*RARRES3*) and of the chemerin receptor (*CMKLR1*).

ABCs' gene expression in eRA patients was also compared to that in age-matched healthy controls (Figure 5.26). Differentially expressed gene analysis between the two groups is shown in the volcano plot (Figure 5.26.A). Gene expression analysis revealed

downregulation in eRA of the transcription factors *BATF* and *IRF5*, as well as the adhesion molecule *PECAM* (Figure 5.26.B). Upregulated genes in eRA comprised interleukin receptors such as *IL4R* and *IL13RA1*, the chemokine receptor *CXCR4* and the transcription factor *IRF1* and transcriptional co-activator *BCL3* (Figure 5.26.C).

Figure 5.27.A shows the upregulated genes when each of the disease groups are compared. There were 12 genes that were shown to be upregulated in ABCs from eRA patients when compared to healthy controls but also upregulated in eRA patients compared to PsA disease controls. The upregulated genes coded for proteins involved in leukocyte activation and migration to inflammatory sites such as *CD6*, as well as receptors related to NK cell cytotoxicity like KIRs and KLRs (Figure 5.27.B). Interestingly, two of the upregulated genes in RA compared to other control groups, *IL13RA1* and *IL4R*, encode a functional receptor for IL-13 (Figure 5.27.B). These genes could represent a RA-specific gene signature as they are increased in RA compared to both control groups. There were some differentially expressed genes in early RA and PsA compared to healthy controls (Figure 5.27.A). As shown in Figure 5.27.B, 8 genes were upregulated in both arthritic diseases compared to healthy controls. Therefore, these genes could be related to general inflammation rather than being disease specific. The upregulated genes included the BCL2 like 11 (*BCL2L11*) and the ligand for T cell activation *ICOSLG* and *CD83*, involved in antigen-presentation and lymphocyte activation. Interestingly, *BCL3* and *SOCS3* appeared upregulated in both disease groups compared to the healthy controls.

Figure 5.28.A shows the downregulated genes when each of the disease groups are compared. There was only one downregulated gene common in the RA versus PsA comparison as well as the RA versus HC comparison (Figure 5.28.B). This gene is *FCGRT*; this gene codes a receptor that binds the Fc region of immunoglobulin G, thus protecting IgG from degradation in addition to facilitating its transport. There were 7 genes downregulated in both arthritic diseases compared to healthy controls. These genes comprised the transcription factors *BATF* and *IRF5* and the inhibitory receptors *FcRL4* and the Leukocyte Immunoglobulin-Like Receptor *LILRA4*. Additionally, the downregulated genes included the pro-apoptosis molecule *CASP1* and the RNA helicase *DDX58* (Figure 5.28.B).

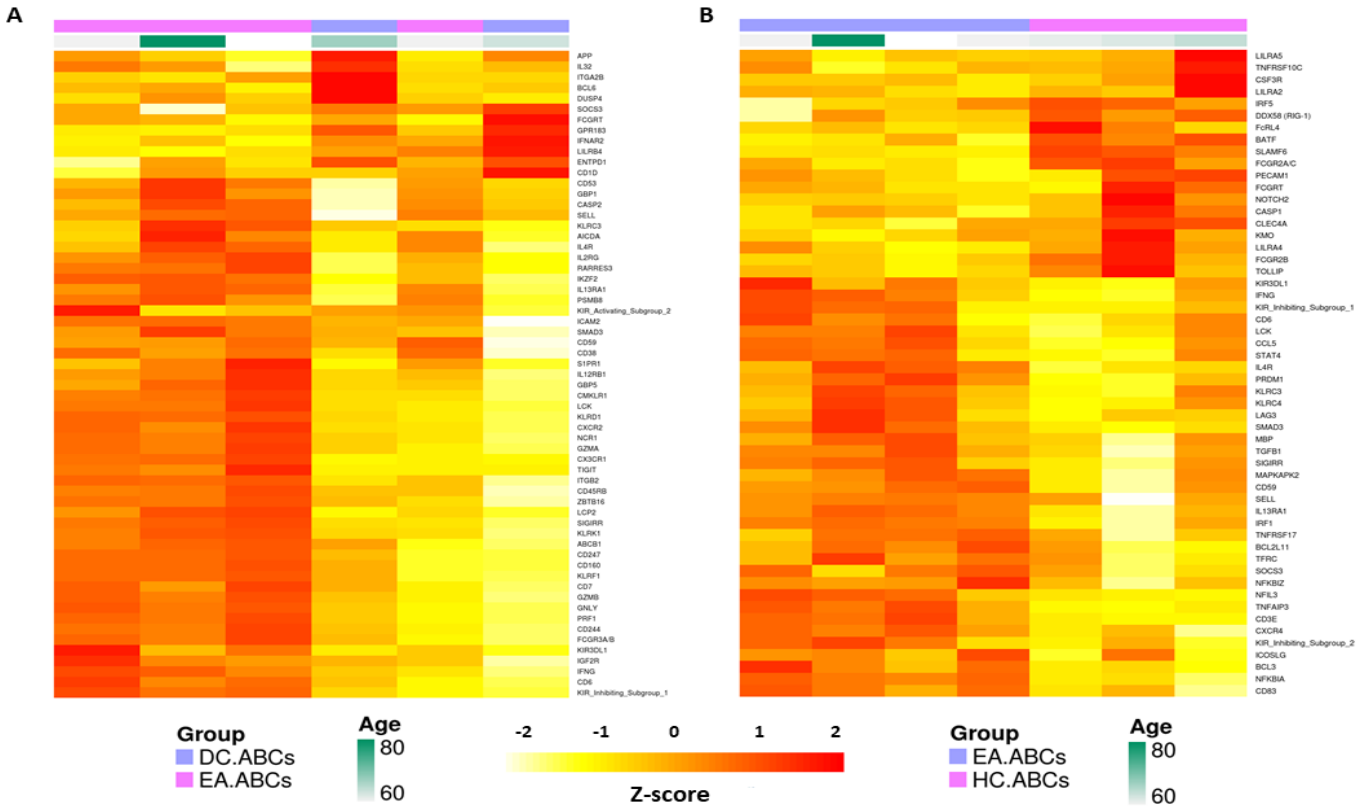

Figure 5. 24. Heatmap of the differentially expressed genes between ABCs from early RA patients, early PsA patients and age-matched healthy controls. Cell lysates from sorted ABCs were loaded to the NanoString nCounter Technologies chip to assess gene expression. Raw counts were normalised to the housekeeping genes. Sample quality was then assessed using the arrayQualityMetrics package Gene expression profiles between different disease groups and healthy controls was assessed using the DESeq2 R package. Gene expression intensities were log10 transformed and are displayed as colours ranging from yellow to red as shown in the key. **A.** Heatmap of the differentially expressed genes between ABCs from eRA patients in pink and ABCs from ePsA patients in purple. **B.** Heatmap of the differentially expressed genes between ABCs from eRA patients in purple and ABCs from healthy controls in pink.

A

B

Gene	Log2 Fold Change	p value
ENTPD1	-0.82182	0.00183
IFNAR2	-0.61671	0.00207
APP	-1.01408	0.00306
GPR183	-1.14478	0.00810
FCGRT	-1.02561	0.00977
BCL6	-0.82290	0.01176
LILRB4	-1.32068	0.02545
SOCS3	-1.13423	0.03181
DUSP4	-1.25508	0.03229
IL32	-0.91869	0.03487

C

Gene	Log2 Fold Change	p value
IL2RG	0.80921	1.13E-06
IL13RA1	2.44517	8.74E-06
CD53	0.66188	0.00021
RARRES3	1.49315	0.00025
PSMB8	0.65936	0.00044
ICAM2	0.95986	0.00061
SIGIRR	1.18836	0.00095
CMKLR1	2.25043	0.00121
CD6	1.67762	0.00142
KIR3DL1	2.06041	0.00158

Figure 5. 25. Gene expression analysis of sorted ABCs from eRA patients compared to ABCs from ePsA patients. Cell lysates from sorted ABCs were loaded to the NanoString nCounter Technologies chip to assess gene expression. Raw counts were normalised to the housekeeping genes. Sample quality was then assessed using the arrayQualityMetrics package Gene expression profiles between different disease groups and healthy controls was assessed using the DESeq2 R package. Genes achieved statistical significance when the unadjusted p value was <0.05 and the fold change was >1.5. **A.** Volcano plot showing the Log2Fold change against the –log10 p value where genes plotted in red are upregulated and genes in green are downregulated in ABCs from eRA patients compared to ABCs from ePsA patients. **B.** Table showing the 10 most significant downregulated genes, with their fold change and p value. **C.** Table showing the 10 most significant upregulated genes, with their fold change and p value.

A

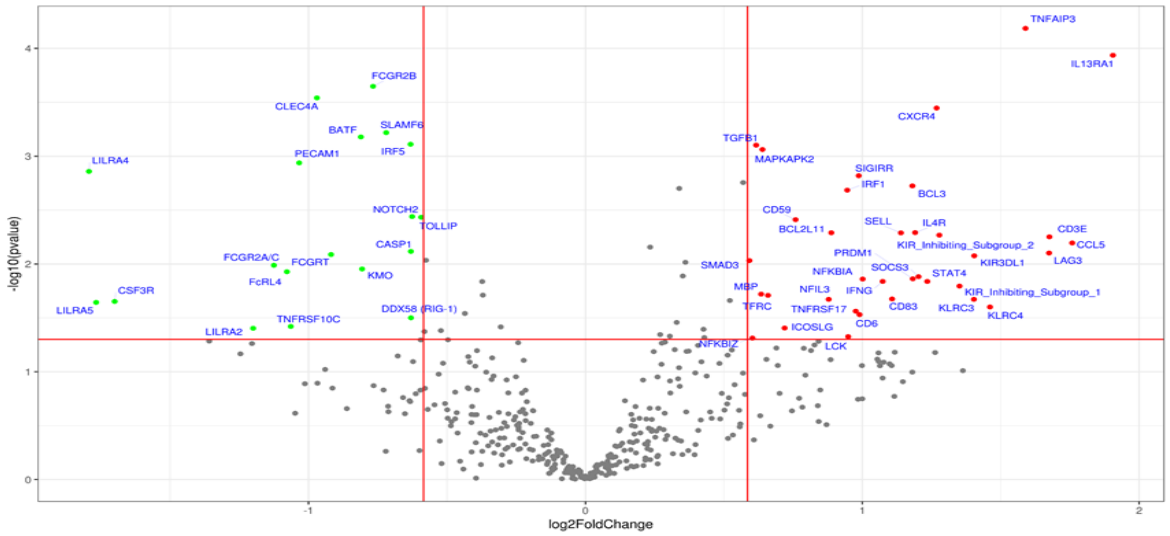

B

Gene	Log2 Fold Change	p value
FCGR2B	-0.76692	0.00022
CLEC4A	-0.96960	0.00028
SLAMF6	-0.71942	0.00060
BATF	-0.81090	0.00066
IRF5	-0.63134	0.00077
PECAM1	-1.03355	0.00115
LILRA4	-1.79269	0.00138
NOTCH2	-0.62571	0.00363
TOLLIP	-0.59297	0.00368
CASP1	-0.63014	0.00764

C

Gene	Log2 Fold Change	p value
TNFAIP3	1.58927	6.52E-05
IL13RA1	1.90512	0.00011
CXCR4	1.26832	0.00035
TGFB1	0.61662	0.00078
MAPKAPK2	0.63940	0.00086
SIGIRR	0.98703	0.00151
BCL3	1.18085	0.00188
IRF1	0.94548	0.00206
CD59	0.75898	0.00387
IL4R	1.19077	0.00511

Figure 5. 26. Gene expression analysis of sorted ABCs from eRA patients compared to ABCs from healthy controls. Cell lysates from sorted ABCs were loaded to the NanoString nCounter Technologies chip to assess gene expression. Raw counts were normalised to the housekeeping genes. Sample quality was then assessed using the arrayQualityMetrics package Gene expression profiles between different disease groups and healthy controls was assessed using the DESeq2 R package. Genes achieved statistical significance when the unadjusted p value was <0.05 and the fold change was >1.5. **A.** Volcano plot showing the Log2Fold change against the –log10 p value where genes plotted in red are upregulated and genes in green are downregulated in ABCs from eRA patients compared to ABCs from healthy controls. **B.** Table showing the 10 most significant downregulated genes, with their fold change and p value. **C.** Table showing the 10 most significant upregulated genes, with their fold change and p value.

A

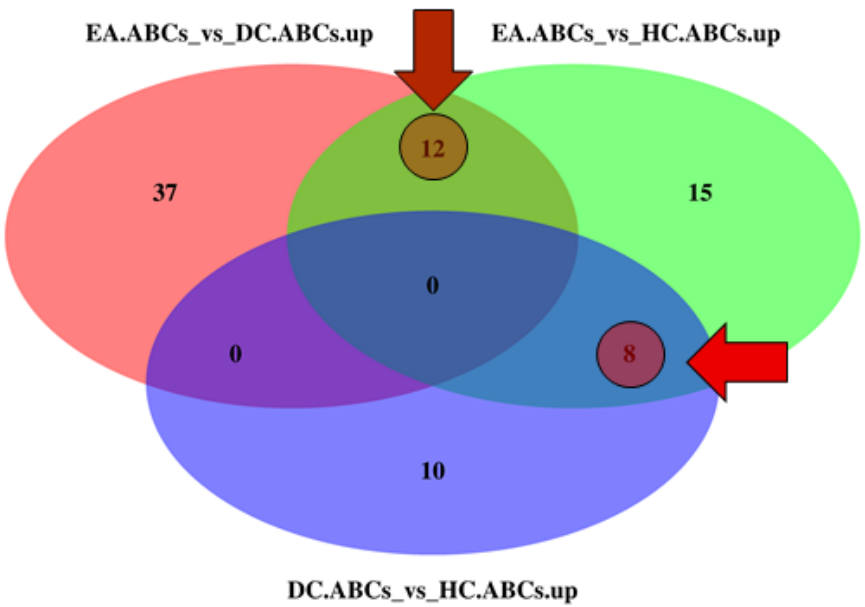

B

Upregulated in eRA compared to DCs and HCs	Upregulated in eRA and DCs compared to HCs
IL13RA1	CXCR4
SIGIRR	BCL3
CD6	BCL2L11
KIR3DL1	SOCS3
CD59	TFRC
LCK	CD83
IL4R	ICOSLG
SMAD3	NFKBIZ
KIR_Inhibiting_Subgroup_1	
KLRC3	
SELL	
IFNG	

Figure 5. 27. Venn diagram of overlapping upregulated genes in early RA, early PsA and healthy controls. Cell lysates from sorted ABCs were loaded to the NanoString nCounter Technologies chip to assess gene expression. Raw counts were normalised to the housekeeping genes. Sample quality was then assessed using the arrayQualityMetrics package Gene expression profiles between different disease groups and healthy controls was assessed using the DESeq2 R package. Genes achieved statistical significance when the unadjusted p value was <0.05 and the fold change was >1.5. **A.** Venn diagram of overlapping upregulated genes in the different disease groups. The red circles and the red arrows mark the genes upregulated in two comparisons. **B.** Table showing the list of upregulated genes for the comparisons highlighted in the Venn's diagram.

A

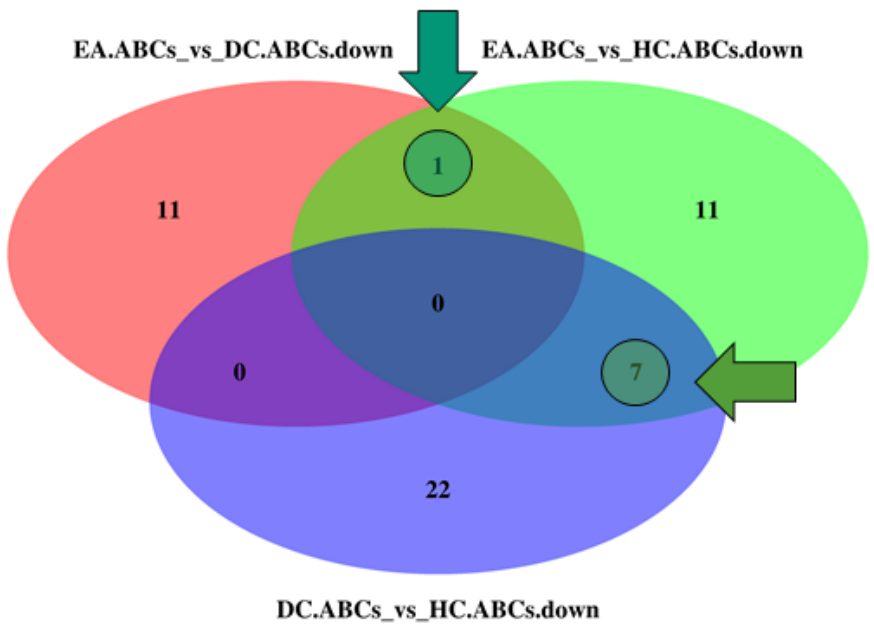

B

Downregulated in eRA compared to DCs and HCs	Downregulated in eRA and DCs compared to HCs
FCGRT	SLAMF6
	BATF
	IRF5
	LILRA4
	CASP1
	FcRL4
	DDX58 (RIG-1)

Figure 5. 28. Venn diagram of overlapping downregulated genes in early RA, early PsA and healthy controls. Cell lysates from sorted ABCs were loaded to the NanoString nCounter Technologies chip to assess gene expression. Raw counts were normalised to the housekeeping genes. Sample quality was then assessed using the arrayQualityMetrics package Gene expression profiles between different disease groups and healthy controls was assessed using the DESeq2 R package. Genes achieved statistical significance when the unadjusted p value was <0.05 and the fold change was >1.5. **A.** Venn diagram of overlapping downregulated genes in the different disease groups. The green circles and the green arrows mark the genes downregulated in two comparisons. **B.** Table showing the list of downregulated genes for the comparisons highlighted in the Venn's diagram

5.4.8 Retroelement expression in different B cell subsets and disease groups

Expression of retroelement sequences in the different B cell subsets and disease and healthy controls was assessed (Figure 5.29.A). When expression of the retroelements is split by B cell subset and donors are pooled, memory B cells show very low expression of the retroelements (Figure 5.29.A). Higher expression is seen in naïve and CD5+ B cells (Figure 5.29.A). Contrary to my hypothesis, ABCs showed low expression of all the retrotransposons (Figure 5.29.A).

Donors were separated into disease and healthy control groups, and expression of the retroelements assessed (Figure 5.29.B-D). In eRA patients, naïve B cells showed higher expression of the retroelements, whereas lower expression was seen in memory B cells and ABCs (Figure 5.29.B). In ePsA patients, higher expression was seen in CD5+ B cells and ABCs while memory B cells showed lower expression (Figure 5.29.C). In heathy controls, higher expression was shown in CD5+ B cells and low expression in memory B cells (Figure 5.29.D).

Expression in each subset comparing the different disease groups and the healthy controls was also examined (Figure 5.30). Naïve B cells showed higher expression of retroelements in eRA patients, whereas expression in ePsA patients was very low (Figure 5.30.A). In memory B cells, high expression was seen in eRA and healthy controls compared to the disease controls which showed very low expression (Figure 5.30.B). CD5+ B cells exhibited a similar pattern, with higher expression in eRA patients and healthy controls compared to disease controls (Figure 5.30.C). Finally, in ABCs, higher expression was seen in healthy controls, while eRA and ePsA patients showed low expression of the retroelements (Figure 5.30.D).

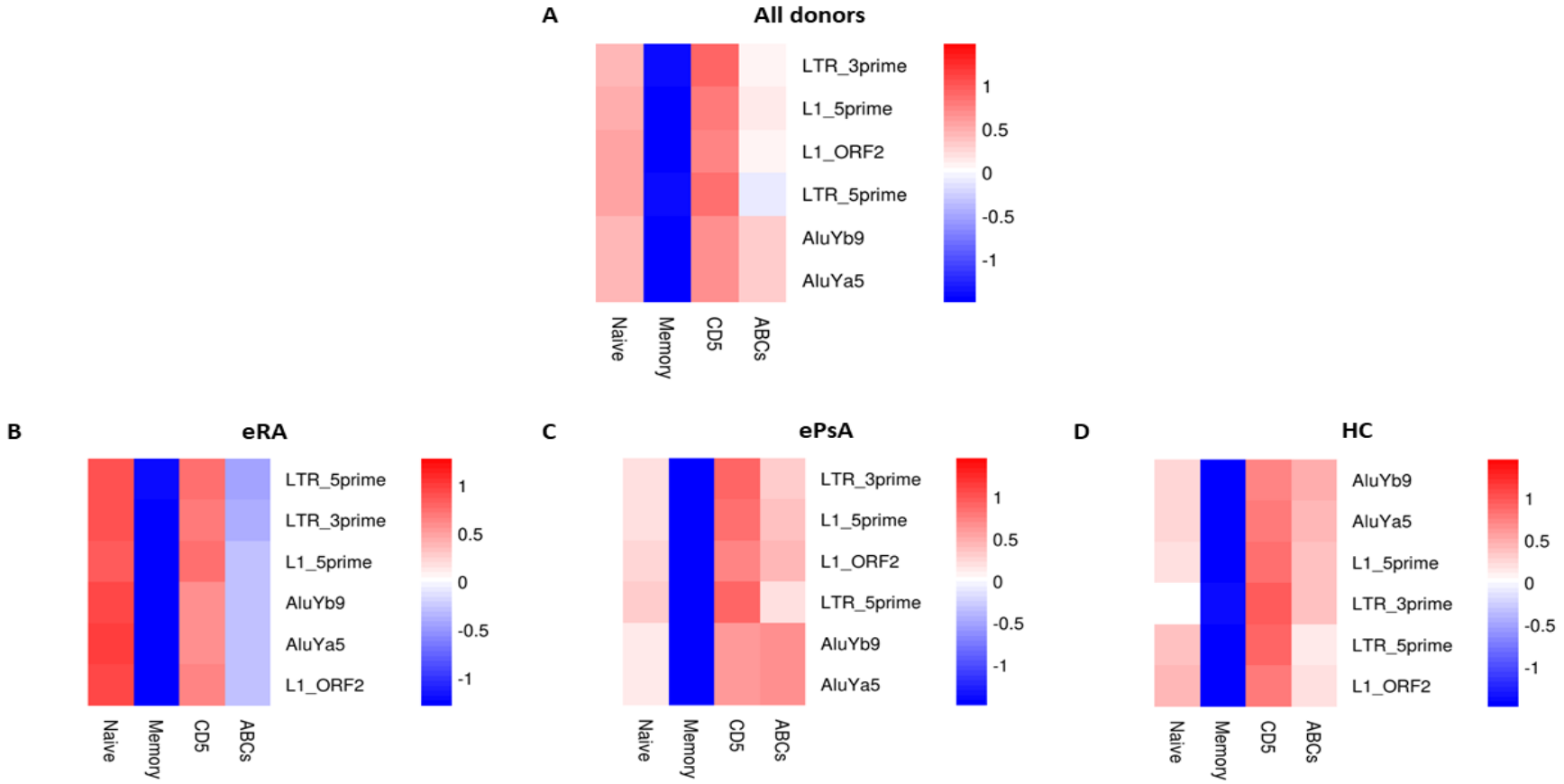

Figure 5. 29. Retroelement expression in the different B cell subsets from all the disease groups as well as the healthy controls. Heat map showing expression pattern of the endogenous retroelements. **A.** Expression of the group of retroelements in the different B cell subsets from all the samples, eRA, ePsA and HC. **B.** Expression of the group of retroelements in the different B cell subsets from only eRA patients. **C.** Expression of the group of retroelements in the different B cell subsets from only ePsA patients. **D.** Expression of the group of retroelements in the different B cell subsets from only healthy controls. For plotting, median log2 expression for each cell population were used. Red indicates higher expression, and blue indicates lower expression. Colour bar indicates Z score or adjusted p value.

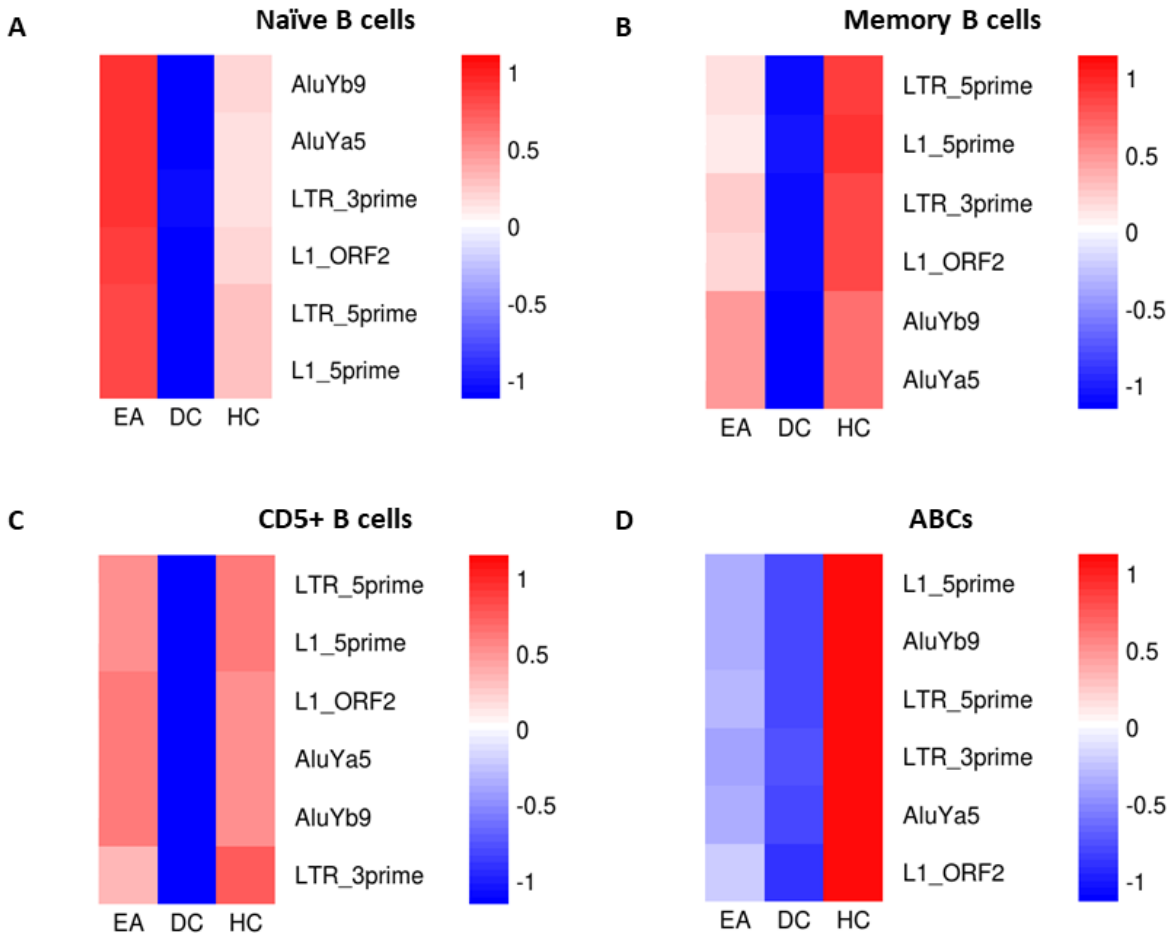

Figure 5. 30 Retroelement expression in the different disease groups and healthy controls plotted by B cell subsets. Heat map showing expression pattern of the endogenous retroelements. **A.** Expression of the group of retroelements in the naïve B cells from each disease group and healthy control group. **B.** Expression of the group of retroelements in the memory B cells from each disease group and healthy control group. **C.** Expression of the group of retroelements in the CD5+ B cells from each disease group and healthy control group. **D.** Expression of the group of retroelements in the ABCs from each disease group and healthy control group. For plotting, median log2 expression for each cell population were used. Red indicates higher expression, and blue indicates lower expression. Colour bar indicates Z score or adjusted p value.

5.5 Discussion

In this chapter I examined the transcriptome profile of ABCs and compared them to other B cell subsets, as well as assessing differences between arthritic diseases and healthy controls. I first optimised a protocol for the sorting of each of the B cell subsets to obtain pure populations for the use in the NanoString Technologies gene expression analysis. NanoString results showed that ABCs are a distinct B cell population with unique transcriptome profile that differs from other B cell subsets. Moreover, ABCs from eRA patients differ from those from PsA patients, as well as healthy controls.

Due to ABCs being found in very low percentages in peripheral blood, I was limited by the number of cells I could obtain after sorting, even when using the largest volume of blood I could obtain under the project ethics (80ml). The NanoString transcriptomic analysis can use RNA or cell lysates as input material. After sorting the highest number of ABCs, which was around 20,000 cells, RNA was extracted and quantified. However, the amount of RNA extracted from these low number of cells was very low (on average 5ng (data not shown)). Because NanoString requires 100ng of purified RNA to run the chip, using such low amounts of RNA would result in the loss of low-expressed genes, which could be very important for the ABCs characterisation. I, therefore, used a cell lysate approach to run the transcriptome analysis. Importantly, for the use of cell lysates, lower numbers of cells are needed (between 5,000 and 10,000). This was an advantage when studying rare subsets, so I optimised a protocol for the sorting and the preparation of the cell lysates from 15,000 cells to load on the chip (see Chapter 2, section 2.5.1 for detailed protocol).

Purity checks were performed in order to make sure that the sorted cells were pure enough as contamination with other cells would lead to erroneous results (Figure 5.4). Although the percentage of positive cells were about 85% in some subsets such as the ABCs, the sorted population was considered pure because the sorted cells had “spread” in terms of fluorescence and the gates were not moved to take this into account. It is known that cells can appear to change fluorescence slightly during sorting, fluorochromes are excited by the flow cytometer sorter and, when they are re-excited during purity checking, their emission can vary slightly with reduced fluorescence intensity (Cossarizza *et al.*, 2017). Moreover, the cells might also change in terms of morphology after sorting, and the way the population appears in the flow cytometry plots can also vary when only sorted cells are plotted. This can result in the cells being slightly outside of the original gates. However, due to the efforts

made to ensure high purity, like the filtering of the cells right before sorting to ensure a single-cell suspension, as well as the use of two excluding doublets gates, purity percentages of 85% were taken to indicate pure populations were being sorted. In addition, gene expression analysis confirmed that the populations were pure as the markers used to sort the cells appeared in the highly expressed gene lists.

Cytospin slides were prepared for the sorted populations to visualise the different subsets of B cells (Figure 5.5). No major differences were seen between the cells, as expected, because all subsets are B cells and there are no major differences detectable by light microscopy. However, there is a hint that naïve and CD5+ B cells are smaller with less cytoplasm (Arce *et al.*, 2001) than memory B cells and ABCs. These results fit with current dogma, as memory B cells are larger due to the fact that when they activate, they blast and increase protein production and therefore, these cells have a larger cytoplasm (Huggins *et al.*, 2007). Because ABCs are phenotypically similar to memory B cells, it was expected that they would look similar to the memory B cells. Moreover, previous studies in mice reported ABCs as slightly larger and more granular than follicular B cells (Rubtsov *et al.*, 2011). These findings are confirmed by the cytospin images compared to naïve B cells. No differences were seen with memory B cells. However, caution needs to be taken when interpreting these results as after sorting, some cells may die or become stressed from the process, and the cytospin process itself may cause some additional physical stress. Therefore, sorting and cytospins could influence the morphology and appearance of cells. Nevertheless, these results further confirm that ABCs resemble memory B cells in terms of morphology and appear to be large and granular cells.

For the gene expression analysis, differences in the expression of 628 genes in the different B cell subsets from early drug-naïve RA patients were examined. My results show that ABCs are a unique B cell subset, which clusters separately from the rest of the B cell subsets analysed (Figure 5.7). Moreover, there is a high number of up and downregulated genes between ABCs and the other B cells (Figure 5.8-10). Further analysis of the involved pathways reveals some interesting potential roles for ABCs. However, it is important to keep in mind that these results are derived from transcriptomic data and gene expression at the mRNA level does not always equate to the protein level. There is not always a relevant link between mRNA expression and function, which is why transcriptomic analysis is usually used as a hypothesis generating tool. Transcriptomics analysis is useful to create an

idea of the function and possible role of cells; however, additional functional work is needed to confirm the role of ABCs in health and disease.

Notwithstanding these caveats, the NanoString results show overexpression of some interesting genes, some of which have previously been reported in the literature and support a relevant role for ABCs in health and disease. Compared to other B cell subsets, ABCs show high expression of adhesion molecules such as integrins, as reported before (Isnardi *et al.*, 2010; Wang *et al.*, 2018). My results report high expression of alpha and beta integrins as well as other adhesion molecules (Figure 5.12). Integrins play a critical role in regulating the interaction between a cell and the microenvironment to control cell fate (Anderson *et al.*, 2014). Integrins initiate a wide range of changes which result in cells attaching to the extracellular matrix and migrating through it to other tissues. Each integrin is formed through the non-covalent association of one α-subunit and one β-subunit (Harburger and Calderwood, 2009). ABCs showed high expression of the two β-subunits, *ITGB1* and *ITGB2* and the α-subunits, *ITGAX*, *ITGAL* and *ITGAM*. The combination of these subunits results in an integrin that can bind different ICAM molecules as well as the iC3b complement fragment and fibrinogen. These combinations have been associated with leukocyte adhesion and transmigration (Bai *et al.*, 2017). The high expression of adhesion molecules by ABCs supports the idea that ABCs might migrate into inflammatory sites, like the synovial fluid in RA, which has been shown to have high percentages of these cells (see Figure 3.11-12 in Chapter 3 and (Amara *et al.*, 2017)). However, integrin function is more complex, and overexpression of integrins does not prove that these molecules will be functionally active. It has been reported that most of the integrins expressed on circulating leukocytes are found in the inactive or low affinity form, until the ligand triggers signalling and adhesion and migration starts (Schittenhelm *et al.*, 2017).

Interestingly, *CD97* expression, another adhesion molecule, was increased in ABCs compared to the other B cell subsets (Figure 5.16). This finding is novel and was confirmed at the protein level when comparing ABCs to naïve and CD5+ B cells (Figure 5.21). CD97 is a member of the EGF-TM7 subfamily of G protein-coupled adhesion receptors; it is known to mediate cell-cell interactions and play a role in cell adhesion, leukocyte recruitment, cell activation and migration to sites of inflammation (Hamann *et al.*, 2010). Moreover, CD97 has been shown to be a receptor for several ligands, including CD55 (Hamann *et al.*, 2016). CD55 is highly expressed by fibroblast-like synoviocytes (FLS) located in the lining layer of the synovium and has been shown to interact with CD97-

expressing macrophages in the rheumatoid synovium (Hamann *et al.*, 1999). Therefore, my findings are consistent with the hypothesis that this receptor-ligand interaction results in the recruitment and retention of CD97-expressing ABCs in the synovium, perpetuating the pro-inflammatory state. I am currently testing this hypothesis with a small grant from the JGW Patterson Foundation, a local charity.

Other differentially expressed pathways included chemokine receptors (Figure 5.12 and Figure 5.15). As shown previously, ABCs show low expression of chemokine receptors that mediate migration to lymphoid organs (Isnardi *et al.*, 2010; Jenks *et al.*, 2018; Wang *et al.*, 2018). My results confirmed these findings with low expression of *CXCR4* and *CXCR5*, as well as *CCR7*, by ABCs. These results were also confirmed at the protein level (Figure 5.17-19), supporting the hypothesis that ABCs are not recruited into lymphoid organs; ligands for these three receptors, CCL19 and CCL21, are found in high concentrations in lymphoid tissues (Mcheik *et al.*, 2019). IL-21, together with IFN-γ, induces an ABC-like phenotype in B cells, and also downregulates CXCR4 expression on centrocytes from germinal centres (Yoshida *et al.*, 2011). This could explain the low expression of this chemokine receptor by ABCs. Conversely, ABCs had high expression of the chemokine receptors, *CXCR3* and *CX3CR1*, both at the RNA and the protein level. These receptors mediate migration into inflammatory sites. Interestingly, CXCR3+ T-bet+ B cells have been reported in other inflammatory diseases, such as multiple sclerosis (van Langelaar *et al.*, 2019). These cells were shown to be enriched in different central nervous system (CNS) compartments of MS patients. Moreover, this study proved that TLR9 triggering upregulated T-bet and CXCR3 and was essential for IgG1 class-switching. This could link ABC expression of T-bet and CXCR3 with the TLR9 and TLR7 responsiveness of ABCs (Rubtsov *et al.*, 2011; Rubtsov *et al.*, 2013). The *CX3CR1* ligand, CX3CL1, is expressed on the surface of endothelial cells near inflamed tissues, attracting CX3CR1+ circulating cells (Lee *et al.*, 2018). Interestingly, some studies have shown that CX3CL1 levels in serum and synovial fluid of patients with RA are higher than in other inflammatory arthritides (Blaschke *et al.*, 2003; Yano *et al.*, 2007). These results support the hypothesis that ABCs migrate into inflammatory sites and promote disease pathogenesis.

The NanoString results also showed high expression of TNF and IFN receptors (Figure 5.12), indicating that ABCs might respond to TNF and IFN stimulation, known to play an important role in autoimmune diseases. Moreover, ABCs overexpress *IL21R* compared to memory B cells. Taken together, these findings support the suggestion that ABCs are

generated through IL-21 and IFN-γ stimulation (Naradikian *et al.*, 2016b). Moreover, TNF is an important pro-inflammatory cytokine, increased in RA synovial fluid, that contributes to the inflammation and joint destruction characteristic of RA (Bradley, 2008).

Interestingly, the ABC transcriptome also showed high expression of genes involved in NK cell cytotoxicity, such as granzymes and NK cell receptors (Figure 5.13). Some of the granzyme genes and perforin were reported previously by others (Rubtsov *et al.*, 2011). However, to my knowledge, this is the first time that NK cell receptors have been described in ABCs and B cells. Expression of some of these receptors outside the NK cell linage, such as the KIRs (Killer-cell Inhibitory Receptors), has been reported in a subset of activated CD8+ T cells (Moretta *et al.*, 1996). These cells had a memory phenotype and the expression of KIRs inhibited TCR mediated functions (Mingari *et al.*, 1998). Expression of the other overexpressed NK receptors, Killer Lectin-like Receptors (KLR), has also been reported in a subset of CD8+ T cells and that study showed that these receptors serve as an alternative pathway for cytotoxic T lymphocyte activation (Guma *et al.*, 2005). These results are of interest as ABCs are known to be unresponsive to BCR stimulation, and KIRs and KLRs on ABCs could provide an alternative activation pathway. Granzyme B and perforin expression could not be validated at the protein level (Figure 5.22-23). It is well known that RNA levels do not always correlate to protein expression levels (Liu *et al.*, 2016), as regulatory mechanisms can prevent RNA translation into protein. It is possible that ABCs express high RNA levels for these cytotoxic proteins but require a danger or activation signal to trigger protein translation. Nevertheless, granzyme B expression showed around 10-25% of positive cells, depending on the B cell subset (Figure 5.22). These percentages are surprisingly high and could be due to the intracellular staining increasing cells autofluorescence and producing a slight shift of the population that was not corrected when setting the gate based on the FMO. These results showing high expression of NK cell markers that could not be proven at the protein level, led me to consider that an NK cell contamination could have happen during sorting. However, this is improbable because although NK cells express CD11c and lack CD21 (like ABCs) they do not express CD19 and they would not be present in the B cell population used to then gate the ABCs as CD19+ CD11c+ CD21low B cells.

Finally, ABCs showed high expression of genes related to apoptosis (Figure 5.13), such as *FAS* and caspases, as well as inhibitory receptors (Figure 5.14), such as *FCGR* and *LILRB*, raising the hypothesis that these cells are refractory to BCR activation and could be an

anergic and exhausted B cell subset. ABCs have been reported as an exhausted B cell subset by other groups (Isnardi *et al.*, 2010). Moreover, high expression of apoptosis related genes supports the hypothesis that these cells might exhibit defective cell survival. Additionally, ABCs show low expression of genes involved in protection against complement-mediated cell lysis, such as *CD59* and the complement receptors *CR1* and *CR2* (CD21). Thus, these cells may be more susceptible to complement lysis and reinforces their susceptibility to cell death (Karnell *et al.*, 2017).

Gene expression in ABCs from different diseases and healthy controls was also assessed (Figure 5.24-28). As disease controls, drug naïve patients newly diagnosed with PsA were recruited. PsA was chosen as a disease control because it is also an autoimmune disease which causes joint destruction and loss of function (Gladman, 2015). PsA is also a good disease control because its pathogenesis differs from RA. In PsA the HLA alleles associated with the disease are from the MHC class I complex rather than MHC class II as in RA (Merola *et al.*, 2018). Moreover, most PsA patients are seronegative for autoantibodies. There were no differences between RA patients, PsA patients and healthy controls in terms of age and sex. The only significant difference, as expected, was in autoantibody seropositivity, as all RA patients recruited were double positive for RF and ACPA and the PsA patients were all seronegative.

Upregulated genes in early RA compared to both control groups, showed enrichment for leukocyte activation and migration (*CD6*), NK cell cytotoxicity (KIRs and KLRs) and IL-13 signalling (*IL13RA1* and *IL4R*) (Figure 5.27). Because these genes are upregulated in RA only, they could represent a RA specific gene signature only found in ABCs from RA patients. Notably, the two upregulated genes *IL13RA1* and *IL4R* form a functional receptor for IL-13 (Murata *et al.*, 1998). Moreover, genetic variants in the *IL4R* gene in RA have been linked to increased joint damage (Krabben *et al.*, 2013). IL-13 has been shown to be increased in synovial fluid in patients with early RA compared to established RA patients and other inflammatory arthritides (Raza *et al.*, 2005). Another study showed that IL-13 decreased the production of pro-inflammatory cytokines by synovial fluid mononuclear cells (Isomaki *et al.*, 1996). Although it has not been reported before, ABCs from RA patients may respond to the cytokines IL-4 and IL-13. However, these results are potentially inconsistent with studies that show that IL-4 antagonises expression of T-bet by B cells (Naradikian *et al.*, 2016b).

Differentially expressed genes were also detected in early RA and PsA patients compared to healthy controls (Figure 5.27). STAT3-inducible genes like *BCL3* and *SOCS3* were upregulated. Interestingly, previous work in our group defined a CD4+ T cell gene signature which implicates interleukin 6-mediated STAT3 signalling in early RA (Pratt *et al.*, 2012; Anderson *et al.*, 2016; Anderson *et al.*, 2019). Both *BCL3* and *SOCS3* were upregulated in CD4+ T cells from patients with early RA compared to other arthritic diseases. In contrast, my results show upregulation of these genes in ABCs from both RA and PsA patients compared to healthy controls. This discrepancy could reflect the examination of different cells (ABCs vs CD4+ T cells), or the inclusion of a healthy control group in my study. Intriguingly, downregulated genes included inhibitory receptors such as *FcRL4*, *LAIR1* and *LILRA4* (Figure 5.28). These receptors are usually associated with dampening of BCR signalling (van der Vuurst de Vries *et al.*, 1999; Sohn *et al.*, 2011). High expression of inhibitory receptors such as FCGR2B and LILRBs has been reported in ABCs before (Karnell *et al.*, 2017), consistent with my results. My supervisor in Birmingham, Professor Dagmar Scheel-Toellner, characterised a subset of B cells with high expression of FcRL4 in the synovial fluid of patients with RA (Yeo *et al.*, 2015), whereas I have found lower expression of *FcRL4* in ABCs from patients with RA and PsA compared to HCs. This could reflect differences in the tissue studied (peripheral blood vs synovial fluid). For example, FcRL4 high cells may have higher migration capacity towards inflamed joints, with FcRL4 low B cells remaining in peripheral blood B cells. Also, the B cells studied by Dagmar are not identical to ABCs in other characteristics. However, it is interesting that these inhibitory receptors are downregulated in inflammatory arthritic diseases compared to healthy controls. This would reinforce the hypothesis that in inflammatory conditions these cells might be more pathogenic due to downregulation of inhibitory mechanisms.

Retroviral expression analysis disproved the hypothesis that ABCs from RA patients have higher retroviral expression, which could have activated them via TLR7. Previous work from our group found higher expression of all six retrotransposons in B cell and CD4+ T cell populations in eRA compared to CD14+ monocytes, plasmacytoid DCs and myeloid DCs (Cooles *et al.*, unpublished results). However, when B cells from eRA patients were split into subsets, the highest expression of these retroelements was seen in the naïve and CD5+ B cell subsets (Figure 5.30). Expression of retroelements in ABCs and memory B cells was low. These results are consistent with the fact that a high proportion of peripheral

blood B cells are naïve B cells (Perez-Andres et al., 2010). The percentage of ABCs in peripheral blood is very low and their gene expression would be masked by that of more abundant subsets. Previous work reported that retroelements are strongly induced during B cell activation (Kassiotis and Stoye, 2016; Attig *et al.*, 2017). This is not in line with my results as memory B cells, which are activated cells, had low expression of the endogenous retroviruses. It is possible, however, that expression of retroelements is transient upon B cell activation. ABCs from healthy controls showed higher expression of retroviral elements than eRA and ePsA patients. Previous studies in MS showed high expression of two human endogenous retrovirus (HERVs) envelop proteins in this neurological and autoimmune disease (Brudek *et al.*, 2009). In contrast with my data, these two viral proteins were detected at higher levels in peripheral blood B cells of patients with active MS compared to healthy controls and other neurological controls. Some studies have described expression of LINE retroelements in RA synovial fluid and synovium (Neidhart *et al.*, 2000; Ali *et al.*, 2003). However, expression of retroelements in RA synovial fluid B cells has not been assessed specifically and it may be a more informative tissue than peripheral blood B cells.

A major consideration, with regard to my findings, is the small sample size used. Only 4 individuals per group were recruited due to the need for age-matched healthy controls, and the isolation of sufficient numbers of subsetted B cells for analysis. Due to the high heterogeneity present in RA, high sample sizes are often needed to overcome individual variability, which needs to be recognised when studying my data.

It is currently unclear whether the ABC subset is anergic or if it plays an important role in autoimmunity and disease pathogenesis. Gene expression analysis is consistent with ABC being a hyporesponsive B cell subset, although the high expression of activation markers, adhesion molecules and chemokine receptors, supports these cells playing an important role in inflammation and autoimmunity. Further functional studies are still needed to unravel the role of ABCs in health and disease.

5.6 Conclusions

In this chapter, I optimised a protocol for sorting different B cell subsets to obtain pure populations. This allowed me to assess the expression of 628 gene using the NanoString Technology nCounter. The transcriptome of ABCs was compared to other B cell subsets. Moreover, I examined gene expression of ABCs from patients suffering from early RA and compared it to the ABC transcriptome in early PsA and age-matched healthy controls.

Purity checks were performed in order to ensure that sorted populations contained the correct subset of B cells. Due to the limiting number of ABCs, cell lysates rather than mRNA were used as the input material for hybridisation chips used in NanoString analysis.

Gene expression analysis of ABCs compared to other B cells revealed a different population of B cells with a unique transcriptome, enriched for adhesion molecules, such as integrins, chemokine receptors involved in leukocyte recruitment to sites of inflammation, and NK cell cytotoxicity enzymes and receptors. This supports the hypothesis that ABCs migrate to sites of inflammation, such as the synovium in RA patients, where they may promote disease pathogenesis. However, ABCs also displayed high expression of apoptosis molecules such as caspases, and inhibitory receptors like LILRs. These data reinforce previous findings that ABCs might be an exhausted and anergic B cell subset, unable to respond to BCR stimulation and prone to die by apoptosis. In addition, a few genes, such as KLRs, were differentially expressed in ABCs from eRA patients compared to ePsA and HCs. Other genes were also up or downregulated in eRA ABCs compared to the control groups, potentially highlighting them as RA specific genes; others were differentially expressed in both arthritic diseases compared to healthy controls, potentially suggesting an inflammation related signature. However, my small sample size means that this work must be viewed as preliminary and hypothesis generating; a bigger sample size would provide more definitive information on the role of ABCs in health and disease.

In summary, ABCs are a novel B cell subset which shows a unique transcriptome profile. My analysis indicates that these cells may migrate to sites of inflammation. However, further functional studies are needed to determine their contribution to health and disease.

Chapter 6. Functional characterisation of ABCs

6.1 Introduction

In addition to the characterisation of ABCs surface phenotype and gene expression, I aimed to investigate the role of these cells through functional studies.

Studies in mice demonstrated that when ABCs were stimulated by a TLR7 agonist, they produced similar levels of IgM as other B cell subsets, but also produced higher levels of IgG (Rubtsov *et al.*, 2013; Rubtsova *et al.*, 2017). This IgG recognised chromatin, suggesting that ABCs may be a source of autoantibodies. Interestingly, simultaneous stimulation with TLR and BCR ligation produced the strongest response, resulting in extensive division and high numbers of responding cells (Hao *et al.*, 2011). Moreover, these ABCs preferentially expressed IL-4 and IL-10 after TLRs stimulation as assessed by qPCR and polarised T cells towards a Th17 response. Studies in mice also showed that generation of CD11c+ T-bet+ B cells required TLR engagement together with a specific cytokine network (Naradikian *et al.*, 2016b). In the absence of IFN-γ signalling, the ratio between IL-4 and IL-21 determines B cell expression of CD11c and T-bet, with low IL-4 and presence of IL-21 driving this expression. So, the generation of ABC-like B cells in autoimmunity and viral infection would depend on TLR engagement together with abundant IFN-γ and IL-21 in absence of IL-4.

In humans only a few studies have investigated the functional role of ABC-like cells of a similar phenotype (CD21low B cells). Some studies showed that these CD21low B cells were unable to activate, proliferate and secrete antibodies after BCR triggering (Isnardi *et al.*, 2010). Moreover, these cells were prone to die by apoptosis. In line with these results, another study found that CD21low CD86+ B cells have impaired BCR-induced signalling, as there was no calcium release detected when the BCR was cross-linked (Shimabukuro-Vornhagen *et al.*, 2017). Although these cells have been shown to be unresponsive to BCR and CD40 signalling, their responses were not globally impaired. In some autoimmune diseases, these cells have been shown to be responsive to TLR7-8 signalling in conjunction with other stimulatory signals such as BCR and IL-2 stimulation (Thorarinsdottir *et al.*, 2016). Overall, these studies suggest that instead of being unresponsive and anergic, these ABC-like cells might exhibit a different response profile, depending on a very specific cytokine milieu, than conventional naïve and memory B cells. Additionally, studies in SLE patients show that CD11c+ B cells were poised to become plasma cells after T cell

activation and had very high secretion of autoantibodies compared to memory B cells (Wang *et al.*, 2018).

Moreover, the FcRL4+ synovial fluid B cell subset with a similar phenotype as ABCs was shown by qPCR to produce RANKL and TNF-α (Yeo *et al.*, 2015). These two cytokines are known to stimulate the differentiation and activation of osteoclasts, suggesting a potential role for FcRL4+ B cells in RA pathogenesis.

However, there is a lack of studies investigating the cytokines secreted by ABC-like B cells. Some mice studies showed ABCs to preferentially secrete IL-4 and IL-10 after TLR7 or TLR9 stimulation (Hao *et al.*, 2011), and TNF-α after TLR4 stimulation (Ratliff *et al.*, 2013). For all that, studies of cytokine secretion after combined TLR and cytokine stimulation are needed to further investigate the role of ABCs in health and disease.

Therefore, I sorted and cultured blood ABCs from patients and controls and assessed phenotype cell marker expression, cytokine production, and immunoglobulin secretion.

6.2 Chapter hypothesis and aims

In this chapter I hypothesised that ABCs are a responsive B cell subset capable of producing proinflammatory cytokines as well as immunoglobulins in response to a B cell stimulation cocktail. Because I hypothesised that ABCs are antigen-experienced B cells and may already be class-switched, the aim was to assess the effect a potent B cell stimuli had on these cells.

Therefore, the aims of this chapter were to:

1. Determine if ABCs show a different cytokine and immunoglobulin production profile than other B cell subsets after potent B cell stimulation.
2. Determine if ABCs from established RA patients respond differently to stimuli compared to those from age-matched healthy controls.

The specific objectives were:

1. Optimise the culturing conditions for the B cell subsets' stimulation assays.
2. Optimise a protocol for the sorting of the B cell subsets that reduced the sorting time.
3. Characterise the phenotype of ABCs compared to other B cell subsets after potent stimulation.
4. Determine the cytokine secretion profile of ABCs compared to other B cells.
5. Compare the cytokine secretion profile in established RA patients and healthy controls.
6. Determine the immunoglobulin production by ABCs and other B cell subsets.
7. Compare the immunoglobulin production profile in established RA patients and healthy controls.

6.3 Methods

All the work completed in Chapter 5 – on ABCs RNA expression profiling was done by sorting B cells from PBMCs. The sorting time from total PBMCs was very long, therefore the cells were exposed to potentially high levels of stress resulting in high cell death. Because the cells were to be used in functional studies the stress the cells were placed under needed to be kept to a minimum to try and keep the cells healthy and viable. Therefore, a protocol was optimised to reduce the sorting time and keep it to a minimum. This was achieved by depleting all the CD3+ cells from the PBMCs fraction using a CD3 MicroBead Kit (Miltenyi Biotech, Germany).

Briefly, PBMCs were isolated from EDTA blood using Lymphoprep (Axis-Shield Diagnostics Ltd, UK). T cells were then depleted using the positive selection CD3 MicroBeads (see Chapter 2 Methods section 2.2.1 for more detail). Because B cells are found in the CD3- fraction, this fraction was then stained for surface antibodies and live/dead dye and sorted on the BD FACSARIA II (Becton Dickinson, NJ, USA). The antibodies used to identify each subset are shown in Table 2.6 in Chapter 2.

Four populations of interest were sorted into 300µl of RF10: ABCs (CD19+CD11c+CD21), CD5+ cells (CD19+ CD5+), naïve B cells (CD19+IgD+CD27-) and memory B cells (CD19+IgD-CD27+). The sorting strategy is shown in Figure 6.1. After excluding dead cells and doublets using two doublet gates, lymphocytes were gated using SSC-A vs FSC-A. From the lymphocyte gate, B cells were gated using CD19 vs CD3/CD33, therefore excluding any remaining T cells and dendritic cells. From the B cell gate, the ABCs were gated using CD11c vs CD21 expression. From the rest of the cells, CD5+ cells were gated using CD5 and CD19 expression. Finally, from the CD5- fraction, naïve (IgD+CD27-) and memory (IgD-CD27+) B cells were gated.

After sorting, cells were counted using a Burker counting chamber (Sigma-Aldrich, MO, USA). Cells were then centrifuged and each cell type was cultured at a density of 20,000 cells per well in 96-well round-bottom plates in a final volume of 200µl of medium. At initiation of culture, B cells were stimulated with a combination of TLR7 ligand Imiquimod, TLR9 agonists ODN 2216 – CpG A and ODN 2006 – CpG B, Poke Weed Mitogen, anti-CD40, human IL-21, human IL-4 and IFN-gamma. B cells were cultured for 5 days at 37°C with 5% CO_2 prior to examination by flow cytometry. Supernatants were frozen at -80°C prior to further analysis by ELISA or MSD assay.

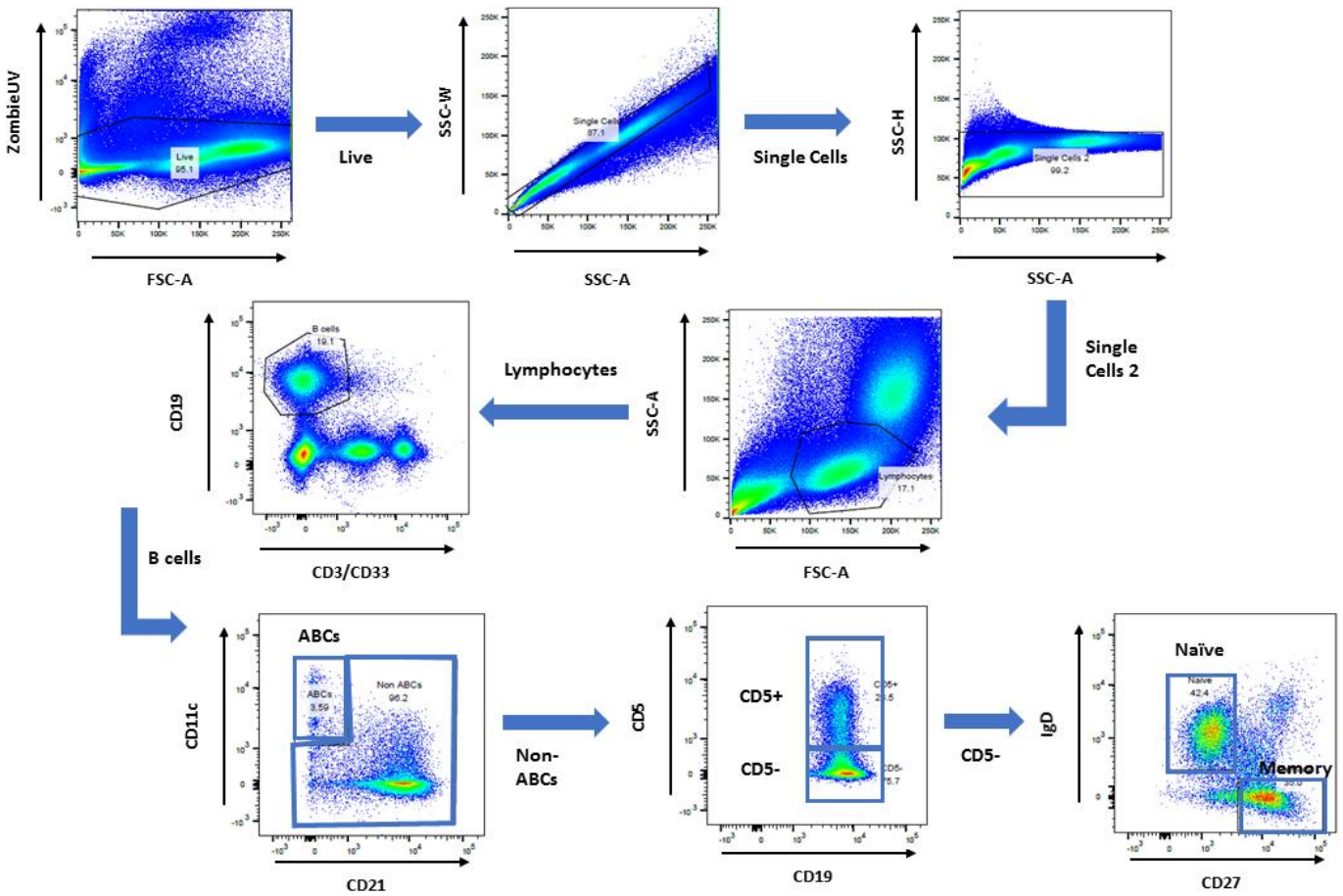

Figure 6. 1. **Gating strategy for the sorting of each B cell subset from the CD3- fraction.** Example of the gating strategy used to sort the B cell populations for the functional work. After excluding dead cells and doublets twice, lymphocytes were gated using SSC-A vs FSC-A. From the lymphocyte gate, B cells were gated using CD19 vs CD3/CD33. From the B cell gate, the ABCs were gated using CD11c vs CD21. From the rest of the cells, CD5+ cells were gated using CD5 and CD19. Finally, from the CD5- fraction, naïve (IgD+CD27-) and memory (IgD-CD27+) B cells were gated.

6.4 Results

6.4.1 Optimisation of the culture volume for sorted B cells

For the functional work I was limited by the small numbers of ABCs in peripheral blood. Therefore, the plate chosen to culture the cells in was a 96-well round-bottom plate. A round bottom plate was chosen over a flat plate because in the round bottom plate the cells are forced closer together to the centre of the well and this is better when working with small number of cells. However, the final volume to culture the cells needed to be optimised. I tested two different culture volumes, 100µl and 200µl. For this, I sorted memory and naïve B cells and cultured the same number of cells, 20,000, in the two volumes with and without the stimulation cocktail. After 6 days, the cells were harvested and their viability was assessed. In addition, the culture supernatants were stored for quantification of IgG production by ELISA. IgG production was chosen over other cytokines as all memory B cells after stimulation are known to secrete class-switched immunoglobulins like IgG. Figure 6.2 shows the results for the memory B cells only. The results from the naïve B cells were not informative as the majority of the cells were dead by day 6 and stimulation for 6 days is not enough for the cells to class switch and produce IgG (data not shown). As shown in Figure 6.2.A, there is a trend for more reproducible and higher percentages of live cells in the stimulated memory B cells when cultured in 200µl compared to 100µl. Moreover, IgG production is also slightly higher and more reproducible in the 200µl volumes of stimulated cells compared to the smaller culture volume. Although being double the volume, IgG production was easily detected in the 200µl cultures, and counterintuitively the concentration detected in the 200µl cultures was not half the concentration detected in the 100µl cultures (Figure 6.2.B). Thus, memory B cells seem to be more viable and healthier and produce more consistent, reliable results in the 200µl culture volume. For this reason, the 200µl culture volume was chosen for the subsequent functional work.

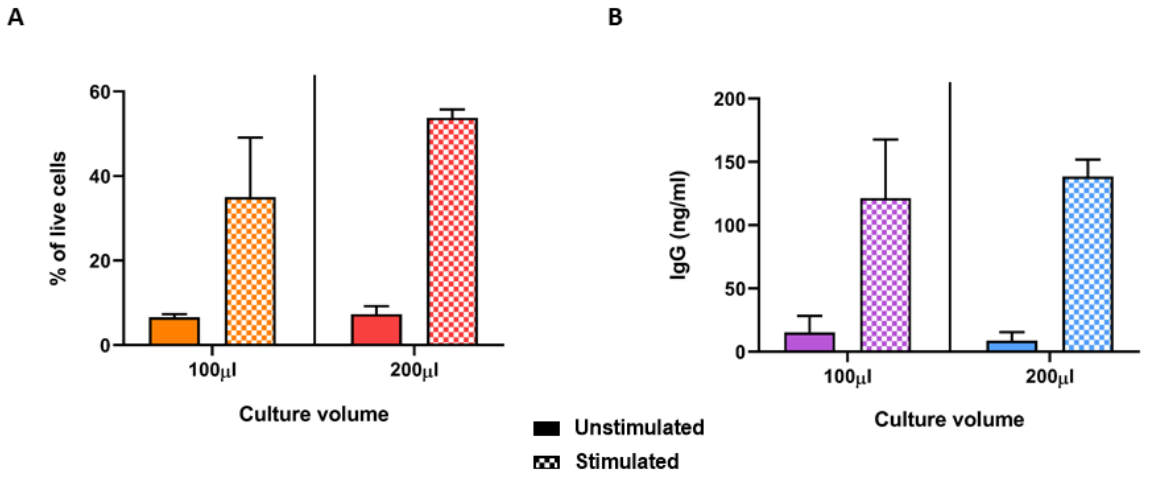

Figure 6. 2. Effect of culture volume on cell viability and IgG production. 20,000 sorted memory B cells were plated in a final volume of 100µl or 200µl culture medium and either left unstimulated or stimulated with a cocktail of stimuli for 6 days. The stimuli cocktail contained TLR7 ligand Imiquimod, TLR9 agonists ODN 2216 – CpG A and ODN 2006 – CpG B, Poke Weed Mitogen, anti-CD40, human IL-21, human IL-4 and IFN-gamma. Unstimulated cells are shown in the filled bars and stimulated in the pattern bars. **A.** Percentage of live cells assessed by Zombie Aqua staining and flow cytometry. **B.** Immunoglobulin G production measured by ELISA from supernatants. No statistical test was performed due to low number of repeats; n = 2, mean values with SEM shown.

6.4.2 Optimisation of the number of cells cultured for the functional work

Due to very small numbers of ABCs in peripheral blood, the number of cells used for the functional assays cell cultures needed to be the minimum which would still produce detectable cytokines and immunoglobulins. Following, the protocol in section 6.3, I sorted memory and naïve B cells and plated two different numbers of cells, 10,000 and 20,000 cells. I then cultured the cells with and without stimulation in a 200µl culture volume for 6 days. As described before, the majority of the naïve B cells died after 6 days, so only the results for the memory B cells are shown (Figure 6.3). There was no difference in the percentage of live cells in the 20,000 cells groups stimulated compared to the 10,000 cells (Figure 6.3.A). In terms of IgG production, there was also no clear difference between the 20,000 stimulated cells compared to the culture containing 10,000 cells (Figure 6.3.A). However, the higher number of cells (20,000) enabled the detection of small concentration of spontaneous IgG production in the unstimulated cells. Consequently, cultures of 20,000 cells were chosen as it would give increased confidence that production of cytokine and immunoglobulin would be within the detection range, and at the same time I would have sufficient numbers of ABCs to include both unstimulated and stimulated conditions.

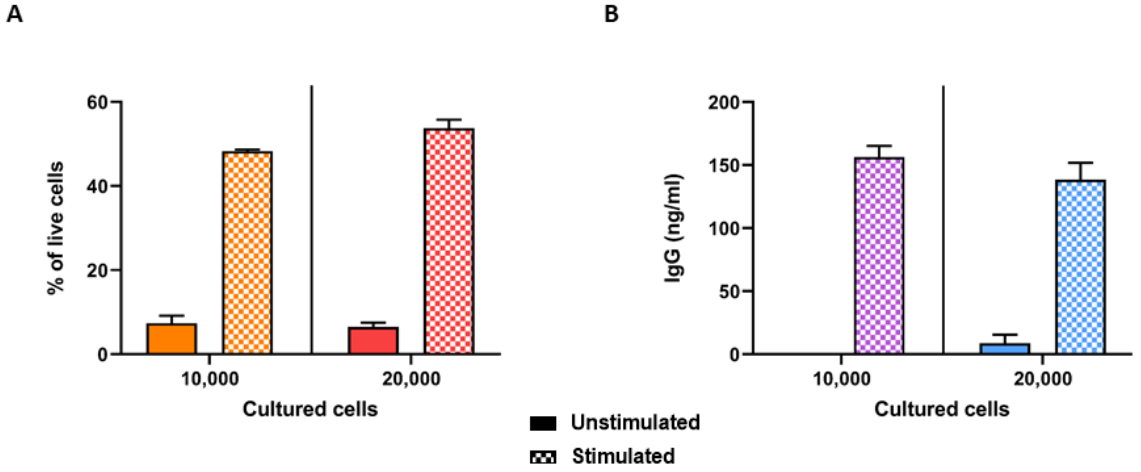

Figure 6. 3. Effect of the number of cultured cells on cell viability and IgG production. Two different numbers of memory B cells, 10,000 cells and 20,000 cells, were plated and either left unstimulated or stimulated with a cocktail of stimuli for 6 days. The stimuli cocktail contained TLR7 ligand Imiquimod, TLR9 agonists ODN 2216 – CpG A and ODN 2006 – CpG B, Poke Weed Mitogen, anti-CD40, human IL-21, human IL-4 and IFN-gamma. Unstimulated cells are shown in the filled bars and stimulated in the pattern bars. **A.** Percentage of live cells assessed by Zombie Aqua staining and flow cytometry. **B.** Immunoglobulin G production measured by ELISA from supernatants. No statistical test was performed due to low number of repeats; n = 2, mean values with SEM shown.

6.4.3 Optimisation of the culture time for the functional work

The culturing time also needed to be optimised. Due to small numbers of ABCs, it was not possible to include different time points for the functional work. I therefore tested incubating naïve and memory B cells for 3 days or for 6 days. Following on from the previous optimisation experiments, naïve and memory B cells were sorted, and 20,000 cells were plated in a 200µl volume. As before, I used an unstimulated and a stimulated condition. Only memory B cells results are shown (Figure 6.4). The results from the naïve B cells were not informative as the majority of the cells were dead by day 6. The percentage of live cells, as expected, was higher after 3 days of culture compared to 6 days, especially in the stimulated B cells (Figure 6.4.A). By day 6, most of the unstimulated cells had died, but the stimulated conditions still had a reasonably high percentage of viable cells. In terms of IgG detection as a functional readout, by day 3 there was some IgG production following stimulation (Figure 6.4.B). Nevertheless, after 6 days, the detectable concentration of secreted IgG was doubled in the stimulated cells. Due to the higher detectable concentrations of IgG by day 6, this time point was chosen over the day 3 time point. However, due to clinic and sample time restrictions, this time point was unfeasible therefore, the final incubation time for the functional work was chosen as 5 days.

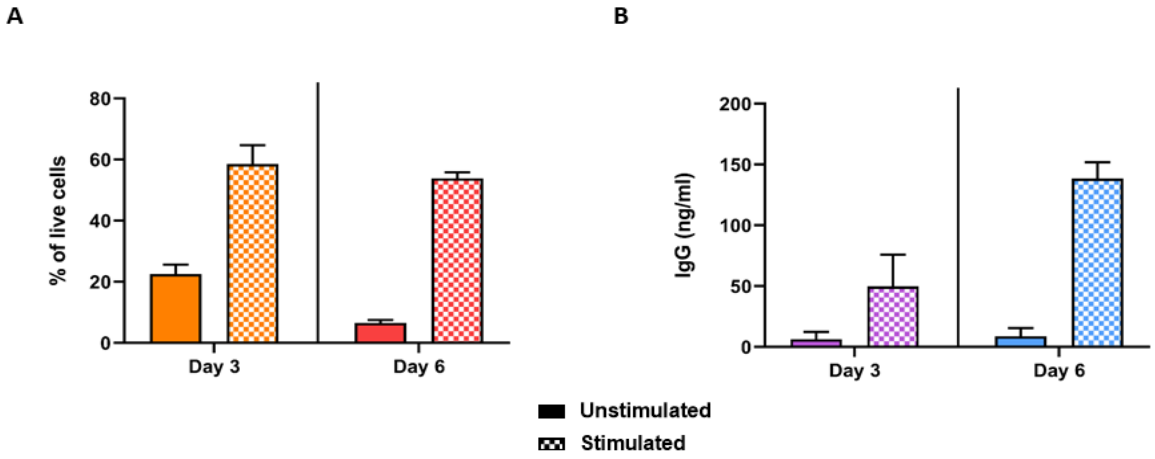

Figure 6. 4. Effect of the incubation time on cell viability and IgG production. 20,000 memory B cells were either left unstimulated or stimulated with a cocktail of stimuli for 3 or 6 days. The stimuli cocktail contained TLR7 ligand Imiquimod, TLR9 agonists CpG A and CpG B, Poke Weed Mitogen, anti-CD40, human IL-21, human IL-4 and IFN-gamma. Unstimulated cells are shown in the filled bars and stimulated in the pattern bars. **A.** Percentage of live cells assessed by Zombie Aqua staining and flow cytometry. **B.** Immunoglobulin G production measured by ELISA from supernatants. No statistical test was performed due to low number of repeats; n = 2, mean values with SEM shown.

6.4.4 Sorting B cell subsets from a pre-enriched B cell population

In order to get the maximum number of ABCs, a large number of PBMCs had to be isolated and sorted. This resulted in very long sorting hours, which in addition to being expensive, also had the potential to impact on cell viability and quality. In order to reduce the sorting time to enable the isolation of viable and healthy cells, I tested a method of sorting from previously enriched B cell population. I isolated PBMCs from the blood of a single donor and then split them in half: One half was used to enrich for B cells using Miltenyi MACS CD19 MicroBeads; the other half was left as PBMCs. Both populations were then stained using my pre-optimised B cell sorting panel and naïve and memory B cells were sorted from each cell preparation. Sorted naïve and memory B cell populations from cell preparations were incubated with and without stimulation. After 6 days, the cells were harvested and their viability and phenotype was assessed. In addition, the culture supernatants were stored for quantification of IgG production by ELISA.

Figure 6.5.A shows the percentage of live cells in the naïve and the memory subsets when cells were sorted from either isolated PBMCs or pre-enriched CD19+ B cells. As expected, the percentage of live cells in the naïve B cell subset, irrespective of the isolation technique, is low, especially when the cells were left unstimulated. However, for the stimulated naïve B cell condition, cells sorted from the pre-enriched CD19+ B cells had a particularly low percentage of live cells compared to the corresponding cells sorted from PBMCs. A similar trend is seen for the memory B cells, although these had a much higher proportion of live cells than in naïve B cells, the difference between the two isolation techniques was minimal (Figure 6.5.A). An informative phenotypic marker which seem to be altered between the two isolation techniques was the co-stimulatory molecule CD40 (Figure 6.5.B). Because I used an anti-CD40 antibody in the stimulation cocktail, CD40 appears to be downregulated in the stimulated conditions. However, in the unstimulated cells sorted from pre-enriched CD19+ B cells, CD40 seems to be greatly downregulated, especially in the naïve B cells (Figure 6.5.B). In terms of IgG production, only the results from the memory B cells are shown, as there was no detectable IgG production by the naïve B cells from any condition (data not shown). IgG production is slightly higher in stimulated memory B cells sorted from PBMCs compared to those sorted from pre-enriched CD19+ B cells (Figure 6.5.C). Similar concentrations of IgG are detected in both isolation techniques for the unstimulated memory B cells.

Taken together, these data suggest that pre-enriching CD19+ B cells using CD19 MicroBeads by positive selection may have an effect on B cell function, as expression of the key co-stimulatory molecule, CD40, appears to be altered.

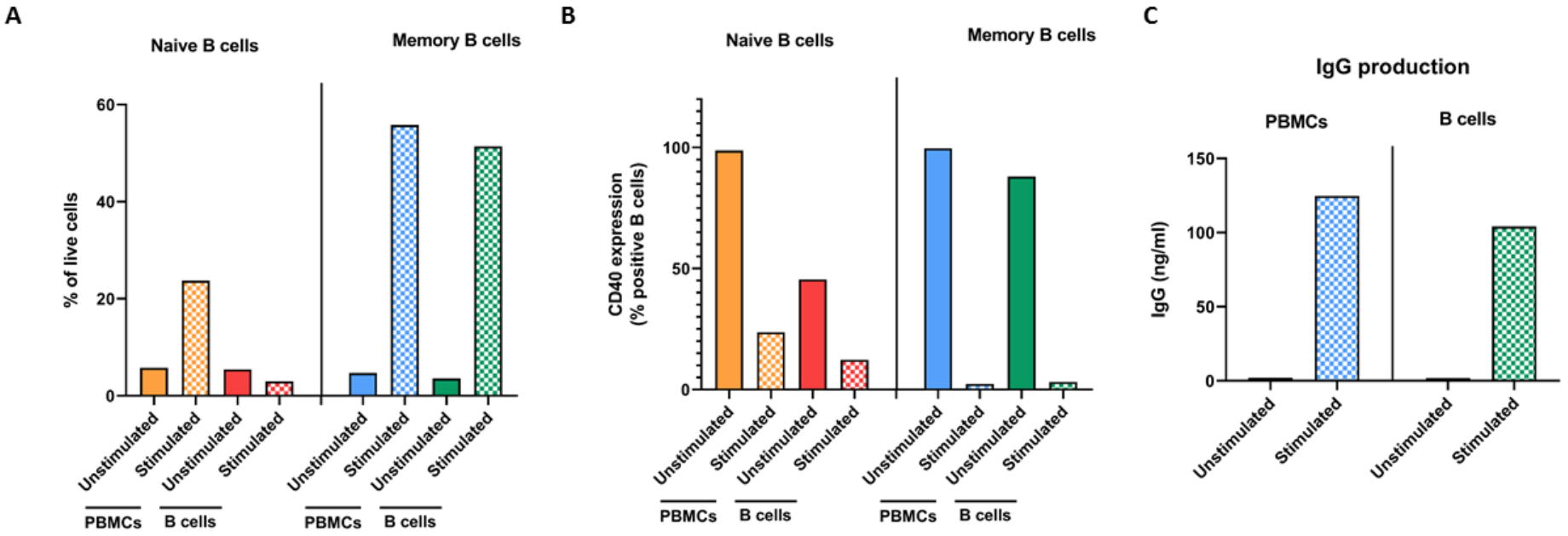

Figure 6. 5. Effect of sorting naïve and memory B cells from PBMCs compared to pre-enriched CD19+ cells on B cell function. Naïve and memory B cells were sorted using two different input populations, PBMCs or pre-enriched CD19+ B cells. Cells were cultured with or without stimulation for 6 days. The stimuli cocktail contained TLR7 ligand Imiquimod, TLR9 agonists CpG A and CpG B, Poke Weed Mitogen, anti-CD40, human IL-21, human IL-4 and IFN-gamma. **A.** Percentage of live cells assessed by Zombie Aqua staining and flow cytometry in naïve and memory B cells sorted using both isolation techniques. **B.** Percentage of CD40 expressing cells determined by flow cytometry in naïve and memory B cells sorted using the two different isolation techniques. The gate was set from the lymphocyte population. **C.** Immunoglobulin G production measured by ELISA from supernatants only on memory B cells. No statistical test was performed due to low number of repeats; n = 1.

6.4.5 Sorting B cell subsets from a CD3-depleted PBMC population

In view of the above results that showed that cultured B cells are potentially altered, for example in terms of CD40 expression, when comparing cells sorted from PBMCs or from pre-enriched CD19+ B cells isolated using a positive selection method, I decided to try an alternative approach. This involved depleting PBMCs of CD3+ cells using Miltenyi MACS CD3 MicroBeads. By depleting the CD3+ cells from the PBMCs, a mix of B cells, NK cells and DCs will remain, with B cell accounting for a large proportion of the remaining cells. This significantly reduces the number of cells that need to be sorted, thus reducing the time, and also leaves the B cells untouched by MicroBeads. Therefore, I isolated PBMCs from the blood of a single donor and split them: One half was used to deplete CD3+ cells using the CD3 MicroBeads; and the other was left as PBMCs. Both populations were then stained using my pre-optimised B cell sorting panel, and naïve and memory B cells were sorted from each cell preparation. Sorted naïve and memory B cell populations from both cell preparations were incubated with and without stimulation. After 6 days, the cells were harvested and their viability and phenotyped was assessed. In addition, the culture supernatants were stored for quantification of IgG production by ELISA.

Figure 6.6.A shows the percentage of live cells in the naïve and memory subsets when cells were sorted from either isolated PBMCs or from CD3-depleted PBMCs. Although the percentage of dead cells in the naïve B cells was high, there was no differences between the two different starting cell preparations. Memory B cells showed higher percentages of live cells than naïve B cells, as expected, and again, there were no differences when cells were sorted from the two different starting cell preparations. With regard to CD40 expression, unlike naïve B cells sorted from pre-enriched CD19+ B cells (Figure 6.5.B), there was no difference in CD40 expression between cells sorted from PBMCs or CD3-depleted PBMCs (Figure 6.6.B). There were also no differences in CD40 expression for the memory B cells. As explained before, in the stimulated conditions there is an apparent downregulation of CD40 because these cells were stimulated with an anti-CD40 antibody. Lastly, in terms of IgG production by the memory B cells (data for the naïve not shown due to low levels of production), there are no differences between the secretion of IgG by memory B cells sorted from PBMCs or CD3-depleted PBMCs (Figure 6.6.C).

Taking all of these results into consideration, for the functional work presented in the rest of this chapter, the four B cell subsets of interest (naïve B cells, memory B cells, CD5+ B

cells and ABCs) were sorted from CD3-depleted PBMCs. This reduced the sorting time of the cells and would hopefully improve cell viability and health.

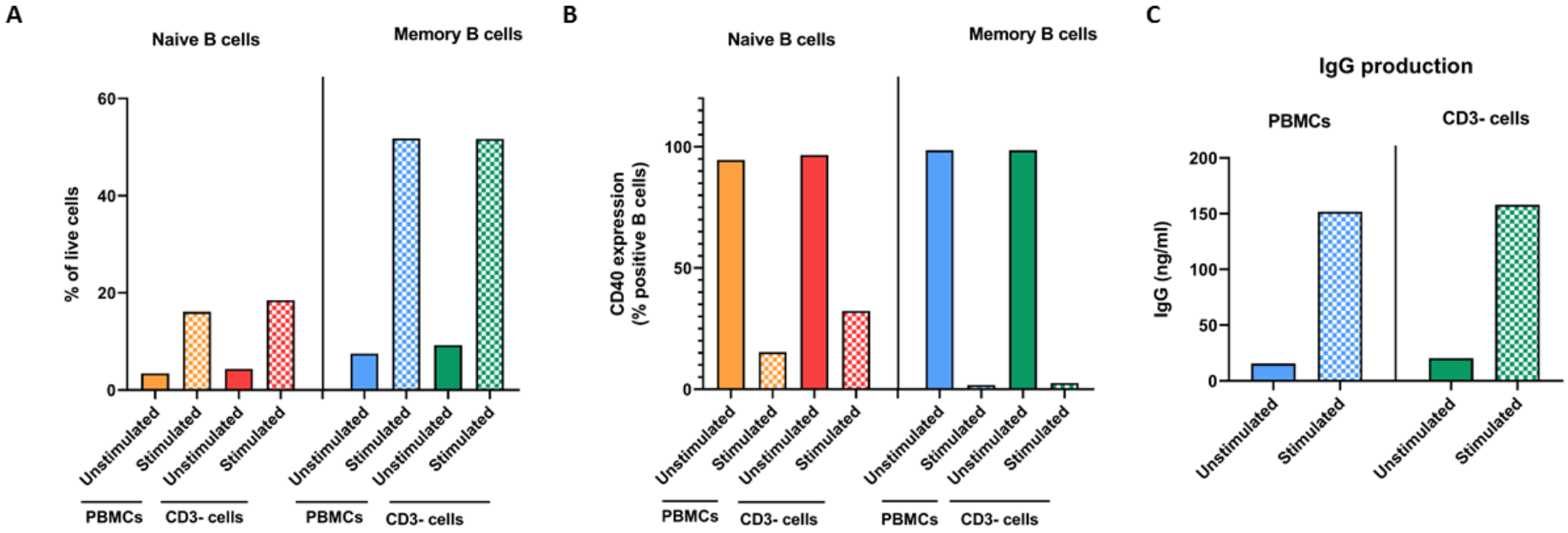

Figure 6. 6. Effect of sorting naïve and memory B cells from PBMCs compared to CD3-depleted PBMCs on B cell function. Naïve and memory B cells were sorted using two different input populations, PBMCs or CD3-depleted PBMCs. Cells were cultured with or without stimulation for 6 days. The stimuli cocktail contained TLR7 ligand Imiquimod, TLR9 agonists CpG A and CpG B, Poke Weed Mitogen, anti-CD40, human IL-21, human IL-4 and IFN-gamma. **A.** Percentage of live cells assessed by Zombie Aqua staining and flow cytometry in naïve and memory B cells sorted using both isolation techniques. **B.** Percentage of CD40 expressing cells determined by flow cytometry in naïve and memory B cells sorted using the two different isolation techniques. The gate was set from the lymphocyte population. **C.** Immunoglobulin G production measured by ELISA from supernatants only on memory B cells. No statistical test was performed due to low number of repeats; n = 1.

6.4.6 Patients cohorts

Once the protocol for sorting and culturing the B cell subsets was optimised, I started recruiting patients with established RA, as well as age-matched healthy controls. Established RA patients were double positive for RF and anti-CCP antibodies. These patients were receiving DMARD therapy but were not on any biological treatment. Healthy controls were age-matched volunteers from the lab who had no previous history of rheumatological or autoimmune disease. Demographic data is shown in Table 6.1. Patient and healthy control demographic data demonstrated no significant differences in the age and the sex of the two cohorts.

	Established RA patients	**Healthy controls**	**Difference between groups**
Number	5	4	-
Age (years; median and range)	57.2 (31 - 72)	56 (50 – 62)	$0.7^{\#}$
Percentage of females (n and percentage)	4 (80%)	3 (75%)	$>0.9^{+}$
Seropositive – anti-CCP+ or RF+ (n and percentage)	5 (100%)	-	

Table 6. 1. Demographic characteristics for the cohorts used for functional work. Flow cytometry cell sorting and B cell culture was performed on two cohorts; RA patients, n = 5 and healthy controls, n = 4, for the functional characterisation of ABCs. # Mann-Whitney test. + Fisher's exact test.

6.4.7 ABCs are less responsive to stimulation and die easily

Viability analysis of the four B cell subsets after 5 days of culture showed that for the unstimulated conditions, almost all cells, no matter which B cell subset, die (Figure 6.7). For the stimulated conditions, a small percentage of cells in the naïve and the CD5+ populations survive the 5 day culture. As expected, memory B cells showed a high percentage of live cells (~60% average) after stimulation for 5 days (Figure 6.7.A). Surprisingly, although ABCs are phenotypically similar to memory B cells, the percentages of live cells in the ABC cultures from both established RA patients and healthy controls after stimulation for 5 days was low (~20% average) (Figure 6.7.A). The number of live cells in the ABC population was even lower than for the stimulated naïve and CD5+ B cells (~30% average for both) (Figure 6.7.A), suggesting that ABCs are potentially more susceptible to cell death or may be unresponsive to stimulation, resulting in fewer live cells.

Viability analysis of each of the four B cell subsets, separately, from established RA patients and healthy controls showed no differences in the percentage of live cells either unstimulated or stimulated in CD5+ B cells, naïve B cells and memory B cells between the RA patients and the healthy controls (Figure 6.7.B-C and E). However, unstimulated memory B cells from established RA patients showed significantly higher percentages of live cells compared to unstimulated memory B cells from healthy controls (Figure 6.7.D).

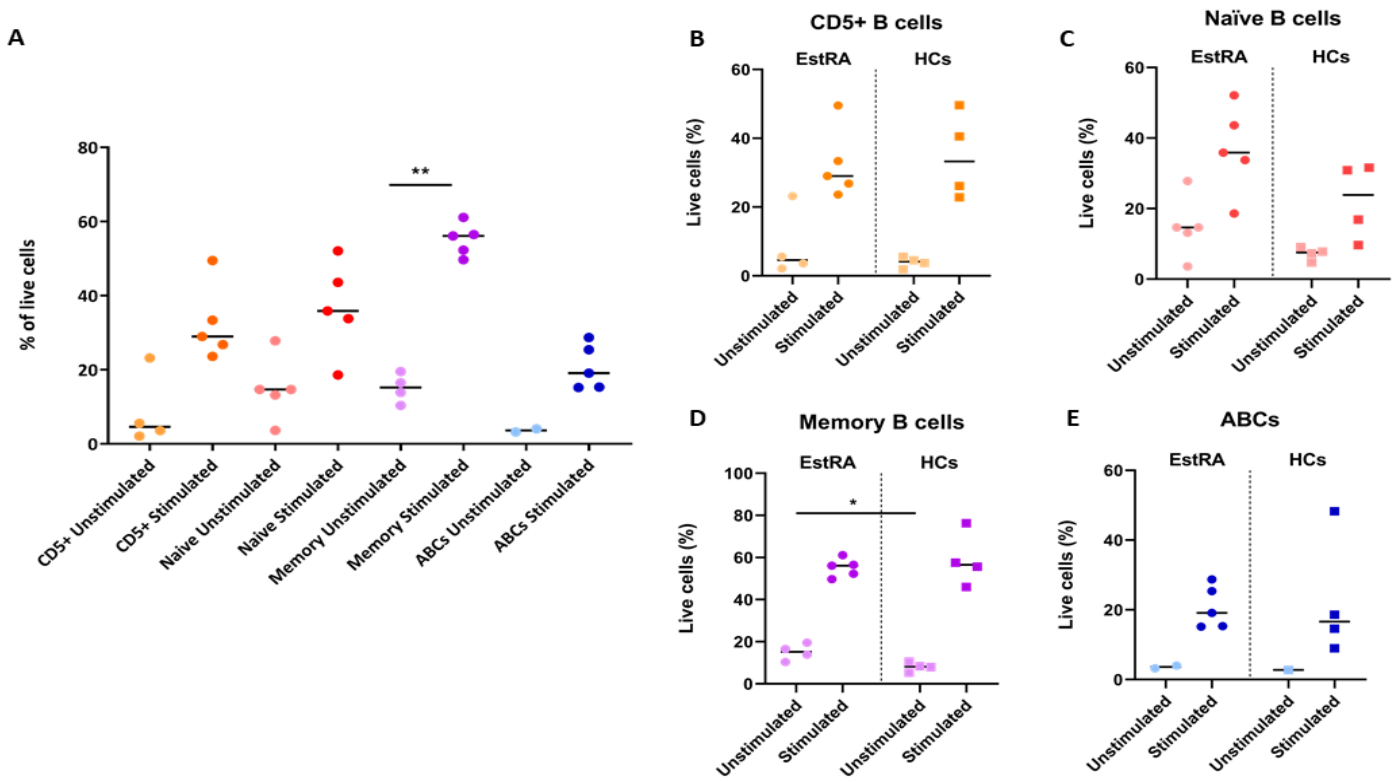

Figure 6. 7. Percentage of live cells in sorted and cultured B cell subsets from established RA patients and healthy controls. The four populations of interest, CD5+ B cells, naïve B cells, memory B cells and ABCs were sorted from CD3-depleted PBMCs. From each subset, 20,000 cells were cultured with or without stimulation (Imiquimod, CpG A, CpG B, PWM, anti-CD40, IL-21, IL-4 and IFN-γ) for 5 days. Cells were harvested and percentage of live cells was determined by flow cytometry using Zombie Aqua staining. **A.** Percentage of live cells in sorted cells from established RA patients are (n= up to 5). Statistical significance was assessed using a Kruskal-Wallis test (p=0.0003) with Dunn's multiple comparisons of the two conditions in each B cell subset; **p < 0.01. **B-E.** Percentage of live cells in each sorted and cultured B cell subset from established RA patients (n= up to 5), shown as circles and healthy controls (n= up to 4), shown as squares. Statistical significance was assessed using a Fit Least Squares comparing RA patients and healthy controls in each B cell subset; *p < 0.05.

6.4.8 Phenotypic characterisation of B cell subsets after stimulation

Expression of certain markers previously used for the phenotypic characterisation of ABCs were used to assess responses of each B cell subset to stimulation. As expected, a large proportion of all B cell subsets from established RA patients express the antigen presentation MHC class II molecule, HLA-DR (Figure 6.8.A-B). Generally, levels of HLA-DR increased after stimulation in all the B cells subsets from established RA patients (Figure 6.8.C), however, this increase was more pronounced in the naïve and the CD5+ B cell subsets (Figure 6.8.B-C). Interestingly, there was a trend for increased percentages of HLA-DR positive cells, and especially HLA-DR expression, as measured by MFI, in healthy controls compared to established RA patients in CD5+, naïve and memory B cells, both unstimulated and stimulated (Figure 6.9.A-B). Stimulated ABCs from healthy controls also showed a higher percentage of HLA-DR positive cells and higher HLA-DR expression.

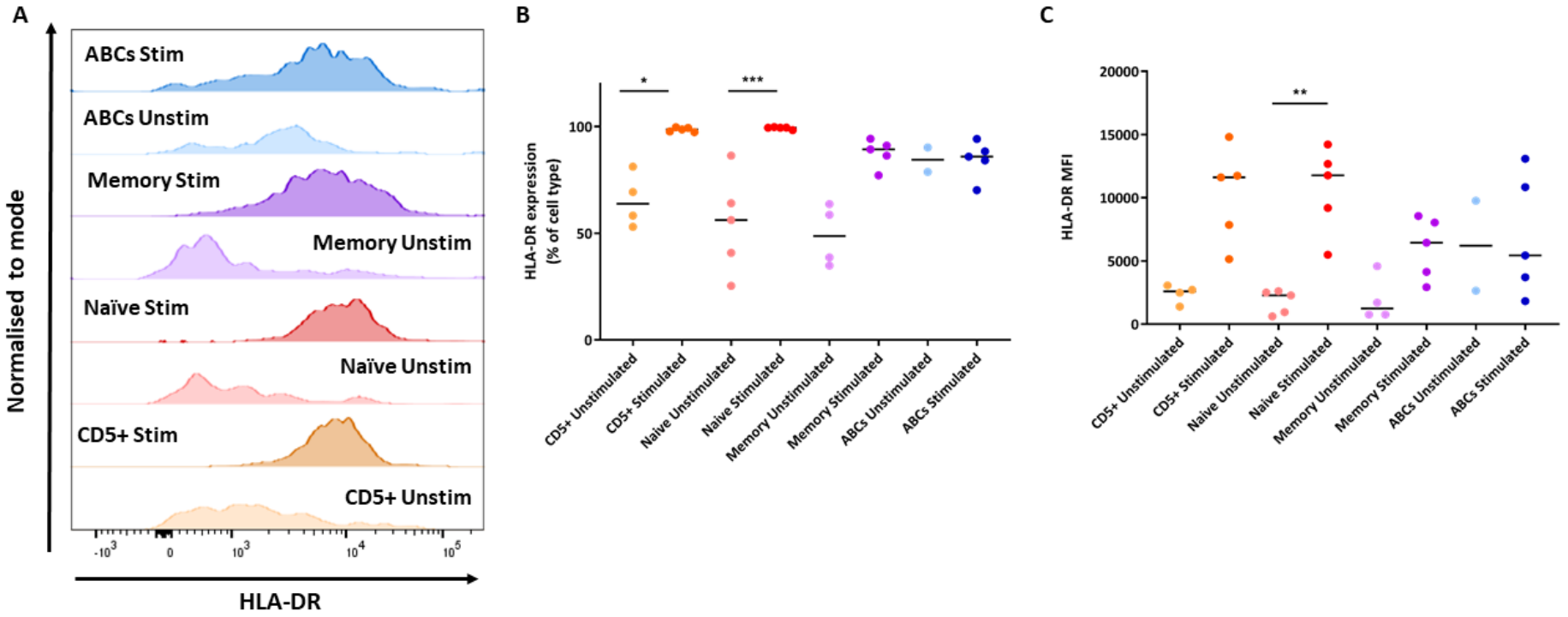

Figure 6. 8. Expression of HLA-DR in unstimulated or stimulated sorted B cell subsets from established RA patients. Sorted cells from established RA patients were incubated with or without stimulation (Imiquimod, CpG A, CpG B, PWM, anti-CD40, IL-21, IL-4 and IFN-γ) for 5 days. The cell phenotype was then assessed by flow cytometry. **A.** HLA-DR expression overlay histograms for each B cell subset and stimulation condition. CD5+ B cells are shown in orange, naïve B cells are shown in red, memory B cells in purple and ABCs in blue. The peaks are normalised to the same height to standardise for different numbers of cells in each population. **B.** Percentage of HLA-DR positive cells in the B cell subsets. The bar represents the median. Gates were set using an unstained sample. **C.** HLA-DR median fluorescence intensity (MFI) in the different B cell subsets. The bar represents the median. N = up to 5. Statistical significance was assessed using a Kruskal-Wallis test (p=0.0002 for B, p=0.0019 for C) with Dunn's multiple comparisons of the two conditions in each B cell subset; * $p < 0.05$, **$p < 0.01$, *** $p < 0.001$.

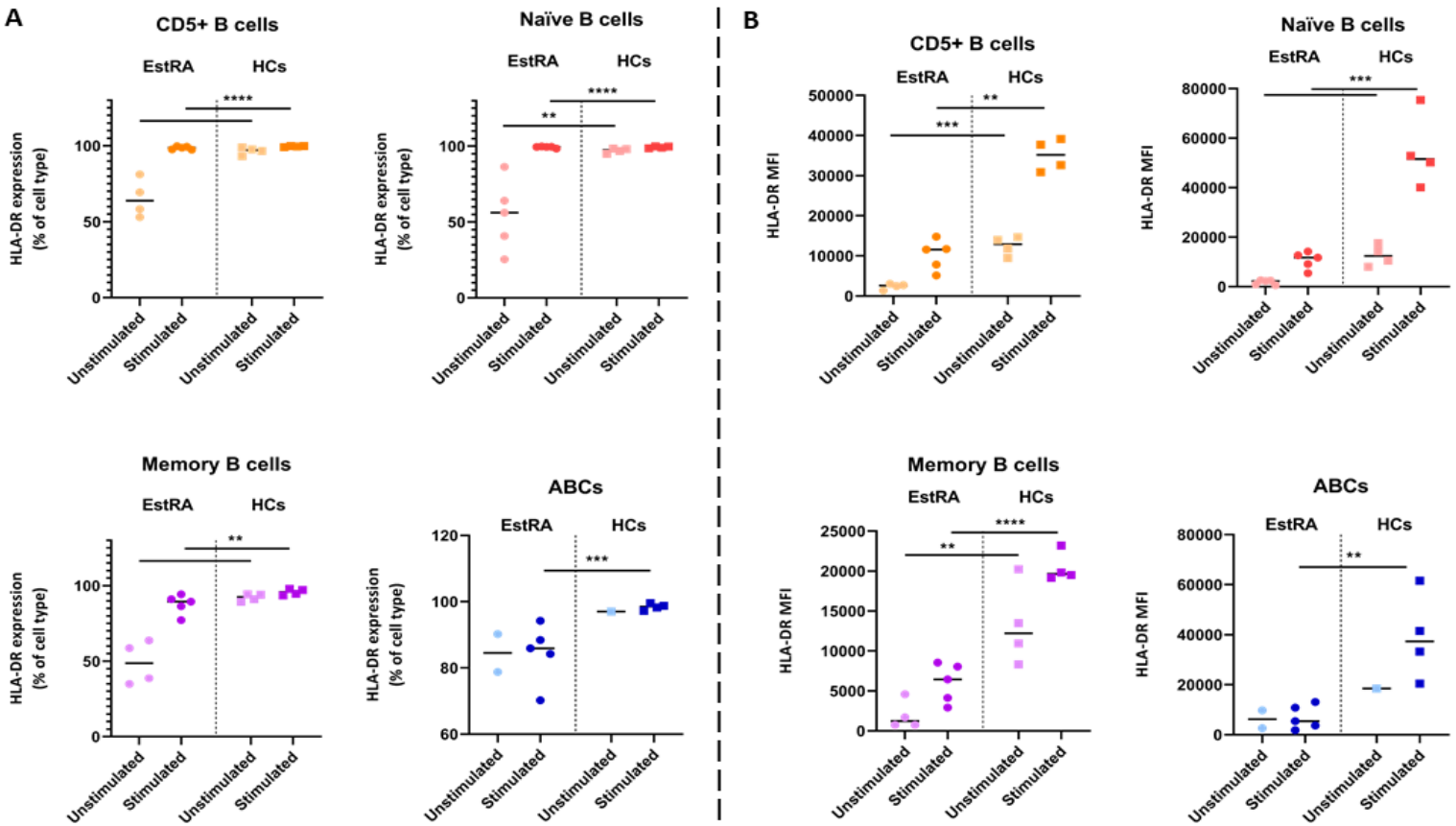

Figure 6. 9. Expression of HLA-DR in unstimulated or stimulated sorted B cell subsets from established RA patients and healthy controls. **A**. Percentage of HLA-DR positive cells in the B cell subsets. The bar represents the median. Gates were set using an unstained sample. **B.** HLA-DR median fluorescence intensity (MFI) in the different B cell subsets. The bar represents the median. Established RA patients (n= up to 5) are shown as circles and healthy controls (n= up to 4) are represented with squares. Statistical significance was assessed using a Fit Least Squares comparing RA patients and healthy controls in each B cell subset; **p < 0.01, *** p < 0.001, **** p < 0.0001.

Expression of CD86, another co-stimulatory molecule, which is known to be upregulated on B cells after stimulation was investigated next. The percentage of CD86 positive cells in the unstimulated cells for all the B cell subsets was quite low, particularly in the naïve B cells and the CD5+ B cells (Figure 6.10.A-B). In keeping with my findings in Chapter 4 (Figure 4.5), memory B cells and ABCs had higher percentages of CD86 positive cells than the other two B cell subsets (Figure 6.10.B). After stimulation, CD86 expression is greatly increased in all B cell subsets (Figure 6.10.B-C). When comparing sorted B cell subsets from established RA patients and healthy controls, only the percentage of CD86 positive cells in the unstimulated naïve B cell subset showed a significant decrease in established RA patients compared to healthy controls (Figure 6.11.A-B).

The expression of the activation molecule, CD69 (a C-type lectin), was also assessed. Unstimulated cells for all B cell subsets showed low percentages of CD69 positive cells (Figure 6.12.A-B). These results are similar to my findings for phenotypic analysis of B cells from peripheral blood, although CD69 expression on ABC assessed using whole blood flow cytometry demonstrated a higher expression of CD69 than that seen here with sorted and cultured ABCs (Chapter 4, Figure 4.6). When the B cell subsets were stimulated, there was a significant increase in both the percentage of CD69 positive cells and CD69 expression, as measured by MFI, in naïve and CD5+ B cells only (Figure 6.12.B-C). However, this increase was not seen in memory B cells and ABCs. No differences in percentage of CD69 positive cells and CD69 MFI values were seen in any of the B cell subsets when B cells from established RA patients were compared to B cells from healthy controls (Figure 6.13.A-B).

The NanoString results (Chapter 5, section 5.4.4) demonstrated that ABCs had high expression of mRNA transcript for the activation molecule CD97 (a G-protein coupled receptor involved in cell adhesion). I therefore, analysed expression of this marker after B cell stimulation (Figure 6.14). Unstimulated B cells, with the exception, as predicated by the NanoString results, of ABCs, showed very low percentages of CD97 positive cells (Figure 6.14.A-B). This marker is greatly upregulated after B cell stimulation in all B cell subsets, but in particular in memory B cells and ABCs, where the percentages of positive cells reach more than 80% (Figure 6.14.B-C). Interestingly, the percentage of CD97 positive cells in stimulated cells from all B cell subsets was higher in healthy controls compared to RA patients (Figure 6.15.A). Same results were found in terms of the MFI values for all the B cell subsets, with the exception of the ABCs (Figure 6.15.B).

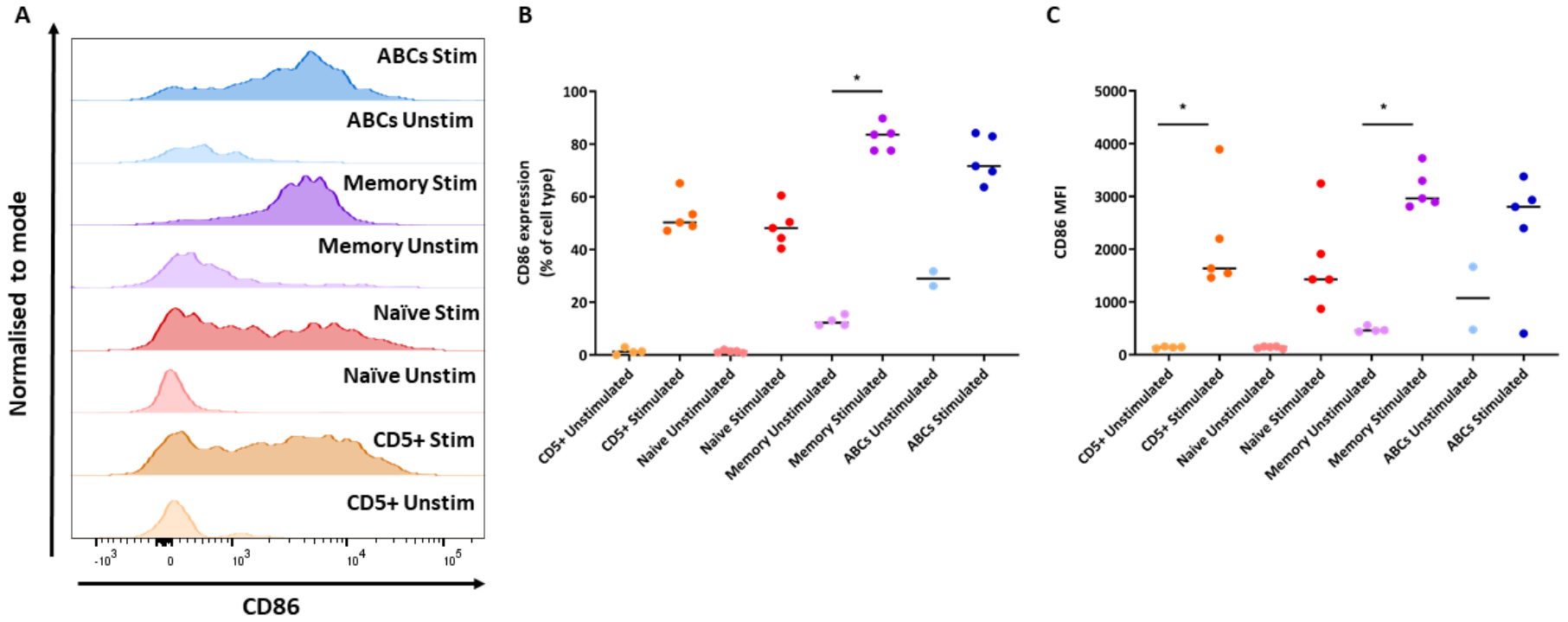

Figure 6. 10. Expression of the co-stimulatory molecule CD86 in unstimulated or stimulated sorted B cell subsets from established RA patients. Sorted cells from established RA patients were incubated with or without stimulation (Imiquimod, CpG A, CpG B, PWM, anti-CD40, IL-21, IL-4 and IFN-γ) for 5 days. The cell phenotype was then assessed by flow cytometry. **A.** CD86 expression overlay histograms for each B cell subset and stimulation condition. CD5+ B cells are shown in orange, naïve B cells are shown in red, memory B cells in purple and ABCs in blue. The peaks are normalised to the same height to standardise for different numbers of cells in each population. **B.** Percentage of CD86 positive cells in the B cell subsets. The bar represents the median. Gates were set using an unstained sample. **C.** CD86 median fluorescence intensity (MFI) in the different B cell subsets. The bar represents the median. N = up to 5. Statistical significance was assessed using a Kruskal-Wallis test ($p<0.0001$ for B, $p=0.0004$ for C) with Dunn's multiple comparisons of the two conditions in each B cell subset; * $p < 0.05$.

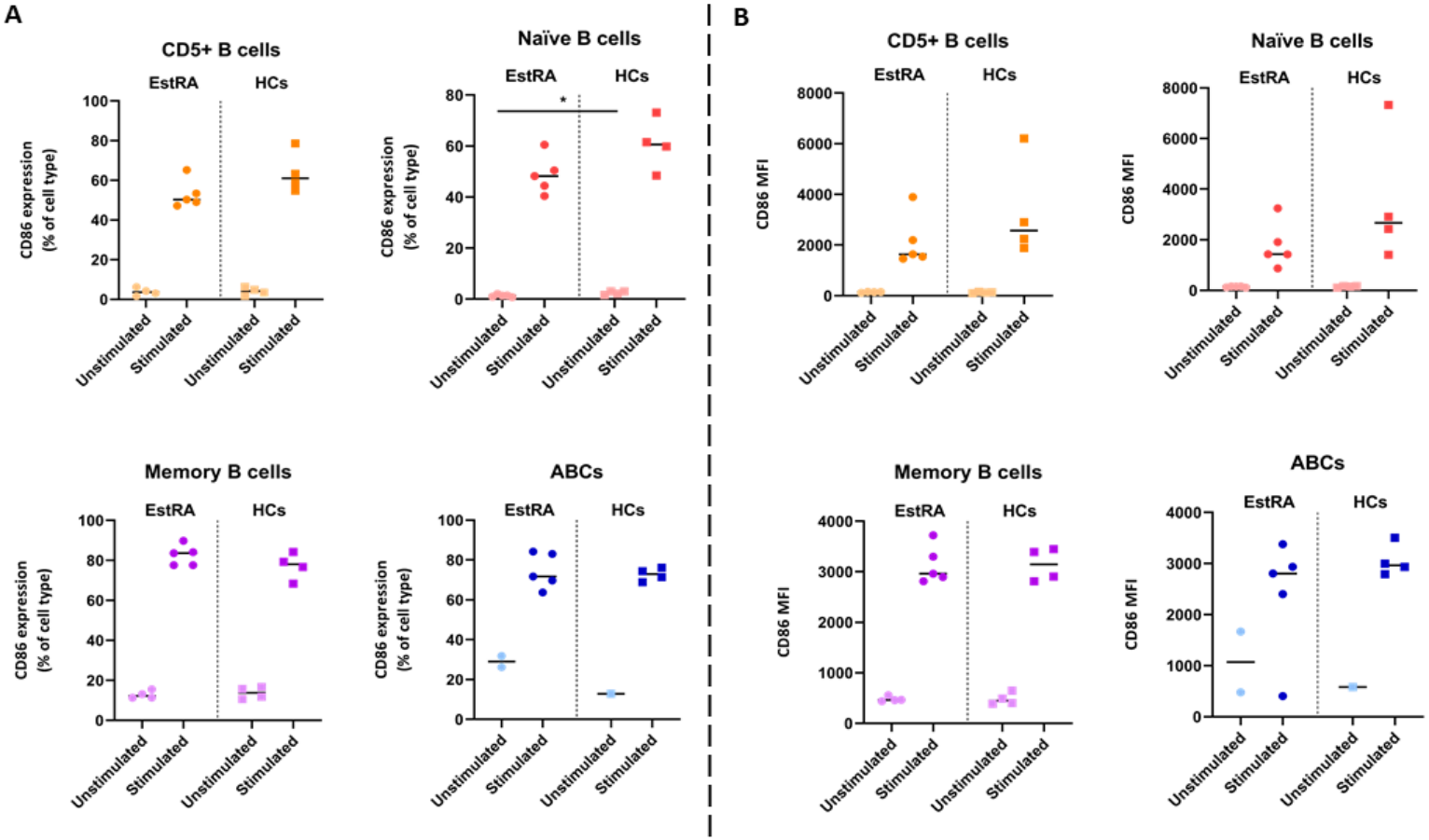

Figure 6. 11. Expression of the co-stimulatory molecule CD86 in unstimulated or stimulated sorted B cell subsets from established RA patients and healthy controls. A. Percentage of CD86 positive cells in the B cell subsets. The bar represents the median. Gates were set using an unstained sample. **B.** CD86 median fluorescence intensity (MFI) in the different B cell subsets. The bar represents the median. Established RA patients (n= up to 5) are shown as circles and healthy controls (n= up to 4) are represented with squares. Statistical significance was assessed using a Fit Least Squares comparing RA patients and healthy controls in each B cell subset; *p < 0.05.

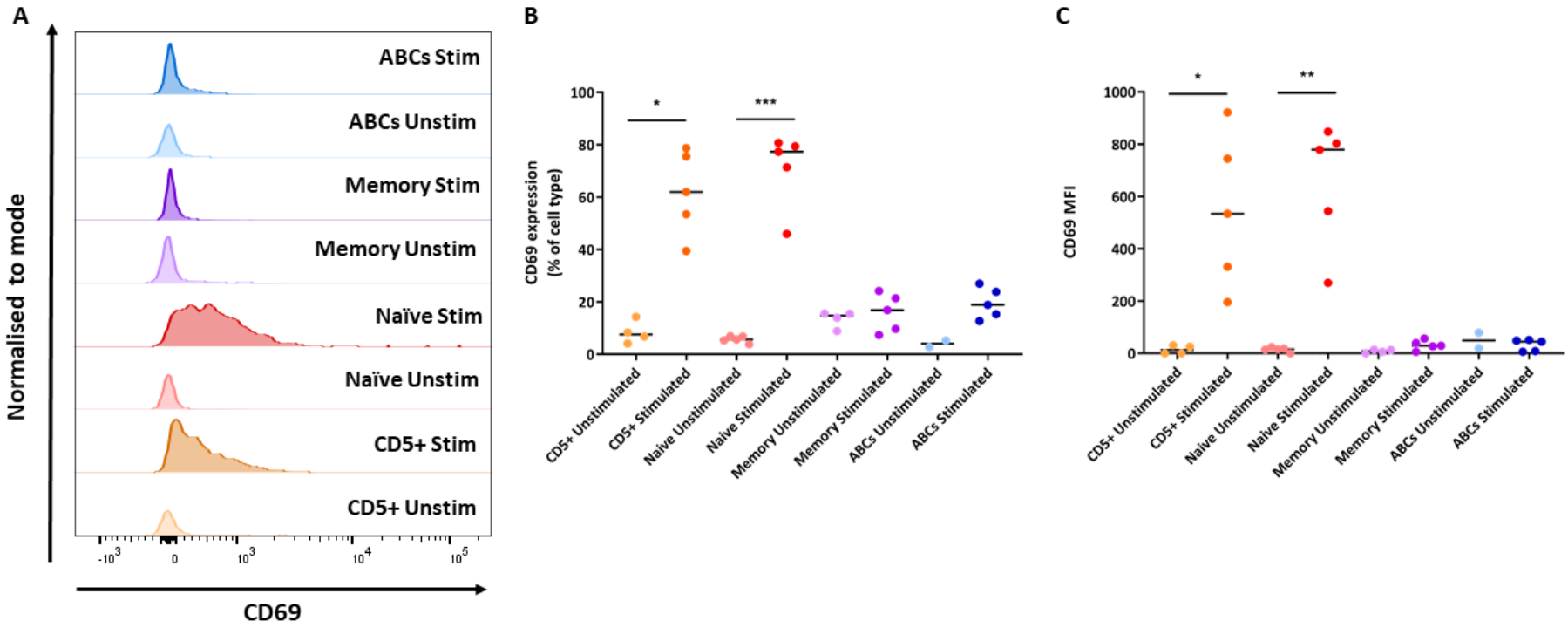

Figure 6. 12. Expression of the activation marker CD69 in unstimulated or stimulated sorted B cell subsets from established RA patients. Sorted cells from established RA patients were incubated with or without stimulation (Imiquimod, CpG A, CpG B, PWM, anti-CD40, IL-21, IL-4 and IFN-γ) for 5 days. The cell phenotype was then assessed by flow cytometry. **A.** CD69 expression overlay histograms for each B cell subset and stimulation condition. CD5+ B cells are shown in orange, naïve B cells are shown in red, memory B cells in purple and ABCs in blue. The peaks are normalised to the same height to standardise for different numbers of cells in each population. **B.** Percentage of CD69 positive cells in the B cell subsets. The bar represents the median. Gates were set using an unstained sample. **C.** CD69 median fluorescence intensity (MFI) in the different B cell subsets. The bar represents the median. N = up to 5. Statistical significance was assessed using a Kruskal-Wallis test (p=0.0001 for B, p=0.0008 for C) with Dunn's multiple comparisons of the two conditions in each B cell subset; * $p < 0.05$, ** $p < 0.01$, ***$p < 0.001$.

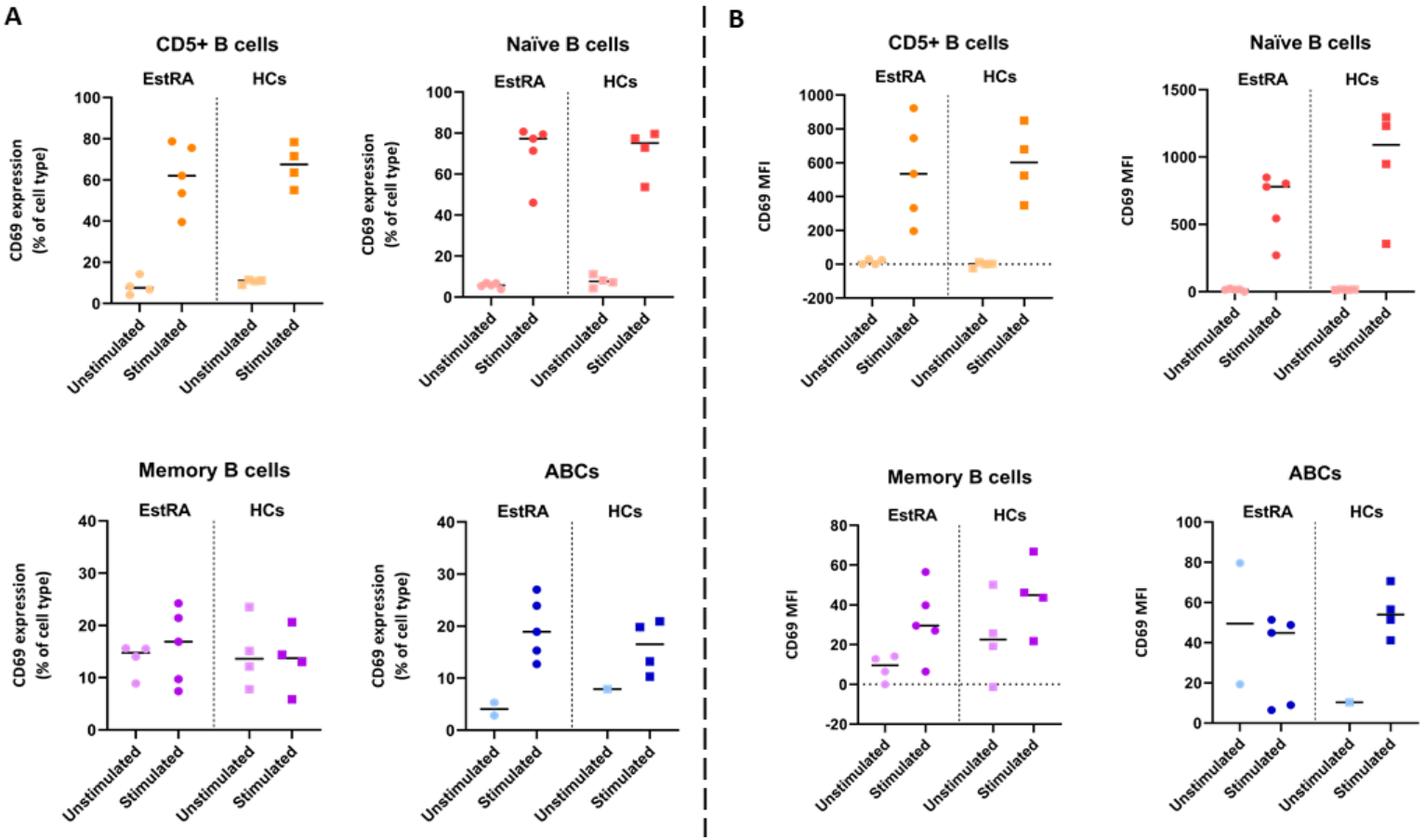

Figure 6. 13. Expression of the activation marker CD69 in unstimulated or stimulated sorted B cell subsets from established RA patients and healthy controls. A. Percentage of CD69 positive cells in the B cell subsets. The bar represents the median. Gates were set using an unstained sample. **B.** CD69 median fluorescence intensity (MFI) in the different B cell subsets. The bar represents the median. Established RA patients (n= up to 5) are shown as circles and healthy controls (n= up to 4) are represented with squares. Statistical significance was assessed using a Fit Least Squares comparing RA patients and healthy controls in each B cell subset.

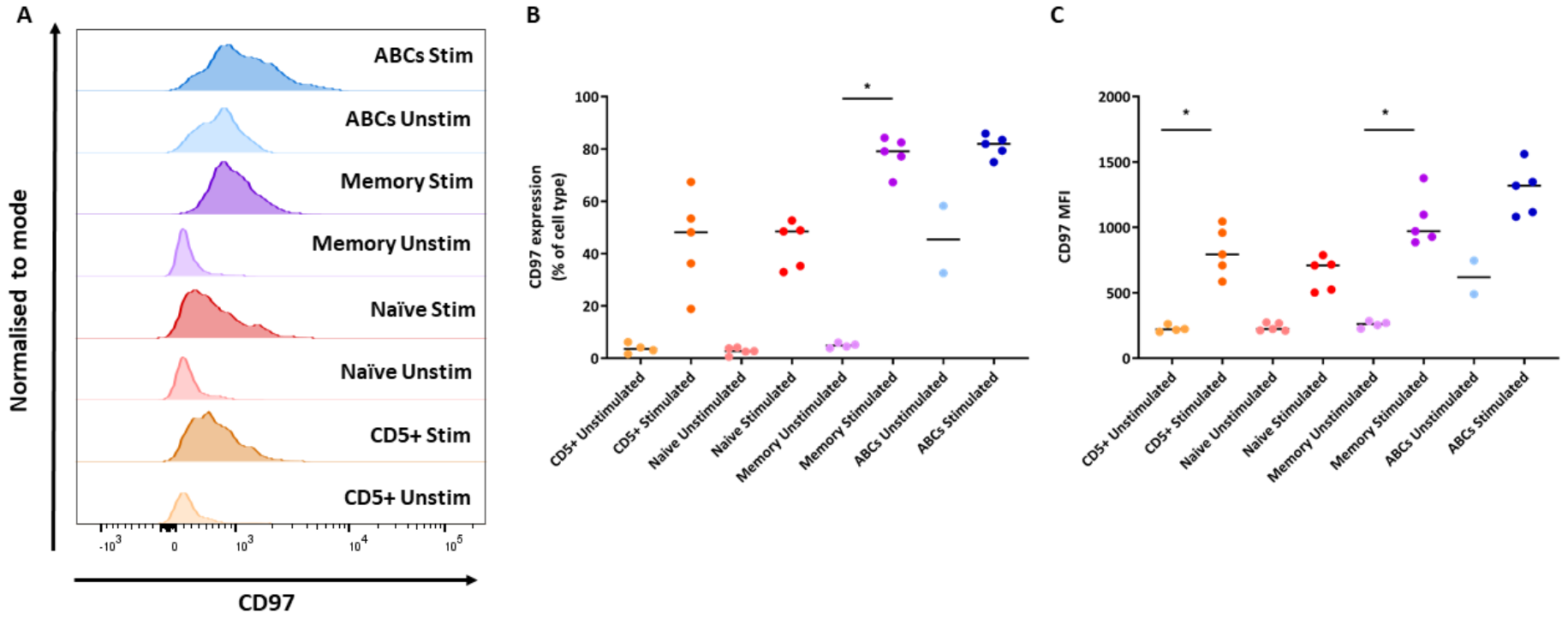

Figure 6. 14. Expression of the activation marker CD97 in unstimulated or stimulated sorted B cell subsets from established RA patients. Sorted cells from established RA patients were incubated with or without stimulation (Imiquimod, CpG A, CpG B, PWM, anti-CD40, IL-21, IL-4 and IFN-γ) for 5 days. The cell phenotype was then assessed by flow cytometry. **A.** CD97 expression overlay histograms for each B cell subset and stimulation condition. CD5+ B cells are shown in orange, naïve B cells are shown in red, memory B cells in purple and ABCs in blue. The peaks are normalised to the same height to standardise for different numbers of cells in each population. **B.** Percentage of CD97 positive cells in the B cell subsets. The bar represents the median. Gates were set using an unstained sample. **C.** CD97 median fluorescence intensity (MFI) in the different B cell subsets. The bar represents the median. N = up to 5. Statistical significance was assessed using a Kruskal-Wallis test ($p<0.0001$ for B, $p<0.0001$ for C) with Dunn's multiple comparisons of the two conditions in each B cell subset; * $p < 0.05$.

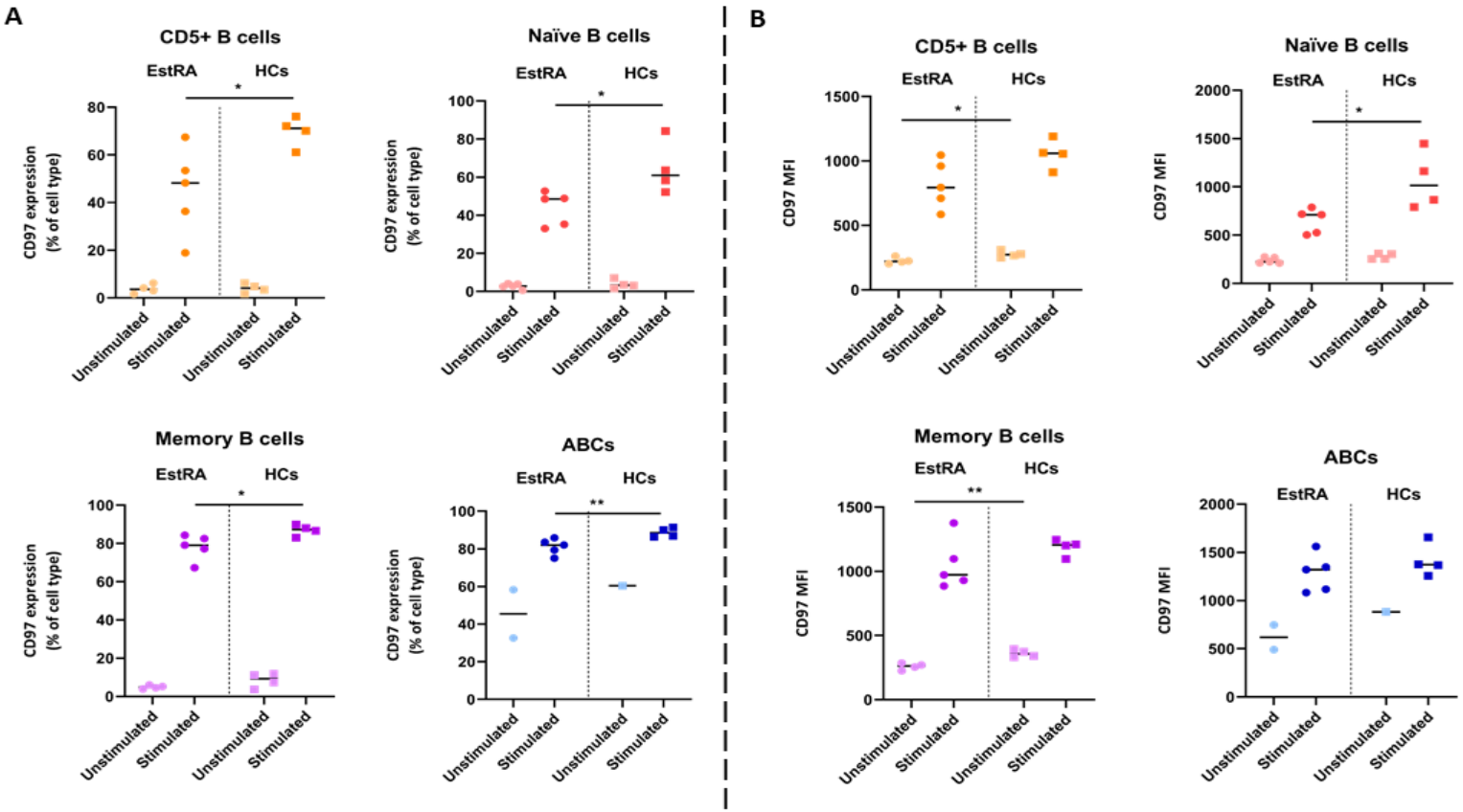

Figure 6. 15. Expression of the activation marker CD97 in unstimulated or stimulated sorted B cell subsets from established RA patients and healthy controls. A. Percentage of CD97 positive cells in the B cell subsets. The bar represents the median. Gates were set using an unstained sample. **B.** CD97 median fluorescence intensity (MFI) in the different B cell subsets. The bar represents the median. Established RA patients (n= up to 5) are shown as circles and healthy controls (n= up to 4) are represented with squares. Statistical significance was assessed using a Fit Least Squares comparing RA patients and healthy controls in each B cell subset; * $p < 0.05$, ** $p < 0.01$.

Expression of the maturation marker CD27 was also assessed. As expected, on unstimulated cells, CD5+ and naïve B cells had lower expression of this marker than ABCs and memory B cells (Figure 6.16.A-C). In ABCs, around 50% of the cells were positive for this marker, and for the memory B cells all the cells were positive for the marker as this subset was sorted based on CD27 expression (i.e. CD19+IgD-CD27+) (Figure 6.16.B). When the B cells were stimulated, the percentage of CD27 positive cells in all the subsets increased, except in the memory B cells as all of the cells were positive initially (Figure 6.16.B). Nevertheless, the MFI data showed that stimulation of memory B cells induced an upregulation of CD27 expression, with a similar effect, albeit not as pronounced, in ABCs (Figure 6.16.C). When comparing sorted B cell subsets from established RA patients and healthy controls, the percentage of CD27 positive cells in the unstimulated and stimulated naïve B cell subset showed a significant decrease in established RA patients compared to healthy controls (Figure 6.17.A). The percentage of CD27 positive cells in stimulated ABCs from established RA patients was also lower than stimulated ABCs from healthy controls (Figure 6.17.A). No differences in MFI values in established RA patients compared to healthy controls were seen in any of the subsets (Figure 6.17.B).

Finally, assessment of surface IgG expression showed no changes in expression after stimulation (Figure 6.18). As expected, and reported in Chapter 4 (Figure 4.11), about 50% of the cells in the unstimulated condition for the memory B cell and the ABC population were IgG positive (Figure 6.18.A-B). The percentage of IgG positive cells in unstimulated and stimulated naïve B cells from RA patients was lower compared to healthy controls (Figure 6.19.A). In terms of the MFI values, there was higher IgG expression in unstimulated CD5+ B cells and stimulated naïve B cells from healthy controls compared to established RA patients (Figure 6.19.B).

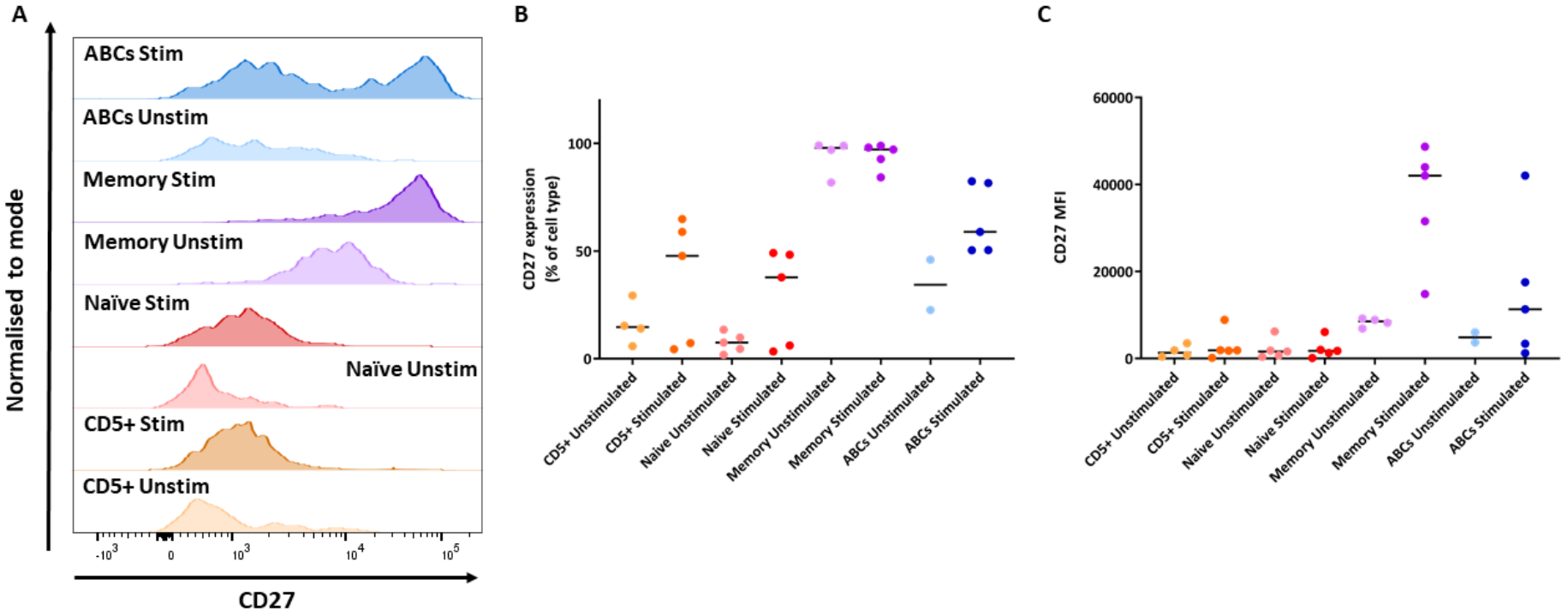

Figure 6. 16. Expression of the maturation marker CD27 in unstimulated or stimulated sorted B cell subsets from established RA patients. Sorted cells from established RA patients were incubated with or without stimulation (Imiquimod, CpG A, CpG B, PWM, anti-CD40, IL-21, IL-4 and IFN-γ) for 5 days. The cell phenotype was then assessed by flow cytometry. **A.** CD27 expression overlay histograms for each B cell subset and stimulation condition. CD5+ B cells are shown in orange, naïve B cells are shown in red, memory B cells in purple and ABCs in blue. The peaks are normalised to the same height to standardise for different numbers of cells in each population. **B.** Percentage of CD27 positive cells in the B cell subsets. The bar represents the median. Gates were set using an unstained sample. **C.** CD27 median fluorescence intensity (MFI) in the different B cell subsets. The bar represents the median. N = up to 5. Statistical significance was assessed using a Kruskal-Wallis test (p=0.0004 for B, p=0.0035 for C) with Dunn's multiple comparisons of the two conditions in each B cell subset.

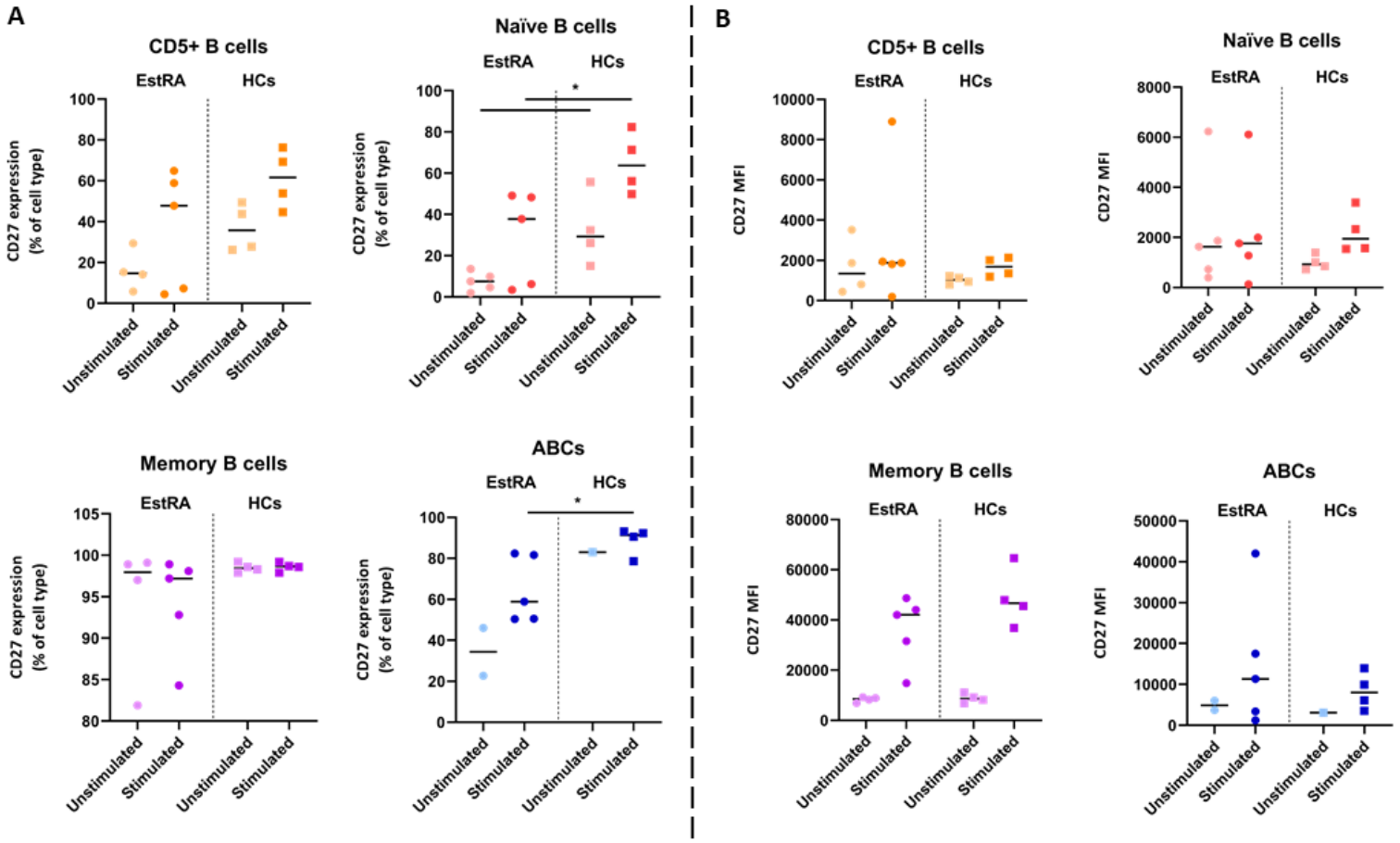

Figure 6. 17. Expression of the maturation marker CD27 in unstimulated or stimulated sorted B cell subsets from established RA patients and healthy controls. A. Percentage of CD27 positive cells in the B cell subsets. The bar represents the median. Gates were set using an unstained sample. **B.** CD27 median fluorescence intensity (MFI) in the different B cell subsets. The bar represents the median. Established RA patients (n= up to 5) are shown as circles and healthy controls (n= up to 4) are represented with squares. Statistical significance was assessed using a Fit Least Squares comparing RA patients and healthy controls in each B cell subset; * $p < 0.05$.

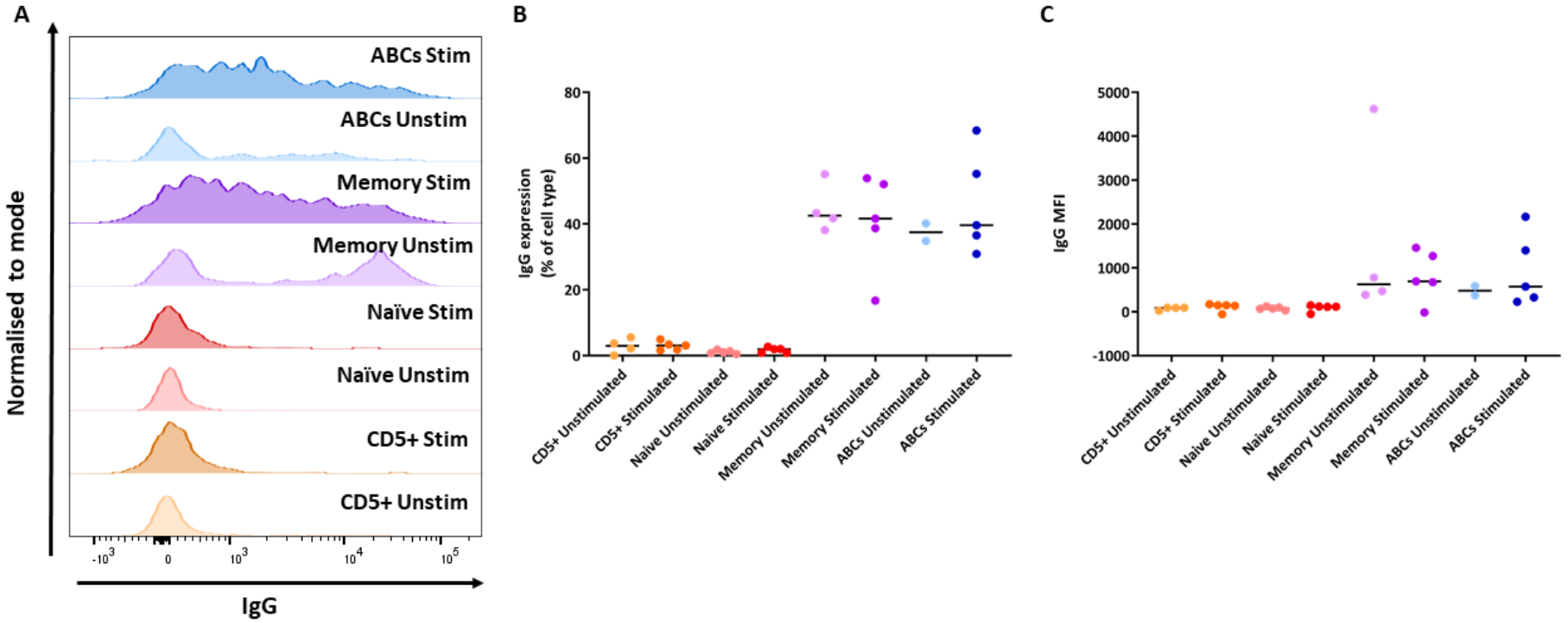

Figure 6. 18. Expression of IgG in unstimulated or stimulated sorted B cell subsets from established RA patients. Sorted cells from established RA patients were incubated with or without stimulation (Imiquimod, CpG A, CpG B, PWM, anti-CD40, IL-21, IL-4 and IFN-γ) for 5 days. The cell phenotype was then assessed by flow cytometry. **A.** IgG expression overlay histograms for each B cell subset and stimulation condition. CD5+ B cells are shown in orange, naïve B cells are shown in red, memory B cells in purple and ABCs in blue. The peaks are normalised to the same height to standardise for different numbers of cells in each population. **B.** Percentage of IgG positive cells in the B cell subsets. The bar represents the median. Gates were set using an unstained sample. **C.** IgG median fluorescence intensity (MFI) in the different B cell subsets. The bar represents the median. N = up to 5. Statistical significance was assessed using a Kruskal-Wallis test (p=0.0003 for B, p=0.0030 for C) with Dunn's multiple comparisons of the two conditions in each B cell subset.

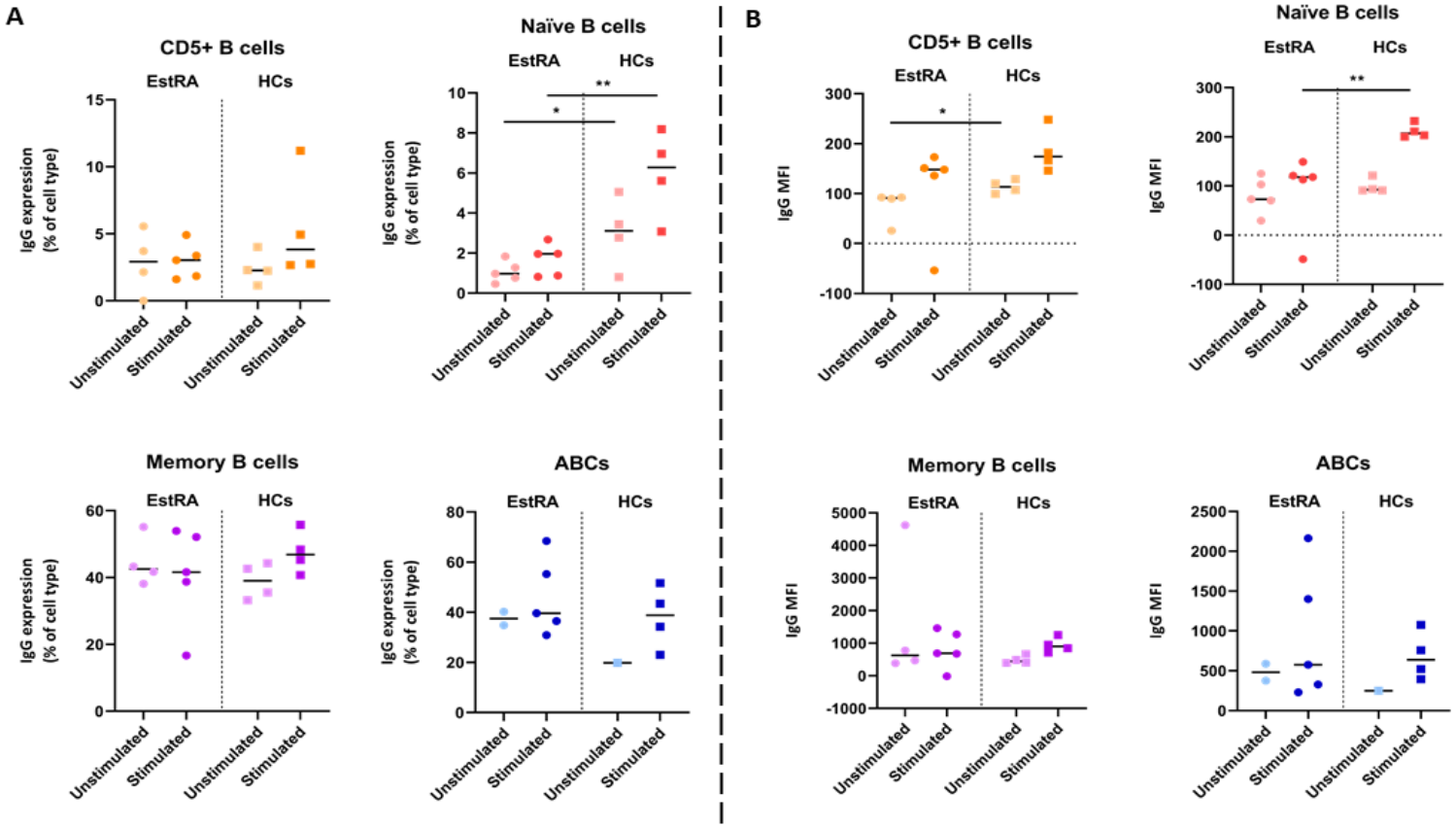

Figure 6. 19. Expression of IgG in unstimulated or stimulated sorted B cell subsets from established RA patients and healthy controls. A. Percentage of IgG positive cells in the B cell subsets. The bar represents the median. Gates were set using an unstained sample. **B.** IgG median fluorescence intensity (MFI) in the different B cell subsets. The bar represents the median. Established RA patients (n= up to 5) are shown as circles and healthy controls (n= up to 4) are represented with squares. Statistical significance was assessed using a Fit Least Squares comparing RA patients and healthy controls in each B cell subset; * $p < 0.05$, ** $p < 0.01$.

6.4.9 Cytokine secretion profiles of each B cell subset after stimulation

Supernatants from the sorted and cultured B cell subsets were analysed on an MSD U-PLEX Custom Biomarker (human) plate. MSD assay allows for the detection of low concentrations of cytokines. The cytokines analysed were: GM-CSF, IL-2, IL-6, IL-10, IL-12p70, IL-23 and TNF-alpha.

Although T cells are considered a major source of IL-2, activated B cells also produce IL-2, which has been proposed to act as an autocrine growth factor (Lagoo *et al.*, 1990; Wojciechowski *et al.*, 2009). In the unstimulated condition all of the B cell subsets produced very low levels of IL-2 (Figure 6.20.A). Production of IL-2 was slightly increased from all the B cell subsets when the B cells were stimulated, however, the concentrations produced were very low. Interestingly, there was increased production of IL-2 by the stimulated CD5+ and naïve B cells from established RA patients compared to heathy controls (Figure 6.20.B-C). Moreover, there was increased production of IL-2 in the unstimulated memory B cell subset from established RA patients compared to heathy controls (Figure 6.20.D).

Another cytokine analysed was IL-6, important in germinal centre formation in autoimmune diseases (Arkatkar *et al.*, 2017). As expected, production of IL-6 was low in the unstimulated conditions for all the B cell subsets (Figure 6.21.A). Interestingly, when the cells were stimulated only the CD5+ and naïve B cells produced significantly high levels of IL-6. There was a small increase in the production of IL-6 from memory B cells but no secretion by ABCs. These data suggest that IL-6 may be a cytokine produced at the initiation of an immune response by naïve B cells. No differences in IL-6 production were seen in any of the B cell subsets when B cells from established RA patients were compared to B cells from healthy controls (Figure 6.21.B-E).

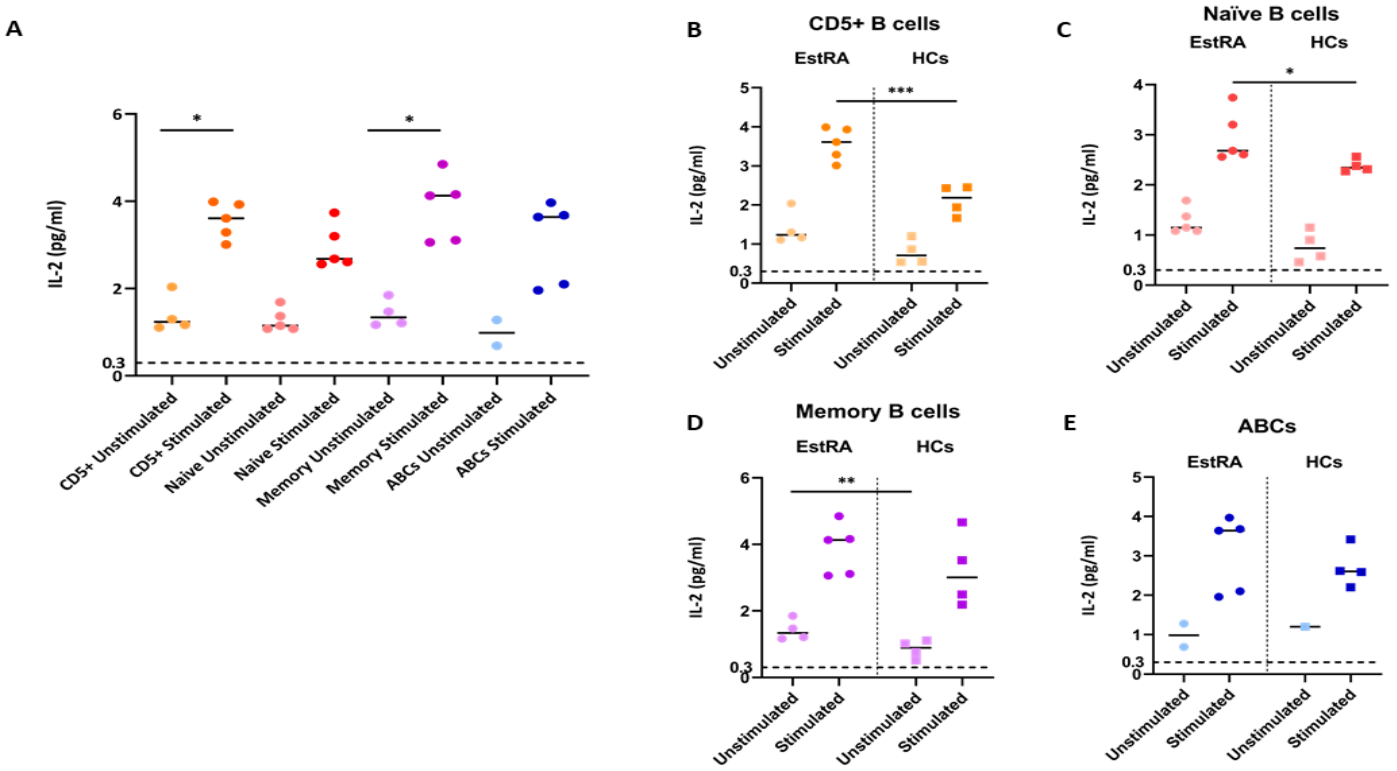

Figure 6. 20. Production of the cytokine IL-2 from unstimulated or stimulated sorted B cell subsets. Sorted cells from established RA patients were incubated with or without stimulation (Imiquimod, CpG A, CpG B, PWM, anti-CD40, IL-21, IL-4 and IFN-γ) for 5 days. **A.** The culture supernatants from established RA patients (n= up to 5) were harvested and the concentration of IL-2 was detected using a U-PLEX Custom Biomarker plate from MSD. The dotted line indicates the lower limit of detection. Statistical significance was assessed using a Kruskal-Wallis test ($p=0.0004$) with Dunn's multiple comparisons of the two conditions in each B cell subset; *$p < 0.05$. **B-E.** IL-2 production from B cells from established RA patients (n= up to 5), shown as circles and healthy controls (n= up to 4), shown as squares. The dotted line indicates the lower limit of detection. Statistical significance was assessed using a Fit Least Squares comparing RA patients and healthy controls in each B cell subset; *$p < 0.05$, ** $p < 0.01$, *** $p < 0.001$.

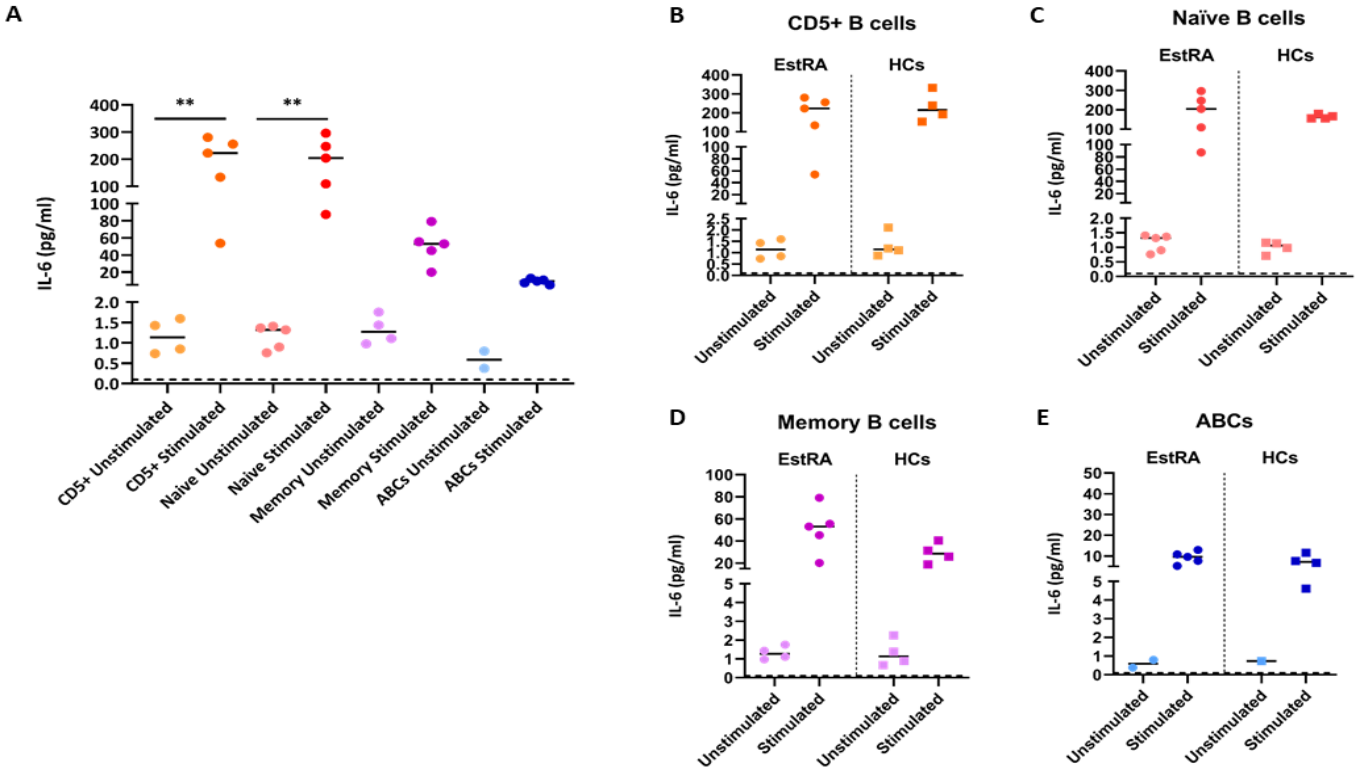

Figure 6. 21. Production of the cytokine IL-6 from unstimulated or stimulated sorted B cell subsets. Sorted cells from established RA patients were incubated with or without stimulation (Imiquimod, CpG A, CpG B, PWM, anti-CD40, IL-21, IL-4 and IFN-γ) for 5 days. **A.** The culture supernatants from established RA patients (n= up to 5) were harvested and the concentration of IL-6 was detected using a U-PLEX Custom Biomarker plate from MSD. The dotted line indicates the lower limit of detection. Statistical significance was assessed using a Kruskal-Wallis test ($p<0.0001$) with Dunn's multiple comparisons of the two conditions in each B cell subset; $^{**}p < 0.01$. **B-E.** IL-6 production from B cells from established RA patients (n= up to 5), shown as circles and healthy controls (n= up to 4), shown as squares. The dotted line indicates the lower limit of detection. Statistical significance was assessed using a Fit Least Squares comparing RA patients and healthy controls in each B cell subset.

Production of the anti-inflammatory cytokine IL-10 was also assessed. IL-10 has been proposed to act as potent growth and differentiation factor for activated B cells (Rousset *et al.*, 1992), as well as acting as a B cell maturation suppressor, depending on the activation stage of the B cells (Itoh and Hirohata, 1995). As was observed for IL-2 and IL-6, production of IL-10 in the unstimulated condition for all the B cell subsets was very low (Figure 6.22.A). However, stimulation enhanced IL-10 production in naïve B cells, CD5+ B cells and memory B cells. Interestingly, stimulation of ABCs did not induce production of IL-10. No differences in IL-10 production were seen in any of the B cell subsets when B cells from established RA patients were compared to B cells from healthy controls (Figure 6.22.B-E).

IL-12 production was also assessed due to its role in skewing T cells towards a Th1 phenotype (Gee *et al.*, 2009). Overall, the concentrations of IL-12p70 that are produced in both the unstimulated and stimulated conditions was quite low (Figure 6.23.A). Production in the unstimulated conditions for all the B cell subsets was almost undetectable. Nonetheless, production of IL-12p70 was slightly increased after stimulation by all the B cell subsets. There were no differences in IL-12p70 production by any of the B cell subsets between the established RA patients and the healthy controls (Figure 6.23.B-E).

Production of IL-23, another cytokine important for T cell skewing, which drives T cell differentiation towards a Th17 phenotype, was assessed. IL-23 production was almost undetectable by the unstimulated cells (Figure 6.24.A). However, similar to IL-12p70, IL-23 production increased when all the B cell subsets were stimulated. Nonetheless, there was increased production of IL-23 by the stimulated CD5+ and naïve B cells from established RA patients compared to heathy controls (Figure 6.24.B-C).

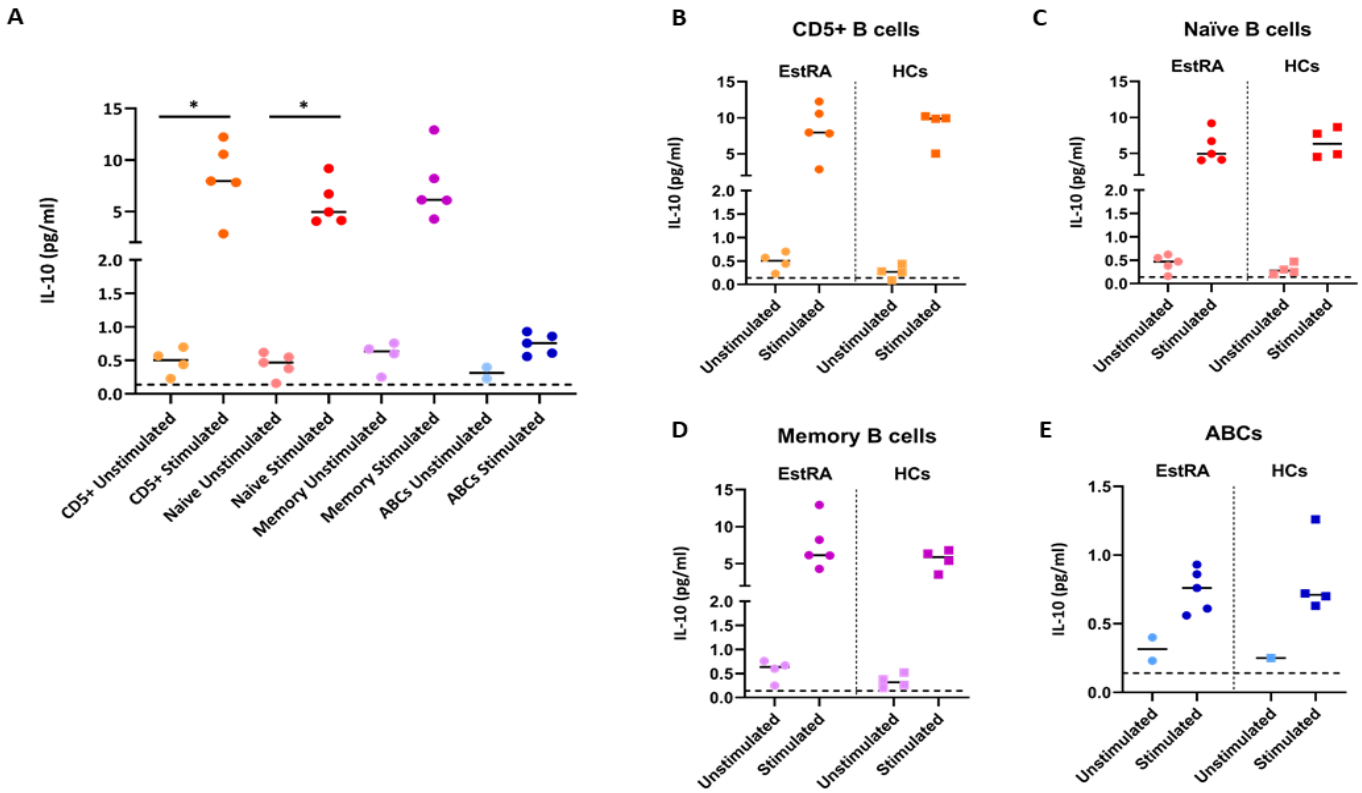

Figure 6. 22. Production of the cytokine IL-10 from unstimulated or stimulated sorted B cell subsets. Sorted cells from established RA patients were incubated with or without stimulation (Imiquimod, CpG A, CpG B, PWM, anti-CD40, IL-21, IL-4 and IFN-γ) for 5 days. **A.** The culture supernatants from established RA patients (n= up to 5) were harvested and the concentration of IL-10 was detected using a U-PLEX Custom Biomarker plate from MSD. The dotted line indicates the lower limit of detection. Statistical significance was assessed using a Kruskal-Wallis test (p=0.0002) with Dunn's multiple comparisons of the two conditions in each B cell subset; *p < 0.05. **B-E.** IL-10 production from B cells from established RA patients (n= up to 5), shown as circles and healthy controls (n= up to 4), shown as squares. The dotted line indicates the lower limit of detection. Statistical significance was assessed using a Fit Least Squares comparing RA patients and healthy controls in each B cell subset.

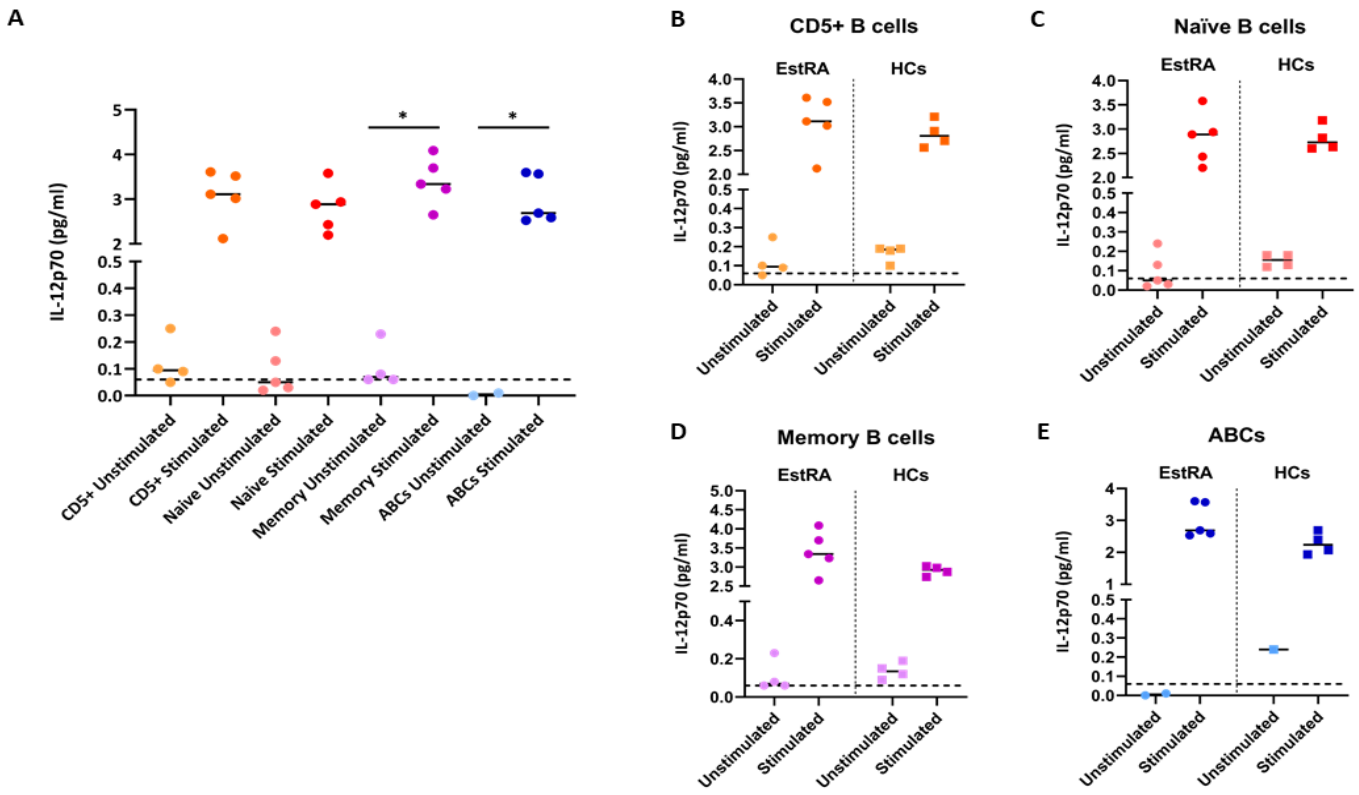

Figure 6. 23. Production of the cytokine IL-12p70 from unstimulated or stimulated sorted B cell subsets. Sorted cells from established RA patients were incubated with or without stimulation (Imiquimod, CpG A, CpG B, PWM, anti-CD40, IL-21, IL-4 and IFN-γ) for 5 days. **A.** The culture supernatants from established RA patients (n= up to 5) were harvested and the concentration of IL-12p70 was detected using a U-PLEX Custom Biomarker plate from MSD. The dotted line indicates the lower limit of detection. Statistical significance was assessed using a Kruskal-Wallis test (p=0.0003) with Dunn's multiple comparisons of the two conditions in each B cell subset; *p < 0.05. **B-E.** IL-12p70 production from B cells from established RA patients (n= up to 5), shown as circles and healthy controls (n= up to 4), shown as squares. The dotted line indicates the lower limit of detection. Statistical significance was assessed using a Fit Least Squares comparing RA patients and healthy controls in each B cell subset.

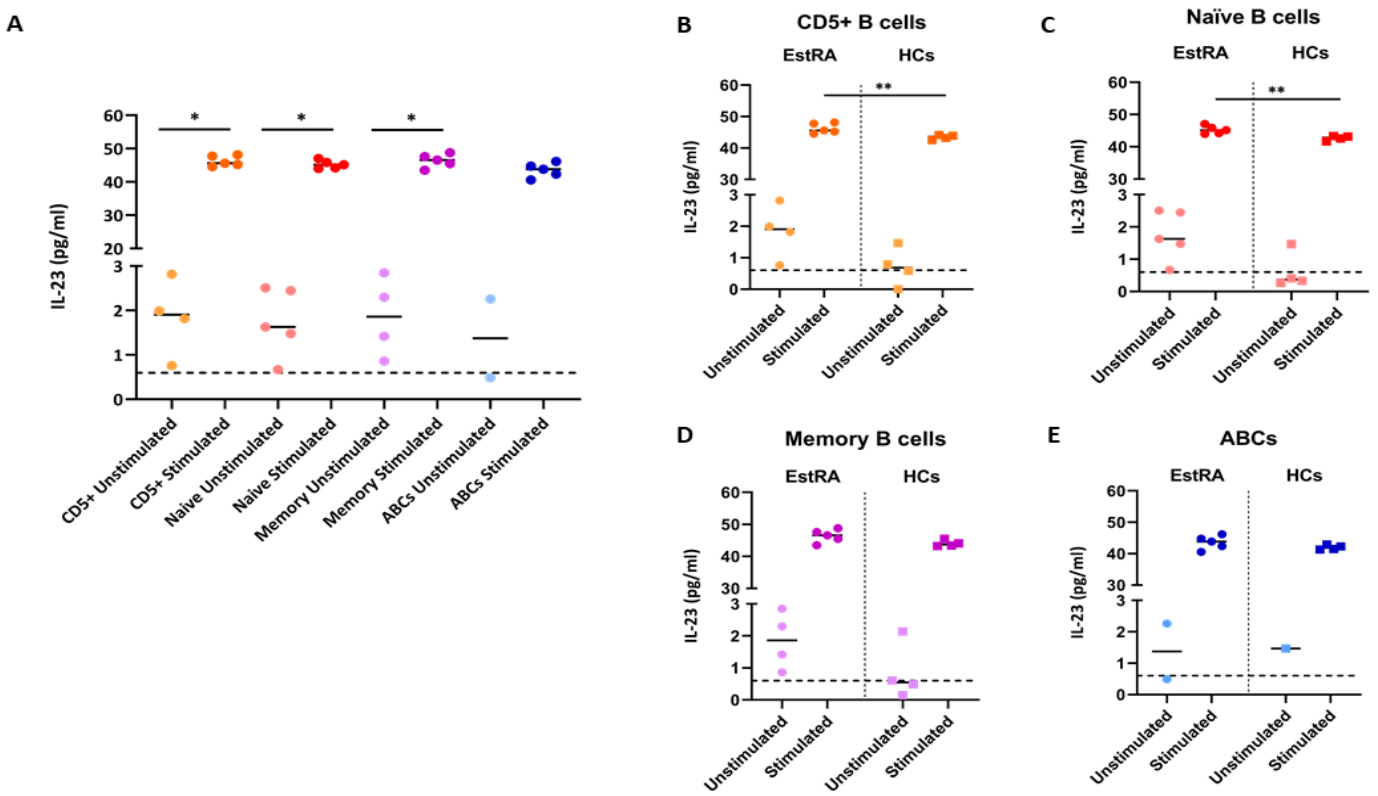

Figure 6. 24. Production of the cytokine IL-23 from unstimulated or stimulated sorted B cell subsets. Sorted cells from established RA patients were incubated with or without stimulation (Imiquimod, CpG A, CpG B, PWM, anti-CD40, IL-21, IL-4 and IFN-γ) for 5 days. **A.** The culture supernatants from established RA patients (n= up to 5) were harvested and the concentration of IL-23 was detected using a U-PLEX Custom Biomarker plate from MSD. The dotted line indicates the lower limit of detection. Statistical significance was assessed using a Kruskal-Wallis test (p=0.0003) with Dunn's multiple comparisons of the two conditions in each B cell subset; *p < 0.05. **B-E.** IL-23 production from B cells from established RA patients (n= up to 5), shown as circles and healthy controls (n= up to 4), shown as squares. The dotted line indicates the lower limit of detection. Statistical significance was assessed using a Fit Least Squares comparing RA patients and healthy controls in each B cell subset; **p < 0.01.

Production of GM-CSF, a cytokine involved in the activation of monocytes and macrophages (Ushach and Zlotnik, 2016), was also assessed. Production of this growth factor was low in the unstimulated conditions for all the B cell subsets (Figure 6.25.A). However, its production was slightly increased after stimulation in all the B cell subsets. Interestingly, production by the CD5+ B cells was more pronounced compared to the other B cell subsets. When the data from the established RA patients was compared to the healthy controls, there were no differences for any of the B cell subsets for either condition (Figure 6.25.B-E).

Finally, TNF-α production was also evaluated. TNF-α was shown to be produced by the synovial FcRL4+ B cell subset, suggesting a possible role for these ABC-like cells in osteoclast activation (Yeo *et al.*, 2015). As for the all other cytokines, production of TNF-α was very low in the unstimulated condition for all the B cell subsets (Figure 6.26.A). However, its production was slightly increased after stimulation in all the B cell subsets, especially in the CD5+ and the naïve B cells. The induction of TNF-α production following stimulation was smaller in ABCs than the other B cell subsets. However, there was increased production of TNF-α by the stimulated memory B cells from established RA patients compared to heathy controls (Figure 6.26.D).

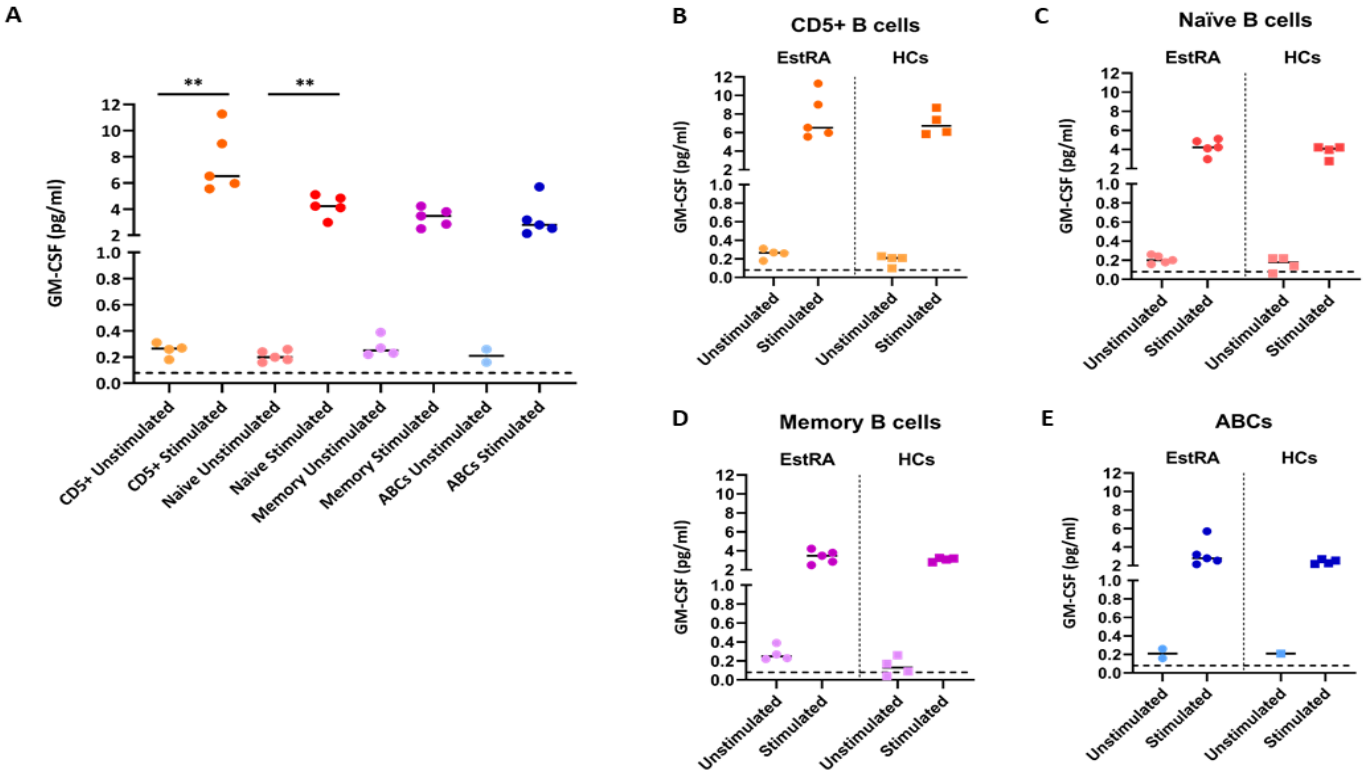

Figure 6. 25. Production of the cytokine GM-CSF from unstimulated or stimulated sorted B cell subsets. Sorted cells from established RA patients were incubated with or without stimulation (Imiquimod, CpG A, CpG B, PWM, anti-CD40, IL-21, IL-4 and IFN-γ) for 5 days. **A.** The culture supernatants from established RA patients (n= up to 5) were harvested and the concentration of GM-CSF was detected using a U-PLEX Custom Biomarker plate from MSD. The dotted line indicates the lower limit of detection. Statistical significance was assessed using a Kruskal-Wallis test (p=0.0001) with Dunn's multiple comparisons of the two conditions in each B cell subset; **p < 0.01. **B-E.** GM-CSF production from B cells from established RA patients (n= up to 5), shown as circles and healthy controls (n= up to 4), shown as squares. The dotted line indicates the lower limit of detection. Statistical significance was assessed using a Fit Least Squares comparing RA patients and healthy controls in each B cell subset.

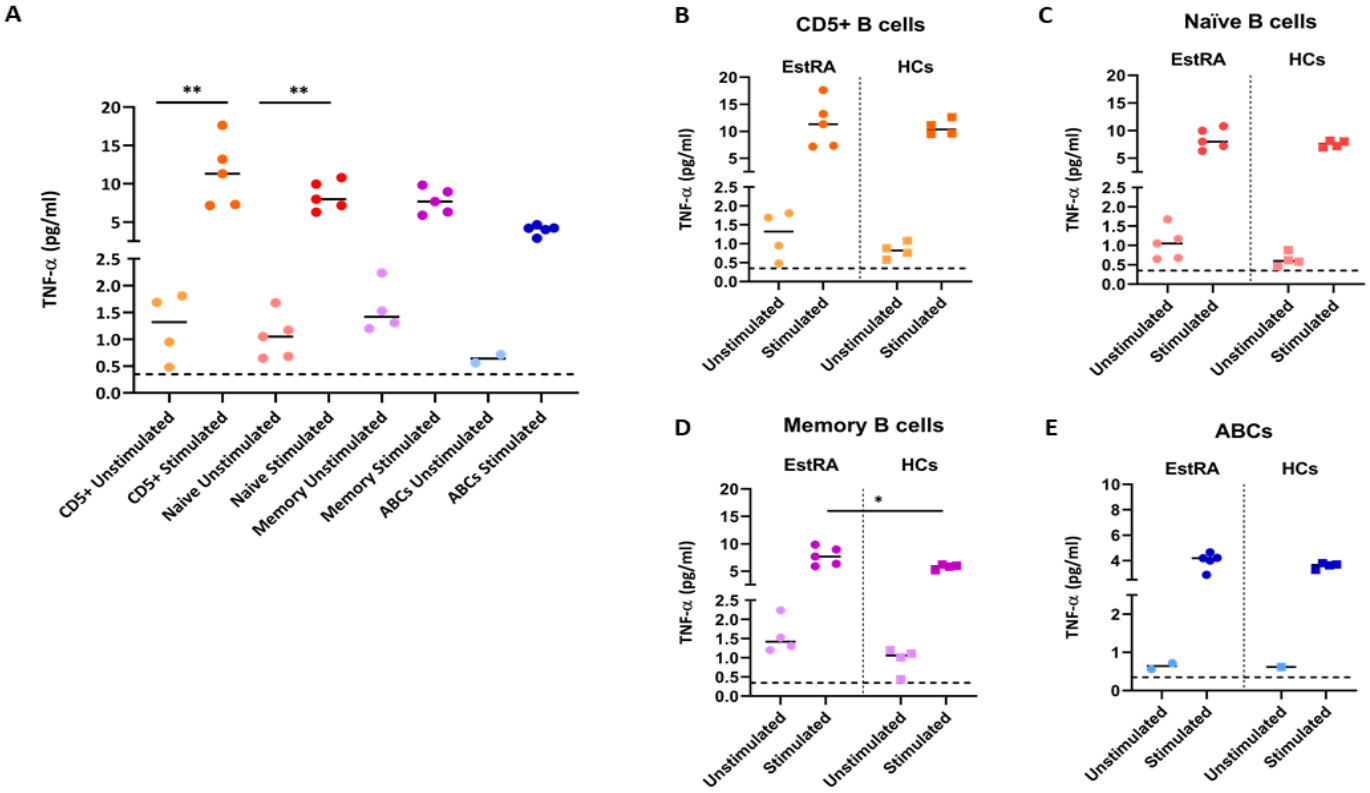

Figure 6. 26. Production of the cytokine TNF-α from unstimulated or stimulated sorted B cell subsets. Sorted cells from established RA patients were incubated with or without stimulation (Imiquimod, CpG A, CpG B, PWM, anti-CD40, IL-21, IL-4 and IFN-γ) for 5 days. **A.** The culture supernatants from established RA patients (n= up to 5) were harvested and the concentration of TNF-α was detected using a U-PLEX Custom Biomarker plate from MSD. The dotted line indicates the lower limit of detection. Statistical significance was assessed using a Kruskal-Wallis test ($p<0.0001$) with Dunn's multiple comparisons of the two conditions in each B cell subset; **$p < 0.01$. **B-E.** TNF-α production from B cells from established RA patients (n= up to 5), shown as circles and healthy controls (n= up to 4), shown as squares. The dotted line indicates the lower limit of detection. Statistical significance was assessed using a Fit Least Squares comparing RA patients and healthy controls in each B cell subset; *$p < 0.05$.

6.4.10 Immunoglobulin production by each B cell subset after stimulation

Supernatants from the cultured B cell subsets were also analysed for the presence of immunoglobulins (total IgM, total IgG and total IgA) using The Isotyping Panel 1 (Human/NHP) Kit from MSD.

There were very low levels of IgM production in the unstimulated condition for all the B cell subsets (Figure 6.27.A). Following stimulation, the level of IgM secreted into the culture supernatant increased and this effect was more enhanced for the memory B cell population. When the data from the established RA patients was compared to the healthy controls, there were no differences for any of the B cell subsets for either condition (Figure 6.27.B-E).

Regarding IgG production, there was no production by the unstimulated condition for all the B cell subsets (Figure 6.28.A). Upon stimulation the CD5+ and naïve B cell subsets did not produce IgG. However, there was detectable levels of this class-switched immunoglobulin by both memory B cells and ABCs, with memory B cells displaying the highest level of induction. Interestingly, there was increased production of IgG by the stimulated ABCs from established RA patients compared to heathy controls (Figure 6.28.E).

In terms of IgA production, there was no detectable levels in the unstimulated conditions for the CD5+ B cells, naïve B cells and ABCs (Figure 6.29.A). Interestingly, there was some spontaneous production of IgA detected in the unstimulated memory cells. Following stimulation, only the memory B cells produced IgA. There were no differences in IgA production by any of the B cell subsets between the established RA patients and the healthy controls (Figure 6.29.B-E).

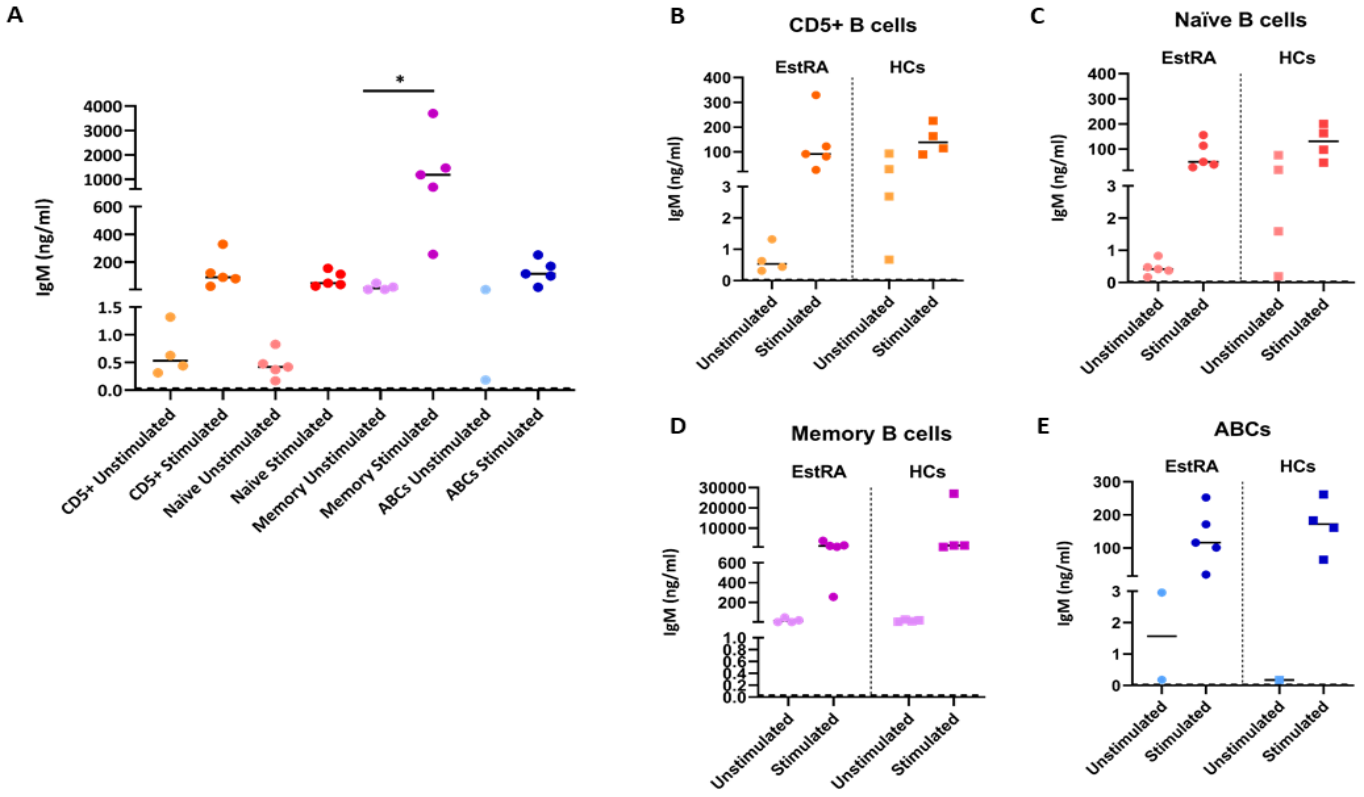

Figure 6. 27. IgM production from unstimulated or stimulated sorted B cell subsets. Sorted cells from established RA patients were incubated with or without stimulation (Imiquimod, CpG A, CpG B, PWM, anti-CD40, IL-21, IL-4 and IFN-γ) for 5 days. **A.** The culture supernatants from established RA patients (n= up to 5) were harvested and the concentration of IgM was detected using the Isotyping Panel 1 Kit from MSD. The dotted line indicates the lower limit of detection. Statistical significance was assessed using a Kruskal-Wallis test (p=0.0001) with Dunn's multiple comparisons of the two conditions in each B cell subset; *p < 0.05. **B-E.** IgM production from B cells from established RA patients (n= up to 5), shown as circles and healthy controls (n= up to 4), shown as squares. The dotted line indicates the lower limit of detection. Statistical significance was assessed using a Fit Least Squares comparing RA patients and healthy controls in each B cell subset.

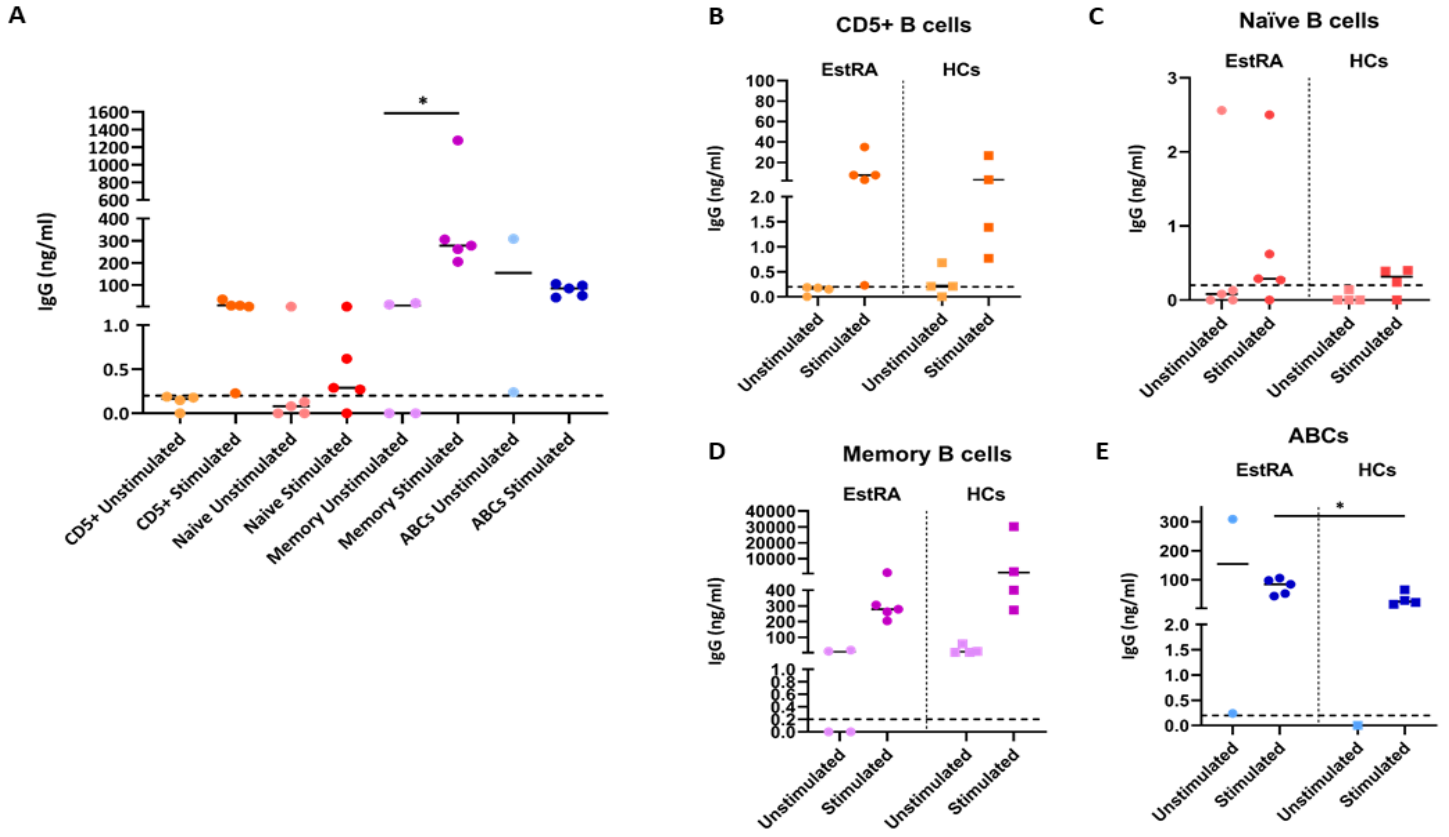

Figure 6. 28. IgG production from unstimulated or stimulated sorted B cell subsets. Sorted cells from established RA patients were incubated with or without stimulation (Imiquimod, CpG A, CpG B, PWM, anti-CD40, IL-21, IL-4 and IFN-γ) for 5 days. **A.** The culture supernatants from established RA patients (n= up to 5) were harvested and the concentration of IgG was detected using the Isotyping Panel 1 Kit from MSD. The dotted line indicates the lower limit of detection. Statistical significance was assessed using a Kruskal-Wallis test (p=0.0009) with Dunn's multiple comparisons of the two conditions in each B cell subset; *p < 0.05. **B-E.** IgG production from B cells from established RA patients (n= up to 5), shown as circles and healthy controls (n= up to 4), shown as squares. The dotted line indicates the lower limit of detection. Statistical significance was assessed using a Fit Least Squares comparing RA patients and healthy controls in each B cell subset; *p < 0.05.

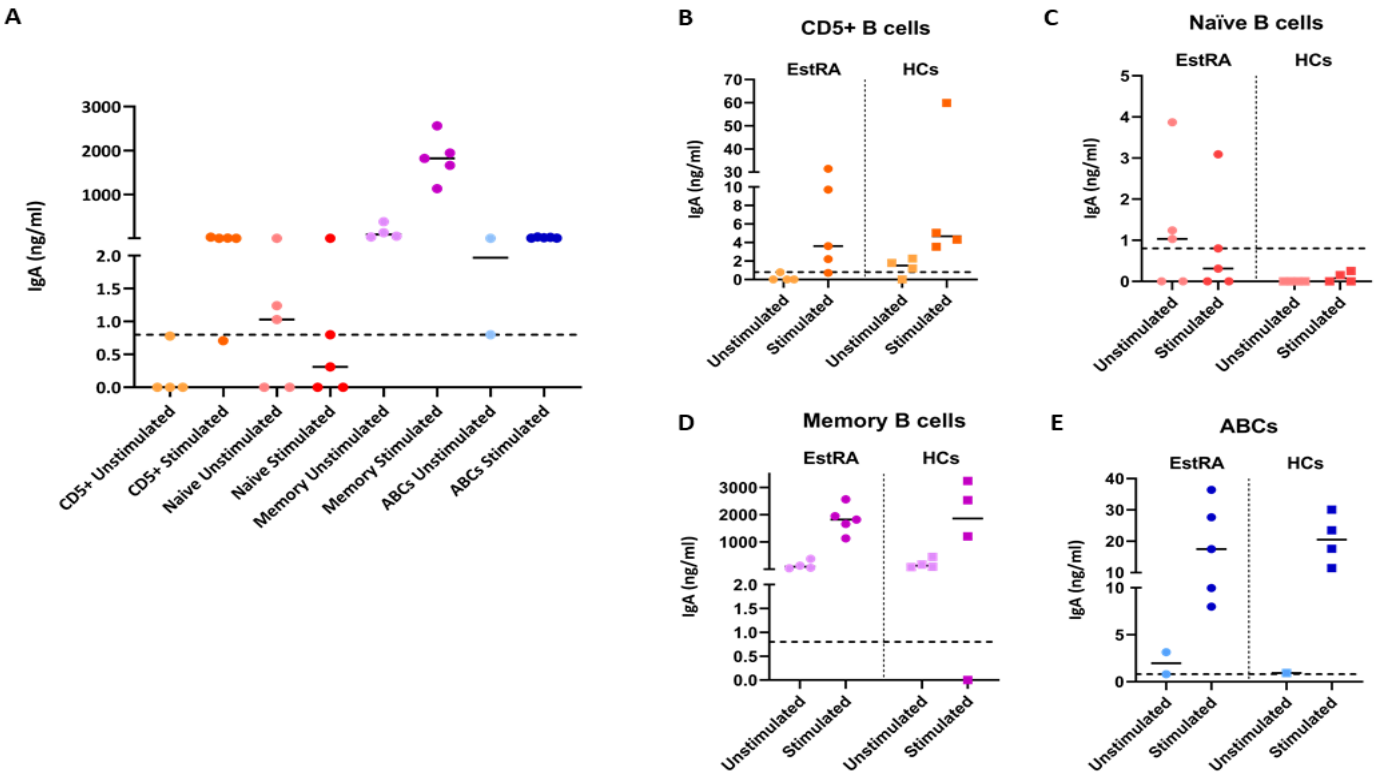

Figure 6. 29. IgA production from unstimulated or stimulated sorted B cell subsets. Sorted cells from established RA patients were incubated with or without stimulation (Imiquimod, CpG A, CpG B, PWM, anti-CD40, IL-21, IL-4 and IFN-γ) for 5 days. **A.** The culture supernatants from established RA patients (n= up to 5) were harvested and the concentration of IgA was detected using the Isotyping Panel 1 Kit from MSD. The dotted line indicates the lower limit of detection. Statistical significance was assessed using a Kruskal-Wallis test (p=0.0001) with Dunn's multiple comparisons of the two conditions in each B cell subset. **B-E.** IgA production from B cells from established RA patients (n= up to 5), shown as circles and healthy controls (n= up to 4), shown as squares. The dotted line indicates the lower limit of detection. Statistical significance was assessed using a Fit Least Squares comparing RA patients and healthy controls in each B cell subset.

6.5 Discussion

In this chapter, I optimised a sorting protocol for the isolation of different B cell subsets and developed a protocol for the culture and stimulation of small numbers of B cells. This optimisation allowed me to perform a few selected functional studies on the ABC population and compare the readout to the other B cell subsets. I phenotyped the cells after culturing with or without a stimulation cocktail containing Imiquimod, CpG A, CpG B, Poke Weed Mitogen, anti-CD40, human IL-21, human IL-4 and IFN-γ, to check for activation marker expression. This stimulation cocktail mimicked signals from a T cell-dependent response such as PWM, which stimulates BCR, and anti-CD40, as well as mimicking innate signals, for a T cell-independent response, using the TLR ligands, Imiquimod and CpG A and B. IL-21 was chosen as it has been shown to induce plasma cell differentiation and Ig secretion (Ettinger *et al.*, 2005). IL-4 is known to induce B cell survival and protect B cells from apoptosis (Wurster *et al.*, 2002), and IFN-γ was added due to its wide range of functions on B cells, such as promoting B cell survival and B cell differentiation into immunoglobulin producing cells (Jurado *et al.*, 1989). In addition to investigating the phenotype of the stimulated cells, I quantified a wide range of cytokines produced by B cells, as well as the profile of immunoglobulins secreted by these cells. Additionally, I compared all these readouts in established RA patients B cell subsets and age-matched healthy controls B cell subsets, albeit there was little difference between the two cohorts.

In order to optimise a protocol for the sorting and culture of B cell subsets, I first tested multiple culture conditions using naïve and memory B cells, as these were readily available in sufficient numbers for optimisation experiments. The first variable I tested was the culture volume. Due to the small numbers of B cells cultured the plate I chose to use was a 96-well round-bottom plate. The reason I wanted to test a smaller volume was due to the fact that culturing low numbers of B cells will likely result in the production of low concentrations of secreted mediators, such as immunoglobulins and cytokines, in the culture supernatant. Therefore, if a too large culture volume is used it would dilute the secreted mediators and could potentially make detection difficult. However, the concentration of IgG detected in the 200µl volumes is slightly higher, and more reproducible, than in the 100µl volumes (Figure 6.2.B). This is probably due to the fact that the cells appeared to be more viable and healthier in the larger volume of culture medium, possibly due to the increased amount of nutrients. Additionally, the slightly reduced

viability of the cells in the lower culture volume could be due to evaporation of culture volume from the plate. There is always some evaporation during incubation at 37°C, but smaller volumes evaporate at a higher rate, resulting in a large reduction of the final volume of culture medium (Esser and Weitzmann, 2011). However, the differences in the detected concentration of secreted IgG in the two culture volumes are very modest and could simply be due to slight differences in the cell composition between the two cultures, i.e. by chance one of the conditions may contain more plasma cells, which would produce more IgG, or may have more responsive cells. Unexpectedly, the concentration of IgG in the 200µl cultures volumes was not half the concentration in the 100µl cultures volumes (Figure 6.2.B). This could be due to the provision of extra nutrients in the 200µl cultures volumes and the cells being healthier and more viable and therefore producing more IgG than the 100µl cultures volumes. From these data I concluded that the 200µl culture volume was optimal, which was further supported by the pragmatic reasoning that having a larger volume of culture supernatant guaranteed that enough supernatants would be available for analysis using two different MSD assays, with spare available for other tests.

The second condition I wanted to optimise was the number of cells plated in each well. According to the manufacturer of the 96-well round-bottom plates, the minimum number of cultured cells in a 96-well plate are 10,000 cells. Once again, as the number of ABCs I could isolate from peripheral blood was very limited, I tested two low numbers (10,000 and 20,000) of B cells to determine if such small cell numbers are able to produce detectable concentrations of cytokines and immunoglobulins. I found that the percentage of live cells was higher in the 20,000 B cell cultures, suggesting that cells are more viable and healthier when cultured in higher numbers (Figure 6.3.A). However, IgG production was slightly higher in the 10,000 B cells cultures (Figure 6.3.B). As explained before, these could be due to having more plasma cells or cells which responded better to stimulation and therefore produced more IgG, in the 10,000 cell cultures just by chance. Because the percentage of live cells was higher in the 20,000 cell cultures and because culturing larger numbers of cells should increase the concentration of detectable cytokines and immunoglobulins, I decided to use 20,000 cells per well for the functional work.

Finally, the last variable I wanted to optimise was the culture time. I tested two different time points: 3 days and 6 days (Figure 6.4). A short time point of 3 days was chosen because B cells are very sensitive and die easily so I wanted to test if I could detect secreted IgG at a short time point. A longer time point of 6 days was chosen to see if a longer culture time

was needed for the cells to activate and secrete IgG and other cytokines. Some studies showed that around 8 days are required for primary B cells to class-switch (Su *et al.*, 2016). Because I hypothesised that ABCs are antigen-experienced B cells and a large proportion has already class-switched, the aim was to assess the effect a potent B cell stimuli had on these cells, and therefore a time point longer than 6 days was deemed unnecessary. As expected, the percentage of live memory B cells was higher at day 3 compared to day 6, however, the live cells did not greatly decrease at day 6 when the memory B cells were stimulated (Figure 6.4.A). In terms of IgG production, secretion of this immunoglobulin was doubled at day 6 compared to day 3 (Figure 6.4.B). Because the number of live stimulated memory B cells did not dramatically decrease and the detection of secreted IgG was much higher at day 6, the later time point was chosen for the functional work. However, due to clinic timings and sample processing time restrictions, the final incubation time for the functional work had to be compromised to 5 days. This time point was chosen as it would provide sufficient culture time for the B cells to activate and secrete cytokines and immunoglobulins, and would maintain a high percentage of live cells when cells were stimulated.

As explained before, in order to isolate a usable number of ABCs, a large volume of blood was needed. This resulted in high numbers of isolated PBMCs and therefore a large number of cells to stain and process through the flow cytometer sorter. This in turn, resulted in very long periods of time sorting the cells, which in addition to being expensive, also had the potential for damaging the sorted cells resulting in high levels of cell stress and ultimately, death. In order to reduce the sorting time, I tried sorting B cell subsets using two different approaches utilising Miltenyi MACS MicroBeads. Positive selection, in which CD19+ B cells are labelled with CD19 MicroBeads and are actively removed from the sample; and negative selection, in which the CD19+ B cells remain "untouched" by MicroBeads. A study comparing different methods, including the use of Miltenyi MACS isolations, found that there was high contamination of platelets when using the Miltenyi MACS system (Moore *et al.,* 2019). This study concludes that the best method for isolating pure B cells for downstream functional assays is by flow cytometry sorting. Nonetheless, because I am interested in different B cell subsets, I needed to sort the cells anyway to obtain pure fractions of the different B cell subsets. Therefore, I tested sorting the subsets from a pre-enriched CD19+ B cell population, obtained using CD19 Miltenyi MACS MicroBeads, as it would decrease the sorting time as only B cells were used as the starting sort population

compared to PBMCs. However, the results showed that B cells sorted from pre-enriched CD19+ B cells were not functionally the same as when sorted directly from PBMCs (Figure 6.5). The B cell subset which seemed more affected were the naïve B cells. These cells showed higher cell death and CD40 downregulation in the unstimulated condition when sorted from the pre-enriched CD19+ B cell population compared to direct sorting from PBMCs. These results suggest that the CD19 MicroBeads isolation process could be inducing downregulation of CD40. A previous study described downregulation of CD20 following CD40 stimulation (Anolik *et al.*, 2003), so it could be possible that stimulation of CD19, via binding of a CD19 MicroBead, may also downregulate CD40. Moreover, production of IgG by the memory B cell subset was ever so slightly lower in cells sorted from the pre-enriched CD19+ B cell population.

Because sorting from pre-enriched CD19+ B cells seemed to affect the function of the cells, a negative selection approach was tested. This method is advantageous as the pre-enriched CD19+ B cells remain untouched by MicroBeads, therefore, potentially functionally unaltered by this process. To this end, a Miltenyi MACS CD3 MicroBead kit was chosen to deplete the T cells from the PBMC fraction. The cells left in the CD3-depleted PBMC sample would include monocytes, NK cells, dendritic cells and B cells. Because T cells constitute around 70% of PBMCs (Corkum *et al.*, 2015), the number of cells remaining for the flow cytometer sort is therefore significantly much less and sort time is significantly reduced. Unlike the results obtained using the B cells sorted from pre-enriched CD19+ B cells, B cells sorted from the CD3-depleted PBMCs showed no difference in B cell function compared to the cells sorted directly from PBMCs (Figure 6.6). Some studies in which functional work on ABC-like cells was performed also used a negative selection approach (Isnardi *et al.*, 2010; Wang *et al.*, 2018). Even though these studies did not just deplete CD3+ cells, other enrichment cocktails which depleted all types except B cells, leaving the B cells untouched, were employed. Taking all of this into account, the functional B cell work was performed using sorted B cell subsets from CD3-depleted PBMCs, allowing for shorter sorting times, and B cells which were functionally similar to the ones sorted directly from PBMCs.

For the functional work, five established RA patients and four age-matched healthy controls were recruited. Because the established RA patients were recruited first, age- and sex-matched healthy controls were picked specifically to match the patients and therefore no significant differences in age and sex were seen (Table 6.1).

In terms of cell viability after sorting and culturing, I expected to see a small number of live cells in the unstimulated conditions, as B cells are known to die quickly in culture if they are not stimulated (Researchgate, 2012). I have demonstrated in the previous chapters that *ex vivo* CD5+ B cells appear to be similar to the naïve B cell subset phenotypically and transcriptionally. In terms of cell viability following stimulation, CD5+ B cells also appear to be similar to naïve B cells as the percentages of live cells are almost identical in the two subsets. In addition, the phenotype and gene expression profile data I have previously shown, suggested that ABCs are quite similar to memory B cells. However, when the ABCs are stimulated, they do not respond as robustly as the memory B cells and they display a high level of cell death (Figure 6.7.A). This could be due to the ABCs being more sensitive to the pressure and stress of cell sorting, resulting in higher cell death. It is known that cell sorting can cause stress to the cells, and the choice of flow cytometer sorter can also influence this. The FACSAria system (BD Biosciences, CA, USA), which I used for this work, interrogates the cells in a cuvette and although it increases optical resolution, cells are slowed down and then sped up and this change in speed can increase cell stress (Harvard, n.d). On the other hand, other cell sorters, such as MoFlo Astrios (Beckman Coulter, CA, USA), maintain velocity, minimising cell stress and improving cell viability. Although all the B cell subsets have been through the same potential stress levels induced by the FACSAria system, ABCs could be more prone to die by apoptosis as highlighted by their expression of apoptotic genes I presented in Chapter 5, as well as in published literature (Isnardi *et al.*, 2010). A study showed that flow cytometry sorting is the best method for transcriptomic analysis as it gives high purity cell yields and avoids the induction of cell stress (Beliakova-Bethell *et al.*, 2014). However, this published study analysed gene expression immediately after sorting the leukocytes, so no assessment of changes which occur after a few days culture, post-sorting, were evaluated. Nevertheless, the only way to feasibly assess cytokine and immunoglobulin production in each of the subsets was by sorting. Another reason for the low cell viability in the ABC population, could be due to the use of IL-4 in the stimulation cocktail. As reported before, IL-4 antagonises ABC formation and could be inhibiting ABC activation, thus leading to increased cell death (Naradikian *et al.*, 2016b). Interestingly, unstimulated memory B cells from established patients showed slightly higher percentages of live cells than unstimulated memory B cells from healthy controls, suggesting that memory B cells from patients with RA may have enhanced survival (Figure 6.7.D). A study showed that in the RA synovia,

V-CAM expressing fibroblast regulated synovial memory B cell survival, preventing apoptosis (Reparon-Schuijt *et al.*, 2000).

A limitation of this experiment was that it was not possible to determine if the cells which responded to stimulation actually proliferated. For future work this could be done by and intracellular staining for Ki67 to assess the percentage of proliferating cells or by labelling the cells with a CellTrace dye. This will help to determine whether the higher percentage of live cells in the memory B cells is due to B cell proliferation or whether the live cells are just more robust and survive.

With regard to the surface marker phenotype, in general, HLA-DR was upregulated following stimulation (Figure 6.8). This is not surprising as HLA-DR is involved in the B cell activation cascade both at an early and late stage (Giudizi *et al.,* 1987). Interestingly, in both unstimulated and stimulated conditions, there is a trend for decreased percentages of HLA-DR+ cells, as well as expression of HLA-DR in all B cell subsets from RA patients compared to healthy controls (Figure 6.9). However, these results are not in line with other studies, which showed a positive correlation between the amount of HLA-DR gene transcripts and the presence of the RA risk alleles, suggesting a correlation between HLA-DR expression and RA susceptibility (Kerlan-Candon *et al.,* 2001; Kampstra and Toes, 2017).

Expression of another co-stimulatory molecule, CD86, which is known to increase after cell activation (Suvas *et al.,* 2002) was assessed. As expected, CD86 expression was upregulated in all B cell subsets after stimulation (Figure 6.10). As reported in Chapter 4 Figure 4.5, resting or unstimulated ABCs, and memory B cells to a lesser extent, have higher expression of CD86 than other resting B cell subsets. CD86 upregulation following stimulation was higher in memory B cells and ABCs, which is in line with a published study showing that CD86 is rapidly upregulated on B cells following activation by cross-linking of the BCR or the addition of a variety of cytokines (Manzoor, 2015). The fact that expression is higher in ABCs and is heavily upregulated after stimulation reinforces the hypothesis that ABCs are an activated B cell subset with a potential role in antigen presentation. Unstimulated naïve B cells from healthy controls showed slightly higher percentages of CD86+ cells than the unstimulated naïve B cells from established RA patients (Figure 6.11.A), suggesting naïve cells from RA patients might require a stronger stimulation to respond and activate.

Expression of the activation marker CD69 was also evaluated. Interestingly, CD69 expression was upregulated after stimulation only on CD5+ and naïve B cells (Figure 6.12). Memory B cells and ABCs showed no change in expression of this activation molecule. However, these results are in keeping with another study looking at the kinetics of CD69 expression, which have shown that CD69 expression increases early after infection in mice (Purtha *et al.*, 2008) and decreases during infection. Therefore, CD69 is an early activation marker, which is upregulated predominantly in naïve B cells. However, CD69 expression did not increase in memory B cells and ABCs following stimulation. This could be due to these cells being already in an activated state or even being exhausted or it might be the case that the kinetics for CD69 might be different in memory B cells and it could be more rapidly downregulated. However, no differences were seen in the percentage of CD69 positive cells or CD69 expression, as measured by MFI, in any of the B cell subsets from established RA patients and healthy controls (Figure 6.13).

Another activation marker, which was of interest based on my NanoString gene expression analysis from Chapter 5 was the activation marker CD97, a G-protein coupled receptor involved in cell adhesion. From my NanoString results CD97 transcript and protein appeared to be upregulated in ABCs compared to the other B cell subsets. Interestingly, CD97 was upregulated by all B cell subsets after stimulation (Figure 6.14). Moreover, as reported in Chapter 5, section 5.4.4, CD97 was highly expressed by resting ABCs, and as demonstrated here, CD97 is greatly upregulated after stimulation. To my knowledge this is the first time that expression of this adhesion molecule is reported in ABCs. Moreover, CD97 has been reported to be expressed at high levels on inflammatory cells and is thought to contribute to inflammation-mediated angiogenesis (Wang *et al.*, 2005). These results, together with the data from Chapter 5 showing high expression of integrins and other chemokine receptors, supports a role for the migration of ABCs to inflammatory sites. Percentage of CD97 positive cells in the stimulated conditions from all the B cell subsets showed higher expression in B cells from healthy controls than established RA patients (Figure 6.15), suggesting that B cells from healthy controls have an increased upregulation of CD97 following stimulation. In terms of MFI values, CD97 expression in the unstimulated CD5+ B cells and memory B cells, as well as the stimulated naïve B cells is higher in healthy controls compared to established RA patients. This decreased expression of CD97 in established RA patients could be explained by the fact that these patients are

being treated with global immune suppressor drugs and activation of the cells could be affected by these.

Expression of the memory B cell marker CD27 was also analysed. CD27 is a type I glycoprotein expressed globally and used to distinguish naïve from memory B cells (Agematsu *et al.*, 2000). Memory B cells express CD27, although expression of this marker also went up with stimulation as CD27 is both a maturation and activation marker. As expected, naïve and CD5+ B cell subsets became positive for CD27 after stimulation, although expression of this marker was not massively upregulated (Figure 6.16). Memory B cells were already positive for CD27 as this marker was used as an identification marker to gate these cells, however, expression of this activation marker was also highly upregulated after stimulation in memory B cells, as evidenced by an increase in the MFI (Figure 6.16.C). Around half of the resting ABC subset were CD27+, however, the percentage of CD27 positive cells increased after stimulation and expression of CD27, measured as MFI, was also slightly upregulated. Interestingly, there was a small trend for unstimulated and stimulated naïve B cells and stimulated ABCs from established RA patients to have a lower percentage of CD27+ cells compared to healthy controls (Figure 6.17.A). This could be due to the increased expression of CD70 by T cells in blood from RA patients (Park *et al.*, 2014). CD70 is the ligand for CD27 and an increased expression in RA could possibly induce downregulation of its receptor, CD27, to help control B cell activation.

The last phenotypic marker assessed was cell surface expression of IgG. IgG expression is not induced after stimulation of naïve and CD5+ B cells (Figure 6.18). These results are expected as 5 days of stimulation culture are not enough to induce class-switching of the naïve B cells (Su *et al.*, 2016). Intriguingly, ABCs showed a similar percentage of IgG+ cells and expression, measured by MFI, of IgG as the memory B cells, supporting the role of ABCs as class-switched memory B cells. These results are in line with the phenotyping of resting ABCs shown in Chapter 4 Figure 4.11, where the percentages of class-switched IgG B cells in the ABC subset were as high as in the memory B cell population. Interestingly, the percentage of IgG positive cells in unstimulated and stimulated naïve B cells from RA patients was lower compared to healthy controls (Figure 6.19). Additionally, there was higher IgG expression, as measured by MFI, in unstimulated CD5+ B cells and stimulated naïve B cells from healthy controls compared to established RA patients (Figure 6.19.B). Although these differences were significant, the percentage of IgG positive cells

and the MFI values in these subsets are very low compared to the memory B cell subset and the ABC population.

In addition to cell surface markers I also assessed the production of cytokines following cell stimulation. IL-2 production was assessed as this cytokine acts as an autocrine growth factor, which has been proven important for B cell proliferation, as well as for T cell survival and for the development of Tregs (Lagoo *et al.*, 1990; Malek, 2003). My results show little secretion of IL-2 by all the B cell subsets (Figure 6.20.A). However, it has been reported before that production of IL-2 by B cells occurs as a late event relative to their activation and proliferation (Kindler *et al.*, 1995). This could explain why such small concentrations of IL-2 were detected from all B cell subsets. A solution to this could be increasing culturing time in order for the B cells to fully activate and secrete IL-2. Moreover, as IL-2 is a growth factor for B cells, it is possible that the B cells are consuming it and therefore small concentrations are detected. Interestingly, unstimulated memory B cells and stimulated CD5+ B cells and naïve B cells from established RA patients showed higher secretion of IL-2 compared to B cells from healthy controls (Figure 6.20.B-D). However, a study found that PBMCs from RA patients produced lower quantities of IL-2 than PBMCs from healthy controls (Combe *et al.*, 1985). Nevertheless, this study was done with PBMCs, so there was a mix of lymphocytes and production by a specific type of cell was not assessed.

IL-6 was also assessed in the culture supernatants following cell stimulation. This cytokine was chosen due to the role it plays in the differentiation of T follicular helper cells and formation of germinal centres (Arkatkar *et al.*, 2017), in addition to our interest in this cytokine stemming from previous work published from our group which described an IL-6 gene signature in CD4 T cells from patients suffering from RA (Pratt *et al.*, 2012; Anderson *et al.*, 2016; Anderson *et al.*, 2019; Ridgley *et al.*, 2019). My results showed high production of IL-6 by naïve and CD5+ B cells after stimulation, however, secretion by memory and ABCs was very low (Figure 6.21.A). As IL-6 production by B cells has been shown to have a function in germinal centre formation and T follicular help cells differentiation, secretion of this cytokine by naïve and CD5+ cells is understandable as when these cells become activated, they should migrate to germinal centres and interact with T follicular helper cells to undergo class-switching (Stebegg *et al.*, 2018). No differences in IL-6 production by all the B cell subsets in established RA patients compared to healthy controls were detected (Figure 6.21.B-E).

Regarding IL-10 production, secretion of this cytokine was assessed due to its properties as anti-inflammatory cytokine (Couper *et al.*, 2008). IL-10 has been proposed to have a dual function, as depending on the activation stage of B cells, this cytokine can act as a growth and differentiation factor (Rousset *et al.*, 1992) or can supress maturation of B cells (Itoh and Hirohata, 1995). Surprisingly, all the B cell subsets except the ABCs secreted this cytokine after stimulation (Figure 6.22.A). CD5+ B cells have been suggested to be potent producers of IL-10 (Dalloul, 2009), and my results showed that they do produce higher levels of this cytokine compared to other B cells. However, to my knowledge, IL-10 production by ABCs have never been investigated, although a study reported CD21low B cells expressed high levels of IL-10 transcript after BCR and TLR stimulation (Hao *et al.*, 2011). Nevertheless, this study did not check secretion of the actual protein. This striking difference between ABCs and the other subsets supports the hypothesis that ABCs may be a pro-inflammatory B cell subset and lack anti-inflammatory capabilities. No differences in IL-10 production by all the B cell subsets in established RA patients compared to healthy controls were detected (Figure 6.22.B-E).

IL-12p70 secretion was also assessed. IL-12 is composed of two subunits, p35 and p40, which combined form the bioactive IL-12p70. Due to the ability of IL-12 to induce IFN-γ production this cytokine is involved in the skewing of T cells towards a Th1 phenotype (Gee *et al.*, 2009). My results showed induction of IL-12p70 production following stimulation by all the B cell subsets (Figure 6.23.A). Although IL-12 production by B cells has been previously reported, the study used much higher numbers of cultured tonsillar B cells rather than peripheral blood B cell subsets (Schultze *et al.*, 1999). Moreover, IL-12p70, the active form peaked on day 2 after stimulation and decreased by day 4, demonstrating that by day 5 of culture, as I used, there might not be very high levels of active IL-12 due to degradation over time. This is in fitting with the low pg/ml levels detected in my B cell subset cultures. As for IL-6 and IL-10, no differences in IL-12p70 production by all the B cell subsets in established RA patients compared to healthy controls were detected (Figure 6.23.B-E).

Another cytokine assessed was IL-23. IL-23 is of interest due to its implication in inducing Th17 cells (Gee *et al.*, 2009). In addition, IL-23 has been proven to play a role in the pathogenesis of different inflammatory conditions, as well as being found in skin lesion in psoriatic arthritis and the synovial membrane in RA patients joints (Duvallet *et al.*, 2011). IL-23 production by stimulated B cells was generally high, however the concentrations

produced by the different B cell subsets were quite similar (Figure 6.24.A). Interestingly, IL-23 production by stimulated CD5+ and naïve B cells from established RA patients was higher than stimulated CD5+ and naïve B cells from healthy controls (Figure 6.24.B-C). Higher levels of serum IL-23 have been reported in RA patients compared to healthy controls (Zaky and El-Nahrery, 2016), therefore, CD5+ and naïve B cells, probably together with other blood cells, might be contributing to the increased levels of IL-23 in serum from RA patients.

Production of GM-CSF was also evaluated. GM-CSF is involved in activation of monocytes and macrophages, as well as mediating their differentiation to other cell types such as dendritic cells (Ushach and Zlotnik, 2016). Although my results showed very low levels of production of GM-CSF (Figure 6.25.A), in the low pg/ml range, upon stimulation, other groups have discovered a subset of B cells in multiple sclerosis that is able to produce GM-CSF (Li *et al.*, 2015). However, in that study GM-CSF production was assessed after a 2 day culture, so as previously mentioned in connection with IL-12, it may be the case that in my cultures by day 5, the GM-CSF secreted by the B cells had been degraded. Even though the amounts of GM-CSF produced were very low, there was a trend for increased production by stimulated CD5+ B cells. As explained before, CD5+ B cells are thought to produce IL-10 (Dalloul, 2009), and some studies in autoimmune diseases have shown that low doses of GM-CSF expand the IL-10 producing regulatory B cells (Sheng *et al.*, 2014). Therefore, CD5+ B cells could be involved in GM-CSF production following activation, which may work in an autocrine manner. No differences in GM-CSF production by all the B cell subsets in established RA patients compared to healthy controls were detected (Figure 6.25.B-E).

The last cytokine assessed was TNF-α. TNF-α is of interest because previous work done by my supervisor in Birmingham (Professor Dagmar Scheel-Toellner) described an FcRL4+ B cell subset, with an ABC-like phenotype. This FcRL4+ B cell subset was found in the synovial fluid of RA patients and had high expression of TNF-α mRNA (Yeo *et al.*, 2015). This high expression of TNF-α, together with the expression of RANKL, suggested a possible role for these cells in osteoclast differentiation and activation. Production of TNF-α by all the B cell subsets was very low after stimulation, levels were only in the low pg/ml range (Figure 6.26.A). In addition, memory B cells and ABCs showed lower production of this cytokine compared to naïve B cells and CD5+ B cells. This is in line with studies in mice which evaluated the production of TNF-α by ABCs compared to

follicular B cells and did not find a significant increase in TNF-α expression in ABCs (Frasca *et al.*, 2012). Interestingly, stimulated memory B cells from established RA patients showed higher TNF-α production than stimulated memory B cells from healthy controls (Figure 6.26.D). High levels of TNF-α have been found in synovial fluid of patients with RA and it has been proven to play an important role in inflammation and joint destruction (Choy and Panayi, 2001). Moreover, anti-TNF therapies have proven effective in the treatment of RA (Feldmann and Maini, 2001), highlighting the importance of this cytokine in RA.

In terms of immunoglobulin production, IgM secretion was assessed. IgM is expressed on naïve B cells and it is the antibody formed during an initial response to an antigen (Goding, 1978). It is a marker of non-class-switched B cells. As expected, my results showed secretion of IgM from all the subsets after stimulation, with memory B cells showing higher secretion (Figure 6.27.A). A study reported CD5+ B cells produced polyreactive IgM, natural antibodies recognising autoantigens (Duan and Morel, 2006). Nevertheless, in my study no increased production of IgM was seen by these cells compared to other subsets, yet no evaluation assessing which epitopes the secreted antibodies recognised was done. Supernatants from stimulated memory and ABCs were sent to the Newcastle clinical laboratories (Newcastle Hospitals NHS Trust) for the detection of RF and CCP antibodies. However, no autoantibodies were detected probably due to the low cell numbers used. Moreover, no differences in IgM production by all the B cell subsets in established RA patients compared to healthy controls were detected (Figure 6.27.B-E).

IgG secretion was also investigated. Contrarily to IgM, IgG is expressed and secreted by antigen-activated B cells which have undergone isotype switching (Rich *et al.*, 2019). Because naïve and CD5+ B cells are not class-switched cells, the low secretion of IgG seen after stimulation was expected (Figure 6.28.A). On the contrary, high production of IgG by memory B cells was as predicted. Regarding the ABCs, as shown before in Chapter 4, Figure 4.11 and in Figure 6.14, around 50% of the B cells in the ABC population showed IgG surface expression. The percentage of IgG+ B cells in the ABC population was similar to the memory B cells, however, secretion of this immunoglobulin was much higher in memory B cells than in ABCs. These results indicate that in the ABC population there are not a lot of effective antibody producing cells, as seen in the memory B cell subset. This lower production of IgG by ABCs could also be due to the low number of live cells after culture. A study describing ABCs as CD11c+ T-bet+ IgM memory B cells demonstrated

that these cells are memory B cells which express IgM but respond quickly to antigen challenge and can undergo class-switching in germinal centres (Winslow *et al.*, 2017). Therefore, the ABC subset found in the peripheral blood may be a heterogeneous population with cells which have undergo isotype class-switching in germinal centres and others which have not. This may also explain the discrepancies reported by other studies in expression of other markers, such as CD27 or T-bet (Thorarinsdottir *et al.*, 2015). Interestingly, stimulated ABCs from established RA patients showed higher IgG production than stimulated ABCs from healthy controls (Figure 6.28.E). These results may suggest that the ABC population in RA patients have a higher percentage of class-switched cells or that these ABCs from RA patients may be more responsive to stimulation, leading to higher concentrations of IgG produced.

Lastly, IgA production was also assessed. This immunoglobulin is of interest for its implication in mucosal immunity, as some studies point at mucosal sites as the trigger of autoimmunity (Catrina *et al.*, 2014). IgA is also expressed and secreted after isotype switching. As expected, naïve B cells and CD5+ B cells secreted very low levels of IgA, even after stimulation (Figure 6.29.A). ABCs showed a similar result. However, the memory B cell population demonstrated some level of IgA secretion upon stimulation and even some without stimulation, suggesting that some spontaneous IgA producing B cells where found in this population. No differences in IgA production by all the B cell subsets in established RA patients compared to healthy controls were detected (Figure 6.29.B-E).

6.6 Conclusions

In this chapter, I performed a functional characterisation of ABCs and other B cell subsets isolated from established RA patients and healthy controls. Previous studies on the functionality of ABCs show discrepancies when describing these cells as an exhausted or an activated B cell subset. Considering, the phenotypic and gene expression characterisation showed in previous chapters, I hypothesised that the ABC subset can respond to a B cell stimulation cocktail and produce immunoglobulins and pro-inflammatory cytokines.

Due to the limiting numbers of ABCs in blood, I optimised a protocol for the sorting and culturing of small numbers of B cells. Culturing 20,000 cells with a B cell stimulation cocktail for 5 days in a final volume of 200µl allowed for the detection of secreted IgG using ELISA. In addition, I optimised a protocol to reduce the sorting time compared to sorting directly from PBMCs, which did not alter the B cell function. After the optimisation of a protocol for the functional work, I sorted and cultured the different B cell subsets from established RA patients and healthy controls, I phenotyped the cells and analysed the supernatants for the detection of secreted immunoglobulins and cytokines. Analysis of the cells after 5 days of culture showed high cell death even in the stimulated conditions for CD5+ B cells, naïve B cells and ABCs. Phenotyping of the stimulated B cell subsets showed upregulation of activation markers, such as CD86, CD97 and CD27, as well as increased expression of the MHC class II molecule, HLA-DR. However, IgG expression was unchanged suggesting that 5 days of stimulation was not enough for the B cells to class-switch. Cytokine secretion revealed, in general, very low concentrations of most of the assessed cytokines, probably due to low cell numbers. Production of the cytokines by the different B cell subsets showed no differences except for the secretion of IL-10, which was mostly undetectable from ABCs. Analysis of the secretion of immunoglobulins showed production of IgM and IgG in ABCs although lower than the concentrations produced by memory B cells.

In summary, to my knowledge this is the first time that cytokine production and immunoglobulin secretion by ABCs has been assessed following cell stimulation. Nevertheless, probably due to small numbers of cells, the amounts of cytokines detected was rather low. All in all, I cannot confirm the hypothesis that ABCs are an active and responsive B cell subset due to the high level of cell death seen. However, further studies

using large number of cells, different time points or different stimuli cocktails could give better B cell responses and would help elucidate the role of ABCs both in health and disease.

Chapter 7. Fc Receptor-Like 3 (FcRL3) functional work

7.1 Introduction

In Chapter 4, section 4.4.6 I assessed expression of the FcRL family of molecules on the ABC population. I demonstrated that higher percentages of cells positive for FcRL2, FcRL3, FcRL4 and FcRL5 were found in the ABC population. Following on from this discovery I next wanted to focus on the functional consequences of this expression.

FcRL1-5, all expressed by B cells, are located in the human *FcRL1-5 cluster*, in chromosome 1. This cluster encodes transmembrane glycoproteins with extracellular Ig-like domains and cytoplasmic tails with immunoreceptor tyrosine-based activating (ITAM), switch (ITSM) and/or inhibitory (ITIM) motifs (Davis *et al.*, 2002) (Figure 7.1). The cytoplasmic properties of FcRLs are complex. The cytoplasmic tail of most FcRLs possess both ITAM-like and ITIM elements. The possession of these intracellular sequences indicates that most of these molecules may be capable of exerting a dual modulation. However, the exact mechanism of how their dual-regulation modulates TLR versus BCR activation of B cells and impacts innate and adaptive immune responses still needs to be explored (Kochi *et al.*, 2009; Sohn *et al.*, 2011). Moreover, expression of FcRLs have been implicated to have potential roles in certain diseases. Several FcRLs have been found upregulated among lymphocyte populations in individuals with chronic viral diseases (Moir *et al.*, 2008) as well as in patients with combined variable immunodeficiency (CVID) (Rakhmanov *et al.*, 2009). Furthermore, disease risk associations for single nucleotide polymorphisms (SNP) located in regions of FcRLs genes have arisen in a variety of disorders (Kochi *et al.*, 2005).

In light of the fact that my supervisor at the University of Birmingham, Professor Dagmar Scheel-Toellner, works on FcRL4+ B cells from RA joints, I decided to focus on one of the others FcRLs and further investigate its potential role in B cell function. Out of the remaining FcRLs that are highly expressed on ABCs I chose to investigate the role of FcRL3 due to the implication that a certain FcRL3 polymorphism acts as a risk factor in RA (Lin *et al.*, 2016). Additionally, previous work published by our group, which reinforces the suggestion that FcRL3 polymorphisms may be risk factors for RA, identified both a methylation and an expression quantitative trait locus (mQTL and eQTL, respectively) in the FcRL3 region on B cells and T cells from patients with RA (Clark *et al.*, 2020).

FcRL3 highest expression is found on memory B cells in the periphery and it marks a circulating innate-like marginal zone (MZ) B cell equivalent (Li *et al.*, 2013). However, FcRL3 is also expressed outside the B cell lineage by subpopulations of cytotoxic NK and CD8+ T cells as well as a dysfunctional population of CD4+ regulatory T cells (Nagata *et al.*, 2009). It has already been reported that FcRL3 engagement augmented TLR9 triggered blood B cell proliferation, survival, and induction of activation markers, in addition to inhibiting Ig production and halting the differentiation of antibody-secreting cells (Li *et al.*, 2013). To expand on this work, I aimed to further investigate the role of FcRL3 on B cell function.

In order to achieve this aim, I created a Ramos B cell line overexpressing FcRL3 to aid in the exploration of B cell function, as well as provide a tool that could aid in the identification of a ligand for FcRL3.

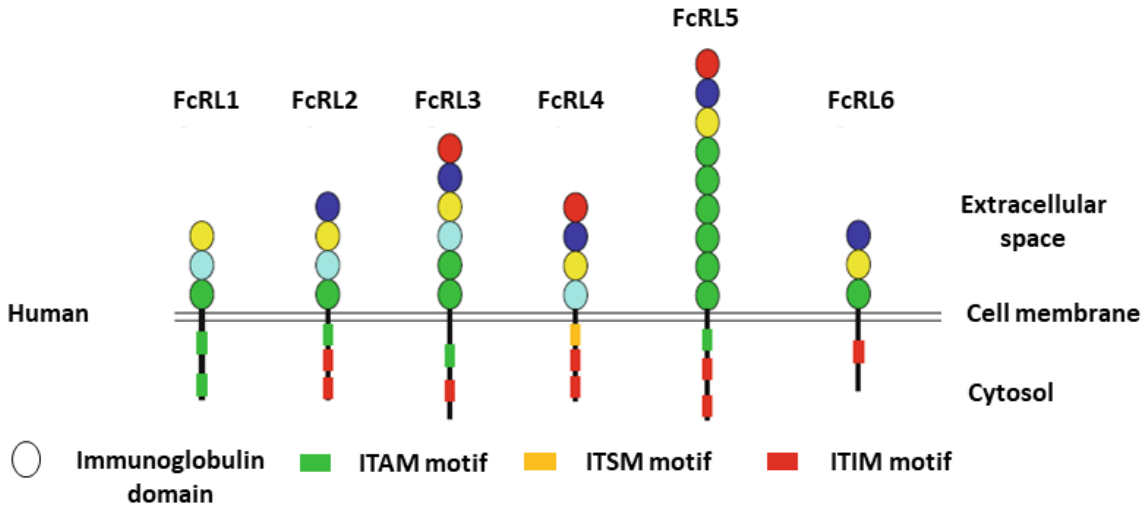

Figure 7. 1. Protein structure of the human FcRL family molecules. In the extracellular space, immunoglobulin domains are shown as circles. These are colour-coded to indicate their phylogenetic relationships. FcRL cytoplasmic tails possess consensus sequences for immunoreceptor tyrosine-based activating motifs (ITAM) in red, immunoreceptor tyrosine-based inhibitory motifs (ITIM) in green and immunoreceptor tyrosine-based switch motifs (ITSM) in orange. Adapted from Li *et al.*, 2014.

7.2 Chapter hypothesis and aims

In this section of my project, I addressed the hypothesis that overexpression of FcRL3 has an impact on B cell proliferation, apoptosis susceptibility and cytokine and immunoglobulin production.

Therefore, the aims of this chapter were to:

1. Stably transduced a B cell line to overexpress FcRL3.
2. Explore the potential role for FcRL3 on B cell function.

The specific objectives were:

1. Stably transduce a B cell line, like the Ramos cell line to overexpress FcRL3.
2. Determine if FcRL3 overexpression changes the Ramos cell phenotype.
3. Determine whether FcRL3 overexpression has any effect on cell proliferation.
4. Investigate if FcRL3 overexpression affects apoptosis susceptibility.
5. Determine if FcRL3 overexpression alters the response of Ramos B cells to stimuli.
6. Assess changes in phenotype, cytokine secretion profile and immunoglobulin production of FcRL3 overexpressing B cells after stimulation.

7.3 Results

7.3.1 FcRL3 overexpression in a B cell line using a retroviral approach

In order to further investigate the role of FcRL3 in B cell biology, I wanted to establish a B cell line which overexpresses FcRL3. Because I already had an expression plasmid (pcDNA3) containing the FcRL3 transcript sequence (a kind gift from Professor Nagata, Osaka University, Japan), I first verified that the FcRL3 transcript sequence in the pcDNA3 expression plasmid was the correct sequence (see Appendix A.5 for sequence BLAST against the reference gene). The sequence in the plasmid was identical to the reference sequence.

Next, two B cell lines were chosen to overexpress FcRL3: Ramos B cells, and Raji B cells. Both B cell lines come from a Burkitt's lymphoma, but Ramos are EBV negative, whereas Raji B cells are EBV positive. The approach used to transfect the cell lines was electroporation using the Neon Kit (Thermo Fisher). The pcDNA3 plasmid contained a neomycin resistance gene, confirming resistance to the G-418 antibiotic to successfully transfected cells. I cultured the transfected cells in culture medium containing G-418 to select only the cells containing the plasmid. Transfection efficacy was checked via flow cytometry using an FcRL3 antibody. Figure 7.2 shows transfection efficiency in the Ramos cells (Figure 7.2.A) and the Raji cells (Figure 7.2.B). For both cell lines, the transfection efficiency was low as the percentage of FcRL3 positive cells at day 3 after selection were less than 1%. Selection with the concentration of G-418 used did not kill the non-transfected cells and, therefore did not select for the transfected cells because the percentage of FcRL3 positive cells did not increase at day 9 or day 18. In Ramos B cells, there was a small increase at day 12 to 14, however the expression was lost in the following days of culture. Due to the fact that the Raji cell line was prone to apoptosis following the transfection procedure (data not shown), and also seemed to have low endogenous expression of FcRL3, I decided that only the Ramos cell line would be used for future overexpression experiments.

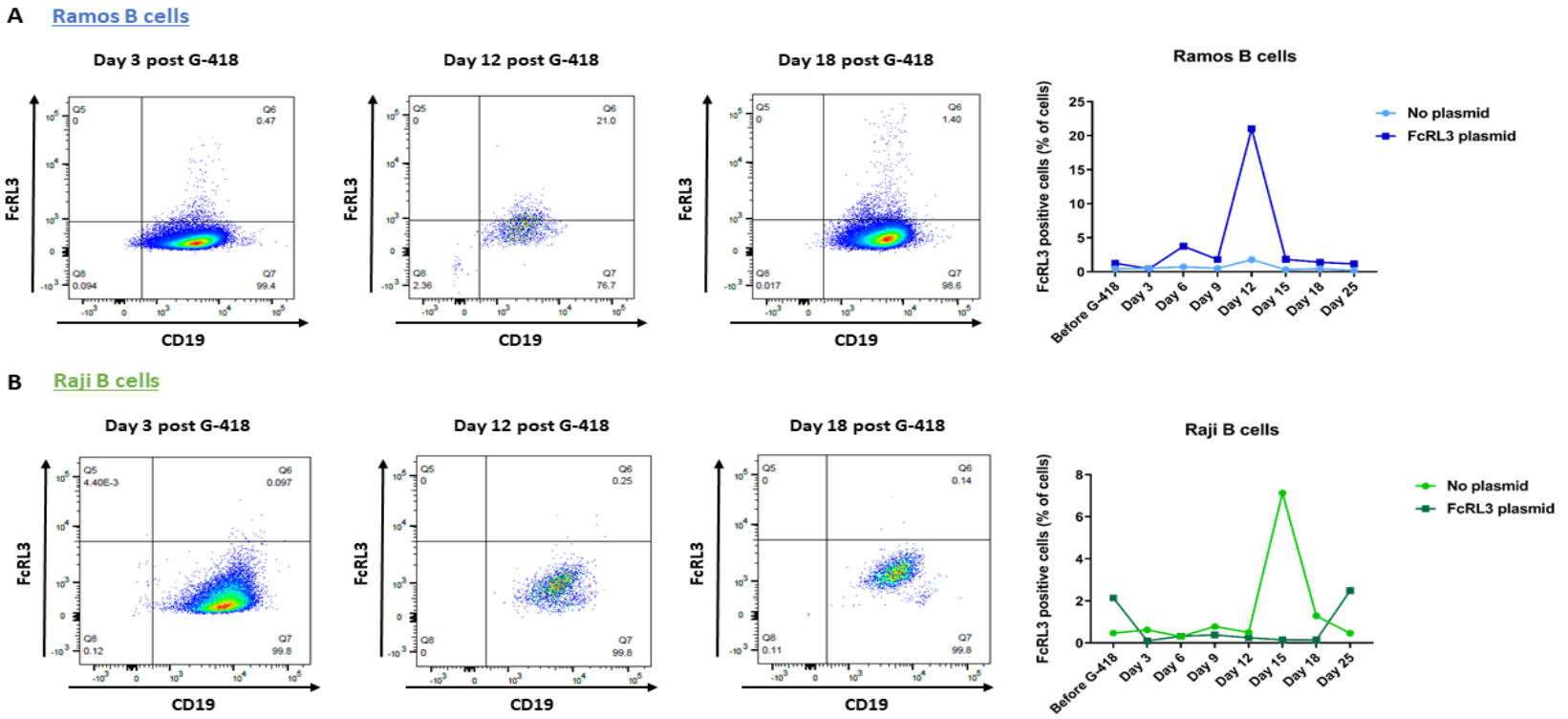

Figure 7. 2. The transfection efficacy of Ramos cells and Rajis cells using electroporation. 2x10^5 Ramos or Raji cells were transfected with a pcDNA3 expression plasmid (at a concentration of 3µg/µl) containing the FcRL3 transcript sequence using the Neon electroporator. After resting the cells for 3 days, the transfected cells were cultured in medium containing G-418 (at a concentration of 600µg/ml). **A.** FcLR3 expression check by flow cytometry of transfected Ramos B cells at day 3, day 12 and day 18 post antibiotic selection. Firstly, dead cells and doublets were excluded and from the cell population, FcRL3 was gated against CD19. Gates were set based on the cells transfected with no plasmid. The graph on the right shows the percentage of FcRL3 positive cells over time in transfected and untransfected cells in Ramos B cells. **B.** FcRL3 expression assessment using flow cytometry on transfected Raji B cells at day 3, day 12 and day 18 post antibiotic selection. As in A, FcRL3 expression was gated against a B cell marker CD19 after excluding dead and doublet cells. Gates were set based on the cells transfected with no plasmid. The graph on the right shows the percentage of FcRL3 positive cells over time in transfected and untransfected Raji cells.

Because electroporation did not work and I could not establish a stably transfected cell line, I decided to try another approach to transfect the cells. Previously in our group, a protocol to transfect Jurkat T cells using a retroviral approach was optimised. In order to create retroviral particles which carried the expression plasmid for FcRL3, I had to clone the FcRL3 gene into the retroviral plasmid pIG (Puro IRES GFP, kind gift from Dr Carmody, Glasgow University, UK). Through the IRES sequence this plasmid enables the expression of the protein of interest (FcRL3), along with expression of GFP as a separate protein product. The plasmid also contains a puromycin resistance gene, allowing for cell selection to create stably transfected cell lines.

A forward and a reverse primer were designed to incorporate restriction enzyme sites, Xho I and Hpa I contained within the pIG plasmid, at the 5' and 3' end of the FcRL3 transcript sequence, respectively (see Chapter 2 methods section 2.8.5 for primers sequence). First, the FcRL3 gene was amplified from the pcDNA3 plasmid (data not shown) and purified from the agarose gel. The gene was then restriction enzyme digested with Xho I and Hpa I, alongside the pIG plasmid to linearise it and create the sticky ends that would allow the gene to be ligated into the plasmid. The digestion products for both the plasmid and FcRL3 gene are shown in Figure 7.3.A. The bands marked by the squares were cut and purified from the agarose gel and then used in a ligation assay with the DNA ligase T4 enzyme. The ligation assay product was then used to transform *E. coli* bacteria which was then cultured on an ampicillin containing agar plate. From the colonies that grew overnight (data not shown), 12 were picked and the plasmid was extracted using a MiniPrep Kit. Purified plasmids from each colony were restriction enzyme digested with Xho I and Hpa I and ran on a gel (Figure 7.3.B). Only one colony, number 8 (the gel image for colonies 1 to 6 not shown) showed two bands which had the expected size for the FcRL3 gene (2,225 bp) and the pIG plasmid backbone (7,649 bp), therefore, colony 8 was transformed with the correct plasmid containing the gene. However, to make sure that the FcRL3 transcript sequence was the correct one and did not contain any mutations, I sent the plasmid for sequencing of the FcRL3 transcript (see Appendix A.6 for sequence BLAST against the reference). The sequence in the plasmid was identical to the reference sequence.

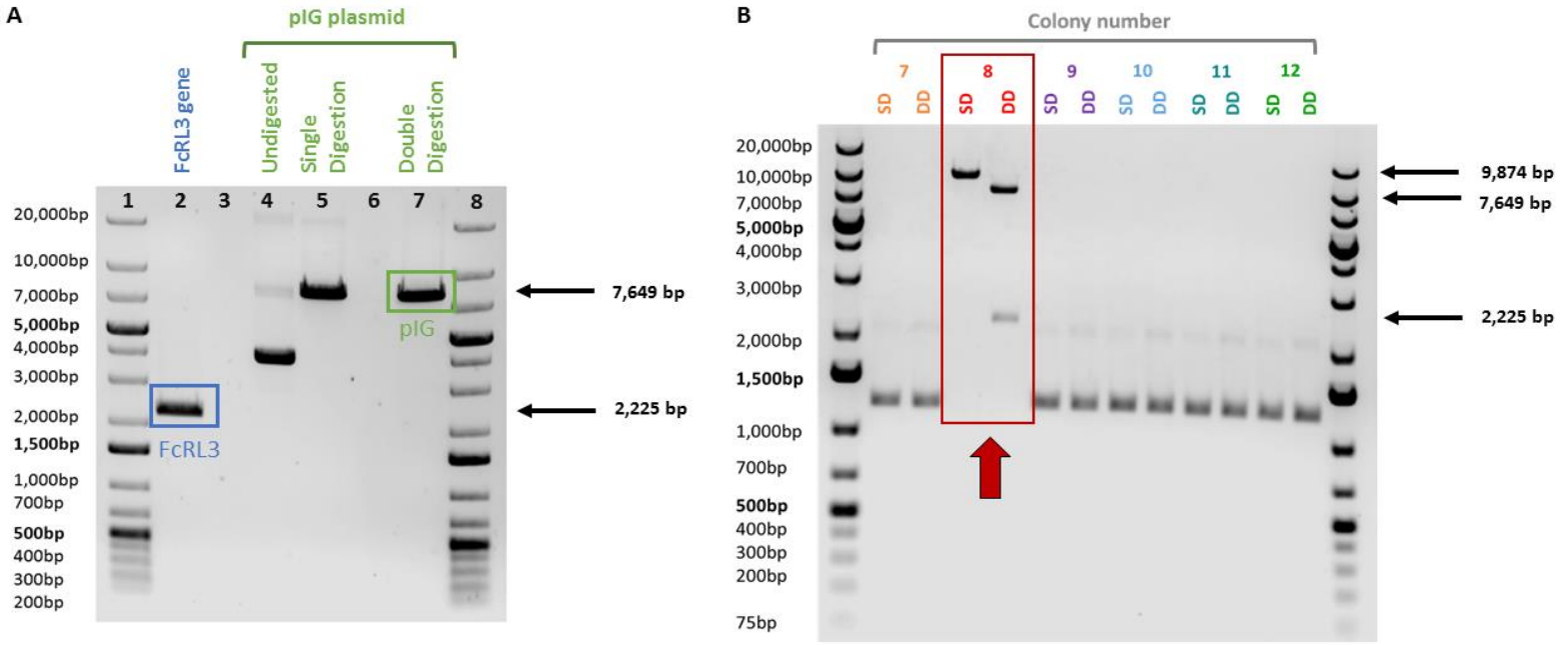

Figure 7. 3. Restriction enzyme digestion products for cloning of FcRL3 into the retroviral plasmid pIG. A. FcRL3 was PCR amplified from the pcDNA plasmid using primers to incorporate an Xho I site at the 5' end of the product and an Hpa I site at the 3' end of the product. Both amplified FcRL3 product and the pIG plasmid were restricted enzyme digested with Xho I and Hpa I and the resultant digests were ran on an agarose gel. Lane 1 and 8 show the DNA size ladder. In lane 2, in blue, the FcRL3 product (expected size of 2,225 bp). Lane 3 is empty. The plasmid was loaded in the lanes marked in green. Different controls were used; one undigested plasmid (lane 4) and a single digested plasmid (lane 5) and double digested plasmid (lane 7) both with an expected size of ~7,649 bp (as the two restriction enzyme sites are only separated by 8 bp in the plasmid). **B.** Plasmids from 12 different transformed *E.coli* colonies were digested with both the restriction enzymes, Xho I and Hpa I, to check that the FcRL3 was successfully ligated in the plasmid. The resultant digestions were run on an agarose gel. The first and last lanes show the DNA ladders. For each colony, labelled with numbers, a single digestion (SD) and a double digestion (DD) were loaded in the gel. Colony number 8 was the only one with the expected size for the plasmid; for the single digestion 9,874 bp was expected and for the double digestion two bands were expected, one corresponding to the plasmid backbone (7,649 bp) and the other one corresponding to the FcRL3 gene (2,225 bp).

After making sure that the plasmid contained the correct sequence of the FcRL3 transcript, I proceeded to the generation of the retroviral particles. In order to create the retroviral particles, I transfected HEK293T cells, a highly transfectable derivate of the human embryonic kidney 293 cell line, with the three plasmids: pIG-FcRL3, pCGP (coding Gag-Pol) and VSVG (coding the vesicular stomatitis glycoprotein) using Lipofectamine (Thermo Fisher). These last two plasmids are translated into protein and the cells then produce retroviral particles containing the pIG-FcRL3 plasmid. The retroviral particles are released by the cells into the culture supernatant. I collected the culture supernatant and added them to the Ramos cells. As a control I also generated retroviral particles containing an empty pIG plasmid. This should result in the overexpression of GFP but no expression of FcRL3 in the successfully transduced cells. These cells will also be puromycin resistant, and were used as a control as they had been through the same transduction process as the FcRL3 overexpressing cells.

As the successful transduction of the pIG plasmid leads to expression of GFP, transfection efficiency of the Ramos cells was assessed by analysis of GFP fluorescence by fluorescent microscopy and flow cytometry. The expression of FcRL3 was also assessed by flow cytometry using an anti-FcRL3 antibody. Transfected cells were selected using the antibiotic puromycin. 8 days after the addition of puromycin, as expected, untransduced Ramos cells (wild type) were double negative (GFP- FcRL3-), Ramos cells transfected with the empty pIG plasmid (termed Ramos GFP control cells) were only positive for GFP (GFP+ FcRL3-), whereas about 50% of the Ramos cells transfected with the FcRL3 plasmid (termed Ramos FcRL3+ cells) were double positive for FcRL3 and GFP (GFP+ FcRL3+), with the other 50% of cells only expressing GFP (GFP+ FcRL3-) (Figure 7.4.A). The fluorescent microscopy image in Figure 7.4.B shows that the Ramos FcRL3+ cells express GFP although some are brighter than others, as confirmed by flow cytometry. Figure 7.4.C shows the change in FcRL3 and GFP expression in the Ramos FcRL3+ cells over time. Because the percentage of double positive cells seemed to decrease over time, possibly due to overgrowth of the culture by the cells only expressing GFP, I decided to flow cytometry sort the different populations to try and enrich for the double positive cells (GFP+ FcRL3+).

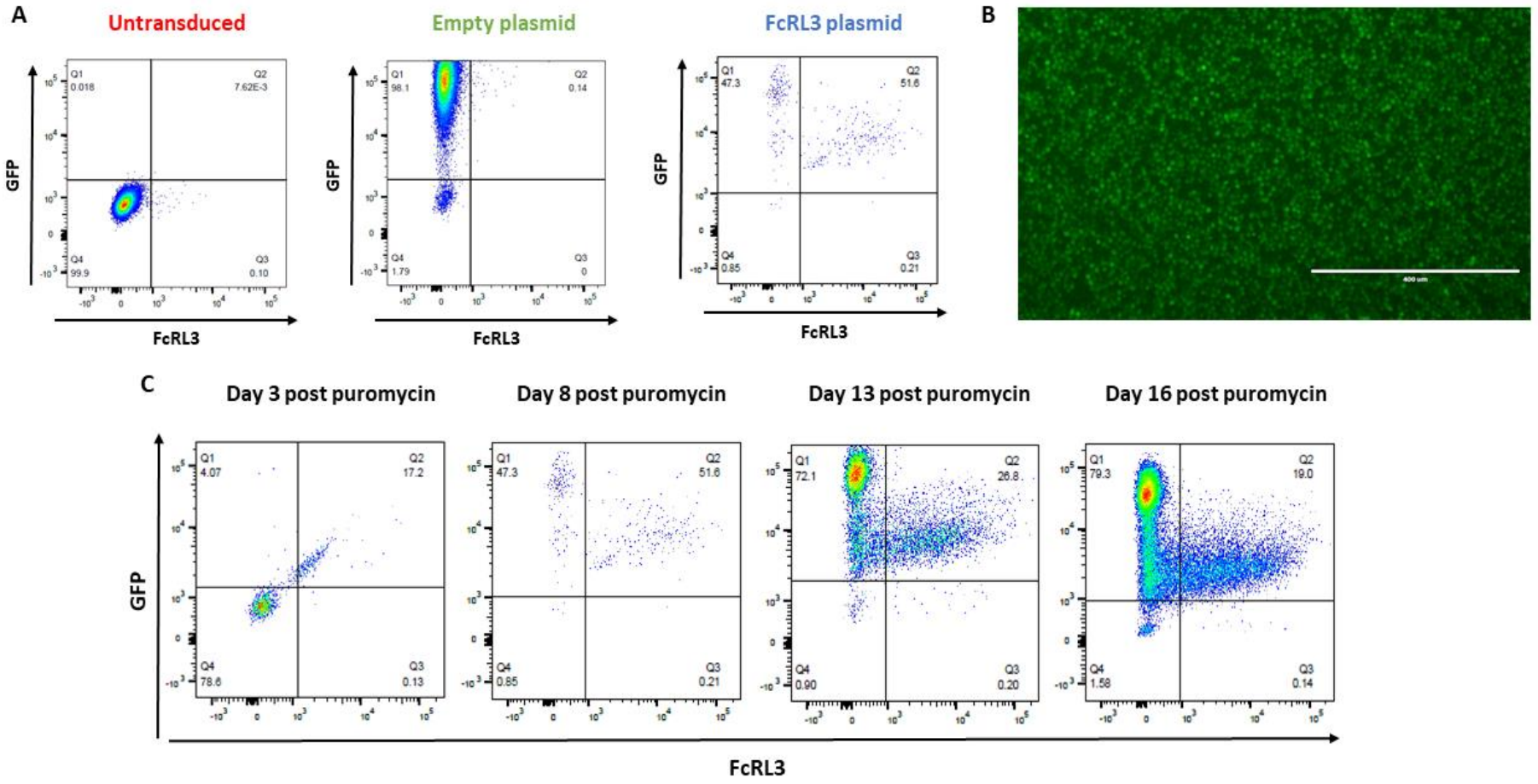

Figure legend in the next page

Figure 7. 4. Retroviral transduction efficacy in Ramos B cells was assessed using flow cytometry and fluorescence microscopy. $5x10^5$ Ramos B cells were either left untransduced (wild type) or were transduced with a HEK293T cell culture supernatant (various volumes: 250µl, 500µl, 750µl and 1000µl) containing retroviral particles expressing an FcRL3 plasmid (Ramos FcRL3+ cells), or as a control, an empty plasmid (Ramos GFP control cells). Both plasmids will lead to expression of GFP and puromycin resistance but only the FcRL3 plasmid will lead to FcRL3 expression. After resting the cells for 3 days the transduced cells were cultured in medium containing puromycin at 1µg/ml. **A.** Transduction efficacy at day 8 post puromycin selection was checked by flow cytometry after staining cells with an anti-FcRL3 antibody and a viability dye. Dead cells and doublets were excluded, and from the alive cell gate, GFP was gated against FcRL3. Gates were set based on the untransduced cells. In red, gating of untransduced cells (wild type), in green empty plasmid transduced cells (Ramos GFP control), and in blue the gating for the FcRL3 plasmid transduced (Ramos FcRL3+ cells) is shown. **B.** Ramos FcRL3+ cells seen under the fluorescence microscope. Image from day 16 post transfection using the 10x objective. **C.** Ramos FcRL3+ cells were assessed for expression of both GFP and FcRL3 over time after the addition of the selection antibiotic puromycin. Dead cells and doublets were excluded, and from the alive cell gate, GFP was gated against FcRL3. Gate based on untransduced cells.

The gating strategy used to sort the transduced Ramos cells is shown in Figure 7.5.A. Three populations were sorted: GFP bright cells (GFP bright FcRL3-), GFP intermediate cells (GFP+ FcRL3-) and double positive cells (FcRL3+ GFP+). Figure 7.5.B shows the sorted populations 12 days after sorting. Some of the GFP intermediate cells seem to become double positive, whereas GFP bright cells stayed only positive for GFP. The FcRL3+GFP+ Ramos cells kept expression of both GFP and FcRL3 (Figure 7.5. B).

Expression of both GFP and FcRL3 was also checked at a later time point (60 days after sorting), and the Ramos cells appear to have stable expression of both GFP and FcRL3 (Figure 7.6.A). The Ramos GFP control cells also had stable expression of only GFP (Figure 7.6.B).

FcRL3 expression in untransduced Ramos cells (wild type), Ramos GFP control cells, and sorted Ramos FcRL3+ cells was also assessed by TaqMan qPCR to confirm overexpression at the gene level (Figure 7.6.C). Normalised expression as compared to wild type cells shows high expression of FcRL3 mRNA by the Ramos FcRL3+ cells (about 150 times more than the wild type), whereas Ramos GFP control cells transfected with the empty plasmid have no expression of FcRL3, similar to the wild type cells.

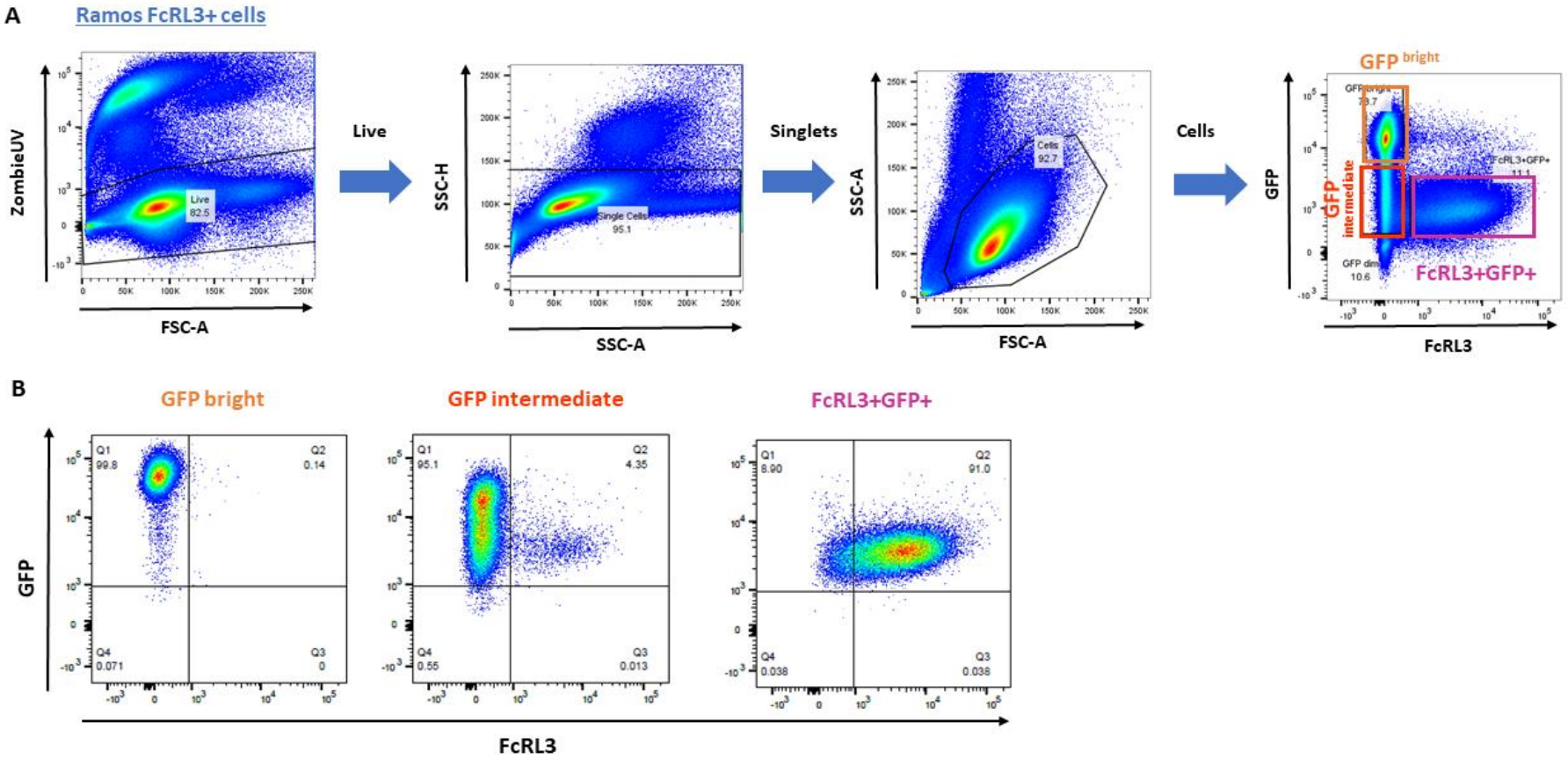

Figure 7. 5. The gating strategy used to sort the FcRL3 transduced Ramos cells and the FcRL3 expression check after sorting. A. Dead cells and doublets were excluded. Alive cells were gated using the SSC-A against the FSC-A. From the cells gate, GFP expression was plotted against FcRL3 expression and three population were gated and sorted: GFP bright cells (GFP bright FcRL3-), GFP intermediate cells (GFP+ FcRL3-) and double positive cells (FcRL3+ GFP+). **B.** GFP and FcRL3 expression was assessed 12 days after of the sort by flow cytometry for each of the sorted subsets. The plots shown are gated cells after excluding dead cells and doublets. Gates were set from the untransduced Ramos cells.

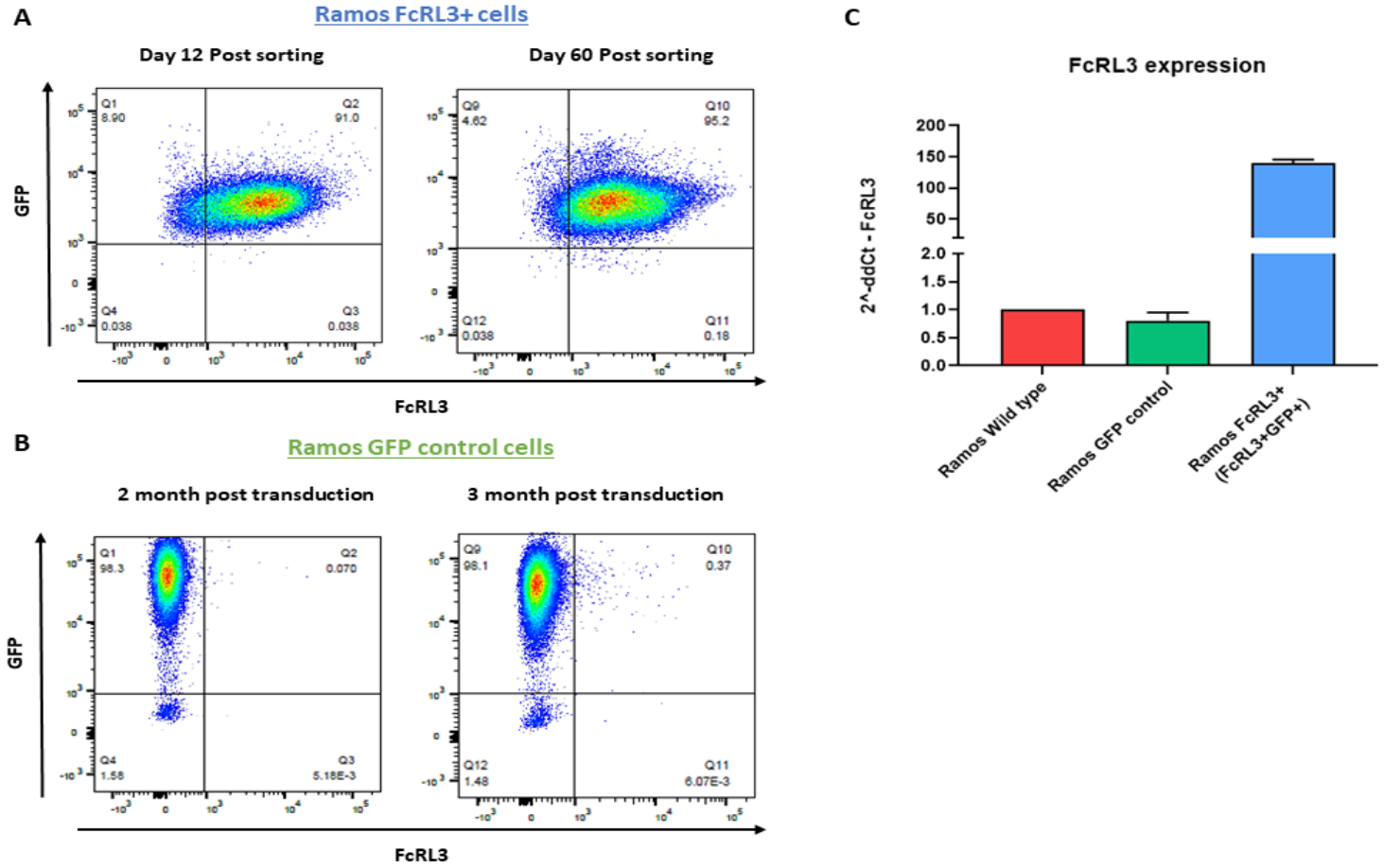

Figure 7. 6. GFP and FcRL3 expression in the double positive (GFP+ FcRL3+) sorted Ramos cells. A-B. GFP and FcRL3 expression check on double positive (GFP+ FcRL3+) sorted Ramos FcRL3+ cells (A) and GFP control transduced Ramos B cells (B), 12 and 60 days after sorting as assessed by flow cytometry following staining with an anti-FcRL3 antibody. The plots shown are gated cells after excluding dead cells and doublets. Gates were set from the untransduced Ramos cells. **C.** FcRL3 gene expression was checked using TaqMan qPCR. Wells were run in duplicate and normalised to the housekeeping gene, POLR2A, followed by normalisation to the wild type cells.

7.3.2 FcRL3 overexpression does not influence the phenotype of Ramos cells

After I had generated a stable Ramos cell line that overexpressed FcRL3 (Ramos FcRL3+ cells), as well as a stable GFP control cell line (Ramos GFP control cells), I firstly wanted to assess if expression of FcRL3 in the transduced cells had an effect on the Ramos phenotype. Therefore, I stained the different cell lines with pre-optimised antibody panels to compare expression of different B cell markers in the Ramos wild type cells, the Ramos GFP control cells, and the Ramos FcRL3+ cells.

Figure 7.7 shows expression of HLA-DR, co-stimulatory molecules and activation markers. In terms of the percentage of the antigen-presenting molecule, HLA-DR, there was variation in expression as not all the cells were positive for this marker (Figure 7.7.A). Moreover, there was little difference in the expression of HLA-DR between the wild type cells and the two transduced cell lines, although the Ramos GFP control cells appeared to have a bigger variation of HLA-DR expression within the population. All Ramos cell lines were positive for the co-stimulatory molecule, CD40, (Figure 7.7.B), and, there was no difference in expression between the different cell lines. Expression of the activation marker, CD69, was low on all the Ramos cell lines, and its expression did not change between the wild type cells and the two transduced cell lines (Figure 7.7.C). All the Ramos cell lines were also positive for the co-stimulatory molecule, CD86, and again, there was no difference in expression between the different cell lines (Figure 7.7.D).

FcRL4 was expressed at very low levels on all the Ramos cell lines (Figure 7.8.A), while none of the Ramos cell lines expressed FcRL5 (Figure 7.8.B). There was no difference in expression of either of these markers between the different Ramos cell lines.

As expected for a cell line, Ki67 was highly expressed in all the Ramos cell lines (Figure 7.9.A), and no difference in Ki67 expression was found between the different cell lines. In addition, all the Ramos cell lines, were negative for the transcription factor T-bet (Figure 7.9. B).

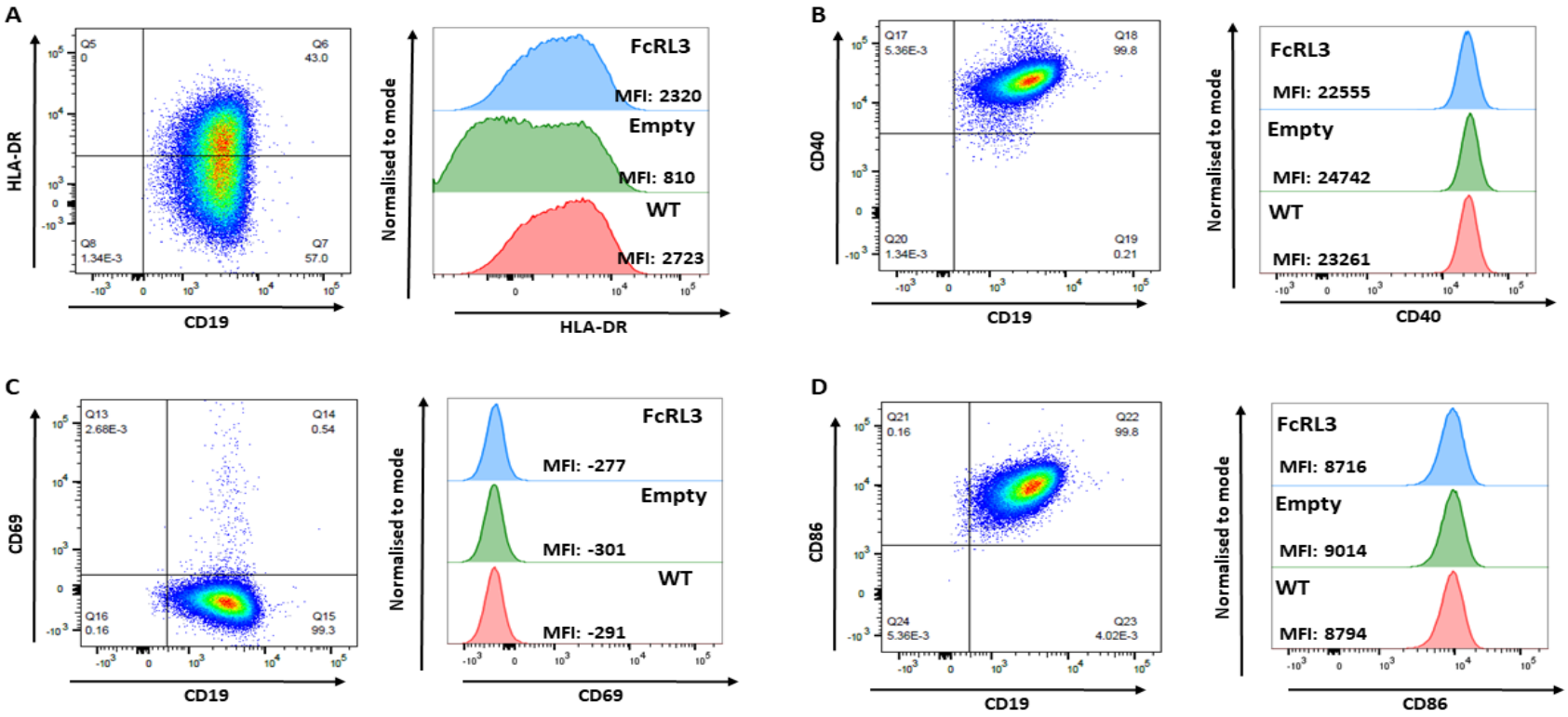

Figure 7. 7. HLA-DR, co-stimulatory molecule and activation marker' expression on Ramos wild type, FcRL3+ cells and GFP control cells. Ramos cell lines were stained with a pre-optimised flow cytometry panel and assessed by flow cytometry. The cells were gated to exclude dead cells and doublets. Gates were set using the unstained cells. An exemplar flow cytometry plot showing HLA-DR expression (**A**, left panel), CD40 expression (**B**, left panel), CD69 expression (**C**, left panel) and CD86 expression (**D**, left panel) in Ramos FcRL3+ cells. Overlay histograms for each of the cell lines is shown for HLA-DR expression (**A**, right panel), CD40 expression (**B**, right panel), CD69 expression (**C**, right panel) and CD86 expression (**D**, right panel). For all the overlay histograms, the peaks are normalised to the same height to standardise for different numbers of cells in each population. MFI values are shown in the histograms. Ramos wild type cells are shown in red; Ramos GFP control are shown in green and Ramos FcRL3+ cells are shown in blue.

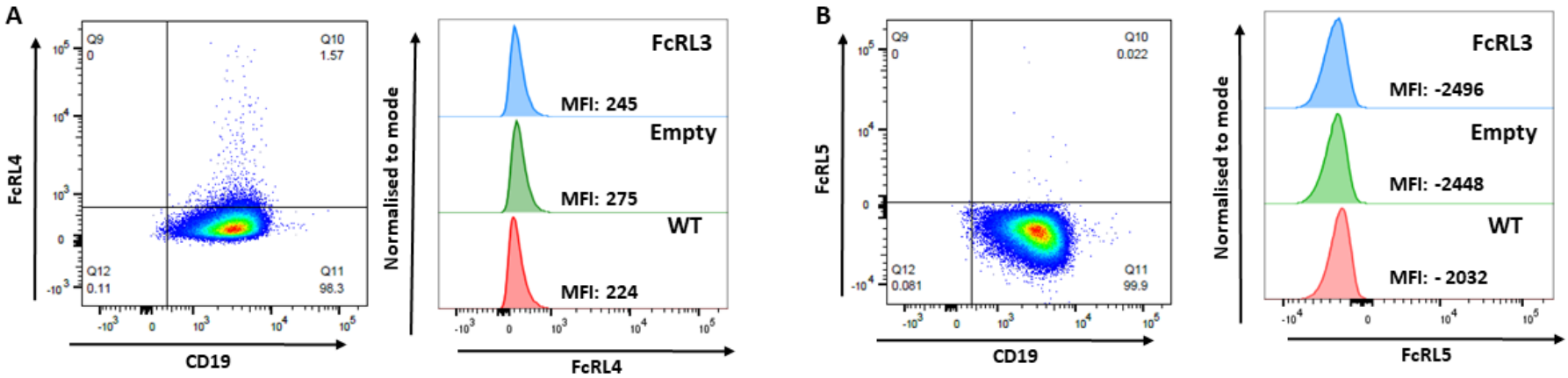

Figure 7. 8. FcRLs expression on Ramos wild type, FcRL3+ cells and GFP control cells. Ramos cell lines were stained with a pre-optimised flow cytometry panel and assessed by flow cytometry. The cells were gated to exclude dead cells and doublets. Gates were set using the unstained cells. An exemplar flow cytometry plot showing FcRL4 expression (**A**, left panel) and FcRL5 expression (**B**, left panel) in Ramos FcRL3+ cells. Overlay histograms for each of the cell lines is shown for FcRL4 expression (**A**, right panel) and FcRL5 expression (**B**, right panel). For all the overlay histograms, the peaks are normalised to the same height to standardise for different numbers of cells in each population. MFI values are shown in the histograms. Ramos wild type cells are shown in red; Ramos GFP control are shown in green and Ramos FcRL3+ cells are shown in blue.

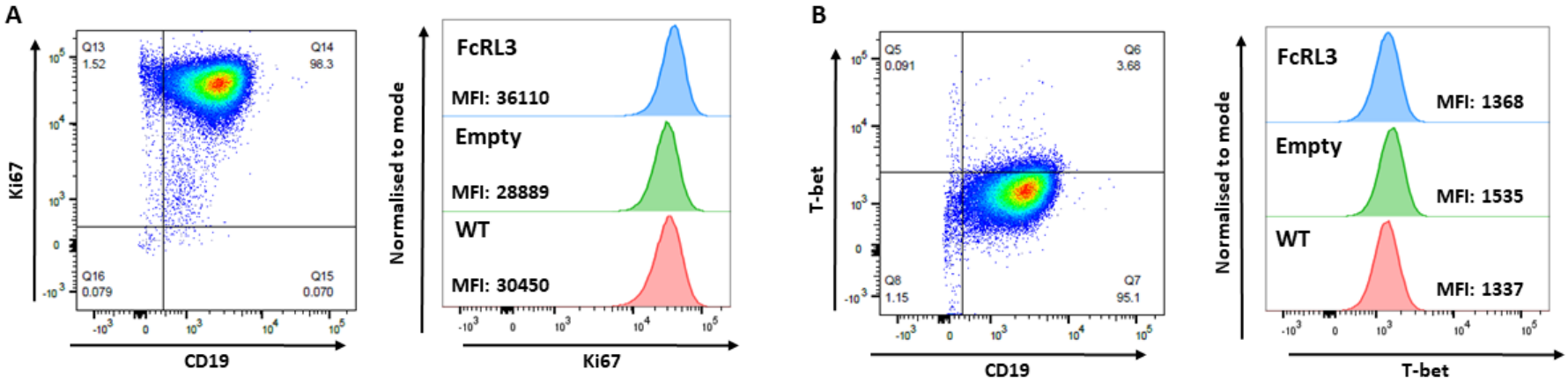

Figure 7. 9. Intracellular markers, Ki67 and T-bet, expression on Ramos wild type, FcRL3+ cells and GFP control cells. Ramos cell lines were stained with a pre-optimised flow cytometry panel and assessed by flow cytometry. The cells were gated to exclude dead cells and doublets. Gates were set using the unstained cells. An exemplar flow cytometry plot showing Ki67 expression (**A**, left panel) and T-bet expression (**B**, left panel) in Ramos FcRL3+ cells. Overlay histograms for each of the cell lines is shown for Ki67 expression (**A**, right panel) and T-bet expression (**B**, right panel). For all the overlay histograms, the peaks are normalised to the same height to standardise for different numbers of cells in each population. MFI values are shown in the histograms. Ramos wild type cells are shown in red; Ramos GFP control are shown in green and Ramos FcRL3+ cells are shown in blue.

As previously reported in the literature (Upton and Unniraman, 2011), Ramos cells were all positive for IgM surface expression and there was no difference between expression in the Ramos wild type cells and both the transduced cell lines (Figure 7.10.A). In terms of IgD expression, all of the Ramos cell lines were negative for this immunoglobulin (Figure 7.10.B). The Ramos cell lines were also negative for the class-switched immunoglobulin, IgG (Figure 7.10.C).

In terms of CD5 expression, none of the Ramos cell lines were found to express this marker (Figure 7.10.D).

I also assessed the B cell lineage markers I used to identify different B cell subsets. CD11c, a marker of ABCs, was expressed at very low levels in all the Ramos cell lines (Figure 7.11.A), and there was no change in expression between the Ramos wild type cells and the two transduced cell lines, although the Ramos GFP control cells appeared to have a small increase in CD11c expression, as measured by the MFI. All the Ramos cell lines were close to 100% positive for the activation markers CD27 and CD97 (Figure 7.11.B-C), and no differences were found between the different cell lines.

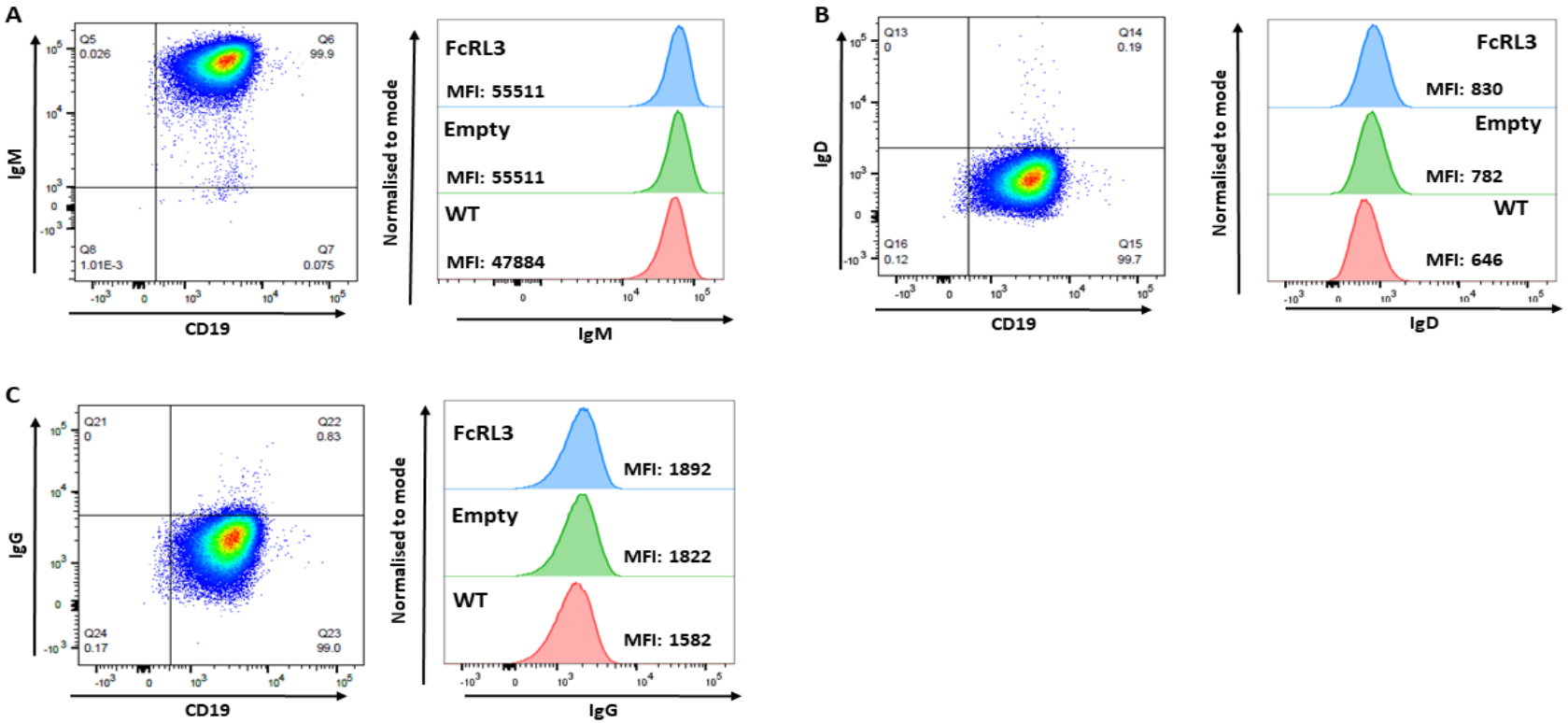

Figure 7. 10. Immunoglobulin expression on Ramos wild type, FcRL3+ cells and GFP control cells. Ramos cell lines were stained with a pre-optimised flow cytometry panel and assessed by flow cytometry. The cells were gated to exclude dead cells and doublets. Gates were set using the unstained cells. An exemplar flow cytometry plot showing IgM expression (**A**, left panel), IgD expression (**B**, left panel) and IgG expression (**C**, left panel) in Ramos FcRL3+ cells. Overlay histograms for each of the cell lines is shown for IgM expression (**A**, right panel), IgD expression (**B**, right panel) and IgG expression (**C**, right panel). For all the overlay histograms, the peaks are normalised to the same height to standardise for different numbers of cells in each population. MFI values are shown in the histograms. Ramos wild type cells are shown in red; Ramos GFP control are shown in green and Ramos FcRL3+ cells are shown in blue.

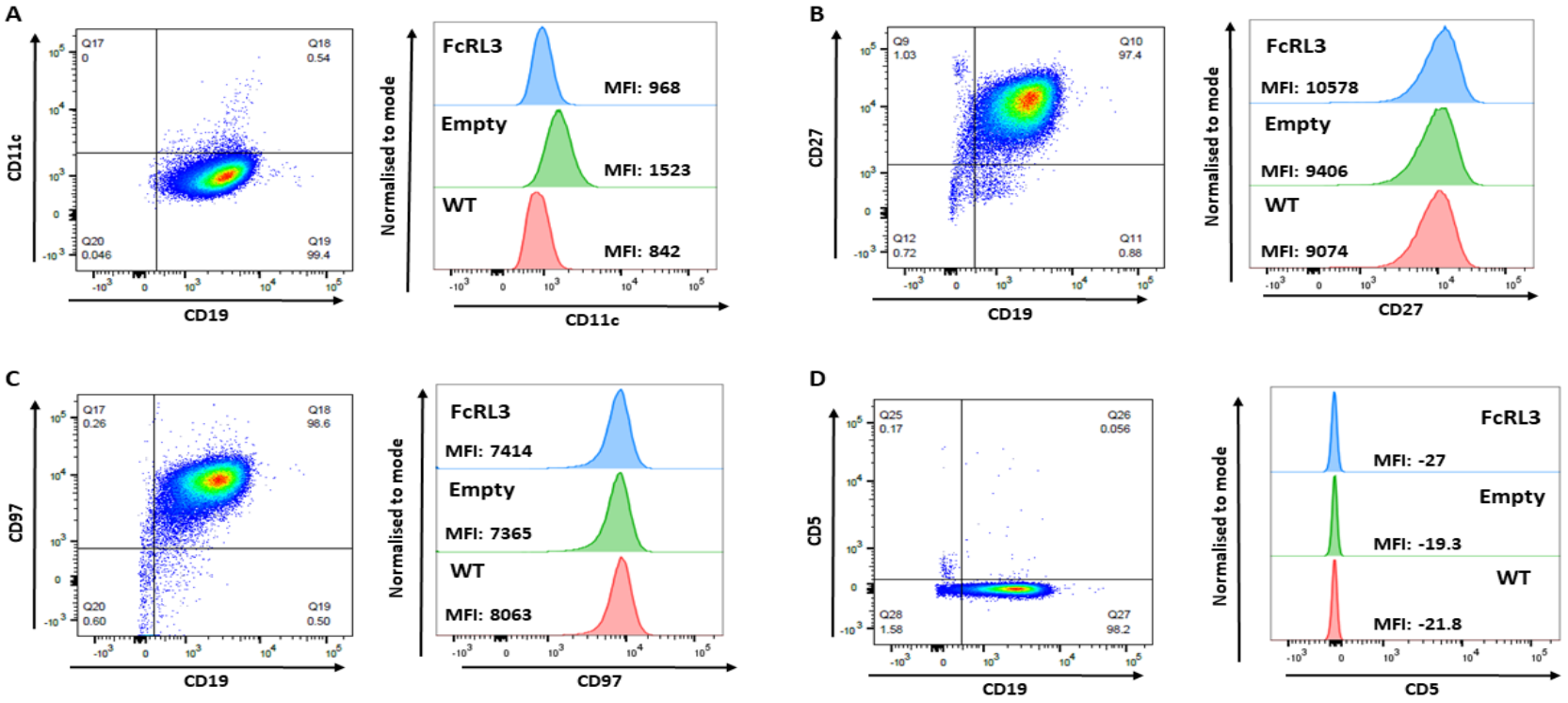

Figure 7. 11. Phenotypic marker's expression on Ramos wild type, FcRL3+ cells and GFP control cells. Ramos cell lines were stained with a pre-optimised flow cytometry panel and assessed by flow cytometry. The cells were gated to exclude dead cells and doublets. Gates were set using the unstained cells. An exemplar flow cytometry plot showing CD11c expression (**A**, left panel), CD27 expression (**B**, left panel), CD97 expression (**C**, left panel) and CD5 expression (**D**, left panel) in Ramos FcRL3+ cells. Overlay histograms for each of the cell lines is shown for CD11c expression (**A**, right panel), CD27 expression (**B**, right panel), CD97 expression (**C**, right panel) and CD5 expression (**D**, right panel). For all the overlay histograms, the peaks are normalised to the same height to standardise for different numbers of cells in each population. MFI values are shown in the histograms. Ramos wild type cells are shown in red; Ramos GFP control are shown in green and Ramos FcRL3+ cells are shown in blue.

7.3.3 Control retroviral transduction increases cell proliferation, whereas FcRL3 overexpression retroviral transduction returns cell proliferation to wild type levels

I assessed cell proliferation using the cell proliferation tracking dye, CellTrace Violet (CTV), to determine whether overexpression of FcRL3 had any effect on cell proliferation and replication. Cells from each of the Ramos cell lines (wild type, GFP control and FcRL3+) were stained with CTV and cultured as normal. At different time points, an aliquot of the cell cultures was removed and the cells were assessed on a flow cytometer to determine CTV dilution, which is indicative of cell proliferation.

Interestingly, the Ramos GFP control cells had a much higher proliferative rate after 12, 24 and 76 hours as compared to the Ramos FcRL3+ cells and Ramos wild type cells (Figure 7.12.A-C). There was no clear difference in the proliferative rate of the Ramos FcRL3+ cells compared to the Ramos wild type cells at these time point. By day 5, most of the cells from all the Ramos cell lines were dim for CTV, indicating that the majority of the cells had undergone multiple rounds of proliferation (Figure 7.12.D).

The Ramos GFP control cells had a higher proliferative rate over time compared to the Ramos FcRL3+ cells and Ramos wild type cells (Figure 7.12.E). However, FcRL3+ Ramos cells had a cell proliferation rate similar to the Ramos wild type cells (Figure 7.12.E).

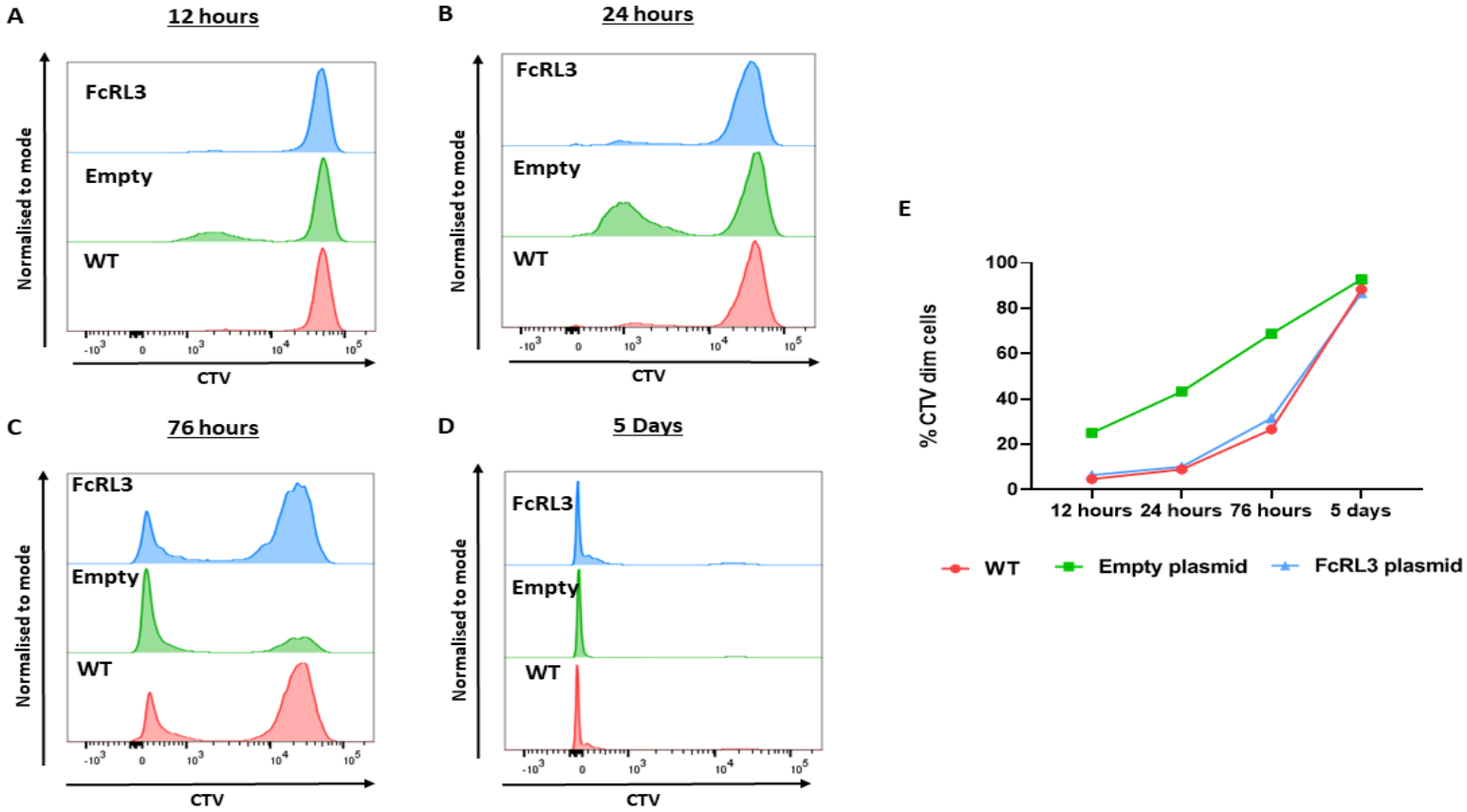

Figure 7. 12. Cell proliferation of Ramos FcRL3+ cells and control cells. The Ramos cell lines were labelled with CellTrace Violet (CTV) and cultured as normal for 24 hours (**A**), 48 hours (**B**), 72 hours (**C**) and 5 days (**D**). CTV expression overlay histograms are shown with Ramos wild type cells in red, Ramos GFP control cells in green and Ramos FcRL3+ cells in blue. The cells were gated to exclude dead cells and doublets. For all the overlay histograms, the peaks are normalised to the same height to standardise for different numbers of cells in each population. **E.** Percentage of divided cells (CTV dim or negative) in the four time points. Ramos wild type cells are shown in red, Ramos GFP control cells are shown in green and Ramos FcRL3+ cells are shown in blue. N = 1.

7.3.4 FcRL3 overexpression increases the susceptibility of Ramos cells to Fas ligand-induced apoptosis

Evidence from the literature suggests that FcRL3+ Tregs might be predisposed to apoptosis due to their high expression of the apoptosis-inducing marker CD95/Fas (Swainson *et al.*, 2010). I decided to investigate whether FcRL3 overexpression had an effect on apoptosis susceptibility in the Ramos cell lines. Cells from each of the Ramos cell lines were incubated without or with different concentrations of an anti-CD95 antibody for 24 hours. Cell death was assessed by flow cytometry using Annexin V and Zombie UV (ZUV) staining. Cells which are only positive for Annexin V (Annexin V+ ZUV-) are in early apoptosis, whereas double positive cells (Annexin V+ ZUV+) are dead.

For the Ramos wild type cell cultures, around 7% of the cells die (are ZUV+ AnnexinV+) without any addition of an anti-CD95 antibody (Figure 7.13.A). However, when the cells were cultured with 100ng/ml of anti-CD95 antibody the percentage of dead cells nearly doubled to 11%. The percentage of early apoptotic cells increases slightly from 1% without anti-CD95 antibody to 1.6% with the anti-CD95 antibody. Similar results were seen for the Ramos GFP control cells, which had 6% dead cells and 1.1% early apoptotic cells without the anti-CD95 antibody and 11% dead cells and 2.3% early apoptotic cells with the anti-CD95 antibody (Figure 7.13.B). Interestingly, the percentage of dead cells in the Ramos FcRL3+ cell cultures without the addition of an anti-CD95 antibody was nearly double that seen in the Ramos GFP control cells and the wild type cells (14% compared to 7% and 6%, respectively) (Figure 7.13.C). The percentage of early apoptotic cells without the addition of anti-CD95 antibody (1.6%) was similar to the Ramos wild type cells and Ramos GFP control cells. When the Ramos FcRL3+ cells are cultured with 100ng/ml of anti-CD95 antibody, the percentage of dead and early apoptotic cells increased considerably to 20% and 3.6% respectably (Figure 7.13.C). Overall Ramos FcRL3+ cells had a higher percentage of early apoptotic cells and dead cells and were more prone to apoptosis both in a resting state and when stimulated via Fas/CD95 than the Ramos wild type cells and the Ramos GFP control cells (Figure 7.14.A-B).

Of general note, Ramos cells appear to be quite resistant to CD95-induced apoptosis as the percentage of dead cells and early apoptotic cells after addition of anti-CD95 antibody was relatively low even after a few days (data not shown).

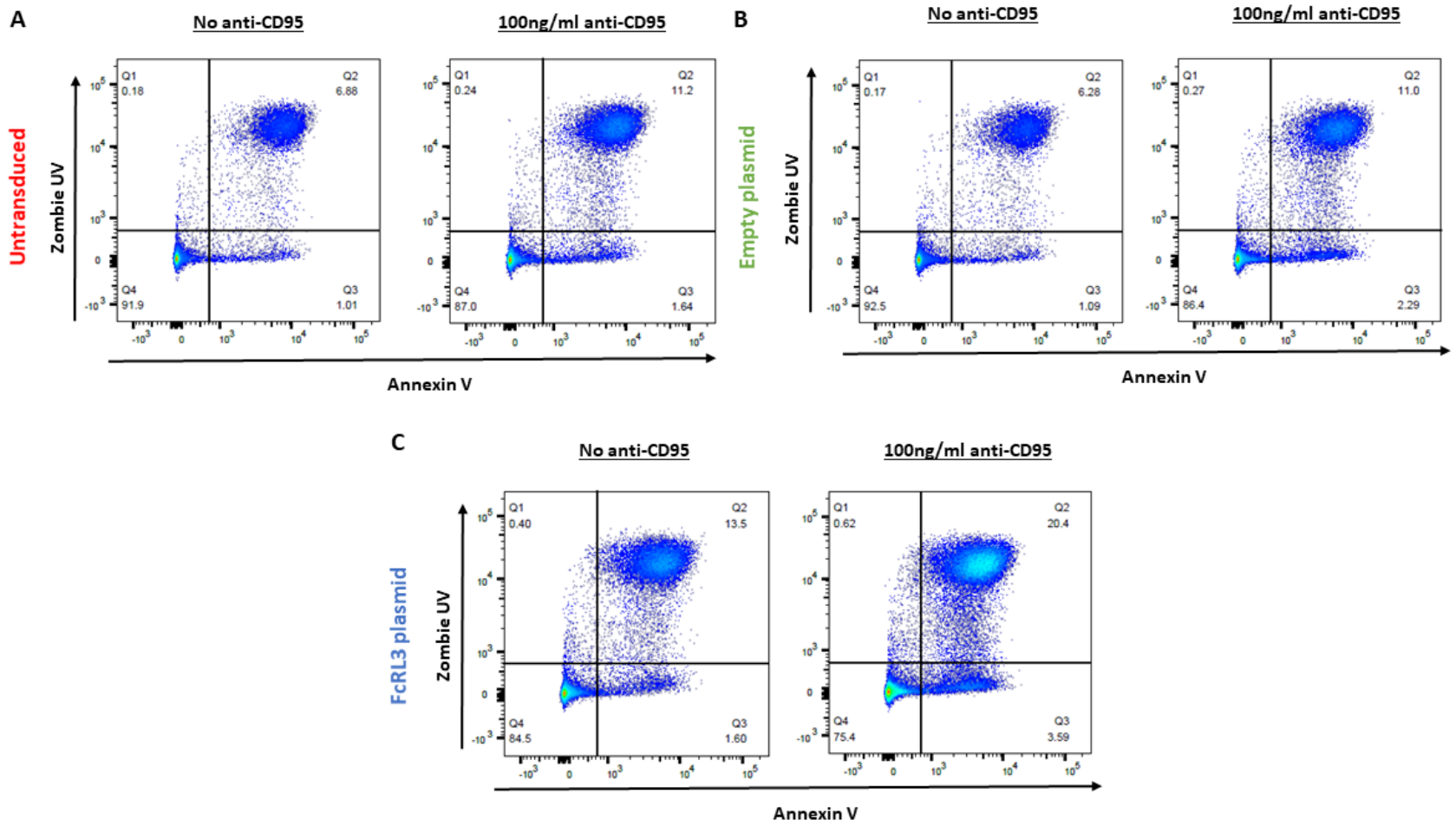

Figure 7. 13. Evaluation of apoptosis induction and cell death following addition of an anti-CD95 antibody to the Ramos cell lines. $1x10^6$ Ramos cell were cultured without or with 100ng/ml anti-CD95 antibody for 24 hours, after which apoptosis and cell death were assessed by flow cytometry. The cells were gated to exclude doublets. An exemplar flow cytometry plot showing Zombie UV against Annexin V in untreated (no anti-CD95 and treated (100ng/ml anti-CD95) in Ramos wild type cells (**A**), Ramos GFP control cells (**B**) and Ramos FcRL3+ cells (**C**). N = 1.

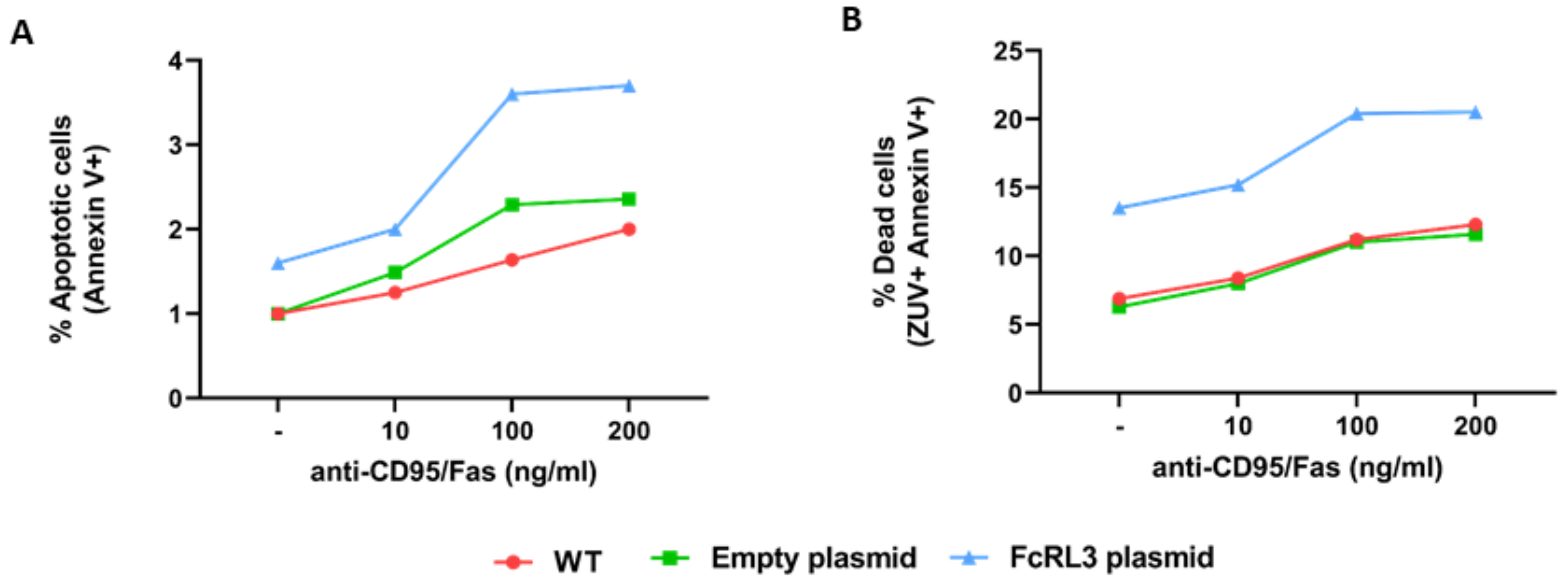

Figure 7. 14. Evaluation of apoptosis induction and cell death following addition of an anti-CD95 antibody to the Ramos cell lines. $1x10^6$ Ramos cell were cultured without or with 100ng/ml anti-CD95 antibody for 24 hours, after which apoptosis and cell death were assessed by flow cytometry. The cells were gated to exclude doublets. **A.** Percentage of early apoptotic cells (Annexin V+ only) using different concentrations of anti-CD95 antibody in the three Ramos cell lines. **B.** Percentage of dead cells (ZUV+ Annexin V+) using different concentrations of anti-CD95 antibody in the three Ramos cell lines. N = 1.

7.3.5 Changes in the phenotype, cytokine secretion profile, and immunoglobulin production of Ramos FcRL3+ cells after B cell stimulation

In order to assess if FcRL3 overexpression alters the Ramos cell response I firstly tested two different stimulation cocktails on Ramos FcRL3+ cells. Stimulation cocktail 1 was the optimised cocktail used for the other B cell stimulation assays using sorted B cell subsets. This stimulation cocktail contained TLR7 ligand Imiquimod, TLR9 agonists ODN 2216 – CpG A and ODN 2006 – CpG B, Poke Weed Mitogen, anti-CD40, human IL-21, human IL-4 and IFN-gamma. Stimulation cocktail 2 contained all the above stimuli but no IL-4. IL-4 was excluded from the stimulation cocktail as it has been shown to inhibit expression of CD11c and T-bet in B cells (Naradikian *et al.*, 2016b). Cells were stimulated for 3 days after which the cell phenotype was assessed by flow cytometry.

Following stimulation with the two different stimulation cocktails there were changes in certain markers with both stimulation conditions (Figure 7.15). There appears to be a slight downregulation in HLA-DR expression (Figure 7.15.A). Although CD86 was already highly expressed in the unstimulated Ramos FcRL3+ cell line, it was slightly increased upon stimulation (Figure 7.15.B). Expression of CD11c was increased (Figure 7.15.C), whereas CD27 expression was decreased with both stimulation cocktails (Figure 7.15.D). IgM appears to be slightly downregulated with both stimulation cocktails (Figure 7.15.E). IgD expression, however, did not change after stimulation (Figure 7.15.F). Even though CD97 expression was high in unstimulated cells, expression of this marker increased after simulation (Figure 7.15.G), as did T-bet (Figure 7.15.H).

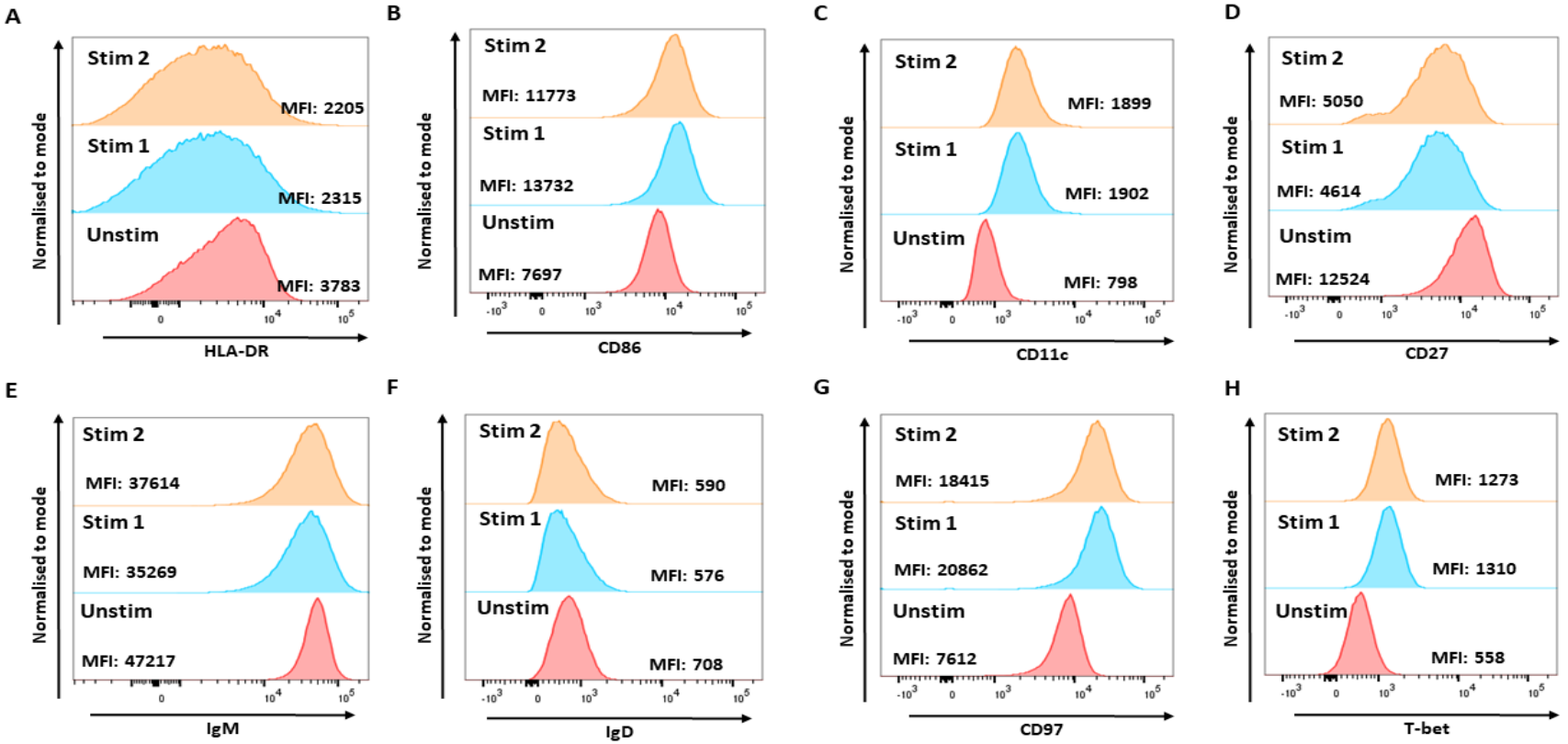

Figure 7. 15. Phenotypic marker expression on unstimulated and stimulated Ramos FcRL3+ cells. $2.5x10^5$ Ramos FcRL3+ cells were left unstimulated or were stimulated with either stimulation cocktail1 (Imiquimod, CpG A and CpG B, PWM, anti-CD40, IL-21, IL-4 and IFN-γ) or stimulation cocktail 2 (Imiquimod, CpG A and CpG B, PWM, anti-CD40, IL-21 and IFN-γ) for 3 days. The cells were then stained with a pre-optimised flow cytometry panel and assessed by flow cytometry. The cells were gated to exclude dead cells and doublets. Flow cytometry overlay histograms are shown displaying unstimulated cells (red), cells stimulated by stimulation cocktail 1 (blue), and cells stimulated by stimulation cocktail 2 (orange) for expression of HLA-DR (**A**), CD86 (**B**), CD11c (**C**), CD27 (**D**), IgM (**E**), IgD (**F**), CD97 (**G**), and T-bet (**H**). For all the overlay histograms, the peaks are normalised to the same height to standardise for different numbers of cells in each population. N = 1.

After testing the two different stimulation cocktails on Ramos FcRL3+ cells I decided to use stimulation cocktail 2 for assessing the phenotype, the cytokine secretion profile and the immunoglobulin production. This cocktail contained TLR7 ligand Imiquimod, TLR9 agonists ODN 2216 – CpG A and ODN 2006 – CpG B, Poke Weed Mitogen, anti-CD40, human IL-21 and IFN-gamma. The different Ramos cell lines were stimulated for 3 days after which the phenotype was assessed by flow cytometry, and culture supernatants were collected for secreted immunoglobulin and cytokine detection.

Figure 7.16 shows expression of the phenotype markers, as displayed in Figure 7.15, comparing Ramos wild type cells, Ramos GFP control cells, and Ramos FcRL3+ cells following stimulation. When the expression profiles of the Ramos wild type cell, Ramos GFP control cells, and Ramos FcRL3+ cells were compared following stimulation there was very little difference between the cell lines for the majority of the markers analysed (Figure 7.16). The only small difference seen was slightly less expression of HLA-DR on the Ramos GFP control and the Ramos FcRL3+ cells compared to the Ramos wild type cells, however, this difference was also seen without stimulation (Figure 7.7.A) so may not be a consequence of stimulation.

In summary, stimulation of the different Ramos cell lines, was not very informative for assessing the effect of FcRL3 overexpression on B cell function. This is possibly due to the fact that in these experiments FcRL3 was not ligated so had little effect on this readout.

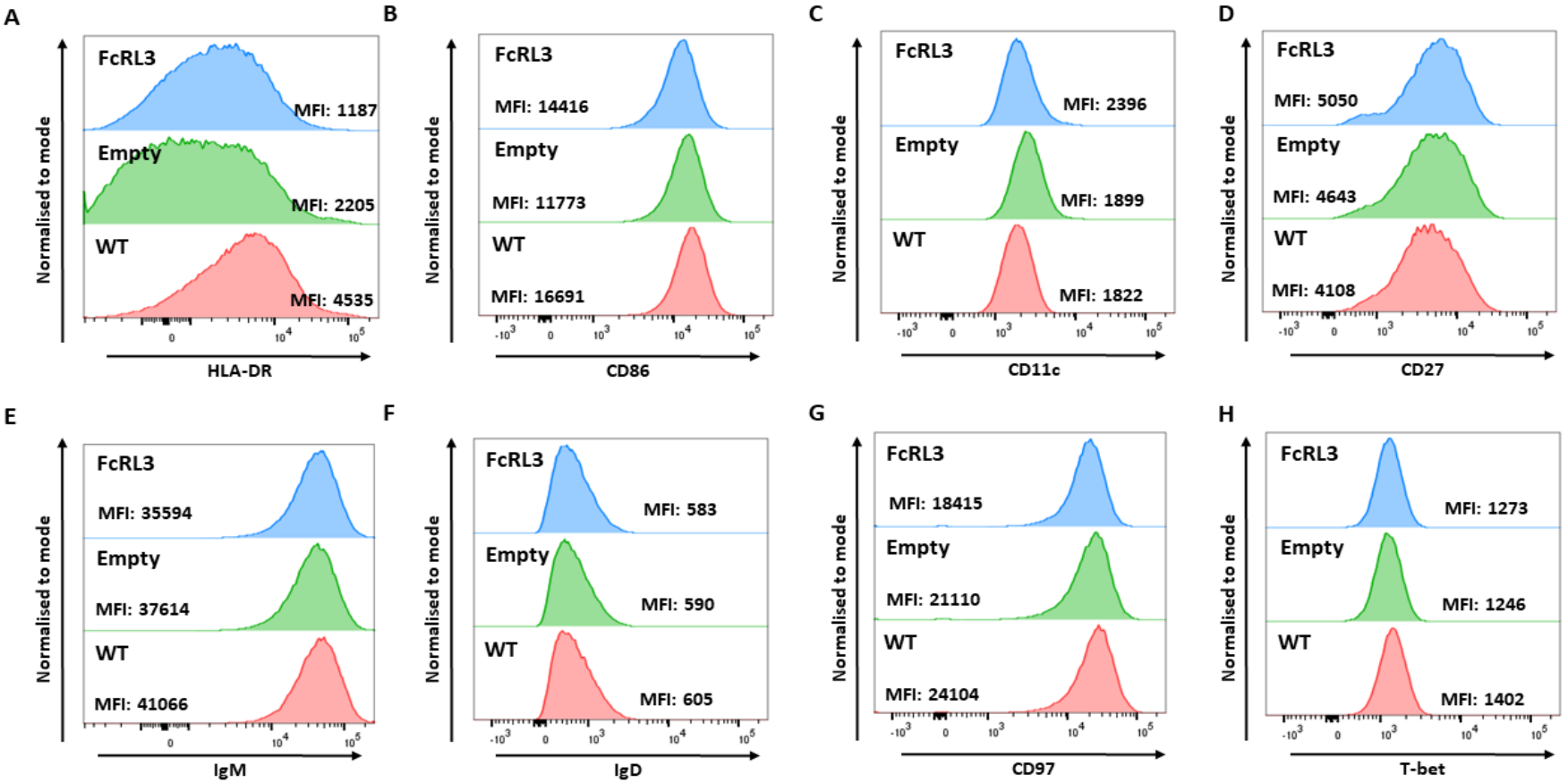

Figure 7. 16. Phenotypic marker expression on stimulated Ramos cell lines. The different Ramos cell lines were stimulated with stimulation cocktail 2 (Imiquimod, CpG A and CpG B, PWM, anti-CD40, IL-21 and IFN-γ) for 3 days. The cells were then stained with a pre-optimised flow cytometry panel and assessed by flow cytometry. The cells were gated to exclude dead cells and doublets. Flow cytometry overlay histograms are shown displaying Ramos wild type cells (red), Ramos GFP control cells (green), and Ramos FcRL3+ cells (blue) for expression of HLA-DR (**A**), CD86 (**B**), CD11c (**C**), CD27 (**D**), IgM (**E**), IgD (**F**), CD97 (**G**), and T-bet (**H**). For all the overlay histograms, the peaks are normalised to the same height to standardise for different numbers of cells in each population. N = 1.

Culture supernatants from the different stimulated Ramos cell lines were used for the detection of secreted immunoglobulins and cytokines. As previously reported in the literature (Benjamin *et al.*, 1982), the Ramos wild type cells were found to spontaneously secrete high levels of IgM (Figure 7.17.A). Stimulation of the cells had no effect on the production of IgM. There were no major differences between the different Ramos cell lines. In terms of IgG secretion, the concentrations detected were very low (Figure 7.17.B), compared to the stimulated primary memory B cells (Chapter 6, Figure 6.30). The amount of IgA produced, similar to IgG, was very low (Figure 7.17.C) when compared to the concentration detected from primary memory B cells (Chapter 6, Figure 6.31). Generally, the Ramos cell lines did not produce IgA, even with stimulation, however, the stimulated Ramos GFP control cells produced a small amount of IgA. Unexpectedly, the unstimulated Ramos wild type cells also produced a small amount of IgA.

Focusing on the cytokines produced by the Ramos cell lines, IL-2 levels were very low (Figure 7.18.A). Interestingly, IL-10 production from the stimulated condition is lower in Ramos FcRL3+ cells compared to the Ramos GFP control and the Ramos wild type cells (Figure 7.18.B). Similar to IL-2, IL-6, IL-23, GM-CSF and TNF-α production was also very low, with no clear differences seen (Figure 7.18.C-F).

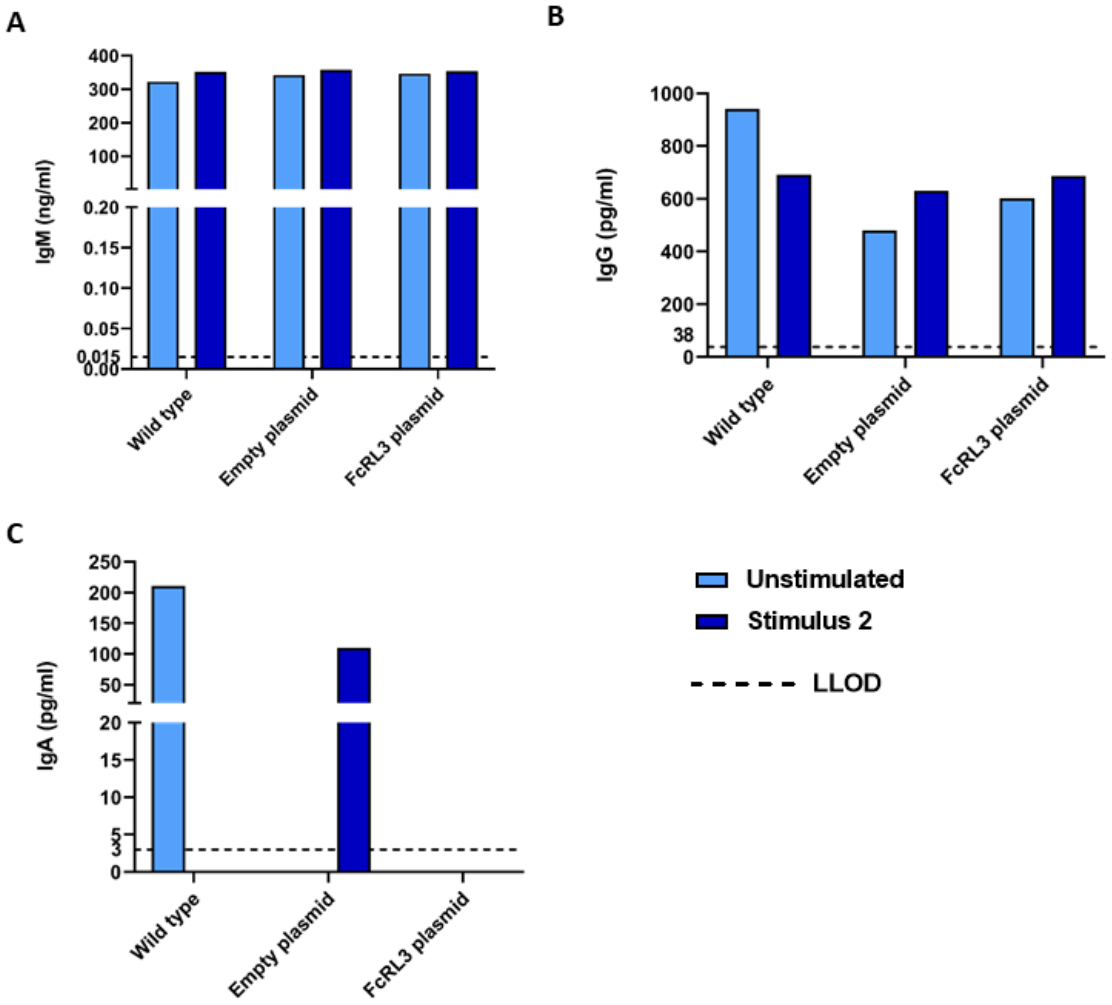

Figure 7. 17. Immunoglobulin production by unstimulated and stimulated Ramos cell lines. The different Ramos cell lines were left unstimulated or were stimulated with stimulation cocktail 2 (Imiquimod, CpG A and CpG B, PWM, anti-CD40, IL-21 and IFN-γ) for 3 days. The culture supernatants were harvested and the concentrations of IgM (**A**), IgG (**B**) and IgA (**C**) were detected using the Isotyping Panel 1 Human Kit from MSD. Unstimulated cells are shown in light blue and cells stimulated with stimulation cocktail 2 are shown in dark blue. The dotted line indicates the lower limit of detection for each immunoglobulin. N = 1.

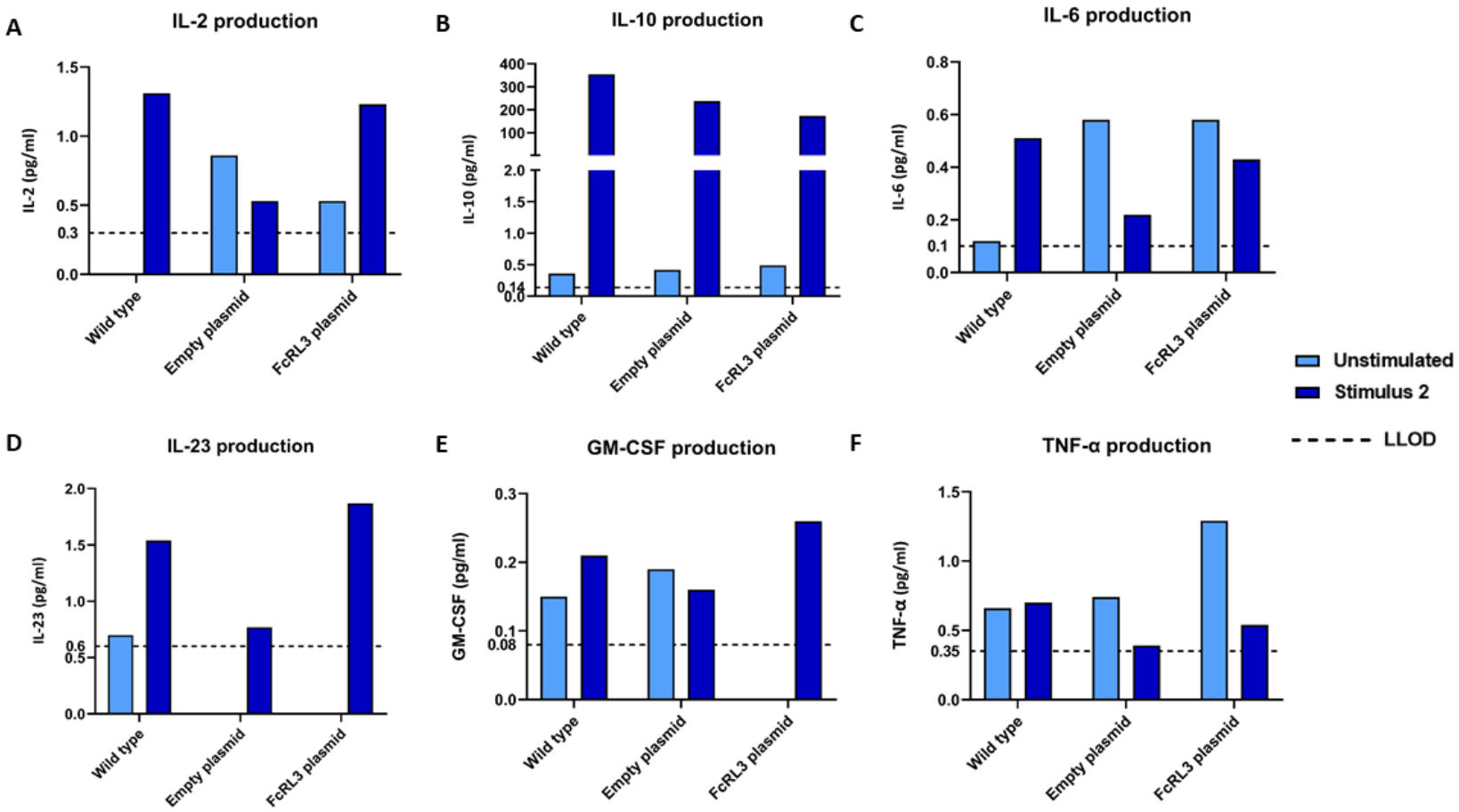

Figure 7. 18. Cytokine production by unstimulated and stimulated Ramos cell lines. The different Ramos cell lines were left unstimulated or were stimulated with stimulation cocktail 2 (Imiquimod, CpG A and CpG B, PWM, anti-CD40, IL-21 and IFN-γ) for 3 days. The culture supernatants were harvested and the concentrations of IL-2 (**A**), IL-10 (**B**), IL-6 (**C**), IL-23 (**D**), GM-CSF (**E**) and TNF-α (**F**) were detected using a U-PLEX Custom Biomarker plate from MSD. Unstimulated cells are shown in light blue and cells stimulated with stimulation cocktail 2 are shown in dark blue. The dotted line indicates the lower limit of detection for each immunoglobulin. N = 1.

7.4 Discussion

I have generated a stably transduced Ramos cell line that overexpresses FcRL3, as well as a Ramos GFP control cell line. These stable B cell lines have enabled me to perform my preliminary experiments to further investigate the effect of FcRL3 overexpression on B cell function, such as apoptosis and cell death, cytokine secretion, and immunoglobulins production. Based on my highly preliminary observation, further work will be needed to bring a deeper understanding of the role of FcRL3 in B cell function, which in turn will aid in determining why ABCs abundantly express FcRL3.

The main aim of this work was to generate a stable transduced B cell line that overexpressed FcRL3. In a stably transfected cell, the introduced genetic material is passed to their daughter cells, either because the introduced genetic material is inserted into the host genome, or, sometimes via stable inheritance of nongenomic DNA. This allows for a sustained expression even after the cell replicates (Kim and Eberwine, 2010). The first approach I used to create a stably transfected cell line overexpressing FcRL3 was electroporation. Electroporation was tried because I already had access to a plasmid containing the FcRL3 transcript sequence (a kind gift from Professor Nagata, Osaka University, Japan). Although I previously used a chemical transfection reagent (lipofectamine) to successfully transfect HEK293T cells with the pcDNA3 FcRL3 plasmid (Chapter 4, section 4.4.6), it has been reported that cells which grow in suspension, like Ramos cells, do not transfect efficiently with lipofectamine (Rahimi *et al.*, 2018). Therefore, I tried a physical method (electroporation) to transfect two different B cell lines, Ramos and Raji cells, with the pcDNA3 FcRL3 plasmid. A group had previously reported success in stably transfecting Ramos B cells with a pcDNA3.1 plasmid using electroporation, followed by selection of transfected cells with G-418 (Zhang *et al.*, 2019a). Unfortunately, even though the protocol followed was as per the manufacturers' instructions and was optimised for Ramos cells, the transfection efficacy I managed to achieve was very low and I could not generate a stably transfected cell line using this method (Figure 7.2).

Previous work done in our group, resulted in the development of an optimised protocol for retroviral transduction of a T cell line, the Jurkat cell line (Natasha West, Newcastle University). Through our RACE collaboration with the University of Glasgow, Dr Ruaidhri

Carmody's group kindly supplied the envelope, packaging and pIG-GFP transfer plasmids (VSVG, pCGP and pIG, respectively) for the retroviral generation.

I successfully cloned the FcRL3 transcript sequence into the pIG-GFP plasmid (Figure 7.3). I used the retroviral transduction protocol developed for the Jurkat cell line and successfully transduced the Ramos cell line to overexpress FcRL3 (Figure 7.6).

Puromycin selection of the transduced cells resulted in a significant number of transduced cells expressing FcRL3, as well as the reporter protein, GFP. Unfortunately, the cultures of transduced cells were heterogeneous, apart from the cell double positive for GFP and FcRL3, a second population expressing only GFP was present (Figure 7.4). One possible explanation for this could be that as the GFP translation is controlled by an IRES element, this may be stronger, resulting in more protein product, than translation of the FcRL3 gene (Addgene, 2014). In addition, GFP is easily visible and has a long half-life at both the mRNA level and the protein level, so expression of GFP may be visible even when the mRNA transcript, which would also include FcRL3, which may not have a long protein half-life, is not actively transcribed or translated anymore (Researchgate, 2013b). Other people have reported that when sorting GFP bright transduced cells, these cells died and had difficulties in expanding to sufficient cell numbers (Researchgate, 2013a). A possible explanation for this phenomenon is these cells are only focused on producing GFP and therefore do not replicate, resulting in cell death. Hence, the recommendation is that only the GFP+ cells, but not the brightest GFP expressing cells, are flow cytometry sorted.

I decided not to use the Raji cell line for the transduction with the FcRL3 plasmid because after the transfection using electroporation the cell viability was very low. Moreover, after the electroporation process, which causes cell stress, the control cells transfected with no plasmid upregulated FcRL3 expression. Raji cells have been reported to be FcRL5 positive (Shabani *et al.*, 2014) and lymphoma cells have high expression of FcRL family members (Polson *et al.*, 2006; Li *et al.*, 2014a). Moreover, Raji cells contain EBV DNA and although DNA synthesis is defective in this cell line, early antigens are expressed (Hatfull *et al.*, 1988). This could interfere with B cell activation and function. For these reasons, Raji cells were not a good cell line to use for overexpression of FcRL3 and this cell line was not transduced with the retrovirus.

Focusing on the outcome of the functional work, I reported that there was no difference in the phenotype of Ramos cells that overexpressed FcRL3 compared to the GFP control cells

(Figure 7.7-11). Ramos cells transduced to overexpress FcRL3 showed the same expression pattern of B cell markers and activation markers as the Ramos wild type and the Ramos GFP control cells. These results could be explained by the fact that the cells have not been stimulated to induce a B cell response, which would lead to potentially alterations in the expression of certain markers.

I therefore, investigated whether FcRL3 overexpression changed how the Ramos cells responded to a B cell stimulation cocktail. Stimulation cocktail 1 contained TLR7 ligand Imiquimod, TLR9 agonists ODN 2216 – CpG A and ODN 2006 – CpG B, Poke Weed Mitogen, anti-CD40, human IL-21, human IL-4 and IFN-gamma. This stimulation cocktail mimicked signals from a T cell-dependent response such as PWM and anti-CD40, as well as innate signals such as TLR ligands (T cell-independent response). Stimulation cocktail 2 contained all the above stimuli but no IL-4. IL-4 was excluded from the stimulation cocktail as it has been shown to inhibit expression of CD11c and T-bet in B cells (Naradikian *et al.*, 2016b). These potent stimulation cocktails were chosen to make sure the cells were fully activated. Although there were no differences in cell activation using the two stimulation cocktails (Figure 7.15), I decided to use stimulation cocktail 2 for the phenotype assessment, the cytokine secretion profile and the immunoglobulin production as this cocktail would more closely resemble the signals that drive the ABC-like phenotype. The differences seen in the stimulated, as compared to the unstimulated cells, confirm that Ramos cells do respond to a B cell stimulation cocktail as there was upregulation of activation markers, such as CD86 and CD97 (Figure 7.15). Sadly, there were no striking differences in expression of co-stimulatory and activation markers between the Ramos wild type, the Ramos GFP control, and the Ramos FcRL3+ cell lines (Figure 7.16). One explanation as to why I did not see any difference in the phenotype between the cells overexpressing FcRL3, as compared to the controls, may be due to the fact that the FcRL3 receptor is not being engaged by its ligand and is therefore not actively signalling and exerting an effect. Thus, without ligation of the FcRL3 receptor no effect on B cell effector function, as measured by changes in the cell phenotype, can be seen. The ligand for FcRL3 has been recently postulated to be secreted IgA (Agarwal *et al.*, 2020). This is in line with the proposed ligands for other FcRL family members, as FcRL4 is proposed to bind IgA and FcRL5 to bind IgG (Wilson *et al.*, 2012). These experiments were done using heat-aggregated serum IgA and IgG, however, the IgA found to bind FcRL3 was secretory IgA from human colostrum.

A more informative experiment for future work would be ligating FcRL3 in conjunction with the addition of a B cell stimuli, such as stimulation of the BCR or addition of TLR ligands, and then assessing B cell phenotype and function. As the ligand for FcRL3 has just been described it would be sensible to try and cross-link FcRL3 using an anti-FcRL3 antibody to induce stimulation of this receptor. A similar experiment was done on TLR9 activated primary B cells (Li *et al.*, 2013). As a different TLR, TLR7, has been proven to be important for ABC generation (Rubtsov *et al.*, 2013), combined with the fact that ABCs have very high expression of FcRL3, elucidating the effect FcRL3 ligation may have on the response to TLR7 stimulation would be very interesting.

In addition to assessing the effect FcRL3 overexpression may have on cell phenotype I also assessed the effect it had on both immunoglobulin production and cytokine secretion (Figure 7.17-18). I found that the Ramos cell lines all had very low production of IgA and IgG, even after stimulation. This is in accordance with another study describing Ramos cells as non-class-switched IgM+ IgD+ B cells (Dussault *et al.*, 2008). However, as reported previously (Benjamin *et al.*, 1982), Ramos cells produced high amounts of IgM. My results showed that this IgM production not only happens after stimulation, but Ramos cells spontaneously secrete this immunoglobulin.

The majority of the cytokines assessed in the culture supernatants following stimulation of the Ramos cell lines were found at very low levels (Figure 7.18). IL-10 was the only cytokine detected at a high level. IL-10 was produced at a lower level in the FcRL3 overexpressing Ramos cells than in the Ramos wild type and the Ramos GFP controls cells. Intriguingly, these results are in line with IL-10 production by FcRL3+ ABCs, which as reported in Chapter 6, section 6.4.9, is almost non-existent. This could mean that FcRL3 expression is a marker of a pro-inflammatory subset of B cells rather than an anti-inflammatory subset. It should be noted that the low levels of secreted cytokines were not surprising, as another study has demonstrated that Ramos cells stimulated with other stimuli, such as an anti-CD40 antibody, produce very little cytokine, and similar to my findings only IL-10 and low levels of TNF-α were detected (Grammer *et al.*, 1998). In addition, it has previously been reported that, Ramos cells, as well as other cancerous B cell lines, exhibit defects in cytokine and immunoglobulin production, and for this reason most of the published studies focus on cell surface marker expression (Van Belle *et al.*, 2016).

As final readouts of B cell function, I decided to investigate if FcRL3 overexpression affected the Ramos cell line in terms of cell proliferation, as well as apoptosis and cell death.

My results investigating cell proliferation showed that the Ramos GFP control cells were proliferating at a faster rate than the Ramos FcRL3+ cell, as well as the Ramos wild type controls (Figure 7.12). This may indicate that retroviral infection of B cell lines may increase cell proliferation. However, the Ramos FcRL3+ cells had been through the same retroviral infection protocol and did not have increased levels of proliferation. In fact, they were similar to the Ramos wild types in terms of proliferation capacity. Therefore, it may be the case that the overexpression of FcRL3 counteracts and reduces the enhanced proliferative effect induced by the retroviral infection. It has been reported previously that in primary B cells some retroviruses stimulate the host cell cycle, increasing cell proliferation (Coffin *et al.*, 1997). However, there are no reports on retroviruses used to transduce having an effect by increasing cell proliferation. The results from the proliferation assay are intriguing as FcRL3 overexpression seems to have some influence on B cell proliferation. Unfortunately, due to time constraints, the functional work using the Ramos cell lines could only be performed once. Future work needs to focus on repeating this experiment to determine reproducibility and robustness of the result.

The apoptosis and viability results highlighted two things: Firstly, FcRL3 overexpressing cells naturally died more easily compared to the two control cell lines; and secondly, when apoptosis was induced using an anti-CD95 antibody, FcRL3 overexpressing cells were more prone to apoptosis (Figure 7.13-14). The method used to induce apoptosis was by directly inducing CD95/FasR cell death by adding an anti-CD95 antibody to the cell cultures. The anti-CD95 antibody stimulates the Fas receptor and activates downstream signalling leading to caspase-induced apoptosis (Nagata, 1999). As shown in my results, induction of apoptosis in Ramos cells using the anti-CD95 antibody was not very effective. It has been reported previously, that CD95 is expressed on activated B cells but not on resting ones (Nagata, 1999). Studies using Ramos cells, found that stimulation with anti-CD40 induced expression of CD95 on these cells (Schattner *et al.*, 1995), perhaps suggesting that Ramos cells do not endogenously express CD95 at a high level. Moreover, a study found that the Ramos cells have different sensitivities to apoptosis and that it was possible to select the ones resistant to CD95-induced apoptosis (Lens *et al.*, 1998). These reports may explain why I see only a small induction of apoptosis in Ramos cells with an

anti-CD95 antibody, even when the cells were left for a few days in culture (data not shown). Prior stimulation of the cells with an anti-CD40 antibody could lead to a better response to an anti-CD95 antibody and could bring more insight into whether FcRL3 overexpression in B cells makes them more sensitive to apoptosis induction. The fact that the Ramos FcRL3+ cells are, in general, more prone to cell death, could also be influencing the proliferation results I discussed earlier. For example, if the Ramos FcRL3+ cells die more easily than the Ramos GFP control cells, this may explain why the proliferation rate is reduced. Of interest, there are studies on T cells connecting FcRL3 expression to cell death. A study described a subpopulation of naturally-occurring regulatory T cells (Tregs) characterised by FcRL3 expression, which are unresponsive to the effects of IL-2 (Nagata *et al.*, 2009). Another study showed that FcRL3 expressing Tregs are dysfunctional and have high expression of the cell death marker Programmed Cell Death-1, PD-1 (Swainson *et al.*, 2010). Although all of these studies have been done in T cells, my results showed that FcRL3 expressed on B cells could have a similar effect and could cause the cells to become more prone to apoptosis and cell death. However, all these results need to be replicated in future experiments as they are very preliminary.

7.5 Conclusions

This chapter illustrates the process of creating a stably transduced FcRL3 overexpressing B cell line using a retroviral approach in order to further investigate the role of FcRL3 in B cell function. Once the cell line was stably overexpressing FcRL3, I performed a few preliminary experiments, checking for differences between the FcRL3 overexpressing cells and control cells.

I demonstrated that when trying to generate a stable FcRL3 overexpressing B cell line the approach which gave the highest transduction efficiency and was the most successful, was a retroviral transduction protocol. I also showed that transduction can result in a heterogeneous population, with cells expressing different levels of FcRL3, as well as the GFP reporter. In order to obtain a pure population of cells overexpressing FcRL3, flow cytometry sorting to enrich for FcRL3+GFP+ cells was needed. Moreover, I confirmed that simply overexpressing FcRL3 had no effect on the Ramos cell phenotype. I also showed that, although the proliferation rate seems to be enhanced in retroviral infected cells, this appears to be reduced in cells overexpressing FcRL3. Furthermore, induction of apoptosis is affected in cells overexpressing FcRL3, with higher susceptibility to apoptosis seen in FcRL3+ cells. Nevertheless, no differences in phenotype, cytokine secretion and immunoglobulins production between FcRL3 overexpressing cells and the control cells were found when cells were stimulated with a B cell stimulation cocktail. The reason why no differences were seen may be due to the fact that in these cultures FcRL3 was not engaged by its ligand. Further work is needed to clarify how ligation of FcRL3, possibly by cross-linking the receptor, affects B cell function.

In summary, I created a B cell line which stably overexpresses FcRL3. This will allow for future work to further explore on how FcRL3 signalling impacts B cell function. Moreover, it may provide insights into why FcRL3 is highly expressed on ABCs and will help elucidate what role it could be playing in these cells.

Chapter 8. General Discussion

8.1 General discussion

For the work performed in this thesis, I used three surface markers, CD19, CD11c and CD21, to identify the ABC subset in peripheral blood. I investigated the frequency of these cells in patients suffering from inflammatory arthritides and healthy controls. Furthermore, I characterised ABCs in depth, phenotypically, by analysing gene expression and functionally, by assessing immunoglobulin and cytokine production. The main outcomes are discussed below.

8.1.1 ABCs activated phenotype

Several studies have investigated ABCs in order to elucidate their potential role in health and disease (Karnell *et al.*, 2017). However, there is a lack of consensus in the way these cells are described. Some studies simply use lack of CD21 expression (Wehr *et al.*, 2004; Thorarinsdottir *et al.*, 2019), others describe them using CD11c expression (Rubtsov *et al.*, 2011), while others define them by the expression of the transcription factor T-bet together with CD11c (Naradikian *et al.*, 2016b; Karnell *et al.*, 2017; Wang *et al.*, 2018). Moreover, as reported in several literature reviews, the name "age-associated B cells", is not very appropriate for three reasons: cells with a similar phenotype also appear in autoimmunity and viral infections, this population is heterogeneous, and their function appears to be distinct in different situations (Phalke and Marrack, 2018). For my PhD project I decided to define the ABC subset as CD11c+CD21- B cells (CD19+CD11c+CD21-) (Rubtsov *et al.*, 2013). The combination of two surface markers, CD11c and CD21, was used in order to make the gated subset more defined because not all CD21- cells are positive for CD11c, and vice versa, not all CD11c+ B cells are negative or low for CD21. Therefore, using two markers I analysed a more distinct population of B cells.

I designed comprehensive flow cytometry panels to fully characterise the ABCs subset and compare these cells with other B cell populations. As reported before in the literature, ABCs have high expression of MHC class II molecules together with co-stimulatory molecules and activation markers. Furthermore, I assessed the expression of the FcRL family on ABCs, which I believe is the first time that a full protein characterisation of this receptor family has been assessed on ABCs. FcRL family member expression on atypical memory B cells (CD10-CD19+CD20+CD21lowCD27-CD11chigh) was reported previously (Portugal *et al.*, 2015), however, other studies have only analysed expression of one or two members of the FcRL family on ABC –like cells (Jenks *et al.*, 2018; Wang *et*

al., 2018; Thorarinsdottir *et al.*, 2019; Zumaquero *et al.*, 2019). My results show that a higher proportion of ABCs express FcRL2 to FcRL5 compared to the other B cell subsets. I also assessed the proliferative marker, Ki67, and found that ABCs contain a high proportion of Ki67 positive cells, indicating that these cells are actively proliferating. A high percentage of ABCs were also positive for the transcription factor T-bet, confirming it as a specific marker for this subset (Rubtsov *et al.*, 2017). However, my results show that not all the cells from the ABC population express T-bet, and this expression varies between individuals. Finally, analysis of immunoglobulin expression revealed that a high proportion of ABCs are class switched B cells as they express IgG. However, a proportion of ABCs are also IgM and/or IgD positive. Figure 8.1 summarises all the markers expressed by ABCs as described in Chapter 4.

Among the described phenotypes, the cells described in this thesis are largely similar to the ABCs described by Rubtsov *et al.*, and differ from the exhausted CD19+CD21- B cells described by Hao *et al.*, in mice and by Isnardi *et al.*, in humans (Isnardi *et al.*, 2010; Hao *et al.*, 2011; Rubtsov *et al.*, 2011). This is due to their high expression of activation and co-stimulatory molecules, such as CD80, CD86, and MHC class II molecules. The CD21low cells described by Hao *et al.*, in mice and by Isnardi *et al.*, in humans showed similar expression levels of these molecules to FO B cells and CD21+ B cells, respectively. Moreover, due to the high percentage of class switched cells in the ABC population, my results, in line with the work by Rubtsov *et al.*, confirm that the ABCs are an antigen-experienced population (Rubtsov *et al.*, 2011).

The data from the literature, as well as my work presented in this thesis, highlight the fact that the cell subset we define as ABC is in fact a heterogeneous population (Phalke and Marrack, 2018; Knox *et al.*, 2019). The best example to illustrate this heterogeneity is the expression of immunoglobulins on ABCs. My results from Chapter 4 show that around half of the cells in the ABC subset are positive for IgD, however, when assessing IgG expression around half of the cells are also positive for this immunoglobulin. IgD+ cells are not positive also for IgG, therefore the ABCs population is heterogeneous and includes class-switched (IgG+) and non-class switched (IgD+) B cells. This is in line with the discrepancies seen in the different studies, as some groups describe these cells as being class-switched (Rubtsov *et al.*, 2011; Shimabukuro-Vornhagen *et al.*, 2017), while others report them to be naïve (Isnardi *et al.*, 2010). Moreover, when assessing expression of other markers, for example T-bet, not all the cells in the ABC population express this marker.

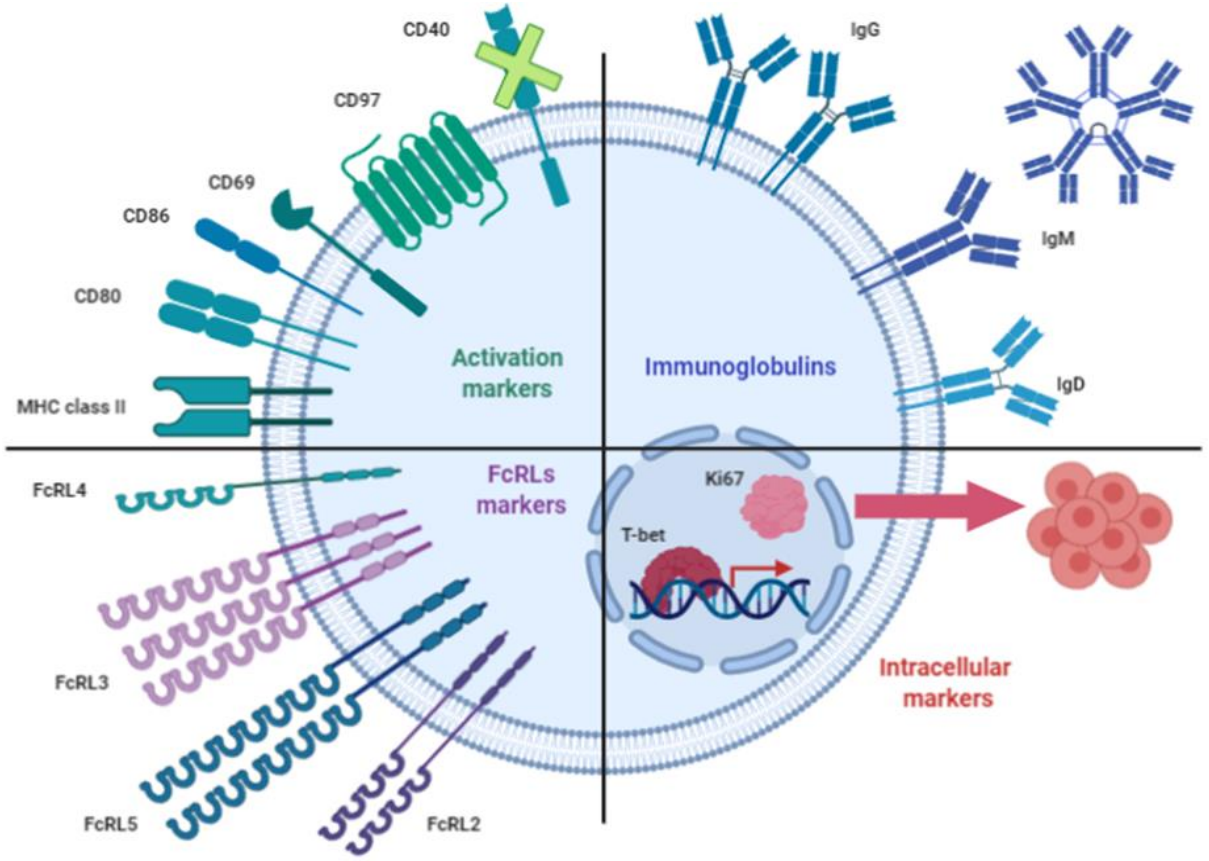

Figure 8. 1. Phenotypic marker expression by ABCs. Graphical representation of the ABCs expression profile determined by flow cytometry. ABCs have high expression of co-stimulatory molecules, CD80 and CD86, in addition to high expression of MHC class II molecules. Moreover, they express the activation markers CD69 and CD97, but have low expression of CD40. ABCs have high expression of FcRLs family members FcRL2 to FcRL5, with a very high expression of FcRL3. In terms of immunoglobulin secretion and expression, some cells in the ABC population are class-switched IgG expressing cells, whereas others express IgD and IgM. Finally, ABCs have high expression of the transcription factor T-bet and are actively proliferating as indicated by Ki67 expression. Created with Biorender.com.

8.1.2 Functional role of ABCs

The role of ABCs both in healthy donors as well as in patients suffering from autoimmune diseases is still unknown. Phenotypic characterisation of these cells has given some insight into what their function may be. The potential roles for ABCs in health and disease, based on my findings, are summarised in Figure 8.2. My work supports the role of ABCs as antigen presenting cells, as they have high expression of co-stimulatory molecules, CD80 and CD86, and high expression of the antigen presentation molecule MHC class II. However, this is an extrapolation from their phenotype while their presentation of antigen and interaction with T cells is yet to be directly tested.

Additionally, the characterisation of surface immunoglobulins expression gives insights into the potential role of ABCs as precursors of antibody secreting plasma cells. Although these cells are not yet plasma cells, as shown by the gene expression analysis, they might be a precursor of antibody secreting cells which rapidly differentiate and secrete antibodies after B cell re-stimulation. Functional work in mice demonstrated that after stimulation, ABCs rapidly differentiate into antibody secreting plasma cells, which produce IgG2a/c despite their high expression of surface IgM and IgD (Rubtsova *et al.*, 2013; Du *et al.*, 2019). ABCs in mice were also shown to contribute to the reduction of B cell lymphopoiesis seen with age and to secrete TNF-α which contributes to the inhibition of survival of the B lineage precursors (Ratliff *et al.*, 2013; Riley *et al.*, 2017). Although ABCs correlate with autoantibody production, B cell development and T cell function, causality is still to be determined (Naradikian *et al.*, 2016a). My transcriptomic and functional results reinforce some of the previously hypothesised role for ABCs, nevertheless, *in vitro* functional work is needed in order to fully determine the function of ABCs.

As shown in Chapter 3, I did not replicate previously published results showing increased frequency of ABCs in patients with RA (Rubtsov *et al.*, 2011; Shimabukuro-Vornhagen *et al.*, 2017). This may be due to the relatively small size of the cohort tested. Nevertheless, I did show that the frequency of ABCs is very high in synovial fluid of patients with inflammatory arthritides, as reported before in the literature (Illges *et al.*, 2000; Yeo *et al.*, 2015; Thorarinsdottir *et al.*, 2019). These results support the hypothesis that ABCs might be migrating into inflammatory sites. Moreover, the results from the gene expression analysis in Chapter 5 showed upregulation of genes involved in cell migration, such as adhesion molecules and chemokine receptors, further supporting the migratory potential of

these cells into inflammatory sites. Additionally, other studies showed that T-bet+ B cells with high expression of CXCR3, akin to the ABCs reported in this thesis, were increased in cerebrospinal fluid from patients with MS and had a higher migration capacity, as assessed in transwell assays (van Langelaar *et al.*, 2019). Interestingly, the cells with a higher migration capacity were also IgG1+, which is the human equivalent to the mouse class switched isotype, IgG2a, shown to be promoted by T-bet expression in B cells (Rubtsova *et al.*, 2013).

The high expression of CD97 by ABCs compared to naïve and CD5+ B cells lead me to hypothesise that these cells may have the ability to interact with synovial fibroblasts. In order for the ABCs to interact with synovial fibroblasts they would need to migrate to the inflamed joint. This migration may be triggered by the high integrin expression, such as CD11c and CD18 and adhesion molecules, such CD97, which would allow them to adhere to the endothelium and migrate through the cell layer (Humphries *et al.*, 2015). The high expression of CXCR3 by ABCs, together with the evidence of increased ligand expression, CXCL10, in RA joints (Patel *et al.*, 2001), would attract these cells to inflammatory sites. Once in the joints, the CD97-expressing ABCs have the potential ability to interact with CD55-expressing fibroblast, as CD97 is known to bind CD55, in addition to another joint component, chondroitin sulfate (Hamann *et al.*, 2016). Further investigation of ABCs migratory ability and their potential interaction with synovial fibroblasts is needed.

Furthermore, my gene expression analysis demonstrated a possible role for cytotoxic activity of ABCs. My NanoString results showed high expression of granzyme A and B, as well as perforin and granulysin. This, together with a high expression of NK cell receptors, supports a potential cytotoxic role for ABCs. Unfortunately, these gene expression results could not be confirmed at the protein level. This could be due to the cells possibly requiring an additional stimulus to initiate translation of the mRNA into protein. Nevertheless, cytotoxic B cells, resulting from insufficient T cell help, have been reported before (Hagn *et al.*, 2012). This study showed that in the absence of CD40L signalling, IL-21 induces differentiation of B cells into granzyme B secreting B cells. These results are in line with the published evidence that ABCs are generated through IL-21 signalling, in addition to IFN-γ and TLR signalling (Naradikian *et al.*, 2016b; Wang *et al.*, 2018).

Intriguingly, my gene expression analysis showed high expression of pro-apoptotic molecules. Expression at the protein level was confirmed for CD95/Fas, reinforcing the

hypothesis that ABCs may be susceptible to cell death by apoptosis. These findings were reported before in literature by other groups, who suggested that the unresponsiveness seen in the ABC population, together with the high expression of caspases and CD95/Fas would lead to death of these cells (Isnardi *et al.*, 2010; Rubtsov *et al.*, 2011; Wang *et al.*, 2018; Du *et al.*, 2019). Functional work using apoptosis assays or B cell stimulation would help determine whether these cells are more prone to apoptosis.

My gene expression results and my phenotypic characterisation showed that ABCs have high expression of the transcription factor T-bet, as confirmed in the literature by others (Rubtsova *et al.*, 2015; Rubtsov *et al.*, 2017). T-bet expression on B cells is induced through IL-21 signalling, together with IFN-γ and in the absence of IL-4 (Naradikian *et al.*, 2016b). Moreover, TLR signalling can also drive T-bet expression in B cells (Knox *et al.*, 2019; Zumaquero *et al.*, 2019). T-bet promotes expression of T-bet inducible genes such as CXCR3, as shown in CD8+ T cells (Groom and Luster, 2011a), which supports a possible role for ABCs migration into inflammatory sites. Additionally, murine studies showed that T-bet expression promotes IgG2a class-switching on B cells (Gerth *et al.*, 2003), which is the equivalent to IgG1 in humans. Figure 8.3 summarises the proposed mechanisms of ABCs generation, and the role T-bet may play in the functional role of ABCs. In the context of autoimmunity, such as in RA, ABCs generated through IL-21, IFN- γ and TLR signalling would lead to T-bet expression, which in turn would drive expression of CXCR3 and class-switching to an IgG1 isotype, supporting their contribution to disease pathogenesis.

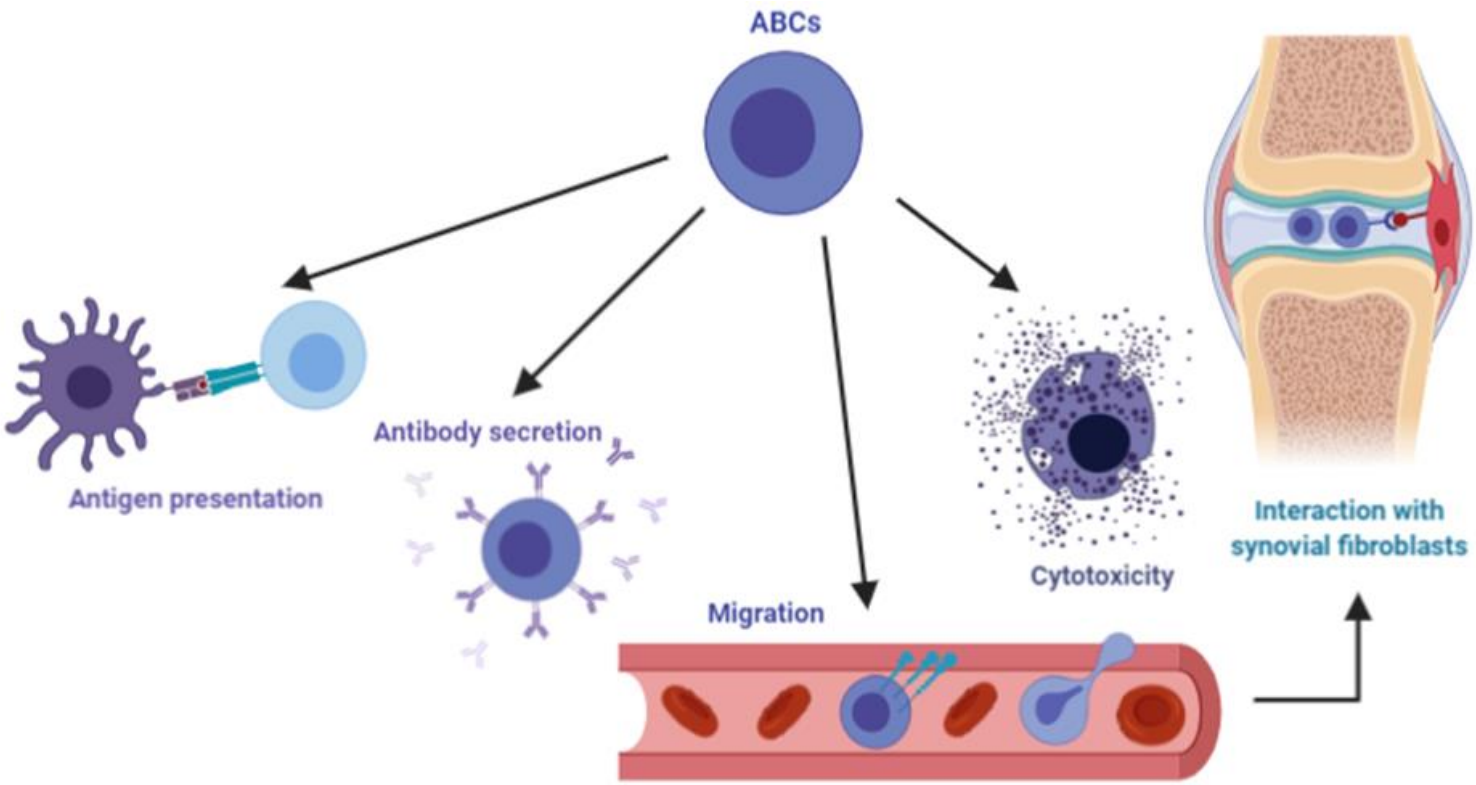

Figure 8. 2. The potential role of ABCs. Graphical summary of the possible functions of ABCs in health and disease. The high expression of both co-stimulatory molecules and HLA-DR suggests a potential role for ABCs in antigen presentation. Due to a high percentage of class-switched ABCs, these cells may be antibody secreting cells or precursors to these cells. Their high expression of integrins and chemokine receptors indicate that ABCs may migrate from the blood into tissues. Once in the inflamed joint, ABCs may interact with synovial fibroblasts through the interaction of CD97 on the ABC with CD55 on the synovial fibroblasts. Finally, gene expression analysis showed high expression of NK cell related cytotoxic mediators, such as granzyme B, suggesting that ABCs may have cytotoxic activity. Created with Biorender.com.

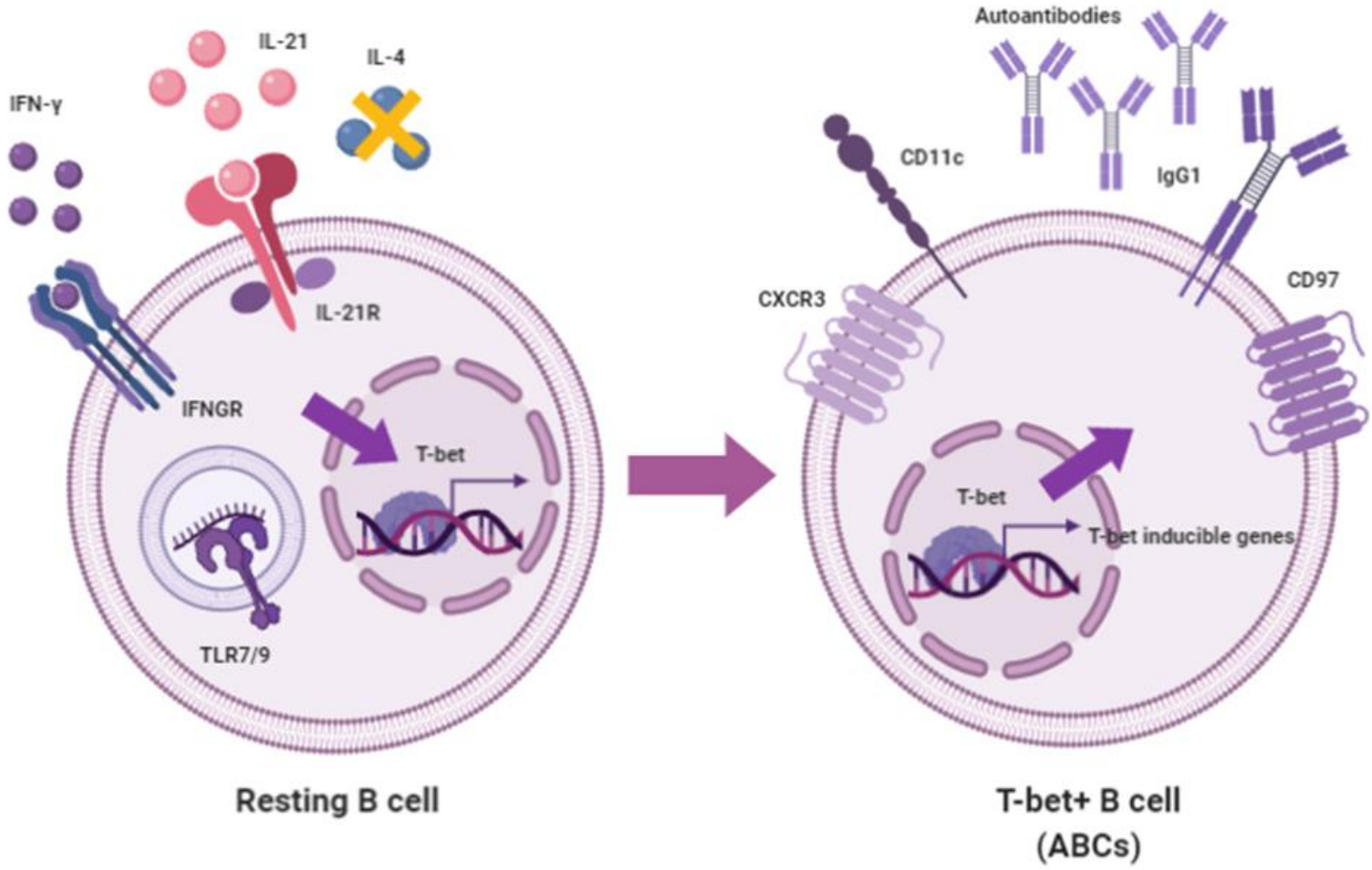

Figure 8. 3. The proposed mechanism involved in ABCs generation. Graphical summary of the generation of ABCs. IFN-γ, together with IL-21 signalling and TLR engagement, in the absence of IL-4, leads to the expression of T-bet. T-bet promotes expression of T-bet inducible genes, leading to expression of the inflammatory homing chemokine receptor, CXCR3, as well as class-switching of the cell to an IgG1 isotype. In the context of autoimmunity, these cells may recognise autoantigens and therefore produce autoantibodies. Created with Biorender.com.

8.1.3 Expression of FcRL family protein on ABCs

I became interested in the FcRL family of receptors and the potential role they play in ABCs function due to the work conducted by my supervisor in Birmingham on a subset of synovial B cells that express FcRL4, which have a similar phenotype to the ABCs (Yeo *et al.*, 2015), in addition to the work performed in our group identifying a mQTL and eQTL for FcRL3 in B cells and T cells from RA patients (Clark *et al.*, 2020). Interestingly, I found that FcRL2-5 expression was enriched in ABCs compared to the other B cell subsets. Expression of certain FcRL members, such as FcRL3, FcRL4 and FcRL5 has previously been reported in ABCs, although mostly at the mRNA level (Isnardi *et al.*, 2010; Lau *et al.*, 2017; Wang *et al.*, 2018). However, none of the studies checked the protein expression of all the FcRL family members, thus my thesis is the first to assess this.

The function of the FcRL family members is still unknown. The presence of both ITAM and ITIM domains in their intracellular tails indicates that most of these receptors may be capable of exerting a dual-modulation by activating or inhibiting responses (Ehrhardt *et al.*, 2007). Some studies have shown that stimulation of the BCR together with one of the FcRL family members (FcRL2-5) leads to an attenuation of antigen receptor-mediated calcium mobilisation and MAPK activation, which results in apoptosis (Haga *et al.*, 2007; Kochi *et al.*, 2009; Jackson *et al.*, 2010). Conversely, in TLR9 activated B cells when FcRL4 and FcRL3 were engaged, there was an enhancement of TLR9-induced proliferation, survival and B cell activation (Sohn *et al.*, 2011; Li *et al.*, 2013). As it has been reported that ABCs do not respond to BCR stimulation but do respond well to TLR engagement (Naradikian *et al.*, 2016b; Thorarinsdottir *et al.*, 2016; Johnson *et al.*, 2019), it may be the case that the high expression of FcRL family members on ABCs contribute to the responsiveness of these cells to TLR ligands.

FcRL3 expression on T cells have been shown to mark an exhausted regulatory T cell subset (Nagata *et al.*, 2009). Interestingly, recent work on Tregs expressing FcRL3 demonstrated that FcRL3 engagement mediates transition of these Tregs to a pro-inflammatory Th17-like phenotype (Agarwal *et al.*, 2020). This would suggest a role for FcRL3 in possibly driving cells to a pro-inflammatory program. Moreover, the authors suggest secretory IgA is a specific FcRL3 ligand which could limit Treg function at mucosal sites in order to control infection. In light of these results, further work is needed

to investigate if secretory IgA binds to FcRL3 on B cells, and, if it does, what the functional outcome of this interaction is.

A subset of memory B cells with a similar phenotype as the ABCs have been described in viral infections. These cells are called atypical memory B cells (Portugal *et al.*, 2017) and express CD11c and T-bet, and lack expression of CD21 (Chang *et al.*, 2017; Obeng-Adjei *et al.*, 2017). Interestingly, these atypical memory B cells have high expression of some of the FcRL family members, such as FcRL3, FcRL4 and FcRL5 (Moir *et al.*, 2008; Sullivan *et al.*, 2015). Additionally, these cells, similar to ABCs, are not a homogeneous population of B cells and show significant heterogeneity between different chronic infections. However, the main reported difference between ABCs and the atypical memory B cell population is in their response to stimulation. Atypical memory B cell are unresponsive to BCR engagement but also do not respond to TLR and cytokine stimulation (Moir *et al.*, 2008; Chang *et al.*, 2017), unlike ABCs which do respond to TLR ligation, IFN-γ and IL-21 (Naradikian *et al.*, 2016b).

8.2 Strengths and weaknesses

The main strengths and weaknesses of this project are summarised in Table 8.1. The main strength of this project is the use of relevant human samples to perform the translational research reported here. Specifically access to peripheral blood samples from early drug naïve RA patients and established RA patients, as well as disease and age-matched healthy controls, allowed a detail characterisation of the ABC population. Although some of the weaknesses would not have been an issue when using animal models, for example isolating sufficient numbers of cells would not have been a challenge, the use of patient samples allowed for a more relevant and accurate characterisation of these cells in human autoimmunity. However, the inclusion of synovial fluid ABCs for phenotypic characterisation and functional work may have been even more informative than peripheral blood ABCs, as blood may be less relevant in RA, which manifests mainly in the joints. Furthermore, RA is a highly heterogeneous disease with a high level of gene – environment interaction. This creates a huge variability between patients and this variability is challenging, requiring sufficiently sized cohorts for both the discovery and the validation of observations. With this in mind, one other weakness of this study is the low numbers of patients and controls used – increased numbers would have enabled more in depth analysis and confidence in the conclusions drawn. Due to the high heterogeneity of human samples, it could have been useful to calculate the sample size prior to recruiting patients. With a few patients recruited as a pilot study, a sample size calculation could have been performed using a statistical test as the 2-Sample t-test. Calculating the sample size would take into account the sample variability and the power of the study and would have allowed me to estimate how many patients are needed to detect significant differences between the frequency of ABCs in the different disease controls and healthy controls. Regarding the FcRL3 functional work, the use of a cell line provides an easy way to overexpress and study the unknown function of proteins. Having a stably transfected B cell line overexpressing FcRL3 will allow for future work which will help elucidating the role of FcRL3 in B cell function. However, cell lines are cancerous cells and their functional properties are altered, therefore it is challenging to use them for functional work.

One of the challenges encountered during this work has been the low number of ABCs that I was able to isolate from peripheral blood. As ABCs are a rare subpopulation of B cells (between 0.5% and 8% of the total B cell population), using the maximum amount of blood that I could collect under our ethical approval, I could only isolate around 40,000 ABCs

per donor. With this number of cells, functional work was very difficult as the number of cultured cells and the production and secretion of cytokines and immunoglobulins was very low. Previous published functional work on ABCs, done in mice, isolated cells from the spleen so cell numbers were not a limiting factor (Hao *et al.*, 2011; Rubtsov *et al.*, 2011; Naradikian *et al.*, 2016b). Other functional studies using human ABCs define this cell population using less phenotypic markers, for example just isolating CD21 low B cells, resulting in a less distinct population which is more abundant (Isnardi *et al.*, 2010; Thorarinsdottir *et al.*, 2019). Some other studies even pooled sorted ABCs from different donors together to reach sufficient cell numbers (Wang *et al.*, 2018).

With the emergence of new techniques, other approaches to investigate the role of ABCs could have been used. CyTOF or mass cytometry tags cells as in flow cytometry but using metals instead of fluorophores, overcoming the limitations of spectral overlap typical from flow cytometry. CyTOF allows for a high number of markers to be analysed in one sample. This would have been useful when phenotyping the ABCs as the number of markers assessed per sample would have been broader and would have allowed for a deeper characterisation of ABCs and discovery of new markers for this subset of B cells.

The use of organoids could also have helped determine the function of ABCs. Organoids are simplified versions of organs produced *in vitro* and derived from stem cells. Organoids can be used for drug testing and for disease modelling. An organoid model of an RA knee could be highly informative to determine how ABCs contribute to joint damage. Moreover, this environment could be favourable for ABCs culturing, which would help elucidating the role of this B cell subset in disease. Organoids would also allow to see how ABCs react to different therapies and how these cells interact with other cell types in the joint.

Strengths	Weaknesses
– Access to peripheral blood from early drug naïve patients – Access to peripheral blood from established RA patients – Use of synovial fluid from inflammatory arthritis patients for ABCs frequency determination – Access to peripheral blood from age-matched disease and healthy controls	– Peripheral blood ABCs used for characterisation work instead of synovial fluid ABCs
– Use of NanoString Technology which allowed analysis of rare subsets and avoided amplification bias – Validation of NanoString transcriptomic candidates at the protein level using flow cytometry	– Due to small patient and control numbers, insufficient power to correlate ABCs with disease – Small number of patients for the transcriptomic analysis – No validation by qRT-PCR of transcriptome findings
– Use of MSD Technology allowed assessment of a multiple cytokines from a small volume of culture supernatant	– Low number of cultured cells
– Generation of a stably transduced FcRL3+ B cell line that can be used for future work	– Use of cell lines for functional work – Insufficient replicates for FcRL3 functional work on the FcRL3+ B cell line

Table 8. 1. Summary of the strengths and the weakness of the work presented in this thesis.

8.3 Future work

The results from the NanoString analysis shown in Chapter 5, demonstrating high expression of chemokine receptors and adhesion molecules further supports the hypothesis that ABCs may migrate into sites of inflammation. Moreover, this hypothesis was reinforced by the high percentages of B cells with an ABC phenotype in the synovial fluid of patients with inflammatory arthritides. In addition, the high expression of CD97, both at the mRNA and the protein level, in ABCs lead me to postulate that once in the joints, ABCs could possibly interact with CD55-expressing synovial fibroblasts, as CD55 is a ligand for CD97, and contribute to the pathogenesis of inflammatory arthritis.

In order to further investigate this hypothesis, I successfully applied for a 1 year project grant from the JGW Patterson Foundation. In this funded project, I will try to elucidate the role of CD97 expression on ABCs in inflammatory arthritis. CD97 is a member of the EGF-TM7 subfamily of adhesion G protein-coupled receptors, which is abundantly expressed on macrophages and dendritic cells, and is upregulated on lymphocytes following activation. CD97 is known to mediate cell-cell interactions and this protein is believed to play a role in cell adhesion, leukocyte recruitment, cell activation and migration to sites of inflammation (Hamann *et al.*, 2010). Interestingly, CD97 neutralisation using a CD97 monoclonal antibody in a murine collagen-induced arthritis model of arthritis (CIA), showed reduced joint damage and inflammation (Kop *et al.*, 2006). Moreover, CD97 has been shown to be a receptor for several ligands other than CD55, including chondroitin sulfate B, CD90 and the integrins α5β1 and αvβ3 (Hamann *et al.*, 2016). CD55 is a glycoprotein involved in the regulation of the complement cascade by accelerating the C3 convertase decay and therefore protecting host cells from complement damage (Dho *et al.*, 2018). CD55 is highly expressed by fibroblast-like synoviocytes (FLS) located in the lining layer of the synovia, and it has been shown that CD55 on FLS interacts with CD97-expressing macrophages in the rheumatoid synovia (Hamann *et al.*, 1999). In addition, CD97 has been shown to bind chondroitin sulfate in the inflamed synovial tissue of patients with RA (Kop *et al.*, 2005), suggesting another receptor-ligand interaction that may result in the recruitment and retention of CD97-expressing leukocytes in the synovium, thus perpetuating the pro-inflammatory state. These findings highlight a potential role for CD97-expressing ABCs interacting with CD55+ synovial fibroblasts in driving the pathogenesis of RA.

Furthermore, it has been reported that interaction of CD97 and CD55 plays an important role in the regulation of T cell responses (Capasso *et al.*, 2006), and blockade of this interaction using monoclonal antibodies impairs both T-cell proliferation and effector cytokine production (Abbott *et al.*, 2007). However, very little is known about the role of CD97-CD55 interactions on B cell function or fibroblast function. Therefore, I hypothesise that the increased expression of pro-inflammatory chemokine receptors and cell adhesion molecules on ABCs promotes their recruitment to sites of inflammation and once there, high expression of CD97 allows them to interact with CD55-expressing fibroblasts, leading to activation of both cell subsets and the promotion of joint inflammation and RA disease pathogenesis.

During this funded project, in order to test this hypothesis, I will address the following aims: 1. Examine whether ABCs co-localise with synovial fibroblasts in RA synovial tissue; 2. Determine whether ABCs can migrate towards RA synovial fibroblasts; and 3. Investigate if interaction of ABCs and RA synovial fibroblasts can drive one or both cell types towards a pro-inflammatory phenotype that may contribute to the joint inflammation seen in RA. This study will provide insights into the interaction between immune cells and stromal cells in the inflamed joint and will elucidate how these cells promote inflammation and joint damage.

Additionally, during this extra year, as a side project, I will also investigate the role of FcRL3 expression on B cell function. By the end of my PhD I managed to stably transfect a B cell line that overexpresses FcRL3 and GFP, as well as a control B cell line just overexpressing GFP. I will, with the help of Undergraduate and Masters students, investigate the effect of FcRL3 co-ligation on downstream phosphorylation cascades. Moreover, I will try to use B cell stimuli, such as TLR7 engagement, and compare the responses with and without FcRL3 ligation. Finally, we will also assess FcRL3 ligation on peripheral blood B cells and check proliferation and survival of the cells.

Due to our group's previous work on the mQTL and eQTL modulating FcRL3 expression on B and T cells from RA patients (Clark *et al.*, 2020), I will also recruit early RA patients and check protein expression of FcRL3 on different B and T cell subsets. These patients will be genotyped to investigate correlation between the genotype and the FcRL3 protein expression in each subset of cells. This will also be done with the help of Masters students.

Additional future work would also include increasing the n numbers for some of the work, for example for the NanoString analysis of gene expression and for the functional work. Due to the heterogeneity of RA and the high variability of the human population, increased numbers of patients and controls would have enabled more in depth analysis and a higher confidence in the conclusions drawn.

Moreover, repeating the characterisation and the functional work on synovial ABCs rather than peripheral blood ABCs would be more informative as RA manifests in the joints. I have already optimised several flow cytometry panels to assess expression of phenotypic markers, which could be used to phenotype matched PBMCs and SFMCs from the same patient and would allow to compare each marker in the ABC population from both tissues. Moreover, sorted cells from peripheral blood and synovial fluid could be cultured and stimulated and cytokine and immunoglobulin production assessed.

The NanoString results could be validated either using qPCR, such as TaqMan PCR at the mRNA level or using flow cytometry to detect protein expression.

Finally, the results from the FcRL3+ B cell line are very preliminary and it is necessary to increase the n numbers. As the B cell line overexpressing FcRL3 is stably transfected, the apoptosis assay could be repeated. Moreover, other experiments crosslinking the FcRL3 receptor and combining different stimuli will help elucidate the role of FcRL3 in B cell function.

8.4 Final conclusions

In conclusion, I have shown that although my study did not show significant differences in the frequency of peripheral blood ABCs between RA patients and other disease and healthy controls, the percentage of cells with an ABC phenotype in the synovial fluid is very high in patients suffering from inflammatory arthritides. I characterised these cells phenotypically and confirmed that they have high expression of activation and co-stimulatory molecules, in addition to expressing high levels of T-bet and the members of the FcRL family (i.e. FcRL2-5). Moreover, these cells are actively proliferating and a high proportion of them have a class-switched memory B cells phenotype expressing IgG. Interestingly, the transcriptome analysis showed that the ABCs are a subset of B cells, distinct from naïve, CD5+ and memory B cell subsets, with a unique transcriptome profile. ABCs had a high expression of chemokine receptors, such as CXCR3, as well as adhesion molecules, such as integrins and CD97, supporting a role for the migration of these cells into inflammatory sites. In addition, ABCs also had high expression of apoptotic markers, such as caspases and Fas. Finally, the functional characterisation of ABCs showed that these cells are capable of secreting IgM and IgG after stimulation. However, due to low cell numbers and high cell death, very low quantities of secreted cytokines were detected; making it very difficult to determine if these cells could contribute to inflammation. Due to the high expression of FcRL3 by ABCs I generated a stably transfected B cell line, which overexpressed FcRL3, in order to determine the role of FcRL3 on B cell function. However, due to time limitations these functional experiments were limited and I was unable to stimulate the FcRL3+ B cell line via FcRL3. I was able to perform a limited number of preliminary experiments simply stimulating the B cell line with a strong B cell stimulation cocktail and the only difference between the control and the FcRL3+ cells was in susceptibility to apoptosis, with FcRL3+ Ramos B cells being more prone to apoptosis. Further work is needed to clarify how cross-linking of the overexpressed FcRL3 receptor affects B cell function.

Overall, I confirmed that the ABC subset is an activated memory-like B cell subset which could potentially migrate into inflammatory sites and promote disease pathogenesis. However, exactly how these cells contribute to RA pathogenesis is still unknown and further functional work will help elucidate their role in autoimmunity. Nevertheless, in the next year I will investigate the possible role of CD97 expression on ABCs and its interaction with its ligand, CD55, expressed on synovial fibroblasts. This will aid in our

understanding of why these cells accumulate in the synovial fluid of patients with inflammatory arthritis.

Appendix A. Additional data

ABCB1	*C6*	*CD164*	*CD96*	*CXCL11*
ABL1	*C7*	*CD19*	*CD97*	*CXCL12*
ADA	*C8A*	*CD1A*	*CD99*	*CXCL13*
AHR	*C8B*	*CD1D*	*CDH5*	*CXCL2*
AICDA	*C8G*	*CD2*	*CDKN1A*	*CYBB*
AIRE	*C9*	*CD209*	*CEACAM1*	*DEFB1*
APP	*CAMP*	*CD22*	*CEACAM6*	*DEFB103A*
ARG1	*CARD9*	*CD24*	*CEACAM8*	*DEFB103B*
ARG2	*CASP1*	*CD244*	*CEBPB*	*DEFB4A*
ARHGDIB	*CASP10*	*CD247*	*CFB*	*DPP4*
ATG10	*CASP2*	*CD27*	*CFD*	*DUSP4*
ATG12	*CASP3*	*CD274*	*CFH*	*EBI3*
ATG16L1	*CASP8*	*CD276*	*CFI*	*EDNRB*
ATG5	*CCBP2*	*CD28*	*CFP*	*EGR1*
ATG7	*CCL11*	*CD34*	*CHUK*	*EGR2*
ATM	*CCL13*	*CD36*	*CIITA*	*ENTPD1*
B2M	*CCL15*	*CD3D*	*CISH*	*EOMES*
B3GAT1	*CCL16*	*CD3E*	*CLEC4A*	*ETS1*
BATF	*CCL18*	*CD3EAP*	*CLEC4E*	*FADD*
BATF3	*CCL19*	*CD4*	*CLEC5A*	*FAS*
BAX	*CCL2*	*CD40*	*CLEC6A*	*FCAR*
BCAP31	*CCL20*	*CD40LG*	*CLEC7A*	*FCER1A*
BCL10	*CCL22*	*CD44*	*CLU*	*FCER1G*
BCL2	*CCL23*	*CD46*	*CMKLR1*	*FCGR1A/B*
BCL2L11	*CCL24*	*CD48*	*CR1*	*FCGR2A*
BCL3	*CCL26*	*CD5*	*CR2*	*FCGR2A/C*
BCL6	*CCL3*	*CD53*	*CRADD*	*FCGR2B*
BID	*CCL4*	*CD55*	*CSF1*	*FCGR3A/B*
BLNK	*CCL5*	*CD58*	*CSF1R*	*FCGRT*
BST1	*CCL7*	*CD59*	*CSF2*	*FKBP5*
BST2	*CCL8*	*CD6*	*CSF2RB*	*FN1*
BTK	*CCND3*	*CD7*	*CSF3R*	*FOXP3*
BTLA	*CCR1*	*CD70*	*CTLA4_all (common probe)*	*FYN*
C14orf166	*CCR10*	*CD74*	*CTLA4-TM (membrane-bound form)*	*GATA3*
C1QA	*CCR2*	*CD79A*	*sCTLA4 (soluble form)*	*GBP1*
C1QB	*CCR5*	*CD79B*	*CTNNB1*	*GBP5*
C1QBP	*CCR6*	*CD80*	*CTSC*	*GFI1*
C1R	*CCR7*	*CD81*	*CTSG*	*GNLY*
C1S	*CCR8*	*CD82*	*CTSS*	*GP1BB*
C2	*CCRL1*	*CD83*	*CUL9*	*GPI*
C3	*CCRL2*	*CD86*	*CX3CL1*	*GPR183*
C4A/B	*CD14*	*CD8A*	*CX3CR1*	*GZMA*
C4BPA	*CD160*	*CD8B*	*CXCL1*	*GZMB*
C5	*CD163*	*CD9*	*CXCL10*	*GZMK*

HAMP	*IKZF3*	*IL4*	*KIR3DL3*	*MAP4K4*
HAVCR2	*IL10*	*IL4R*	*KIT*	*MAPK1*
HFE	*IL10RA*	*IL5*	*KLRAP1*	*MAPK11*
HLA-A	*IL11RA*	*IL6*	*KLRB1*	*MAPK14*
HLA-B	*IL12A*	*IL6R*	*KLRC1*	*MAPKAPK2*
HLA-C	*IL12B*	*IL6ST*	*KLRC2*	*MARCO*
HLA-DMA	*IL12RB1*	*IL7*	*KLRC3*	*MASP1*
HLA-DMB	*IL13*	*IL7R*	*KLRC4*	*MASP2*
HLA-DOB	*IL13RA1*	*IL8*	*KLRD1*	*MBL2*
HLA-DPA1	*IL15*	*IL9*	*KLRF1*	*MBP*
HLA-DPB1	*IL16*	*ILF3*	*KLRF2*	*MCL1*
HLA-DQA1	*IL17A*	*IRAK1*	*KLRG1*	*MIF*
HLA-DQB1	*IL17B*	*IRAK2*	*KLRG2*	*MME*
HLA-DRA	*IL17F*	*IRAK3*	*KLRK1*	*MR1*
HLA-DRB1	*IL18*	*IRAK4*	*LAG3*	*MRC1*
HLA-DRB3	*IL18R1*	*IRF1*	*LAIR1*	*MS4A1*
HRAS	*IL18RAP*	*IRF3*	*LAMP3*	*MSR1*
ICAM1	*IL19*	*IRF4*	*LCK*	*MUC1*
ICAM2	*IL1A*	*IRF5*	*LCP2*	*MX1*
ICAM3	*IL1B*	*IRF7*	*LEF1*	*MYD88*
ICAM4	*IL1R1*	*IRF8*	*LGALS3*	*NCAM1*
ICAM5	*IL1R2*	*IRGM*	*LIF*	*NCF4*
ICOS	*IL1RAP*	*ITGA2B*	*LILRA1*	*NCR1*
ICOSLG	*IL1RL1*	*ITGA4*	*LILRA2*	*NFATC1*
IDO1	*IL1RL2*	*ITGA5*	*LILRA3*	*NFATC2*
IFI16	*IL1RN*	*ITGA6*	*LILRA4*	*NFATC3*
IFI35	*IL2*	*ITGAE*	*LILRA5*	*NFIL3*
IFIH1	*IL20*	*ITGAL*	*LILRA6*	*NFKB1*
IFIT2	*IL21*	*ITGAM*	*LILRB1*	*NFKB2*
IFITM1	*IL21R*	*ITGAX*	*LILRB2*	*NFKBIA*
IFNA1/13	*IL22*	*ITGB1*	*LILRB3*	*NFKBIZ*
IFNA2	*IL22RA2*	*ITGB2*	*LILRB4*	*NLRP3*
IFNAR1	*IL23A*	*ITLN1*	*LILRB5*	*NOD1*
IFNAR2	*IL23R*	*ITLN2*	*LITAF*	*NOD2*
IFNB1	*IL26*	*JAK1*	*LTA*	*NOS2*
IFNG	*IL27*	*JAK2*	*LTB4R*	*NOTCH1*
IFNGR1	*IL28A*	*JAK3*	*LTB4R2*	*NOTCH2*
IGF2R	*IL28A/B*	*KCNJ2*	*LTBR*	*NT5E*
IKBKAP	*IL29*	*KIR_Activating _ Subgroup_1*	*LTF*	*PAX5*
IKBKB	*IL2RA*	*KIR_Activating _ Subgroup_2*	*LY96*	*PDCD1*
IKBKE	*IL2RB*	*KIR_Inhibiting _ Subgroup_1*	*MAF*	*PDCD1LG2*
IKBKG	*IL2RG*	*KIR_Inhibiting _ Subgroup_2*	*MALT1*	*PDCD2*
IKZF1	*IL3*	*KIR3DL1*	*MAP4K1*	*PDGFB*
IKZF2	*IL32*	*KIR3DL2*	*MAP4K2*	*PDGFRB*

PECAM1	*SELL*	*TLR3*	*ZEB1*
PIGR	*SELPLG*	*TLR4*	
PLA2G2A	*SERPING1*	*TLR5*	
PLA2G2E	*SH2D1A*	*TLR7*	
PLAU	*SIGIRR*	*TLR8*	
PLAUR	*SKI*	*TLR9*	
PML	*SLAMF1*	*TMEM173*	
POU2F2	*SLAMF6*	*TNF*	
PPARG	*SLAMF7*	*TNFAIP3*	
PPBP	*SLC2A1*	*TNFAIP6*	
PRDM1	*SMAD3*	*TNFRSF10C*	
PRF1	*SMAD5*	*TNFRSF11A*	
PRKCD	*SOCS1*	*TNFRSF13B*	
PSMB10	*SOCS3*	*TNFRSF13C*	
PSMB5	*SPP1*	*TNFRSF14*	
PSMB7	*SRC*	*TNFRSF17*	
PSMB8	*STAT1*	*TNFRSF1B*	
PSMB9	*STAT2*	*TNFRSF4*	
PSMC2	*STAT3*	*TNFRSF8*	
PSMD7	*STAT4*	*TNFRSF9*	
PTAFR	*STAT5A*	*TNFSF10*	
PTGER4	*STAT5B*	*TNFSF11*	
PTGS2	*STAT6*	*TNFSF12*	
PTK2	*SYK*	*TNFSF13B*	
PTPN2	*TAGAP*	*TNFSF15*	
PTPN22	*TAL1*	*TNFSF4*	
PTPN6	*TAP1*	*TNFSF8*	
PTPRC_all (common probe)	*TAP2*	*TOLLIP*	
CD45R0	*TAPBP*	*TP53*	
CD45RA	*TBK1*	*TRAF1*	
CD45RB	*TBX21*	*TRAF2*	
PYCARD	*TCF4*	*TRAF3*	
RAF1	*TCF7*	*TRAF4*	
RAG1	*TFRC*	*TRAF5*	
RAG2	*TGFB1*	*TRAF6*	
RARRES3	*TGFBI*	*TYK2*	
RELA	*TGFBR1*	*UBE2L3*	
RELB	*TGFBR2*	*VCAM1*	
RORC	*THY1*	*VTN*	
RUNX1	*TICAM1*	*XBP1*	
S100A8	*TIGIT*	*XCL1*	
S100A9	*TIRAP*	*XCR1*	
S1PR1	*TLR1*	*ZAP70*	
SELE	*TLR2*	*ZBTB16*	

Appendix A. 1. Full list of genes included on NanoString nCounter Human Immunology V2 Panel.

Customised probe	Sequence
AluYa5	GGAAGAAGGGGGCCGGGCGCGGTGGCTCACGCCTGTAA TCCCAGCACTTTGGGAGGCCGAGGCGGGCGGATCACGA GGTCAGGAGATCGAGACCATCCCGGCTAAAACGGTGAA ACCCCGTCTCTACTAAAAATACAAAAAATTAGCCGGGC GTAGTGGCGGGCGCCTGTAGTCCCAGCTACTTGGGAGG CTGAGGCAGGAGAATGGCGTGAACCCGGGAGGCGGAG CTTGCAGTGAGCCGAGATCCCGCCACTGCACTCCAGCCT GGGCGACAGAGCGAGACTCCGTC
AluYb9	GTAGGCAATGGGCCGGGCGCGGTGGCTCACGCCTGTAA TCCCAGCACTTTGGGAGGCCGAGGCGGGTGGATCATGA GGTCAGGAGATCGAGACCATCCTGGCTAACAAGGTGAA ACCCCGTCTCTACTAAAAATACAAAAAATTAGCCGGGC GCGGTGGCGGGCGCCTGTAGTCCCAGCTACTGGGGAGG CTGAGGCAGGAGAATGGCGTGAACCCGGGAAGCGGAG CTTGCAGTGAGCCGAGATTGCGCCACTGCAGTCCGCAG TCCGGCCTGGGCGACAGAGCGAGACTCCGTC
LTR5 5' end	AAGGGGGAAATGTGGGGAAAAGCAAGAGAGATCAGAT TGTTACTGTGTCTGTGTAGAAAGAAGTAGACATAGGAG ACTCCATTTTGTTATGTACTAAGAAAAATTCTTCTGCCTT GAGATTCTGTTAATCTATGACCTTACCCCCAACCCCGTG CTCTCTGAAACATGTGCTGTGTCCACTCAGAGTTGAATG GATTAAGGGCGGTGCAGGATGTGCTTTGTTAAACAGAT GCTTGAAGGCAGCATGCTCCTTAAGAGTCATCACCACTC CCTAATCTCAAGTACCCAGGGACACAAAAA
LTR5 3'end	GGTGGGACCTGCGGGCAGCAATACTGCTTTGTAAAGCA CTGAGATGTTTATGTGTATGCATATCTAAAAGCACAGCA CTTAATCCTTTACATTGTCTATGATGCAAAGACCTTTGTT CACATGTTTGTCTGCTGACCCTCTCCCCACAATTGTCTT GTGACCCTGACACATCCCCCTCTTCGAGAAACACCCAC AGATGATCAATAAATACTAAGGGAACTCAGAGGCTGGC GGGATCCTCCATATGCTGAACGCTGGTTCCCCGGGTCCC CTTCTTTCTTTCTCTATACTTTGTCTCTGTGTCTTTTTCTT TTCCAAATCTCTCGTCCCACCTTACGAGAAACACCCACA GGTGTG
L1 5'UTR	GGGGGAGGAGCCAAGATGGCCGAATAGGAACAGCTCC GGTCTACAGCTCCCAGCGTGAGCGACGCAGAAGACGGT GATTTCTGCATTTCCATCTGAGGTACCGGGTTCATCTCA CTAGGGAGTGCCAGACAGTGGGCGCAGGCCAGTGTGTG TGCGCACCGTGCGCGAGCCGAAGCAGGGCGAGGCATTG CCTCACCTGGGAAGCGCAAGGGGTCAGGGAGTTCCCTT TCCGAGTCAAAGAAAGGGGTGACGGACGCACCTGGAA AATC
L1 ORF2	GTAGGGACATGGATGAAATTGGAAACCATCATTCTCAG TAAACTATCGCAAGAACAAAAAACCAAACACCGCATAT TCTCACTCATAGGTGGGAATTGAACAATGAGATCACAT GGACACAGGAAGGGGAATATCACACTCTGGGGACTGTG GTGGGGTCGGGGGAGGGGGGAGGGATAGCATTGGGAG ATATACCTAATGCTAGATGACACATTAGTGGGTGCAGC GCACCAGCATGGCACATGTATACATATGTAACTAACCT GCACAATGTGCACATGTACCCTAAAACTTAGAGTATAA

Appendix A. 2. Sequences of customised probes, designed by Dr Faye Cooles, and used in NanoString panel plus nCounter to identify retroelement activity.

Appendix A.3. Demographic characteristics in each phenotypic panel in eRA patients.

All panels in eRA	Activation	FcRLs	Intracellular	Igs	Difference between groups
Number	8	11	11	15	-
Age (years; median and range)	64.5 (33 - 84)	69 (33 - 84)	69 (33 - 84)	73 (51 - 82)	0.74[#]
Percentage of females (n and percentage)	5 (62.5%)	7 (63.6%)	7 (63.6%)	11 (73.3%)	0.92[+]
DAS28 (median and range)	4.97 (1.33 - 7.01)	5.24 (1.33 – 7.01)	5.24 (1.33 – 7.01)	5.14 (2.4 – 6.21)	0.96[#]
Seropositive – anti-CCP+ or RhF+ (n and percentage)	5 (62.5%)	7 (63.6%)	7 (63.6%)	10 (66.6%)	0.99[+]

Appendix A. 3. Comparison of the demographic characteristics for each phenotypic panel in eRA patients. Early RA patients' demographic characteristics were recorded and the characteristics for each cohort of patients used for the different flow cytometry panels was compared. # Kruskal-Wallis test with Dunn's multiple comparisons. + Chi-square test.

Appendix A.4. Demographic characteristics for each phenotypic panel.

Activation panel

Activation panel	Early RA patients	Early DC patients	Established RA patients	Healthy controls	Difference between groups
Number	8	14	8	6	-
Age (years; median and range)	64.5 (33 - 84)	52 (20 - 93)	62.5 (50 - 84)	61.5 (53 - 64)	0.03#
Percentage of females (n and percentage)	5 (62.5%)	8 (57%)	5 (62.5%)	3 (50%)	0.96+
DAS28 (median and range)	4.97 (1.33 - 7.01)	3.4 (1.54 – 7.06)	2.58 (0.68 – 3.74)	-	0.058#
Seropositive – anti-CCP+ or RhF+ (n and percentage)	5 (62.5%)	2 (14%)	7 (87.5%)	-	0.0024+

Table A. 1. Demographic characteristics for all the cohorts used for the activation panel. Demographical data for the disease cohorts: early RA patients, n=8; early DC patients, n=14; established RA patients, n=8; and the healthy control cohort (n=6) used for the activation panel. # Kruskal-Wallis test with Dunn's multiple comparisons. + Chi-square test.

FcRLs panel

FcRLs panel	Early RA patients	Early DC patients	Established RA patients	Healthy controls	Difference between groups
Number	11	15	8	8	-
Age (years; median and range)	69 (33 - 84)	52 (20 - 93)	62.5 (50 - 84)	61 (51 - 64)	0.024#
Percentage of females (n and percentage)	7 (63.6%)	8 (53.3%)	5 (62.5%)	5 (62.5%)	0.94+
DAS28 (median and range)	5.24 (1.33 – 7.01)	3.3 (1.54 – 7.06)	2.58 (0.68 – 3.74)	-	0.015#
Seropositive – anti-CCP+ or RhF+ (n and percentage)	7 (63.6%)	4 (26.6%)	7 (87.5%)	-	0.014+

Table A. 2. Demographic characteristics for all the cohorts used for the FcRLs panel. Demographical data for the disease cohorts: early RA patients, n=11; early DC patients, n=15; established RA patients, n=8; and the healthy control cohort (n=8) used for the FcRLs panel. # Kruskal-Wallis test with Dunn's multiple comparisons. + Chi-square test.

Immunoglobulins panel

Immunoglobulins panel	Early RA patients	Early DC patients	Established RA patients	Healthy controls	Difference between groups
Number	15	12	4	8	-
Age (years; median and range)	73 (51 - 82)	48.5 (32 - 74)	67.5 (48 - 72)	59.5 (50 - 73)	0.0006#
Percentage of females (n and percentage)	11 (73.3%)	4 (33.3%)	3 (75%)	5 (62.5%)	0.17+
DAS28 (median and range)	5.14 (2.4 – 6.21)	3.42 (1.05 – 5.17)	-	-	0.006‡
Seropositive – anti-CCP+ or RhF+ (n and percentage)	10 (66.6%)	3 (25%)	4 (100%)	-	0.014+

Table A. 3. Demographic characteristics for all the cohorts used for the immunoglobulins panel. Demographical data for the disease cohorts: early RA patients, n=15; early DC patients, n=12; established RA patients, n=4; and the healthy control cohort (n=8) used for the immunoglobulins panel. # Kruskal-Wallis test with Dunn's multiple comparisons. + Chi-square test.

Intracellular panel

Intracellular panel	Early RA patients	Early DC patients	Established RA patients	Healthy controls	Difference between groups
Number	11	15	10	8	-
Age (years; median and range)	69 (33 - 84)	52 (20 - 93)	65.5 (50 - 84)	61 (51 - 64)	0.013#
Percentage of females (n and percentage)	7 (63.6%)	8 (53.3%)	6 (60%)	5 (62.5%)	0.95+
DAS28 (median and range)	5.24 (1.33 – 7.01)	3.3 (1.54 - 7.06)	2.58 (0.68 – 3.74)	-	0.016#
Seropositive – anti-CCP+ or RhF+ (n and percentage)	7 (63.6%)	3 (20%)	9 (90%)	-	0.002+

Table A. 4. Demographic characteristics for all the cohorts used for the intracellular panel. Demographical data for the disease cohorts: early RA patients, n=11; early DC patients, n=15; established RA patients, n=10; and the healthy control cohort (n=8) used for the intracellular panel. # Kruskal-Wallis test with Dunn's multiple comparisons. + Chi-square test.

FcRL1 panel

FcRL1 panel	Early RA patients	Early DC patients	Established RA patients	Healthy controls	Difference between groups
Number	9	7	11	8	-
Age (years; median and range)	62 (28 - 82)	39 (20 - 57)	64 (48 - 84)	61.5 (50 - 64)	0.009#
Percentage of females (n and percentage)	8 (88.8%)	4 (57.1%)	8 (72.7%)	4 (50%)	0.32+
DAS28 (median and range)	5.11 (3.2 – 6.37)	3.3 (2.03 – 7.06)	2.58 (0.68 – 3.74)	-	0.006#
Seropositive – anti-CCP+ or RhF+ (n and percentage)	6 (66.6%)	0 (0%)	10 (90%)	-	0.0006+

Table A. 5. Demographic characteristics for all the cohorts used for the FcRL1 panel. Demographical data for the disease cohorts: early RA patients, n=9; early DC patients, n=7; established RA patients, n=11; and the healthy control cohort (n=8) used for the FcRL1 panel. # Kruskal-Wallis test with Dunn's multiple comparisons. + Chi-square test.

FcRL2 panel

FcRL2 panel	Early RA patients	Early DC patients	Established RA patients	Healthy controls	Difference between groups
Number	10	10	5	6	-
Age (years; median and range)	57 (31 - 89)	40.5 (22 - 76)	68 (48 - 73)	57 (50 - 62)	0.22#
Percentage of females (n and percentage)	3 (30%)	5 (50%)	4 (80%)	4 (66.6%)	0.26+
DAS28 (median and range)	3.8 (1.9 – 5)	4.2 (1.05 – 5.89)	-	-	0.54ǂ
Seropositive – anti-CCP+ or RhF+ (n and percentage)	7 (70%)	3 (30%)	5 (100%)	-	0.02+

Table A. 6. Demographic characteristics for all the cohorts used for the FcRL2 panel. Demographical data for the disease cohorts: early RA patients, n=10; early DC patients, n=10; established RA patients, n=5; and the healthy control cohort (n=6) used for the FcRL2 panel. # Kruskal-Wallis test with Dunn's multiple comparisons. + Chi-square test. ǂ Mann Whitney test.

Appendix A.5. BLAST analysis of the FcRL3 transcript contained in the pcDNA3 plasmid using the EMBOSS Needle Tool (EMBL-EBI, Hinxton, UK).

Forward sequencing alignment:

```
EMBOSS_001        85 GGTACCGAGCTCGGATCCACTAGTAACGGCCGCCAGTGTGCTGGAATTCT    134
                     ||||||||||||||||||||||||||||||||||||||||||||||||||||
EMBOSS_001       951 GGTACCGAGCTCGGATCCACTAGTAACGGCCGCCAGTGTGCTGGAATTCT   1000

EMBOSS_001       135 GCAGATATCAAAGCCACCATGCTTCTGTGGCTGCTGCTGCTGATCCTGAC    184
                     ||||||||||||||||||||||||||||||||||||||||||||||||||||
EMBOSS_001      1001 GCAGATATCAAAGCCACCATGCTTCTGTGGCTGCTGCTGCTGATCCTGAC   1050

EMBOSS_001       185 TCCTGGAAGAGAACAATCAGGGGTGGCCCCAAAAGCTGTACTTCTCCTCA    234
                     ||||||||||||||||||||||||||||||||||||||||||||||||||||
EMBOSS_001      1051 TCCTGGAAGAGAACAATCAGGGGTGGCCCCAAAAGCTGTACTTCTCCTCA   1100

EMBOSS_001       235 ATCCTCCATGGTCCACAGCCTTCAAAGGAGAAAAAGTGGCTCTCATATGC    284
                     ||||||||||||||||||||||||||||||||||||||||||||||||||||
EMBOSS_001      1101 ATCCTCCATGGTCCACAGCCTTCAAAGGAGAAAAAGTGGCTCTCATATGC   1150

EMBOSS_001       285 AGCAGCATATCACATTCCCTAGCCCAGGGAGACACATATTGGTATCACGA    334
                     ||||||||||||||||||||||||||||||||||||||||||||||||||||
EMBOSS_001      1151 AGCAGCATATCACATTCCCTAGCCCAGGGAGACACATATTGGTATCACGA   1200

EMBOSS_001       335 TGAGAAGTTGTTGAAAATAAAACATGACAAGATCCAAATTACAGAGCCTG    384
                     ||||||||||||||||||||||||||||||||||||||||||||||||||||
EMBOSS_001      1201 TGAGAAGTTGTTGAAAATAAAACATGACAAGATCCAAATTACAGAGCCTG   1250

EMBOSS_001       385 GAAATTACCAATGTAAGACCCGAGGATCCTCCCTCAGTGATGCCGTGCAT    434
                     ||||||||||||||||||||||||||||||||||||||||||||||||||||
EMBOSS_001      1251 GAAATTACCAATGTAAGACCCGAGGATCCTCCCTCAGTGATGCCGTGCAT   1300

EMBOSS_001       435 GTGGAATTTTCACCTGACTGGCTGATCCTGCAGGCTTTACATCCTGTCTT    484
                     ||||||||||||||||||||||||||||||||||||||||||||||||||||
EMBOSS_001      1301 GTGGAATTTTCACCTGACTGGCTGATCCTGCAGGCTTTACATCCTGTCTT   1350

EMBOSS_001       485 TGAAGGAGACAATGTCATTCTGAGATGTCAGGGGAAAGACAACAAAAACA    534
                     ||||||||||||||||||||||||||||||||||||||||||||||||||||
EMBOSS_001      1351 TGAAGGAGACAATGTCATTCTGAGATGTCAGGGGAAAGACAACAAAAACA   1400

EMBOSS_001       535 CTCATCAAAAGGTTTACTACAAGGATGGAAAACAGCTTCCTAATAGTTAT    584
                     ||||||||||||||||||||||||||||||||||||||||||||||||||||
EMBOSS_001      1401 CTCATCAAAAGGTTTACTACAAGGATGGAAAACAGCTTCCTAATAGTTAT   1450

EMBOSS_001       585 AATTTAGAGAAGATCACAGTGAATTCAGTCTCCAGGGATAATAGCAAATA    634
                     ||||||||||||||||||||||||||||||||||||||||||||||||||||
EMBOSS_001      1451 AATTTAGAGAAGATCACAGTGAATTCAGTCTCCAGGGATAATAGCAAATA   1500

EMBOSS_001       635 TCATTGTACTGCTTATAGGAAGTTTTACATACTTGACATTGAAGTAACTT    684
                     ||||||||||||||||||||||||||||||||||||||||||||||||||||
EMBOSS_001      1501 TCATTGTACTGCTTATAGGAAGTTTTACATACTTGACATTGAAGTAACTT   1550

EMBOSS_001       685 CAAAACCCCTAAATATCCAAGTTCAAGAGCTGTTTCTACATCCTGTGCTG    734
                     ||||||||||||||||||||||||||||||||||||||||||||||||||||
EMBOSS_001      1551 CAAAACCCCTAAATATCCAAGTTCAAGAGCTGTTTCTACATCCTGTGCTG   1600

EMBOSS_001       735 AGAGCCAGCTCTTCCACGCCCATAGAGGGGAGTCCCATGACCCTGACCTG    784
                     ||||||||||||||||||||||||||||||||||||||||||||||||||||
EMBOSS_001      1601 AGAGCCAGCTCTTCCACGCCCATAGAGGGGAGTCCCATGACCCTGACCTG   1650

EMBOSS_001       785 TGAGACCCAGCTCTCTCCACAGAGGCCAGATGTCCAGCTGCAATTCTCCC    834
                     ||||||||||||||||||||||||||||||||||||||||||||||||||||
EMBOSS_001      1651 TGAGACCCAGCTCTCTCCACAGAGGCCAGATGTCCAGCTGCAATTCTCCC   1700
```

```
EMBOSS_001       835 TCTTCAGAGATAGCCAGACCCTCGGATTGGGCTGGAGCAGGTCCCCCAGA   884
                     ||||||||||||||||||||||||||||||||||||||||||||||||||
EMBOSS_001      1701 TCTTCAGAGATAGCCAGACCCTCGGATTGGGCTGGAGCAGGTCCCCCAGA  1750

EMBOSS_001       885 CTCCAGATCCCTGCCATGTGGACTGAAGACTCAGGGTCTTACTGGTGTGA   934
                     ||||||||||||||||||||||||||||||||||||||||||||||||||
EMBOSS_001      1751 CTCCAGATCCCTGCCATGTGGACTGAAGACTCAGGGTCTTACTGGTGTGA  1800

EMBOSS_001       935 GGTGGAGACAGTGACTCACAGCATCAAAAAAAGGAGCCTGAGATCTCAGA   984
                     ||||||||||||||||||||||||||||||||||||||||||||||||||
EMBOSS_001      1801 GGTGGAGACAGTGACTCACAGCATCAAAAAAAGGAGCCTGAGATCTCAGA  1850

EMBOSS_001       985 TACGTGTACAGAGAGTCCCTGTGTCTAATGTGAATCTAGAGATCCGGCCC   1034
                     ||||||||||||||||||||||||||||||||||||||||||||||||||
EMBOSS_001      1851 TACGTGTACAGAGAGTCCCTGTGTCTAATGTGAATCTAGAGATCCGGCCC  1900

EMBOSS_001      1035 ACCGGAGGGCAGCTGATTGAAGGAGAAAATATGGTCCTTATTTGCTCAGT  1084
                     ||||||||||||||||||||||||||||||||||||||||||||||||||
EMBOSS_001      1901 ACCGGAGGGCAGCTGATTGAAGGAGAAAATATGGTCCTTATTTGCTCAGT  1950

EMBOSS_001      1085 AGCCCAGGGTTCAGGGACTGTCACATTCTCCTGGCACAAAGAAGGAAGAG  1134
                     ||||||||||||||||||||||||||||||||||||||||||||||||||
EMBOSS_001      1951 AGCCCAGGGTTCAGGGACTGTCACATTCTCCTGGCACAAAGAAGGAAGAG  2000

EMBOSS_001      1135 TAAGAAGCCTGGGTAGAAAGACCCAGCGTTCCCTGTTGGCAGAGCTGCAT  1184
                     ||||||||||||||||||||||||||||||||||||||||||||||||||
EMBOSS_001      2001 TAAGAAGCCTGGGTAGAAAGACCCAGCGTTCCCTGTTGGCAGAGCTGCAT  2050

EMBOSS_001      1185 GTTCTCACCGTGAAGGAGAGTGATGCAGGGAGATACTACTGTGCAGCTGA  1234
                     ||||||||||||||||||||||||||||||||||||||||||||||||||
EMBOSS_001      2051 GTTCTCACCGTGAAGGAGAGTGATGCAGGGAGATACTACTGTGCAGCTGA  2100

EMBOSS_001      1235 TAACGTTCACAGCCCCATCCTCAGCACGTGGATTCGAGTCACCGTGAGAA  1284
                     ||||||||||||||||||||||||||||||||||||||||||||||||||
EMBOSS_001      2101 TAACGTTCACAGCCCCATCCTCAGCACGTGGATTCGAGTCACCGTGAGAA  2150

EMBOSS_001      1285 TTCCGGTATCTCACCCTGTCCTCACCTTCAGGGCTCCCAGGGCCCACACT  1334
                     ||||||||||||||||||||||||||||||||||||||||||||||||||
EMBOSS_001      2151 TTCCGGTATCTCACCCTGTCCTCACCTTCAGGGCTCCCAGGGCCCACACT  2200

EMBOSS_001      1335 GTGGTGGGGGACCTGCTGGAGCTTCACTGTGAGTCCCTGAGAGGCTCTCC  1384
                     ||||||||||||||||||||||||||||||||||||||||||||||||||
EMBOSS_001      2201 GTGGTGGGGGACCTGCTGGAGCTTCACTGTGAGTCCCTGAGAGGCTCTCC  2250

EMBOSS_001      1385 CCCGATCCTGTACCGATTTTATCATGAGGATGTCACCCTGGGGAACAGCT  1434
                     ||||||||||||||||||||||||||||||||||||||||||||||||||
EMBOSS_001      2251 CCCGATCCTGTACCGATTTTATCATGAGGATGTCACCCTGGGGAACAGCT  2300

EMBOSS_001      1435 CAGCCCCCTCTGGAGGAGGAGCCTCCTTCAACCTCTCTCTGACTGCAGAA  1484
                     ||||||||||||||||||||||||||||||||||||||||||||||||||
EMBOSS_001      2301 CAGCCCCCTCTGGAGGAGGAGCCTCCTTCAACCTCTCTCTGACTGCAGAA  2350

EMBOSS_001      1485 CATTCTGGAAACTACTCCTGTGATGCAGACAATGGCCTGGGGGCCCAGCA  1534
                     ||||||||||||||||||||||||||||||||||||||||||||||||||
EMBOSS_001      2351 CATTCTGGAAACTACTCCTGTGATGCAGACAATGGCCTGGGGGCCCAGCA  2400

EMBOSS_001      1535 CAGTCATGGAGTGAGTCTCAGGGTCACAGTTCCGGTGTCTCGCCCCGTCC  1584
                     ||||||||||||||||||||||||||||||||||||||||||||||||||
EMBOSS_001      2401 CAGTCATGGAGTGAGTCTCAGGGTCACAGTTCCGGTGTCTCGCCCCGTCC  2450

EMBOSS_001      1585 TCACCCTCAGGGCTCCCGGGGCCCAGGCTGTGGTGGGGGACCTGCTGGAG  1634
                     ||||||||||||||||||||||||||||||||||||||||||||||||||
EMBOSS_001      2451 TCACCCTCAGGGCTCCCGGGGCCCAGGCTGTGGTGGGGGACCTGCTGGAG  2500

EMBOSS_001      1635 CTTCACTGTGAGTCCCTGAGAGGCTCCTTCCCGATCCTGTACTGGTTTTA  1684
                     ||||||||||||||||||||||||||||||||||||||||||||||||||
EMBOSS_001      2501 CTTCACTGTGAGTCCCTGAGAGGCTCCTTCCCGATCCTGTACTGGTTTTA  2550
```

```
EMBOSS_001      1685 TCACGAGGATGACACCTTGGGGAACATCTCGGCCCACTCTGGAGGAGGGG   1734
                     ||||||||||||||||||||||||||||||||||||||||||||||||||
EMBOSS_001      2551 TCACGAGGATGACACCTTGGGGAACATCTCGGCCCACTCTGGAGGAGGGG   2600

EMBOSS_001      1735 CATCCTTCAACCTCTCTCTGACTACAGAACATTCTGGAAACTACTCATGT   1784
                     ||||||||||||||||||||||||||||||||||||||||||||||||||
EMBOSS_001      2601 CATCCTTCAACCTCTCTCTGACTACAGAACATTCTGGAAACTACTCATGT   2650

EMBOSS_001      1785 GAGGCTGACAATGGCCTGGGGGCCCAGCACAGTAAAGTGGTGACACTCAA   1834
                     ||||||||||||||||||||||||||||||||||||||||||||||||||
EMBOSS_001      2651 GAGGCTGACAATGGCCTGGGGGCCCAGCACAGTAAAGTGGTGACACTCAA   2700

EMBOSS_001      1835 TGTTACAGGAACTTCCAGGAACAGAACAGGCCTTACCGCTGCGGGAATCA   1884
                     ||||||||||||||||||||||||||||||||||||||||||||||||||
EMBOSS_001      2701 TGTTACAGGAACTTCCAGGAACAGAACAGGCCTTACCGCTGCGGGAATCA   2750

EMBOSS_001      1885 CGGGGCTGGTGCTCAGCATCCTCGTCCTTGCTGCTGCTGCTGCTCTGCTG   1934
                     ||||||||||||||||||||||||||||||||||||||||||||||||||
EMBOSS_001      2751 CGGGGCTGGTGCTCAGCATCCTCGTCCTTGCTGCTGCTGCTCTGCTG     2800

EMBOSS_001      1935 CATTACGCCAGGGCCCGAAGGAAACCAGGAGGACTTTCTGCCACTGGAAC   1984
                     ||||||||||||||||||||||||||||||||||||||||||||||||||
EMBOSS_001      2801 CATTACGCCAGGGCCCGAAGGAAACCAGGAGGACTTTCTGCCACTGGAAC   2850

EMBOSS_001      1985 ATCTAGTCACAGTCCTAGTGAGTGTCAGGAGCCTTCCTCGTCCAGGCCTT   2034
                     ||||||||||||||||||||||||||||||||||||||||||||||||||
EMBOSS_001      2851 ATCTAGTCACAGTCCTAGTGAGTGTCAGGAGCCTTCCTCGTCCAGGCCTT   2900

EMBOSS_001      2035 CCAGGATAGACCCTCAAGAGCCCACTCACTCTAAACCACTAGCCCCAATG   2084
                     ||||||||||||||||||||||||||||||||||||||||||||||||||
EMBOSS_001      2901 CCAGGATAGACCCTCAAGAGCCCACTCACTCTAAACCACTAGCCCCAATG   2950

EMBOSS_001      2085 GAGCTGGAGCCAATGTACAGCAATGTAAATCCTGGAGATAGCAACCCGAT   2134
                     ||||||||||||||||||||||||||||||||||||||||||||||||||
EMBOSS_001      2951 GAGCTGGAGCCAATGTACAGCAATGTAAATCCTGGAGATAGCAACCCGAT   3000
```

Reverse sequencing alignment:

```
EMBOSS_001       981 CGCCAGTGTGCTGGAATTCTGCAGATATCAAAGCCACCATGCTTCTGTGG   1030
                     ||     ||||                          ||||||||||||||
EMBOSS_001       285 CG-----GTGC-------------------------CCATGCTTCTGTGG    304

EMBOSS_001      1031 CTGCTGCTGCTGATCCTGACTCCTGGAAGAGAACAATCAGGGGTGGCCCC   1080
                     ||||||||||||||||||||||||||||||||||||||||||||||||||
EMBOSS_001       305 CTGCTGCTGCTGATCCTGACTCCTGGAAGAGAACAATCAGGGGTGGCCCC    354

EMBOSS_001      1081 AAAAGCTGTACTTCTCCTCAATCCTCCATGGTCCACAGCCTTCAAAGGAG   1130
                     ||||||||||||||||||||||||||||||||||||||||||||||||||
EMBOSS_001       355 AAAAGCTGTACTTCTCCTCAATCCTCCATGGTCCACAGCCTTCAAAGGAG    404

EMBOSS_001      1131 AAAAAGTGGCTCTCATATGCAGCAGCATATCACATTCCCTAGCCCAGGGA   1180
                     ||||||||||||||||||||||||||||||||||||||||||||||||||
EMBOSS_001       405 AAAAAGTGGCTCTCATATGCAGCAGCATATCACATTCCCTAGCCCAGGGA    454

EMBOSS_001      1181 GACACATATTGGTATCACGATGAGAAGTTGTTGAAAATAAAACATGACAA   1230
                     ||||||||||||||||||||||||||||||||||||||||||||||||||
EMBOSS_001       455 GACACATATTGGTATCACGATGAGAAGTTGTTGAAAATAAAACATGACAA    504

EMBOSS_001      1231 GATCCAAATTACAGAGCCTGGAAATTACCAATGTAAGACCCGAGGATCCT   1280
                     ||||||||||||||||||||||||||||||||||||||||||||||||||
EMBOSS_001       505 GATCCAAATTACAGAGCCTGGAAATTACCAATGTAAGACCCGAGGATCCT    554

EMBOSS_001      1281 CCCTCAGTGATGCCGTGCATGTGGAATTTTCACCTGACTGGCTGATCCTG   1330
                     ||||||||||||||||||||||||||||||||||||||||||||||||||
EMBOSS_001       555 CCCTCAGTGATGCCGTGCATGTGGAATTTTCACCTGACTGGCTGATCCTG    604
```

```
EMBOSS_001      1331 CAGGCTTTACATCCTGTCTTTGAAGGAGACAATGTCATTCTGAGATGTCA  1380
                     ||||||||||||||||||||||||||||||||||||||||||||||||||
EMBOSS_001       605 CAGGCTTTACATCCTGTCTTTGAAGGAGACAATGTCATTCTGAGATGTCA   654

EMBOSS_001      1381 GGGGAAAGACAACAAAAACACTCATCAAAAGGTTTACTACAAGGATGGAA  1430
                     ||||||||||||||||||||||||||||||||||||||||||||||||||
EMBOSS_001       655 GGGGAAAGACAACAAAAACACTCATCAAAAGGTTTACTACAAGGATGGAA   704

EMBOSS_001      1431 AACAGCTTCCTAATAGTTATAATTTAGAGAAGATCACAGTGAATTCAGTC  1480
                     ||||||||||||||||||||||||||||||||||||||||||||||||||
EMBOSS_001       705 AACAGCTTCCTAATAGTTATAATTTAGAGAAGATCACAGTGAATTCAGTC   754

EMBOSS_001      1481 TCCAGGGATAATAGCAAATATCATTGTACTGCTTATAGGAAGTTTTACAT  1530
                     ||||||||||||||||||||||||||||||||||||||||||||||||||
EMBOSS_001       755 TCCAGGGATAATAGCAAATATCATTGTACTGCTTATAGGAAGTTTTACAT   804

EMBOSS_001      1531 ACTTGACATTGAAGTAACTTCAAAACCCCTAAATATCCAAGTTCAAGAGC  1580
                     ||||||||||||||||||||||||||||||||||||||||||||||||||
EMBOSS_001       805 ACTTGACATTGAAGTAACTTCAAAACCCCTAAATATCCAAGTTCAAGAGC   854

EMBOSS_001      1581 TGTTTCTACATCCTGTGCTGAGAGCCAGCTCTTCCACGCCCATAGAGGGG  1630
                     ||||||||||||||||||||||||||||||||||||||||||||||||||
EMBOSS_001       855 TGTTTCTACATCCTGTGCTGAGAGCCAGCTCTTCCACGCCCATAGAGGGG   904

EMBOSS_001      1631 AGTCCCATGACCCTGACCTGTGAGACCCAGCTCTCTCCACAGAGGCCAGA  1680
                     ||||||||||||||||||||||||||||||||||||||||||||||||||
EMBOSS_001       905 AGTCCCATGACCCTGACCTGTGAGACCCAGCTCTCTCCACAGAGGCCAGA   954

EMBOSS_001      1681 TGTCCAGCTGCAATTCTCCCTCTTCAGAGATAGCCAGACCCTCGGATTGG  1730
                     ||||||||||||||||||||||||||||||||||||||||||||||||||
EMBOSS_001       955 TGTCCAGCTGCAATTCTCCCTCTTCAGAGATAGCCAGACCCTCGGATTGG  1004

EMBOSS_001      1731 GCTGGAGCAGGTCCCCCAGACTCCAGATCCCTGCCATGTGGACTGAAGAC  1780
                     ||||||||||||||||||||||||||||||||||||||||||||||||||
EMBOSS_001      1005 GCTGGAGCAGGTCCCCCAGACTCCAGATCCCTGCCATGTGGACTGAAGAC  1054

EMBOSS_001      1781 TCAGGGTCTTACTGGTGTGAGGTGGAGACAGTGACTCACAGCATCAAAAA  1830
                     ||||||||||||||||||||||||||||||||||||||||||||||||||
EMBOSS_001      1055 TCAGGGTCTTACTGGTGTGAGGTGGAGACAGTGACTCACAGCATCAAAAA  1104

EMBOSS_001      1831 AAGGAGCCTGAGATCTCAGATACGTGTACAGAGAGTCCCTGTGTCTAATG  1880
                     ||||||||||||||||||||||||||||||||||||||||||||||||||
EMBOSS_001      1105 AAGGAGCCTGAGATCTCAGATACGTGTACAGAGAGTCCCTGTGTCTAATG  1154

EMBOSS_001      1881 TGAATCTAGAGATCCGGCCCACCGGAGGGCAGCTGATTGAAGGAGAAAAT  1930
                     ||||||||||||||||||||||||||||||||||||||||||||||||||
EMBOSS_001      1155 TGAATCTAGAGATCCGGCCCACCGGAGGGCAGCTGATTGAAGGAGAAAAT  1204

EMBOSS_001      1931 ATGGTCCTTATTTGCTCAGTAGCCCAGGGTTCAGGGACTGTCACATTCTC  1980
                     ||||||||||||||||||||||||||||||||||||||||||||||||||
EMBOSS_001      1205 ATGGTCCTTATTTGCTCAGTAGCCCAGGGTTCAGGGACTGTCACATTCTC  1254

EMBOSS_001      1981 CTGGCACAAAGAAGGAAGAGTAAGAAGCCTGGGTAGAAAGACCCAGCGTT  2030
                     ||||||||||||||||||||||||||||||||||||||||||||||||||
EMBOSS_001      1255 CTGGCACAAAGAAGGAAGAGTAAGAAGCCTGGGTAGAAAGACCCAGCGTT  1304

EMBOSS_001      2031 CCCTGTTGGCAGAGCTGCATGTTCTCACCGTGAAGGAGAGTGATGCAGGG  2080
                     ||||||||||||||||||||||||||||||||||||||||||||||||||
EMBOSS_001      1305 CCCTGTTGGCAGAGCTGCATGTTCTCACCGTGAAGGAGAGTGATGCAGGG  1354

EMBOSS_001      2081 AGATACTACTGTGCAGCTGATAACGTTCACAGCCCCATCCTCAGCACGTG  2130
                     ||||||||||||||||||||||||||||||||||||||||||||||||||
EMBOSS_001      1355 AGATACTACTGTGCAGCTGATAACGTTCACAGCCCCATCCTCAGCACGTG  1404

EMBOSS_001      2131 GATTCGAGTCACCGTGAGAATTCCGGTATCTCACCCTGTCCTCACCTTCA  2180
                     ||||||||||||||||||||||||||||||||||||||||||||||||||
EMBOSS_001      1405 GATTCGAGTCACCGTGAGAATTCCGGTATCTCACCCTGTCCTCACCTTCA  1454
```

```
EMBOSS_001      2181 GGGCTCCCAGGGCCCACACTGTGGTGGGGGACCTGCTGGAGCTTCACTGT   2230
                     ||||||||||||||||||||||||||||||||||||||||||||||||||
EMBOSS_001      1455 GGGCTCCCAGGGCCCACACTGTGGTGGGGGACCTGCTGGAGCTTCACTGT   1504

EMBOSS_001      2231 GAGTCCCTGAGAGGCTCTCCCCCGATCCTGTACCGATTTTATCATGAGGA   2280
                     ||||||||||||||||||||||||||||||||||||||||||||||||||
EMBOSS_001      1505 GAGTCCCTGAGAGGCTCTCCCCCGATCCTGTACCGATTTTATCATGAGGA   1554

EMBOSS_001      2281 TGTCACCCTGGGGAACAGCTCAGCCCCCTCTGGAGGAGGAGCCTCCTTCA   2330
                     ||||||||||||||||||||||||||||||||||||||||||||||||||
EMBOSS_001      1555 TGTCACCCTGGGGAACAGCTCAGCCCCCTCTGGAGGAGGAGCCTCCTTCA   1604

EMBOSS_001      2331 ACCTCTCTCTGACTGCAGAACATTCTGGAAACTACTCCTGTGATGCAGAC   2380
                     ||||||||||||||||||||||||||||||||||||||||||||||||||
EMBOSS_001      1605 ACCTCTCTCTGACTGCAGAACATTCTGGAAACTACTCCTGTGATGCAGAC   1654

EMBOSS_001      2381 AATGGCCTGGGGGCCCAGCACAGTCATGGAGTGAGTCTCAGGGTCACAGT   2430
                     ||||||||||||||||||||||||||||||||||||||||||||||||||
EMBOSS_001      1655 AATGGCCTGGGGGCCCAGCACAGTCATGGAGTGAGTCTCAGGGTCACAGT   1704

EMBOSS_001      2431 TCCGGTGTCTCGCCCCGTCCTCACCCTCAGGGCTCCCGGGGCCCAGGCTG   2480
                     ||||||||||||||||||||||||||||||||||||||||||||||||||
EMBOSS_001      1705 TCCGGTGTCTCGCCCCGTCCTCACCCTCAGGGCTCCCGGGGCCCAGGCTG   1754

EMBOSS_001      2481 TGGTGGGGGACCTGCTGGAGCTTCACTGTGAGTCCCTGAGAGGCTCCTTC   2530
                     ||||||||||||||||||||||||||||||||||||||||||||||||||
EMBOSS_001      1755 TGGTGGGGGACCTGCTGGAGCTTCACTGTGAGTCCCTGAGAGGCTCCTTC   1804

EMBOSS_001      2531 CCGATCCTGTACTGGTTTTATCACGAGGATGACACCTTGGGGAACATCTC   2580
                     ||||||||||||||||||||||||||||||||||||||||||||||||||
EMBOSS_001      1805 CCGATCCTGTACTGGTTTTATCACGAGGATGACACCTTGGGGAACATCTC   1854

EMBOSS_001      2581 GGCCCACTCTGGAGGAGGGGCATCCTTCAACCTCTCTCTGACTACAGAAC   2630
                     ||||||||||||||||||||||||||||||||||||||||||||||||||
EMBOSS_001      1855 GGCCCACTCTGGAGGAGGGGCATCCTTCAACCTCTCTCTGACTACAGAAC   1904

EMBOSS_001      2631 ATTCTGGAAACTACTCATGTGAGGCTGACAATGGCCTGGGGGCCCAGCAC   2680
                     ||||||||||||||||||||||||||||||||||||||||||||||||||
EMBOSS_001      1905 ATTCTGGAAACTACTCATGTGAGGCTGACAATGGCCTGGGGGCCCAGCAC   1954

EMBOSS_001      2681 AGTAAAGTGGTGACACTCAATGTTACAGGAACTTCCAGGAACAGAACAGG   2730
                     ||||||||||||||||||||||||||||||||||||||||||||||||||
EMBOSS_001      1955 AGTAAAGTGGTGACACTCAATGTTACAGGAACTTCCAGGAACAGAACAGG   2004

EMBOSS_001      2731 CCTTACCGCTGCGGGAATCACGGGGCTGGTGCTCAGCATCCTCGTCCTTG   2780
                     ||||||||||||||||||||||||||||||||||||||||||||||||||
EMBOSS_001      2005 CCTTACCGCTGCGGGAATCACGGGGCTGGTGCTCAGCATCCTCGTCCTTG   2054

EMBOSS_001      2781 CTGCTGCTGCTGCTCTGCTGCATTACGCCAGGGCCCGAAGGAAACCAGGA   2830
                     ||||||||||||||||||||||||||||||||||||||||||||||||||
EMBOSS_001      2055 CTGCTGCTGCTGCTCTGCTGCATTACGCCAGGGCCCGAAGGAAACCAGGA   2104

EMBOSS_001      2831 GGACTTTCTGCCACTGGAACATCTAGTCACAGTCCTAGTGAGTGTCAGGA   2880
                     ||||||||||||||||||||||||||||||||||||||||||||||||||
EMBOSS_001      2105 GGACTTTCTGCCACTGGAACATCTAGTCACAGTCCTAGTGAGTGTCAGGA   2154

EMBOSS_001      2881 GCCTTCCTCGTCCAGGCCTTCCAGGATAGACCCTCAAGAGCCCACTCACT   2930
                     ||||||||||||||||||||||||||||||||||||||||||||||||||
EMBOSS_001      2155 GCCTTCCTCGTCCAGGCCTTCCAGGATAGACCCTCAAGAGCCCACTCACT   2204

EMBOSS_001      2931 CTAAACCACTAGCCCCAATGGAGCTGGAGCCAATGTACAGCAATGTAAAT   2980
                     ||||||||||||||||||||||||||||||||||||||||||||||||||
EMBOSS_001      2205 CTAAACCACTAGCCCCAATGGAGCTGGAGCCAATGTACAGCAATGTAAAT   2254

EMBOSS_001      2981 CCTGGAGATAGCAACCCGATTTATTCCCAGATCTGGAGCATCCAGCATAC   3030
                     ||||||||||||||||||||||||||||||||||||||||||||||||||
EMBOSS_001      2255 CCTGGAGATAGCAACCCGATTTATTCCCAGATCTGGAGCATCCAGCATAC   2304
```

Appendix A.6. BLAST analysis of the FcRL3 transcript contained in the pIG plasmid using the EMBOSS Needle Tool (EMBL-EBI, Hinxton, UK).

Forward sequencing alignment:

```
EMBOSS_001         1 -------ATGCTTCTGTGGCTGCTGCTGCTGATCCTGACTCCTGGAAGAG     43
                           |||||||||||||||||||||||||||||||||||||||||||
EMBOSS_001         1 TCTCGAGATGCTTCTGTGGCTGCTGCTGCTGATCCTGACTCCTGGAAGAG     50

EMBOSS_001        44 AACAATCAGGGGTGGCCCCAAAAGCTGTACTTCTCCTCAATCCTCCATGG     93
                     ||||||||||||||||||||||||||||||||||||||||||||||||||
EMBOSS_001        51 AACAATCAGGGGTGGCCCCAAAAGCTGTACTTCTCCTCAATCCTCCATGG    100

EMBOSS_001        94 TCCACAGCCTTCAAAGGAGAAAAAGTGGCTCTCATATGCAGCAGCATATC    143
                     ||||||||||||||||||||||||||||||||||||||||||||||||||
EMBOSS_001       101 TCCACAGCCTTCAAAGGAGAAAAAGTGGCTCTCATATGCAGCAGCATATC    150

EMBOSS_001       144 ACATTCCCTAGCCCAGGGAGACACATATTGGTATCACGATGAGAAGTTGT    193
                     ||||||||||||||||||||||||||||||||||||||||||||||||||
EMBOSS_001       151 ACATTCCCTAGCCCAGGGAGACACATATTGGTATCACGATGAGAAGTTGT    200

EMBOSS_001       194 TGAAAATAAAACATGACAAGATCCAAATTACAGAGCCTGGAAATTACCAA    243
                     ||||||||||||||||||||||||||||||||||||||||||||||||||
EMBOSS_001       201 TGAAAATAAAACATGACAAGATCCAAATTACAGAGCCTGGAAATTACCAA    250

EMBOSS_001       244 TGTAAGACCCGAGGATCCTCCCTCAGTGATGCCGTGCATGTGGAATTTTC    293
                     ||||||||||||||||||||||||||||||||||||||||||||||||||
EMBOSS_001       251 TGTAAGACCCGAGGATCCTCCCTCAGTGATGCCGTGCATGTGGAATTTTC    300

EMBOSS_001       294 ACCTGACTGGCTGATCCTGCAGGCTTTACATCCTGTCTTTGAAGGAGACA    343
                     ||||||||||||||||||||||||||||||||||||||||||||||||||
EMBOSS_001       301 ACCTGACTGGCTGATCCTGCAGGCTTTACATCCTGTCTTTGAAGGAGACA    350

EMBOSS_001       344 ATGTCATTCTGAGATGTCAGGGGAAAGACAACAAAAACACTCATCAAAAG    393
                     ||||||||||||||||||||||||||||||||||||||||||||||||||
EMBOSS_001       351 ATGTCATTCTGAGATGTCAGGGGAAAGACAACAAAAACACTCATCAAAAG    400

EMBOSS_001       394 GTTTACTACAAGGATGGAAAACAGCTTCCTAATAGTTATAATTTAGAGAA    443
                     ||||||||||||||||||||||||||||||||||||||||||||||||||
EMBOSS_001       401 GTTTACTACAAGGATGGAAAACAGCTTCCTAATAGTTATAATTTAGAGAA    450

EMBOSS_001       444 GATCACAGTGAATTCAGTCTCCAGGGATAATAGCAAATATCATTGTACTG    493
                     ||||||||||||||||||||||||||||||||||||||||||||||||||
EMBOSS_001       451 GATCACAGTGAATTCAGTCTCCAGGGATAATAGCAAATATCATTGTACTG    500

EMBOSS_001       494 CTTATAGGAAGTTTTACATACTTGACATTGAAGTAACTTCAAAACCCCTA    543
                     ||||||||||||||||||||||||||||||||||||||||||||||||||
EMBOSS_001       501 CTTATAGGAAGTTTTACATACTTGACATTGAAGTAACTTCAAAACCCCTA    550

EMBOSS_001       544 AATATCCAAGTTCAAGAGCTGTTTCTACATCCTGTGCTGAGAGCCAGCTC    593
                     ||||||||||||||||||||||||||||||||||||||||||||||||||
EMBOSS_001       551 AATATCCAAGTTCAAGAGCTGTTTCTACATCCTGTGCTGAGAGCCAGCTC    600

EMBOSS_001       594 TTCCACGCCCATAGAGGGGAGTCCCATGACCCTGACCTGTGAGACCCAGC    643
                     ||||||||||||||||||||||||||||||||||||||||||||||||||
EMBOSS_001       601 TTCCACGCCCATAGAGGGGAGTCCCATGACCCTGACCTGTGAGACCCAGC    650

EMBOSS_001       644 TCTCTCCACAGAGGCCAGATGTCCAGCTGCAATTCTCCCTCTTCAGAGAT    693
                     ||||||||||||||||||||||||||||||||||||||||||||||||||
EMBOSS_001       651 TCTCTCCACAGAGGCCAGATGTCCAGCTGCAATTCTCCCTCTTCAGAGAT    700

EMBOSS_001       694 AGCCAGACCCTCGGATTGGGCTGGAGCAGGTCCCCCAGACTCCAGATCCC    743
                     ||||||||||||||||||||||||||||||||||||||||||||||||||
EMBOSS_001       701 AGCCAGACCCTCGGATTGGGCTGGAGCAGGTCCCCCAGACTCCAGATCCC    750
```

```
EMBOSS_001      744 TGCCATGTGGACTGAAGACTCAGGGTCTTACTGGTGTGAGGTGGAGACAG   793
                    ||||||||||||||||||||||||||||||||||||||||||||||||||
EMBOSS_001      751 TGCCATGTGGACTGAAGACTCAGGGTCTTACTGGTGTGAGGTGGAGACAG   800

EMBOSS_001      794 TGACTCACAGCATCAAAAAAAGGAGCCTGAGATCTCAGATACGTGTACAG   843
                    ||||||||||||||||||||||||||||||||||||||||||||||||||
EMBOSS_001      801 TGACTCACAGCATCAAAAAAAGGAGCCTGAGATCTCAGATACGTGTACAG   850

EMBOSS_001      844 AGAGTCCCTGTGTCTAATGTGAATCTAGAGATCCGGCCCACCGGAGGGCA   893
                    ||||||||||||||||||||||||||||||||||||||||||||||||||
EMBOSS_001      851 AGAGTCCCTGTGTCTAATGTGAATCTAGAGATCCGGCCCACCGGAGGGCA   900

EMBOSS_001      894 GCTGATTGAAGGAGAAAATATGGTCCTTATTTGCTCAGTAGCCCAGGGTT   943
                    ||||||||||||||||||||||||||||||||||||||||||||||||||
EMBOSS_001      901 GCTGATTGAAGGAGAAAATATGGTCCTTATTTGCTCAGTAGCCCAGGGTT   950

EMBOSS_001      944 CAGGGACTGTCACATTCTCCTGGCACAAAGAAGGAAGAGTAAGAAGCCTG   993
                    ||||||||||||||||||||||||||||||||||||||||||||||||||
EMBOSS_001      951 CAGGGACTGTCACATTCTCCTGGCACAAAGAAGGAAGAGTAAGAAGCCTG  1000

EMBOSS_001      994 GGTAGAAAGACCCAGCGTTCCCTGTTGGCAGAGCTGCATGTTCTCACCGT  1043
                    ||||||||||||||||||||||||||||||||||||||||||||||||||
EMBOSS_001     1001 GGTAGAAAGACCCAGCGTTCCCTGTTGGCAGAGCTGCATGTTCTCACCGT  1050

EMBOSS_001     1044 GAAGGAGAGTGATGCAGGGAGATACTACTGTGCAGCTGATAACGTTCACA  1093
                    ||||||||||||||||||||||||||||||||||||||||||||||||||
EMBOSS_001     1051 GAAGGAGAGTGATGCAGGGAGATACTACTGTGCAGCTGATAACGTTCACA  1100

EMBOSS_001     1094 GCCCCATCCTCAGCACGTGGATTCGAGTCACCGTGAGAATTCCGGTATCT  1143
                    ||||||||||||||||||||||||||||||||||||||||||||||||||
EMBOSS_001     1101 GCCCCATCCTCAGCACGTGGATTCGAGTCACCGTGAGAATTCCGGTATCT  1150

EMBOSS_001     1144 CACCCTGTCCTCACCTTCAGGGCTCCCAGGGCCCACACTGTGGTGGGGGA  1193
                    ||||||||||||||||||||||||||||||||||||||||||||||||||
EMBOSS_001     1151 CACCCTGTCCTCACCTTCAGGGCTCCCAGGGCCCACACTGTGGTGGGGGA  1200

EMBOSS_001     1194 CCTGCTGGAGCTTCACTGTGAGTCCCTGAGAGGCTCTCCCCCGATCCTGT  1243
                    ||||||||||||||||||||||||||||||||||||||||||||||||||
EMBOSS_001     1201 CCTGCTGGAGCTTCACTGTGAGTCCCTGAGAGGCTCTCCCCCGATCCTGT  1250

EMBOSS_001     1244 ACCGATTTTATCATGAGGATGTCACCCTGGGGAACAGCTCAGCCCCCTCT  1293
                    ||||||||||||||||||||||||||||||||||||||||||||||||||
EMBOSS_001     1251 ACCGATTTTATCATGAGGATGTCACCCTGGGGAACAGCTCAGCCCCCTCT  1300

EMBOSS_001     1294 GGAGGAGGAGCCTCCTTCAACCTCTCTCTGACTGCAGAACATTCTGGAAA  1343
                    ||||||||||||||||||||||||||||||||||||||||||||||||||
EMBOSS_001     1301 GGAGGAGGAGCCTCCTTCAACCTCTCTCTGACTGCAGAACATTCTGGAAA  1350

EMBOSS_001     1344 CTACTCCTGTGATGCAGACAATGGCCTGGGGGCCCAGCACAGTCATGGAG  1393
                    ||||||||||||||||||||||||||||||||||||||||||||||||||
EMBOSS_001     1351 CTACTCCTGTGATGCAGACAATGGCCTGGGGGCCCAGCACAGTCATGGAG  1400

EMBOSS_001     1394 TGAGTCTCAGGGTCACAGTTCCGGTGTCTCGCCCCGTCCTCACCCTCAGG  1443
                    ||||||||||||||||||||||||||||||||||||||||||||||||||
EMBOSS_001     1401 TGAGTCTCAGGGTCACAGTTCCGGTGTCTCGCCCCGTCCTCACCCTCAGG  1450

EMBOSS_001     1444 GCTCCCGGGGCCCAGGCTGTGGTGGGGGACCTGCTGGAGCTTCACTGTGA  1493
                    ||||||||||||||||||||||||||||||||||||||||||||||||||
EMBOSS_001     1451 GCTCCCGGGGCCCAGGCTGTGGTGGGGGACCTGCTGGAGCTTCACTGTGA  1500

EMBOSS_001     1494 GTCCCTGAGAGGCTCCTTCCCGATCCTGTACTGGTTTTATCACGAGGATG  1543
                    ||||||||||||||||||||||||||||||||||||||||||||||||||
EMBOSS_001     1501 GTCCCTGAGAGGCTCCTTCCCGATCCTGTACTGGTTTTATCACGAGGATG  1550

EMBOSS_001     1544 ACACCTTGGGGAACATCTCGGCCCACTCTGGAGGAGGGGCATCCTTCAAC  1593
                    ||||||||||||||||||||||||||||||||||||||||||||||||||
EMBOSS_001     1551 ACACCTTGGGGAACATCTCGGCCCACTCTGGAGGAGGGGCATCCTTCAAC  1600
```

```
EMBOSS_001      1594 CTCTCTCTGACTACAGAACATTCTGGAAACTACTCATGTGAGGCTGACAA  1643
                     ||||||||||||||||||||||||||||||||||||||||||||||||||
EMBOSS_001      1601 CTCTCTCTGACTACAGAACATTCTGGAAACTACTCATGTGAGGCTGACAA  1650

EMBOSS_001      1644 TGGCCTGGGGGCCCAGCACAGTAAAGTGGTGACACTCAATGTTACAGGAA  1693
                     ||||||||||||||||||||||||||||||||||||||||||||||||||
EMBOSS_001      1651 TGGCCTGGGGGCCCAGCACAGTAAAGTGGTGACACTCAATGTTACAGGAA  1700

EMBOSS_001      1694 CTTCCAGGAACAGAACAGGCCTTACCGCTGCGGGAATCACGGGGCTGGTG  1743
                     ||||||||||||||||||||||||||||||||||||||||||||||||||
EMBOSS_001      1701 CTTCCAGGAACAGAACAGGCCTTACCGCTGCGGGAATCACGGGGCTGGTG  1750

EMBOSS_001      1744 CTCAGCATCCTCGTCCTTGCTGCTGCTGCTGCTCTGCTGCATTACGCCAG  1793
                     ||||||||||||||||||||||||||||||||||||||||||||||||||
EMBOSS_001      1751 CTCAGCATCCTCGTCCTTGCTGCTGCTGCTGCTCTGCTGCATTACGCCAG  1800

EMBOSS_001      1794 GGCCCGAAGGAAACCAGGAGGACTTTCTGCCACTGGAACATCTAGTCACA  1843
                     ||||||||||||||||||||||||||||||||||||||||||||||||||
EMBOSS_001      1801 GGCCCGAAGGAAACCAGGAGGACTTTCTGCCACTGGAACATCTAGTCACA  1850

EMBOSS_001      1844 GTCCTAGTGAGTGTCAGGAGCCTTCCTCGTCCAGGCCTTCCAGGATAGAC  1893
                     ||||||||||||||||||||||||||||||||||||||||||||||||||
EMBOSS_001      1851 GTCCTAGTGAGTGTCAGGAGCCTTCCTCGTCCAGGCCTTCCAGGATAGAC  1900

EMBOSS_001      1894 CCTCAAGAGCCCACTCACTCTAAACCACTAG------------------  1924
                     ||||||||||||||||||||||||||||||
EMBOSS_001      1901 CCTCAAGAGCCCACTCACTCTAAACCACTAGCCCCAATGGAGCTGGAGCC  1950
```

Reverse sequencing alignment:

```
EMBOSS_001         1 -------------ATGCTTCTGTGGCTGCTGCTGCTGATCCTGACTCCTG    37
                                   |||||||||||||||||||||||||||||||||||||
EMBOSS_001       651 TAGATCTCTCGAGATGCTTCTGTGGCTGCTGCTGCTGATCCTGACTCCTG    700

EMBOSS_001        38 GAAGAGAACAATCAGGGGTGGCCCCAAAAGCTGTACTTCTCCTCAATCCT    87
                     ||||||||||||||||||||||||||||||||||||||||||||||||||||
EMBOSS_001       701 GAAGAGAACAATCAGGGGTGGCCCCAAAAGCTGTACTTCTCCTCAATCCT    750

EMBOSS_001        88 CCATGGTCCACAGCCTTCAAAGGAGAAAAAGTGGCTCTCATATGCAGCAG    137
                     ||||||||||||||||||||||||||||||||||||||||||||||||||||
EMBOSS_001       751 CCATGGTCCACAGCCTTCAAAGGAGAAAAAGTGGCTCTCATATGCAGCAG    800

EMBOSS_001       138 CATATCACATTCCCTAGCCCAGGGAGACACATATTGGTATCACGATGAGA    187
                     ||||||||||||||||||||||||||||||||||||||||||||||||||||
EMBOSS_001       801 CATATCACATTCCCTAGCCCAGGGAGACACATATTGGTATCACGATGAGA    850

EMBOSS_001       188 AGTTGTTGAAAATAAAACATGACAAGATCCAAATTACAGAGCCTGGAAAT    237
                     ||||||||||||||||||||||||||||||||||||||||||||||||||||
EMBOSS_001       851 AGTTGTTGAAAATAAAACATGACAAGATCCAAATTACAGAGCCTGGAAAT    900

EMBOSS_001       238 TACCAATGTAAGACCCGAGGATCCTCCCTCAGTGATGCCGTGCATGTGGA    287
                     ||||||||||||||||||||||||||||||||||||||||||||||||||||
EMBOSS_001       901 TACCAATGTAAGACCCGAGGATCCTCCCTCAGTGATGCCGTGCATGTGGA    950

EMBOSS_001       288 ATTTTCACCTGACTGGCTGATCCTGCAGGCTTTACATCCTGTCTTTGAAG    337
                     ||||||||||||||||||||||||||||||||||||||||||||||||||||
EMBOSS_001       951 ATTTTCACCTGACTGGCTGATCCTGCAGGCTTTACATCCTGTCTTTGAAG   1000

EMBOSS_001       338 GAGACAATGTCATTCTGAGATGTCAGGGGAAAGACAACAAAAACACTCAT    387
                     ||||||||||||||||||||||||||||||||||||||||||||||||||||
EMBOSS_001      1001 GAGACAATGTCATTCTGAGATGTCAGGGGAAAGACAACAAAAACACTCAT   1050

EMBOSS_001       388 CAAAAGGTTTACTACAAGGATGGAAAACAGCTTCCTAATAGTTATAATTT    437
                     ||||||||||||||||||||||||||||||||||||||||||||||||||||
EMBOSS_001      1051 CAAAAGGTTTACTACAAGGATGGAAAACAGCTTCCTAATAGTTATAATTT   1100
```

```
EMBOSS_001       438 AGAGAAGATCACAGTGAATTCAGTCTCCAGGGATAATAGCAAATATCATT    487
                     ||||||||||||||||||||||||||||||||||||||||||||||||||||
EMBOSS_001      1101 AGAGAAGATCACAGTGAATTCAGTCTCCAGGGATAATAGCAAATATCATT   1150

EMBOSS_001       488 GTACTGCTTATAGGAAGTTTTACATACTTGACATTGAAGTAACTTCAAAA    537
                     ||||||||||||||||||||||||||||||||||||||||||||||||||||
EMBOSS_001      1151 GTACTGCTTATAGGAAGTTTTACATACTTGACATTGAAGTAACTTCAAAA   1200

EMBOSS_001       538 CCCCTAAATATCCAAGTTCAAGAGCTGTTTCTACATCCTGTGCTGAGAGC    587
                     ||||||||||||||||||||||||||||||||||||||||||||||||||||
EMBOSS_001      1201 CCCCTAAATATCCAAGTTCAAGAGCTGTTTCTACATCCTGTGCTGAGAGC   1250

EMBOSS_001       588 CAGCTCTTCCACGCCCATAGAGGGGAGTCCCATGACCCTGACCTGTGAGA    637
                     ||||||||||||||||||||||||||||||||||||||||||||||||||||
EMBOSS_001      1251 CAGCTCTTCCACGCCCATAGAGGGGAGTCCCATGACCCTGACCTGTGAGA   1300

EMBOSS_001       638 CCCAGCTCTCTCCACAGAGGCCAGATGTCCAGCTGCAATTCTCCCTCTTC    687
                     ||||||||||||||||||||||||||||||||||||||||||||||||||||
EMBOSS_001      1301 CCCAGCTCTCTCCACAGAGGCCAGATGTCCAGCTGCAATTCTCCCTCTTC   1350

EMBOSS_001       688 AGAGATAGCCAGACCCTCGGATTGGGCTGGAGCAGGTCCCCCAGACTCCA    737
                     ||||||||||||||||||||||||||||||||||||||||||||||||||||
EMBOSS_001      1351 AGAGATAGCCAGACCCTCGGATTGGGCTGGAGCAGGTCCCCCAGACTCCA   1400

EMBOSS_001       738 GATCCCTGCCATGTGGACTGAAGACTCAGGGTCTTACTGGTGTGAGGTGG    787
                     ||||||||||||||||||||||||||||||||||||||||||||||||||||
EMBOSS_001      1401 GATCCCTGCCATGTGGACTGAAGACTCAGGGTCTTACTGGTGTGAGGTGG   1450

EMBOSS_001       788 AGACAGTGACTCACAGCATCAAAAAAAGGAGCCTGAGATCTCAGATACGT    837
                     ||||||||||||||||||||||||||||||||||||||||||||||||||||
EMBOSS_001      1451 AGACAGTGACTCACAGCATCAAAAAAAGGAGCCTGAGATCTCAGATACGT   1500

EMBOSS_001       838 GTACAGAGAGTCCCTGTGTCTAATGTGAATCTAGAGATCCGGCCCACCGG    887
                     ||||||||||||||||||||||||||||||||||||||||||||||||||||
EMBOSS_001      1501 GTACAGAGAGTCCCTGTGTCTAATGTGAATCTAGAGATCCGGCCCACCGG   1550

EMBOSS_001       888 AGGGCAGCTGATTGAAGGAGAAAATATGGTCCTTATTTGCTCAGTAGCCC    937
                     ||||||||||||||||||||||||||||||||||||||||||||||||||||
EMBOSS_001      1551 AGGGCAGCTGATTGAAGGAGAAAATATGGTCCTTATTTGCTCAGTAGCCC   1600

EMBOSS_001       938 AGGGTTCAGGGACTGTCACATTCTCCTGGCACAAAGAAGGAAGAGTAAGA    987
                     ||||||||||||||||||||||||||||||||||||||||||||||||||||
EMBOSS_001      1601 AGGGTTCAGGGACTGTCACATTCTCCTGGCACAAAGAAGGAAGAGTAAGA   1650

EMBOSS_001       988 AGCCTGGGTAGAAAGACCCAGCGTTCCCTGTTGGCAGAGCTGCATGTTCT   1037
                     ||||||||||||||||||||||||||||||||||||||||||||||||||||
EMBOSS_001      1651 AGCCTGGGTAGAAAGACCCAGCGTTCCCTGTTGGCAGAGCTGCATGTTCT   1700

EMBOSS_001      1038 CACCGTGAAGGAGAGTGATGCAGGGAGATACTACTGTGCAGCTGATAACG   1087
                     ||||||||||||||||||||||||||||||||||||||||||||||||||||
EMBOSS_001      1701 CACCGTGAAGGAGAGTGATGCAGGGAGATACTACTGTGCAGCTGATAACG   1750

EMBOSS_001      1088 TTCACAGCCCCATCCTCAGCACGTGGATTCGAGTCACCGTGAGAATTCCG   1137
                     ||||||||||||||||||||||||||||||||||||||||||||||||||||
EMBOSS_001      1751 TTCACAGCCCCATCCTCAGCACGTGGATTCGAGTCACCGTGAGAATTCCG   1800

EMBOSS_001      1138 GTATCTCACCCTGTCCTCACCTTCAGGGCTCCCAGGGCCCACACTGTGGT   1187
                     ||||||||||||||||||||||||||||||||||||||||||||||||||||
EMBOSS_001      1801 GTATCTCACCCTGTCCTCACCTTCAGGGCTCCCAGGGCCCACACTGTGGT   1850

EMBOSS_001      1188 GGGGGACCTGCTGGAGCTTCACTGTGAGTCCCTGAGAGGCTCTCCCCCGA   1237
                     ||||||||||||||||||||||||||||||||||||||||||||||||||||
EMBOSS_001      1851 GGGGGACCTGCTGGAGCTTCACTGTGAGTCCCTGAGAGGCTCTCCCCCGA   1900

EMBOSS_001      1238 TCCTGTACCGATTTTATCATGAGGATGTCACCCTGGGGAACAGCTCAGCC   1287
                     ||||||||||||||||||||||||||||||||||||||||||||||||||||
EMBOSS_001      1901 TCCTGTACCGATTTTATCATGAGGATGTCACCCTGGGGAACAGCTCAGCC   1950
```

```
EMBOSS_001      1288 CCCTCTGGAGGAGGAGCCTCCTTCAACCTCTCTCTGACTGCAGAACATTC   1337
                     |||||||||||||||||||||||||||||||||||||||||||||||||||
EMBOSS_001      1951 CCCTCTGGAGGAGGAGCCTCCTTCAACCTCTCTCTGACTGCAGAACATTC   2000

EMBOSS_001      1338 TGGAAACTACTCCTGTGATGCAGACAATGGCCTGGGGGCCCAGCACAGTC   1387
                     |||||||||||||||||||||||||||||||||||||||||||||||||||
EMBOSS_001      2001 TGGAAACTACTCCTGTGATGCAGACAATGGCCTGGGGGCCCAGCACAGTC   2050

EMBOSS_001      1388 ATGGAGTGAGTCTCAGGGTCACAGTTCCGGTGTCTCGCCCCGTCCTCACC   1437
                     |||||||||||||||||||||||||||||||||||||||||||||||||||
EMBOSS_001      2051 ATGGAGTGAGTCTCAGGGTCACAGTTCCGGTGTCTCGCCCCGTCCTCACC   2100

EMBOSS_001      1438 CTCAGGGCTCCCGGGGCCCAGGCTGTGGTGGGGGACCTGCTGGAGCTTCA   1487
                     |||||||||||||||||||||||||||||||||||||||||||||||||||
EMBOSS_001      2101 CTCAGGGCTCCCGGGGCCCAGGCTGTGGTGGGGGACCTGCTGGAGCTTCA   2150

EMBOSS_001      1488 CTGTGAGTCCCTGAGAGGCTCCTTCCCGATCCTGTACTGGTTTTATCACG   1537
                     |||||||||||||||||||||||||||||||||||||||||||||||||||
EMBOSS_001      2151 CTGTGAGTCCCTGAGAGGCTCCTTCCCGATCCTGTACTGGTTTTATCACG   2200

EMBOSS_001      1538 AGGATGACACCTTGGGGAACATCTCGGCCCACTCTGGAGGAGGGGCATCC   1587
                     |||||||||||||||||||||||||||||||||||||||||||||||||||
EMBOSS_001      2201 AGGATGACACCTTGGGGAACATCTCGGCCCACTCTGGAGGAGGGGCATCC   2250

EMBOSS_001      1588 TTCAACCTCTCTCTGACTACAGAACATTCTGGAAACTACTCATGTGAGGC   1637
                     |||||||||||||||||||||||||||||||||||||||||||||||||||
EMBOSS_001      2251 TTCAACCTCTCTCTGACTACAGAACATTCTGGAAACTACTCATGTGAGGC   2300

EMBOSS_001      1638 TGACAATGGCCTGGGGGCCCAGCACAGTAAAGTGGTGACACTCAATGTTA   1687
                     |||||||||||||||||||||||||||||||||||||||||||||||||||
EMBOSS_001      2301 TGACAATGGCCTGGGGGCCCAGCACAGTAAAGTGGTGACACTCAATGTTA   2350

EMBOSS_001      1688 CAGGAACTTCCAGGAACAGAACAGGCCTTACCGCTGCGGGAATCACGGGG   1737
                     |||||||||||||||||||||||||||||||||||||||||||||||||||
EMBOSS_001      2351 CAGGAACTTCCAGGAACAGAACAGGCCTTACCGCTGCGGGAATCACGGGG   2400

EMBOSS_001      1738 CTGGTGCTCAGCATCCTCGTCCTTGCTGCTGCTGCTGCTCTGCTGCATTA   1787
                     |||||||||||||||||||||||||||||||||||||||||||||||||||
EMBOSS_001      2401 CTGGTGCTCAGCATCCTCGTCCTTGCTGCTGCTGCTGCTCTGCTGCATTA   2450

EMBOSS_001      1788 CGCCAGGGCCCGAAGGAAACCAGGAGGACTTTCTGCCACTGGAACATCTA   1837
                     |||||||||||||||||||||||||||||||||||||||||||||||||||
EMBOSS_001      2451 CGCCAGGGCCCGAAGGAAACCAGGAGGACTTTCTGCCACTGGAACATCTA   2500

EMBOSS_001      1838 GTCACAGTCCTAGTGAGTGTCAGGAGCCTTCCTCGTCCAGGCCTTCCAGG   1887
                     |||||||||||||||||||||||||||||||||||||||||||||||||||
EMBOSS_001      2501 GTCACAGTCCTAGTGAGTGTCAGGAGCCTTCCTCGTCCAGGCCTTCCAGG   2550

EMBOSS_001      1888 ATAGACCCTCAAGAGCCCACTCACTCTAAACCACTAG-------------   1924
                     |||||||||||||||||||||||||||||||||||
EMBOSS_001      2551 ATAGACCCTCAAGAGCCCACTCACTCTAAACCACTAGCCCCAATGGAGCT   2600
```

Appendix B. Presentations pertaining to this thesis

Presentations:

Oral - internationally

- American Association of Immunologist (AAI) Annual Meeting, San Diego, USA. May 2019. *Age-associated B cells in early drug-naïve rheumatoid arthritis patients*.

Poster - internationally

- American Association of Immunologist (AAI) Annual Meeting, San Diego, USA. May 2019. *Age-associated B cells in early drug-naïve rheumatoid arthritis patients*.
- European Workshop on Rheumatology Research (EWRR), Lyon, France. February 2019. *Age-associated B cells in early drug-naïve rheumatoid arthritis patients*.
- Keystone Symposia on B cells, Dresden Germany. June 2018. *Age-associated B cells in early drug-naïve rheumatoid arthritis patients*.
- EMBO B cell workshop, Girona, Spain. September 2017. *Age-associated B cells in early drug-naïve rheumatoid arthritis patients*.

Poster and oral – regional and local

- Immunology North East AGM and Research Symposium, Newcastle, UK. June 2019. *Age-associated B cells in early drug-naïve rheumatoid arthritis patients*.
- RACE renewal meeting, Glasgow, UK. January 2019. *Age-associated B cells in early drug-naïve rheumatoid arthritis patients*. Poster and oral presentation.
- Inflammation Immunology and Immunotherapy Away Day, Newcastle University, UK. October 2018. *Age-associated B cells in early drug-naïve rheumatoid arthritis patients*. Poster and lightning talk.
- Intitule of Cellular Medicine (ICM) Director's Research Day, Newcastle University, UK. September 2018. *Age-associated B cells in early drug-naïve rheumatoid arthritis patients*.
- RACE Scientific Advisory Board (SAB) meeting, Glasgow, UK. September 2018. *Age-associated B cells in early drug-naïve rheumatoid arthritis patients*. Poster and oral presentation.
- British Society of Immunology (BSI) Congress, Brighton, UK. December 2017. *Age-associated B cells in early drug-naïve rheumatoid arthritis patients*.
- Annual Northern and Yorkshire Rheumatology Meeting, York, UK. September 2017. *Age-associated B cells in early drug-naïve rheumatoid arthritis patients*.

- Immunology North East AGM and Research Symposium, Newcastle, UK. June 2017. *Age-associated B cells in early drug-naïve rheumatoid arthritis patients*.

Prizes

- Best Poster Prize. *Age-associated B cells in early drug-naïve rheumatoid arthritis patients*. Immunology North East AGM and Research Symposium. Newcastle, UK. June 2019.
- Best Oral Presentation Prize. *Age-associated B cells in early drug-naïve rheumatoid arthritis patients*. ICM Director's Research Day. Newcastle University, UK. September 2018.

References

Abbott, R.J., Spendlove, I., Roversi, P., Fitzgibbon, H., Knott, V., Teriete, P., McDonnell, J.M., Handford, P.A. and Lea, S.M. (2007) 'Structural and functional characterization of a novel T cell receptor co-regulatory protein complex, CD97-CD55', *J Biol Chem*, 282(30), pp. 22023-32.

Addgene (2014) *Plasmids 101: Multicistronic Vectors*. Available at: https://blog.addgene.org/plasmids-101-multicistronic-vectors (Accessed: February 26, 2020).

Agarwal, S., Kraus, Z., Dement-Brown, J., Alabi, O., Starost, K. and Tolnay, M. (2020) 'Human Fc Receptor-like 3 Inhibits Regulatory T Cell Function and Binds Secretory IgA', *Cell Rep*, 30(5), pp. 1292-1299.e3.

Agematsu, K., Hokibara, S., Nagumo, H. and Komiyama, A. (2000) 'CD27: a memory B-cell marker', *Immunol Today*, 21(5), pp. 204-6.

Ahmed, R. and Gray, D. (1996) 'Immunological memory and protective immunity: understanding their relation', *Science*, 272(5258), pp. 54-60.

Aletaha, D., Neogi, T., Silman, A.J., Funovits, J., Felson, D.T., Bingham, C.O., 3rd, Birnbaum, N.S., Burmester, G.R., Bykerk, V.P., Cohen, M.D., Combe, B., Costenbader, K.H., Dougados, M., Emery, P., Ferraccioli, G., Hazes, J.M., Hobbs, K., Huizinga, T.W., Kavanaugh, A., Kay, J., Kvien, T.K., Laing, T., Mease, P., Menard, H.A., Moreland, L.W., Naden, R.L., Pincus, T., Smolen, J.S., Stanislawska-Biernat, E., Symmons, D., Tak, P.P., Upchurch, K.S., Vencovsky, J., Wolfe, F. and Hawker, G. (2010) '2010 Rheumatoid arthritis classification criteria: an American College of Rheumatology/European League Against Rheumatism collaborative initiative', *Arthritis Rheum*, 62(9), pp. 2569-81.

Aleyd, E., Al, M., Tuk, C.W., van der Laken, C.J. and van Egmond, M. (2016) 'IgA Complexes in Plasma and Synovial Fluid of Patients with Rheumatoid Arthritis Induce Neutrophil Extracellular Traps via FcalphaRI', *J Immunol*, 197(12), pp. 4552-4559.

Ali, M., Veale, D.J., Reece, R.J., Quinn, M., Henshaw, K., Zanders, E.D., Markham, A.F., Emery, P. and Isaacs, J.D. (2003) 'Overexpression of transcripts containing LINE-1 in the synovia of patients with rheumatoid arthritis', *Ann Rheum Dis*, 62(7), pp. 663-6.

Alivernini, S., Tolusso, B., Fedele, A.L., Di Mario, C., Ferraccioli, G. and Gremese, E. (2019) 'The B side of rheumatoid arthritis pathogenesis', *Pharmacol Res*, 149, p. 104465.

Amara, K., Clay, E., Yeo, L., Ramskold, D., Spengler, J., Sippl, N., Cameron, J.A., Israelsson, L., Titcombe, P.J., Gronwall, C., Sahbudin, I., Filer, A., Raza, K., Malmstrom, V. and Scheel-Toellner, D. (2017) 'B cells expressing the IgA receptor FcRL4 participate in the autoimmune response in patients with rheumatoid arthritis', *J Autoimmun*, 81, pp. 34-43.

Anders, S. and Huber, W. (2010) 'Differential expression analysis for sequence count data', *Genome Biol*, 11(10), p. R106.

Anderson, A.E., Lorenzi, A.R., Pratt, A., Wooldridge, T., Diboll, J., Hilkens, C.M. and Isaacs, J.D. (2012) 'Immunity 12 years after alemtuzumab in RA: CD5(+) B-cell depletion, thymus-dependent T-cell reconstitution and normal vaccine responses', *Rheumatology (Oxford)*, 51(8), pp. 1397-406.

Anderson, A.E., Maney, N.J., Nair, N., Lendrem, D.W., Skelton, A.J., Diboll, J., Brown, P.M., Smith, G.R., Carmody, R.J., Barton, A., Isaacs, J.D. and Pratt, A.G. (2019) 'Expression of STAT3-

regulated genes in circulating CD4+ T cells discriminates rheumatoid arthritis independently of clinical parameters in early arthritis', *Rheumatology (Oxford)*, 58(7), pp. 1250-1258.

Anderson, A.E., Pratt, A.G., Sedhom, M.A., Doran, J.P., Routledge, C., Hargreaves, B., Brown, P.M., Le Cao, K.A., Isaacs, J.D. and Thomas, R. (2016) 'IL-6-driven STAT signalling in circulating CD4+ lymphocytes is a marker for early anticitrullinated peptide antibody-negative rheumatoid arthritis', *Ann Rheum Dis*, 75(2), pp. 466-73.

Anderson, L.R., Owens, T.W. and Naylor, M.J. (2014) 'Structural and mechanical functions of integrins', *Biophys Rev*, 6(2), pp. 203-213.

Anolik, J., Looney, R.J., Bottaro, A., Sanz, I. and Young, F. (2003) 'Down-regulation of CD20 on B cells upon CD40 activation', *Eur J Immunol*, 33(9), pp. 2398-409.

Arce, E., Jackson, D.G., Gill, M.A., Bennett, L.B., Banchereau, J. and Pascual, V. (2001) 'Increased frequency of pre-germinal center B cells and plasma cell precursors in the blood of children with systemic lupus erythematosus', *J Immunol*, 167(4), pp. 2361-9.

Arkatkar, T., Du, S.W., Jacobs, H.M., Dam, E.M., Hou, B., Buckner, J.H., Rawlings, D.J. and Jackson, S.W. (2017) 'B cell-derived IL-6 initiates spontaneous germinal center formation during systemic autoimmunity', *J Exp Med*, 214(11), pp. 3207-3217.

Attig, J., Young, G.R., Stoye, J.P. and Kassiotis, G. (2017) 'Physiological and Pathological Transcriptional Activation of Endogenous Retroelements Assessed by RNA-Sequencing of B Lymphocytes', *Front Microbiol*, 8, p. 2489.

Bai, M., Grieshaber-Bouyer, R., Wang, J., Schmider, A.B., Wilson, Z.S., Zeng, L., Halyabar, O., Godin, M.D., Nguyen, H.N., Levescot, A., Cunin, P., Lefort, C.T., Soberman, R.J. and Nigrovic, P.A. (2017) 'CD177 modulates human neutrophil migration through activation-mediated integrin and chemoreceptor regulation', *Blood*, 130(19), pp. 2092-2100.

Barnett, B.E., Staupe, R.P., Odorizzi, P.M., Palko, O., Tomov, V.T., Mahan, A.E., Gunn, B., Chen, D., Paley, M.A., Alter, G., Reiner, S.L., Lauer, G.M., Teijaro, J.R. and Wherry, E.J. (2016) 'Cutting Edge: B Cell-Intrinsic T-bet Expression Is Required To Control Chronic Viral Infection', *J Immunol*, 197(4), pp. 1017-22.

Beliakova-Bethell, N., Massanella, M., White, C., Lada, S., Du, P., Vaida, F., Blanco, J., Spina, C.A. and Woelk, C.H. (2014) 'The effect of cell subset isolation method on gene expression in leukocytes', *Cytometry A*, 85(1), pp. 94-104.

Benjamin, D., Magrath, I.T., Maguire, R., Janus, C., Todd, H.D. and Parsons, R.G. (1982) 'Immunoglobulin secretion by cell lines derived from African and American undifferentiated lymphomas of Burkitt's and non-Burkitt's type', *J Immunol*, 129(3), pp. 1336-42.

Berland, R. and Wortis, H.H. (2002) 'Origins and functions of B-1 cells with notes on the role of CD5', *Annu Rev Immunol*, 20, pp. 253-300.

Blaschke, S., Koziolek, M., Schwarz, A., Benohr, P., Middel, P., Schwarz, G., Hummel, K.M. and Muller, G.A. (2003) 'Proinflammatory role of fractalkine (CX3CL1) in rheumatoid arthritis', *J Rheumatol*, 30(9), pp. 1918-27.

Bonilla, F.A. and Oettgen, H.C. (2010) 'Adaptive immunity', *J Allergy Clin Immunol*, 125(2 Suppl 2), pp. S33-40.

Bradley, J.R. (2008) 'TNF-mediated inflammatory disease', *J Pathol*, 214(2), pp. 149-60.

Brink, M., Verheul, M.K., Ronnelid, J., Berglin, E., Holmdahl, R., Toes, R.E., Klareskog, L., Trouw, L.A. and Rantapaa-Dahlqvist, S. (2015) 'Anti-carbamylated protein antibodies in the pre-symptomatic phase of rheumatoid arthritis, their relationship with multiple anti-citrulline peptide antibodies and association with radiological damage', *Arthritis Res Ther*, 17, p. 25.

Brown, P.B., Nardella, F.A. and Mannik, M. (1982) 'Human complement activation by self-associated IgG rheumatoid factors', *Arthritis Rheum*, 25(9), pp. 1101-7.

Brudek, T., Christensen, T., Aagaard, L., Petersen, T., Hansen, H.J. and Moller-Larsen, A. (2009) 'B cells and monocytes from patients with active multiple sclerosis exhibit increased surface expression of both HERV-H Env and HERV-W Env, accompanied by increased seroreactivity', *Retrovirology*, 6, p. 104.

Bugatti, S., Vitolo, B., Caporali, R., Montecucco, C. and Manzo, A. (2014) 'B cells in rheumatoid arthritis: from pathogenic players to disease biomarkers', *Biomed Res Int*, 2014, p. 681678.

Burska, A.N., Hunt, L., Boissinot, M., Strollo, R., Ryan, B.J., Vital, E., Nissim, A., Winyard, P.G., Emery, P. and Ponchel, F. (2014) 'Autoantibodies to posttranslational modifications in rheumatoid arthritis', *Mediators Inflamm*, 2014, p. 492873.

Capasso, M., Durrant, L.G., Stacey, M., Gordon, S., Ramage, J. and Spendlove, I. (2006) 'Costimulation via CD55 on human CD4+ T cells mediated by CD97', *J Immunol*, 177(2), pp. 1070-7.

Carsetti, R., Rosado, M.M. and Wardmann, H. (2004) 'Peripheral development of B cells in mouse and man', *Immunol Rev*, 197, pp. 179-91.

Catrina, A.I., Ytterberg, A.J., Reynisdottir, G., Malmstrom, V. and Klareskog, L. (2014) 'Lungs, joints and immunity against citrullinated proteins in rheumatoid arthritis', *Nat Rev Rheumatol*, 10(11), pp. 645-53.

Chang, L.Y., Li, Y. and Kaplan, D.E. (2017) 'Hepatitis C viraemia reversibly maintains subset of antigen-specific T-bet+ tissue-like memory B cells', *J Viral Hepat*, 24(5), pp. 389-396.

Charles, E.D., Brunetti, C., Marukian, S., Ritola, K.D., Talal, A.H., Marks, K., Jacobson, I.M., Rice, C.M. and Dustin, L.B. (2011) 'Clonal B cells in patients with hepatitis C virus-associated mixed cryoglobulinemia contain an expanded anergic CD21low B-cell subset', *Blood*, 117(20), pp. 5425-37.

Chatzidionysiou, K., Lie, E., Nasonov, E., Lukina, G., Hetland, M.L., Tarp, U., Gabay, C., van Riel, P.L., Nordstrom, D.C., Gomez-Reino, J., Pavelka, K., Tomsic, M., Kvien, T.K. and van Vollenhoven, R.F. (2011) 'Highest clinical effectiveness of rituximab in autoantibody-positive patients with rheumatoid arthritis and in those for whom no more than one previous TNF antagonist has failed: pooled data from 10 European registries', *Ann Rheum Dis*, 70(9), pp. 1575-80.

Cherukuri, A., Cheng, P.C. and Pierce, S.K. (2001) 'The role of the CD19/CD21 complex in B cell processing and presentation of complement-tagged antigens', *J Immunol*, 167(1), pp. 163-72.

Cheung, T.T. and McInnes, I.B. (2017) 'Future therapeutic targets in rheumatoid arthritis?', *Semin Immunopathol*, 39(4), pp. 487-500.

Choy, E.H. and Panayi, G.S. (2001) 'Cytokine pathways and joint inflammation in rheumatoid arthritis', *N Engl J Med*, 344(12), pp. 907-16.

Ciechomska, M., Lennard, T.W., Kirby, J.A. and Knight, A.M. (2011) 'B lymphocytes acquire and present intracellular antigens that have relocated to the surface of apoptotic target cells', *Eur J Immunol*, 41(7), pp. 1850-61.

Clark, A.D., Nair, N., Anderson, A.E., Thalayasingam, N., Naamane, N., Skelton, A.J., Diboll, J., Barton, A., Eyre, S., Isaacs, J.D., Pratt, A.G. and Reynard, L.N. (2020) 'Lymphocyte DNA methylation mediates genetic risk at shared immune mediated disease loci', *J Allergy Clin Immunol*.

Coffin, J., Hughes, S. and Varmus, H. (1997) 'Effect of Infection on Cell Division and Differentiation', in *Retroviruses*. Cold Spring Harbor (NY): Cold Spring Harbor Laboratory Press.

Combe, B., Pope, R.M., Fischbach, M., Darnell, B., Baron, S. and Talal, N. (1985) 'Interleukin-2 in rheumatoid arthritis: production of and response to interleukin-2 in rheumatoid synovial fluid, synovial tissue and peripheral blood', *Clin Exp Immunol*, 59(3), pp. 520-8.

Conigliaro, P., Chimenti, M.S., Triggianese, P., Sunzini, F., Novelli, L., Perricone, C. and Perricone, R. (2016) 'Autoantibodies in inflammatory arthritis', *Autoimmun Rev*, 15(7), pp. 673-83.

Cooles, F.A., Anderson, A.E., Drayton, T., Harry, R.A., Diboll, J., Munro, L., Thalayasingham, N., Ostor, A.J. and Isaacs, J.D. (2016) 'Immune reconstitution 20 years after treatment with alemtuzumab in a rheumatoid arthritis cohort: implications for lymphocyte depleting therapies', *Arthritis Res Ther*, 18(1), p. 302.

Cooles, F.A., Isaacs, J.D. and Anderson, A.E. (2013) 'Treg cells in rheumatoid arthritis: an update', *Curr Rheumatol Rep*, 15(9), p. 352.

Cooper, M.D. (2015) 'The early history of B cells', *Nat Rev Immunol*, 15(3), pp. 191-7.

Cope, A.P. (2008) 'T cells in rheumatoid arthritis', *Arthritis Res Ther*, 10 Suppl 1, p. S1.

Corkum, C.P., Ings, D.P., Burgess, C., Karwowska, S., Kroll, W. and Michalak, T.I. (2015) 'Immune cell subsets and their gene expression profiles from human PBMC isolated by Vacutainer Cell Preparation Tube (CPT) and standard density gradient', *BMC Immunol*, 16, p. 48.

Cossarizza, A., Chang, H.D., Radbruch, A., Akdis, M., Andra, I., Annunziato, F., Bacher, P., Barnaba, V., Battistini, L., Bauer, W.M., Baumgart, S., Becher, B., Beisker, W., Berek, C., Blanco, A., Borsellino, G., Boulais, P.E., Brinkman, R.R., Buscher, M., Busch, D.H., Bushnell, T.P., Cao, X., Cavani, A., Chattopadhyay, P.K., Cheng, Q., Chow, S., Clerici, M., Cooke, A., Cosma, A., Cosmi, L., Cumano, A., Dang, V.D., Davies, D., De Biasi, S., Del Zotto, G., Della Bella, S., Dellabona, P., Deniz, G., Dessing, M., Diefenbach, A., Di Santo, J., Dieli, F., Dolf, A., Donnenberg, V.S., Dorner, T., Ehrhardt, G.R.A., Endl, E., Engel, P., Engelhardt, B., Esser, C., Everts, B., Dreher, A., Falk, C.S., Fehniger, T.A., Filby, A., Fillatreau, S., Follo, M., Forster, I., Foster, J., Foulds, G.A., Frenette, P.S., Galbraith, D., Garbi, N., Garcia-Godoy, M.D., Geginat, J., Ghoreschi, K., Gibellini, L., Goettlinger, C., Goodyear, C.S., Gori, A., Grogan, J., Gross, M., Grutzkau, A., Grummitt, D., Hahn, J., Hammer, Q., Hauser, A.E., Haviland, D.L., Hedley, D., Herrera, G., Herrmann, M., Hiepe, F., Holland, T., Hombrink, P., Houston, J.P., Hoyer, B.F., Huang, B., Hunter, C.A., Iannone, A., Jack, H.M., Javega, B., Jonjic, S., Juelke, K., Jung, S., Kaiser, T., Kalina, T., Keller, B., Khan, S., Kienhofer, D., Kroneis, T., et al. (2017) 'Guidelines for the use of flow cytometry and cell sorting in immunological studies', *Eur J Immunol*, 47(10), pp. 1584-1797.

Couper, K.N., Blount, D.G. and Riley, E.M. (2008) 'IL-10: the master regulator of immunity to infection', *J Immunol*, 180(9), pp. 5771-7.

Curtsinger, J.M. and Mescher, M.F. (2010) 'Inflammatory cytokines as a third signal for T cell activation', *Curr Opin Immunol*, 22(3), pp. 333-40.

Dalloul, A. (2009) 'CD5: a safeguard against autoimmunity and a shield for cancer cells', *Autoimmun Rev*, 8(4), pp. 349-53.

Davis, R.S., Dennis, G., Jr., Odom, M.R., Gibson, A.W., Kimberly, R.P., Burrows, P.D. and Cooper, M.D. (2002) 'Fc receptor homologs: newest members of a remarkably diverse Fc receptor gene family', *Immunol Rev*, 190, pp. 123-36.

Davis, R.S., Wang, Y.H., Kubagawa, H. and Cooper, M.D. (2001) 'Identification of a family of Fc receptor homologs with preferential B cell expression', *Proc Natl Acad Sci U S A*, 98(17), pp. 9772-7.

Deane, K.D., Demoruelle, M.K., Kelmenson, L.B., Kuhn, K.A., Norris, J.M. and Holers, V.M. (2017) 'Genetic and environmental risk factors for rheumatoid arthritis', *Best Pract Res Clin Rheumatol*, 31(1), pp. 3-18.

Deane, K.D. and El-Gabalawy, H. (2014) 'Pathogenesis and prevention of rheumatic disease: focus on preclinical RA and SLE', *Nat Rev Rheumatol*, 10(4), pp. 212-28.

Deane, K.D. and Holers, V.M. (2019) 'The Natural History of Rheumatoid Arthritis', *Clin Ther*, 41(7), pp. 1256-1269.

Defrance, T., Taillardet, M. and Genestier, L. (2011) 'T cell-independent B cell memory', *Curr Opin Immunol*, 23(3), pp. 330-6.

Dement-Brown, J., Newton, C.S., Ise, T., Damdinsuren, B., Nagata, S. and Tolnay, M. (2012) 'Fc receptor-like 5 promotes B cell proliferation and drives the development of cells displaying switched isotypes', *J Leukoc Biol*, 91(1), pp. 59-67.

Dempsey, P.W., Vaidya, S.A. and Cheng, G. (2003) 'The art of war: Innate and adaptive immune responses', *Cell Mol Life Sci*, 60(12), pp. 2604-21.

den Haan, J.M., Arens, R. and van Zelm, M.C. (2014) 'The activation of the adaptive immune system: cross-talk between antigen-presenting cells, T cells and B cells', *Immunol Lett*, 162(2 Pt B), pp. 103-12.

Dho, S.H., Lim, J.C. and Kim, L.K. (2018) 'Beyond the Role of CD55 as a Complement Component', *Immune Netw*, 18(1), p. e11.

Du, S.W., Arkatkar, T., Al Qureshah, F., Jacobs, H.M., Thouvenel, C.D., Chiang, K., Largent, A.D., Li, Q.Z., Hou, B., Rawlings, D.J. and Jackson, S.W. (2019) 'Functional Characterization of CD11c(+) Age-Associated B Cells as Memory B Cells', *J Immunol*, 203(11), pp. 2817-2826.

Duan, B. and Morel, L. (2006) 'Role of B-1a cells in autoimmunity', *Autoimmun Rev*, 5(6), pp. 403-8.

Duke, O., Panayi, G.S., Janossy, G. and Poulter, L.W. (1982) 'An immunohistological analysis of lymphocyte subpopulations and their microenvironment in the synovial membranes of patients with rheumatoid arthritis using monoclonal antibodies', *Clin Exp Immunol*, 49(1), pp. 22-30.

Dussault, N., Ducas, E., Racine, C., Jacques, A., Pare, I., Cote, S. and Neron, S. (2008) 'Immunomodulation of human B cells following treatment with intravenous immunoglobulins involves increased phosphorylation of extracellular signal-regulated kinases 1 and 2', *Int Immunol*, 20(11), pp. 1369-79.

Duvallet, E., Semerano, L., Assier, E., Falgarone, G. and Boissier, M.C. (2011) 'Interleukin-23: a key cytokine in inflammatory diseases', *Ann Med*, 43(7), pp. 503-11.

Edwards, J.C. and Cambridge, G. (2006) 'B-cell targeting in rheumatoid arthritis and other autoimmune diseases', *Nat Rev Immunol*, 6(5), pp. 394-403.

Ehrhardt, G.R. and Cooper, M.D. (2011) 'Immunoregulatory roles for fc receptor-like molecules', *Curr Top Microbiol Immunol*, 350, pp. 89-104.

Ehrhardt, G.R., Hsu, J.T., Gartland, L., Leu, C.M., Zhang, S., Davis, R.S. and Cooper, M.D. (2005) 'Expression of the immunoregulatory molecule FcRH4 defines a distinctive tissue-based population of memory B cells', *J Exp Med*, 202(6), pp. 783-91.

Ehrhardt, G.R., Leu, C.M., Zhang, S., Aksu, G., Jackson, T., Haga, C., Hsu, J.T., Schreeder, D.M., Davis, R.S. and Cooper, M.D. (2007) 'Fc receptor-like proteins (FCRL): immunomodulators of B cell function', *Adv Exp Med Biol*, 596, pp. 155-62.

Elgueta, R., Benson, M.J., de Vries, V.C., Wasiuk, A., Guo, Y. and Noelle, R.J. (2009) 'Molecular mechanism and function of CD40/CD40L engagement in the immune system', *Immunol Rev*, 229(1), pp. 152-72.

Elliott, M.J., Maini, R.N., Feldmann, M., Kalden, J.R., Antoni, C., Smolen, J.S., Leeb, B., Breedveld, F.C., Macfarlane, J.D., Bijl, H. and et al. (1994) 'Randomised double-blind comparison of chimeric monoclonal antibody to tumour necrosis factor alpha (cA2) versus placebo in rheumatoid arthritis', *Lancet*, 344(8930), pp. 1105-10.

Esser, P. and Weitzmann, L. (2011) *Evaporation from Cell Culture Plates* Available at: http://www.labobaza.pl/download/artykulplik/parowaniezplytekdohodowlikomorkowych.pdf.

Ettinger, R., Sims, G.P., Fairhurst, A.M., Robbins, R., da Silva, Y.S., Spolski, R., Leonard, W.J. and Lipsky, P.E. (2005) 'IL-21 induces differentiation of human naive and memory B cells into antibody-secreting plasma cells', *J Immunol*, 175(12), pp. 7867-79.

Eyre, S., Bowes, J., Potter, C., Worthington, J. and Barton, A. (2006) 'Association of the FCRL3 gene with rheumatoid arthritis: a further example of population specificity?', *Arthritis Res Ther*, 8(4), p. R117.

Falini, B., Tiacci, E., Pucciarini, A., Bigerna, B., Kurth, J., Hatzivassiliou, G., Droetto, S., Galletti, B.V., Gambacorta, M., Orazi, A., Pasqualucci, L., Miller, I., Kuppers, R., Dalla-Favera, R. and Cattoretti, G. (2003) 'Expression of the IRTA1 receptor identifies intraepithelial and subepithelial marginal zone B cells of the mucosa-associated lymphoid tissue (MALT)', *Blood*, 102(10), pp. 3684-92.

Feldmann, M. and Maini, R.N. (2001) 'Anti-TNF alpha therapy of rheumatoid arthritis: what have we learned?', *Annu Rev Immunol*, 19, pp. 163-96.

Firestein, G.S. and McInnes, I.B. (2017) 'Immunopathogenesis of Rheumatoid Arthritis', *Immunity*, 46(2), pp. 183-196.

Forthal, D.N. (2014) 'Functions of Antibodies', *Microbiol Spectr*, 2(4), pp. Aid-0019-2014.

Franco, A., Damdinsuren, B., Ise, T., Dement-Brown, J., Li, H., Nagata, S. and Tolnay, M. (2013) 'Human Fc receptor-like 5 binds intact IgG via mechanisms distinct from those of Fc receptors', *J Immunol*, 190(11), pp. 5739-46.

Frasca, D., Romero, M., Diaz, A., Alter-Wolf, S., Ratliff, M., Landin, A.M., Riley, R.L. and Blomberg, B.B. (2012) 'A molecular mechanism for TNF-alpha-mediated downregulation of B cell responses', *J Immunol*, 188(1), pp. 279-86.

Gee, K., Guzzo, C., Che Mat, N.F., Ma, W. and Kumar, A. (2009) 'The IL-12 family of cytokines in infection, inflammation and autoimmune disorders', *Inflamm Allergy Drug Targets*, 8(1), pp. 40-52.

Geiss, G.K., Bumgarner, R.E., Birditt, B., Dahl, T., Dowidar, N., Dunaway, D.L., Fell, H.P., Ferree, S., George, R.D., Grogan, T., James, J.J., Maysuria, M., Mitton, J.D., Oliveri, P., Osborn, J.L., Peng, T., Ratcliffe, A.L., Webster, P.J., Davidson, E.H., Hood, L. and Dimitrov, K. (2008) 'Direct multiplexed measurement of gene expression with color-coded probe pairs', *Nat Biotechnol*, 26(3), pp. 317-25.

Gerth, A.J., Lin, L. and Peng, S.L. (2003) 'T-bet regulates T-independent IgG2a class switching', *Int Immunol*, 15(8), pp. 937-44.

Gibson, A.W., Li, F.J., Wu, J., Edberg, J.C., Su, K., Cafardi, J., Wiener, H., Tiwari, H., Kimberly, R.P. and Davis, R.S. (2009) 'The FCRL3-169CT promoter single-nucleotide polymorphism, which is associated with systemic lupus erythematosus in a Japanese population, predicts expression of receptor protein on CD19+ B cells', *Arthritis Rheum*, 60(11), pp. 3510-2.

Giudizi, M.G., Biagiotti, R., Almerigogna, F., Alessi, A., Tiri, A., Del Prete, G.F., Ferrone, S. and Romagnani, S. (1987) 'Role of HLA class I and class II antigens in activation and differentiation of B cells', *Cell Immunol*, 108(1), pp. 97-108.

Gladman, D.D. (2015) 'Clinical Features and Diagnostic Considerations in Psoriatic Arthritis', *Rheum Dis Clin North Am*, 41(4), pp. 569-79.

Goding, J.W. (1978) 'Allotypes of IgM and IgD receptors in the mouse: a probe for lymphocyte differentiation', *Contemp Top Immunobiol*, 8, pp. 203-43.

Grammer, A.C., Swantek, J.L., McFarland, R.D., Miura, Y., Geppert, T. and Lipsky, P.E. (1998) 'TNF receptor-associated factor-3 signaling mediates activation of p38 and Jun N-terminal kinase, cytokine secretion, and Ig production following ligation of CD40 on human B cells', *J Immunol*, 161(3), pp. 1183-93.

Gray, D., Gray, M. and Barr, T. (2007a) 'Innate responses of B cells', *Eur J Immunol*, 37(12), pp. 3304-10.

Gray, M., Miles, K., Salter, D., Gray, D. and Savill, J. (2007b) 'Apoptotic cells protect mice from autoimmune inflammation by the induction of regulatory B cells', *Proc Natl Acad Sci U S A*, 104(35), pp. 14080-5.

Grimaldi, C.M., Hicks, R. and Diamond, B. (2005) 'B cell selection and susceptibility to autoimmunity', *J Immunol*, 174(4), pp. 1775-81.

Groom, J.R. and Luster, A.D. (2011a) 'CXCR3 in T cell function', *Exp Cell Res*, 317(5), pp. 620-31.

Groom, J.R. and Luster, A.D. (2011b) 'CXCR3 ligands: redundant, collaborative and antagonistic functions', *Immunology and cell biology*, 89(2), pp. 207-215.

Guma, M., Busch, L.K., Salazar-Fontana, L.I., Bellosillo, B., Morte, C., Garcia, P. and Lopez-Botet, M. (2005) 'The CD94/NKG2C killer lectin-like receptor constitutes an alternative activation pathway for a subset of CD8+ T cells', *Eur J Immunol*, 35(7), pp. 2071-80.

Haga, C.L., Ehrhardt, G.R., Boohaker, R.J., Davis, R.S. and Cooper, M.D. (2007) 'Fc receptor-like 5 inhibits B cell activation via SHP-1 tyrosine phosphatase recruitment', *Proc Natl Acad Sci U S A*, 104(23), pp. 9770-5.

Hagn, M., Sontheimer, K., Dahlke, K., Brueggemann, S., Kaltenmeier, C., Beyer, T., Hofmann, S., Lunov, O., Barth, T.F., Fabricius, D., Tron, K., Nienhaus, G.U., Simmet, T., Schrezenmeier, H. and Jahrsdorfer, B. (2012) 'Human B cells differentiate into granzyme B-secreting cytotoxic B lymphocytes upon incomplete T-cell help', *Immunol Cell Biol*, 90(4), pp. 457-67.

Hajizadeh, S., DeGroot, J., TeKoppele, J.M., Tarkowski, A. and Collins, L.V. (2003) 'Extracellular mitochondrial DNA and oxidatively damaged DNA in synovial fluid of patients with rheumatoid arthritis', *Arthritis Res Ther*, 5(5), pp. R234-40.

Hamann, J., Hsiao, C.C., Lee, C.S., Ravichandran, K.S. and Lin, H.H. (2016) 'Adhesion GPCRs as Modulators of Immune Cell Function', *Handb Exp Pharmacol*, 234, pp. 329-350.

Hamann, J., Veninga, H., de Groot, D.M., Visser, L., Hofstra, C.L., Tak, P.P., Laman, J.D., Boots, A.M. and van Eenennaam, H. (2010) 'CD97 in leukocyte trafficking', *Adv Exp Med Biol*, 706, pp. 128-37.

Hamann, J., Wishaupt, J.O., van Lier, R.A., Smeets, T.J., Breedveld, F.C. and Tak, P.P. (1999) 'Expression of the activation antigen CD97 and its ligand CD55 in rheumatoid synovial tissue', *Arthritis Rheum*, 42(4), pp. 650-8.

Hao, Y., O'Neill, P., Naradikian, M.S., Scholz, J.L. and Cancro, M.P. (2011) 'A B-cell subset uniquely responsive to innate stimuli accumulates in aged mice', *Blood*, 118(5), pp. 1294-304.

Harburger, D.S. and Calderwood, D.A. (2009) 'Integrin signalling at a glance', *J Cell Sci*, 122(Pt 2), pp. 159-63.

Hardy, R.R. and Hayakawa, K. (2001) 'B cell development pathways', *Annu Rev Immunol*, 19, pp. 595-621.

Harvard (n.d) *Guideline for choosing a sorter*. Available at: https://immunology.hms.harvard.edu/resources/flow-cytometry/sorting-guidlines (Accessed: September 17, 2019).

Hatfull, G., Bankier, A.T., Barrell, B.G. and Farrell, P.J. (1988) 'Sequence analysis of Raji Epstein-Barr virus DNA', *Virology*, 164(2), pp. 334-40.

Hatzivassiliou, G., Miller, I., Takizawa, J., Palanisamy, N., Rao, P.H., Iida, S., Tagawa, S., Taniwaki, M., Russo, J., Neri, A., Cattoretti, G., Clynes, R., Mendelsohn, C., Chaganti, R.S. and Dalla-Favera, R. (2001) 'IRTA1 and IRTA2, novel immunoglobulin superfamily receptors expressed in B cells and involved in chromosome 1q21 abnormalities in B cell malignancy', *Immunity*, 14(3), pp. 277-89.

Hayakawa, K., Hardy, R.R., Honda, M., Herzenberg, L.A., Steinberg, A.D. and Herzenberg, L.A. (1984) 'Ly-1 B cells: functionally distinct lymphocytes that secrete IgM autoantibodies', *Proc Natl Acad Sci U S A*, 81(8), pp. 2494-8.

Herlands, R.A., Christensen, S.R., Sweet, R.A., Hershberg, U. and Shlomchik, M.J. (2008) 'T cell-independent and toll-like receptor-dependent antigen-driven activation of autoreactive B cells', *Immunity*, 29(2), pp. 249-60.

Huber, W., Carey, V.J., Gentleman, R., Anders, S., Carlson, M., Carvalho, B.S., Bravo, H.C., Davis, S., Gatto, L., Girke, T., Gottardo, R., Hahne, F., Hansen, K.D., Irizarry, R.A., Lawrence, M., Love, M.I., MacDonald, J., Obenchain, V., Oles, A.K., Pages, H., Reyes, A., Shannon, P., Smyth, G.K., Tenenbaum, D., Waldron, L. and Morgan, M. (2015) 'Orchestrating high-throughput genomic analysis with Bioconductor', *Nat Methods*, 12(2), pp. 115-21.

Huggins, J., Pellegrin, T., Felgar, R.E., Wei, C., Brown, M., Zheng, B., Milner, E.C., Bernstein, S.H., Sanz, I. and Zand, M.S. (2007) 'CpG DNA activation and plasma-cell differentiation of CD27- naive human B cells', *Blood*, 109(4), pp. 1611-9.

Humphreys, J.H., Verstappen, S.M., Hyrich, K.L., Chipping, J.R., Marshall, T. and Symmons, D.P. (2013) 'The incidence of rheumatoid arthritis in the UK: comparisons using the 2010 ACR/EULAR classification criteria and the 1987 ACR classification criteria. Results from the Norfolk Arthritis Register', *Ann Rheum Dis*, 72(8), pp. 1315-20.

Humphries, J.D., Paul, N.R., Humphries, M.J. and Morgan, M.R. (2015) 'Emerging properties of adhesion complexes: what are they and what do they do?', *Trends Cell Biol*, 25(7), pp. 388-97.

Illges, H., Braun, M., Peter, H.H. and Melchers, I. (2000) 'Reduced expression of the complement receptor type 2 (CR2, CD21) by synovial fluid B and T lymphocytes', *Clin Exp Immunol*, 122(2), pp. 270-6.

Innala, L., Sjoberg, C., Moller, B., Ljung, L., Smedby, T., Sodergren, A., Magnusson, S., Rantapaa-Dahlqvist, S. and Wallberg-Jonsson, S. (2016) 'Co-morbidity in patients with early rheumatoid arthritis - inflammation matters', *Arthritis Res Ther*, 18, p. 33.

Isaak, A., Prechl, J., Gergely, J. and Erdei, A. (2006) 'The role of CR2 in autoimmunity', *Autoimmunity*, 39(5), pp. 357-66.

Ise, T., Maeda, H., Santora, K., Xiang, L., Kreitman, R.J., Pastan, I. and Nagata, S. (2005) 'Immunoglobulin superfamily receptor translocation associated 2 protein on lymphoma cell lines and hairy cell leukemia cells detected by novel monoclonal antibodies', *Clin Cancer Res*, 11(1), pp. 87-96.

Isnardi, I., Ng, Y.S., Menard, L., Meyers, G., Saadoun, D., Srdanovic, I., Samuels, J., Berman, J., Buckner, J.H., Cunningham-Rundles, C. and Meffre, E. (2010) 'Complement receptor 2/CD21- human naive B cells contain mostly autoreactive unresponsive clones', *Blood*, 115(24), pp. 5026-36.

Isomaki, P., Luukkainen, R., Toivanen, P. and Punnonen, J. (1996) 'The presence of interleukin-13 in rheumatoid synovium and its antiinflammatory effects on synovial fluid macrophages from patients with rheumatoid arthritis', *Arthritis Rheum*, 39(10), pp. 1693-702.

Itoh, K. and Hirohata, S. (1995) 'The role of IL-10 in human B cell activation, proliferation, and differentiation', *J Immunol*, 154(9), pp. 4341-50.

Jackson, T.A., Haga, C.L., Ehrhardt, G.R., Davis, R.S. and Cooper, M.D. (2010) 'FcR-like 2 Inhibition of B cell receptor-mediated activation of B cells', *J Immunol*, 185(12), pp. 7405-12.

Jacob, J. and Kelsoe, G. (1992) 'In situ studies of the primary immune response to (4-hydroxy-3-nitrophenyl)acetyl. II. A common clonal origin for periarteriolar lymphoid sheath-associated foci and germinal centers', *J Exp Med*, 176(3), pp. 679-87.

Janeway, C.A., Jr. and Medzhitov, R. (2008) 'Innate immune recognition', *Annu Rev Immunol*, 20, pp. 197-216.

Jenks, S.A., Cashman, K.S., Zumaquero, E., Marigorta, U.M., Patel, A.V., Wang, X., Tomar, D., Woodruff, M.C., Simon, Z., Bugrovsky, R., Blalock, E.L., Scharer, C.D., Tipton, C.M., Wei, C., Lim, S.S., Petri, M., Niewold, T.B., Anolik, J.H., Gibson, G., Lee, F.E., Boss, J.M., Lund, F.E. and Sanz, I. (2018) 'Distinct Effector B Cells Induced by Unregulated Toll-like Receptor 7 Contribute to Pathogenic Responses in Systemic Lupus Erythematosus', *Immunity*, 49(4), pp. 725-739.e6.

Johnson, J.L., Scholz, J.L., Marshak-Rothstein, A. and Cancro, M.P. (2019) 'Molecular pattern recognition in peripheral B cell tolerance: lessons from age-associated B cells', *Curr Opin Immunol*, 61, pp. 33-38.

Jurado, A., Carballido, J., Griffel, H., Hochkeppel, H.K. and Wetzel, G.D. (1989) 'The immunomodulatory effects of interferon-gamma on mature B-lymphocyte responses', *Experientia*, 45(6), pp. 521-6.

Kampstra, A.S.B. and Toes, R.E.M. (2017) 'HLA class II and rheumatoid arthritis: the bumpy road of revelation', *Immunogenetics*, 69(8-9), pp. 597-603.

Karnell, J.L., Kumar, V., Wang, J., Wang, S., Voynova, E. and Ettinger, R. (2017) 'Role of CD11c(+) T-bet(+) B cells in human health and disease', *Cell Immunol*, 321, pp. 40-45.

Kassiotis, G. and Stoye, J.P. (2016) 'Immune responses to endogenous retroelements: taking the bad with the good', *Nat Rev Immunol*, 16(4), pp. 207-19.

Katikaneni, D.S. and Jin, L. (2019) 'B cell MHC class II signaling: A story of life and death', *Hum Immunol*, 80(1), pp. 37-43.

Kauffmann, A., Gentleman, R. and Huber, W. (2009) 'arrayQualityMetrics--a bioconductor package for quality assessment of microarray data', *Bioinformatics*, 25(3), pp. 415-6.

Kerlan-Candon, S., Combe, B., Vincent, R., Clot, J., Pinet, V. and Eliaou, J.F. (2001) 'HLA-DRB1 gene transcripts in rheumatoid arthritis', *Clin Exp Immunol*, 124(1), pp. 142-9.

Kim, T.K. and Eberwine, J.H. (2010) 'Mammalian cell transfection: the present and the future', *Anal Bioanal Chem*, 397(8), pp. 3173-8.

Kindler, V., Matthes, T., Jeannin, P. and Zubler, R.H. (1995) 'Interleukin-2 secretion by human B lymphocytes occurs as a late event and requires additional stimulation after CD40 cross-linking', *Eur J Immunol*, 25(5), pp. 1239-43.

Kinne, R.W., Brauer, R., Stuhlmuller, B., Palombo-Kinne, E. and Burmester, G.R. (2000) 'Macrophages in rheumatoid arthritis', *Arthritis Res*, 2(3), pp. 189-202.

Knox, J.J., Myles, A. and Cancro, M.P. (2019) 'T-bet(+) memory B cells: Generation, function, and fate', *Immunol Rev*, 288(1), pp. 149-160.

Koch, M.A., Tucker-Heard, G., Perdue, N.R., Killebrew, J.R., Urdahl, K.B. and Campbell, D.J. (2009) 'The transcription factor T-bet controls regulatory T cell homeostasis and function during type 1 inflammation', *Nat Immunol*, 10(6), pp. 595-602.

Kochi, Y., Myouzen, K., Yamada, R., Suzuki, A., Kurosaki, T., Nakamura, Y. and Yamamoto, K. (2009) 'FCRL3, an autoimmune susceptibility gene, has inhibitory potential on B-cell receptor-mediated signaling', *J Immunol*, 183(9), pp. 5502-10.

Kochi, Y., Yamada, R., Suzuki, A., Harley, J.B., Shirasawa, S., Sawada, T., Bae, S.C., Tokuhiro, S., Chang, X., Sekine, A., Takahashi, A., Tsunoda, T., Ohnishi, Y., Kaufman, K.M., Kang, C.P., Kang, C., Otsubo, S., Yumura, W., Mimori, A., Koike, T., Nakamura, Y., Sasazuki, T. and Yamamoto, K. (2005) 'A functional variant in FCRL3, encoding Fc receptor-like 3, is associated with rheumatoid arthritis and several autoimmunities', *Nat Genet*, 37(5), pp. 478-85.

Kop, E.N., Adriaansen, J., Smeets, T.J., Vervoordeldonk, M.J., van Lier, R.A., Hamann, J. and Tak, P.P. (2006) 'CD97 neutralisation increases resistance to collagen-induced arthritis in mice', *Arthritis Res Ther*, 8(5), p. R155.

Kop, E.N., Kwakkenbos, M.J., Teske, G.J., Kraan, M.C., Smeets, T.J., Stacey, M., Lin, H.H., Tak, P.P. and Hamann, J. (2005) 'Identification of the epidermal growth factor-TM7 receptor EMR2 and its ligand dermatan sulfate in rheumatoid synovial tissue', *Arthritis Rheum*, 52(2), pp. 442-50.

Krabben, A., Wilson, A.G., de Rooy, D.P., Zhernakova, A., Brouwer, E., Lindqvist, E., Saxne, T., Stoeken, G., van Nies, J.A., Knevel, R., Huizinga, T.W., Toes, R., Gregersen, P.K. and van der Helm-van Mil, A.H. (2013) 'Association of genetic variants in the IL4 and IL4R genes with the severity of joint damage in rheumatoid arthritis: a study in seven cohorts', *Arthritis Rheum*, 65(12), pp. 3051-7.

Kremer, J.M., Westhovens, R., Leon, M., Di Giorgio, E., Alten, R., Steinfeld, S., Russell, A., Dougados, M., Emery, P., Nuamah, I.F., Williams, G.R., Becker, J.C., Hagerty, D.T. and Moreland, L.W. (2003) 'Treatment of rheumatoid arthritis by selective inhibition of T-cell activation with fusion protein CTLA4Ig', *N Engl J Med*, 349(20), pp. 1907-15.

Kumar, V., Abbas, A. and Aster, J. (2017) 'Diseases of the Immune System', in Sciences, E.H. (ed.) *Robbins Basic Pathology*. 10 edn. Canada, p. 928.

Kvien, T.K., Uhlig, T., Odegard, S. and Heiberg, M.S. (2006) 'Epidemiological aspects of rheumatoid arthritis: the sex ratio', *Ann N Y Acad Sci*, 1069, pp. 212-22.

Lagoo, A., Tseng, C.K. and Sell, S. (1990) 'Interleukin 2 produced by activated B lymphocytes acts as an autocrine proliferation-inducing lymphokine', *Cytokine*, 2(4), pp. 272-9.

Lard, L.R., Visser, H., Speyer, I., vander Horst-Bruinsma, I.E., Zwinderman, A.H., Breedveld, F.C. and Hazes, J.M. (2001) 'Early versus delayed treatment in patients with recent-onset rheumatoid arthritis: comparison of two cohorts who received different treatment strategies', *Am J Med*, 111(6), pp. 446-51.

Lau, D., Lan, L.Y., Andrews, S.F., Henry, C., Rojas, K.T., Neu, K.E., Huang, M., Huang, Y., DeKosky, B., Palm, A.E., Ippolito, G.C., Georgiou, G. and Wilson, P.C. (2017) 'Low CD21 expression defines a population of recent germinal center graduates primed for plasma cell differentiation', *Sci Immunol*, 2(7).

Leadbetter, E.A., Rifkin, I.R., Hohlbaum, A.M., Beaudette, B.C., Shlomchik, M.J. and Marshak-Rothstein, A. (2002) 'Chromatin-IgG complexes activate B cells by dual engagement of IgM and Toll-like receptors', *Nature*, 416(6881), pp. 603-7.

LeBien, T.W. and Tedder, T.F. (2008) 'B lymphocytes: how they develop and function', *Blood*, 112(5), pp. 1570-80.

Lee, M., Lee, Y., Song, J., Lee, J. and Chang, S.Y. (2018) 'Tissue-specific Role of CX3CR1 Expressing Immune Cells and Their Relationships with Human Disease', *Immune Netw*, 18(1), p. e5.

Lens, S.M., den Drijver, B.F., Potgens, A.J., Tesselaar, K., van Oers, M.H. and van Lier, R.A. (1998) 'Dissection of pathways leading to antigen receptor-induced and Fas/CD95-induced apoptosis in human B cells', *J Immunol*, 160(12), pp. 6083-92.

Leu, C.M., Davis, R.S., Gartland, L.A., Fine, W.D. and Cooper, M.D. (2005) 'FcRH1: an activation coreceptor on human B cells', *Blood*, 105(3), pp. 1121-6.

Li, F.J., Ding, S., Pan, J., Shakhmatov, M.A., Kashentseva, E., Wu, J., Li, Y., Soong, S.J., Chiorazzi, N. and Davis, R.S. (2008) 'FCRL2 expression predicts IGHV mutation status and clinical progression in chronic lymphocytic leukemia', *Blood*, 112(1), pp. 179-87.

Li, F.J., Schreeder, D.M., Li, R., Wu, J. and Davis, R.S. (2013) 'FCRL3 promotes TLR9-induced B-cell activation and suppresses plasma cell differentiation', *Eur J Immunol*, 43(11), pp. 2980-92.

Li, F.J., Won, W.J., Becker, E.J., Jr., Easlick, J.L., Tabengwa, E.M., Li, R., Shakhmatov, M., Honjo, K., Burrows, P.D. and Davis, R.S. (2014a) 'Emerging roles for the FCRL family members in lymphocyte biology and disease', *Curr Top Microbiol Immunol*, 382, pp. 29-50.

Li, R., Rezk, A., Miyazaki, Y., Hilgenberg, E., Touil, H., Shen, P., Moore, C.S., Michel, L., Althekair, F., Rajasekharan, S., Gommerman, J.L., Prat, A., Fillatreau, S. and Bar-Or, A. (2015) 'Proinflammatory GM-CSF-producing B cells in multiple sclerosis and B cell depletion therapy', *Sci Transl Med*, 7(310), p. 310ra166.

Li, X., Gibson, A.W. and Kimberly, R.P. (2014b) 'Human FcR polymorphism and disease', *Curr Top Microbiol Immunol*, 382, pp. 275-302.

Lin, X., Zhang, Y. and Chen, Q. (2016) 'FCRL3 gene polymorphisms as risk factors for rheumatoid arthritis', *Hum Immunol*, 77(2), pp. 223-9.

Liu, N., Ohnishi, N., Ni, L., Akira, S. and Bacon, K.B. (2003) 'CpG directly induces T-bet expression and inhibits IgG1 and IgE switching in B cells', *Nat Immunol*, 4(7), pp. 687-93.

Liu, Y., Beyer, A. and Aebersold, R. (2016) 'On the Dependency of Cellular Protein Levels on mRNA Abundance', *Cell*, 165(3), pp. 535-50.

Lorenzi, A.R., Clarke, A.M., Wooldridge, T., Waldmann, H., Hale, G., Symmons, D., Hazleman, B.L. and Isaacs, J.D. (2008) 'Morbidity and mortality in rheumatoid arthritis patients with prolonged therapy-induced lymphopenia: twelve-year outcomes', *Arthritis Rheum*, 58(2), pp. 370-5.

Love, M.I., Huber, W. and Anders, S. (2014) 'Moderated estimation of fold change and dispersion for RNA-seq data with DESeq2', *Genome Biol*, 15(12), p. 550.

Ma, K., Du, W., Wang, X., Yuan, S., Cai, X., Liu, D., Li, J. and Lu, L. (2019) 'Multiple Functions of B Cells in the Pathogenesis of Systemic Lupus Erythematosus', *Int J Mol Sci*, 20(23).

Ma, L., Liu, B., Jiang, Z. and Jiang, Y. (2014) 'Reduced numbers of regulatory B cells are negatively correlated with disease activity in patients with new-onset rheumatoid arthritis', *Clin Rheumatol*, 33(2), pp. 187-95.

MacLennan, I.C. (1994) 'Germinal centers', *Annu Rev Immunol*, 12, pp. 117-39.

Malek, T.R. (2003) 'The main function of IL-2 is to promote the development of T regulatory cells', *J Leukoc Biol*, 74(6), pp. 961-5.

Malmstrom, V., Catrina, A.I. and Klareskog, L. (2017) 'The immunopathogenesis of seropositive rheumatoid arthritis: from triggering to targeting', *Nat Rev Immunol*, 17(1), pp. 60-75.

Maltais, L.J., Lovering, R.C., Taranin, A.V., Colonna, M., Ravetch, J.V., Dalla-Favera, R., Burrows, P.D., Cooper, M.D. and Davis, R.S. (2006) 'New nomenclature for Fc receptor-like molecules', *Nat Immunol*, 7(5), pp. 431-2.

Manni, M., Gupta, S., Ricker, E., Chinenov, Y., Park, S.H., Shi, M., Pannellini, T., Jessberger, R., Ivashkiv, L.B. and Pernis, A.B. (2018) 'Regulation of age-associated B cells by IRF5 in systemic autoimmunity', *Nat Immunol*, 19(4), pp. 407-419.

Manzoor, A.M. (2015) 'Introduction to Costimulation and Costimulatory Molecules', in *Developing Costimulatory Molecules for Immunotherapy of Diseases*. Elsevier, p. 322.

Martin, F., Oliver, A.M. and Kearney, J.F. (2001) 'Marginal zone and B1 B cells unite in the early response against T-independent blood-borne particulate antigens', *Immunity*, 14(5), pp. 617-29.

Masilamani, M., Kassahn, D., Mikkat, S., Glocker, M.O. and Illges, H. (2003) 'B cell activation leads to shedding of complement receptor type II (CR2/CD21)', *Eur J Immunol*, 33(9), pp. 2391-7.

Mason, U., Aldrich, J., Breedveld, F., Davis, C.B., Elliott, M., Jackson, M., Jorgensen, C., Keystone, E., Levy, R., Tesser, J., Totoritis, M., Truneh, A., Weisman, M., Wiesenhutter, C., Yocum, D. and Zhu, J. (2002) 'CD4 coating, but not CD4 depletion, is a predictor of efficacy with primatized monoclonal anti-CD4 treatment of active rheumatoid arthritis', *J Rheumatol*, 29(2), pp. 220-9.

Mcheik, S., Van Eeckhout, N., De Poorter, C., Galés, C., Parmentier, M. and Springael, J.-Y. (2019) 'Coexpression of CCR7 and CXCR4 during B cell development controls CXCR4 responsiveness and bone marrow homing', *bioRxiv*, p. 689372.

McInnes, I.B. and Schett, G. (2007) 'Cytokines in the pathogenesis of rheumatoid arthritis', *Nat Rev Immunol*, 7(6), pp. 429-42.

McInnes, I.B. and Schett, G. (2011) 'The pathogenesis of rheumatoid arthritis', *N Engl J Med*, 365(23), pp. 2205-19.

Mechetina, L.V., Najakshin, A.M., Volkova, O.Y., Guselnikov, S.V., Faizulin, R.Z., Alabyev, B.Y., Chikaev, N.A., Vinogradova, M.S. and Taranin, A.V. (2002) 'FCRL, a novel member of the leukocyte Fc receptor family possesses unique structural features', *Eur J Immunol*, 32(1), pp. 87-96.

Medzhitov, R. (2001) 'Toll-like receptors and innate immunity', *Nat Rev Immunol*, 1(2), pp. 135-45.

Mensah, K.A., Chen, J.W., Schickel, J.N., Isnardi, I., Yamakawa, N., Vega-Loza, A., Anolik, J.H., Gatti, R.A., Gelfand, E.W., Montgomery, R.R., Horowitz, M.C., Craft, J.E. and Meffre, E. (2019) 'Impaired ATM activation in B cells is associated with bone resorption in rheumatoid arthritis', *Sci Transl Med*, 11(519).

Merola, J.F., Espinoza, L.R. and Fleischmann, R. (2018) 'Distinguishing rheumatoid arthritis from psoriatic arthritis', *RMD Open*, 4(2), p. e000656.

Miller, I., Hatzivassiliou, G., Cattoretti, G., Mendelsohn, C. and Dalla-Favera, R. (2002) 'IRTAs: a new family of immunoglobulinlike receptors differentially expressed in B cells', *Blood*, 99(8), pp. 2662-9.

Mingari, M.C., Moretta, A. and Moretta, L. (1998) 'Regulation of KIR expression in human T cells: a safety mechanism that may impair protective T-cell responses', *Immunol Today*, 19(4), pp. 153-7.

Moir, S., Ho, J., Malaspina, A., Wang, W., DiPoto, A.C., O'Shea, M.A., Roby, G., Kottilil, S., Arthos, J., Proschan, M.A., Chun, T.W. and Fauci, A.S. (2008) 'Evidence for HIV-associated B cell exhaustion in a dysfunctional memory B cell compartment in HIV-infected viremic individuals', *J Exp Med*, 205(8), pp. 1797-805.

Moore, D.K., Motaung, B., du Plessis, N., Shabangu, A.N. and Loxton, A.G. (2019) 'Isolation of B-cells using Miltenyi MACS bead isolation kits', *PLoS One*, 14(3), p. e0213832.

Moretta, A., Bottino, C., Vitale, M., Pende, D., Biassoni, R., Mingari, M.C. and Moretta, L. (1996) 'Receptors for HLA class-I molecules in human natural killer cells', *Annu Rev Immunol*, 14, pp. 619-48.

Mu, X., Ahmad, S. and Hur, S. (2016) 'Endogenous Retroelements and the Host Innate Immune Sensors', *Adv Immunol*, 132, pp. 47-69.

Murata, T., Obiri, N.I. and Puri, R.K. (1998) 'Structure of and signal transduction through interleukin-4 and interleukin-13 receptors (review)', *Int J Mol Med*, 1(3), pp. 551-7.

Myles, A., Sanz, I. and Cancro, M.P. (2019) 'T-bet(+) B cells: A common denominator in protective and autoreactive antibody responses?', *Curr Opin Immunol*, 57, pp. 40-45.

Nagata, S. (1999) 'Fas ligand-induced apoptosis', *Annu Rev Genet*, 33, pp. 29-55.

Nagata, S., Ise, T. and Pastan, I. (2009) 'Fc receptor-like 3 protein expressed on IL-2 nonresponsive subset of human regulatory T cells', *J Immunol*, 182(12), pp. 7518-26.

Naradikian, M.S., Hao, Y. and Cancro, M.P. (2016a) 'Age-associated B cells: key mediators of both protective and autoreactive humoral responses', *Immunol Rev*, 269(1), pp. 118-29.

Naradikian, M.S., Myles, A., Beiting, D.P., Roberts, K.J., Dawson, L., Herati, R.S., Bengsch, B., Linderman, S.L., Stelekati, E., Spolski, R., Wherry, E.J., Hunter, C., Hensley, S.E., Leonard, W.J. and Cancro, M.P. (2016b) 'Cutting Edge: IL-4, IL-21, and IFN-gamma Interact To Govern T-bet and CD11c Expression in TLR-Activated B Cells', *J Immunol*, 197(4), pp. 1023-8.

Neidhart, M., Rethage, J., Kuchen, S., Kunzler, P., Crowl, R.M., Billingham, M.E., Gay, R.E. and Gay, S. (2000) 'Retrotransposable L1 elements expressed in rheumatoid arthritis synovial tissue: association with genomic DNA hypomethylation and influence on gene expression', *Arthritis Rheum*, 43(12), pp. 2634-47.

Obeng-Adjei, N., Portugal, S., Holla, P., Li, S., Sohn, H., Ambegaonkar, A., Skinner, J., Bowyer, G., Doumbo, O.K., Traore, B., Pierce, S.K. and Crompton, P.D. (2017) 'Malaria-induced interferon-gamma drives the expansion of Tbethi atypical memory B cells', *PLoS Pathog*, 13(9), p. e1006576.

Page, G. and Miossec, P. (2004) 'Paired synovium and lymph nodes from rheumatoid arthritis patients differ in dendritic cell and chemokine expression', *J Pathol*, 204(1), pp. 28-38.

Park, J.K., Han, B.K., Park, J.A., Woo, Y.J., Kim, S.Y., Lee, E.Y., Lee, E.B., Chalan, P., Boots, A.M. and Song, Y.W. (2014) 'CD70-expressing CD4 T cells produce IFN-gamma and IL-17 in rheumatoid arthritis', *Rheumatology (Oxford)*, 53(10), pp. 1896-900.

Parkin, J. and Cohen, B. (2001) 'An overview of the immune system', *Lancet*, 357(9270), pp. 1777-89.

Patel, D.D., Zachariah, J.P. and Whichard, L.P. (2001) 'CXCR3 and CCR5 ligands in rheumatoid arthritis synovium', *Clin Immunol*, 98(1), pp. 39-45.

Perez-Andres, M., Paiva, B., Nieto, W.G., Caraux, A., Schmitz, A., Almeida, J., Vogt, R.F., Jr., Marti, G.E., Rawstron, A.C., Van Zelm, M.C., Van Dongen, J.J., Johnsen, H.E., Klein, B. and Orfao, A. (2010) 'Human peripheral blood B-cell compartments: a crossroad in B-cell traffic', *Cytometry B Clin Cytom*, 78 Suppl 1, pp. S47-60.

Phalke, S. and Marrack, P. (2018) 'Age (autoimmunity) associated B cells (ABCs) and their relatives', *Curr Opin Immunol*, 55, pp. 75-80.

Plenge, R.M., Padyukov, L., Remmers, E.F., Purcell, S., Lee, A.T., Karlson, E.W., Wolfe, F., Kastner, D.L., Alfredsson, L., Altshuler, D., Gregersen, P.K., Klareskog, L. and Rioux, J.D. (2005) 'Replication of putative candidate-gene associations with rheumatoid arthritis in >4,000 samples from North America and Sweden: association of susceptibility with PTPN22, CTLA4, and PADI4', *Am J Hum Genet*, 77(6), pp. 1044-60.

Polson, A.G., Zheng, B., Elkins, K., Chang, W., Du, C., Dowd, P., Yen, L., Tan, C., Hongo, J.A., Koeppen, H. and Ebens, A. (2006) 'Expression pattern of the human FcRH/IRTA receptors in normal tissue and in B-chronic lymphocytic leukemia', *Int Immunol*, 18(9), pp. 1363-73.

Ponchel, F., Brown, A.K., Field, S.L., Quinn, M., Conaghan, P., Emery, P. and Isaacs, J.D. (2005) 'T-bet expression in rheumatoid arthritis patients with early, disease-modifying anti-rheumatic drug naïve disease is low and correlates with low levels of IL-7 and T-cell dysfunctions.', *Arthritis Research & Therapy*, 7, p. 18.

Portugal, S., Obeng-Adjei, N., Moir, S., Crompton, P.D. and Pierce, S.K. (2017) 'Atypical memory B cells in human chronic infectious diseases: An interim report', *Cell Immunol*, 321, pp. 18-25.

Portugal, S., Tipton, C.M., Sohn, H., Kone, Y., Wang, J., Li, S., Skinner, J., Virtaneva, K., Sturdevant, D.E., Porcella, S.F., Doumbo, O.K., Doumbo, S., Kayentao, K., Ongoiba, A., Traore, B., Sanz, I., Pierce, S.K. and Crompton, P.D. (2015) 'Malaria-associated atypical memory B cells exhibit markedly reduced B cell receptor signaling and effector function', *Elife*, 4.

Postigo, A.A., Corbi, A.L., Sanchez-Madrid, F. and de Landazuri, M.O. (1991) 'Regulated expression and function of CD11c/CD18 integrin on human B lymphocytes. Relation between attachment to fibrinogen and triggering of proliferation through CD11c/CD18', *J Exp Med*, 174(6), pp. 1313-22.

Pratt, A.G., Swan, D.C., Richardson, S., Wilson, G., Hilkens, C.M., Young, D.A. and Isaacs, J.D. (2012) 'A CD4 T cell gene signature for early rheumatoid arthritis implicates interleukin 6-mediated STAT3 signalling, particularly in anti-citrullinated peptide antibody-negative disease', *Ann Rheum Dis*, 71(8), pp. 1374-81.

Prieto, J.M.B. and Felippe, M.J.B. (2017) 'Development, phenotype, and function of non-conventional B cells', *Comp Immunol Microbiol Infect Dis*, 54, pp. 38-44.

Purtha, W.E., Chachu, K.A., Virgin, H.W.t. and Diamond, M.S. (2008) 'Early B-cell activation after West Nile virus infection requires alpha/beta interferon but not antigen receptor signaling', *J Virol*, 82(22), pp. 10964-74.

Rahimi, P., Mobarakeh, V.I., Kamalzare, S., SajadianFard, F., Vahabpour, R. and Zabihollahi, R. (2018) 'Comparison of transfection efficiency of polymer-based and lipid-based transfection reagents', *Bratisl Lek Listy*, 119(11), pp. 701-705.

Rajewsky, K. (1996) 'Clonal selection and learning in the antibody system', *Nature*, 381(6585), pp. 751-8.

Rakhmanov, M., Keller, B., Gutenberger, S., Foerster, C., Hoenig, M., Driessen, G., van der Burg, M., van Dongen, J.J., Wiech, E., Visentini, M., Quinti, I., Prasse, A., Voelxen, N., Salzer, U., Goldacker, S., Fisch, P., Eibel, H., Schwarz, K., Peter, H.H. and Warnatz, K. (2009) 'Circulating CD21low B cells in common variable immunodeficiency resemble tissue homing, innate-like B cells', *Proc Natl Acad Sci U S A*, 106(32), pp. 13451-6.

Ratliff, M., Alter, S., Frasca, D., Blomberg, B.B. and Riley, R.L. (2013) 'In senescence, age-associated B cells secrete TNFalpha and inhibit survival of B-cell precursors', *Aging Cell*, 12(2), pp. 303-11.

Raza, K., Falciani, F., Curnow, S.J., Ross, E.J., Lee, C.Y., Akbar, A.N., Lord, J.M., Gordon, C., Buckley, C.D. and Salmon, M. (2005) 'Early rheumatoid arthritis is characterized by a distinct and transient synovial fluid cytokine profile of T cell and stromal cell origin', *Arthritis Res Ther*, 7(4), pp. R784-95.

Reparon-Schuijt, C.C., van Esch, W.J., van Kooten, C., Rozier, B.C., Levarht, E.W., Breedveld, F.C. and Verweij, C.L. (2000) 'Regulation of synovial B cell survival in rheumatoid arthritis by vascular cell adhesion molecule 1 (CD106) expressed on fibroblast-like synoviocytes', *Arthritis Rheum*, 43(5), pp. 1115-21.

Researchgate (2012) *Recommendations for primary B cell isolation*. Available at: https://www.researchgate.net/post/Can_anyone_share_recommendations_for_primary_B_cell_isolation_human_and_also_how_you_best_keep_them_growing_in_culture_over_time (Accessed: September 17, 2019).

Researchgate (2013a) *Ramos cells dying after FACS sorting*. Available at: https://www.researchgate.net/post/Ramos_cells_dying_after_FACS_sorting (Accessed: September 9, 2019).

Researchgate (2013b) *Trouble in lentiviral expression*. Available at: https://www.researchgate.net/post/Can_someone_advise_on_a_trouble_in_lentiviral_expression_GFP_expressed_target_gene_not (Accessed: February 26, 2020).

Rich, R., Fleisher, T., Shearer, W., Schroeder, H., Frew, A. and Weyand, C. (2019) *Clinical Immunology: Principles and Practice*. 5th edn. Elsevier.

Ridgley, L.A., Anderson, A.E., Maney, N.J., Naamane, N., Skelton, A.J., Lawson, C.A., Emery, P., Isaacs, J.D., Carmody, R.J. and Pratt, A.G. (2019) 'IL-6 Mediated Transcriptional Programming of Naive CD4+ T Cells in Early Rheumatoid Arthritis Drives Dysregulated Effector Function', *Front Immunol*, 10, p. 1535.

Riley, R.L., Khomtchouk, K. and Blomberg, B.B. (2017) 'Age-associated B cells (ABC) inhibit B lymphopoiesis and alter antibody repertoires in old age', *Cell Immunol*, 321, pp. 61-67.

Rousset, F., Garcia, E., Defrance, T., Peronne, C., Vezzio, N., Hsu, D.H., Kastelein, R., Moore, K.W. and Banchereau, J. (1992) 'Interleukin 10 is a potent growth and differentiation factor for activated human B lymphocytes', *Proc Natl Acad Sci U S A*, 89(5), pp. 1890-3.

Rubtsov, A.V., Marrack, P. and Rubtsova, K. (2017) 'T-bet expressing B cells - Novel target for autoimmune therapies?', *Cell Immunol*, 321, pp. 35-39.

Rubtsov, A.V., Rubtsova, K., Fischer, A., Meehan, R.T., Gillis, J.Z., Kappler, J.W. and Marrack, P. (2011) 'Toll-like receptor 7 (TLR7)-driven accumulation of a novel CD11c(+) B-cell population is important for the development of autoimmunity', *Blood*, 118(5), pp. 1305-15.

Rubtsov, A.V., Rubtsova, K., Kappler, J.W. and Marrack, P. (2013) 'TLR7 drives accumulation of ABCs and autoantibody production in autoimmune-prone mice', *Immunol Res*, 55(1-3), pp. 210-6.

Rubtsova, K., Rubtsov, A.V., Cancro, M.P. and Marrack, P. (2015) 'Age-Associated B Cells: A T-bet-Dependent Effector with Roles in Protective and Pathogenic Immunity', *J Immunol*, 195(5), pp. 1933-7.

Rubtsova, K., Rubtsov, A.V., Thurman, J.M., Mennona, J.M., Kappler, J.W. and Marrack, P. (2017) 'B cells expressing the transcription factor T-bet drive lupus-like autoimmunity', *J Clin Invest*, 127(4), pp. 1392-1404.

Rubtsova, K., Rubtsov, A.V., van Dyk, L.F., Kappler, J.W. and Marrack, P. (2013) 'T-box transcription factor T-bet, a key player in a unique type of B-cell activation essential for effective viral clearance', *Proc Natl Acad Sci U S A*, 110(34), pp. E3216-24.

Saadoun, D., Terrier, B., Bannock, J., Vazquez, T., Massad, C., Kang, I., Joly, F., Rosenzwajg, M., Sene, D., Benech, P., Musset, L., Klatzmann, D., Meffre, E. and Cacoub, P. (2013) 'Expansion of autoreactive unresponsive CD21-/low B cells in Sjogren's syndrome-associated lymphoproliferation', *Arthritis Rheum*, 65(4), pp. 1085-96.

Schattner, E.J., Elkon, K.B., Yoo, D.H., Tumang, J., Krammer, P.H., Crow, M.K. and Friedman, S.M. (1995) 'CD40 ligation induces Apo-1/Fas expression on human B lymphocytes and facilitates apoptosis through the Apo-1/Fas pathway', *J Exp Med*, 182(5), pp. 1557-65.

Schittenhelm, L., Hilkens, C.M. and Morrison, V.L. (2017) 'beta2 Integrins As Regulators of Dendritic Cell, Monocyte, and Macrophage Function', *Front Immunol*, 8, p. 1866.

Scholzen, T. and Gerdes, J. (2000) 'The Ki-67 protein: from the known and the unknown', *J Cell Physiol*, 182(3), pp. 311-22.

Schultze, J.L., Michalak, S., Lowne, J., Wong, A., Gilleece, M.H., Gribben, J.G. and Nadler, L.M. (1999) 'Human non-germinal center B cell interleukin (IL)-12 production is primarily regulated by T cell signals CD40 ligand, interferon gamma, and IL-10: role of B cells in the maintenance of T cell responses', *J Exp Med*, 189(1), pp. 1-12.

Schwarting, R., Gerdes, J., Niehus, J., Jaeschke, L. and Stein, H. (1986) 'Determination of the growth fraction in cell suspensions by flow cytometry using the monoclonal antibody Ki-67', *J Immunol Methods*, 90(1), pp. 65-70.

Seifert, M. and Kuppers, R. (2016) 'Human memory B cells', *Leukemia*, 30(12), pp. 2283-2292.

Shabani, M., Bayat, A.A., Jeddi-Tehrani, M., Rabbani, H., Hojjat-Farsangi, M., Ulivieri, C., Amirghofran, Z., Baldari, C.T. and Shokri, F. (2014) 'Ligation of human Fc receptor like-2 by

monoclonal antibodies down-regulates B-cell receptor-mediated signalling', *Immunology*, 143(3), pp. 341-53.

Shapiro-Shelef, M. and Calame, K. (2005) 'Regulation of plasma-cell development', *Nat Rev Immunol*, 5(3), pp. 230-42.

Sheng, J.R., Quan, S. and Soliven, B. (2014) 'CD1d(hi)CD5+ B cells expanded by GM-CSF in vivo suppress experimental autoimmune myasthenia gravis', *J Immunol*, 193(6), pp. 2669-77.

Shimabukuro-Vornhagen, A., Garcia-Marquez, M., Fischer, R.N., Iltgen-Breburda, J., Fiedler, A., Wennhold, K., Rappl, G., Abken, H., Lehmann, C., Herling, M., Wolf, D., Fatkenheuer, G., Rubbert-Roth, A., Hallek, M., Theurich, S. and von Bergwelt-Baildon, M. (2017) 'Antigen-presenting human B cells are expanded in inflammatory conditions', *J Leukoc Biol*, 101(2), pp. 577-587.

Shlomchik, M.J., Craft, J.E. and Mamula, M.J. (2001) 'From T to B and back again: positive feedback in systemic autoimmune disease', *Nat Rev Immunol*, 1(2), pp. 147-53.

Shokat, K.M. and Goodnow, C.C. (1995) 'Antigen-induced B-cell death and elimination during germinal-centre immune responses', *Nature*, 375(6529), pp. 334-8.

Smolen, J.S., Aletaha, D., Barton, A., Burmester, G., Emery, P., Firestein, G.S., Kavanaugh, A., McInnes, I.B., Solomon, D.H., Strand, V. and Yamamoto, K. (2018) 'Rheumatoid arthritis', *Nat Rev Dis Primers*, 4, p. 18002.

Smolen, J.S., Collaud Basset, S., Boers, M., Breedveld, F., Edwards, C.J., Kvien, T.K., Miossec, P., Sokka-Isler, T., van Vollenhoven, R.F., Abadie, E.C., Bruyere, O., Cooper, C., Makinen, H., Thomas, T., Tugwell, P. and Reginster, J.Y. (2016) 'Clinical trials of new drugs for the treatment of rheumatoid arthritis: focus on early disease', *Ann Rheum Dis*, 75(7), pp. 1268-71.

Sohn, H.W., Krueger, P.D., Davis, R.S. and Pierce, S.K. (2011) 'FcRL4 acts as an adaptive to innate molecular switch dampening BCR signaling and enhancing TLR signaling', *Blood*, 118(24), pp. 6332-41.

Stebegg, M., Kumar, S.D., Silva-Cayetano, A., Fonseca, V.R., Linterman, M.A. and Graca, L. (2018) 'Regulation of the Germinal Center Response', *Front Immunol*, 9, p. 2469.

Stoffer, M.A., Schoels, M.M., Smolen, J.S., Aletaha, D., Breedveld, F.C., Burmester, G., Bykerk, V., Dougados, M., Emery, P., Haraoui, B., Gomez-Reino, J., Kvien, T.K., Nash, P., Navarro-Compan, V., Scholte-Voshaar, M., van Vollenhoven, R., van der Heijde, D. and Stamm, T.A. (2016) 'Evidence for treating rheumatoid arthritis to target: results of a systematic literature search update', *Ann Rheum Dis*, 75(1), pp. 16-22.

Stone, S.L., Peel, J.N., Scharer, C.D., Risley, C.A., Chisolm, D.A., Schultz, M.D., Yu, B., Ballesteros-Tato, A., Wojciechowski, W., Mousseau, B., Misra, R.S., Hanidu, A., Jiang, H., Qi, Z., Boss, J.M., Randall, T.D., Brodeur, S.R., Goldrath, A.W., Weinmann, A.S., Rosenberg, A.F. and Lund, F.E. (2019) 'T-bet Transcription Factor Promotes Antibody-Secreting Cell Differentiation by Limiting the Inflammatory Effects of IFN-gamma on B Cells', *Immunity*, 50(5), pp. 1172-1187.e7.

Strand, V., Kimberly, R. and Isaacs, J.D. (2007) 'Biologic therapies in rheumatology: lessons learned, future directions', *Nat Rev Drug Discov*, 6(1), pp. 75-92.

Su, K.Y., Watanabe, A., Yeh, C.H., Kelsoe, G. and Kuraoka, M. (2016) 'Efficient Culture of Human Naive and Memory B Cells for Use as APCs', *J Immunol*, 197(10), pp. 4163-4176.

Sullivan, R.T., Kim, C.C., Fontana, M.F., Feeney, M.E., Jagannathan, P., Boyle, M.J., Drakeley, C.J., Ssewanyana, I., Nankya, F., Mayanja-Kizza, H., Dorsey, G. and Greenhouse, B. (2015) 'FCRL5 Delineates Functionally Impaired Memory B Cells Associated with Plasmodium falciparum Exposure', *PLoS Pathog*, 11(5), p. e1004894.

Suvas, S., Singh, V., Sahdev, S., Vohra, H. and Agrewala, J.N. (2002) 'Distinct role of CD80 and CD86 in the regulation of the activation of B cell and B cell lymphoma', *J Biol Chem*, 277(10), pp. 7766-75.

Suzuki, K., Grigorova, I., Phan, T.G., Kelly, L.M. and Cyster, J.G. (2009) 'Visualizing B cell capture of cognate antigen from follicular dendritic cells', *J Exp Med*, 206(7), pp. 1485-93.

Swainson, L.A., Mold, J.E., Bajpai, U.D. and McCune, J.M. (2010) 'Expression of the autoimmune susceptibility gene FcRL3 on human regulatory T cells is associated with dysfunction and high levels of programmed cell death-1', *J Immunol*, 184(7), pp. 3639-47.

Szabo, S.J., Kim, S.T., Costa, G.L., Zhang, X., Fathman, C.G. and Glimcher, L.H. (2000) 'A novel transcription factor, T-bet, directs Th1 lineage commitment', *Cell*, 100(6), pp. 655-69.

Tan, E.M. and Smolen, J.S. (2016) 'Historical observations contributing insights on etiopathogenesis of rheumatoid arthritis and role of rheumatoid factor', *J Exp Med*, 213(10), pp. 1937-50.

Tavakolpour, S., Alesaeidi, S., Darvishi, M., GhasemiAdl, M., Darabi-Monadi, S., Akhlaghdoust, M., Elikaei Behjati, S. and Jafarieh, A. (2019) 'A comprehensive review of rituximab therapy in rheumatoid arthritis patients', *Clin Rheumatol*.

Thorarinsdottir, K., Camponeschi, A., Cavallini, N., Grimsholm, O., Jacobsson, L., Gjertsson, I. and Martensson, I.L. (2016) 'CD21(-/low) B cells in human blood are memory cells', *Clin Exp Immunol*, 185(2), pp. 252-62.

Thorarinsdottir, K., Camponeschi, A., Gjertsson, I. and Martensson, I.L. (2015) 'CD21 -/low B cells: A Snapshot of a Unique B Cell Subset in Health and Disease', *Scand J Immunol*, 82(3), pp. 254-61.

Thorarinsdottir, K., Camponeschi, A., Jonsson, C., Granhagen Onnheim, K., Nilsson, J., Forslind, K., Visentini, M., Jacobsson, L., Martensson, I.L. and Gjertsson, I. (2019) 'CD21(-/low) B cells associate with joint damage in rheumatoid arthritis patients', *Scand J Immunol*, 90(2), p. e12792.

Treanor, B. (2012) 'B-cell receptor: from resting state to activate', *Immunology*, 136(1), pp. 21-7.

Upton, D.C. and Unniraman, S. (2011) 'Assessing somatic hypermutation in Ramos B cells after overexpression or knockdown of specific genes', *J Vis Exp*, (57), p. e3573.

Ushach, I. and Zlotnik, A. (2016) 'Biological role of granulocyte macrophage colony-stimulating factor (GM-CSF) and macrophage colony-stimulating factor (M-CSF) on cells of the myeloid lineage', *J Leukoc Biol*, 100(3), pp. 481-9.

Van Belle, K., Herman, J., Boon, L., Waer, M., Sprangers, B. and Louat, T. (2016) 'Comparative In Vitro Immune Stimulation Analysis of Primary Human B Cells and B Cell Lines', *J Immunol Res*, 2016, p. 5281823.

van de Sande, M.G., Thurlings, R.M., Boumans, M.J., Wijbrandts, C.A., Modesti, M.G., Gerlag, D.M. and Tak, P.P. (2011) 'Presence of lymphocyte aggregates in the synovium of patients with

early arthritis in relationship to diagnosis and outcome: is it a constant feature over time?', *Ann Rheum Dis*, 70(4), pp. 700-3.

van der Vuurst de Vries, A.R., Clevers, H., Logtenberg, T. and Meyaard, L. (1999) 'Leukocyte-associated immunoglobulin-like receptor-1 (LAIR-1) is differentially expressed during human B cell differentiation and inhibits B cell receptor-mediated signaling', *Eur J Immunol*, 29(10), pp. 3160-7.

van Langelaar, J., Rijvers, L., Janssen, M., Wierenga-Wolf, A.F., Melief, M.J., Siepman, T.A., de Vries, H.E., Unger, P.A., van Ham, S.M., Hintzen, R.Q. and van Luijn, M.M. (2019) 'Induction of brain-infiltrating T-bet-expressing B cells in multiple sclerosis', *Ann Neurol*, 86(2), pp. 264-278.

Wang, S., Wang, J., Kumar, V., Karnell, J.L., Naiman, B., Gross, P.S., Rahman, S., Zerrouki, K., Hanna, R., Morehouse, C., Holoweckyj, N., Liu, H., Manna, Z., Goldbach-Mansky, R., Hasni, S., Siegel, R., Sanjuan, M., Streicher, K., Cancro, M.P., Kolbeck, R. and Ettinger, R. (2018) 'IL-21 drives expansion and plasma cell differentiation of autoreactive CD11c(hi)T-bet(+) B cells in SLE', *Nat Commun*, 9(1), p. 1758.

Wang, T., Ward, Y., Tian, L., Lake, R., Guedez, L., Stetler-Stevenson, W.G. and Kelly, K. (2005) 'CD97, an adhesion receptor on inflammatory cells, stimulates angiogenesis through binding integrin counterreceptors on endothelial cells', *Blood*, 105(7), pp. 2836-44.

Wardemann, H., Yurasov, S., Schaefer, A., Young, J.W., Meffre, E. and Nussenzweig, M.C. (2003) 'Predominant autoantibody production by early human B cell precursors', *Science*, 301(5638), pp. 1374-7.

Warnatz, K., Wehr, C., Drager, R., Schmidt, S., Eibel, H., Schlesier, M. and Peter, H.H. (2002) 'Expansion of CD19(hi)CD21(lo/neg) B cells in common variable immunodeficiency (CVID) patients with autoimmune cytopenia', *Immunobiology*, 206(5), pp. 502-13.

Wehr, C., Eibel, H., Masilamani, M., Illges, H., Schlesier, M., Peter, H.H. and Warnatz, K. (2004) 'A new CD21low B cell population in the peripheral blood of patients with SLE', *Clin Immunol*, 113(2), pp. 161-71.

Weller, S., Faili, A., Garcia, C., Braun, M.C., Le Deist, F.F., de Saint Basile, G.G., Hermine, O., Fischer, A., Reynaud, C.A. and Weill, J.C. (2001) 'CD40-CD40L independent Ig gene hypermutation suggests a second B cell diversification pathway in humans', *Proc Natl Acad Sci U S A*, 98(3), pp. 1166-70.

William, J., Euler, C., Christensen, S. and Shlomchik, M.J. (2002) 'Evolution of autoantibody responses via somatic hypermutation outside of germinal centers', *Science*, 297(5589), pp. 2066-70.

Williams, M.A. and Bevan, M.J. (2007) 'Effector and memory CTL differentiation', *Annu Rev Immunol*, 25, pp. 171-92.

Wilson, T.J., Fuchs, A. and Colonna, M. (2012) 'Cutting edge: human FcRL4 and FcRL5 are receptors for IgA and IgG', *J Immunol*, 188(10), pp. 4741-5.

Winslow, G.M., Papillion, A.M., Kenderes, K.J. and Levack, R.C. (2017) 'CD11c+ T-bet+ memory B cells: Immune maintenance during chronic infection and inflammation?', *Cell Immunol*, 321, pp. 8-17.

Wojciechowski, W., Harris, D.P., Sprague, F., Mousseau, B., Makris, M., Kusser, K., Honjo, T., Mohrs, K., Mohrs, M., Randall, T. and Lund, F.E. (2009) 'Cytokine-producing effector B cells regulate type 2 immunity to H. polygyrus', *Immunity*, 30(3), pp. 421-33.

Wong, P.K., Quinn, J.M., Sims, N.A., van Nieuwenhuijze, A., Campbell, I.K. and Wicks, I.P. (2006) 'Interleukin-6 modulates production of T lymphocyte-derived cytokines in antigen-induced arthritis and drives inflammation-induced osteoclastogenesis', *Arthritis Rheum*, 54(1), pp. 158-68.

Wurster, A.L., Rodgers, V.L., White, M.F., Rothstein, T.L. and Grusby, M.J. (2002) 'Interleukin-4-mediated protection of primary B cells from apoptosis through Stat6-dependent up-regulation of Bcl-xL', *J Biol Chem*, 277(30), pp. 27169-75.

Yano, R., Yamamura, M., Sunahori, K., Takasugi, K., Yamana, J., Kawashima, M. and Makino, H. (2007) 'Recruitment of CD16+ monocytes into synovial tissues is mediated by fractalkine and CX3CR1 in rheumatoid arthritis patients', *Acta Med Okayama*, 61(2), pp. 89-98.

Yap, H.Y., Tee, S.Z., Wong, M.M., Chow, S.K., Peh, S.C. and Teow, S.Y. (2018) 'Pathogenic Role of Immune Cells in Rheumatoid Arthritis: Implications in Clinical Treatment and Biomarker Development', *Cells*, 7(10).

Yatim, K.M. and Lakkis, F.G. (2015) 'A brief journey through the immune system', *Clin J Am Soc Nephrol*, 10(7), pp. 1274-81.

Yeo, L., Lom, H., Juarez, M., Snow, M., Buckley, C.D., Filer, A., Raza, K. and Scheel-Toellner, D. (2015) 'Expression of FcRL4 defines a pro-inflammatory, RANKL-producing B cell subset in rheumatoid arthritis', *Ann Rheum Dis*, 74(5), pp. 928-35.

Yeo, L., Toellner, K.M., Salmon, M., Filer, A., Buckley, C.D., Raza, K. and Scheel-Toellner, D. (2011) 'Cytokine mRNA profiling identifies B cells as a major source of RANKL in rheumatoid arthritis', *Ann Rheum Dis*, 70(11), pp. 2022-8.

Yoshida, N., Kitayama, D., Arima, M., Sakamoto, A., Inamine, A., Watanabe-Takano, H., Hatano, M., Koike, T. and Tokuhisa, T. (2011) 'CXCR4 expression on activated B cells is downregulated by CD63 and IL-21', *J Immunol*, 186(5), pp. 2800-8.

Yoshida, T., Mei, H., Dorner, T., Hiepe, F., Radbruch, A., Fillatreau, S. and Hoyer, B.F. (2010) 'Memory B and memory plasma cells', *Immunol Rev*, 237(1), pp. 117-39.

Yurasov, S. and Nussenzweig, M.C. (2007) 'Regulation of autoreactive antibodies', *Curr Opin Rheumatol*, 19(5), pp. 421-6.

Zaky, D.S. and El-Nahrery, E.M. (2016) 'Role of interleukin-23 as a biomarker in rheumatoid arthritis patients and its correlation with disease activity', *Int Immunopharmacol*, 31, pp. 105-8.

Zhang, L., Zhao, X., Xin, M., Wang, L., Wen, D., Gao, Y., Luo, B. and Sun, M. (2019a) '[Establishment of human B lymphocyte strain overexpressing Epstein-Barr virus latent membrane protein 1 (LMP1)]', *Xi Bao Yu Fen Zi Mian Yi Xue Za Zhi*, 35(3), pp. 206-210.

Zhang, W., Zhang, H., Liu, S., Xia, F., Kang, Z., Zhang, Y., Liu, Y., Xiao, H., Chen, L., Huang, C., Shen, N., Xu, H. and Li, F. (2019b) 'Excessive CD11c(+)Tbet(+) B cells promote aberrant TFH differentiation and affinity-based germinal center selection in lupus', *Proc Natl Acad Sci U S A*, 116(37), pp. 18550-18560.

Zhao, Y., Chen, B., Li, S., Yang, L., Zhu, D., Wang, Y., Wang, H., Wang, T., Shi, B., Gai, Z., Yang, J., Heng, X., Yang, J. and Zhang, L. (2018) 'Detection and characterization of bacterial nucleic

acids in culture-negative synovial tissue and fluid samples from rheumatoid arthritis or osteoarthritis patients', *Sci Rep*, 8(1), p. 14305.

Ziff, M. (1989) 'Pathways of mononuclear cell infiltration in rheumatoid synovitis', *Rheumatol Int*, 9(3-5), pp. 97-103.

Zumaquero, E., Stone, S.L., Scharer, C.D., Jenks, S.A., Nellore, A., Mousseau, B., Rosal-Vela, A., Botta, D., Bradley, J.E., Wojciechowski, W., Ptacek, T., Danila, M.I., Edberg, J.C., Bridges, S.L., Jr., Kimberly, R.P., Chatham, W.W., Schoeb, T.R., Rosenberg, A.F., Boss, J.M., Sanz, I. and Lund, F.E. (2019) 'IFNgamma induces epigenetic programming of human T-bet(hi) B cells and promotes TLR7/8 and IL-21 induced differentiation', *Elife*, 8.